

AFRICAN PALAEOENVIRONMENTS AND GEOMORPHIC
LANDSCAPE EVOLUTION

Palaeoecology of Africa

International Yearbook of Landscape Evolution
and Palaeoenvironments

Volume 30

Editor in Chief

J. Runge, Frankfurt, Germany

Editorial board

G. Botha, Pietermaritzburg, South Africa

E. Cornellissen, Tervuren, Belgium

F. Gasse, Aix-en-Provence, France

P. Giresse, Perpignan, France

S. Kröpelin, Köln, Germany

K. Heine, Regensburg, Germany

T. Huffmann, Johannesburg, South Africa

E. Latrubesse, Austin, Texas, USA

J. Maley, Montpellier, France

J.-P. Mund, Bonn, Germany

D. Olago, Nairobi, Kenya

F. Runge, Altendiez, Germany

L. Scott, Bloemfontein, South Africa

I. Stengel, Pretoria, South Africa

F.A. Street-Perrott, Oxford, UK

M.R. Talbot, Bergen, Norway

African Palaeoenvironments and Geomorphic Landscape Evolution

Editor

Jürgen Runge

Centre for Interdisciplinary African Studies (CIAS/ZIAF)

Johann Wolfgang Goethe University, Frankfurt am Main, Germany



CRC Press

Taylor & Francis Group

Boca Raton London New York Leiden

CRC Press is an imprint of the
Taylor & Francis Group, an **informa** business

A BALKEMA BOOK

Front cover: Geomorphic landscape evolution in South Africa: Gully erosion (donga) in multilayered Quaternary colluvia with palaeosols at St. Paul's, KwaZulu-Natal. Photograph by Jürgen Runge, September 16th, 2001.

Financially supported by CIAS/ZIAF (Centre for Interdisciplinary African Studies/Zentrum für interdisziplinäre Afrikaforschung)



CRC Press/Balkema is an imprint of the Taylor & Francis Group, an informa business

© 2010 Taylor & Francis Group, London, UK

Typeset by Vikatan Publishing Solutions (P) Ltd., Chennai, India

Printed and bound in USA by Antony Rowe (a CPI group Company), Chippenham, Wiltshire

All rights reserved. No part of this publication or the information contained herein may be reproduced, stored in a retrieval system, or transmitted in any form or by any means, electronic, mechanical, by photocopying, recording or otherwise, without written prior permission from the publisher.

Although all care is taken to ensure integrity and the quality of this publication and the information herein, no responsibility is assumed by the publishers nor the author for any damage to the property or persons as a result of operation or use of this publication and/or the information contained herein.

Published by: CRC Press/Balkema

P.O. Box 447, 2300 AK Leiden, The Netherlands

e-mail: Pub.NL@taylorandfrancis.com

www.crcpress.com – www.taylorandfrancis.co.uk – www.balkema.nl

Library of Congress Cataloging-in-Publication Data

African palaeoenvironments and geomorphic landscape evolution / Jürgen Runge, [editor].

p. cm.—(Palaeoecology of Africa : International yearbook of landscape evolution and palaeoenvironments ; volume 30)

Includes index.

ISBN 978-0-415-58789-1 (hard cover : alk. paper)

1. Paleoecology—Africa. 2. Geomorphology—Africa. 3. Landscape changes—Africa. 4. Africa—Environmental conditions. I. Runge, Jürgen. II. Title. III. Series.

QE720.2.A352A37 2010

560'.45096—dc22

2010042534

ISBN: 978-0-415-58789-1 (Hbk)

ISBN: 978-0-203-84527-1 (eBook)

Contents

FOREWORD	vii
— <i>Jürgen Runge</i>	
IN MEMORIAM TIMOTHY COOPER PARTRIDGE (1942–2009)	ix
— <i>Phillip V. Tobias</i>	
PREFACE AND INTRODUCTION	xix
— <i>Jürgen Runge</i>	
CONTRIBUTORS	xxiii
CHAPTER 1 HOW IT ALL BEGAN—EDUARD VAN ZINDEREN BAKKER AND <i>PALAEOECOLOGY OF AFRICA</i>	1
— <i>Klaus Heine</i>	
CHAPTER 2 RECONSTRUCTING ENVIRONMENTAL CHANGES SINCE THE LAST GLACIAL MAXIMUM (LGM) IN THE GEBA BASIN, NORTHERN ETHIOPIA, BY GEOMORPHIC PROCESS INTERPRETATION AND LAND MANAGEMENT EVALUATION	9
— <i>Jan Moeyersons, Jean Poesen, Jan Nyssen, Jozef Deckers & Mitiku Haile</i>	
CHAPTER 3 CLIMATE RECONSTRUCTIONS BASED ON FLUVIAL DEPOSITS IN HYPER-ARID DESERT ENVIRONMENTS: THE NAMIB CASE	27
— <i>Klaus Heine</i>	
CHAPTER 4 A SEDIMENTARY RECORD OF ENVIRONMENTAL CHANGE AT TSODILO HILLS WHITE PAINTINGS ROCK SHELTER, NORTHWEST KALAHARI DESERT, BOTSWANA	53
— <i>Andrew H. Ivester, George A. Brook, Lawrence H. Robbins, Alec C. Campbell, Michael L. Murphy & Eugene Marais</i>	
CHAPTER 5 ECOSYSTEM CHANGE DURING MIS 4 AND EARLY MIS 3: EVIDENCE FROM MIDDLE STONE AGE SITES IN SOUTH AFRICA	79
— <i>Grant Hall & Stephan Woodborne</i>	

CHAPTER 6	THE POTENTIAL OF POACEAE, CYPERACEAE AND RESTIONACEAE PHYTOLITHS TO REFLECT PAST ENVIRONMENTAL CONDITIONS IN SOUTH AFRICA — <i>Carlos E. Cordova & Louis Scott</i>	107
CHAPTER 7	TOPOGRAPHIC AND HYDROLOGIC CONTROL OF GULLY EROSION PHENOMENA IN PALAEOLANDSCAPES OF SWAZILAND, SOUTHERN AFRICA — <i>Samanta Pelacani & Michael Märker</i>	135
CHAPTER 8	GYPSUM IN DESERT SOILS, SUBSURFACE CRUSTS AND HOST SEDIMENTS (WESTERN DESERT OF EGYPT) — <i>Ashraf Mohamed, Konrad Rögner & Sixten Bussemer</i>	151
CHAPTER 9	NEW FINDINGS FROM GEOLOGICAL, GEOMORPHOLOGICAL AND SEDIMENTOLOGICAL STUDIES ON THE PALAEOENVIRONMENTAL CONDITIONS IN SOUTHERN CAMEROON — <i>Mark Sangen, Joachim Eisenberg, Jürgen Runge, Boniface Kankeu & Mesmin Tchindjang</i>	165
CHAPTER 10	PALAEOCLIMATE OF ONDIRI SWAMP, KIKUYU, KENYA, FROM 1.350 TO 1.810 AD — <i>Julian A. Ogondo, Daniel O. Olago & Eric O. Odada</i>	189
CHAPTER 11	A CLUSTER-ANALYSIS-BASED CLIMATE CLASSIFICATION FOR NE AFRICA — <i>Brigitta Schütt, Katharina Ducke & Jan Krause</i>	199
CHAPTER 12	CLIMATE AND PALAEOENVIRONMENT EVOLUTION IN NORTH TROPICAL AFRICA FROM THE END OF THE TERTIARY TO THE UPPER QUATERNARY — <i>Jean Maley</i>	227
CHAPTER 13	AN ASSESSMENT OF THE SPATIAL AND TEMPORAL DISTRIBUTION OF NATURAL HAZARDS IN CENTRAL AFRICA — <i>Ine Vandecasteele, Jan Moeyersons & Philippe Trefois</i>	279
REGIONAL INDEX		301
SUBJECT INDEX		303

Foreword

I take pleasure in presenting the “jubilee” edition “30” of the new *Palaeoecology of Africa*. This meanwhile historic series started some 44 years ago in 1966 under the auspices of Eduard van Zinderen Bakker (1907–2002). In these early days research on former climates, ecosystem changes and landscape dynamics (palaeoecology) was still a new topic in South Africa. This was also true for other African regions in lower latitudes where less was known on the palaeoenvironmental conditions especially during the northern hemisphere glaciations. Professor van Zinderen Bakker started by introducing Palynology as a scientific tool for studying vegetation and climate evolution. However, it was soon realized that the study of fossil pollen and spores is so strongly connected to other scientific disciplines that it would be useful to include biogeography, archaeology, geology, geomorphology, pedology and related fields which have a bearing on the study of the past and present environment. In the course of the time the area covered by numerous articles has been extended from South Africa to the whole of the continent, its surrounding islands and Antarctica. Since then *Palaeoecology of Africa* has become an independent international medium for palaeoenvironmental studies in Africa, and one of the first multi- and interdisciplinary oriented journals. The growing awareness of potential threats by “Global Change” during recent years has emphasized once more the importance of palaeoecological research and knowledge. Aside from the past and present history of landscapes, predictions on future climate developments will be only possible when we know what had happened already once during earth history. With this in mind the past can be considered as to be the key to understand the nearby future.

The “jubilee” edition of the series offers the occasion to include on the one hand several longer review articles that illustrate the growing knowledge on African palaeoenvironments (and will give an orientation on the extensive literature), on the other hand it contains a broad variety of different interdisciplinary case studies from all over Africa. It is now already the third volume of *Palaeoecology of Africa* since 2007 when the series was undertaken large scale modernization. Formatting of the papers to the PoA layout was reliably done by Erik Hock to whom I am most grateful. Ursula Olbrich revised numerous figures and assisted by carrying out cartographic work on the book. The Taylor & Francis team in Leiden with senior editor Janjaap Bloom supported the editorial work. The Frankfurt Centre for Interdisciplinary Research (CIRA) assisted by financial support to print this volume. Many thanks go to all colleagues for submitting their papers to *Palaeoecology of Africa*.

The volume also serves to the memory of Professor Timothy Cooper Partridge who suddenly died on 8th December 2009. He is honored within the series by an obituary of Professor Phillip V. Tobias. Regarded as the leading South African geomorphologist the international scientific community has lost a distinguished scholar and leader in palaeoenvironmental research. This book is devoted to Tim.

Jürgen Runge
Bangui and Frankfurt
May 2010

OBITUARY

In Memoriam Timothy Cooper Partridge¹ 7th December 1942–8th December 2009

Phillip V. Tobias

*Institute for Human Evolution, School of Anatomical Sciences,
University of the Witwatersrand, South Africa*

The untimely and sudden death of Professor Timothy Cooper Partridge (Figures 1 and 2) on 8th December 2009 has robbed the community of geomorphologists, geographers, palaeoclimatologists, palaeontologists and archaeologists of a distinguished scholar and leader in his fields.

Timothy Cooper Partridge was born in Pretoria, South Africa, on 7th December 1942. In 1959, Tim Partridge matriculated from Parktown Boys' High School, Johannesburg, with four distinctions.



Figure 1. Professor Timothy Cooper Partridge (1942–2009).

¹Published in the South African Geographical Journal 2010 (slightly modified version).

After his initial graduation from the University of the Witwatersrand, he pursued graduate studies at the University of Natal under geomorphologist Professor Lester King. Among King's well-known works, he had studied the geomorphology of the South African *Australopithecus*-bearing dolomitic limestone caves. This must have played a part in determining at least one of Partridge's research directions, for he spent some forty years of his life elucidating the geology, stratigraphy and geomorphology of these cave deposits.

He served on the lecturing staff of the Department of Geography at the Witwatersrand University from 1965. For several years he was a research officer in geotechnics with the South African Council for Scientific and Industrial Research. He was Chief Engineering Geologist to Loxton, Hunting and Associates, before setting up his own consultancy, T.C. Partridge and Associates. He headed this consultancy for more than a quarter of a century and it produced over five hundred professional reports in engineering geology, pedology, hydrogeology and photogeology. The specialist activities included the geotechnical classification of land for housing and industrial development, the exploitation of groundwater resources for rural development and site evaluation for large dams. He was a photogeologist of international repute. Using aerial photographs, and other remote sensing imagery, he mapped and analysed some 600.000 square kilometres in Western Australia and the Australian Northern Territory. Nearer home, he made similar surveys covering some 100.000 square kilometres in South Africa, as well as substantial areas of Botswana and Angola.

In his deep interest in the processes that gave rise to the unique landforms of Africa, with its elevated interior plateaux, lengthy marginal escarpments and the eastern Rift Valley, Partridge followed in the footsteps of two eminent geomorphologists of the 1940s and 1950s, Sir Frank Dixey and Lester King, but there was a difference. Whereas the findings of these early pioneers were largely limited to the recognition of flights of planation surfaces and the inferences from them of successive tectonic uplifts, Partridge systematically mapped the distribution of these erosional remnants and assessed the deformations which they had experienced since their creation, as well as the timing of both warping and uplift events. This was achieved through wide-ranging field-work, as well as through his interpretation of remote sensing imagery, in which he was highly skilled. Partridge paid especial attention to the timing and magnitude of tectonic movements in the East African Rift System. A major motivation for this focus was the fundamental importance which these movements have had in providing the ecological backdrop and environmental stimuli that materially influenced the evolutionary pathways along which the genus, *Homo*, evolved from early hominid progenitors. He claimed that much of the vertical uplift of up to 2.000 metres, that had given rise to the elevated plateaux of eastern and southern Africa, was relatively recent, namely post-Miocene. This claim placed Partridge at loggerheads with a cohort of international colleagues, who repeatedly denied the possibility of geologically recent continental uplifts in passive marginal settings. However, in his Alex du Toit Memorial Lecture of 1997, Partridge gathered together and consolidated the evidence delimiting the timing of these movements.

In defending over more than ten years, in the face of widespread international opposition, his assertion that large-scale uplift of major areas in Africa had occurred during the Neogene, and through his subsequent vindication, on the basis of his own and of independent evidence, Partridge belonged in a small coterie of scientists who were responsible for what has been called "premature discoveries". The validity of their hypotheses and paradigms was, in each case, acknowledged by the scientific world only much later. As examples, Raymond Dart's claim in 1925 that the Taung child represented a creature transitional to humankind was accepted only 25 years

later; the pivotal rôle played by *Homo habilis*, that L.S.B. Leakey and his colleagues proclaimed in 1964, took close on twenty years to gain wide acceptance; whilst Alex du Toit's evidence encapsulated in *Our Wandering Continents* (1937), following the work of Taylor (1910), and Wegener (1912), was resuscitated and supported not before the 1960s when the scientific basis of plate tectonics was established.

Partridge tenaciously maintained his position on the importance of neotectonics, until opposition crumbled in the face of overwhelming evidence. His scientific input seems to have revolutionised conventional wisdom on the geomorphic history of a large part of this continent.

The hominid-bearing cave and tufa deposits of South Africa have, since 1924, produced more early hominid specimens than any other area of the world. However, despite their large number and undeniable importance for an understanding of human origins, these finds have, until recently, been somewhat eclipsed by those from the Rift Valley of East Africa. This was owing in part to the impact of the academic boycott on South African science and scientists, and in part to the fact that, with few exceptions, the Rift Valley deposits were securely dated, in contradistinction with the dolomitic cave deposits of South Africa.

In the 1970s he was appointed Honorary Research Associate attached to the author's Palaeo-anthropological Research Unit at the University of the Witwatersrand, and he occupied a similar position in the Sterkfontein Research Unit since its inception. These two research organisations recovered more than six hundred specimens of early hominid fossils since 1966. Partridge was early confronted by the difficulties of dating the South African cave-sites. Yet he knew that it was crucial to place these hominid fossils, and the contemporaneous fauna, in the correct stratigraphic and chronological sequence.

In addition, he determined which materials within the deposits retained an unambiguous palaeomagnetic signal and helped to derive magnetostratigraphies for the important Sterkfontein and Makapansgat sites. Most recently, he headed the team that provided the first absolute dates for major new finds at Sterkfontein, using cosmogenic nuclides.

Tim Partridge made seminal contributions by systematically placing these uniquely important finds within stratigraphic, palaeo-environmental and geochronological frameworks. In this virtually lifelong endeavour, the successive breakthroughs that Partridge achieved or catalysed made a fundamental contribution to the placement of the early South African hominids in time, and thus to the establishment of phylogenies linking them to their East African counterparts. Equally important was his work on the depositional environments and sedimentologies of these deposits, which, together with evidence gleaned from the species composition of the faunas, plant remains and the stable light isotopes present in tooth enamel, permitted the reconstruction of palaeo-environmental conditions at the times when the deposits were formed. To this evidence Partridge added that derived from the reconstruction of uplift histories for the interior plateaux of South and East Africa. As he observed in several publications, these uplifts were of sufficient amplitude to have had major impacts on African environments during some intervals when species turnover was rapid among animals including hominids. These findings were important, too, for an understanding of the circumstances underlying significant changes in hominid demography.

Partridge's seminal research encompassed most of the important South African sites, including Sterkfontein, Makapansgat, Kromdraai and Taung (Figure 2). He was instrumental in providing a date (based on magnetostratigraphy) for what is arguably the most important hominid specimen yet discovered in South Africa, the 3.3 million year old virtually complete skeleton from Sterkfontein, Stw 573, which is presently

being exhumed by R.J. Clarke and co-workers. The recently announced $^{26}\text{Al}/^{10}\text{Be}$ dates, confirming the age of this specimen and of other early hominid remains from Sterkfontein, owe much to Partridge's input, particularly the three-dimensional stratigraphy that he established for this site, which permitted sampling in parallel sections.

Since the mid-1980s Tim Partridge has been deeply immersed in research on Quaternary palaeoclimates. The rapidly increasing importance of his contributions in this field was acknowledged when he was appointed to the Scientific Steering Committee of the PAGES (Past Global Changes) Core Project of the International Geosphere-Biosphere Programme in 1989. Partridge's contributions to the deliberations of this influential committee over six years were significant, especially in decisions on the scientific strategy for the analysis of the PAGES third Pole-Equator-Pole transect through Europe and Africa. A book synthesising the results of this work, entitled *Past Climate Variability through Europe and Africa*, included an important review of southern Africa by Partridge and co-workers.

Arguably the single most important palaeoclimate project initiated by Partridge has been an investigation of the long terrestrial record contained within the



Figure 2. Professor Tim Partridge in 1990 on an excursion of the South African Association of Geomorphologists (SAAG) explaining the geomorphic evolution of the Vaal River's terraces. In the foreground left Professor Jürgen Hövermann (Photo: J. Runge).

sedimentary infilling of the Tswaing impact crater (previously the Pretoria Saltpan). Drilling of the crater began under Partridge's direction in 1988, and by 1989 a lacustrine sequence 90 metres thick had been cored and the impact origin of the crater confirmed. Further analysis showed the sediments to span the past 200,000 years. Apart from important chemical, mineralogical and biological evidence preserved in this sequence, the sediments themselves have yielded one of the best proxy rainfall records from anywhere within the world's mid-latitudes. The transfer function that gave rise to this record was based on granulometry, with calibration from soils sampled along a transect spanning the full range of present Southern African climates. This unique contribution is widely accepted as an important aid in palaeoclimatic reconstruction.

From this record Partridge was able to show that, when insolation forcing due to precessional changes in the earth's orbit was strong, rainfall fluctuations occurred at precessional frequency (23,000 years). When the insolation signal weakened, changes associated with variations in the intensity of the oceanic thermohaline circulation around Southern Africa, and in the extent of the circum-Antarctic atmospheric vortex, became dominant. This highly significant finding is contributing materially to an understanding of the global climate system in the tropics and sub-tropics.

Even more arresting in its vision and implications was Partridge's proposition, announced during a conference in Aix-en-Provence in August 2001. This was based on careful analysis of significant leads and lags in the onset of climatic changes during the Last Glacial Period, observed in Antarctica, in the Kalahari (where they were signalled by the beginning of periods of dune mobility, defined by series of luminescence dates), and in oceanic records from the North Atlantic. He interpreted these substantial and consistent discrepancies as indicating that major climatic events during the Last Glacial were forced from the high latitudes of the southern hemisphere. In particular, he argued that Heinrich Events, associated with massive discharges of icebergs from the ice-sheets fringing the North Atlantic, which repeatedly stalled the oceanic circulation that drives the Gulf Stream, were initiated by an increase in the range and intensity of moisture-bearing winds blowing northwards across the equator. These large-scale changes in atmospheric circulation, in his view, caused the rapid enlargement and ultimate collapse of extensive segments of the northern ice-sheets.

This highly original interpretation is not without its critics, but if correct, as growing evidence appears to indicate, it needs to be taken into account by analysts concerned with scenarios of future climate change in a greenhouse world. Natural changes triggered from the southern hemisphere, particularly those causing variations in oceanic heat transfer, may critically and unexpectedly alter the course of events predicted from modelling experiments based on current paradigms of global atmospheric circulation and the progressive build-up of greenhouse gases. Partridge's proposition that the Antarctic plays a more important role in climatic change than has been acknowledged hitherto is being echoed by others and may yet help to promote a switch of regional focus in the study of global climate change.

Tim Partridge was an earth scientist whose extensive research output over 38 years bore testimony to a broad range of skills. His principal focus was on the recent geological past and his area of interest was Africa, particularly the region south of the equator. His reputation among earth scientists with research interests in this area is unrivalled. But his standing as a scientist of exceptional originality extended far beyond Africa's shores and stemmed from major inputs to several fields of geology. His contributions to an understanding of the geological setting within which our earliest ancestors evolved are admired worldwide—indeed such is his reputation in this field that he was invited to present the opening public address at a conference

of the Royal Swedish Academy of Sciences on *The Origin of Humankind and the Environment* in May 2000. The placement of the world's most important assemblage of early hominid fossils—that from South Africa—within an increasingly precise chronological framework is largely the result of his efforts, and culminated in his announcement early in the new millennium, of the first absolute dates for specimens from Sterkfontein.

Partridge's contributions to an understanding of the mechanisms underlying the evolution of passive continental margins, and of palaeoclimatic processes that have impacted the African continent, and, in some cases, sent ripples across the globe, are well known within the relevant international communities and were acknowledged by his election to high office within international and national scientific bodies.

Among the honours that have been accorded to Tim Partridge are fellowships of the South African Geographical Society (1980), the S.A. Institute of Engineering Geologists (1994) and the Royal Society of South Africa (1995). His achievements have further been recognised through the award in 2001 of the Fellowship of the Geological Society of South Africa, and the award of the Geological Society's Jubilee Medal in 1989, which he shared with Dr. Rodney R. Maud, for an article entitled *Geomorphic Evolution of Southern Africa since the Mesozoic*.

Tim Partridge's greatest gift lay in his ability to grasp the broad picture without compromising attention to detail or the application of conceptual models of the highest sophistication. He was always mindful of the importance of good field evidence and was quickly able, through his highly developed skills, to comprehend its implications in the regional or even global context. This stamped him as a world leader in geology, remarkable for the depth and breadth of his vision in an age of increasingly narrow specialisation (Figure 2).

Tim Partridge at various times held many national and international positions. These included chairmanship of the Cainozoic Task Group of the S.A. Committee on Stratigraphy and of the S.A. National Committee for INQUA. He was President of the Institute for the Study of Mankind in Africa and of the Southern African Society for Quaternary Research (SASQUA). He was leader of the Palaeoclimates of the Southern Hemisphere Project of INQUA, and co-leader of the Pilot Project on Climates of the Past of UNESCO and the International Union of Geological Sciences. As part of the INQUA Commission on Stratigraphy, he chaired the Working Group on the Plio-Pleistocene Boundary. Seriously topical today, he led the project on Long-term Climatic Change of the Foundation for Research Development Special Programme on Southern African Climatic Change. Likewise he led the FRD Special Programme on Palaeoclimates of Southern Africa during the Quaternary. He was a member of the Board of Control of the Bernard Price Institute for Palaeontological Research of the Witwatersrand University.

It would be quite wrong to leave readers with the impression that Tim Partridge was purely a scientist's scientist. He loved life, sparkled at dinner parties—or around a camp-fire—could expound knowledgeably and often passionately on music, history, art and photography, people, wine and food. He loved travel and he loved people. His gentle and kindly manner, his human skills, made it a joy to work with him, to savour his breadth of experience, his originality of mind and his love of literature and language, and to enjoy his friendship.

He married Marilyn Phillips, a medical practitioner and specialist anaesthetist, in 1973 and they spent 31 years happily and creatively complementing each other's careers. Tim was predeceased by Marilyn and by their son, Astley. Tim Partridge was married to Susan Jordan on 26th September 2009. Less than three months later, they were putting the finishing touches to a book, *Caves of the Ape-men*. He turned 67

on Monday, 7th December 2009: a day later, while working on the book with his long-time devoted assistant, Mrs Pat Moon, he was smitten with a severe heart attack and died within minutes. So the last of his books will perforce appear posthumously. This book and his other 150 published works (see selected publications) will help to keep Tim Partridge's memory green.

SELECTED PUBLICATIONS

- Partridge, T.C. and Brink, A.B.A., 1963, Soils for South African Students. Department of Geology, University of the Witwatersrand, 120 p.
- Partridge, T.C., 1964, Some geomorphological considerations in the collation and storage of information on terrain. *Proc. 1st Symp. on Soil Engineering Mapping and Data Storage*, CSIR, Appendix 1, pp. 1–2.
- Partridge, T.C. and Brink, A.B.A., 1965, Transvaal karst: some considerations on morphology and development with special reference to sinkholes and subsidences on the Far West Rand. *S. Afr. Geog. J.*, **47**, pp. 11–34.
- Partridge, T.C., 1965, Legend units, mapping units and land facets. *Proc. 2nd Symp. on Soil Engineering Mapping and Data Storage*, CSIR, pp. 7–9.
- Partridge, T.C. and Brink, A.B.A., 1967, Kyalami Land System: an example of physiographic classification for the storage of terrain data. *Proc. 4th Reg. Conf. for Africa on Soil Mechanics and Foundation Engineering*, **1**, Balkema, Cape Town, pp. 9–14.
- Partridge, T.C., 1967, Some aspects of the water table in South Africa. *Proc. 4th Reg. Conf. for Africa on Soil Mechanics and Foundation Engineering*, **1**, Balkema, Cape Town, pp. 41–44.
- Partridge, T.C., 1967, Statistical variability within soil materials of the Kyalami Land System. *Proc. 4th Ref. Conf. for Africa on Soil Mechanics and Foundation Engineering*, **2**, Balkema, Cape Town, pp. 320–323.
- Partridge, T.C. and Brink, A.B.A., 1967, Gravels and terraces of the lower Vaal River basin. *S. Afr. Geog. J.*, **49**, pp. 21–38.
- Partridge, T.C., Brink, A.B.A., Webster, R. and Williams, A.A.B., 1968, Terrain classification and data storage for the engineering usage of natural materials. *Proc. 4th Conf. Australian Road Research Board*, **4**(2), pp. 1624–1647.
- Partridge, T.C., Brink, A.B.A. and Williams, A.A.B., 1971, The production of soil engineering maps for roads in South Africa and the storage of materials data. *CSIR Technical Recommendations for Highways Series*, **2**.
- Partridge, T.C. and Wilson, J.G., 1970, A regional approach to groundwater prospecting and utilization in South Africa. *Proc. Conv. on Water for the Future*, pp. 1–8.
- Partridge, T.C., 1970, Airphoto interpretation in South Africa. *Photointerpretation*, **5**.
- Partridge, T.C., Brink, A.B.A. and Mallows, E.W.N., 1973, Morphological classification and mapping as a basis for development planning. *S. Afr. Geog. J.*, **55**(1), pp. 69–80.
- Partridge, T.C., 1974, *The Witwatersrand: a study in metropolitan research and analysis undertaken to assist the Central Guideplan Committees for the East and West Rand 1972–73: terrain and engineering geological constraints. Special Report*. Urban and Regional Research Unit, University of the Witwatersrand, 66 p.
- Partridge, T.C., 1975, Some geomorphic factors influencing the formation and engineering properties of soil materials in South Africa. *Proc. 6th Ref. Conf. for Africa on Soil Mechanics and Foundation Engineering*, **1**, Balkema, Cape Town, pp. 37–42.
- Partridge, T.C. 1978, Re-appraisal of lithostratigraphy of Sterkfontein hominid site. *Nature*, **275**(5678), pp. 282–287.

- Partridge, T.C. and Normen, J.W., 1978, Fracture analysis in the determination of sub-unconformity structure: a photogeological study. *J. of Petrol. Geol.* **1**(1), pp. 43–63.
- Partridge, T.C. and Harris, G.M., 1980, Engineering properties of a delta deposit of Lake Malawi. *Proc. 7th Reg. Conf. for Afr. on Soil Mechanics and Foundation Engineering*, Accra, Ghana, pp. 33–41.
- Partridge, T.C., 1981, Terrain and environmental data requirements for metropolitan planning in South Africa. *Proc. 3rd Symp. on Terrain Evaluation and Data Storage, Division of Soil Mechanics and Foundation Engineering*, South African Institution of Civil Engineers, Kyalami Ranch, Transvaal, pp. 49–55.
- Partridge, T.C., Brink, A.B.A. and Williams, A.A.B., 1981, *Soil Survey for Engineering*. Clarendon Press, Oxford, 420 p.
- Partridge, T.C., Diesel, V.A. and Harris, G.M., 1981, Construction upon dolomites of the south-western Transvaal. *Bull. Internat. Assoc. Eng. Geol.*, **24**, pp. 125–135.
- Partridge, T.C. and Dison, L., 1983, Collapse of a railway tunnel through deeply weathered Dwyka tillite associated with slumping on an undercut slope. *Engineering Geology of Southern Africa*, **3**, pp. 55–56.
- Partridge, T.C., 1983, Rehabilitation after strip mining. *Engineering Geology of Southern Africa*, **3**, pp. 130–136.
- Partridge, T.C., 1985, Cretaceous Sediments. *Engineering Geology of Southern Africa*, **4**, pp. 34–36.
- Partridge, T.C., 1985, Tertiary to Recent Coastal Deposits: *Engineering Geology of Southern Africa*, **4**, pp. 57–87.
- Partridge, T.C. and Weinert, H.H., 1985, Colluvium. *Engineering Geology of Southern Africa*, **4**, pp. 154–160.
- Partridge, T.C. and van der Walt, P.J., 1985, Use of coarse and fine alluvia for construction of earthfill dam: Ngotwane River Dam. *Engineering Geology of Southern Africa*, **4**, pp. 169–170.
- Partridge, T.C. and van der Walt, P.J., 1985, Use of fine clayey colluvium for core of earthfill dam: Middle Letaba River Dam. *Engineering Geology of Southern Africa*, **4**, pp. 171–173.
- Partridge, T.C., Robson, J.F., Harris, G.M. and Hamilton, D.J., 1985, Surface mine plant on alluvium mantled by transported soils of mixed origin: Beatrix Gold Mine, Orange Free State. *Engineering Geology of Southern Africa*, **4**, pp. 248–251.
- Partridge, T.C. and Maud, R.R., 1987, *Geomorphic evolution of Southern Africa since the Mesozoic*. *South African Journal of Geology*, **90**, pp. 179–208.
- Partridge, T.C. and Maud, R.R., 1987, An Early Tertiary marine deposit at Pato's Kop, Ciskei. *South African Journal of Geology*, **90**(3), pp. 231–238.
- Bousman, C.B., Partridge, T.C., Scott, L., Metcalfe, S.E., Vogel, J.C., Seaman, M. and Brink, J.S., 1988, Palaeoenvironmental implications of Late Pleistocene and Holocene valley fills in Blydefontein basin, Noupoort, C.P., South Africa. *Palaeoecology of Africa* **19**, pp. 43–67.
- Partridge, T.C., 1988, Geomorphic perspectives on recent environmental change in southern Africa. *Proceedings of National Conference on Long-Term Data Series Relating to South Africa's Renewable Natural Resources, South African Scientific Programmes*, **157**, pp. 367–378.
- Partridge, T.C., 1989, *The significance of origin for the identification of engineering problems in Quaternary transported soils*. In: *Applied Quaternary Research*, edited by de Mulder, E.F.J. and Hageman, B.S., Balkema, Rotterdam, pp. 119–128.
- Partridge, T.C., Brink, A.B.A. and Williams, A.A.B., 1989, Appropriate methods of engineering geological evaluation for rapid urbanization in developing countries. *Proceedings of the 28th International Geological Congress*, Washington D.C., pp. 1–202.

- Partridge, T.C., Brink, A.B.A. and Williams, A.A.B., 1989, Appropriate technology for the design and construction of low-cost unsurfaced roads in developing countries. *Proceedings of the 12th International Conference of International Society for Soil Mechanics and Foundation Engineering, Rio de Janeiro*. A.A.Balkema, Rotterdam, pp. 2101–2105.
- du Pisani, A.L. and Partridge, T.C., 1990, Effects of global warming on crop production in South Africa. *S. Afr. J. Sci.*, **86**, pp. 306–311.
- Partridge, T.C., Avery, D.M., Botha, G.A., Brink, J.S., Deacon, J., Herbert, R.S., Maud, R.R., Scholtz, A., Scott, L., Talma, A.S. and Vogel, J.C., 1990, Late Pleistocene and Holocene climatic change in southern Africa. *S. Afr. J. Sci.*, **86**, pp. 302–306.
- Partridge, T.C. and Watt, I.B., 1991, The stratigraphy of the Sterkfontein hominid deposit and its relationship to the underground cave system, *Palaeontologia Africana*, **28**, pp. 35–40.
- Schmidt, V.A., and Partridge, T.C., 1991, An attempt to establish a magnetostratigraphic framework for sediments deposited in Sterkfontein Cave, South Africa. *Palaeoanthropology Research Unit (PARU) 25th Annual Report*, University of the Witwatersrand, Johannesburg.
- Partridge, T.C., 1997, Cainozoic environmental change in southern Africa, with special reference on the last 200,000 years. *Prog. Phys. Geogr.*, **21**, pp. 3–22.
- Partridge, T.C., de Menocal, P., Lorenz, S.A., Paiker, M.J., Vogel, J.C., 1997, Orbital forcing of climate over South Africa: a 200,000-year rainfall record from the Pretoria Saltpan. *Quat. Sci. Rev.* **16**, pp. 1125–1133.
- Partridge, T.C., 1999, The sedimentary record and its implication for rainfall fluctuations in the past. *Mem. Geol. Survey South Africa*, **85**, pp. 127–143.
- Partridge, T.C., Shaw, J., Heslop, D. and Clarke, R.J., 1999, The new hominid skeleton from Sterkfontein, South Africa: age and preliminary assessment, *J. Quat. Sci.* **14**, pp. 293–298.
- Partridge, T.C. and Maud, R.R., 2000, The Cenozoic of Southern Africa. *Oxford Monographs on Geology & Geophysics*, **40**, Oxford University Press, Oxford.
- Partridge, T.C., 2000, Hominid-bearing cave and Tufa deposits. In: *The Cenozoic in Southern Africa. Oxford Monographs on Geology and Geophysics*, **40**, Oxford University Press, pp. 100–125.
- Partridge, T.C., 2002, Were Heinrich events forced from the southern hemisphere? *S. Afr. J. Sci.* **98**, pp. 43–46.
- Holmgren, K., Lee-Thorp, J.A., Cooper, G.R.J., Lundblad, K., Partridge, T.C., Scott, L. *et al.*, 2003, Persistent millennial-scale climatic variability over the past 25,000 years in southern Africa. *Quaternary Science Reviews*, **22**, pp. 2311–2326.
- Partridge, T.C., Granger, D.E., Caffee, M.W. and Clarke, R.J., 2003, Lower Pliocene hominid remains from Sterkfontein, *Science*, **300**, pp. 607–612.
- Partridge, T.C., Lowe, J.J., Barker, P., Hoelzmann, P., Magri, D., Saarnisto, M., Vandenberghe, J., Street-Perrott, F.A., Gasse, F., 2004, Climate variability in Europe and Africa: a PAGES-PEP III time stream II synthesis. In: *Past climate variability through Europe and Africa. Developments in Palaeoenvironmental Research*, **6**, pp. 583–603.
- Scott L., Holmgren K. and Partridge T.C., 2008, Reconciliation of vegetation and climatic interpretations of pollen profiles and other regional records from the last 60 thousand years in the Savanna Biome of Southern Africa. *Palaeogeography, Palaeoclimatology, Palaeoecology*, **257**, pp. 198–206.
- Holzkämper, S., Holmgren, K., Lee-Thorp, J., Talma, S., Mangini, A. and Partridge, T.C., 2009, Late Pleistocene stalagmite growth in Wolkberg Cave, South Africa. *Earth and Planetary Science Letters*, **282**, 1–4, pp. 212–221.

Norström, E., Scott, L., Partridge, T.C., Risberg, J. and Holmgren, K., 2009, Reconstruction of environmental and climate changes at Braamhoek Wetland, eastern escarpment South Africa, during the last 16.000 years with emphasis on the Pleistocene–Holocene transition. *Palaeogeography, Palaeoclimatology, Palaeoecology*, **271**, pp. 240–258.

Preface and Introduction

With the presentation of volume 30 of *Palaeoecology of Africa* (PoA) the series celebrates its 44th anniversary since starting in 1966. The jubilee edition of the yearbook looks back and forward, showing the history of the series, and former as well as recent trends and developments in palaeoenvironmental research. The 13 papers gathered together in this volume are covering numerous aspects, ideas and regions on former climates, vegetation cover, ecosystems and landscape dynamics all over Africa applying a huge variety of scientific methods (Figure 1). The reader will find complex reviews and new assessments as well as recent manuscripts on the former dynamics of ecosystems. Aside from natural changes in climate the human impact on landscapes and ecosystems is highlighted by some contributions. The concern and growing public awareness of recent and future Global Climate Change has underlined the importance and necessity of a better knowledge on past climate conditions to gain a better understanding of future processes that will probably change earth's environments within a relatively short time span. The past is the key to the future!

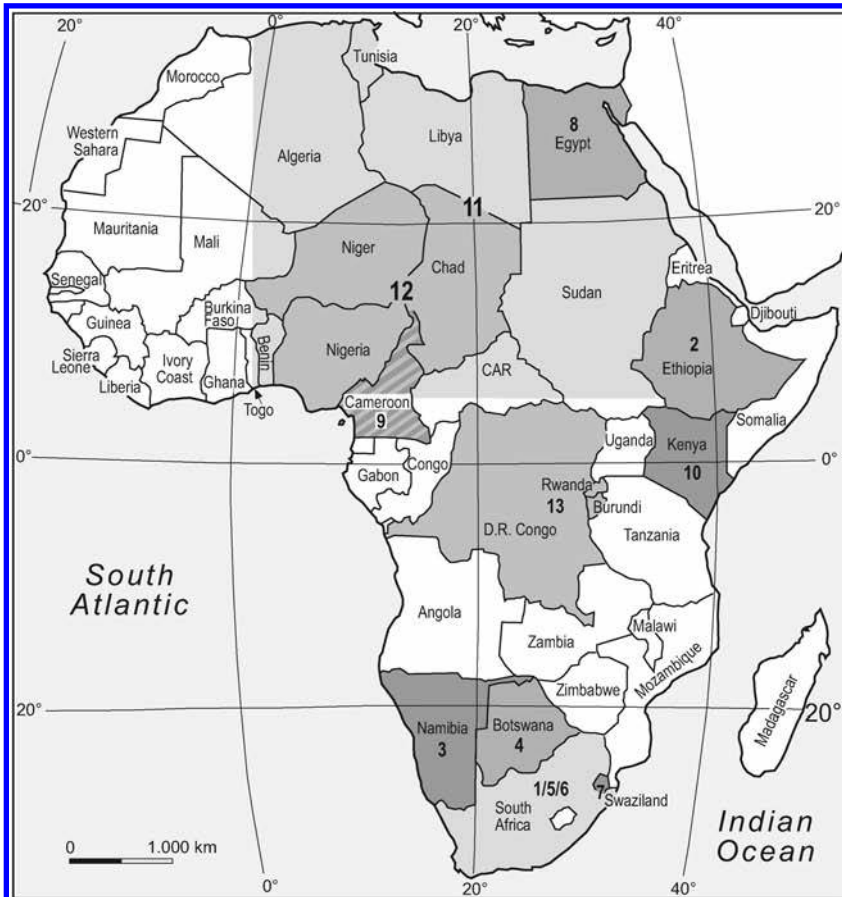
“How it all began” is the title of a short retrospective paper written by Klaus Heine (chapter 1) on the history of the PoA series founded by Professor Eduard M. van Zinderen Bakker. In 1993 the late van Zinderen Bakker published his reminiscences. Some of the introductory pages (“In praise of dust and mud”) are re-published in this volume showing the early days of palynological research in South Africa.

A Belgian and Ethiopian research team around Jan Moeyersons is reconstructing environmental changes since the Late Glacial Maximum in the Geba basin of Northern Ethiopia (chapter 2) highlighting the early and today's influence by humans on the environment. Klaus Heine is concerned with climate reconstructions on the basis of fluvial deposits in the Namib desert (chapter 3) doing a critical reappraisal on how proxy data can be gained from complex fluvial sediment facies—often more than only one palaeoecological interpretation is possible.

Terrestrial rockshelter sediments at Tsodilo Hills in the Kalahari Desert of Botswana are analyzed by Andrew Ivester and his team (chapter 4) using optically stimulated luminescence (OSL) dating methods giving a series of soil stratigraphic units evidencing changing conditions over a period of the past 100/120 ka. Aside from the local findings their interpretations are done within a global context.

Grant Hall and Stephan Woodborne (chapter 5) document by other cave sediments from Sibudu, Kwa-Zulu-Natal and OSL datations severe ecosystem changes in South Africa for the oxygen isotope stages 3 and 4 similar to the Last Glacial Maximum. Correlations to archaeological findings for the Middle Stone Age have become possible. For interpretation they look at these terrestrial observations in a regional context focusing on ocean/atmosphere interactions and a weakening of the palaeo Agulhas current.

A palaeobotanical approach is applied by Carlos Cordova and Louis Scott (chapter 6) studying the potential of phytoliths from C₃ and C₄ plants (Poaceae, Cyperaceae, Restionaceae) in South Africa. They evidence that the dynamics of some climate



- 1 - Klaus Heine, How it all began—Eduard van Zinderen Bakker and PALAEOECOLOGY OF AFRICA.
- 2 - Jan Moeyersons *et al.*, Reconstructing environmental changes in Northern Ethiopia.
- 3 - Klaus Heine, Climate reconstructions in hyper-arid desert environments: the Namib case.
- 4 - Andrew H. Ivester *et al.*, A sedimentary record of environmental change at Tsodilo Hills White Paintings Rock, Botswana.
- 5 - Grant Hall & Stephan Woodborne, Ecosystem change during MIS4 and early MIS 3, South Africa.
- 6 - Carlos E. Cordova & Louis Scott, The palaeoenvironmental potential of phytoliths, South Africa.
- 7 - Samanta Pelacani & Michael Märker, Gully erosion phenomena, Swaziland.
- 8 - Ashraf Mohamed *et al.*, Gypsum in desert soils, Egypt.
- 9 - Mark Sangen *et al.*, Palaeoenvironmental conditions in Southern Cameroon.
- 10 - Julian A. Ogondo *et al.*, Palaeoclimate of Ondiri Swamp, Kikuyu-Kenya.
- 11 - Brigitta Schütt *et al.*, A cluster-analysis-based climate classification for NE Africa.
- 12 - Jean Maley, Climate and palaeoenvironment evolution in north tropical Africa.
- 13 - Ine Vandecasteele *et al.*, Spatial and temporal distribution of natural hazards in Central Africa.

Figure 1. Location map of study sites and short title according to PoA-chapters.

variables such as total annual precipitation, rainfall seasonality and variability and summer temperatures can be documented by grass phytoliths and that they therefore provide a useful tool for palaeoclimatic reconstructions in this study area.

Geomorphic, pedologic and hydrologic aspects of recent to subrecent donga/gully erosion phenomena (see cover photo of PoA 30) in palaeolandscapes in Swaziland are discussed by Samanta Pelacani and Michael Märker in chapter 7. Spatio-temporal dynamics of gullies and rates of headcut retreat for several forms were calculated by using aerial photograph comparison and setting up high resolution digital terrain models (DTM).

In chapter 8 Ashraf Mohamed, Konrad Rögner and Sixten Bussemer contribute to overall palaeoenvironmental questions by studying the occurrence of gypsum in soils and in crusts emphasizing that the formation of crusts must have had occurred under a more humid climate than the hyper arid climate of today. However, the authors do not give a concrete interpretation neither an ecosystem history hypothesis for these findings from the Western Desert of Egypt.

Chapter 9 summarizes comprehensive palaeoenvironmental findings and proxy data generation from fluvial sediments of several rivers in the rain forest zone of Southern Cameroon by a team around Mark Sanguen. These terrestrial records in a humid tropical environment date back to almost 50 ka. Numerous radiocarbon data (^{14}C) and $\delta^{13}\text{C}$ figures allowed the reconstruction of former Late Quaternary environments in the western Atlantic part of Central Africa.

Julian A. Ogondo, Daniel Olago and Eric O. Odada summarize in chapter 10 the results on a pollen-diatom and geochemistry study from a near to surface core at Ondiri Swamp in Kenya that evidence historic environmental conditions close to the equator between 1350 to 1810 AD. By comparison with other proxy data from the region (e.g. Lake Naivasha) they confirm shorter climatic fluctuations and subrecent environmental/landscape disturbances. However, this paper also illustrates that it is often a problem to transfer local findings on a wider regional scale, what means that it is also possible that they are more the expression of effects in places.

The region of Northern and Central Africa is covered by the study of Brigitta Schütt, Katharina Ducke and Jan Krause on a cluster-analysis-based climate classification comparing conventional and established climate classifications of Köppen-Geiger, Troll-Paffen and others with their own approach in chapter 11. This paper can have some relevance to the understanding to recent and to short time climate dynamics based on empirical data and is therefore useful to be included in a book on palaeoenvironments.

Chapter 12 is a very comprehensive review paper by the editorial board member of PoA Jean Maley concerning the evolution of climate and palaeoenvironment in the northern hemisphere of Africa from the end of the Tertiary to the Upper Quaternary. Especially the extensive studies on the Lake Chad basin give an excellent overview what has been done so far and what open questions future research is facing.

Finally, chapter 13 by Ine Vandecasteele, Jan Moeyersons and Phillipe Trefois is concerned with climate controlled natural hazards in Central Africa. This paper gives on the one hand an overview of the spatial and temporal distribution of geomorphic and hydrologic hazards by introducing a new data base on these phenomena, on the other hand it shows that research on palaeo-relief and landscape dynamics has a large potential for applied science and for further research.

Contributors

George A. Brook

Department of Geography, University of Georgia, GG Building, 210 Field St., Room 204, Athens, GA 30602, U.S.A. Email: gabrook@uga.edu

Sixten Bussemer

Institut für Geographie und Geologie, Lehrstuhl Geoökologie und Bodengeographie, Universität Greifswald, F.-L.-Jahnstr. 17a, D-17489 Greifswald, Germany. Email: sixten.bussemer@uni-greifswald.de

Alec C. Campbell

P.O. Box 306, Crocodile Pools, Gaborone, Botswana. Email: acpeba@home.co.bw

Carlos E. Cordova

Department of Geography, 337 Murray Hall, Oklahoma State University, Stillwater, OK 74078, U.S.A. Email: carlos.cordova@okstate.edu

Jozef Deckers

Soil and Water Management, K.U. Leuven, Celestijnenlaan 200e-bus 2411, 3001 Heverlee, Belgium. Email: Seppe.Deckers@ees.kuleuven.be

Katharina Dücke

Physical Geography, Department of Earth Sciences, Freie Universität Berlin, Malteserstr. 74-100, Haus H, 12249 Berlin, Germany. Email: kducke@googlemail.com

Joachim Eisenberg

Institute of Physical Geography, Johann Wolfgang Goethe University Frankfurt am Main, Altenhöfer Allee 1, D-60438 Frankfurt, Germany. Email: j.eisenberg@em.uni-frankfurt.de

Grant Hall

Ecosystem Processes and Dynamics, CSIR, P.O. Box 395, Pretoria, 0001, South Africa. Email: ghall@csir.co.za

Mitiku Haile

Mekelle University, P.O. Box 231, Mekelle, Tigray, Ethiopia. Email: gualmitiku@yahoo.com

Klaus Heine

Philosophische Fakultät I, Universität Regensburg, D-93040 Regensburg, Germany. Email: klaus.heine@geographie.uni-regensburg.de

Andrew H. Ivester

Department of Geosciences, University of West Georgia, 1601 Maple Street, Carrollton, GA, 30108-3100, U.S.A. Email: aivester@westga.edu

Boniface Kankeu

Institut de Recherches Géologiques et Minières (IRGM), BP 4110, Yaoundé, Cameroon. Email: bonifacekankeu@yahoo.fr

Jan Krause

Physical Geography, Department of Earth Sciences, Freie Universität Berlin, Malteserstr. 74-100, Haus H, 12249 Berlin, Germany. Email: jan.krause@fu-berlin.de

Michael Märker

Heidelberger Akademie der Wissenschaften Forschungsstelle: The role of culture in the early expansions of humans c/o Geographisches Institut der Eberhard Karls Universität Tübingen, Rümelinstr 19-21, D-72070 Tübingen, Germany. Email: michael.maerker@geographie.uni-tuebingen.de

Jean Maley

Departement Paléoenvironnements & Paléoclimatologie, ISEM-CNRS, UMR 5554, Université de Montpellier-2, Montpellier-34095, France. Email: jmaley@univ-montp2.fr

Eugene Marais

National Museum of Namibia, P.O. Box 1203, Windhoek, Namibia. Email: insects@natmus.cul.na

Jan Moeyersons

Geomorphology and Remote sensing, Royal Museum for Central Africa, Leuvensesteenweg 13, 3080 Tervuren, Belgium, Email: Jan.moeyersons@africamuseum.be

Ashraf Mohamed

Fayoum University, Said Soliman St., University Region, Fayoum 63514, Egypt. Email: ashraf96@hotmail.com

Michael L. Murphy

Kalamazoo Valley Community College, Texas Township Campus, 6767 West O Avenue, P.O. Box 4070, Kalamazoo, MI 49003-4070, U.S.A. Email: michaellmurphy@aol.com

Jan Nyssen

Department of Geography, Ghent University, Krijgslaan 281 (S8), B 9000 Gent, Belgium. Email: jan.nyssen@ugent.be

Eric O. Odada

University of Nairobi, Department of Geology, P.O. Box 30197, Nairobi, Kenya. Email: africanness@uonbi.ac.ke

Julian Awuor Ogondo

National Museums of Kenya, P.O. Box 40658-00100, Nairobi, Kenya. Email: jogondo@museums.or.ke

Daniel Ochieng Olago

University of Nairobi, Department of Geology, P.O. Box 30197, Nairobi, Kenya. Email: dolago@uonbi.co.ke

Samanta Pelacani

Department of Plant, Soil and Environmental Science University of Florence, P.le delle Cascine 15, 50114 Firenze, Italy. Email: samanta.pelacani@unifi.it

Jean Poesen

Physical and Regional Geography Research Group, Department Earth and Environmental Sciences, K.U. Leuven, GEO-INSTITUTE, Bus 2409, Room 03.246, Celestijnenlaan 200 E, B-3001 Heverlee, Belgium.
Email: jean.poesen@ees.kuleuven.be

Lawrence H. Robbins

Department of Anthropology, Michigan State University, 355 Baker Hall, East Lansing, MI 48824, U.S.A. Email: lrobbins@msu.edu

Konrad Rögner

Department für Geographie, LMU München, Luisenstr. 37, D-80333 München.
Email: k.roegner@geographie.uni-muenchen.de

Jürgen Runge

Institute of Physical Geography, Johann Wolfgang Goethe University Frankfurt am Main, Altenhöfer Allee 1, D-60438 Frankfurt, Germany.
Email: j.runge@em.uni-frankfurt.de

Mark Sangen

Institute of Physical Geography, Johann Wolfgang Goethe University Frankfurt am Main, Altenhöfer Allee 1, D-60438 Frankfurt, Germany.
Email: m.sangen@em.uni-frankfurt.de

Brigitta Schütt

Physical Geography, Department of Earth Sciences, Freie Universität Berlin, Malteserstr. 74-100, Haus H, 12249 Berlin, Germany. Email: brigitta.schuett@fu-berlin.de

Louis Scott

Department of Plant Sciences, University of the Free State, Nelson Mandela Avenue, PO Box 339, Bloemfontein, 9300, South Africa. Email: scottl@ufs.ac.za

Mesmin Tchindjang

Department of Geography, University of Yaoundé I, BP 755, Yaoundé, Cameroon.
Email: mtchind@yahoo.fr

Phillip V. Tobias

Institute for Human Evolution, School of Anatomical Sciences, University of the Witwatersrand, Johannesburg, South Africa.

Philippe Trefois

Geomorphology and Remote sensing, Royal Museum for Central Africa, Leuvensesteenweg 13, 3080 Tervuren, Belgium, Email: philippe.trefois@africamuseum.be

Ine Vandecasteele

Geomorphology and Remote sensing, Royal Museum for Central Africa, Leuvensesteenweg 13, 3080 Tervuren, Belgium, Email: ine.vandecasteele@africamuseum.be

Stephan Woodborne

Ecosystem Processes and Dynamics, CSIR, P.O. Box 395, Pretoria, 0001, South Africa. Email: swoodbor@csir.co.za

CHAPTER 1

How it all began—Eduard van Zinderen Bakker and *Palaeoecology of Africa*

Klaus Heine

*Department of Geography, Universität Regensburg,
Regensburg, Germany*

1.1 INTRODUCTION

There are several reasons why it seems to me both appropriate and opportune that a chapter of Eduard M. van Zinderen Bakker's *Reminiscences* will be published in volume 30 of *Palaeoecology of Africa*. The *Reminiscences of biological travels in Africa and to south polar islands* are not a book in the accepted sense of the word and this book is not a publication which is available in bookshops. The *Reminiscences* are memories which are intended for lovers of nature and adventure, for those who admire the birds and beasts, the rain and the wind, the forests and the mountains. But the *Reminiscences* also document why van Zinderen Bakker became absorbed in Quaternary studies, plant ecology and palynology. In the first chapter which is "In praise of dust and mud", van Zinderen Bakker introduces into palynology. For van Zinderen Bakker palynology was the starting-point of all his palaeoecological research. Very early, van Zinderen Bakker realised that the future of a sound Earth depends on an ecological understanding of all compartments and interferences of Earth's nature and that by understanding natural processes mankind will be able to manage future environmental problems.

The series *Palaeoecology of Africa*, established by van Zinderen Bakker, started in 1966. From the beginning it was a rich collection of ideas and facts. Volume 1 presented a compilation of reports which have been published over the years 1950–1963 under the title of *Palynology in Africa* written by Eduard van Zinderen Bakker. After more than 50 years of the study of fossil pollen and spores together with many other disciplines which consider past and present environments in all their bearings, *Palaeoecology of Africa* is a platform for the growing interest in the sustainable use of natural resources in Africa (relief, soils, water, vegetation, atmosphere) as well as in global change issues. With the publication of 30 volumes of *Palaeoecology of Africa* van Zinderen Bakker's hope came true that this series might be of value to a great number of scientists and that it might assist in correlating research in many different fields.

Born in 1907 in the Netherlands, the country that according to van Zinderen Bakker's friend Richard Foster Flint exports tulip bulbs and palynologists, van Zinderen Bakker emigrated in 1947 to South Africa together with his wife and two young sons when he was offered a university position at Bloemfontein. In those days, palynological research in South Africa was still in a preliminary stage. During the decades before 1950 only a few papers had been published on this subject. Furthermore, the first contributions to the study of pollen had been in connection with hay-fever. Van Zinderen Bakker first made a collection of pollen samples which represents most of the important genera of South African plants. A slide collection had been started

and a pollen atlas was published in sections. After the morphology of the South African pollen had been investigated by van Zinderen Bakker and his co-workers, results were achieved in pollen analysis. He held the opinion that the demand for presenting these results had been so heavy that it had been necessary to print them. By the many reports published in *Palaeoecology of Africa* over the years, gradually an image of the vegetation and climate of the past of southern Africa and adjacent regions was obtained and the difficult coordination of the results gathered from various sites by different disciplines was possible.

Dedicated to relatives and friends, van Zinderen Bakker wrote his *Reminiscences of biological travels in Africa and to south polar islands*. The *Reminiscences* start and end with a remark by Voltaire “La science est comme la terre, on n’en peut posséder qu’un peu”. As far as I know Eduard van Zinderen Bakker, this remark was the leitmotiv for his research. His experience and knowledge was respected world-wide in the scientific community. His scientific work brought him into contact with many colleagues who were specialists in related fields, such as geomorphology, radiometric dating, archaeology and climatology. Looking for the global causes of the profound environmental changes that had occurred in the past in Africa he also came into fruitful contact with oceanographers and glaciologists. The culmination of these interdisciplinary personal meetings, van Zinderen Bakker wrote in his *Reminiscences*, was his nomination as Convenor of the Group of Specialists on Late Cenozoic Studies of the Antarctic. To van Zinderen Bakker it was a privilege to have met the many pioneers and inquisitive minds of this group who opened new horizons to him as a botanist. I remember the evening of October 4, 1978 when we were sitting near our tents in the Namib Desert watching the sun-set over the dune crests in the far distance. Van Zinderen Bakker concluded our discussion, remarking that it is so easy and so tempting to believe that we have found the key or the solution. The presumption that there is only one answer to a problem runs counter to our experience of the natural world, where several keys may fit to the same lock, so that no one theory, however original or attractive, can ever claim to represent more than a very modest and provisional part of reality.

After retirement as professor of Botany at the University of the Orange Free State (OFS), Bloemfontein, in 1972 he became director of the Institute for Environmental Research, Bloemfontein, until 1976, and from 1976 until 1988 he was research officer at the University of the OFS. Reconsidering shortly the aim of *Palaeoecology of Africa*, the most important results certainly were “to somewhat raise the veil which

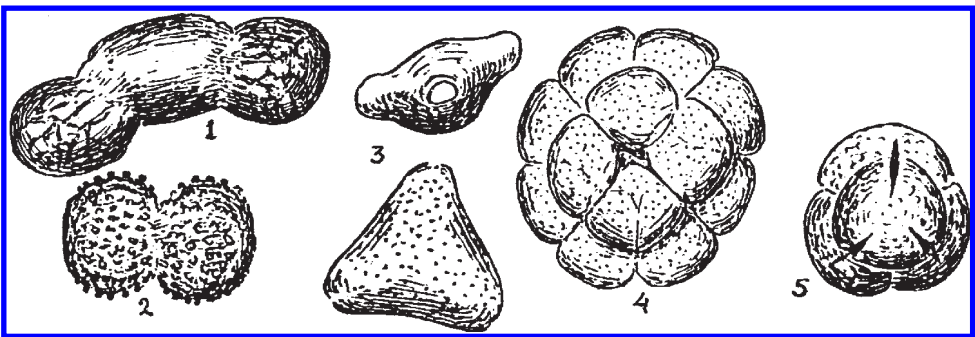


Figure 1. Some African pollen grains. 1. Podocarpus, Yellowwood, 70 μ long, a grain with two air bladders: 2. Sphaerothylox, 35 μ long, a waterfall plant: 3. Protea, 30 μ , two different views: 4. Acacia horrida, 50 μ , a polyad of 16 grains: 5. Erica, 33 μ , a tetrad (four grain united). (1 μ = 0,001 mm).

obscured the mysteries of environmental change in Africa' (van Zinderen Bakker, 1993).

The following pages and pictures are reprinted in the present volume with respect of the person and scientist Eduard van Zinderen Bakker Sr. They show how (palaeo) ecological research began in Africa.

1.1.1 In praise of dust and mud

Eduard M. van Zinderen Bakker, Sr. (1993)

This short introduction has been written for those readers who are not acquainted with the research method known as palynology. These lines are certainly not intended to represent a scientific discourse, but are a popular presentation belonging to the 'biologie amusante'.

What is palynology? The meaning of the term is 'knowledge about fine dust' and microscopic plant particles which can occur floating in the air. A palynologist is mostly interested in the pollen rains, the yellow powder, which is always found in the 'aerial plankton'. He studies these tiny cells in the recent state as well as those that have become fossilised and are hundreds of thousands of years old. The intriguing fact is that plants produce these valuable reproductive cells wrapped in a flimsy wall consisting of an extremely resistant substance, called sporopollenin. These peculiar plant cells, which range in size from 20–100 micron (one micron being a thousandth of a millimetre) and are therefore practically invisible to the naked eye but reveal with microscopic examination a miraculous array of shapes and an incredibly refined and beautiful ornamentation. The infinite variation of these wall patterns is certainly one of the perplexing wonders of nature. As these microscopic features are characteristic to plant families, genera and even in some cases to plant species, they are fingerprints by which the palynologist can identify the plants which produced them. But to be able to do this the scientist has to possess reference collections of thousands of well known pollen types as well as a large collection of photographs made with a photomicroscope.

So far, so good—but this is only the beginning of the hard work which awaits the researcher who is studying an assemblage of fossil grains he has extracted from a deep geological core taken on land or in the ocean. His task is to read these old archives of nature's history. The pollen grains are the letters of his alphabet and the number of the letter-types is infinitely larger than that of the Chinese language. His memory of forms and details often needs the assistance of a computer to decode the story told on every page of the valuable document he is reading.

As the first page of his archival document is present at the bottom of the deep core, his study resembles the reading of a Hebrew book, namely from the back to the front. Once his analysis of the pollen language has provided a picture of the former vegetation the palynologist has also obtained a very valuable assessment of the former climate as the vegetation is a very sensitive parameter of climate. This work is extremely time-consuming and a good 'palyno' must have the patience of a mediaeval monk who is not interested in time but only in perfection. For his investigations he is able to cut ultrathin sections of the 'invisible' pollen grains in order to study its intricate wall structure. He can also examine his grains under the scanning electron microscope which will produce three-dimensional pictures with an enlargement of several thousand times. In short palynology is a fascinating method of studying the past vegetation and climate and its application has revealed and explained a large number of mysteries of the history of our planet.

My first steps as a student in this field date back to the pre-war years when I had finished my Doctor's thesis and turned my mind more and more towards ecology and the Quaternary geology of the Netherlands. The very small section of the Earth's surface occupied by that country has in geological times been formed on the southeastern side of the North Sea by the interplay of rivers and the sea which accumulated horizons of sand, clay and peat. Glaciers descending from the north finally bulldozed and reshaped part of the surface of this delta. As the geological history of these processes was of great interest to my friends and enthusiastic colleagues from different disciplines a study group was formed and leading scientists were invited to give guidance in discussions and to lecture on a variety of subjects, such as: glacial geology, former vegetation and fauna, archaeology, etc.

During field work in those days I discovered a strange configuration in a soil profile near the town of Apeldoorn, which could represent an example of so-called cryoturbation. The experienced pedologist Professor C.H. Edelman agreed that the dark peaty horizon of warped and convoluted bands in the sandy profile was the result of conditions which had prevailed in a polar climate not far away from glaciers and was a so-called periglacial phenomenon.

The tortuous configuration must have been formed in a tundra where, during severe cold conditions, the soil was frozen to great depth, while the surface thawed in summer. When I boiled some peaty material in potassium hydroxide and examined the residue under my microscope, I was amazed to see hundreds of fossil pollen grains from the former tundra vegetation. In those days my interest in pollen studies was stimulated by my mentor Professor F. Florschütz, the Netherlands pioneer in this field. In the deposits he found small well-preserved leaves of the cold-loving alpine rose (*Dryas octopetala*), a mat-forming plant covered with a profusion of small white flowers.

This experience opened my eyes to the fascinating fields of climatic change, ecology of former times (palaeoecology) and especially the ice ages and was in later years an incentive to my search for evidence of the ice age in equatorial Africa. As a consequence I gave some demonstrations of fossil pollen to the gifted students in the higher grades of the grammar school at which I taught. This was apparently appreciated as later on two of these young men published scientific papers on this subject and one of them, Professor W. van Zeist, became a leading palaeobotanist and palynologist working in Europe and the Near East. One of the many finds he described was the interesting discovery in the extensive peat country in the province of Drenthe of the remains of a leather pouch containing 312 Roman coins (van Zeist, 1956). The purse

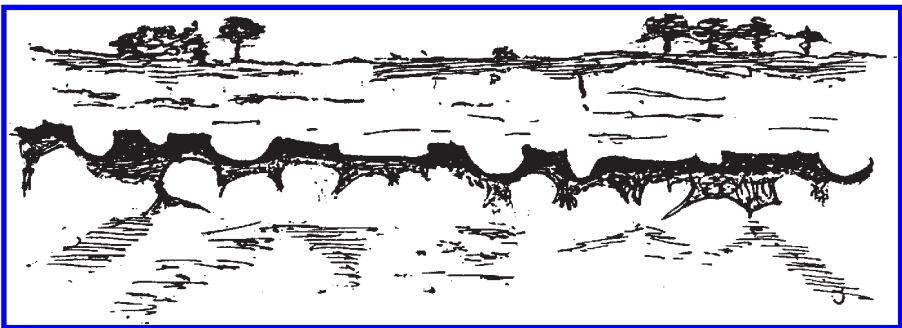


Figure 2. Cryoturbation. Convoluted peat bands in a soil profile indicating former glacial conditions.

had apparently been hidden by a Roman soldier in a tussock of cotton-sedge (*Eriophorum*) with the intention to retrieve it later on. As the lost purse gradually became engulfed in the accumulating peat it was well preserved for posterity. The peat adhering to the pouch contained enough fossil pollen grains to give a valuable picture of the former vegetation which had surrounded the wandering Roman. The 312 coins with the effigy of the cruel, bloodthirsty Roman emperor Comodus (180–192 AD), a son of the famous Marcus Aurelius, marked the date of the event. The age of the peat layer could be assessed by measuring the radioactivity of the peat (the radiocarbon method), which confirmed the other findings. This remarkable find was a lucky and a very rare coincidence which shows how studies of fossil pollen can assist in reconstructing the past.

So far my short discourse on ‘the praise of dust and mud’ has only partly explained the mud-part of the title. The dust-part needs some consideration. For this purpose I invite the reader to join me on an excursion into the Namib Desert, that elongated sand sea situated along the coast of Namibia. On one of my trips there I wanted to assess the pollen production of the desert vegetation. This may sound as odd as looking for palmtrees in the Arctic. However, on getting to know the desert more intimately, one realises that there is much more vegetation, especially in the wadi’s and along the dune slopes, than one expects. Collecting pollen produced by this sparse vegetation seemed at first sight to be an impossible task. Furthermore, to trap this extremely rare pollen floating in the air or recovering it from the soil surface was like searching for a needle in a haystack. For statistical purposes it is further important to obtain a random sample representing the production of a fairly large area. The ingenious method I used to trap the pollen had been developed by Dr. P. Cour, a botanist from the palynological laboratory at Montpellier, who gave me his full co-operation for my studies. Cour used multiple-layered medicinal gauze impregnated with silicone oil to catch dust and pollen behind a moving vehicle. The gauze is fixed on a frame behind the rear wheels of the motorcar, which travels over a distance of 5–10 km at a speed of 30–40 km/h. In the laboratory the inorganic dust particles and the gauze are dissolved in a very aggressive chemical, viz. 70% hydrofluoric acid. The sporopollenin, which forms the wall of the pollen grains, stands up to this drastic treatment and the residual pollen concentrate can then be identified and counted. Cour and others, like German palynologist E. Schultz, have obtained remarkable results with this method in Europe and in the Sahara. Research of this kind shows that dust is an extremely important source of pollen grains, while all kinds of mud are invaluable depositories of these little plant cells.

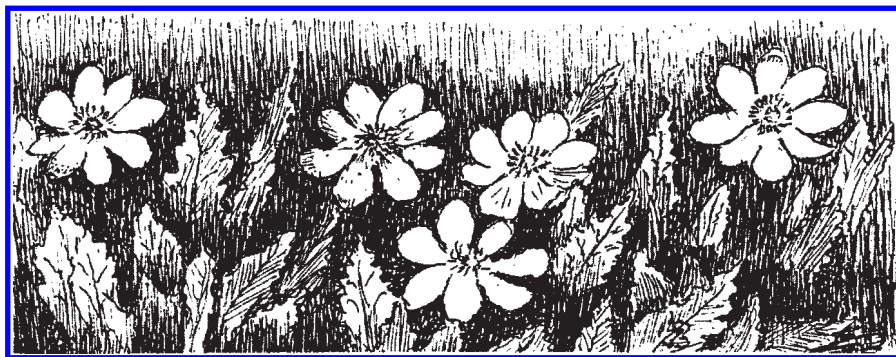


Figure 3. *Dryas octopetala*.

Embarking on pollen analysis in Africa gave me mixed feelings of excitement and bewilderment as the field of research was so large and unknown. Around my native town in the Netherlands my area of study was very small and I could take my auger on a bicycle on a short trip and make borings in a variety of small bogs. Besides that the number of different pollen types, one had to know, was very limited. Facing my problems in Africa I realised that practically nobody had seriously looked at fossil pollen grains between Cape Town and Cairo. A bicycle would also not bring me to any swamp and the rich flora with its tens of thousands of plant species and pollen grains presented me with 'une mer à boire'. I had to make a large reference collection

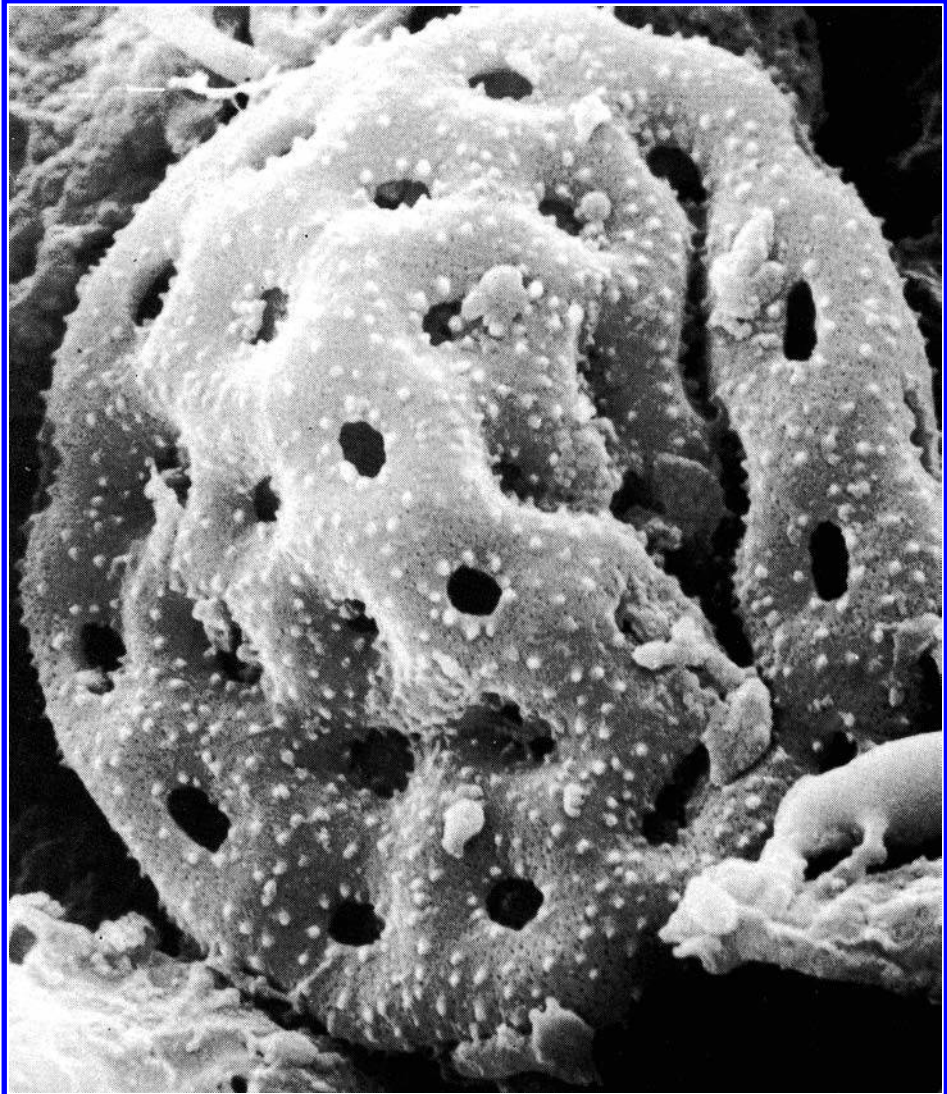


Figure 4. Three-dimensional picture of a salt bush pollen grain of the Chenopodiaceae family with many germination pores, taken with the scanning electron microscope.
Size of the grain 0,02 mm.

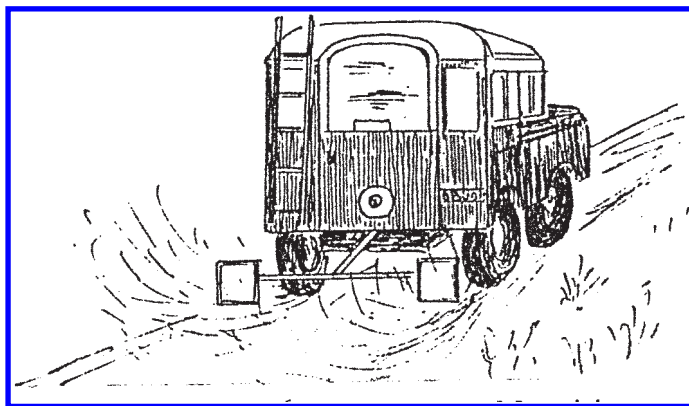


Figure 5. Cour-method for collecting pollen.

of pollen types and had to collect colleagues in related fields from archaeologists to geologists who could give me information on promising sites.

A serious handicap was that, unlike in Europe, large parts of the African continent have on many occasions in recent geological time been exposed to severe aridity. Under such circumstances pollen often disintegrates fairly soon as the very resistant sporopollenin of their wall does not withstand such hot-dry-oxidising conditions. This is the reason for the absence of pollen in important deposits where one hoped to find it.

This short introduction explains why I travelled so far and wide to remote swamps, barren tundra and high mountains. From now onward I will mainly limit myself to the description of those safaris which have left lasting impressions on my mind and which form the ‘raison d’être’ for this book.

REFERENCES

van Zeist, W., 1956, *Palaeohistoria*, 5, pp. 93–99.

van Zinderen Bakker, E.M., 1993, *Reminiscences of biological travels in Africa and to south polar islands*, (Somerset West: Private edition).

CHAPTER 2

Reconstructing environmental changes since the Last Glacial Maximum (LGM) in the Geba Basin, Northern Ethiopia, by geomorphic process interpretation and land management evaluation

Jan Moeyersons

Geomorphology and Remote sensing, Royal Museum for Central Africa, Tervuren, Belgium

Jean Poesen

Physical and Regional Geography Research Group, K. U. Leuven, Heverlee, Belgium

Jan Nyssen

Department of Geography, Ghent University, Gent, Belgium

Jozef Deckers

Soil and Water Management, K. U. Leuven, Heverlee, Belgium

Mitiku Haile

Mekelle University, Mekelle, Ethiopia

ABSTRACT: The palaeoenvironmental evolution of the Geba Basin in Northern Ethiopia since the Last Glacial Maximum (LGM) certainly is a good indicator for the climatic conditions, but there is evidence that climate has been affected by the interference of humans with the hydrological cycle, especially since the second half of the Holocene. Before ~15 cal ky BP, Ethiopia knew a dry climate in the lower parts and cold and also dry conditions in the Simen and Bale Mountains, in phase with the LGM. But while elsewhere in Ethiopia the cold/dry conditions continued till ~10–11 cal ky BP, the Geba Basin enjoyed moist conditions from ~15 cal ky BP onwards and no clear explanation can be given for this. These conditions continued in Tsigaba till ~3 cal ky BP and in many valley bottoms, till 50 years ago or even nowadays. This article presents evidence suggesting that the ‘arid environmental conditions’ which started in some places as early as ~5 cal ky BP, in other places only very recently, are more a human-induced than an astronomically steered phenomenon. Our research indicates that man has the necessary tools to bend off the present tendency towards aridification.

2.1 INTRODUCTION

The timing of late glacial events in the tropical mountains of Africa corresponds to the one in higher latitudes (Shanahan *et al.*, 2006). The Last Glacial Maximum (LGM) is linked to relatively cold and dry climatic conditions in West Africa (Petit-Maire, 1989) and in the Main Ethiopian Rift (MER) (Butzer *et al.*, 1972). However, there remain doubts whether climatic evolution in the high plateaus of the African Horn, is in phase with the evolution in the lower lying MER bottom (Moeyersons *et al.*, 2006; Marshall *et al.*, 2009) and further with the one in South and West Africa and the Congo basin.

Doubts are also raised about the climatic indicator value of MER lake levels alone because changes in water supply are also influenced by the tectonically induced rearrangement of the fluvial drainage network in the MER (Sagri *et al.*, 2007). Furthermore, a glance at the recent literature reveals that Mid- to Late-Holocene climatic variations appear to be less well coupled with changes across Africa and elsewhere (Shanahan, 2006). It has been suggested (Nyssen *et al.*, 2004), that humans became a factor increasingly important in environmental management, obliterating the precessional forcing of climate since middle to Late Holocene times.

Palaeoclimatic understanding in Ethiopia is of uttermost importance because this country occupies a geographical key position between the northern and central African 'lowlands', climatically phased with the LGM-Holocene transition, and the so-called Southern African Superswell (Summerfield, 1996).

This article presents evidence of Late Pleistocene and Holocene palaeoclimatic conditions and timing in the Geba Basin in Tigray, Northern Ethiopia (Figure 1). This basin is located in altitude below 3.000 m asl, meaning that no indications of palaeoglaciations are expected to be present. On the other hand, it is located on the shoulder of the Danakil Depression (DD), and it has been questioned recently to what degree palaeoclimatic indications from the lakes in the MER-bottom are representative for this area (Moeyersons *et al.*, 2006).

This paper addresses two major problems: 1) the definition of the LGM environment in Tigray and the timing of the transition between the Pleistocene and the Holocene; 2) the reason and nature of the Late Holocene 'aridification' which has affected the highlands from between ~5 to ~4 ky BP onwards and which culminates in the 'desertification' of today. Data and arguments were collected in the frame work of geomorphological, agricultural and hydrogeological research over the last decade.

2.2 MATERIALS AND METHODS

2.2.1 The study area

The Geba Basin is a banana shaped 5.200 km² region in Tigray, Northern Ethiopia. From upstream to downstream, the basin dips southwards in the northern part and turns westward in the south-western part (Figure 1). The Geba River is a tributary of the Tekeze which joins the Nile in Atbara, Sudan. The outlet of the basin is at ca 900 m asl, and the highest point, in the North, reaches ca 3.000 m asl.

The geology of the basin comprises in the central part, between lines A and B (Figure 1), the Mesozoic succession of the Mekelle Outlier (Bosellini *et al.*, 1995), composed of the Antalo Supersequence. This slightly eastward dipping succession of mostly limestones and shales is about 600 m thick in the area. A number of Mekelle dolerite sills appear in this succession (Arkin *et al.*, 1971; Merla *et al.*, 1979).

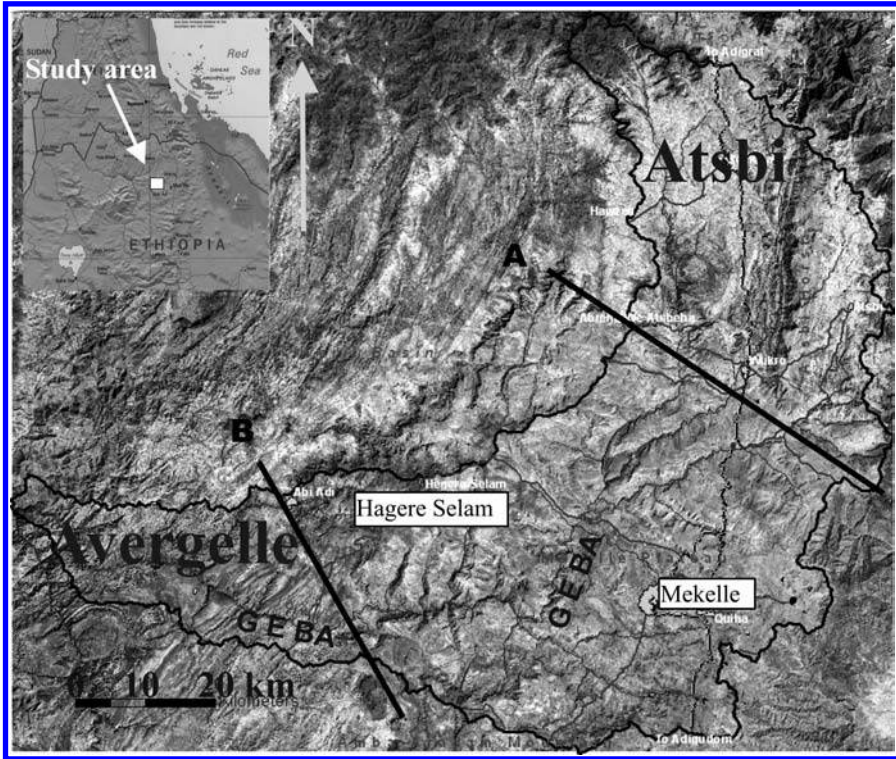


Figure 1. The Geba River Basin, indicated by a thin black line on a false colour ETM image (bands 123). The region of Hagere Selam has been studied for landsliding, tufa dam building and the effectiveness of soil and water conservation. Lines A and B delimit the middle basin, with mainly Mesozoic rocks, from the Atsbi highlands and the Avergelle lowlands, both underlain by Proterozoic rocks.

The Antalo Supersequence rests on Adigrat sandstone and is unconformably overlain by the Amba Aradam sandstone, considered as Cretaceous in age. In the Avergelle lowlands to the South-West of line B and on the Atsbi Highlands to the North of line A (Figure 1), Palaeozoic sedimentary rocks, described by Beyth (1972), Tesfaye and Gebretsadik (1982) and Garland (1980) crop out. Tertiary basalts occur in the extreme North of the basin and on a few massifs along the water divide between the Geba Basin and the Werei Basin, to the North and North-East of Hagere Selam. In the frame work of our studies, the geological map of the Geba Basin has been worked out in detail (Tsfamichael *et al.*, 2009).

The topography of the central part of the catchment is mainly structurally controlled by the subhorizontal geological stratigraphy. This gives rise to the characteristic high cliffs, escarpments and structural subhorizontal surfaces. The Avergelle lowlands and the Atsbi highlands, where Palaeozoic rocks appear, show both a topography characterized by SSW-NNE oriented ridges, reflecting the folded structure of the basement. The granite intrusion of Negash, in the North of the basin, forms a dome-like relief.

Climatic data are summarized by Tsfamichael (2009). Because of the altitude, mean maximum air temperatures are moderate, reaching ca 20°C to 23°C in the northern and central part of the basin, while in the 'lowlands' of Avergelle the mean max air temperature goes up to 32°C. The mean annual rainfall varies from ca 400 mm y⁻¹

in the North to well above 900 mm y^{-1} in the South of the basin. 77% of the annual rainfall is confined to the 'kiremt' rainy season, which extends from June to September. The eight other months of the year give only occasionally light 'belg' rains in some parts of the basin during the months March to May. Nyssen *et al.* (2005) have shown that the short duration high intensity rain storms in Hagera Selam are among the world's most energetic ones because of the big rain drop size. According to the International Convention to Combat Desertification (UNEP, 1994), the region should be considered as being affected by desertification because the proportion of the annual precipitation over the potential evapotranspiration is below 0,65.

The natural vegetation in the Geba Basin is highly degraded by human activities. On the eastern water divide with the DD, the Des'a forest is present. It is a degraded remnant of the Afromontane forest with *Juniperus* and *Olea* (Friis, 1992). If the landscape is nowadays largely deforested, small patches of forest around churches as well as in places, which are difficult to access, are secondarized remnants of a former climax vegetation (Descheemaeker *et al.*, 2006).

2.2.2 A review of the current Late Quaternary palaeoclimatic knowledge in Ethiopia

Late Pleistocene conditions and the transition to Early Holocene times

Pre-Holocene conditions have been studied in several regions in Ethiopia (Figure 2). Hurni (1989) and Messerli and Rognon (1980) discussed palaeoclimatic conditions of the Ethiopian highlands of Bale and Simen during the Quaternary. They described glacier cirques, moraines and periglacial solifluction deposits. This combination of landforms indicates that part of the high mountains above 3.000 m asl was glaciated during the LGM. Cores from the Bale Mountains, dated by ^{14}C from inside and outside the glaciated area suggest that the northern valley glaciers may date from the LGM. Estimated equilibrium line altitudes for these glaciers and the ice-cap are 3.750–4.230 m asl (Osmaston *et al.*, 2005). The beginning of deglaciation has been estimated at 14 to 13 ^{14}C cal ky BP (Umer and Bonnefille, 1998) and ice melting ended progressively between 12,6 and 11,8 ^{14}C cal ky BP (Tiercelin *et al.*, 2008). The pre-Holocene vegetation in the Bale Mountains was sparse and consisted mainly of grasses, Amaranthaceae, Chenopodiaceae and *Artemisia*, indicating an arid climate. The first start

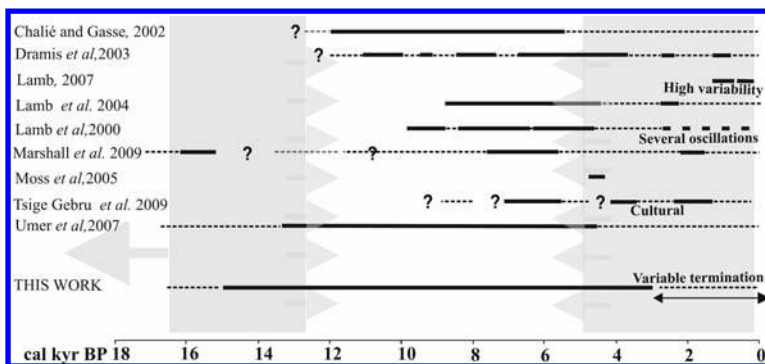


Figure 2. Recent palaeoclimatic interpretations for Ethiopia. Thick lines: relatively moist; thin dashed lines: relatively arid; Question marks: uncertainty about extent in time; grey belt to the left: generally accepted LGM-arid conditions; grey belt to the right: often considered as late-Holocene climatic aridification.

The results of Moeyersons *et al.* (2006), discussed further in this work are added as a comparison.

for moister conditions at 13,4 cal ky BP was interrupted by the Younger Dryas interval and moist conditions prevailed since 11,2 cal ky BP (Umer *et al.*, 2007).

Recent work at Lake Ashenge, located on the verge of the DD-shoulder at about 80 km to the South of the Geba Basin shows a high lake level, linked to a more humid climatic pulsation between 16,2 to 15,2 cal ky BP (Marshall *et al.*, 2009). This pulsation interrupted a dry period which ended at 11,8 cal ky BP. This humid pulsation could not be registered in the sediments of Lake Tana. This lake had a low water level without overflow to the Blue Nile before 14,7 cal ky (Lamb *et al.*, 2007).

Since Street, (1980), lake levels in the MER and elsewhere have been considered as a proxy for climatic conditions, low stands being related to dry environmental conditions. According to Butzer *et al.* (1972), lake levels in the MER were often low before early Holocene high stands. Wherever information is available for the period preceding 12 ky BP, it has been consistently shown that lakes were much smaller. This has been confirmed a few years ago for Lake Abiyata (Chalié and Gasse, 2002).

The Holocene

The Holocene record subsequent to the maximum of 10 to 8 ky BP is more complex. During this maximum, it seems that lakes in many parts of tropical Africa were greatly enlarged. Where evidence for the previous span of time is well resolved, it appears that lake level rises leading to this high stand began about 12 ky BP (Butzer *et al.*, 1972).

For a long time it was believed that Early Holocene conditions were relatively moist and that this humid period results from orbital forcing. But an overview of work done since 2000 (Figure 2) suggests that changes from Late Pleistocene dry conditions to a humid Early Holocene climate are not in phase everywhere. Most authors find also that the wet conditions during Early Holocene times were interrupted by dry spells (Lamb *et al.*, 2000; Dramis *et al.*, 2003; Tsige Gebru *et al.*, 2009; Marshall *et al.*, 2009).

The phased climatic evolution is completely lost at the end of the Early Holocene humid interval when relatively drier conditions arrive. This transition took place at lake Tilo at ~4,5 ky BP (Lamb *et al.*, 2004), but it clearly appears (Figure 2) that this climatic change was spread over some 2000 years in the different localities, and hence was far from being simultaneous over the whole country. Furthermore, the subsequent environmental evolution differs much from place to place and is generally characterized by short but severe oscillations in the same place (Lamb *et al.*, 2000, 2007) or by dry environments created by human activities (Tsige Gebru *et al.*, 2009). The Holocene environmental evolution has been related not only to climate change but also to land use changes introduced since 7 cal ky BP (Philipson, 1998). The role of prehistoric man in the environmental history of Tigray has been summarized by Bard *et al.* (2000) as follows: (1) the plateau experienced a more humid climate with a denser vegetation cover during the Early Holocene; (2) soil erosion due to vegetation clearing began in the Middle Holocene; (3) agricultural activity was intensified in the Late Holocene, as a consequence of the rise of a state; (4) demographic pressure increased from the early first millennium BC to the mid-first millennium AD, causing soil erosion; (5) environmental degradation and demographic decline occurred in the late first millennium AD; (6) the vegetation cover was regenerated in the early second millennium AD; and (7) progressive vegetation clearance started again in the second half of the second millennium AD. In the context of archaeological investigations, it is noteworthy to mention the presence of important concentrations of lithic assemblages of Middle Stone Age artifacts (Aerts *et al.*, 2010) in Northern Ethiopia.

Also pollen and charcoal analysis confirms that the vegetation in the highlands of Northern Ethiopia has changed in response to human impact during the last 3 ky (Darbyshire *et al.*, 2003). Although the role of man on the environment is generally recognized, archaeological research has worked long time with the idea of climatic determinism to explain the rise and fall of prehistoric societies, as done by Butzer (1981) in the case of Aksum. Recent research, however, admits that growing population and agricultural intensification have played an important role in forest cutting and landscape stability management (French *et al.*, 2009). In all Tigray, the period of forest disappearance and of the end of tufa dam build-up varies from one locality to another. Ancient soils, related to the presence of the primary forest (Brancaccio *et al.*, 1997), were covered by colluvium after $5,16 \pm 0,08$ cal ky (May Makden, Tigray) to $0,3 \pm 0,06$ cal ky BP (Adi Kolen, Tigray). Finally, the end of tufa build-up in May Makden is estimated to have occurred after 4,23–3,76 cal ky BC (Ogbaghebriel Bera-khi *et al.*, 1998).

Also outside Ethiopia, Mid- to Late-Holocene variations in West-Africa and South-Africa appear to be less coupled with changes across Africa and elsewhere (Shanahan *et al.*, 2006; Scott and Nyakale, 2002).

2.2.3 Strategies to gain palaeoclimatic information

Over the last decade multidisciplinary research programmes have addressed the following research topics:

- Geomorphologic mapping and study of landslides and their distribution in the Hagere Selam region (Moeyersons *et al.*, 2008a; Nyssen *et al.*, 2002a; Van Den Eckhaut *et al.*, 2008)
- Geomorphologic mapping, study and ^{14}C and U/Th dating on tufa dams (Moeyersons *et al.*, 2006)
- A throughout revision, completion and compilation in GIS of the geological map of the Geba Basin (Tsfamichael *et al.*, 2009)
- Regional groundwater flow modelling (Tsfamichael, 2009)
- Studies on the specific sediment yield and sediment bound nutrient export in 8 reservoir catchments (Nigussie Haregeweyn *et al.*, 2008)
- Studies on the efficiency of several soil and water conservation techniques (Nyssen *et al.*, 2008; Nyssen *et al.*, 2004; Vancampenhout *et al.*, 2006; Desta Gebremichael *et al.*, 2005)
- Assessment of spatial and temporal variability of river discharge, sediment yield and sediment-fixed nutrient export in Geba River catchment (Zenebe Abraha, 2009)
- Studies of the causal factors of gullying (Nyssen *et al.*, 2002b; Nyssen *et al.*, 2006; Veyret-Picot *et al.*, 2004)
- Studies on the restoration of dry Afromontane forest by using several techniques (Aerts *et al.*, 2008)
- Studies on the regrowth of woody vegetation in exclosures and the buffering capacities of exclosures to concentrated runoff (Descheemaeker *et al.*, 2006; 2009).

Although these studies did not directly intend to study the palaeoclimatic history of the highlands, most of them provide a lot of information about the points of discussion addressed below.

2.3 RESULTS

2.3.1 Late Quaternary environments and timing in the Geba Basin

In the Geba Basin, eight freshwater tufa dams, considered to be of Holocene age have been studied in detail (Moeyersons *et al.*, 2006). These phytoherms developed in formerly existing river beds, estimated to be of Late Pleistocene age. The river beds supporting the tufa dams contain thick deposits of river pebbles, rounded stones and even boulders up to some decimetres in size. These beds indicate a river regime, characterized by high energy floods, much alike the flash flood dynamics of braided rivers in arid or degraded savannah conditions.

The freshwater tufa deposits are the sedimentary response to karstic system activity (Magnin *et al.*, 1991; Peña *et al.*, 2000). Their presence is related to relatively wet environmental conditions, with significant plant cover and with nearly perennial river flow and percolation (Goudie *et al.*, 1993). U/Th ages on tufa and on speleothems in tufa dams suggest that this drastic change in river regime from highly seasonal to nearly perennial base flow took place before 15 U/Th ky BP. This is 4 to 5 ky before the first signs of post-LGM humid conditions deduced from former lake extensions in the Ethiopian and Kenyan rift (Moeyersons *et al.*, 2006). The occurrence of long lasting moist conditions long before 10 to 11 ky BP has also been found at Lake Ashenge (Marshall *et al.*, 2009). It can not be excluded that during the LGM forest refugia (Prentice and Jolly, 2000) were present on the heights below the glaciation equilibrium line. Important is also that tufa build up is related to underwater growth of algae and mosses. This means that photosynthesis is needed in the building process, which implies a low turbidity content of the river flow (Ford and Pedley, 1996). This is supplementary strong evidence for a river regime with much less pronounced peaks than today and thus with a consistent base flow.

2.3.2 Late Holocene environmental evolution in the Geba Basin

In the Geba Basin, the gradual disappearance of forest since a short time before the end of tufa dam build-up is evidenced by the following combination of arguments: (1) the change in dominance by dicotyledon to monocotyledon phytoliths at the period of tufa growth ending; (2) the accelerated sediment redistribution since that time and several gravel layers of the infillings of the barrier lakes behind the tufa dams, confirming a low vegetation density and soil truncation by runoff; (3) bush fires of grasses in Tukhul, stratigraphically equivalent to or younger than the top of the tufa dam. These arguments suggest that the area became gradually deforested by firing. In Moeyersons *et al.* (2006) the hypothesis is put forward that deforestation and bush fires were the main reasons for important sediment production, leading to increasing river turbidity inhibiting photosynthesis by algae and thus also precipitation of tufa, as shown by Ford and Pedley (1996) in NW Europe.

Another important source of sediments in the rivers probably were—and still are—the many landslides which have occurred at Hagere Selam and towards the North-East (Nyssen *et al.*, 2002a; Moeyersons *et al.*, 2008a). It is known that landslides, especially debris flows (Dikau *et al.*, 1996) can result in very high turbidities. Furthermore, research, complementary to Nigussie Haregeweyn *et al.* (2008) has shown a clear statistical relationship between the presence of landslide lobes and specific sediment yield (SSY) in reservoir catchments in the Geba Basin. The landslides in the Hagere Selam

region have never been well dated, but they were tentatively placed within the moist period of tufa dam building, because their triggering needs high hydrostatic pressures, which can be expected during a period of high water tables. But recent studies in natural hazards in Uvira (DR Congo) confirm that landslides rather occur in conditions of lower water tables, showing sudden and short living surges of rise (Moeyersons *et al.*, 2009). Because they create high sediment loads and because their occurrence depends mostly on important oscillations in the water tables, landslides are hydrologically incompatible with tufa dam growth. This is the reason why the landslide activity in the Hagere Selam region is historically placed from the start of tufa dam breakdown up to now. Risk assessment studies (Van Den Eeckhaut *et al.*, 2008) show the imminent risk of landsliding today, which suggests that water table surges at present might be still of the same magnitude as at the time of the start of tufa dam destruction.

At Tsigaba tufa dam, the degradation phase is situated at 3,09 cal ky BP. Both the presence of layered slope deposits and of a burnt soil tend to indicate that deforestation in that area locally started before 1,43–1,26 cal ky BC (Moeyersons *et al.*, 2006).

2.3.3 Nature of the current aridity in the Geba Basin

Forests and present-day climate in the Geba Basin and in Ethiopia

The Geba Basin does only count a restricted number of forest relicts, and this is sometimes ascribed to the arid conditions. The yearly energy received by earth has slightly diminished since the start of the Holocene as a result of astronomical forcing (Crucifix *et al.*, 2002). But ample evidence exists that forests can still survive and even develop in the environmental conditions of today. Cases of natural reforestation after emigration in northern Ethiopia (Darbyshire *et al.*, 2003) show that the evolution of the forest cover was not always towards increasing degradation. Moreover, the strongest arguments for a non-climatically driven deforestation in the Ethiopian Highlands since 5 cal ky BP are that the actual climate still easily supports forest, that forest recovery can be quick in enclosure areas where free grazing for cattle is forbidden (Moeyersons *et al.*, 2006), that reforestation operations are envisaged by foresters (Aerts *et al.*, 2008; Descheemaeker *et al.*, 2009) and can be successful (Eshetu Zewdu and Hogberg, 2000). Moreover, it is just a biased idea that arborescent vegetation should be on retreat. A recent study (Nyssen *et al.*, 2009) shows that overall there has been a remarkable recovery of tree and shrub vegetation and also improved soil protection over the last 140 years.

The reversible nature of current aridity in the Geba Basin

As shown in Figure 2, the aridification in the last half of the Holocene started between ~5 cal ky BP and recently, depending on local situations of deforestation and other land use. This change went hand in hand with a change in river regime which throws some light on the changes in hydrological landscape response. It is known that in many parts of Africa, including most parts of Ethiopia, relicts of the ancient valley network exist (Figure 3), characterized by small channelless valleys, commonly called 'dam-bos' (Acres *et al.*, 1985), 'tropical valley bottoms' or 'inland valley swamps' (Raunet, 1985). These valleys, mostly with grass or gallery forest vegetation were—and their relicts today still are—characterized by seasonal or even perennial water logging due to the rise of the water table to the surface of the valley bottom. The dense grassy or woody vegetation slows down valley surface water flow. Stratigraphically the channelless



Figure 3. Dambo at the fringe of Des'a forest. An initial stone fragment mulch and the polygonal structures, Gilgai undulations micro-relief, suggest the presence of a thick vertisol in this channelless valley. (Photo: Jean Poesen).

valley bottoms are marked by wedges of alluvial/colluvial valley fills, mostly clayey, sometimes in the form of vertic horizons, sometimes also peat layers, occupying the valley bottom in superposed position. Carnicelli *et al.* (2009) give splendid descriptions of the successions of flat valley bottom deposits along Lake Ziway and dated the present palaeosoils between $\sim 8,3$ and $4,7$ cal ky BP. According to descriptions by Acres *et al.* (1985) and Raunet (1985), and based on our own experience in Rwanda, the hydrograph of a dambo shows a relatively constant perennial base discharge with retarded and restricted flood response to rains, either individual storms or a rainy season (Figure 4). This delay is due to the fact that channelless valleys are mainly spring fed. We consider this type of river as hydrologically compatible with the humid conditions in the Geba Basin until the Late Holocene. Today, rivers in the Geba Basin show very important flash floods and only restricted base flow (Zenebe Abraha, 2009). This change in river regime reflects a change in the general hydrological behaviour of the landscape with river discharge fed by direct runoff from the hillslopes to a much higher proportion than before. The flat morphology of valley bottoms is no longer in equilibrium with the unprecedented current peak flow discharges, especially when the valley bottoms are devoid of the ancient flow retarding vegetation. Habitants reported how some 60 years ago, a small swampy channelless stream at Dingilet, close to Hagere Selam (Figure 1) cut a 6 m deep channel after runoff coefficients increased as a result of deforestation and agriculture intensification on the surrounding slopes and desiccation induced by Eucalyptus plantation in the valley (Veyret-Picot *et al.*, 2004;

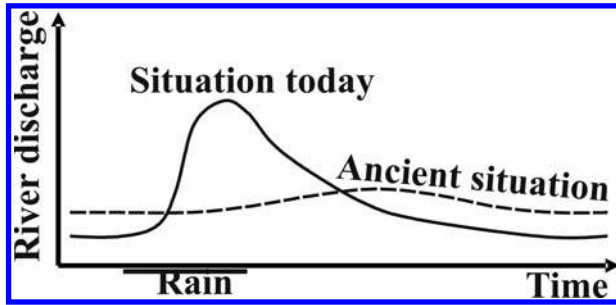


Figure 4. Change in river regime in the Geba Basin in Ethiopia and elsewhere in Africa.

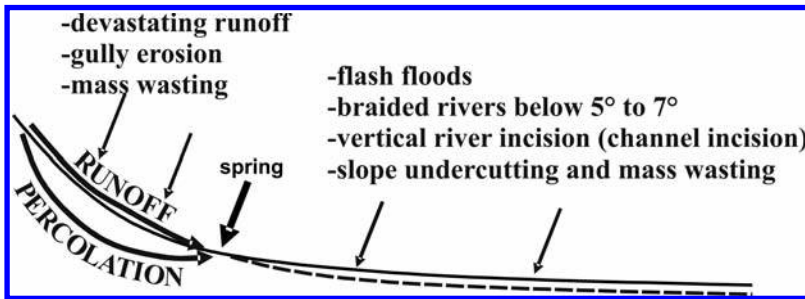


Figure 5. Increase in hydrological risks as a result of runoff increase at the partial expense of the infiltration-exfiltration water circulation.

Nyssen *et al.*, 2006). It seems, therefore, that the aridification since Mid-Holocene times can be characterized by an increasing hillslope runoff production.

Moeyersons and Trefois (2008b) assess the natural risks involved with increasing runoff in Central Africa (Figure 5) and this assessment seems to be valid for the Geba Basin as well. Land use change has certainly played an important role in the increase of hillslope runoff production as a result of an increasing runoff coefficient.

Descheemaeker *et al.* (2006, 2009) show that church forests and enclosure forests are able to trap important sediment and water volumes from upslope and so implicitly demonstrate that deforestation in the Geba Basin should have strongly contributed to the increase of the runoff coefficient. It is known that the construction of roads and houses and urbanisation in general contribute to a very considerable increase in runoff coefficient and, above all, can concentrate runoff to higher than natural discharges. The latter is an important factor in valley side and valley bottom gullying in the Geba Basin along newly constructed roads (Nyssen *et al.*, 2002b) or in flooding in urbanized areas. Nyssen *et al.* (2008) show that all measures delaying runoff, taken region-wide in Tigray counteract the present desertification, even if some of the runoff increase was due to astronomically forced climatic effects of extreme rainfalls.

2.4 CONSIDERATIONS ABOUT DEFORESTATION-CLIMATE COUPLING

Forest plays an important role in the inland alimentation of the hydrological cycle with vapour and vegetation-climate coupling is generally applied in atmospheric general

circulation models (Crucifix *et al.*, 2002). Whitmore (1998) and Zhang *et al.* (2001) confirm that in ideal conditions evapotranspiration of forest can be about 1.5 times the evapotranspiration of grassland or grassy crops. But empirical evidence suggests that evapotranspiration by lowland tropical forest in Africa should be higher and reach about the same amount of evapotranspiration per unit of surface as the Atlantic Ocean by evaporation. This stems from the empirical observation that the Aw and Bsh climatic belts of Köppen-Geiger (Peel *et al.*, 2007) cross the African continent straight from West to East, while the Atlantic coast turns to the South at Mount Cameroon. To the West of Cameroon the climatic belts are parallel to the Atlantic coast. This is generally ascribed to the flux of humid air masses to the West African continent, due to the SW trade winds during the Boreal summer. These winds also steer the West African hydrological cycle further inland. But the Aw and Bsh climatic belts East of Cameroon receive trade winds, which have only a restricted trajectory over the Atlantic Ocean. According to Leroux (1983), the trajectory of the July trade winds to the western part of Ethiopia is even mainly continental (Figure 6). It is known that water vapour flux transport from the oceans to the continental land masses only accounts for 1/3 of the precipitation actually recorded (Oki, 1999). But in Eastern Sudan and Western Ethiopia the rainfall coming from the West (Rudloff, 1981) should be mainly ‘continental’ around the end of June, when the ITCZ is situated at its most northerly position (16–20°N). The uptake of vapour above the forest in the Congo basin and above the Atlantic Ocean and the coastal forest in West-Africa should be of the same order of magnitude because of the general parallelism between the northern tropical forest fringe, as given by Ady and Hazlewood (1965) and the AW and Bsh climatic belts (Figure 5). Less vapour production above the Congolese forest would result in climatic belts, narrowing and/or coming closer to the northern forest limit north of DR Congo.

The climatic impact of massive tropical deforestation is regularly addressed (Whitmore, 1998). In Amazonia Gash *et al.* (1996) observed reduced rainfall and higher rainfall irregularities downwind of deforested zones. In West-Africa, it has been suggested by Roose (1994) that the exploitation of mangroves and savannah along the coast will hamper rainfall in the Sahel. Claussen *et al.* (1999) explain the abrupt desertification in

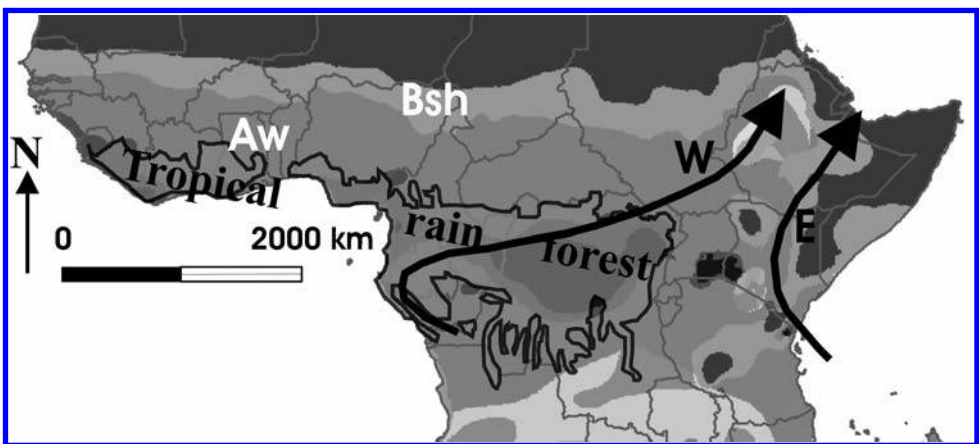


Figure 6. Extension of the tropical rain forest and climatic Köppen belts Aw and Bsh to the North. The W arrow indicates the mean trajectory of the western trade winds in the month of July. The E arrow gives the approximate path of the trade winds from the Indian Ocean.

North-Africa during the Mid-Holocene in terms of vegetation-atmosphere feedbacks in the climate system. Zeng *et al.* (1999) confirm that variations in vegetation enhance climate variability in the Sahel and Taylor *et al.* (2002) show that changes in vegetation in the Sahel can cause substantial reductions in rainfall. In the case of Ethiopia, there is no doubt that deforestation either along the path of the western or eastern trade winds will have contributed to less rainfall in the study area. Human-induced land changes since 7 cal ky BP (Philipson, 1998) started about thousand years before the first local manifestations of the more dry to arid conditions (Figure 2).

2.5 CONCLUSIONS

This study reveals the following information about the environmental evolution in the Geba Basin in Northern Ethiopia since the LGM:

1. Before 15 U/Th ky BP most tributaries of the Geba were of the braided or winding river type. These rivers are indicators for an irregular river regime with flash flooding, probably as a result of an important contribution from hillslope runoff.
2. From 15 U/Th ky BP to ~3 cal ky BP the river regime was markedly opposite. The building up of numerous tufa herms in the old river channels shows that the river regime was characterized by consistent base flow. Mechanical erosion, resulting in high sediment loads, was replaced by chemical karstic erosion types, depending on the presence of a rather luxurious vegetation. Tentatively we see rivers whose knick points on cliffs were stabilised by tufa dams. Upslope of Tsigaba dam a lake existed and we attribute the development of channel-less valleys upstream of tufa dam lakes to this period. Because the transition from seasonal to more perennial hydrologic landscape behaviour at 15 U/Th ky BP has only been locally observed, astronomical forcing for the environmental transition at that particular moment remains questionable. The recent finding by Marshall *et al.* (2009) of moist conditions around Lake Ashenge between 16,2 and 15,2 cal ky BP shows that environmental conditions in Tigray locally oscillated during the LGM. The post LGM overflow of Lake Tana is situated between 15,2 and 14,75 cal ky BP (Lamb *et al.*, 2007).
3. The gradual change, first to less humid environmental conditions and later to aridity, was dated at Tsigaba around ~3 cal ky BP. This period is up to the present characterized by important geomorphic activity. Landslides, often of the debris flow type occur. The tufa dams degrade by river incision and weathering and the flat bottom river sections behind the dams or elsewhere are actively incised as a result of flash flooding. Increased hillslope runoff creates gullies and sheet and rill wash. The original forest cover has nearly completely disappeared. Although the astronomical energy balance is somewhat lower today than during the Holocene optimum, there does not exist any ground of evidence that forest cover reduction is the result of decreasing rainfall. On the other hand increasing evidence points to the negative impact of regional or generalized anthropogenic deforestation on annual precipitation. We agree that climatic conditions became gradually drier during the second part of the Holocene, but they should be due to forest cutting locally as well as in regions to the South of the study area where the trade winds are passing. Forest cutting and regrowth history can be responsible for the variation over time of the start of increasing aridity since ~5 cal ky BP in the Geba Basin.

This is probably one of the earliest interventions of humans in the hydrological cycle and hence in climate.

ACKNOWLEDGEMENTS

This article is a spin-off of the following projects: 1) research programme G006598 N funded by the Fund for Scientific Research—Flanders, Belgium (1998–2001); 2) The Flemish Inter-University Council Own Initiatives Zala Daget project EIN2001PR237 (2002–2008); 3) The Flemish Inter-University Council Institutional University Cooperation Mekelle University—Land Management and Hydrogeology Projects (2003–2013).

REFERENCES

- Acres, B.D., Rains, A.B., King, R.B., Lawton, R.M., Mitchell, A.J.B. and Rackham, L.J., 1985, African dambos: their distribution, characteristics and use. *Zeitschrift für Geomorphologie, Supplementband*, **52**, pp. 63–86.
- Ady, P.H. and Hazlewood, A.H., 1965, *Oxford regional economic atlas Africa*, (Oxford: Clarendon Press).
- Aerts, R., Finneran, N., Haile, M. and Poesen, J., 2010, The accumulation of stone age lithic artifacts in rock fragment mulches in northern Ethiopia. *Geoarchaeologie*, **25**, pp. 137–148.
- Aerts, R., November, E., Maes, W. and Van der Borght, I., 2008, In situ persistence of African wild olive and forest restoration in degraded semiarid savanna. *Journal of Arid Environments* **72**, pp. 1131–1136.
- Arkin, Y., Beyth, M., Dow, D.B., Levitte, D., Temesgen, H. and Tsegaye, H., 1971, Geological map of Mekele sheet area ND 37–11, Tigre province, 1:250.000, *Imperial Ethiopian Government, Ministry of Mines, Geological Survey*, Addis Ababa.
- Bard, K.A., Coltorti, M., DiBlasi, M.C., Dramis, F. and Fattovich, R., 2000, The Environmental History of Tigray (Northern Ethiopia) in the Middle and Late Holocene: A Preliminary Outline. *African Archaeological Review*, **17**, pp. 65–86.
- Beyth, M., 1972, Paleozoic–Mesozoic sedimentary basin of Makalle outlier. *American Association of Petroleum Geologists Bulletin* **56**, pp. 2426–2439.
- Bosellini, A., Russo, A., Fantozzi, P.L., Getaneh, Assefa, Tadesse, Solomon, 1997, The Mesozoic succession of the Mekele Outlier (Tigre Province, Ethiopia). *Memorie di Scienze Geologiche*, **49**, pp. 95–116.
- Branaccio, L., Calderoni, G., Coltorti, M. and Dramis, F., 1997, Phases of soil erosion during the Holocene in the Highlands of Western Tigray (Northern Ethiopia): a preliminary report. In *The Environmental History and Human Ecology of Northern Ethiopia in the Late Holocene*, edited by Bard, K., (Napoli: Istituto Universitario Orientale), pp. 30–48.
- Butzer, K.W., 1981, Rise and fall of Axum, Ethiopia: a geo-archaeological interpretation. *American Antiquity*, **46**, pp. 471–495.
- Butzer, K.W., Isaac, G.L., Richardson, J.L. and Washbourn-Kamau, C., 1972, Radio carbon dating of East African lake levels. *Science*, **175**, pp. 1069–1076.
- Carnicelli, S., Benvenuto, M., Ferrari, G. and Sagri, M., 2009, Dynamics and driving factors of late Holocene gullying in the Main Ethiopian Rift (MER). *Geomorphology*, **103**, pp. 541–554.

- Chalié, F. and Gasse, F., 2002, Late glacial-Holocene diatom record of water chemistry and lake level change from the tropical East African Rift Lake Abiyata (Ethiopia). *Palaeogeography, Palaeoclimatology, Palaeoecology*, **187**, pp. 259–283.
- Claussen, M., Kubatzki, C., Brovkin, V., Ganopolski, A., Hoelzmann, P. and Pachur, H.-J., 1999, Simulation of an abrupt change in Saharan vegetation in the Mid-Holocene, *Geophysical Research Letters*, **26**, pp. 2037–2040.
- Crucifix, M., Loutre, M.-F., Tulkens, P., Fichet, T. and Berger, A., 2002, Climate evolution during the Holocene: a study with an earth system model of intermediate complexity. *Climate Dynamics*, **19**, pp. 43–60.
- Darbyshire, I., Lamb, H.F. and Umer, M., 2003, Forest clearance and regrowth in northern Ethiopia during the last 3,000 years. *The Holocene*, **13**, pp. 537–546.
- Descheemaeker, K., Raes, D., Nyssen, J., Poesen, J., Haile, M. and Deckers, J., 2009, Changes in water flows and water productivity upon vegetation regeneration on degraded hillslopes in Northern Ethiopia: a water balance modelling exercise. *The Rangeland Journal*, **31**, pp. 237–249.
- Descheemaeker, K., Nyssen, J., Rossi, J., Poesen, J., Haile, M., Raes, D., Muys, B., Moeyersons, J. and Deckers, J., 2006, Sediment deposition and pedogenesis in exclosures in the Tigray highlands. *Geoderma*, **132**(3–4), pp. 291–314.
- Desta, G., Nyssen, J., Poesen, J., Deckers, J., Haile, M., Govers, G. and Moeyersons, J., 2005, Effectiveness of stone bunds in controlling soil erosion on cropland in the Tigray Highlands, Northern Ethiopia. *Soil Use and Management*, **21**(3), pp. 287–297.
- Dikau, R., Brunsten, D., Schrott, L. and Ibsen, M.-L., 1996, *Landslide recognition*. (Chichester: Wiley).
- Dramis, F., Umer, M., Calderoni, G. and Haile, M., 2003, Holocene climate phases from buried soils in Tigray (Northern Ethiopia): comparison with lake level fluctuations in the Main Ethiopian Rift. *Quaternary Research*, **60**, pp. 274–283.
- Eshetu Zewdu, and Hogberg, P., 2000, Reconstruction of forest site history in Ethiopian Highlands based on (super 13) C natural abundance of soils. *Ambio*, **29**, pp. 83–89.
- French, C., Sulas, F. and Madella, M., 2009, New geoarchaeological investigations of the valley systems in the Aksum area of Northern Ethiopia. *Catena*, **78**, pp. 218–233.
- Friis, I., 1992, *Forests and forest trees of Northeast tropical Africa. Their natural habitats and distribution patterns in Ethiopia, Djibouti and Somalia*. Kew Bulletin Additional series xv, HMSO (London: Royal Botanic Gardens) pp. 1–396.
- Ford, T. and Pedley, H.M., 1996, A review of tufa and travertine deposits of the world. *Earth Science Reviews*, **41**, pp. 117–175.
- Garland, C., 1980, *Geology of the Adigrad Area*. Ministry of Mines, Energy and Water Resources, Geological Survey of Ethiopia, Addis Ababa. 51 p.
- Gash, J.H.C., Nobre, C.A., Roberts, J.M. and Victoria, R.L., 1996, *Amazonian Deforestation and Climate* (Chichester: Wiley).
- Goudie, A.S., Viles, H.A. and Pentecost, A., 1993, The late-Holocene tufa decline in Europe. *The Holocene*, **3**, pp. 181–186.
- Hurni, H., 1989, Late Quaternary of Simen and other mountains in Ethiopia. In *Quaternary and Environmental Research on East African Mountains*, edited by Mahaney, W. (Balkema, Rotterdam), pp. 105–120.
- Lamb, H.F., 2007, Oxygen and carbon isotope composition of authigenic carbonate from an Ethiopian lake: a climate record of the last 2,000 years. *The Holocene*, **17**, pp. 517–526.

- Lamb, H.F., Bates, C.R., Coombes, P.V., Marshall, M.H., Umer, M., Davies, S.J. and Dejen, E., 2007, Late Pleistocene desiccation of Lake Tana, source of the Blue Nile. *Quaternary Science Reviews*, **26**, pp. 287–299.
- Lamb, A.L., Leng, M.J., Umer, M. and Lamb, H.F., 2004, Holocene climate and vegetation change in the Main Ethiopian Rift Valley, inferred from the composition (C/N and $\delta^{13}\text{C}$) of lacustrine organic matter. *Quaternary Science Reviews*, **7–8**, pp. 881–891.
- Lamb, A.L., Leng, M.J., Lamb, H.F. and Umer, M., 2000, A 9,000-year oxygen and carbon isotope record of hydrological change in a small Ethiopian crater lake. *The Holocene*, **10.2**, pp. 167–177.
- Leroux, M., 1983, *Le climat de l'Afrique tropicale*, Atlas, (Paris: Champion).
- Magnin, F., Guendon, J.L., Vaudour, J. and Martin, Ph., 1991, Les travertins: accumulations carbonatées associées aux systèmes karstiques, séquences sédimentaires et paléoenvironnements quaternaires. *Bulletin de la Société Géologique de France*, **162**, pp. 585–594.
- Marshall, M.H., Lamb, H.F., Davies, S.J., Leng, M.J., Kubsa, Z., Umer, M. and Bryant, C., 2009, Climatic Change in Northern Ethiopia during the past 17,000 years: A diatom and stable isotope record from Lake Ashenge. *Palaeogeography, Palaeoclimatology, Palaeoecology*, **279**, pp. 114–127.
- Merla, G., Abbate, E., Azzaroli, A., Bruni, P., Canuti, P., Fazzuoli, M., Sagri, M. and Tacconi, P., 1979, A geological map of Ethiopia and Somalia (1973) 1:2,000,000 and comment. *University of Florence*, Italy.
- Messerli, B. and Rognon, P., 1980, The Saharan and East African uplands during the Quaternary. In *The Sahara and the Nile; Quaternary environments and prehistoric occupation in Northern Africa*, edited by Williams, M., Faure, H. (Balkema, Rotterdam), pp. 87–132.
- Moeyersons, J., Trefois, Ph., Nahimana, L., Ilunga, L., Vandecasteele, I., Biyzigiro, V. and Sadiki, S., 2009, River and landslide dynamics on the western Tanganyika rift border, Uvira, D.R.Congo: diachronic observations and a GIS inventory of traces of extreme geomorphic activity. *Natural Hazards*. DOI 10.1007/s11069-009-9430-z.
- Moeyersons, J., Van Den Eeckhaut, M., Nyssen, J., Tesfamichael, G.Y., Van de Wauw, J., Hofmeister, J., Poesen, J., Deckers, J. and Haile, M., 2008a, Mass movement mapping for geomorphological understanding and sustainable development: Tigray, Ethiopia. *Catena*, **75**, pp. 45–54.
- Moeyersons, J. and Trefois Ph., 2008b, Desertification and changes in river regime in Central Africa: possible ways to prevention and remediation. In: *Proceedings of the Conference on Desertification, Ghent, 23 January 2008*. UNESCO Centre for Eremology, Ghent, edited by Gabriels, D., Cornelis, W., Eyletters, M., Hollebosch, P., (Ghent: Ghent University), pp. 144–156.
- Moeyersons, J., Nyssen, J., Poesen, J., Deckers, J. and Haile, M., 2006, Age and back-fill/overfill stratigraphy of two tufa dams, Tigray Highlands, Ethiopia: Evidence for Late Pleistocene and Holocene wet conditions. *Palaeogeography, Palaeoclimatology, Palaeoecology*, **230**, pp. 165–181.
- Moss, J., Baker, A., Leng, M., Umer, M., Asfawossen Asrat, Gilmour, M. and Smith, C., 2005, A Mid Holocene high resolution ^{18}O stalagmite record from Ethiopia. *Cave and Karst Science*, **32**, p. 45.
- Nigussie Haregeweyn, Poesen, J., Nyssen, J., Govers, G., Verstraeten, G., de Vente, J., Deckers, J., Moeyersons, J. and Haile, M., 2008, Sediment yield variability in Northern Ethiopia: A quantitative analysis of its controlling factors, *Catena*, **75**, 1, pp. 65–76.

- Nyssen, J., Haile, M., Naudts, J., Munro, N., Poesen, J., Moeyersons, J., Frankl, A., Deckers, J. and Pankhurst, R., 2009, Desertification? Northern Ethiopia re-photographed after 140 years, *Science of the total environment*, *STOTEN-11080*.
- Nyssen, J., Poesen, J., Descheemaeker, K., Haregeweyn, N., Haile, M., Moeyersons, J., Frankl, A., Govers, G., Munro, R.N. and Deckers, J., 2008, Effects of region-wide soil and water conservation in semi-arid areas: the case of Northern Ethiopia. *Zeitschrift für Geomorphologie N.F.*, **52**, pp. 291–315.
- Nyssen, J., Poesen, J., Veyret-Picot, M., Moeyersons, J., Haile, M., Deckers, J., Dewit, J., Naudts, J., Kassa Teka, and Govers, G., 2006, Assessment of gully erosion rates through interviews and measurements: a case study from Northern Ethiopia. *Earth Surface Processes and Landforms*, **31**, (2), pp. 167–185.
- Nyssen, J., Vandenreyken, H., Poesen, J., Moeyersons, J., Deckers, J., Haile, M., Salles, C. and Govers, G., 2005, Rainfall erosivity and variability in the Northern Ethiopian Highlands. *Journal of Hydrology*, **311**, pp. 172–187.
- Nyssen, J., Veyret-Picot, M., Poesen, J., Moeyersons, J., Haile, M., Deckers, J. and Govers, G., 2004, The effectiveness of loose rock check dams for gully control in Tigray, Northern Ethiopia. *Soil Use and Management*, **20**, pp. 55–64.
- Nyssen, J., Moeyersons, J., Poesen, J., Deckers, J. and Haile, M., 2002a, The environmental significance of the remobilization of ancient mass movements in the Atbara-Tekeze headwaters, Northern Ethiopia. *Geomorphology*, **49**, (3–4), pp. 303–322.
- Nyssen, J., Poesen, J., Moeyersons, J., Luyten, E., Veyret-Picot, M., Deckers, J., Haile, M. and Govers, G., 2002b, Impact of road building on gully erosion risk: a case study from the Northern Ethiopian highlands. *Earth Surface Processes and Landforms*, **27**, pp. 1267–1283.
- Ogbaghebriel Berakhi, Brancaccio, L., Calderoni, G., Coltorti, M., Dramis, F. and Mohammed Umer, 1998, The Mai Makden sedimentary sequence: a reference point for the environmental evolution of the Highlands of Northern Ethiopia. *Geomorphology*, **23**, pp. 127–138.
- Oki, T., 1999, The global water cycle. In *Global energy and water cycles*, edited by Browning, K.A. and Gurney, R.J., (Cambridge: University Press), pp. 10–29.
- Osmaston, H.A., Mitchell, W.A. and Osmaston, J.A.N., 2005, Quaternary glaciation of the Bale Mountains, Ethiopia. *Journal of Quaternary Science*, **20**, pp. 593–606.
- Peel, M.C., Finlayson, B.L. and McMahon, T.A., 2007, Updated world map of the Köppen-Geiger climate classification. *Hydrology and Earth Systems Sciences*, **11**, pp. 1633–1644.
- Peña, J.L., Sancho, C. and Lozano, M.V., 2000, Climatic and tectonic significance of late Pleistocene and Holocene tufa deposits in the Mijares River canyon, eastern Iberian range, Northeast Spain. *Earth Surface Processes and Landforms*, **25**, pp. 1403–1417.
- Petit-Maire, N., 1989, Interglacial environments in presently hyperarid Sahara: Palaeoclimatic interpretations. In *Palaeoclimatology and Palaeometeorology: Modern and past patterns of global atmospheric transport*, edited by Leinen, M., Sarnthein, M., (Dordrecht, Neth.), pp. 637–661.
- Philipson, D.W., 1998, Ancient Ethiopia, Aksum: *Its antecedents and Successors*, (London, British Museum Press).
- Prentice, I.C. and Jolly, D., 2000, Mid-Holocene and glacial-maximum vegetation geography of the northern continents and Africa. *Journal of Biogeography*, **27**, pp. 507–519.
- Raunet, M., 1985, Les bas-fonds en Afrique et à Madagascar, *Zeitschrift für Geomorphologie N.F.*, **52**, pp. 25–62.
- Roose, E., Introduction à la gestion conservatoire de l'eau, de la biomasse et de la fertilité des sols (GCS), *Bulletin pédologique. FAO*, **70**, 420 p.

- Rudloff, W., 1981. *World climates*, (Stuttgart: Wissenschaftliche Verlagsgesellschaft).
- Sagri, M., Bartolini, C., Billi, P., Ferrari, G., Benvenuti, M., Carnicelli, S. and Barbano, F., 2008, Latest Pleistocene and Holocene river network evolution in the Ethiopian lakes region, *Geomorphology*, **94**, pp. 79–97.
- Scott, L. and Nyakale, M., 2002, Pollen indications of Holocene palaeoenvironments at Florisbad spring in the central Free State, South Africa, *The Holocene*, **12**, pp. 497–503.
- Shanahan, T.M., Overpeck, J.T., Wheeler, C.W., Beck, J.W., Pigati, J.S., Talbot, M.R., Scholz, C.A., Peck, J. and King, J.W., 2006, Paleoclimatic variations in West Africa from a record of late Pleistocene and Holocene lake level stands of Lake Bosumtwi, Ghana. *Palaeogeography, Palaeoclimatology, Palaeoecology*, **242**, pp. 287–302.
- Street, F.A., 1980, The relative importance of climate and local hydrogeological factors in influencing lake-level fluctuations. *Palaeoecology of Africa*, **12**, pp. 137–158.
- Summerfield, M.A., 1996, Tectonics, geology and long-term landscape development. In *The physical geography of Africa*, edited by Adams, W.M., Goudie, A.S. and Orme, A.R., (Oxford University Press), pp. 1–17.
- Taylor, C.M., Lambin, E.F., Stephenne, N., Harding, R.J. and Essery, R.L.H., The Influence of Land Use Change on Climate in the Sahel. *Journal of Climate*, **15**, pp. 3615–3629.
- Tesfamichael, G.Y., 2009, Regional groundwater flow modeling of the Geba Basin, Northern Ethiopia, Free University of Brussels (VUB). *Series of VUB-Hydrology*, **56**, 256 p.
- Tesfamichael, G.Y., de Smedt, F., Miruts, H., Kassa, A., Kurkura, K., Abdulwassie, H., Nyssen, J., Bauer, H., Moeyersons, J., Deckers, J. and Nurhussein, T., 2009, Large-Scale Geological mapping of the Geba Basin, Northern Ethiopia. *Tigray livelihood Papers*, January 2009.
- Tesfaye, C. and Gebretsadik, E., 1982, *Hydrogeology of the Mekele area*. Ministry of Mines and Energy, Addis Ababa. 50 p.
- Tiercelin, J.-J., Gibert, E., Umer, M., Bonnefille, R., Disnar, J.-R., Lezine, A.-M., Hureau-Mazaudier, D., Travi, Y., Keravis, D. and Lamb, H.F., 2008, High-resolution sedimentary record of the last deglaciation from a high-altitude lake in Ethiopia. *Quaternary Science Reviews*, **27**, pp. 449–467.
- Tsige, G., Eshetu, Z., Huang, Y., Woldemariam, T., Strong, N., Umer, M., Diblasi, M. and Terwilliger, V.J., 2009, Holocene palaeovegetation of the Tigray Plateau in Northern Ethiopia from charcoal and stable organic carbon isotopic analyses of gully sediments. *Palaeogeography, Palaeoclimatology, Palaeoecology*, **282**, pp. 67–80.
- Umer, M. and Bonnefille, R., 1998, A late Glacial/Late Holocene pollen record from a highland peat at Tamsaa, Bale Mountains, S. Ethiopia. *Global and Planetary Change*, **16**, pp. 121–129.
- Umer, M., Lamb, H.F., Bonnefille, R., Lezine, A.-M., Tiercelin, J.-J., Gibert, E., Cazet, J.-P. and Watrin, J., 2007, Late Pleistocene and Holocene vegetation history of the Bale Mountains, Ethiopia. *Quaternary Science Reviews*, **26**, pp. 2229–2246.
- UNEP, 1994, United Nations convention to combat desertification, 71 p.
- Vancampenhout, K., Nyssen, J., Desta, G., Deckers, J., Poesen, J., Haile, M. and Moeyersons, J., 2006, Stone bunds for soil conservation in the Northern Ethiopian highlands: impacts on soil fertility and crop yields. *Soil & Tillage Research*, **90**, pp. 1–15.
- Van Den Eeckhaut, M., Moeyersons, J., Nyssen, J., Amanuel Abraha, Poesen, J., Haile, M. and Deckers, J., 2008, Spatial patterns of old, deep-seated landslides: A case-study in the Northern Ethiopian highlands. *Geomorphology*, **105**, pp. 239–252.

- Veyret-Picot, M., Nyssen, J., Poesen, J., Moeyersons, J., Haile, M. and Deckers, J., 2004, L'effet de l'affectation du sol sur l'origine du ravin de Dingilet (Ethiopie du Nord). *Bulletin du Réseau Erosion*, **23**, pp. 50–59.
- Whitmore, T.C., 1998, *An introduction to tropical rain forests*, (Oxford: University Press).
- Zenebe, A., 2009, *Assessment of spatial and temporal variability of river discharge, sediment yield and sediment-fixed nutrient export in Geba River catchment Northern Ethiopia*. PhD thesis, Department of Geography, K.U. Leuven, Belgium (Heverlee-Belgium: Procopia N.V.), 346 p.
- Zeng, N., Neelin, J.D., Lau, K.-M. and Tucker, C.J., 1999, Enhancement of inter-decadal climate variability in the Sahel by vegetation interaction. *Science*, **286**, pp. 1537–1540.
- Zhang, L., Dawes, W.R. and Walker, G.R., 2001, Response of mean annual evapotranspiration to vegetation changes at catchment scale. *Water Resources Research*, **37**, pp. 701–708.

CHAPTER 3

Climate reconstructions based on fluvial deposits in hyper-arid desert environments: The Namib case

Klaus Heine

*Department of Geography, Universität Regensburg,
Regensburg, Germany*

ABSTRACT: This review focuses on arid fluvial sedimentary systems of the Namib Desert. The fluvial deposits of the Namib Desert can provide proxy data for palaeoclimates assuming that critical reappraisal is done of all sediment facies previously interpreted as having been deposited under flash floods, still water, dammed lakes, waning floods, and the like. Furthermore, it is important to critically evaluate the ages of the fluvial deposits. If well-dated and poor-dated climate records from the Namib region are compared chronologically without evaluating the quality on which the records depend, errors in palaeoclimatic interpretations cannot be avoided. The review of the Homeb Silts (Kuisseb River) and the Amspoort Silts (Hoanib River) should urge future researchers to critically reexamine existing palaeoclimate databases from the Namib (and Southern Africa) and to generate much subtler interpretations to explain their palaeoclimatic evidence.

3.1 INTRODUCTION

Over the last three decades, a great number of contributions dealt with fluvial processes and sediments of the Namib Desert valleys and palaeoclimatic implications. Reconstruction of the fluvial style present during deposition of a fluvial sedimentary succession is a primary objective to solve the problems arising with palaeoclimatic interpretations. The fluvial style influences the relative proportion, internal arrangement and three-dimensional geometry of channel and overbank deposits (Tooth, 2009).

Significant advances in the investigation of arid zone fluvial systems have been made in process-orientated studies on the nature and impact of flash floods (Nash, 1999). Slackwater deposits and floodout deposits are reported to document big flood events in the valleys and on the plains of arid to semi-arid environments (Baker, 1987; Baker *et al.*, 1988; Kochel and Baker, 1982, 1988; Ely and Baker, 1985; Ward, 1987; Tooth, 1999; Smith 1992a; Pickup, 1989; Greenbaum *et al.*, 2000; Srivastava *et al.*, 2005; Eitel *et al.*, 2006). Slackwater deposits and floodout deposits represent the most accurate palaeoflood evidence for reconstructing the magnitude and recurrence frequency of floods that are hundreds to thousands of years old (Zawada, 1995, 1997, 2000; Baker *et al.*, 1987). Slackwater deposits occur in many valleys of the Namib Desert (Namibia). Until recently, Late Quaternary slackwater deposits from the Namib Desert valleys have been interpreted as sediments representing river endpoint accumulations (Blümel *et al.*, 2000; Eitel *et al.*, 2002, 2004, 2005), as deposits of an aggrading

river system (Smith *et al.*, 1993; Srivastava *et al.*, 2006), or as deposits controlled by a change in the hydrological regime in the catchment area towards more aridity (Rust, 1989b; Vogel, 1989; Vogel and Rust, 1990; Partridge, 1993; Dollar, 1998). Heine and Heine (2002) pointed out that the Late Pleistocene slackwater deposits of the Kuiseb Valley in the Namib Desert were likely deposited in areas of the floodplain that are sheltered from high-velocity flood flows and thus represent extreme flood events. Nevertheless, some authors interpret the valley-fills in a different palaeohydrological scenario deducing from their observations an increased aridity for the catchments (Eitel and Zöller, 1996; Vogel and Rust, 1987, 1990; Hüser *et al.*, 1998; Blümel *et al.*, 2000; Eitel *et al.*, 1999b, 2000, 2002, 2004, 2005). It is the aim of this paper, to present additional evidence that slackwater deposits and floodout deposits of the Namib Desert valleys are caused by Late Quaternary palaeofloods.

Palaeoflood hydrology, and therefore palaeoclimatic interpretations of alluvial sedimentary sequences, begins with real data that indicate the properties of real flood events (Baker, 2003a). Based on the concept of *desert flash flood series* (Heine and Völkel, 2009), fluvial deposits of Namibian desert valleys are analysed and interpreted. The *desert flash flood series* model is a concept of a hierarchical dynamic stratigraphy to investigate the relationships between heterogeneous deposits of ephemeral desert streams.

Here I present an improved analysis of drivers of fluvial deposition in three Namib Desert valleys, making use of information from data of fluvial deposits itself and of the *desert flash flood series* model. The purpose is to avoid errors in palaeoclimatic interpretations.

3.1.1 Study area

The Namib Desert stretches from South Africa to Southern Angola along the Atlantic coast between 29° and 16° S latitude and 12° and 17° E longitude (Figure 1). The area is characterized by a great variety of rock formations, which usually are exposed in a rugged landscape of valleys, escarpments, mountains and large plains (Mendelsohn *et al.*, 2002; Hüser *et al.*, 2001). In the Namib Desert and adjacent areas, dominant soils are arenosols, gypsisols, leptosols, together with dune sands, gravel plains, and rock outcrops. In the escarpment areas and mountains, soils consist mostly of leptosols and regosols. On calcareous rocks, calcisols are common. Fluvisols are found along the margins and valleys of larger river courses. The clay mineral assemblages of the Namib Desert were investigated by Heine and Völkel (2010). They delineated four soil clay mineral provinces in the Namib Desert and many individual clay mineral assemblages in fluvial, pan, cave and other environments.

The region's climate is heavily influenced by its location. The area is exposed to air movements of the Intertropical Convergence Zone (ITC), of the Subtropical High Pressure Zone, and of the Temperate Zone. The relative positions of these systems determine the rainfall pattern. The cold Benguela Current modifies the subtropical climate of Southwestern Africa. As a result, the coastal regions of the Namib Desert see little rainfall, relatively low temperatures, strong winds, frequent fogs, relatively high humidity, less radiation and no frost along the Atlantic coast. The regional significance of thermo-topographic airflows over the central Namib Desert frequently equals or exceeds that of the general circulation. The mean annual rainfall is less than 20 mm yr⁻¹ along the coast and reaches >100 mm yr⁻¹ in the eastern parts of the desert. The larger river catchments extend to the Namibian highland and receive greater amounts of rainfall in their upper reaches (Ugab up to 500 mm yr⁻¹, Swakop up to

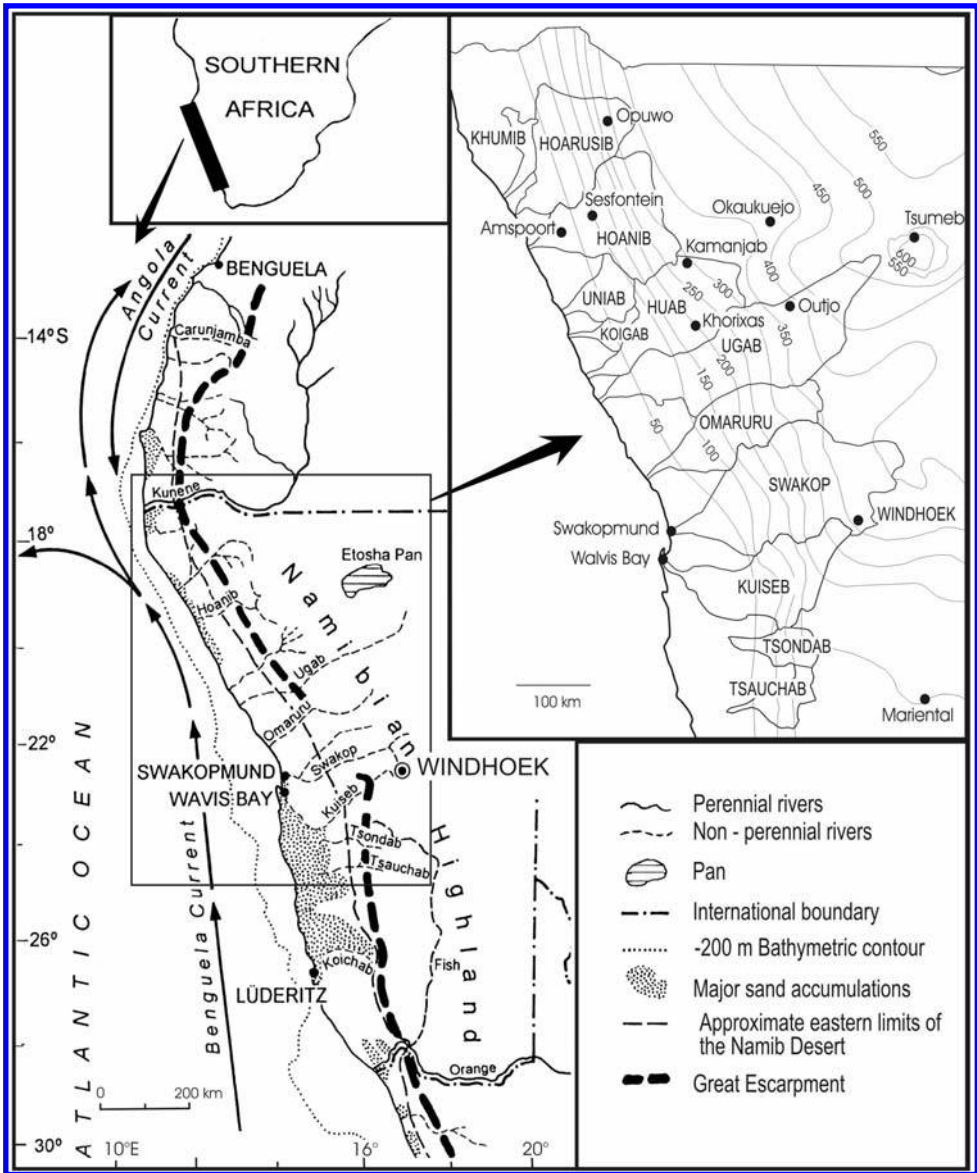


Figure 1. Twelve major ephemeral rivers flow across Western Namibia. Apart from Tsauchab and Tsondab all ephemeral rivers may discharge into the Atlantic Ocean after extreme precipitation events. Inset map shows major drainage systems and isohyets (mm a^{-1}).

400 mm yr^{-1}). Vegetation patterns mostly depend on climate. From the coast to the east the vegetation types change progressively from desert to dwarf shrub savanna, and shrub-and-Acacia-tree-savanna,

Twelve major ephemeral rivers are found in the central and northern Namib Desert of Namibia (Figure 1). A number of smaller rivers originate within the arid desert itself. The frequency of flooding in the valleys is dependent on catchment size,

average rainfall, and, in some areas, upstream dams (Jacobson *et al.*, 1995). Empirical observations on valleys in Namibia that experience flooding remain scarce. This is especially the case for extremely high flood variabilities in the Namib Desert. Today, the frequency of flooding varying from catchment to catchment, markedly affects vegetation and water resources each river supports. These geographical, climatic and biological features, in addition to the specific geology, make each catchment unique, as described in detail by Jacobson *et al.* (1995).

In the Namib Desert, fluvial deposits of the following valleys were considered: Kuiseb, Hoanib and lower Orange River (Figure 1). In the river channels, characteristics of braided river sedimentation are observed (Heine and Völkel, 2009). Today, the river beds are filled by sand and gravel up to an equilibrium gradient. This prevents linear erosion and incision of the rivers (Martin, 1950). In overbank areas slackwater deposits are deposited. They consist of sedimentary particles with high settling velocities (sand and silt, sometimes gravel) that accumulate from suspension in extreme floods at local sites of reduced flow velocity (Baker, 1989). On unchannelled desert surfaces (desert plains) floodout deposits occur where channel capacity is reduced abruptly, causing flows to become unconfined and to spread across the (alluvial) plain.

3.2 METHODS AND SOURCES

Fluvial deposits of the Namib Desert valleys are particularly heterogeneous and their sediments are quite variable over a wide range of scales. Sedimentologic studies focus on inn-channel and off-channel processes to improve our understanding of the links between river channel and floodplain interactions. While channel facies at best may harbor only weak climatic signals, floodplains may host more climatically diagnostic features (e.g., palaeosols, bioturbation features, trace fossil assemblages, R.M.H. Smith *et al.*, 1993; J.J. Smith *et al.*, 2008) that can be of greater use in palaeoenvironmental reconstructions (Tooth, 2009). In-channel and off-channel sedimentary sequences combined with stratigraphic mapping are used to reconstruct their palaeohydrology. We analysed the grain size distribution (standard techniques, sieve, pipette), carbonate content (Scheibler and Finkener technique, see Ellerbrock, 2000), content of organic material (UV-VIS spectrometer Lambda 2), colour (Munsell) and clay mineral associations (X-ray diffraction, Philips APD-10, Philips PW 1730 and Siemens X-ray unit D 5000, see Heine and Völkel, 2010) to describe and classify stratinomic features (Miall, 1985; Reineck and Singh, 1980), to differentiate flood sediments of different provenance and to reconstruct potential fluvial palaeoenvironments, enabling us to calculate the most likely palaeohydrological parameters, such as discharge and sedimentation rates.

Ground Penetrating Radar (GPR) was used in fluvial and vlei sediments (gravel, sand, silt, clay) to establish their subsurface architecture. The geometric patterns of depositional elements of ancient river systems were classified into so-called radar facies. A radar facies can be defined as a mappable, three dimensional sediment unit composed of radar reflections having characteristic properties which therefore can be used to differentiate this unit from adjacent ones in a profile (Völkel *et al.*, 2006; Leopold *et al.*, 2006; Heine and Völkel, 2010). Different radar facies were related to specific accretionary elements, such as gravel sheets, silts, dune sand, etc.).

By using conventional ^{14}C and AMS (accelerator mass spectroscopy) ^{14}C age determinations, a Late Quaternary chronology was established for the palaeoflood record for the Namib Desert valleys. The analyses were conducted by laboratories in Hannover (M.A. Geyh, M. Frechen) and Erlangen (W. Kretschmer, A. Scharf). Ages

younger than AD 1951, were inferred from a diagram elaborated by M.A. Geyh. OSL (optically stimulated luminescence) age determinations were carried out by laboratories in Hannover (M. Frechen), Cologne (U. Radtke, A. Hilgers), Pretoria (J.C. Vogel) and Ahmedabad (A. Singhvi). Applied optical dating protocols are described in detail in Kale *et al.* (2000). Furthermore, many ^{14}C , AMS ^{14}C , TL (thermally stimulated luminescence) and OSL age determinations were gathered by reviewing the literature.

Detailed investigations of the desert soils of the central Namib plains north of the Kuiseb River (Heine and Walter, 1996; Wartbichler 1998; Bao *et al.* 2000, 2001) allow reconstructions of extreme sheet floods.

Published descriptions and analyses dealing with fluvial deposits of the Namib Desert valleys that complement our studies, are considered and evaluated with regard to the concept of *desert flash flood series* (Heine and Völkel, 2009), and to provide facts and arguments for or against our interpretations. Much information was assembled by reading the publications of Rust (1987, 1989a, 1989b, 1999), Rust and Wieneke (1974, 1980), Marker and Müller (1978), Hövermann (1978), Vogel (1982, 1989), Ward (1987), Vogel and Rust (1990), Smith *et al.* (1993), Eitel *et al.* (2002, 1999a,b, 2001, 2004), Krapf *et al.* (2003), Pradeep *et al.* (2004), Brook *et al.* (2006) and Srivastava *et al.* (2004, 2005, 2006).

3.3 MODEL-DRIVEN VERSUS EVIDENCE-LED INTERPRETATION

In a recently published progress report on arid fluvial sedimentary systems Tooth (2009) directed attention to the debate of model-driven versus evidence-led interpretations of dryland river systems. Many facies models have been developed almost exclusively on the basis of humid examples and may not be representative for desert environments. Furthermore, detailed research on sediments of modern ephemeral rivers that decrease in size downstream are restricted to a small number of examples from a limited variety of geographical settings (Tooth, 2009). In Namibia, no detailed studies on the transport of sediment through desert river channels exist. Little is known about hydraulic conditions at overbank flow, whether in the channel or in the floodplain (see Knighton and Nanson, 2002), about mass flux and its relation to water flow or the components of sediment load transported in a channel and in contact with the stream bed, about the influence of overbank sedimentation on the decrease of the downstream rate in channels (see Frings, 2008), and about the depositional character of fluvial deposits formed by individual floods (see Laronne and Shlomi, 2007). It is therefore difficult to evaluate the impact of big floods on the channel. Better insight comes from GPR profiles (Leopold *et al.*, 2006). Only a few systematic and detailed studies of Late Quaternary sediments along the Namib Desert river courses exist. Limited independent evidence for palaeoenvironmental reconstructions based on fluvial deposits is currently available only for the Kuiseb Valley (e.g., Marker and Müller, 1978; Ward, 1987; Smith *et al.*, 1993; Heine and Heine, 2002; Srivastava *et al.*, 2006), the Hoanib Valley (e.g., Rust, 1999; Vogel and Rust, 1990; Heine, 2004a, 2004b; Eitel *et al.*, 2005, 2006), the Khumib River (Srivastava *et al.*, 2004) and the Hoarusib Valley (Srivastava *et al.*, 2005). Therefore, in the Namib Desert, palaeoenvironmental and palaeoclimatic reconstructions based on fluvial deposits are often model-driven interpretations (see Leser, 2000; Rust, 1989b; Rust and Vogel, 1988). Such approaches run the risk of creating errors in palaeoclimatic reconstructions, e.g., situations that clearly are counterproductive for advancing knowledge (Tooth, 2009).

3.4 THE NAMIB DESERT RIVERS

This paper reviews the best-analysed fluvial palaeoclimatic records from the Namib Desert from the LGM to the Little Ice Age, and evaluates the evidence from selected fluvial records from three Namib Desert rivers: The Kuiseb with the Homeb Silt sequence, the Hoanib with the Amspoort Silts and the lower Orange River with Late Holocene flood deposits. This paper does not refer to the sedimentary sequences that accumulated in basins such as the basins of Opuwo (Brunotte and Sander, 2000a, 2000b), Dieprivier (Eitel and Zöller, 1996), the upper Hoanib Valley (Eitel *et al.*, 2006) or the Khumib valley (Srivastava *et al.*, 2004). Neither are potential silt-generating processes for such environments discussed (Haberlah, 2007, 2009).

3.4.1 The Kuiseb River

The Kuiseb River, rising on the interior plateau of Namibia some 20 km southwest of Windhoek (Figure 1), is one of the ephemeral watercourses traversing the Namib Desert towards the Atlantic Ocean. The catchment has an area of 15.500 km² (Jacobson *et al.*, 1995). In a detailed study Ward (1987) investigated the Cenozoic history of the Kuiseb valley and its major tributaries west of the Great Escarpment. Ward (1987) describes the nomenclature, distribution, composition, origin, age and correlation of the Cenozoic succession which consists of ten sedimentary units. Here, I only will relate to the Late Quaternary fluvial deposits.

The *Homeb Silts* (Figure 2) are remnants of flat-lying, fine-grained silty deposits that are preserved up to 45 m above the present Kuiseb River in sheltered localities adjacent to the lower canyon/upper valley section of the main river course (Ward, 1987). Distribution, thickness, lithology and structure are described by Smith *et al.* (1993), Ward (1987), Marker (1977), Marker and Müller (1978), Rust and Wieneke (1974, 1980), Ollier (1977), Hövermann (1978), Goudie (1972), Heine and Heine (2002), amongst others.

Previous authors have proposed different explanations for the origin of the Homeb Silts: (i) sediments deposited behind a dune dam(s) (Goudie, 1972; Scholz, 1972; Rust and Wieneke, 1974, 1980); (ii) fluvial river terrace accumulation (Hövermann, 1978); (iii) river endpoint accumulations (Marker, 1977; Marker and Müller, 1978; Vogel, 1982, 1989; Blümel *et al.*, 2000); (iv) silt deposits of an aggrading river during flashflood events by rapid sedimentation from eddying currents as the floodwaters inundated the side valleys (Ollier, 1977; Ward, 1987); (v) flood deposits of an aggrading river that resemble slackwater deposits, accumulated episodically as a result of successive back-flooding into embayments and tributary valleys (Smith *et al.*, 1993; Srivastava *et al.*, 2006); (vi) stacked slackwater deposits, no aggradation in the main Kuiseb channel (Heine and Heine, 2002).

Aside from many other observations in the field (Srivastava *et al.*, 2006; Heine and Heine, 2002; Heine *et al.*, 2000; Smith *et al.*, 1993; Ward, 1987), the concomitance of the following evidence exclude the explanations (i), (ii) and (iii) for the origin: (a) The flat-lying deposits show layers that can be traced over hundreds of metres to some kilometers and an inclination (1–2°) parallel to the Kuiseb River bed, thereby indicating accumulation of sediments by a river (and not in a lake of a dammed valley); (b) in the tributary valleys, the palaeo-flow direction is up-valley; at the base the flat-lying deposits ascend up-valley and show in the contact area with the rock slopes a bending upward together with a thinning of the layers, thereby indicating that flashfloods occupied the tributaries and that the silty sediments were laid down in a water

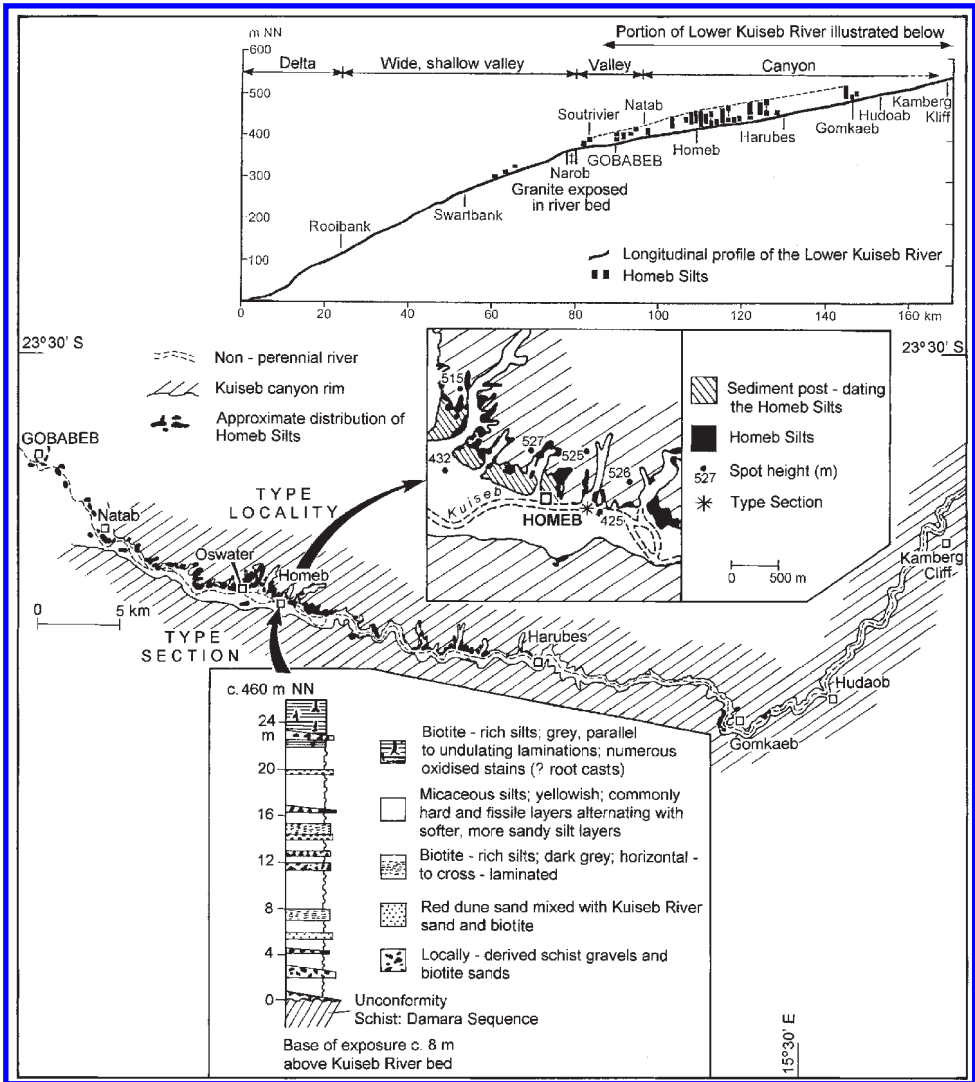


Figure 2. Distribution of the Homeb Silt deposits of the Kuiseb River. The type locality and section is shown, as is the distribution relative to the longitudinal profile of the Lower Kuiseb Valley (after Ward, 1987).

column that decreased towards the head of the tributaries (Klarl, 1999). The explanation (iv) 'flood deposits of an aggrading river' considered by Ollier (1977) does not correspond in internal bedding structures to an aggrading braided river with sandy bars and channels. Field evidence (a) and (b) document that explanation (iv) has to be rejected. Smith *et al.* (1993) and Srivastava *et al.* (2006) note that the Homeb Silts were predominantly deposited from suspension by backflooding water and that they closely resemble slackwater deposits.

Heine and Heine (2002) argued that the Homeb Silts are slackwater deposits within the meaning of Baker (1983, 1987), Kochel and Baker (1982, 1988) and Zawada

(1997); slackwater deposits consist of sedimentary particles with high settling velocities, such that they accumulate relatively rapidly from suspension during extreme floods (Baker, 2003b). The height of the slackwater deposits in tributary valleys and embayments can be used to make a conservative estimate of the peak palaeoflood stage (Kochel and Baker, 1982). The slackwater deposits would not have accumulated if the palaeofloods had not occurred more frequently with a higher stage than current floods, so that inundation and backflooding of the tributary mouths and embayments were possible. Heine and Heine (2002) concluded that during slackwater deposition in low-energy areas (off-channel processes) sediment infilling and/or erosion was insignificant in the main channel. The authors calculated the palaeodischarge values for the Kuiseb Valley during the Homeb Silt accumulation. Although the Kuiseb palaeofloods match the world's and Southern African recorded flood peaks (Figure 3), the palaeohydrologic reconstruction of the Kuiseb Valley during the Homeb Silt deposition was questioned. Srivastava *et al.* (2006) argued that the massive floods postulated by Heine and Heine (2002) to explain silts ~45 m above the present Kuiseb channel are not necessary if backflooding of tributaries was accompanied by aggradation of the main channel.

No studies deal with inbank and overbank velocity/sedimentary conditions in Namibia's arid ephemeral rivers. Field observations and GPR research on fluvial deposits, whether in the channel or in overbank areas (Leopold *et al.*, 2006; Völkel *et al.*, 2006), reveal sharp discontinuities in velocity at the inbank/overbank transition. The hydrologic processes increase the complexity of flow behavior as within-channel, and off-channel waters interact. In the Kuiseb valley, the GPR research shows that high-energy floods moved and deposited boulders, cross-bedded gravel and sand in the main channel and accumulated horizontally bedded fine, silty deposits on the floodplain (Leopold *et al.*, 2006). The high-energy runoff in the main channel and low-flow

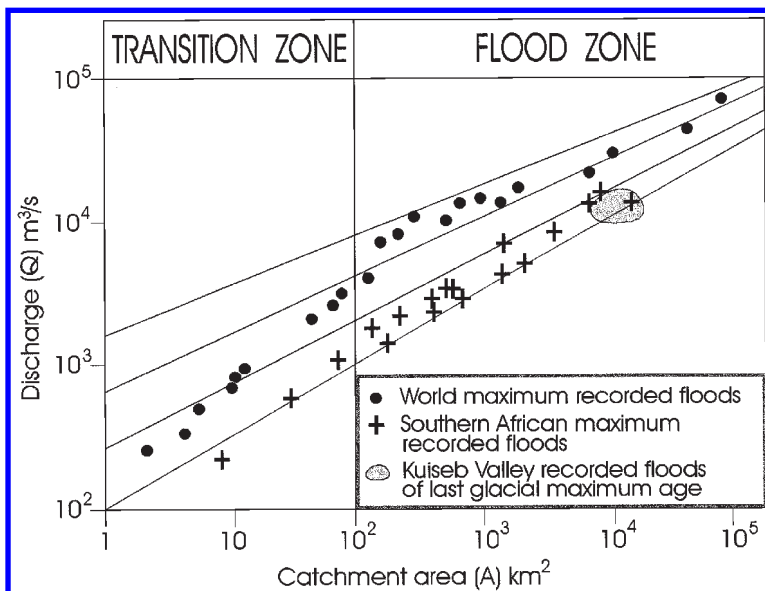


Figure 3. The palaeodischarge value calculated from the Homeb slackwater deposits plotted on the Francou-Rodier diagram together with world and Southern African flood peaks. For explanation see Zawada (1997: 114–115) and Heine and Heine (2002).

sedimentary conditions in the floodplain areas are characteristic while slackwater sediments deposited. The simultaneous transport and deposition of fine-grained material on the river banks and gravel and sand in the main river course was observed during and after the 1962–1963, 1995 and 1997 floods in various Namib Desert valleys (see also Ward, 1988). During major floods discharge capacities, required to move the gravel-sand mixture, are about equal to those needed to transport the sand fraction alone. Gravel particles in a mixture with more than 50% sand seem to have little effect on the overall mobility of the mixture (see also Hassan *et al.*, 1999). Lately, in the channel, the transport of gravel and sand was equal to the transport energy, so that equilibrium conditions existed and that no erosion or sedimentation occurred (see also Martin, 1950). GPR results from channel fills yield insights into sediment transport at river beds (Leopold *et al.*, 2006) and add to these observations: It seems that bedload transport moves material with a very wide range of grain sizes and shapes only to a depth of several grain diameters. Yet, during flash floods slackwater deposits were laid down in inundated areas, but the channels remained essentially stable despite large floods. As to the sedimentation of the Homeb Silts, we do not know whether gravel and sand aggraded within the main channel resulting in an upward accumulation of both, the in-channel gravel/sand deposits and the off-channel slackwater deposits. If this was the case, the reconstruction of the peak palaeoflood stages (Heine and Heine, 2002; Figure 3) shows too high discharge values and the palaeoclimatic inferences have to be revised.

The Homeb Silt sediments occur from below the channel level up to ~45 m above the present river bed. In the lower canyon they are mainly covered by Holocene fluvial sediments (Gobabeb Gravels) up to 30 m above the recent channel. The deposits contain not only bedrock material derived locally from the tributary washes but also gravels composed predominantly of (well)rounded vein quartz, metaquartzite and quartzite clasts (Ward, 1987). The Gobabeb Gravels partly truncate the Homeb Silts. The distribution, thickness, lithology and structure of the Gobabeb Gravels in the Kuiseb Valley are described in detail by Ward (1987). According to the observations compiled by Korn and Martin (1957), Ward (1987) and our team, the *desert flash flood series* model (Heine and Völkel, 2009) can help to understand and interpret the Homeb Silts and Gobabeb Gravels. The following presents a new interpretation with respect to the mode of origin for the Gobabeb Gravels and their relationship to the Homeb Silts.

During the accumulation of the Homeb Silts a gravel-sand mixture of local and upstream material was transported in the main channel. The channel deposits show characteristics of braided river sedimentation. At the end of the confined canyon valley where channel capacity is reduced abruptly, causing flows to become unconfined, the floods deposited so-called floodout sediments. The stratigraphic architecture of these floodout deposits is not preserved. Supposedly, the Homeb Silt flood events are responsible for the accumulation of the Gobabeb Gravels in the main channel and in the braided channels of the floodout area. While the floods caused slackwater sedimentation in off-channel areas up to 45 m above the present Kuiseb bed, the channels were filled with gravels and sand. The rate of sedimentation was greater in the overbank areas than in the channel itself, resulting in a more rapid build-up of the slackwater deposits than of the channel bed gravels. After many flood events, in the channel of the Kuiseb canyon, the sequence of the coarse fluvial material was up to 30 m thick. In the floodout area, fills of braided flood channels and anabranching channels, overbank sand, silt and mud layers, slackwater deposits and aeolian dunes built a stratigraphic architecture with various interrelationships of the lithological units. After the period of the Homeb Silt deposition (including the channel-fill deposits),

erosion occurred. The bulk of the fine sediments of the Homeb Silts and the floodout deposits were eroded. The coarser gravels were redistributed; thereby a thin layer of Gobabeb Gravels was spread over the slopes of the canyon, over river terraces and over the Homeb Silts preventing them from further erosion.

Our approach combines the field evidences described by many researchers with our own observations. By referring to the *desert flash flood series* model we interpret the Homeb Silts of the Kuiseb River as evidence for extreme flash floods and the Gobabeb Gravels as redeposited material that was primarily transported and accumulated at Homeb times, but was later eroded, mixed with local sheet wash and slope debris, and partly scattered over Homeb Silts, surface rocks and river terraces.

Before and after the Homeb Silt accumulation, smaller floods of the Kuiseb River and tributaries caused erosion. According to various efforts to date the Homeb Silt accumulation phase, the age of the Homeb flash flood period is disputed. Vogel (1982) radiocarbon dated gastropod shells, thin calcareous crusts and a wood fragment of the Homeb Silts and derived ages between 23.000 and 19.000 ^{14}C years BP (= $\sim 27\text{--}22$ cal ka BP; peak of Antarctic ice extent: 30.000–24.000 cal yr BP, see Chase and Meadows, 2007). Eitel and Zöller (1996) presented thermoluminescence ages of $20,3 \pm 3,2$ ka for a base sand layer and $19,3 \pm 1,8$ ka for a top sand layer. Bourke *et al.* (2003) used optical age estimates which indicate that the Homeb Silts were deposited between 6,3 and 9,8 ka; these ages may be too young because of methodological problems. Srivastava *et al.* (2006) identified by OSL dating two phases of sedimentation ~ 15 ka and ~ 6 ka. The ages determined by Vogel (1982) suit best with the observations by many authors (e.g., Ward, 1987; Heine and Heine, 2002). The proposed age for the Homeb Silts corresponds closely to the *last glacial maximum* (LGM). Ward (1987) and Smith *et al.* (1993) argued that aggradation of the Homeb Silts was probably controlled either by a base level change in the lower reaches of the Kuiseb Valley (eustatic control) or, more likely, a change in the hydrological regime in the catchment area (climatic control). The TL ages (Eitel and Zöller, 1996) and the ^{14}C ages (Vogel, 1982) are not confirmed by the OSL ages (Bourke *et al.*, 2003; Srivastava *et al.*, 2006). The big difference in ages may record different phases of sediment accumulation between the LGM and the early/middle Holocene.

Although the Homeb Silt sequences document repeated flash flood events in the Kuiseb catchment area during the LGM, it is questionable whether the Homeb Silts represent a more humid climate during times of the silt accumulation. The Homeb Silts stand for a phase of some thousand years with low-frequency high-magnitude precipitation events causing floods not only in the upper catchment of the Kuiseb but also in the Namib Desert. These floods are documented by the slackwater deposits and the sheetwash breccias composed of locally derived bedrock fragments that occur throughout the Homeb succession. The floods could have occurred in an overall arid climate (like today) as well as in a semiarid climate. The fluvial evidence from the Homeb Silts alone does not allow a reconstruction of a certain climate that was drier or wetter than the present one. Definitely, the Homeb Silts do not represent river endpoint accumulations and, thus, do not document an increase in aridity in the upper catchment as was maintained by some authors (Marker, 1977; Marker and Müller, 1978; Vogel, 1982, 1989; Blümel *et al.*, 2000) and referred to in many summaries of the climate history in Southern Africa (e.g., Partridge, 1993; Dollar, 1998). The ages obtained for the Homeb Silts by various methods differ considerably from one another. Unfortunately, the samples were taken from different sites of the Homeb sequence. Furthermore, none of the authors observed or described several accumulation sequences at Homeb that are separated by erosion, documenting cut and fill processes of the silts in tributary valleys and embayments. If the accumulation of the

Homeb Silts occurred during many thousand years (between the LGM and the middle Holocene), climatic and/or hydrological changes must have led to deposition and erosion of the Homeb Silt sequence. To date it is impossible to correlate the Homeb Silt aggradation phase(s) with relatively well established palaeoclimate chronologies from the marine environment off the Namib coast (Gasse *et al.*, 2008).

To yield more palaeoenvironmental information from the Homeb Silt sequence, Smith *et al.* (1993) investigated the ichnofacies of the Homeb Silts and paid attention to gastropods from both aquatic and terrestrial habitats, carbonate encrusted rhizocretions, gypsum rosettes and rates of pedogenesis. Although many scientists looked for fossils, body fossils are very scarce in the Homeb Silts. Smith *et al.* (1993) suggest that the climate was less harsh and arid when the silts accumulated, because the ancient ichnofauna was a much more diverse assemblage compared to the impoverished one of the modern Kuiseb. Their palaeoclimatic conclusions (wetter phase) are based on the palaeontologic evidence.

Our understanding of the past climates reconstructed from the Homeb fluvial archive is still very limited by a poor chronology and by questionable palaeoenvironmental interpretations of the deposits. Additional insight may be obtained by comparing the Homeb Silts with similar valley-fill deposits in the Australian Flinders Range. The Flinders Silts aggraded throughout the last glacial cycle during intervals of rapid aggradation alternating with intervals of relative surface stability and erosion (Haberlah, 2009). Haberlah (2009) noticed that the bulk of the fine-grained material consists of wind-blown dust, and interpreted the fine-grained valley-fill formations as the fluvial response to glacial aridity-induced dust deposition and devegetation. The results of Haberlah (2009) can help resolving debates on the age, source and nature of the Homeb Silts. The Homeb Silt sequence is >45 m thick. To provide such great quantities of fine-grained material in the Kuiseb catchment, aridity of the LGM was a prior condition together with low-frequency high-magnitude precipitation events.

3.4.2 The Hoanib River

The Hoanib catchment (Figure 1) comprises 17,200 km², stretches far to the east (Namibian highland, ~1,200 m asl), and contains narrow gorges as well as wide basins (Jacobson *et al.*, 1995; Leser, 2000). The present precipitation ranges from nearly zero at the Atlantic coast to 325 mm a⁻¹ in the east. In the Hoanib valley and basins fine-grained, mainly silty deposits are found that—according to many authors—indicate periods of less rainfall and reduced sediment transport capacity of the rivers (e.g., Rust, 1989a; Eitel *et al.*, 2004, 2005, 2006).

Geomorphological and chronological investigations of the fluvial deposits of the Hoanib River were done in the upper catchment by Heine (2004a, 2004b) and Eitel *et al.* (2006), in the lower catchment around Amspoort by Vogel and Rust (1987; 1990), Rust (1999), Eitel *et al.* (2005) and Leopold *et al.* (2006), amongst others. Near the Hoanib mouth a dune field dams the westward flowing ephemeral river and river flood deposits are accumulated between aeolian dunes (Krapf *et al.*, 2003; Stanistreet and Stollhofen, 2002).

In the following the Amspoort Silts (Figures 4 and 5) as palaeoenvironmental archive will be discussed, because the palaeoclimatic interpretation is disputed. Eitel *et al.* (2005) argue that the Amspoort Silts are evidence of palaeohydrological fluctuations and that they are river end accumulations indicating decreased precipitation during the Little Ice Age (Rust, 1999; Vogel and Rust, 1990). Moreover, the authors conclude that the subsequent incision of the river channel documents—contrary to the

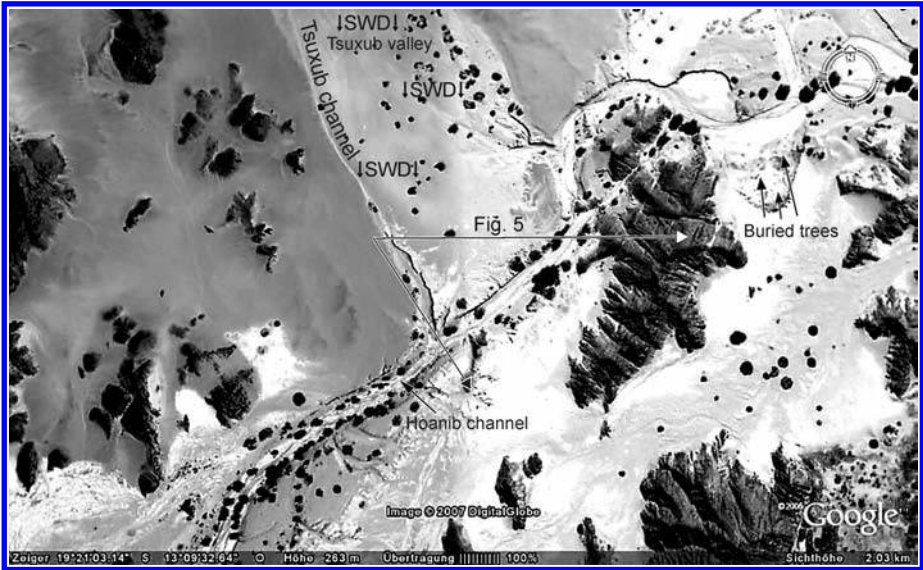


Figure 4. Satellite image of the Amspoort site. The Hoanib River channel runs from above right to lower left. The distribution of the Amspoort slackwater deposits is shown. The slackwater deposits reach upvalley in the Tsuxub tributary. In the tributary mouth they are covered by sheet flood sediments of the Tsuxub (↓SWD↓). Occasionally (little) floods caused backward erosion and formed the Hoanib main channel and the small gullies of the tributaries. The view shown in Figure 5 is indicated. (Google, 2006).



Figure 5. The Amspoort Silts (AS) are characterized by horizontal bedding and deposition in back-flooding embayments. The gully is the tributary mouth of the Tsuxub River. The persons are working on the GPR profile of the site which is described in detail by Leopold *et al.* (2006). AS, Amspoort Silts; HC, Hoanib channel, TG, Tsuxub gully. (Photo: K. Heine, 16 March 2004).

aridification of northwestern Namibia (e.g., Heine, 2005)—more monsoonal rainfall; deposition and erosion of the Amspoort Silts show that the landscape degradation in northwestern Namibia is primarily anthropogenically induced and most probably not accelerated by a decrease in precipitation (Eitel *et al.*, 2005).

The Amspoort Silts were deposited during the Little Ice Age according to ^{14}C age determinations of buried trees (Vogel and Rust, 1990) and OSL dating on fluvial silt and aeolian sand (Eitel *et al.*, 2005). To contribute to a better understanding Leopold *et al.* (2006) have combined the published sedimentological and chronological data with the interpretation of radar images. The Amspoort Silts are characterized by the horizontal bedding and deposition in back-flooding embayments and tributary mouths (e.g., Tsuxub Valley) which is typical of slackwater deposits, whereas the Amspoort Silts described by Rust (1987), Vogel and Rust (1990) and Eitel *et al.* (2005) were accumulated in areas either off or near the main channel or, downstream, of abrupt channel expansion. The study sites of all these researchers can clearly be correlated in the field, and the sections described belong to the same stratigraphic unit with three facies types (Leopold *et al.*, 2006): (i) mid-facies, which comprises the main sequence of the Amspoort Silts; (ii) lateral facies, which comprises silty and clayey deposits in backflooding areas (Figures 5 and 6); (iii) distal facies, which comprises fan-like sediments that are spread to the west on the Namib surface (Figure 7) ('floodout' *sensu* Tooth, 1999). The distribution of these three facies shows that only very large, sediment-laden floods could have caused these fluvial deposits as is described by the *desert flash flood series* (Heine and Völkel, 2009). Waning floods as assumed by Rust



Figure 6. Amspoort Silt section. The horizontally fine-grained slackwater deposits (SWD) accumulated on top of tributary valley sheet flood deposits (TSFD). Both facies units are separated by a 0,3 m thick fluvial sand layer (S). OSL-1, OSL age ~4 ka BP; OSL-2, OSL age ~1 ka BP. (Photo: K. Heine, 16 March 2004).



Figure 7. Gravel, coarse sand, fine-grained sand and silt of the distal facies, which comprises fan-like sediments that are spread to the west on the Namib surface ('floodout' *sensu* Tooth, 1999). These deposits correlate with the Amspoort Silts (Figure 6). Ca. 13°06'E, 19°22,5'S. (Photo: K. Heine, 27 September 1999).

(1989a), Vogel and Rust (1990), Eitel *et al.* (2005) and other authors are not capable of transporting such large quantities of sediments and forming massive, well-sorted silt layers that can be traced over hundreds of metres and that were laid down during inundation (low-energy flow) in tributary mouths and embayments (Leopold *et al.*, 2006). The upstream shift of the main sedimentation area during the Little Ice Age, documented by ^{14}C and OSL dating, was *not* caused by gradually decreasing runoff resulting from aridification of the upper reaches of the catchment as assumed by Eitel *et al.* (2005), but is the result of floods carrying big sediment loads and—where the valley widens—of rapid sediment accretion which started downstream and moved slowly upstream (headward aggradation, 'rückschreitende Aufschüttung' *sensu* Ahnert, 1999). After the Little Ice Age the big floods ceased more or less and runoff decreased which led to headward gullying of the floodout/slackwater deposits (see Brooks *et al.*, 2009) and the development of the present shallow Hoanib channel. Fine-grained sand, silt and clay sediments are deposited in the basin of the Gui-uin east of the dune belt and between the dunes itself which confirm that considerable floods have passed through the dunefield during the last centuries to spill into the Atlantic (Vogel and Rust, 1987). In average, every nine years exceptional rainfall in the Hoanib catchment caused floods that break through the dune belt. Therefore, during extreme floods the sediment load was carried to the Atlantic and only part of it was accumulated in the Gui-uin basin and the adjacent dune area (Krapf *et al.*, 2003; Stanistreet and Stollhofen, 2002; Svendsen *et al.*, 2003).

All field observations and laboratory data corroborate the interpretation of the Amspoort Silts as sediments of big floods in the sense of the *desert flash flood series*. Interestingly, Sea Surface Temperatures (SST) and sedimentary fish scale record

(Altenbach and Struck, 2006; Struck and Altenbach, 2006) from the Benguela Current off the Namib Desert show that during the Little Ice Age the sea surface temperatures dropped and that the population of several fish species altered indicating wetter conditions in the 'hinterland' (see also Baumgartner *et al.*, 2004). More extreme Little Ice Age flash floods in the central Namib Desert are also documented by sheet flood sediments and flood transported tree trunks on the Namib surface (Heine, 2004b).

3.4.3 Orange River Valley

The most detailed palaeoflood hydrological investigation published to date in Southern Africa has been on the middle and lower reaches of the Orange River (Zawada, 1995, 1997, 2000). The Orange River originates in the Drakensberg area of Lesotho and flows west for about 2,200 km to the Atlantic Ocean. The catchment comprises ~0,973 million km² and is situated in different climatic regions (most of it in the subtropical summer rain area, the lower catchment in the southern Namib Desert with occasional winter rains). The Orange River is one of the World's most turbid, delivering annually ~60 million tons of sediment to the western margin of South Africa (Compton and Maake, 2007). While most of the Orange River water suspended sediment is derived from Karoo sedimentary rocks rather than from Drakensberg Basalt (Compton and Maake, 2007), the Late Holocene slackwater deposits of the lower reaches are dominated by clay mineral assemblages from soils developed on the basalts of the Drakensberg (Heine and Völkel, 2010).

The Orange River 'palaeoflood deposits' as described by Zawada (1995, 1997, 2000) and Herbert and Compton (2007) provide a direct evidence that these sediments are slackwater deposits and that they document extreme flood events which contributed to the sediment transport into the Atlantic. Zawada (1997) identified, dated and flow-modelled 13 palaeofloods over a period of 5,500 years (Figure 8). The Little Ice Age had significantly stronger/extremes floods. About 100 km south of the lower Orange River, slackwater deposits of the Buffels River were investigated by Benito *et al.* (2009). The palaeoflood record with more than 25 flood events over the last 600 years (during the Little Ice Age), shows clusters of floods AD 1,400–1,500 (five events) and AD 1,700–1,900 (≥10 events). Since AD 1900 a decrease in both, frequency and magnitude, of big floods occurred. These observations add to the Orange River record.

While the Orange River slackwater deposits of the Little Ice Age document catastrophic precipitation events in the upper reaches of the catchment, they do not stand for a climate change to more humid conditions. The Little Ice Age floods were possibly the result of tropical cyclonic activity which at that time occasionally reached farther south (Smith, 1992b). Anyhow, the LIA Orange River floods were *not* produced by snowmelt events during the transition from the cooler-wetter LIA to the warmer period which followed as assumed by Smith (1992a).

3.5 IMPLICATIONS AND CONCLUSIONS

Apart from the reviewed fluvial archives of the Kuiseb, Hoanib and Orange River, many papers were published to provide data about Late Quaternary climate change in the Namib Desert and adjacent regions. Most authors assembled both, well-dated and poor-dated, climate records from the Namib-Kalahari regions and nearby areas (often from different climatic realms of Southern Africa) and compared them

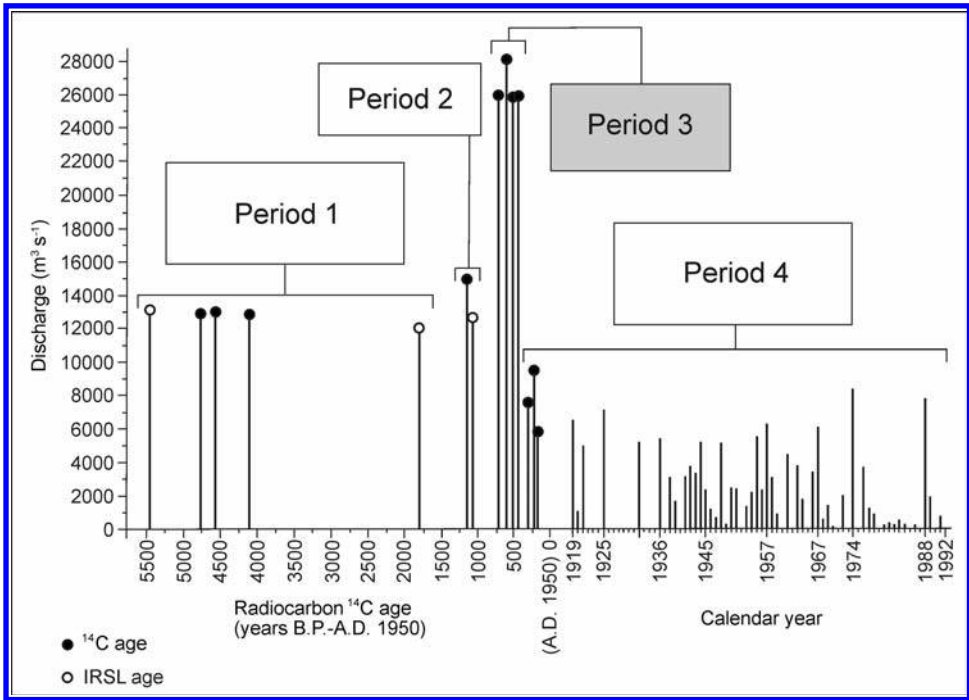


Figure 8. Compilation of the palaeoflood record for the lower Orange River with the annual peak-flow series gauged at Violdrift for the period 1919–1992. The entire record is subdivided into four palaeoflood periods characterized by a threshold discharge value (after Zawada, 2000). Period 1: 1.797 ^{14}C years (AD 961)–minimum older age of 450 ^{14}C years; the Orange did not experience a flood that exceeded the threshold discharge of $12.800 \text{ m}^3 \text{ s}^{-1}$. Period 2: 1.160 ± 80 ^{14}C years (AD 961)–565 ^{14}C years BP; the Orange did not experience a flood that exceeded the threshold discharge of $14.700 \text{ m}^3 \text{ s}^{-1}$. Period 3 (Little Ice Age): AD 1453–AD 1785; the Orange did not experience a flood that exceeded the threshold discharge of $27.000 \text{ m}^3 \text{ s}^{-1}$. Period 4: AD 1.785–AD 1.992; the Orange did not experience a flood that exceeded the threshold discharge of $9.500 \text{ m}^3 \text{ s}^{-1}$.

chronologically without evaluating the quality on which the records depend. By doing so, errors in palaeoclimatic interpretations cannot be avoided.

- i. Fluvial deposits of desert rivers can provide proxy data for palaeoclimates assuming that critical reappraisal is done of all sediment facies previously interpreted as having been deposited under flash floods, still water, dammed lakes, waning floods, and the like. A variety of sediment transport processes have been observed in desert rivers from different areas on earth. Earlier, we adapted a simple process-based approach (*desert flash flood series* model, Heine and Völkel, 2009) to analyse highly variable fluvial deposits of desert rivers by separately analysing the following six characteristics: (1) particles, (2) strata, (3) depositional elements, (4) facies bodies, (5) sequences and (6) basin fills. Combination and integration of various methodologies (e.g. sedimentology, geophysics, geochemistry, morphostratigraphy) allowed to identify all these sedimentary units and correlate them in a bigger palaeoclimatic context.
- ii. This review indicates that many of the preconceptions about chronologies are naïve. Most researchers did not consider it important to critically evaluate the published ages, although some had recognized the vital role that sound

chronologies play. (In their comprehensive review of palaeoclimatic evidence from Southern Africa, Chase and Meadows [2007:131] include ‘all available evidence, excluding only the Namibian silt records, for which a consensus of interpretation has not yet been reached’.) Figure 9 shows ages for the Namib Desert flash flood deposits.

- iii. This review should urge us to critically reexamine existing palaeoclimate databases from adjacent Southern African areas and to extract maximal information from them (see Gasse *et al.*, 2008; Chase, 2009).
- iv. The researchers will have to revisit the fluvial deposits of the Namib Desert valleys and generate much subtler interpretations to explain their palaeoclimatic evidence.

By considering the variety of evidence available for Namibia, and the debates concerning the reliability and palaeoclimatic interpretations of these proxies, a Holocene history of Namibia’s climate has been calculated by Heine (2005) (Figure 10). In Namibia’s desert environments, fluvial deposits cannot be used as palaeoclimatic archives; yet, they document flashflood conditions caused by extreme precipitation events. During the Late Quaternary, these events concentrated during certain periods of which only the Holocene periods can be dated with reliability. The ages published for the Pleistocene fluvial deposits are either disputable with regard to additional observations and evidence or methodically doubtful.

Although there have certainly been wetter and drier phases, Namibia’s climate has been rather similar to what it is today for the Holocene with only little climatic fluctuations (Heine, 2005). The LGM of the Namib Desert seems to have been slightly wetter according to the reconstruction of Chase and Meadows (2007), but drier according to the evaluation of the palaeoclimate records by Heine (1998a, 1998b, 2002; see also Gasse *et al.*, 2008). Because of problematic validity of many dates (^{14}C , TL, OSL) of Late Quaternary fluvial deposits (e.g., Homeb Silts), these sediments cannot be used as geoarchive for palaeoenvironmental reconstructions (see also Chase and Meadows, 2007). The early Holocene was slightly wetter; short dry episodes occurred around 8 ka BP and around 4–3 ka BP. Since about 500 years the Namib Desert experienced more arid conditions. Fluvial deposits of the Namib Desert, however, were dated to the early Holocene and the Little Ice Age, showing that fluvial deposits were accumulated during both, slightly wetter and drier climatic phases. The *desert flash flood series* model is a concept of a hierarchical dynamic stratigraphy to investigate the relationships between heterogeneous deposits of ephemeral desert streams. Fluvial deposits in deserts are geoarchives representing *a priori* not the climate, but atmospheric conditions prevailing at an area and a time (weather).

For the southwestern Kalahari, Heine (1981, 2002) discussed the frequent LGM discordance of aeolian activity with other terrestrial records indicating coeval increases in humidity and the correlation of these phases with wind strength proxies. Heine’s (1981) conclusions are now confirmed in a comprehensive study by Chase (2009) who evaluated the use of dune sediments as a proxy for palaeoclimatic reconstructions. As discussed above, fluvial aggradation in deserts does not show a clear, consistent relationship with humidity (or wetter phases), so does desert dune activity not document a consistent relationship with aridity. Chase (2009) suggested that aridity is unlikely to be the sole, or even primary, forcing mechanism for aeolian activity, and that the palaeoclimatic significance of these sedimentary archives needs to be reassessed (see also Heine, 1981). By excluding the Namib Desert fluvial deposits and records of aridity based on aeolian proxies, the palaeoclimatic reconstructions for Southern Africa become much more coherent (see Heine, 1981, 2002; Chase, 2009; Chase and Meadows, 2007; Gasse *et al.*, 2008).

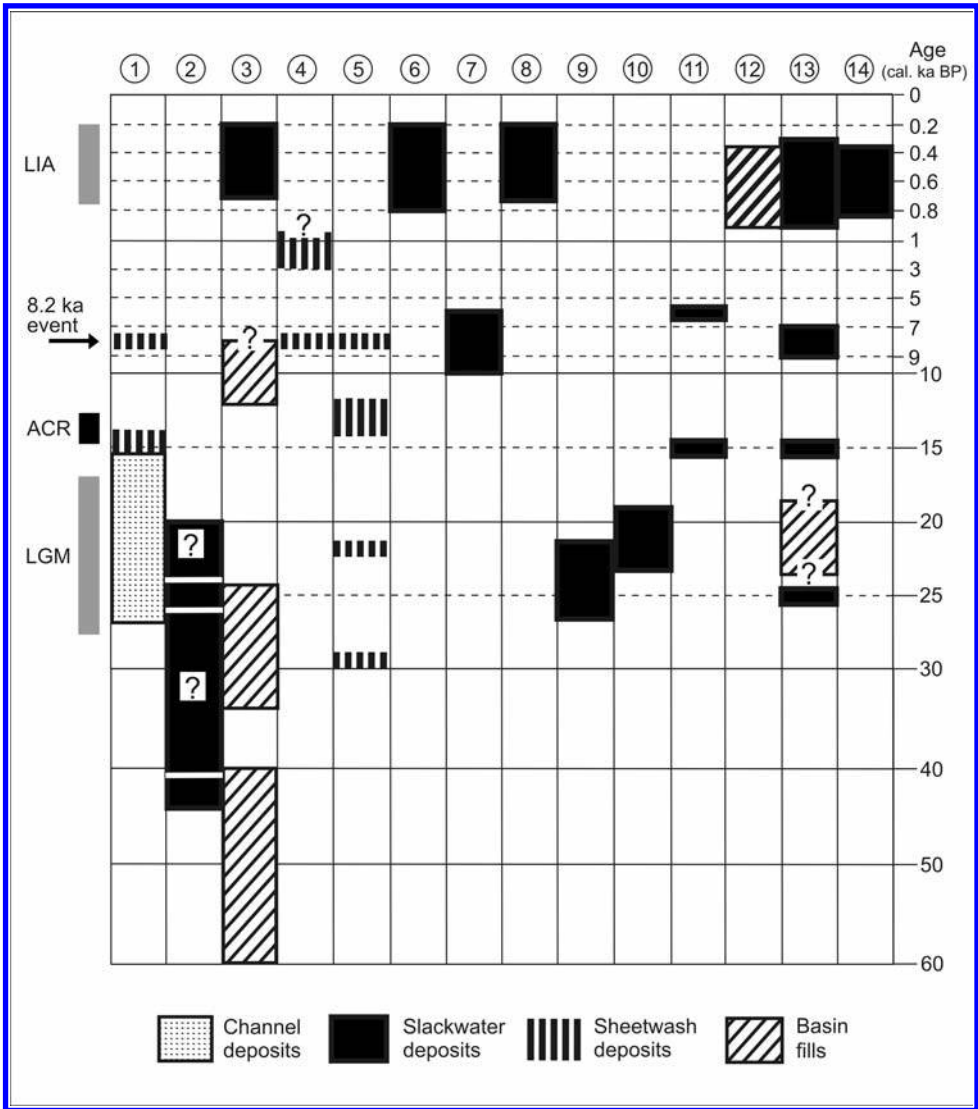


Figure 9. Ages for the Namib Desert flash flood deposits. The numbers (1 to 14) refer to different catchments. Authors, valleys and dating methods are mentioned. ^{14}C (and AMS ^{14}C) ages are given in ‘cal yr BP’. Note the different vertical scales. LIA, Little Ice Age; ACR, Antarctic Cold Reversal; LGM, Last Glacial Maximum. (After Heine and Völkel, 2009). 1, Srivastava *et al.* (2004): Khumib – OSL; 2, Srivastava *et al.* (2005): Hoarusib/Clay Castle Silts – OSL; 3, Eitel *et al.* (2006): Upper Hoanib/Basin fills – OSL; Heine (2004b): Upper Hoanib-Amspoort/SWD – ^{14}C ; Eitel *et al.* (2005): Amspoort Silts – OSL; 4, Brunotte and Sander (2000a, b): Opuwo area – TL; 5, Eitel and Zöller (1996): Aba Huab – TL; 6, Heine (2004b): Swakop-Khan/SWD – ^{14}C ; 7, Bourke *et al.* (2003): Kuiseb/Homeb Silts – OSL; 8, Leopold *et al.* (2006), Mizuno (2005): Kuiseb – ^{14}C ; 9, Vogel (1982): Kuiseb/Homeb Silts – ^{14}C ; 10, Eitel and Zöller (1996): Kuiseb/Homeb Silts – TL; 11, Srivastava *et al.* (2006): Kuiseb/Homeb Silts – OSL; 12, Heine (2004b): Namib surface – ^{14}C ; 13, Heine (1998): Tsauchab/Basin fills – ^{14}C ; Brook *et al.* (2006): Sossus Vlei – OSL; 14, Heine (unpubl.), Zawada (2000): Orange River/SWD – ^{14}C .

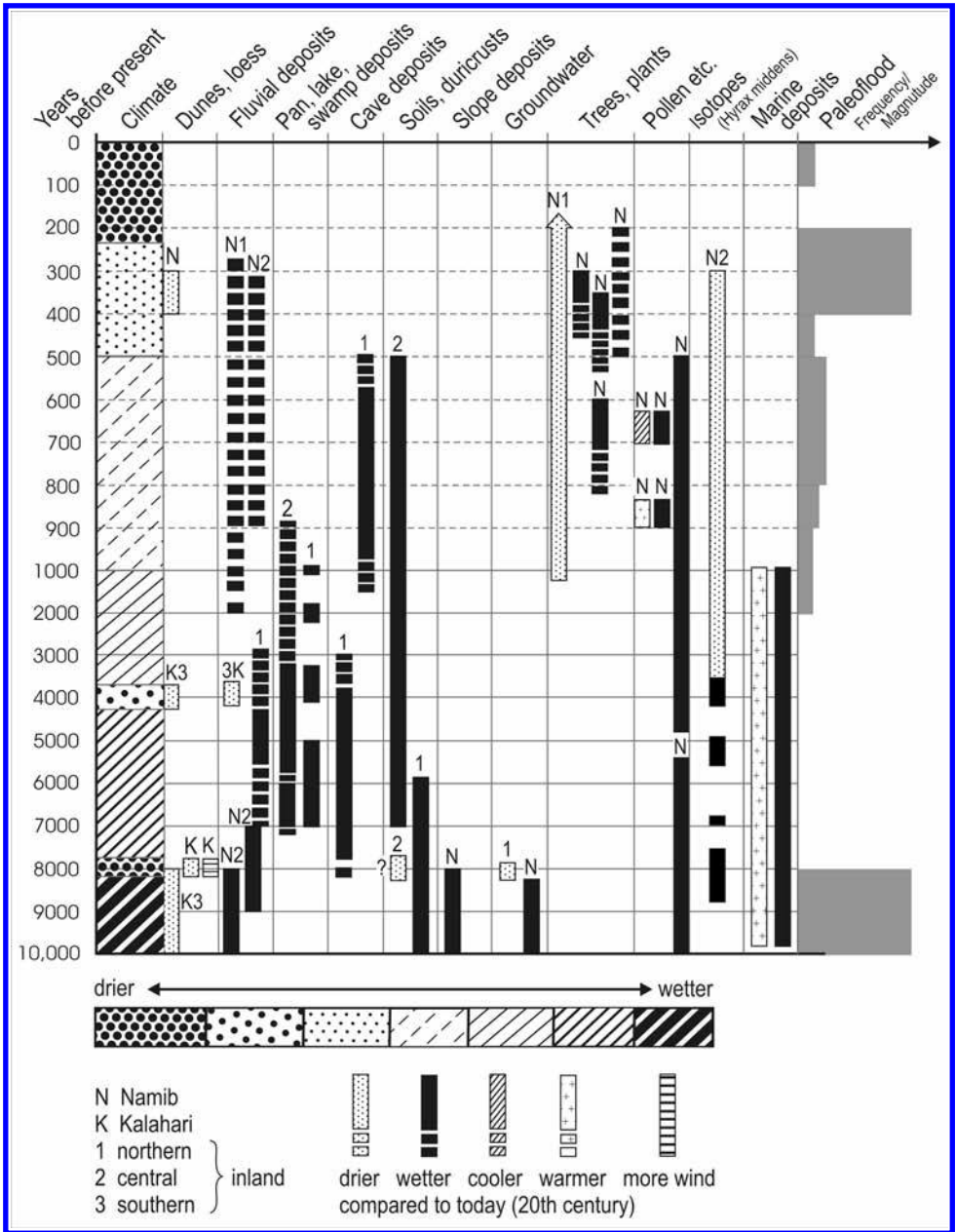


Figure 10. Summary of weighted evidence from different dated geoarchives for periods of increased and decreased moisture, phases with intensification of wind velocity, lowering of ground water table, soil formation phases etc. in Namibia (after Heine, 2005, supplemented).

ACKNOWLEDGEMENTS

The author thanks the German Science Foundation (DFG) for continuous support of his research in the Namib Desert. Research funding by the Japanese Ministry of Education, Science, Sports and Culture (Project No. 13371013) is also highly acknowledged. The author is grateful for the support, help and discussions of many persons during field and laboratory work and scientific meetings.

REFERENCES

- Ahnert, F., 1999, *Einführung in die Geomorphologie*, (Stuttgart: Eugen Ulmer).
- Altenbach, A. and Struck, U., 2006, Some remarks on Namibia's shelf environments, and a possible teleconnection to the Hinterland. In *The Changing Culture and Nature of Namibia: Case Studies*, edited by Leser, H., (Basel, Windhoek: Basler Afrika Bibliographien), pp. 109–124.
- Baker, V., 1983, Palaeoflood hydrology techniques for the extension of stream flow records. *Transportation Research Record (Transportation Research Board, Washington, D.C.)*, **922**, pp. 18–23.
- Baker, V., 1987, Palaeoflood hydrology and extraordinary flood events. *Journal of Hydrology*, **96**, pp. 79–99.
- Baker, V., 1989, Magnitude and Frequency of Palaeofloods. In *Floods: Hydrological, Sedimentological and Geomorphological Implications*, edited by Beven, K. and Carling, P., (Chichester: Wiley), pp. 171–183.
- Baker, V., 2003a, Palaeofloods and Extended Discharge Records. In *Palaeohydrology: Understanding Global Change*, edited by Gregory, K.J. and Benito, G., (Chichester: Wiley), pp. 307–323.
- Baker, V., 2003b, A bright future for old flows: origins, status and future of palaeoflood hydrology. In *Palaeofloods, Historical Floods and Climatic Variability: Applications in Flood Risk Assessment*, edited by Thorndycraft, V.R., Benito, G., Barriendos, M. and Llasat, M.C., (Barcelona: Proceedings of the PHEFRA Workshop, 16–19th October 2002), pp. 13–18.
- Baker, V.R., Ely, L.L., O'Connor, J.E. and Partridge, J.B., 1987, Palaeoflood hydrology and design applications. In *Regional Flood Frequency Analysis*, edited by Singh, V.P., (Dordrecht: Reidel), pp. 339–353.
- Baker, V.R., Kochel, R.C. and Patton, P.C., (eds.), 1988, *Flood Geomorphology*, (New York, Chichester: Wiley).
- Bao, H., Thiemens, M.H., Farquhar, J., Campbell, D.A., Chi-Woo Lee, C., Heine, K. and Loope, D.B., 2000, Anomalous ¹⁷O composition in massive sulphate deposits on the Earth. *Nature*, **406**, pp. 176–178.
- Bao, H., Thiemens, M.H. and Heine, K., 2001, Oxygen-17 excesses of the Central Namib gypcretes: spatial distribution. *Earth Planetary Science Letters*, **192**, pp. 125–135.
- Baumgartner, T.R., Struck, U. and Alheit, J., 2004, GLOBEC Investigation of Interdecadal to Multi-Centennial Variability in Marine Fish Populations. *PAGES Newsletter*, **12**(1), pp. 19–23.
- Benito, G., Botero, B.A., Thorndycraft, V.R., Rico, M.T., Sánchez Moya, Y., Sopena, A. and Pérez González, A., 2009, Palaeoflood records applied to estimate aquifer recharge in ephemeral rivers (Buffels River, Namaqualand, South Africa). In *GLOCOPH Israel 2009 (Oct 25—Nov 3, 2009), Program and Abstracts*, edited by

- Enzel, Y., Greenbaum, N. and Laskow, M., (Jerusalem: The Hebrew University of Jerusalem), p. 25.
- Blümel, W.-D., Hüser, K. and Eitel, B., 2000, Landschaftsveränderungen in der Namib. *Geographische Rundschau*, **52**, pp. 17–23.
- Bourke, M.C., Child, A. and Stokes, S., 2003, Optical age estimates for hyper-arid fluvial deposits at Homeb, Namibia. *Quaternary Science Reviews*, **22**, pp. 1099–1103.
- Brook, G.A., Srivastava, P. and Marais, E., 2006, Characteristics and OSL minimum ages of relict fluvial deposits near Sossus Vlei, Tsauchab River, Namibia, and a regional climate record for the last 30 ka. *Journal of Quaternary Science*, **21**, pp. 347–362.
- Brooks, A.P., Shellberg, J.G., Knight, J. and Spencer, J., 2009, Alluvial gully erosion: an example from the Mitchell fluvial megafan, Queensland, Australia. *Earth Surface Processes and Landforms*, **34**, pp. 1951–1969.
- Brunotte, E. and Sander, H., 2000a, Bodenerosion in lößartigen Sedimenten Nordnamibias (Becken von Opuwo) hervorgerufen durch Gullybildung und Mikropedimentation. *Zeitschrift für Geomorphologie, N.F.*, **44**, pp. 249–267.
- Brunotte, E. and Sander, H., 2000b, Loess accumulation and soil formation in Kaokoland (Northern Namibia) as indicators of Quaternary climatic change. *Global and Planetary Change*, **26**, pp. 67–75.
- Chase, B., 2009, Evaluating the use of dune sediments as a proxy for palaeo-aridity: A Southern African case study. *Earth-Science Reviews*, **93**, pp. 31–45.
- Chase, B.M. and Meadows, M.E., 2007, Late Quaternary dynamics of Southern Africa's winter rainfall zone. *Earth-Science Reviews*, **84**, pp. 103–138.
- Chase, B.M., Meadows, M.E., Scott, L., Thomas, D.S.G., Marais, E., Sealy, J. and Reimer, P.J., 2009, A record of rapid Holocene climate change preserved in hyrax middens from southwestern Africa. *Geology*, **37**, pp. 703–706.
- Compton, J.S. and Maake, L., 2007, Source of the suspended load of the upper Orange River, South Africa. *South African Journal of Geology*, **110**, pp. 339–348.
- Dollar, E.S.J., 1998, Palaeoflood geomorphology in Southern Africa: a review. *Progress in Physical Geography*, **22**, pp. 325–349.
- Eitel, B., Blümel, W.-D. and Hüser, K., 1999a, River silt terraces at the eastern margin of the Namib Desert (NW-Namibia): Genesis and palaeoclimatic evidence. *Zentralblatt für Geologie und Paläontologie, Teil I*, 1998, H. 5/6, pp. 243–254.
- Eitel, B., Blümel, W.-D., Hüser, K. and Zöller, L., 1999b, Dust and river silt terraces at the eastern margin of the Skeleton Coast Desert (northwestern Namibia): genetic relations and palaeoclimatic evidence. In *Loessfest '99. Loess: Characterization, Stratigraphy, Climate and Societal Significance*, edited by Derbyshire, E., (London: Centre for Quaternary Research (CQR), Royal Holloway University), pp. 56–59.
- Eitel, B., Blümel, W.-D., and Hüser, K., 2000, The Early to Mid-Holocene Climatic Change in Southwestern Africa: Evidence from dunes, loess-like deposits and soils based on TL and OSL-data. In *Environmental Changes During the Holocene*, edited by Diaz del Olmo, F., Faust, D. and Porras, A.I., (Seville, Spain: INQUA Commission on the Holocene Meeting 27–31 March 2000), pp. 41–43.
- Eitel, B., Blümel, W.-D., Hüser, K. and Mauz, B., 2001, Dust and loessic alluvial deposits in northwestern Namibia (Damaraland, Kaokoveld): sedimentology and palaeoclimatic evidence based on luminescence data. *Quaternary International*, **76/77**, pp. 57–65.
- Eitel, B., Blümel, W.-D., and Hüser, K., 2002, Environmental transition between 22 ka and 8 ka in monsoonally influenced Namibia—A preliminary chronology. *Zeitschrift für Geomorphologie, NF*, **126**, pp. 31–57.

- Eitel, B., Blümel, W.-D., and Hüser, K., 2004, Palaeoenvironmental Transition Between 22 ka and 8 ka in Monsoonally Influenced Namibia. In *Palaeoecology of Quaternary Drylands*, edited by Smykatz-Kloss, W. and Felix-Henningsen, P., (Berlin, Heidelberg etc.: Springer), pp. 167–194.
- Eitel, B., Kadereit, A., Blümel, W.-D., Hüser, K. and Kromer, B., 2005, The Amspoort Silts, northern Namib desert (Namibia): formation, age and palaeoclimatic evidence of river-end deposits. *Geomorphology*, **64**, pp. 299–314.
- Eitel, B., Kadereit, A., Blümel, W.-D., Hüser, K., Lomax, J. and Hilgers, A., 2006, Environmental changes at the eastern Namib Desert margin before and after the Last Glacial Maximum: New evidence from fluvial deposits in the upper Hoanib River catchment, northwestern Namibia. *Palaeogeography, Palaeoclimatology, Palaeoecology*, **234**, pp. 201–222.
- Eitel, B. and Zöller, L., 1996, Soils and Sediments in the Basin of Dieprivier-Uitskot (Khorixas District, Namibia): Age, geomorphic and sedimentological investigation, palaeoclimatic interpretation. *Palaeoecology of Africa*, **24**, pp. 159–172.
- Ellerbrock, R., 2000, Carbonatgehalt in Boden und Wasser. In *Arbeitsmethoden in Physiogeographie und Geoökologie*, edited by Barsch, H., Billwitz, K. and Bork, H.-R., (Gotha: Perthes), pp. 328–332.
- Ely, L.L. and Baker, V.R., 1985, Reconstructing palaeoflood hydrology with slackwater deposits: Verde River, Arizona. *Physical Geography*, **5**, pp. 103–126.
- Frings, R.M., 2008, Downstream fining in large sand-bed rivers. *Earth-Science Reviews*, **87**, pp. 39–60.
- Gasse, F., Chalié, F., Vincens, A., Williams, M.A.J. and Williamson, D., 2008, Climatic patterns in equatorial and Southern Africa from 30,000 to 10,000 years ago reconstructed from terrestrial and near-shore proxy data. *Quaternary Science Reviews*, **27**, pp. 2316–2340.
- Goudie, A., 1972, Climate, weathering, crust formation, dunes and fluvial features of the Central Namib Desert, near Gobabeb, South West Africa. *Madoqua*, **II**(54–64), pp. 15–31.
- Greenbaum, N., Schick, A.P. and Baker, V.R., 2000, The palaeoflood record of a hyperarid catchment, Nahal Zin, Negev Desert, Israel. *Earth Surface Processes and Landforms*, **25**, pp. 951–971.
- Haberlah, D., 2007, A call for Australian loess. *Area*, **39**(2), pp. 224–229.
- Haberlah, D., 2009, *Loess and floods: Late Pleistocene fine-grained valley-fill deposits in the Flinders Ranges, South Australia*. (Adelaide: PhD Thesis, Faculty of Science, The University of Adelaide, Australia), pp. 1–317.
- Hassan, M.A., Schick, A.P. and Shaw, P.A., 1999, The transport of gravel in an ephemeral sandbed river. *Earth Surface Processes and Landforms*, **24**, pp. 623–640.
- Heine, K., 1981, Aride und pluviale Bedingungen während der letzten Kaltzeit in der Südwest-Kalahari (südliches Afrika). Ein Beitrag zur klimagenetischen Geomorphologie der Dünen, Pfannen und Täler. *Zeitschrift für Geomorphologie, N.F., Supplement vol.*, **38**, pp. 1–37.
- Heine, K., 1998a, Neue Ergebnisse der Paläoklimaforschung in den Tropen und Subtropen (Lateinamerika, südliches Afrika). In *Globaler Wandel – Welterbe. HGG-Journal*, **13**, edited by Karrasch, H., Gamerith, W., Schwan, T., Sachs, K. and Krause, U., (Heidelberg: Heidelberger geographische Gesellschaft), pp. 19–44.
- Heine, K., 1998b, Climate change over the past 135,000 years in the Namib Desert (Namibia) derived from proxy data. *Palaeoecology of Africa*, **25**, pp. 171–198.
- Heine, K., 2002, Sahara and Namib/Kalahari during the Late Quaternary—inter-hemispheric contrasts and comparisons. *Zeitschrift für Geomorphologie, N.F., Supplement vol.*, **126**, pp. 1–29.

- Heine, K., 2004a, Flood Reconstructions in the Namib Desert, Namibia and Little Ice Age Climatic Implications: Evidence from Slackwater Deposits and Desert Soil Sequences.—*Journal of the Geological Society of India*, **64**, pp. 535–547.
- Heine, K., 2004b, Little Ice Age climatic fluctuations in the Namib Desert, Namibia, and adjacent areas: evidence of exceptionally large floods from slack water deposits and desert soil sequences. In *Palaeoecology of Quaternary Drylands, Lecture Notes of Earth Sciences*, **102**, edited by Smykatz-Kloss, W. and Felix-Henningsen, P. (Berlin, Heidelberg: Springer), pp. 137–165.
- Heine, K., 2005, Holocene Climate of Namibia: a Review Based on Geoarchives. *African Study Monographs, Supplement, Kyoto*, **30**, pp. 119–133.
- Heine, K. and Heine, J.T., 2002, A palaeohydrologic reinterpretation of the Homeb Silts, Kuiseb River, central Namib Desert (Namibia) and palaeoclimatic implications. *Catena*, **48**, pp. 107–130.
- Heine, K., Heine, C. and Kühn, T., 2000, Slackwater Deposits der Namib-Wüste (Namibia) und ihr paläoklimatischer Aussagewert. *Zentralblatt für Geologie und Paläontologie, Teil I*, 1999, Heft 5/6, pp. 587–613.
- Heine, K. and Völkel, J., 2009, Desert flash flood series—Slackwater deposits and floodouts in Namibia: their significance for palaeoclimatic reconstructions. *Zentralblatt für Geologie und Paläontologie, Teil I*, 2007, Heft 3/4, pp. 287–308.
- Heine, K. and Völkel, J., 2010, Soil clay minerals in Namibia and their significance for the terrestrial and marine past global change research. *African Study Monographs, Supplement, Kyoto*, **40**, pp. 15–34.
- Heine, K. and Walter, R., 1996, Gypcretes of the central Namib Desert (Namibia). *Palaeoecology of Africa*, **24**, pp. 173–201.
- Herbert, C.T. and Compton, J.S., 2007, Geochronology of Holocene sediments on the western margin of South Africa. *South African Journal of Geology*, **110**, pp. 327–338.
- Hövermann, J., 1978, Formen und Formung in der Pränamib (Flächen-Namib). *Zeitschrift für Geomorphologie, N.F.*, **30**, pp. 55–73.
- Hüser, K., Besler, H., Blümel, W.-D., Heine, K., Leser, H. and Rust, U., 2001, *Namibia. Bilder seiner Landschaften geographisch kommentiert*, (Göttingen, Windhoek: Hess).
- Hüser, K., Blümel, W.-D. and Eitel, B., 1998, Geomorphologische Untersuchungen an Rivierterrassen im Mündungsbereich des Uniab (Skelettküste/NW-Namibia). *Zentralblatt für Geologie und Paläontologie, Teil I*, 1997, Heft 1/2, pp. 243–254.
- Jacobson, P.J., Jacobson, K.M. and Seely, M., 1995, *Ephemeral Rivers and their Catchments. Sustaining People and Development in Western Namibia*, (Desert Research Foundation of Namibia [DRFN]: Windhoek).
- Kale, V.S., Singhvi, A.K., Mishra, P.K. and Banerjee, D., 2000, Sedimentary records and luminescence chronology of Late Holocene palaeofloods in the Luni River, Thar Desert, northwest India. *Catena*, **40**, pp. 337–358.
- Klarl, H., 1999, *Die Homeb-Silte im Kuiseb-Tal, zentrale Namib, Namibia: Untersuchungen zur Genese und paläoklimatischen Interpretation*, (Regensburg: Unpublished M.A. Thesis, Institute of Geography, University of Regensburg), 97 p.
- Knighton, A.D. and Nanson, G.C., 2002, Inbank and overbank velocity conditions in an arid zone anastomosing river. *Hydrological Proceedings*, **16**, pp. 1771–1791.
- Kochel, R.C. and Baker, V.R., 1982, Palaeoflood hydrology. *Science*, **215**, pp. 353–361.
- Kochel, R.C. and Baker, V.R., 1988, Palaeoflood analysis using slackwater deposits. In *Flood Geomorphology*, edited by Baker, V.R., Kochel, R.C. and Patton, P.C., (New York: Wiley), pp. 357–376.

- Korn, H. and Martin, H., 1957, The Pleistocene in South West Africa. In *Proc. 3rd Pan-African Congress Prehistory, Livingstone*, edited by Clarke, D.J. and Cole, S., (London: Chatto and Windus), pp. 14–22.
- Krapf, C.B.E., Stollhofen, H. and Stanistreet, I.G., 2003, Contrasting styles of ephemeral river systems and their interaction with dunes of the Sceleton Coast erg (Namibia). *Quaternary International*, **104**, pp. 41–52.
- Laronne, J.B. and Shlomi, Y., 2007, Depositional character and preservation potential of coarse-grained sediments deposited by flood events in hyper-arid braided channels in the Rift Valley, Arava, Israel. *Sedimentary Geology*, **195**, pp. 21–37.
- Leopold, M., Völkel, J. and Heine, K., 2006, A ground-penetrating radar survey of Late Holocene fluvial sediments in NW Namibian river valleys: characterization and comparison. *Journal of the Geological Society of London*, **163**, pp. 923–936.
- Leser, H., 2000, Methodische Probleme sedimentologischer Untersuchungen pleistozäner Sedimente im Kaokoveld (Namibia). *Regensburger geographische Schriften*, **33**, pp. 19–36.
- Marker, M.E., 1977, Aspects of the geomorphology of the Kuiseb River, South West Africa. *Madoqua*, **10**(3), pp. 199–206.
- Marker, M.E. and Müller, D., 1978, Relict vlei silts of the middle Kuiseb River valley, South West Africa. *Madoqua*, **11**(2), pp. 151–162.
- Martin, H., 1950, Südwestafrika. *Geologische Rundschau*, **38**, pp. 6–14.
- Mendelsohn, J., Jarvis, A., Roberts, C. and Robertson, T., 2002, *Atlas of Namibia. A Portrait of the Land and its People*, (David Philip: Cape Town).
- Miall, A.D., 1985, Architectural-element analysis: a new method of facies analysis applied to fluvial deposits. *Earth Science Reviews*, **22**, pp. 261–308.
- Mizuno, K., 2005, Environmental changes in relation to tree death along the Kuiseb River in the Namib Desert. *African Studies Monographs, Supplement*, **30**, pp. 27–41.
- Nash, D.J., 1999, Arid geomorphology. *Progress in Physical Geography*, **23**, pp. 429–439.
- Ollier, C.D., 1977, Outline geological and geomorphological history of the Central Namib Desert. *Madoqua*, **10**(3), pp. 207–212.
- Partridge, T.C., 1993, The evidence for Cainozoic aridification in Southern Africa. *Quaternary International*, **17**, pp. 105–110.
- Pickup, G., 1989, Palaeoflood Hydrology and Estimation of the Magnitude, Frequency and Areal Extent of Extreme Floods—An Australian Perspective. *Civil Engineering Transactions, I.E. Australia*, vol. **CE 34**, pp. 19–29.
- Pradeep, S., Brook, G.A. and Marais, E., 2004, A record of fluvial aggradation in the northern Namib Desert during the Late Quaternary. *Zeitschrift für Geomorphologie, Supplement*, **133**, pp. 1–18.
- Reineck, H.-E. and Singh, I.B., 1980, *Depositional Sedimentary Environments. With Reference to Terrigenous Clastics*, (Berlin, Heidelberg, New York: Springer).
- Rust, U., 1987, Geomorphologische Forschungen im südwestafrikanischen Kaokoveld zum angeblichen vollariden quartären Kernraum der Namibwüste. *Erdkunde*, **41**, pp. 118–133.
- Rust, U., 1989a, (Palão)-Klima und Relief: Das Reliefgefüge der südwestafrikanischen Namibwüste (Kunene bis 27°s. Br.). *Münchner geographische Abhandlungen*, **7**, pp. 1–158.
- Rust, U., 1989b, Grundsätzliches über Flußterrassen als paläoklimatische Zeugen in der südwestafrikanischen Namibwüste. *Palaeoecology of Africa*, **20**, pp. 119–132.
- Rust, U., 1999, River-end deposits along the Hoanib-River, northern Namib: archives of Late Holocene climatic variation on a subregional scale. *South African Journal of Science*, **95**, pp. 205–208.

- Rust, U. and Vogel, J.C., 1988, Late Quaternary environmental changes in the northern Namib Desert as evidenced by fluvial landforms. *Palaeoecology of Africa*, **19**, pp. 127–137.
- Rust, U. and Wieneke, F., 1974, Studies on gramadulla formation in the middle part of the Kuiseb River, South West Africa. *Madoqua*, **II** (3), pp. 5–15.
- Rust, U. and Wieneke, F., 1980, A reinvestigation of some aspects of the evolution of the Kuiseb River valley upstream of Gobabeb, South West Africa. *Madoqua*, **12**(3), pp. 163–173.
- Scholz, H., 1972, The soils of the central Namib Desert with special consideration of the soils in the vicinity of Gobabeb. *Madoqua*, **II**–1(54–62), pp. 33–51.
- Smith, A.M., 1992a, Holocene palaeoclimatic trends from palaeoflood analysis. *Palaeogeography, Palaeoclimatology, Palaeoecology*, **97**, pp. 235–240.
- Smith, A.M., 1992b, Palaeoflood hydrology of the lower Umgeni River from a reach south of the Inanda Dam, Natal. *South African Geographical Journal*, **74**, pp. 63–68.
- Smith, J.J., Hasiotis, S.T., Kraus, M.J. and Woody, D.T., 2008, Relationship of floodplain ichnocoenoses to palaeopedology, palaeohydrology, and palaeoclimate in the Willwood Formation, Wyoming, during the Palaeocene-Eocene Thermal Maximum. *Palaios*, **23**, pp. 683–699.
- Smith, R.M.H., Mason, T.R. and Ward, J.D., 1993, Flash-flood sediments and ichnofacies of the Late Pleistocene Homeb Silts, Kuiseb River, Namibia. *Sedimentary Geology*, **85**, pp. 579–599.
- Srivastava, P., Brook, G.A. and Marais, E., 2004, A record of fluvial aggradation in the northern Namib Desert during the Late Quaternary. *Zeitschrift für Geomorphologie, N.F.*, **133**, pp. 1–18.
- Srivastava, P., Brook, G.A. and Marais, E., 2005, Depositional environment and luminescence chronology of the Hoarusib River Clay Castles sediments, northern Namib Desert, Namibia. *Catena*, **59**, pp. 187–204.
- Srivastava, P., Brook, G.A., Marais, E., Morthekai, P. and Singhvi, A.K., 2006, Depositional environment and OSL chronology of the Homeb silt deposits, Kuiseb River, Namibia. *Quaternary Research*, **65**, pp. 478–491.
- Stanistreet, I.G. and Stollhofen, H., 2002, Hoanib River flood deposits of Namib Desert interdunes as analogues for thin permeability barrier mudstone layers in aeolian reservoir. *Sedimentology*, **49**, pp. 719–736.
- Struck, U. and Altenbach, A., 2006, Palaeoclimatological investigations in upwelling sediments off Namibia. In *The Changing Culture and Nature of Namibia: Case Studies*, edited by Leser, H., (Basel, Windhoek: Basler Afrika Bibliographien), pp. 165–169.
- Svendsen, J., Stollhofen, H., Krapf, C.B.E. and Stanistreet, I.G., 2003, Mass and hyperconcentrated flow deposits record, dune damming and catastrophic breakthrough of ephemeral rivers, Skeleton Coast Erg, Namibia. *Sedimentary Geology*, **160**, pp. 7–31.
- Tooth, S., 1999, Floodouts in Central Australia. In *Varieties in Fluvial Forms*, edited by Miller, A.J. and Gupta, A., (Chichester: Wiley), pp. 219–247.
- Tooth, S., 2009, Arid geomorphology: emerging research themes and new frontiers. *Progress in Physical Geography*, **33**(2), pp. 251–287.
- Vogel, J.C., 1982, The age of the Kuiseb River silt terrace at Homeb. *Palaeoecology of Africa*, **15**, pp. 201–209.
- Vogel, J.C., 1989, Evidence of past climatic change in the Namib Desert. *Palaeogeography, Palaeoclimatology, Palaeoecology*, **70**, pp. 355–364.
- Vogel, J.C. and Rust, U., 1987, Environmental changes in the Kaokoland Namib Desert during the present millennium. *Madoqua*, **15**(1), pp. 5–16.

- Vogel, J.C. and Rust, U., 1990, Ein in der Kleinen Eiszeit (Little Ice Age) begrabener Wald in der nördlichen Namib. *Berliner geographische Studien*, **30**, pp. 15–34.
- Völkel, J., Leopold, M. and Heine, K., 2006, Studying fluvial sediments using Ground Penetrating Radar—a case study from Namibia. In *The Changing Culture and Nature of Namibia: Case Studies*, edited by Leser, H., (Basel, Windhoek: Basler Afrika Bibliographien), pp. 153–157.
- Ward, J.D., 1987, The Cenozoic succession in the Kuiseb Valley, central Namib Desert. *Geological Survey of SWA/Namibia, Memoir*, **9**, pp. 1–124.
- Ward, J.D., 1988, On the interpretation of the Oswater Conglomerate Formation, Kuiseb Valley, Namib Desert. *Palaeoecology of Africa*, **19**, pp. 119–125.
- Wartbichler, S., 1998, *Untersuchungen zur Ausprägung und Mächtigkeit von Gipskrusten in Abhängigkeit vom Relief, in einem ausgewählten, begrenzten Areal bei Gobabeb in der zentralen Namib, Namibia*. (Regensburg: Unpublished M.A. Thesis, Institute of Geography, University of Regensburg), 113 p.
- Zawada, P.K., 1995, Palaeoflood hydrology of South African Rivers: evidence for Holocene catastrophic flooding in the Lower Orange River valley. *Terra Nostra, (INQUA Abstracts)*, **2/95**, p. 310.
- Zawada, P.K., 1997, Palaeoflood hydrology: method and application on flood-prone Southern Africa. *South African Journal Science*, **93**, pp. 111–132.
- Zawada, P.K., 2000, Slackwater Sediments and Palaeofloods. Their significance for Holocene Palaeoclimatic Reconstruction and Flood Prediction. In *The Cenozoic of Southern Africa*, edited by Partridge, T.C. and Maud, R.R., (New York: Oxford Univ. Press), pp. 219–247.

CHAPTER 4

A sedimentary record of environmental change at Tsodilo Hills White Paintings Rock Shelter, Northwest Kalahari Desert, Botswana

Andrew H. Ivester

Department of Geosciences, University of West Georgia, Carrollton, GA, USA

George A. Brook

Department of Geography, University of Georgia, Athens, GA, USA

Lawrence H. Robbins

Department of Anthropology, Michigan State University, East Lansing, MI, USA

Alec C. Campbell

Crocodile Pools, Gaborone, Botswana

Michael L. Murphy

Kalamazoo Valley Community College, Kalamazoo, MI, USA

Eugene Marais

National Museum of Namibia, Windhoek, Namibia

ABSTRACT: New optically stimulated luminescence ages, in combination with detailed analysis of sediment from White Paintings rock shelter provide a basis for reconstructing palaeoenvironment and site formation processes at the longest archaeological sequence in the Kalahari. The new data resolve previous ambiguities related to the site's chronology. A series of soil stratigraphic units documents changing conditions at the site over the past 100/120 ka. Millennial-scale periods of increased moisture availability, occupation intensity, and landscape stability alternate with periods characterized by more arid conditions, aeolian sedimentation, and lower site occupation intensity. Broader trends in the sediment data suggest a general transition from greater moisture availability in the Pleistocene and Early to Mid Holocene toward more arid conditions in the Late Holocene. Wetter climates occurred at the time of Heinrich events in the North Atlantic due to slowing or cessation of the North Atlantic Deep Water flow (NADW) that resulted in warming of Southern Hemisphere oceans and the associated weakening of the South Atlantic and South African anticyclones.

4.1 INTRODUCTION

4.1.1 Background

White Paintings shelter in the Tsodilo Hills of Northwestern Botswana (Figure 1) has been the site of intense archaeological investigations and is notable for the depth and age-span of its archaeological record (Robbins *et al.*, 2000). The sequence includes Historic through Middle Stone Age cultural materials, extending to a depth of 7 meters, and to an age of around 100/120 ka. The sequence features some of the earliest evidence for fresh water fishing, ornament production, and other activities in the Kalahari and in Southern Africa. The sedimentary record of the site is valuable in suggesting distinct variations in local palaeoenvironment. However, problems with the site's chronology have obfuscated interpretation of portions of the archaeological and sedimentary record. In an effort to resolve some of the dating issues nine additional samples were collected from a single vertical profile for optically stimulated luminescence (OSL) analysis. Here we present new dates and a clarified chronology for the site. We also examine selected physical and chemical properties of the sedimentary units at the site in order to reconstruct site formation processes and temporal changes in environmental conditions.

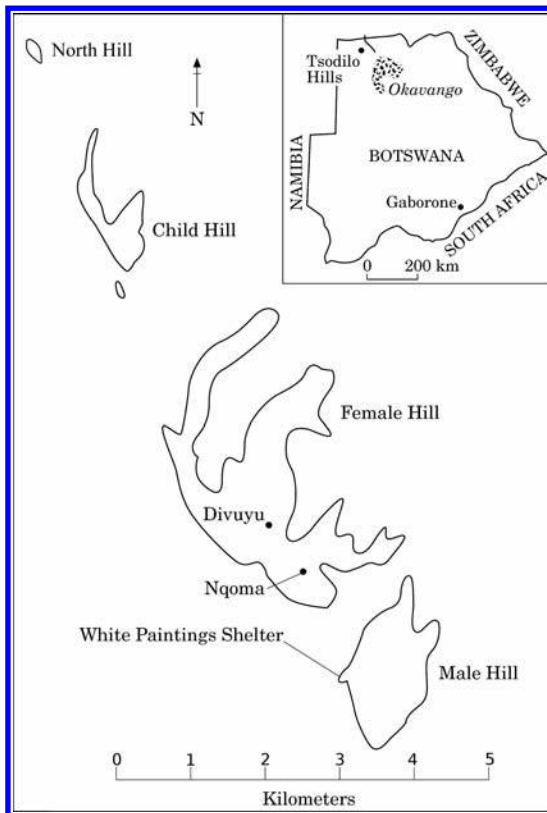


Figure 1. Location of White Paintings rock shelter in Tsodilo Hills, Northwestern Botswana (modified from Robbins *et al.*, 2000).

4.1.2 Study Area

The Tsodilo Hills (21°45'E, 18°45'S) are composed of four outcrops of Upper Proterozoic Damara Sequence micaceous schists, quartzite, and dolomitic marble, metamorphosed to varying extents (Figure 2). The highest, Male Hill, peaks at 1.394 m asl, with a relief of 410 m from base to top. Relict linear dunes surrounding Tsodilo are up to 25 m high and spaced apart by 1 to 2.5 km; they have been active periodically during the last 100 ka (Thomas *et al.*, 2003). Dune crests and slopes are covered by an open savanna with trees and shrubs, while interdune swales support a grass and scrub vegetation. An east-southeasterly dune-forming wind deposited sand against the east side of the hills, leaving a sand shadow extending 40 km to the West.

Immediately west of Male Hill there is a sheet of lacustrine carbonate that is overlain by a few centimeters of sandy soil. The carbonate contains gastropods and freshwater diatoms, indicating the former existence of a lake that reached a maximum extent of around 8 × 5 km. Radiocarbon ages indicate standing water in this lake from 36–22, 26,5–22,5, and 19–11 ka (Brook, 1998; Robbins *et al.*, 2000; Thomas *et al.*, 2003). Today the nearest permanent body of water is the Okavango River, 45 km to the East.

White Paintings rock shelter is located beneath a large outcrop of bedrock projecting from the western base of Male Hill. The shelter is named after the many calcareous-pigmented paintings covering the shelter wall, the most prominent of which is a large white elephant. The shelter's drip line lies around six meters from the base of the shelter wall. Today, the main sources of sediment to the shelter are aeolian sands, colluvial materials from the adjacent hill, and detrital material from the shelter wall and ceiling. About one meter to the right of the elephant painting there is a near-vertical joint in the shelter wall that is stained dark and presumably acts as a seepage point for flowing water. Exfoliation is more noticeable along this joint. Sediment of the shelter floor consists of gray sands, scattered schist granules and schist pebble fragments, some of them more than 0,5 cm in diameter, and large pieces of charcoal.

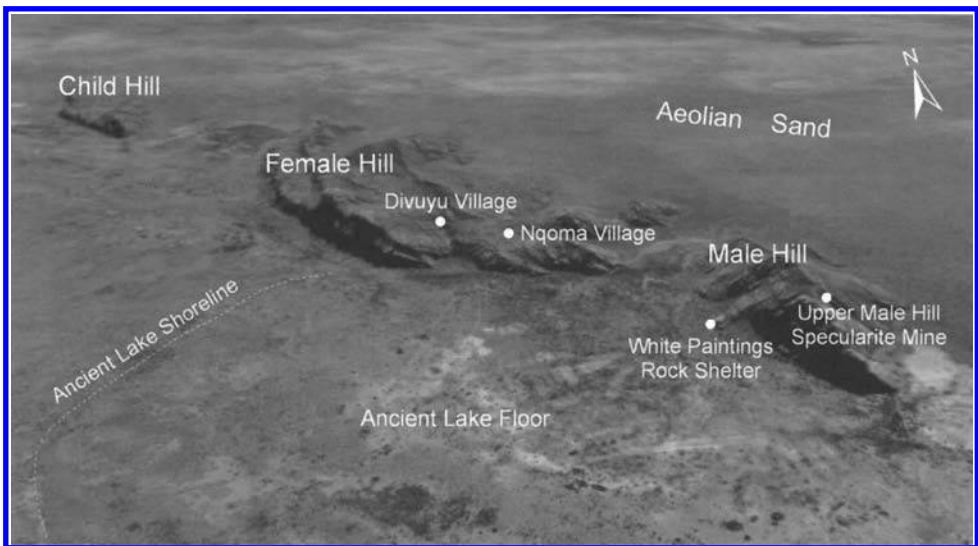


Figure 2. Oblique view of the Tsodilo Hills showing the location of White Paintings Shelter on the western side of Male Hill (annotated Google Earth image).

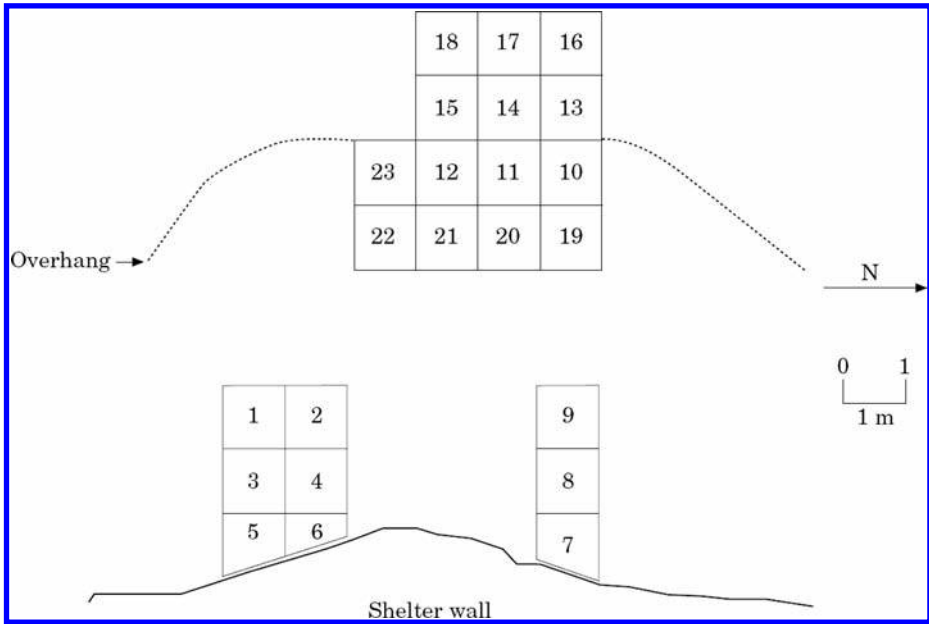


Figure 3. Map showing the locations of squares excavated at White Paintings. Sediment samples were collected from the south wall of Square 12 for depths 0–547,5 cm and from the south wall of Square 23 for depths 547,5 to 705 cm. OSL samples were collected from the south wall of Square 23 (modified from Robbins *et al.*, 2000).

4.1.3 Chronology

The chronology of strata at White Paintings has been somewhat problematic (Robbins *et al.*, 2000). A wide variety of materials and methods have previously been employed in dating the site with mixed results. Several radiocarbon dates on ostrich eggshell have ages that are older than expected given the associated diagnostic artefact assemblages. Existing age determinations for the Lower Fish deposits, for example, suggest an age of ca. 48 ka, although there is no evidence for a lake at Tsodilo at that time, and these deposits contain LSA assemblages that typically date to <39 ka in Southern Africa (Robbins *et al.*, 2000). The lack of a rigorous chronology has hampered important archaeological interpretations at the site such as the timing of the early use of bone harpoon points, ostrich eggshell for beads and other uses, and the timing of other cultural transitions reflected in changing tool assemblages. The sedimentary record of palaeoenvironmental changes has also suffered from a lack of a reliable chronological framework.

There are several reasons for the dating difficulties at the site. The sandy nature of the matrix allows post-depositional mobility of cultural and datable materials. Refits of broken ceramics and bone points document maximum vertical displacements on the order of 20–30 cm. In some places the sedimentary matrix is less disturbed. Articulated fish vertebrae were found to be intact at 250 cm depth (Robbins *et al.*, 2000). The matrix can therefore be considered as a mosaic, with some regions intact since deposition and others disturbed, to a greater or lesser extent, by pedoturbative processes. A discontinuity in sedimentation at around 1 m depth, for example, is marked by a sloped surface between the younger and older sediments. The dip of the

buried surface, combined with the long duration of its exposure and the intensity of occupation allowed older materials to move laterally into younger sedimentary units. The presence of humans at the site throughout the late Quaternary introduces the possibility of many activities that might introduce older materials into younger strata or vice versa. Elsewhere, intact, laterally extensive schist fall horizons indicate little post-depositional mobility.

Other limitations to the efficacy of radiocarbon dating this site are associated with age range limitations. The lower half of the excavation is beyond the effective range of radiocarbon dating (ca. 40 ka). Many of the dates produced from ostrich eggshell at the site are near this limit, in the range of 30–40 ka. Some of these should be considered minimum age estimates, and might explain why some of the dates appear younger than the apparent age of their surrounding matrix. The net effect is that some radiocarbon dates on small pieces of charred material, bone fragments, or ostrich eggshell are unreliable for dating the depositional age of their sedimentary matrix.

Optically stimulated luminescence dating avoids some of the problems with radiocarbon by providing a direct age for burial. Initial success with OSL ages from samples at 120, 250, and 440 cm (Feathers, 1997) prompted the collection of nine additional OSL samples in an attempt to resolve remaining chronological ambiguities. The samples were collected from a single vertical profile (the south face of square 23), so as to be directly related to the continuous column of sediment samples.

4.2 METHODS

4.2.1 Luminescence dating methods

Samples were collected for OSL dating by hammering an opaque plastic pipe horizontally into the vertical face of the exposure. In dating, a 4 mm-diameter aliquot size was used and the central aliquot age was taken as the best estimate of the true age of the sample.

Sample preparation and handling for OSL dating was carried out in the laboratory under controlled red-light conditions. Five centimeters of sediment was removed from each end of the PVC sample tubes for dose rate estimation. Luminescence measurements were made on the central section of the sediment cylinder that was least likely to have been exposed to sunlight during sampling.

Core sediments for OSL analysis were washed with water and then treated with 10% HCl and 30% H₂O₂ to remove carbonates and organic material. Sieving isolated the 120–150 µm-size fraction and then density separation using Na-Polytungstate ($\rho = 2.58 \text{ g/cm}^3$) was used to separate quartz from feldspar minerals. The quartz fraction was etched with 48% HF for 80 min followed by 36% HCl for 40 min to remove the alpha skin. Quartz grains were mounted on stainless steel discs with the help of *Silkospray*TM. Light stimulation of quartz mineral extracts was undertaken with a RISØ array of combined blue LEDs centered at 470 nm. Detection optics comprised two Hoya 2,5 mm thick U340 filters and a 3 mm thick Schott GG420 filter coupled to an EMI 9635 QA photomultiplier tube. Measurements were taken with a RISØ TL-DA-15 reader. A 25-mCi ⁹⁰Sr/⁹⁰Y built-in source was used for sample irradiation. A thick source Daybreak alpha counting system was used to estimate U and Th for dose rate calculation. Potassium was measured by ICP90, with a detection limit of 0,01%, using the sodium peroxide fusion technique at the SGS Laboratory in Toronto, Canada. The cosmic-ray dose was estimated for each sample as a function of depth and altitude following Prescott and Hutton (1994).

The SAR protocol (Murray and Wintle, 2000) was used to determine palaeodose. Fifteen 4 mm diameter aliquots from each sample were analyzed. A five-point regenerative dose strategy was adopted with three dose points to bracket the palaeodose, a fourth zero dose to test for recuperation effects, and a fifth repeat dose, usually of the smallest regenerative dose. The OSL response to the repeat dose was measured to monitor whether the sensitivity change correction incorporated in the SAR protocol was successful. All measurements were made at 125°C for 100 s after a pre-heat to 220°C for 60 s. For all aliquots the recycling ratio between the first and fifth point ranged within 0,95–1,05. Data were analyzed using the ANALYST program of Duller (1999).

4.2.2 Granulometric methods

In the field a continuous column was sampled at 7,5 cm intervals from excavation squares 12 and 23, underneath the drip line, for a total of 94 samples. Sediment samples were collected from the south wall of square 12 to a depth of 547,5 cm, and continued on the south wall of square 23 for depths from 547,5 to 705 cm. OSL samples were taken from the south wall of square 23. The 1-meter horizontal offset in the sediment column meant that small adjustments in depths were required to synchronize the OSL and sediment samples in a few sedimentary zones where the strata are slightly inclined. Additional samples from the slope of Male Hill and from dunes to the south were also collected for comparison.

A 60 g subsample was pretreated for granulometric analyses. Macro-organic material was removed by hand and the samples oven-dried overnight and weighed after cooling for 30 minutes. Gravel was removed using a 2 mm sieve. Each sample was treated with 0,5 N HCl to remove carbonates following Jackson (1969) and the mass loss used as a measure of carbonate content. Samples above 142,5 cm were treated with hydrogen peroxide to remove organics following the method of Janitzky (1986). Treatment was not necessary for deeper samples which contained no significant amounts of organic material.

Each sample was placed in a 400 ml fleaker with 200 ml of distilled water and 25 ml of hexametaphosphate solution (50 g/l) and dispersed on a shaker table for at least 8 hours. The dispersed samples were wet sieved over a 62,5 µm sieve. The sand fraction was dried and sieved at half phi intervals from -1 to 4 phi on a mechanical shaker for 5 minutes. Silt and clay fractions were determined at 16 µm and 2 µm by pipette as described in Gee and Bauder (1986). Gravel was pretreated with HCl to remove precipitated carbonate and to disassociate any gravel fragments cemented together. Gravels were sieved over a 2 mm screen and weighed. Clasts more than 3 cm long were weighed separately as cobbles. Grain size statistics were calculated using mathematical moments.

4.2.3 Geochemical methods

Geochemical analysis was done on alternate samples (at 15 cm intervals) to help identify sediment provenance and to provide evidence of post-depositional alteration. An acid extraction was performed as described in Van Loon and Barefoot (1989) by exposing sediment samples to HCl-HNO₃ (2:1). Concentrations of 20 elements were determined in parts per million at the Institute of Ecology, University of Georgia, using an inductively coupled argon plasma (ICAP) spectrometer.

Subsamples of the <2 mm fraction were sent to Brooks Ellwood, Department of Geology, University of Texas at Arlington for magnetic susceptibility measurements.

Measurements were made with a Maxwell bridge calibrated to the National Bureau of Standards using MnF_2 salts, MnO_2 salts, and magnetite standard samples (Swartzen-druher, 1992). Results are given in units of m^3/kg . Each sample was measured three times with an average precision of $\pm 0,02 \times 10^{-7}$ or 10^{-8} , depending on the magnitude of the susceptibility. The worst precision was $0,06 \times 10^{-7}$ or 10^{-8} .

Organic carbon was determined for depths 0 to 142,5 cm by wet oxidation with the Walkley-Black method as described in Janitzky (1986) in order to check for possible buried soil horizons.

4.3 RESULTS

4.3.1 Luminescence dating results

Radio-isotope concentrations used in the dose rate calculation are listed in Table 1 with palaeodose and age estimates. Dose rates range from 1–2 Gy/ka. Palaeodose distributions (Figure 4) indicate well defined modes for each sample. In all cases but one, a unimodal palaeodose distributions suggests that the samples were adequately bleached on deposition, and that the mean is more appropriate than the minimum age model for age determinations. An exception is the sample from 75 cm (UGA03OSL-102) where the distinct bi-modal distribution suggests mixing or incomplete bleaching during the most recent depositional event. For this sample, the minimum age model is considered more appropriate. The ages are in correct chronostratigraphic sequence and consistent with previous OSL ages determined for the site (Feathers, 1997; Figure 5). These new ages resolve some of the dating issues at White Paintings and are discussed further by soil stratigraphic unit below.

4.3.2 Radiocarbon dating of fish and mollusc remains

Bone collagen in four of five fish vertebrae from the Upper and Lower Fish Horizons at White Paintings was dated by AMS radiocarbon at the University of Arizona. The four C^{14} ages for the fish bones, corrected for $\delta^{13}C$, were calibrated using CALIB 6,0

Table 1. Dosimetry data for OSL samples, White Paintings Rock Shelter square 23, south face.

Lab No.	Depth (cm)	U (ppm)	Th (ppm)	K (%)	Palaeodose (Gy)	Age (ka)
UGA03OSL-102	75	2,0 ± 0,4	5,2 ± 1,4	0,12	5,56 ± 0,1*	5,2 ± 09,7*
UGA03OSL-103	125	2,9 ± 0,4	4,0 ± 1,4	0,18	21,9 ± 4,7	17,6 ± 4,3
UGA03OSL-101	162	3,4 ± 0,6	5,5 ± 2,2	0,13	31,0 ± 5,5	21,7 ± 5,1
UGA03OSL-88	215	4,8 ± 1,3	8,0 ± 4,5	0,13	55,8 ± 10,5	29,2 ± 8,7
UGA03OSL-94	275	6,5 ± 0,5	3,8 ± 1,8	0,14	71,1 ± 4,5	35,6 ± 4,1
UGA03OSL-89	360	5,1 ± 1,3	6,8 ± 4,3	0,13	85,4 ± 14,8	45,2 ± 12,6
UGA03OSL-95	415	5,4 ± 0,8	4,7 ± 2,7	0,13	97,7 ± 9,5	54,2 ± 9,5
UGA03OSL-96	450	6,1 ± 0,9	5,5 ± 3,0	0,12	118,3 ± 17,5	58,5 ± 12,2
UGA03OSL-98	510	5,0 ± 0,7	3,5 ± 2,5	0,18	102,3 ± 14,4	61,2 ± 12,4

* Palaeodose and age for this sample based on the minimum age model. All other ages are based on the mean.

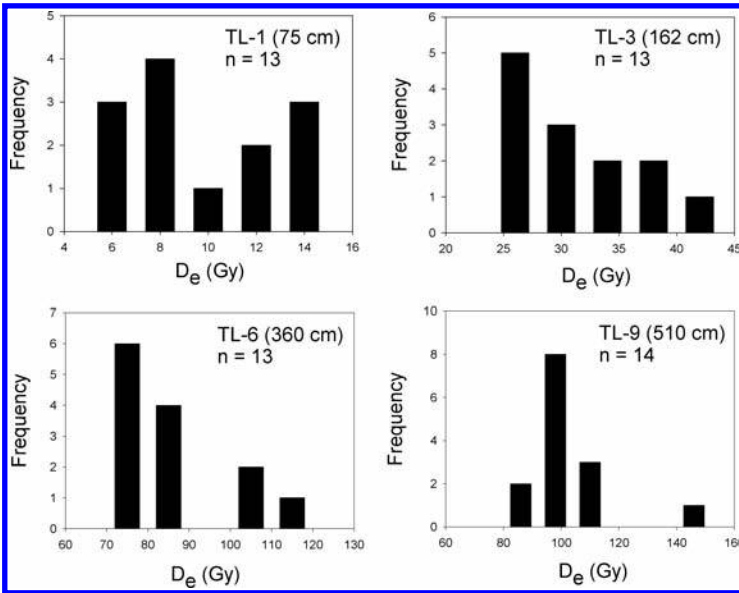


Figure 4. Representative histograms of palaeodose distribution.

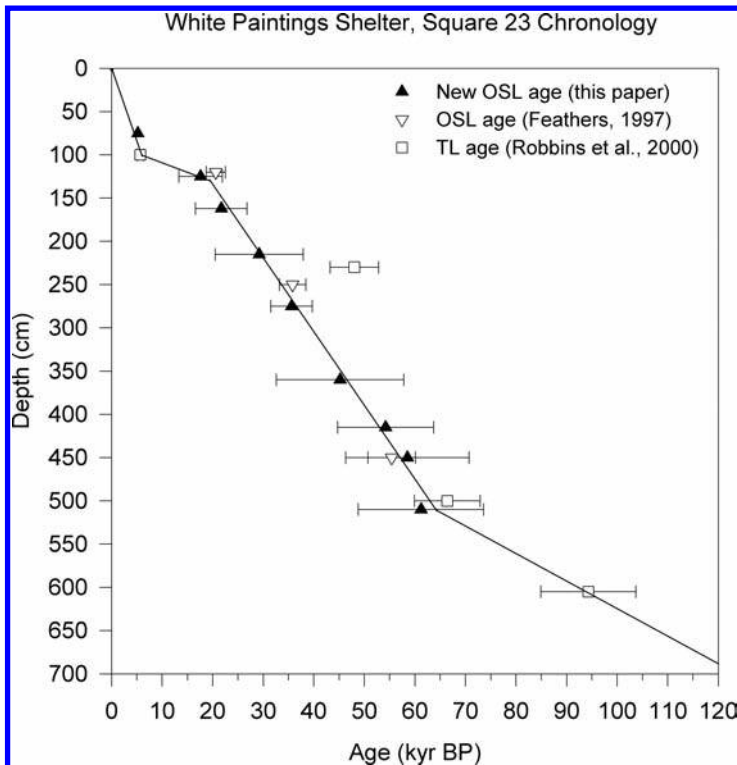


Figure 5. Revised White Paintings chronology based only on OSL and TL ages for the sediment matrix.

Table 2. Radiocarbon and calibrated ages for fish vertebrae and a mollusk shell from fish-rich layers at White Paintings rock shelter.

Lab Number	Material	Square	Depth	Sample ID*	Radiocarbon		Calibrated Age (cal yr BP)**
					Age C ¹⁴ yr BP	δ ¹³ C (‰)	
AA38920	Fish	12	240–250	WPS-12L	6.789 ± 193	–26,5	7.761–7.431 (1σ; 0,979)
AA38921	Fish	11	250–260	WPS-11L	8.250 ± 380	–24,1	9.528–8.634 (1σ; 1,00)
AA38922	Fish	23	120–130	WPS-23U	insufficient collagen	–25,4	
AA38923	Fish	12	120–130	WPS-12U	7.231 ± 151	–26,2	8.316–7.699 (2σ; 1,00)
AA38924	Fish	11	120–130	WPS-11U	6.330 ± 130	–25,5	7.433–6.858 (2σ; 0,998)
AA38925	Shell	22	240–250	WPS-22L	34.460 ± 690	–5,3	36.958–35.224 (1σ; 1,00)

* U = Upper Fish Unit; L = Lower Fish Unit.

** Probability and area under curve given in parentheses.

(Stuiver and Reimer, 1993) and the SHCal04 Southern Hemisphere calibration curve of McCormac *et al.* (2004). The carbonate of the mollusk shell from the Lower Fish Horizon was dated by CALIB 6.0 and the Intcal09 calibration curve based on Northern Hemisphere data (Reimer *et al.*, 2009). The calibrated ages suggest that fish were consumed at White Paintings during the Early Holocene from ca. 9,5–6,9 ka, suggesting greater availability of fish resources within a short distance of the site. The most likely possibility is that the fish were obtained from the Ncamaseri/Xeidum River 17 km north of the Tsodilo Hills at a time when this river flowed considerably more than it does today. The Early Holocene must have been substantially wetter than today as the upper sections of the Ncamaseri/Xeidum that are accessible from Tsodilo are fed by local rainfall. In fact the ages of the fish bones correspond with evidence from the Makgadikgadi Basin of high lake levels ca. 8,5 ka (Burrough *et al.*, 2009).

The new OSL age sequence places the age of the deposit at ca. 125 cm around 8 ka, which is not much different from the ages of the fish bones recovered from this depth. Likewise, the OSL chronology indicates that sediments at ca. 245 cm date to ca. 34 ka, which is about 2 ka younger than the central calibrated age of the mollusk shell recovered from this depth. This difference may be due to incorporation of old carbon into the carbonate of the shell from calcrete deposits that are common in the area. The much younger ages of fish bones recovered from this depth (ca. 9,5–7,5 ka) suggest that they may have been intruded into the sands from above.

4.3.3 Results of the sediment analysis

The excavation at White Paintings rock shelter (Figure 6) features soil stratigraphic units that are observable in the field and further characterized by laboratory analysis. The shelter sediments are composed predominately of aeolian sands with varying admixtures of locally-derived colluvium and spalled detrital contributions from the adjacent Male Hill. Several laterally extensive spall horizons, marked by coarse sands

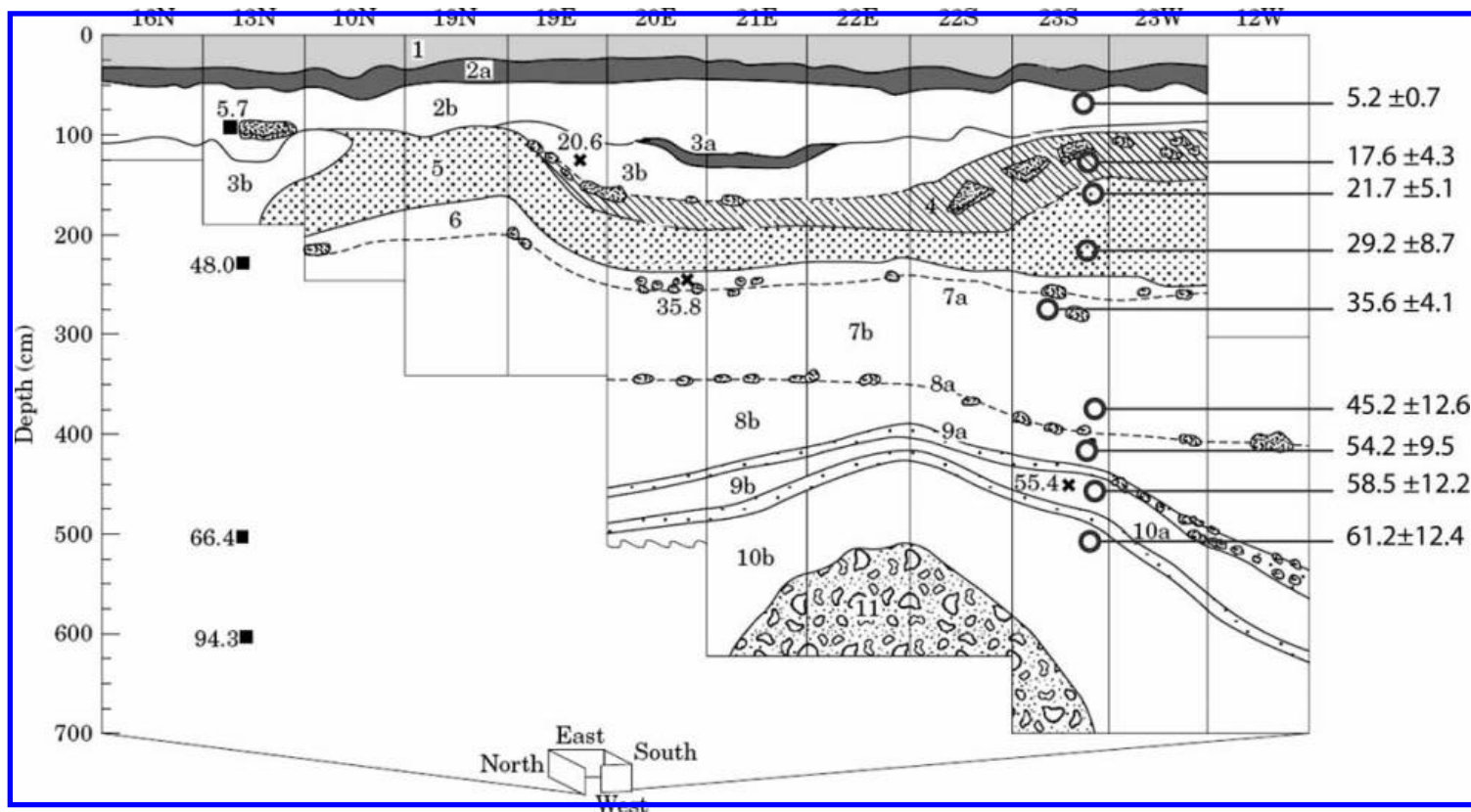


Figure 6. Soil stratigraphic units with new OSL ages from square 23. Also shown are TL ages from square 13 (Robbins *et al.*, 2000) and OSL ages from squares 19, 20, and 23 (Feathers, 1997). Figure is modified from Robbins *et al.* (2000).

and gravels, alternate with thicker units of medium to fine, well-sorted aeolian sands. Multiple stacked, buried soil profiles are observed in association with the spall horizons. In particular, two buried A horizons, soil stratigraphic Units 2a and 3a, are quite visible in the upper part of the section due to their darker colors compared with the surrounding sediments. In Unit 5 and deeper, the sands are pale brown with no visible changes in color. The soil stratigraphic units are numbered sequentially (1–11) from the surface downward. The subscript “a” is used to indicate a visible buried soil A horizon or spall horizon throughout the sequence. Unit 11 at the base of the section is an indurated, carbonate-cemented breccia.

Key granulometric measures—gravel, mean size of the sand fraction and sorting of the sand fraction—are graphed in Figure 7 along with the interpreted soil stratigraphic units and cultural levels. The estimated age on the right-hand axis of the graph is based on the age-depth model of Figure 5. Throughout the profile sand comprises 93–97% of the <2 mm fraction. Most of the sand (more than 80%) is in the medium and fine sand fractions of 500–125 μm diameter, with a consistent mode in the fine sand fraction at 250–180 μm , slightly finer than the better-sorted dune sands in the vicinity, which have a medium sand mode at 355–250 μm . Surface soils on the hill above the rock shelter differ by containing more coarse sands and gravels and being more poorly-sorted, though the modal sand size is also in the medium and fine sand fraction.

Figure 7 also indicates variations in carbonate, magnetic susceptibility and organic carbon with depth. Carbonate percentage varies from 2 to 11% of the untreated sand, silt, and clay weight. Higher carbonate concentrations occur at 160–360 cm, 420–440 cm, and 560–660 cm. Carbonate peaks around 200–250 cm depth, making up just over 10% of the total sample weight, and again in the indurated breccia below 600 cm. Minimum carbonate amounts of 2–3% occur in the leached near-surface samples. Surface sediment samples from the hill were 1–2% carbonate, whereas the dunes to the south of the hill contained less than 0,5% carbonate.

Magnetic susceptibility ranged from $0,70\text{--}3,49 \times 10^{-7} \text{ m}^3/\text{kg}$, generally decreasing with depth, although exhibiting slight peaks in the upper levels of each soil stratigraphic unit. In the surrounding dune fields, susceptibility values were very low, between $0,158$ and $0,063 \times 10^{-7} \text{ m}^3/\text{kg}$. Hill samples ranged from $2,20\text{--}4,63 \times 10^{-7} \text{ m}^3/\text{kg}$. Organic carbon is highest near the surface, decreasing quickly with depth, with peaks at soil stratigraphic Units 2a and 3a.

Figure 8 shows acid extractable element concentrations with depth for several key major and trace elements. Only alternate samples were measured for geochemistry, at 15 cm intervals instead of the 7,5 cm interval used for the other analyses. Although other elements were measured (Ivester, 1995), the ones highlighted here are relatively immobile and useful as pedogenic indicators for delineating soil stratigraphic boundaries.

Organic carbon in the shelter ranges from near zero to 2% of the total sample weight. A peak in organic carbon at 37,5–45 cm marks the Unit 2a buried soil. Below 60 cm the percent organic carbon is less than 0,5%. Equivalent percent organic matter can be estimated by multiplying Walkley-Black figures by 1,75.

4.4 DISCUSSION

4.4.1 Basis for interpretation of the sedimentary record

At White Paintings shelter, each stratigraphic unit is a mixture of varying proportions of material from the hill and from the sand dunes. The relative proportion of dune to

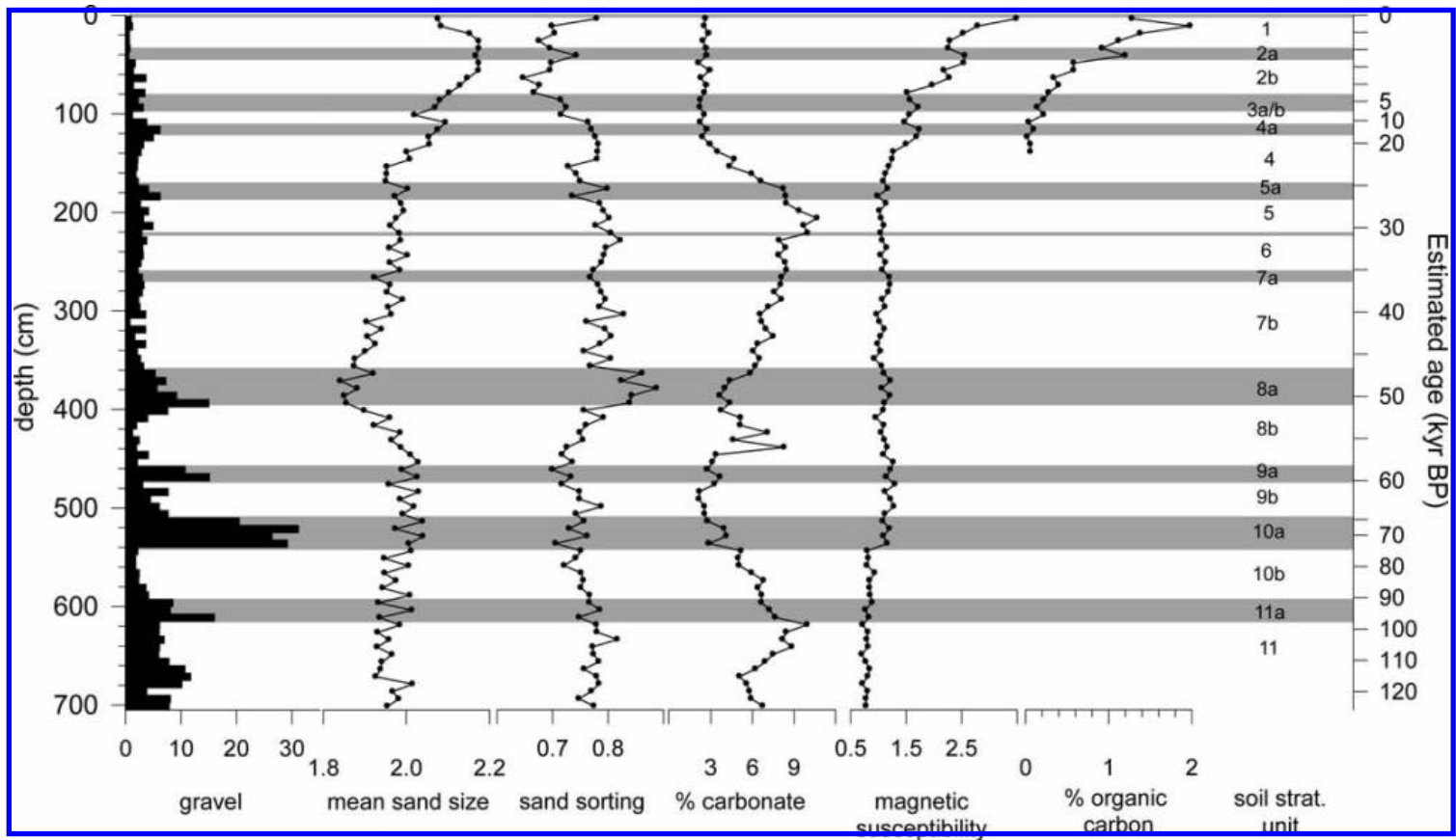


Figure 7. Key measures of particle size with soil stratigraphic units and archaeostratigraphic zones. Gravel is a percent of the total sample weight. Mean sand size (higher values = finer sands) and sorting (higher values = more poorly sorted) are in phi units. Carbonate and organic carbon are given as a percentage of total sample weight, and magnetic susceptibility is in $10^{-7} \text{ m}^3/\text{kg}$.

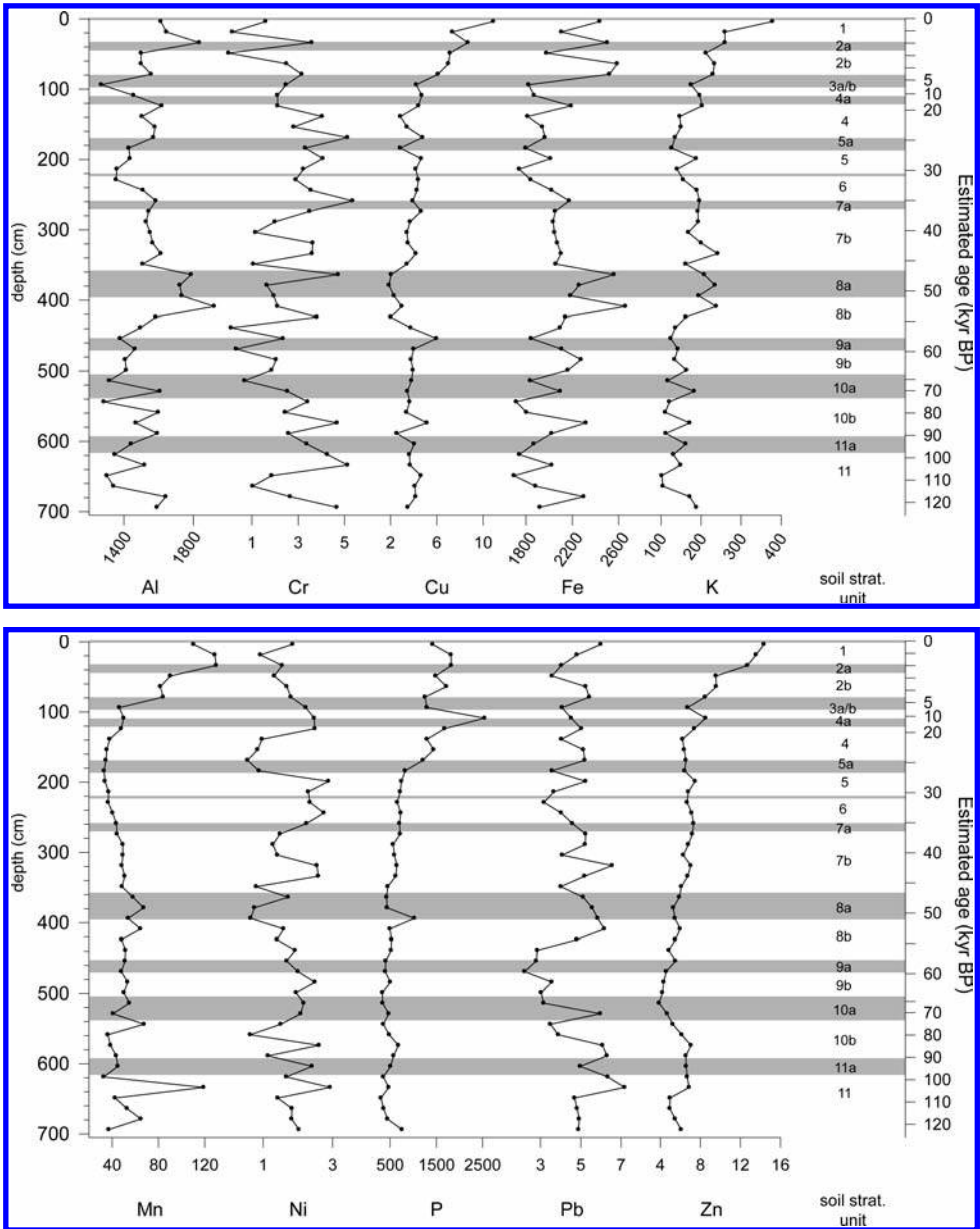


Figure 8. Acid (HCl-HNO₃) extractable element concentrations (ppm) measured by ICAP spectrometer.

hill sediment can be estimated based on differences in the source materials, and is a function of climate at the time of deposition. During wetter periods the dunes would have been stabilized by increased vegetation and the basin west of Male Hill may have contained water, either slowing or completely blocking aeolian contributions to the shelter. Enhanced chemical weathering and mass wasting of the bedrock would increase the relative contribution of coarse clasts via colluviation from the hill and

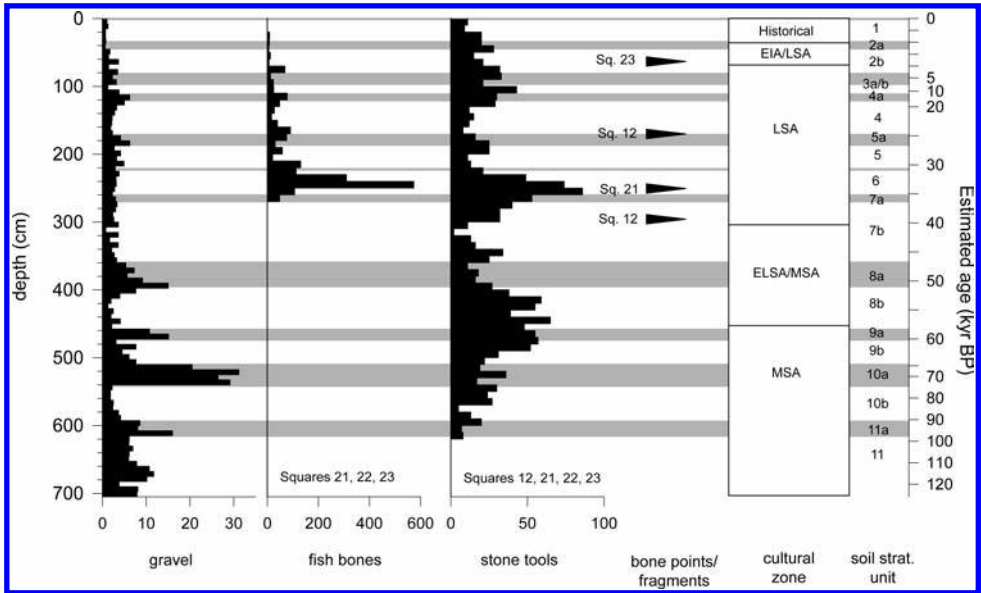


Figure 9. Fish bones, stone tools, and bone points or point fragments, by 10 cm level. Estimated cultural boundaries are from Robbins *et al.* (2000). Gravel percentages are shown for comparison.

spalling from the shelter ceiling. Such units would have greater amounts of gravel and coarse sand, a greater magnetic susceptibility, concentrations of certain extractable elements, and would be less well sorted. A relatively dry period would allow increased aeolian contributions, with decreased weathering and colluviation, resulting in better sorted sediment with less gravel and coarse sand. The high sand input would dilute certain elemental concentrations, while the lack of pedogenesis would result in lower magnetic susceptibility. In the interpretation of the White Paintings sediment column, an estimate of the relative contribution of each source is a useful climatic indicator.

Though evidence of past moisture conditions can be assessed, temperature changes are more problematic. Today there is limited freeze/thaw action at Tsodilo because the winter season, when temperatures sometimes dip below freezing, is also the dry season. A climatic regime with a wetter cold season with more effective freeze/thaw cycles would produce more gravel from the easily broken schist bedrock. Lower temperatures would also affect moisture to some extent by decreasing evapotranspiration, and thus enhance freeze/thaw action. Thus coarse materials may indicate wetter conditions and lower temperatures. Marked peaks in gravel could reflect a combination of cold and wet conditions, while minor peaks could reflect slightly increased water. In any case water is the crucial factor; changes in temperature have little effect on gravel production without sufficient water.

Of the sedimentary characteristics examined, percent gravel provides the simplest and clearest evidence for past wetter and possibly colder conditions. During a dry period coarser material would quickly be covered by aeolian sand. Therefore higher gravel percentages indicate wetter periods characterized by a vegetated and stabilized landscape and increased weathering of the bedrock at Male Hill into gravel-sized clasts. The rock shelter sediments are composed of varying amounts of gravel, making up anywhere from 1 to 31% of the total clastic weight. Certain levels have

particularly high gravel concentrations, most noticeably at around 4 m depth and again just below 5 m.

The significance of variations in gravel amounts from one spall horizon to the next is not certain, though it might indicate weathering intensity, with higher peaks in gravel amounts resulting from exceptionally large increases in rainfall or decreases in temperature. Another uncertainty is the significance of the cobble amounts; for example, during Unit 8a fewer cobble sized clasts were deposited than in Unit 10a. This could also result from varying intensities of the weathering periods. In any case, the gravel percentage curve is perhaps the simplest and most direct indicator of palaeoclimate at White Paintings.

Compared to gravel amounts there is little variation in the <2 mm fraction; sand makes up between 93% and 97% of the total weight. For the non-gravel clastics, mean grain size ranges from 1,95 to 2,28 phi. Sorting varies between 0,69 (moderately well sorted) to 1,35 phi (poorly sorted). Skewness ranges from -0,06 (near symmetrical) to 0,22 phi (fine-skewed). Kurtosis ranges from 1,17 (leptokurtic) to 2,43 phi (very leptokurtic). Sorting values, however, are significantly higher for the hill sediments, while the dune samples are much better sorted. Sediment from the rock shelter has intermediate values, as would be expected as the shelter sediment is a mixture of the two source materials. Sorting is then a good indicator of provenance, with better sorting resulting from increased aeolian input from the dunes and poor sorting a result of the increased input of coarse sands and clays from the hill during wetter periods. Sorting correlates well with the gravel amounts.

Elevated organic carbon and magnetic susceptibility indicate both human occupation and pedogenesis. At White Paintings, since the hill sediments have higher susceptibility values than the dune sands, susceptibility can also be an indicator of provenance. Peaks may therefore be partially attributable to wetter conditions. Higher carbonate amounts tend to cause a decrease in magnetic susceptibility; and at White Paintings, all of the peaks in magnetic susceptibility (except for the one at 260–280 cm) are at depths with less than 5% carbonate.

Acid-extractable elements vary in mobility in soils. Those that are relatively immobile in the profile may serve as indicators of pedogenesis and of provenance, if there are significant differences between their concentrations in the two source materials. (Kabata-Pendias and Pendias, 1984). Aluminum and iron are not very mobile in well-aerated sediments and can be used to identify buried soils. At Tsodilo their concentrations are much higher for hill and bedrock samples than for dune samples, making their distributions in the stratigraphy also useful for identifying relative aeolian/colluvial contributions.

Chromium, copper, nickel and zinc are relatively stable in soils and can be used as indicators of former organic matter in sediment where organics have been lost to oxidation. Amounts of these elements were low in the dune samples, so they can also indicate more colluviation and spalling. Lead is relatively stable in sediments. It is almost completely absent in the dune samples, with much higher concentrations in the hill and bedrock samples, and so can be an indicator of provenance. Manganese has medium to high mobility and is often fixed by organic matter and associated with iron. Phosphorous and potassium are often associated with human occupation. Both of these elements show a decrease in concentration with time due to their moderate mobility. Potassium and phosphorous values are low in the dune sands.

Magnetic susceptibility is the ratio of the intensity of magnetization produced in a substance to the magnetizing force or intensity of the field to which it is subjected. Susceptibility is a function of both the fraction of iron oxides that have been converted to maghemite and the concentration of iron oxide and detrital magnetite available.

Humans can increase the magnetic susceptibility of the soil by building fires. Iron oxide in the soil is reduced to form hematite. Fire later causes oxidation and the hematite is transformed to maghemite, which is strongly magnetic. This process can occur under a fire hearth, under decaying plants, or in a time of quickly alternating wet and dry periods (Tite, 1972). Increased susceptibility may also result from pedogenesis and so can be used as an indicator of palaeoclimate (Verosub *et al.*, 1993). At White Paintings rock shelter, high values of magnetic susceptibility correlate with buried soil A horizons and with higher artifact densities.

4.4.2 Soil stratigraphic interpretations

In the following discussion the chronological, sedimentological, and archaeological evidence in each of the soil stratigraphic units delineated in the profile at White Paintings is examined. The discussion is framed in terms of the soil stratigraphic units and cultural levels identified by Robbins *et al.* (2000), bringing to bear the new OSL data and palaeoenvironmental implications revealed in the sedimentary record. All radiocarbon dates referenced below are from Robbins *et al.* (2000) but have been re-calibrated using CALIB 6.0 (Stuiver and Reimer, 1993) and either the SHCal04 Southern Hemisphere calibration curve (0–11 ka) of McCormac *et al.* (2004) or the IntCal09 calibration curve (0–50 ka based on Northern Hemisphere data) of Reimer *et al.* (2009) so as to be comparable to the OSL ages.

Unit 1: Late Prehistoric/Historic (0–30 cm)

Unit 1 is the modern A horizon and has the highest amount of organic carbon (1–2%) of the whole profile. Carbonate amounts are low here at around 2%, as would be expected in a leached surface horizon. The relatively darker color of Unit 2a might mean that the surface that this horizon represents was stable for longer than the present surface has been.

Unit 1 was likely deposited during the last thousand years or so based on cultural materials and radiocarbon data. There are no luminescence dates for this unit. This interpretation is unchanged from that presented in Robbins *et al.* (2000). Artifacts supporting the age include a nylon button (10–20 cm), European glass trade beads with colors indicating an age of circa 150 years (0–20 cm), iron and copper beads, and maize kernels/ear indicating an age of less than 500 years (0–20 cm). LSA lithics in this zone could be several hundred years older than the beads and maize. A calibrated AMS radiocarbon date (200 ± 50 C¹⁴ yr BP) of 301–56 cal yr BP (probability 2 σ ; area under curve 0,874; central age 178 cal yr BP or 0,2 ka BP) was determined from ostrich eggshell at 20–30 cm in excavation square 17. The underlying unit has a radiocarbon age for bone (1.225 ± 60 C¹⁴ yr BP) of 1.186–962 cal yr BP (probability 2 σ ; area under curve 0,905; central age .1074 cal yr BP or 1,1 ka BP) at 40–50 cm, which helps to constrain the age of Unit 1.

Units 2a and upper 2b: Later Stone Age/Early Iron Age (30–80 cm)

Ceramics from Units 2a and the upper part of 2b, most from above 60 cm, are Early Iron Age, and indicate an age about 1,450–900 years (Robbins *et al.*, 2000). An AMS radiocarbon date (1.225 ± 60 C¹⁴ yr BP) on a sheep jawbone from square 23 at 40–50 cm yielded a calibrated age of 1.186–962 cal yr BP (central age 1.074 cal yr BP or 1,1 ka BP). Another AMS radiocarbon age (3.570 ± 60 C¹⁴ yr BP) yielded a

calibrated age of 3.933–3.632 cal yr BP (probability 2σ ; area under curve 0,968; central age 3.782 cal yr BP or 3,8 ka BP) at 60–70 cm and this helps to date the lower part of this deposit.

A new OSL age from 75 cm (UGA03OSL-102) yielded a mean age of $9,0 \pm 3,2$ ka, and a minimum age of $5,2 \pm 0,7$ ka. This sample has a mode at the minimum of the dose distribution histogram, indicating that the minimum age is more likely associated with the last episode of reworking of this sand. The broad palaeodose distribution suggests incomplete bleaching on deposition. The age closely corresponds to the age of underlying Unit 3a, suggesting that older material may have been reworked by small-scale, localized remobilization.

The presence of a buried A horizon (Unit 2a; 30–50 cm) indicates a period of stability after the deposition of Unit 2. A peak in organic carbon occurs at 37,5–45 cm, while the magnetic susceptibility peak is broader and extends from 37,5 to 52,5 cm. This buried A horizon is also expressed in geochemical indicators from 30–37,5 cm as peaks in Al, Cr, Cu, Fe, and Mn, although there are no peaks in K or P. All geochemical measures return to lower values at 45–52,5 cm, suggesting that the base of the Unit 2a buried A horizon is at 45 cm. Peaks in ceramic sherd counts (30–40 cm), stone tool counts (30–50 cm), and lithic debitage totals (40–50 cm) also indicate stability and higher occupational intensity at the surface represented by this buried A horizon.

Both the buried (2a) and the modern A horizon share similarities in the ways they deviate from the aeolian signature of their less-altered parent materials. They have more coarse sands, and therefore are slightly less well-sorted. These characteristics are consistent with a period of stability—a slowing or cessation of aeolian deposition that allowed soil forming processes to differentiate the A horizon, and allowed for a greater input of locally-derived coarse sands in the form of colluviation or roof-spall. Both A horizons have relatively high levels of very-coarse sand that decrease with depth, although compared with the underlying 6 meters, even the A horizons have low coarse sand and gravel amounts. The more pronounced geochemical signature, darker color, and greater stone tool concentrations in Unit 2a suggest that it was stable for longer than the 1.000 years or so that the modern A horizon has been.

Unit 2b (50–100 cm) is a less-weathered and lighter-colored (10YR 4/2) sub-surface horizon associated with the overlying A horizon of Unit 2a. Clay does not increase in this horizon relative to the A—in fact, clay percentages drop from around 3,5% in Unit 2a to around 2,5% in Unit 2b, suggesting some degree of eluviation while 2a was the surface horizon. Carbonate percentages also remain low throughout 2b, as they are in the entire upper 1,5 m of the profile. Unit 2b has a higher color value and higher chroma than the overlying A horizon. Due to the lack of illuvial characteristics, Unit 2b is more characteristic of a relatively unaltered C, or incipient E horizon rather than a B horizon. An increased concentration of artifacts and debitage between 70 and 80 cm may indicate either lower sedimentation rates or more intense occupation during the time that level 2b was deposited, albeit with insufficient pedogenesis to leave evidence of an A horizon.

Units 1, 2a, and 2b have an aeolian signature and appear to contain relatively little colluvially-derived sediment. Apart from the modern surface sample (0–7,5 cm) gravel and coarse sand percentages are low. This zone is characterized by well-sorted sands—finer sands than anywhere else in the profile—with a high percentage sand in the 180–125 μm fraction, and a low percentage of sand $>710 \mu\text{m}$. Units 1 and 2 are less like colluvial sand than any other unit in the profile, suggesting that local colluviation has been minimal and aeolian deposition dominant during the last 1.000 years. The upper-most meter, and especially the upper 60 cm also have the lowest gravel amounts of the profile. Between 60–100 cm gravel amounts are slightly more than in the upper

60 cm. This suggests that during the past 4,000 years aeolian deposition has been a more important process than colluviation and roof-spalling at White Paintings. At least two phases of aeolian deposition, of unknown duration, are indicated: one prior to and one after the time when Unit 2a was the stable land surface.

Upper Fish deposits lower Units 2b, 3a, and upper 3b (80–120 cm)

This zone is marked by another buried A horizon, high tool counts, and an abundance of fish bones. Late Stone Age (LSA) microlithic artifacts and other tool assemblages suggest a Holocene age for the occupation of this surface (Robbins *et al.*, 2000). This interpretation is supported by radiocarbon dates. In square 23 at 110–120 cm an AMS radiocarbon date (3.555 ± 45 C¹⁴ yr BP) on a nut shell fragment yielded a calibrated age of 3,895–3,641 cal yr BP (probability 2 σ ; area under curve 1,00; central age 3,768 cal yr BP or 3,8 ka BP). From the same level a bulk date from several fragments of ostrich eggshell (6.840 ± 40 C¹⁴ yr BP) dated to 7,691–7,572 cal yr BP (probability 2 σ ; area under curve 1,00; central age 7,632 cal yr BP or 7,6 ka BP), though the dated sample may have been a mix of younger and older eggshell fragments (Robbins *et al.*, 2000).

Unit 3 was likely deposited sometime between 21 ka and 5 ka, and its surface exposed and occupied until 4 ka. The interval of 18 to 5 ka is not represented by any dates at White Paintings and represented by at most 5–15 cm of sediment. Dates from immediately underlying units are much older and indicate that Unit 3a was the surface for a long period of time. Feathers (1997) reported an OSL age of 20,6 ka for a sample from 120 cm in Square 19 (in Unit 3b). A new OSL age, reported here, of $17,6 \pm 4,3$ ka (UGA03OSL-103) is from 125 cm in Unit 4. The error terms on these ages from Unit 4 suggest that they are not significantly different, both dating to the Last Glacial Maximum.

The much older ages for sediments immediately beneath the 3a surface, along with the high concentration of artifacts and fish bones suggests that this was a stable to slowly aggrading occupation surface from about the Pleistocene/Holocene transition until about 4,1 ka. Deposition rates were either very slow or stopped altogether during the deglacial period, and there may have been some erosion. Occupation of this surface likely began in the early to Mid-Holocene, as suggested by the radiocarbon ages from fish bones of 9,5–6,9 ka and the lack of other dates prior to ca. 9,5 ka. The termination of the fish deposits in lower Unit 2b occurred sometime around 3,8 ka BP (3.570 ± 60 C¹⁴ yr BP) based on a calibrated ostrich eggshell radiocarbon age of 3,933–3,632 cal yr BP (central age 3,782 cal yr BP or 3,8 ka BP) at 60–70 cm.

On the south face of Square 12, where the sediment column was collected, Unit 3a and 3b are represented by only two samples (97,5–112,5 cm) because the unit thins toward the South and West as the underlying Unit 4 slopes upward toward the crest of the Unit 4/5 ridge around the drip line of the shelter. To the North and East, in Squares 21 and 22, the Unit 4 surface drops by around 50 cm and Unit 3a/3b is thicker here. Gravel amounts are still around 3%, rising to a peak of 6% in the top of the underlying Unit 4. Fish bones are concentrated both in Unit 3 and in the lowest levels of Unit 2b. The intense occupation might have allowed some disturbance of the surface and allowed localized erosion and mobilization of sediment to bury and mix with Unit 3a to form the lower part of Unit 2b. This is also consistent with the 10 ka age discontinuity between 110/120 and 125 cm and helps to explain some of the mixed ages found in Unit 3.

Other evidence substantiates 3a as a long-term stable surface represented by sediment at 90–127,5 cm. Magnetic susceptibility values in this zone peak at 90–97,5 cm and again at 112,5–127,5 cm, then drop to background levels below 135 cm. Organic

carbon peaks at 97,5–105 cm. The surface is also well-represented in the geochemical data: Al and Fe peak at 120–127,5 cm, while Cu, K, Mn, Ni, P, and Zn peak at 105–127,5 cm. The phosphorous peak is more pronounced here than anywhere else in the profile as would be expected given the concentration of fish bones.

The delineation of the upper fish sediments is also well-marked by granulometry. Below 82,5 cm, the sands are coarser and more poorly sorted than in the above Unit 2b. As for the lower boundary, there is an increase in gravel, coarse sands, very fine sands, and coarse silt below 105 cm compared to the zone above. The lithologic break is therefore about 15–20 cm higher than the break in geochemistry and archaeology. This suggests that Unit 3 was aggraded up to the 105 cm level as a discrete depositional unit before being occupied as a surface. Subsequent exposure and occupation of the surface modified the upper 20 cm of Unit 3. The surface then became cumulic, receiving locally reworked materials from the drip line crest, and perhaps some exogenic materials, to extend properties of the A horizon up to the 80 or 90 cm level. Subsequent more rapid sedimentation buried the fish zone.

Low density LSA: Units 3b, 4, and 5 (130/140–210 cm)

As mentioned above, Unit 3 is thin in the vicinity of the sediment column. So in Square 23 the fish zone sits directly on top of Unit 4, which extends from about 112,5 to 170 cm. The upper part of Unit 4, to a depth of 127,5 cm is somewhat overprinted and modified by the pedogenic processes that affected Unit 3. These pedogenic modifications complement pre-existing modifications that occurred prior to the deposition of Unit 3, when the top of Unit 4 was at the surface for some unknown duration. The pedogenic indicators listed for 3a apply also to Unit 4 and suggest that the surfaces of first Unit 4 and next Unit 3a were exposed for long durations during the interval from ca. 20 ka until the Middle-Holocene. Unit 4 is dated by two OSL ages: $17,6 \pm 4,3$ ka from 125 cm as discussed in the preceding section, and $21,7 \pm 5,1$ ka at 162 cm (UGA03OSL-101). Unit 4 was therefore deposited during OIS Stage 2 and remained exposed until some time during the Pleistocene/Holocene transition.

Gravel amounts peak at the base of the upper fish zone and in the top of the underlying Unit 4, with a peak concentration from 112,5 to 127,5 cm. This peak occurs at the age discontinuity, suggesting that these gravels represent erosion on the sloped upper surface of Unit 4, remobilizing some of the Unit 4 sediment to form the 3b fill in adjacent squares toward the Northeast. Unit 4 sediments are coarser and more poorly sorted than the overlying sediments.

Unit 5 (170–225 cm) is dated by an OSL age of $29,2 \pm 8,7$ ka at 215 cm (UGA03OSL-88). Ostrich eggshell ages of 31.220 ± 320 C¹⁴ yr BP (36.460–35.036 cal yr BP; 2σ with area under curve 1.00; central age 35.748 or 35,7 ka BP) at 150–160 and 33.470 ± 250 C¹⁴ yr BP (38.891–37.347 cal yr BP; 2σ with area under curve 1,00; central age 38.119 or 38,1 ka BP) at 160–170 cm are older than the associated OSL dates (Robbins *et al.*, 2000). It is likely that these shell fragments were reworked from older deposits in underlying units given the evidences for erosion and the consistency of these ages with OSL ages from Units 6 and 7. The upper part of Unit 5 is characterized by higher gravel amounts, a finer mean sand size, more poorly sorted sands, and by peaks in Cr and Cu. These suggest a period of stability of unknown duration after the deposition of Unit 5.

The base of Unit 5 at 225 cm is delineated by several textural and chemical indicators. Standard deviation and coarse sand amounts increase to peaks at 225–232,5 cm. Carbonate amounts peak at around 10% of the total sediment weight at 202,5–225 cm. It is likely that this calcic horizon formed at least partially during the late Pleistocene

and early to Mid-Holocene. Based on the modern rainfall for this area in the Kalahari, around 56 cm/yr, the depth to the top of the calcic horizon should be somewhere between 40 and 100 cm below surface (based on data in Schaetzl and Anderson, 2005). Of course the expected depth can vary greatly depending on slope, landscape position, soil texture, climate change, etc. In any case, the top of the observed calcic horizon at White Paintings is at roughly 175–200 cm, suggesting that the past ground surface below which it formed would be located between 75 and 160 cm depth below modern surface. This depth range includes both the Unit 4 and Unit 3a surfaces, and provides yet another line of evidence that one or both of these surfaces were stable for long periods of time.

Lower Fish deposits: Unit 6 and upper surface of Unit 7 (210–280 cm)

A second concentration of fish bones and LSA artifacts occurs in this zone which corresponds to depths at the sediment column of 225–280 cm, taking into account the dip of bounding strata. A peak in tool counts occurs at 240–270 cm for square 12. Feathers (1997) reported an OSL age of $35,8 \pm 2,6$ from Unit 6 at 250 cm. A new OSL sample from the Unit 7a/7b boundary at 275 cm provides an age of $35,6 \pm 4,1$ ka (UGA03-94). This is equivalent to the ages of ostrich eggshell in the overlying Unit 5 that were possibly reworked from Unit 6. Ostrich eggshell from Unit 7a was previously dated to >48 ka (Robbins *et al.*, 2000). As in Unit 5, the OSL age estimates are younger than the corresponding eggshell ages. However 48 ka is close to the limit of radiocarbon dating. It is considered that the OSL ages are more reliable for dating these units. Robbins *et al.* (2000) reported that the LSA microlithic assemblages in this zone likely date between 39 and 19 ka, further substantiating the OSL age estimates. Early Holocene radiocarbon dates of the fish bones in this deposit, along with the slope of the strata boundaries, suggest that the fish bones were intruded downward into this level.

Unit 7a is evident at 262,5 to 277,5 cm. This stable surface is weakly expressed in the textural data as higher clay amounts (around 3,5%) and lower total sand (93% at 262,5–270 cm). The 7a buried surface also shows up in magnetic susceptibility as a subtle peak at 262,5–285 cm and is marked by elevated Cu, K, Pb, and Zn. Gravel amounts are low for this unit, suggesting short term stability of surface 7a relative to other buried surfaces at this site. The peak in fish bones and stone tools farther from the less-disturbed vicinity of the sediment column reflects downward intrusion of younger materials.

Early LSA/Transitional MSA: Units 7b and 8a (300–410/420 cm)

A major shift in several sedimentary characteristics occurs near the base of Unit 7a, below about 280 cm in the sediment column. Unit 7b extends from 277,5 to 360 cm and is characterized by a lower concentration of lithic materials. Below around 300 cm, large blades occur and continue downward into the MSA horizons. The zone from 300 to 320 in particular has low tool and lithic totals. There is nothing particularly notable in the textural or geochemical data for these depths except for a general coarsening with depth of the samples from 300 to 400 cm depth. The tight palaeodose distribution of sample UGA03-94 ($35,6 \pm 4,1$ ka at the 7a/7b boundary at 275 cm) indicates good bleaching on deposition. All these characteristics suggest a fairly rapid depositional rate for Unit 7b, dominated by aeolian contributions.

Unit 8a is expressed as a higher concentration of gravels at 360–400 cm and a slight peak in artifact concentration in Square 12 at 350–360 cm. Unit 8a also shows up in magnetic susceptibility (360–400 cm), Al and Fe (360–376,5 and below),

Cr (360–367,5), K and Mn (375–382,5), and P (390–397,5). Therefore it is assumed that 8a represents a fairly substantial period of stability. The Unit 7b/8a boundary, at 360 cm, is dated by OSL to $45,2 \pm 12,6$ ka (UGA03OSL-89). The relatively large standard deviation in the palaeodose estimate suggests a colluvial depositional environment or, perhaps some mixing of differently aged grains in a stable soil. This is consistent with Unit 8a having been a stable surface. Unit 8b extends from 405 to 457,5 cm and is dated at 415 cm (equivalent to a depth of about 435 cm in the sediment column) to $54,2 \pm 9,5$ ka (UGA03OSL-95). There is a peak in carbonate at 420–442,5 cm that could be associated pedogenically with the Unit 8a surface.

MSA levels: 410/420–700 cm, Units 9–11

Two prominent schist spall horizons occur as Units 9a and 10a. These horizons and the MSA horizons in general probably formed during periods of increased precipitation and have higher artifact densities compared to units above and below. Unit 9a (457,5–472,5 cm) has higher magnetic susceptibility values from 450–502,5 cm, higher gravel content (up to 15% of the total sample), and high Cu, Fe, Ni, Pb, and Zn, but less of a distinct signature in the sand fractions. Tool counts peak between 440 and 480 cm in Square 12. Unit 9b (472,5–510 cm) is characterized by lower gravel amounts. Unit 10a at 510–540 cm has high gravel content and a peak in tool concentrations in Square 12 at 520–530 cm. Unit 10b at 540–600 cm has lower gravel amounts and suggests an increase in aeolian sedimentation. Unit 11 at 600–705 cm is in the indurated breccia and contains few artifacts.

The age of these levels is based on three OSL samples. Unit 9b was dated by OSL to $55,4 \pm 4,7$ ka (Feathers, 1997). Two new OSL samples also help to date these levels: a sample from 450 cm (equivalent to sediment at 490) was dated to $58,5 \pm 12,2$ ka (UGA03OSL-96) and a sample from 510 cm (sedimentary column 550 cm) was dated to $61,2 \pm 12,4$ ka (UGA03OSL-98). These dates are consistent with other MSA sites in the Kalahari. Given the fairly large standard deviations in the estimates, the ages of the two schist spall horizons at 9a and 10a, and of the increased gravel amounts at 11a, are not precisely known. A TL age of 94,3 ka at 605 cm (Robbins *et al.*, 2000) may help date the lowest portions of the profile. Extrapolation of sedimentation rates to the base of the excavation suggests a basal age of ≥ 100 ka at seven meters.

4.5 REGIONAL AND GLOBAL RELATIONSHIPS

The stratigraphy of the White Paintings rock shelter shows eleven phases of greater surface stability accompanied by weak soil formation. These periods are indicated by a series of buried soil A horizons dating to ca. 2,5, 5–7,5, 15, 25–26, 31, 36, 47–51, 58–60, 65–73, 97, and 115 ka (Table 3). Six of these A horizons (3a, 4a, 5a, 7a, 9a, and 11a), as well as a coarse sediment zone in Unit 11 at 770 cm, correspond in age with lake high-stands in the Makgadikgadi Basin of Botswana (~500 km SE of Tsodilo Hills) at ca. $8,5 \pm 0,2$, $17,1 \pm 1,6$, $26,8 \pm 1,2$, $38,7 \pm 1,8$, $64,2 \pm 2,0$, $92,2 \pm 1,5$, and $104,6 \pm 3,1$ ka (Burrough *et al.*, 2009). This correspondence confirms that the buried soils at White Paintings formed during periods of increased rainfall, or at least increased effective moisture, in the region. The ages of the buried soils also correlate with evidence from Tsodilo Hills of a large lake that existed immediately west of the White Paintings rock shelter during the Late Pleistocene (Thomas *et al.*, 2003). Luminescence ages for lake shore sediments indicate a sizeable body of water ca. 12–13 and 18 ka. In addition, calibrated AMS radiocarbon ages for freshwater mollusc shells embedded in lacustrine

marls indicate high lake phases at ca. 14–17, 23, 32, and 36 ka. Together, the OSL and AMS radiocarbon ages define five lake intervals that correlate in time with the formation of buried A horizons 4a–7a (Table 3).

Other evidence supporting the White Paintings climate record comes from submerged speleothems in flooded caves and cenotes in NE Namibia that were recovered by divers from depths varying from 3–40 m below present ground water levels. Uranium-series ages for these deposits indicate periods with lower ground water levels, and therefore significantly drier climate, at 7–11, 13–15, 28–31, 62, and 107–112 ka (Brook *et al.*, 1998). The two most recent drier intervals date to the period between the formation of buried soil horizons 3a and 4a at White Paintings rock shelter while the dry periods at 28–31 and ca. 62 ka fall in the periods separating soil horizons 5a and 6a, and 9a and 10a, respectively. The dry interval at 107–112 ka pre-dated the formation of soil horizon 11a and post-dated a coarse sediment layer, possibly another buried A horizon, dating to ca. 115 ka (Table 3).

Luminescence ages for a number of linear dunes south of Tsodilo Hills provide evidence of past aeolian activity in this area that would have affected the accumulation and nature of sediments at White Paintings shelter. Thomas *et al.* (2003) report ages of $28,1 \pm 4,6$, $35,1 \pm 4,2$, and $35,4 \pm 4,1$ ka at 0,7, 1,1, and 1,75 m depth for one dune, $29,8 \pm 4,4$ ka (1,2 m) for a second dune, and $33,8 \pm 2,8$ (1,0 m) and $98,1 \pm 9,2$ ka (4,9 m) for a third dune. Additional ages have been obtained for sand at depths of 1,0–7,0 m at a 1,0 m interval in a fourth dune. In order of increasing depth these are: $28,8 \pm 6,9$, $53,6 \pm 8,8$, $54,4 \pm 14,7$, $50,5 \pm 8,8$, $63,1 \pm 10,5$, $78,5 \pm 14,5$, and $88,1 \pm 14,0$ ka. Thus, there are now thirteen OSL ages for linear dunes in the Tsodilo area. The distribution of these ages suggests periods of drier climate and increased aeolian activity at 28–30, 34–35, 50–54, 63, 78, 88, and 98 ka (Table 3). Importantly, dunes were active in the time intervals separating periods of soil A horizon development in the sediments at White Paintings rock shelter (e.g. between 5a and 6a, and between 10a and 11a).

The separate records of wet and dry intervals of climate at Tsodilo Hills, the Makgadikgadi pans, and NE Namibia match extremely well and when combined produce a detailed 115 ka palaeoenvironmental history for the region. Significantly, wetter events in this record correlate strongly with Heinrich (H) events in the North Atlantic and with Antarctic warmings (A) in the Southern Hemisphere (see Blunier and Brook, 2001). Heinrich event 1 (H1) correlates with White Paintings buried A horizon 4a, while H2 and H3 correlate with soil horizons 5a and 6a. Soil horizon 7a dates to the time of the H4 event and A1 warming while horizon 8a correlates with H5 and A2/3. Soil A horizons 9a and 10a were formed at the times of the H6/A4 and A5/A6 events, respectively (Table 3).

In contrast, drier intervals of climate in the terrestrial record correlate with N. *pachyderma* (s) or PS events in marine core GeoB 1711 off the Namibian coast. Little *et al.* (1997) have identified nine such events (PS1–PS9) in the last 135 ka when the percentage of the cold-water foraminifer N. *pachyderma* (s) increased substantially. These PS or *pachyderma* sinistral events are thought to indicate increased upwelling of the Benguela Current in the SE Atlantic triggered by stronger SE Trade winds. It is particularly noteworthy that upwelling events PS1–PS6 occur in the intervals between buried soil horizons 4a–5a up to 9a–10a, respectively. Therefore, the marine evidence for upwelling due to strong SE Trade winds corresponds with terrestrial evidence of aeolian activity and also more arid conditions.

The association between Heinrich events in the North Atlantic and wet intervals of climate in southern Africa is due to antiphasing of climate changes between the Northern and Southern Hemisphere as indicated by oceanic and Greenland and Antarctic Ice Sheet records (e.g. Little *et al.*, 1997; Blunier *et al.*, 1998; Blunier and Brook,

Table 3. Comparison of the White Paintings sediment record with data on wet or dry conditions from other sites in the region. Ages are in ka. (a) this paper showing the age of each “A” horizon (2a, 3a, etc) depicted in Fig. 5, (b) Burrough *et al.* (2009), (c) Thomas *et al.* (2003), (d) Blunier and Brook (2001), (e) Little *et al.* (1997), (f) Brook *et al.* (1998), (g) Thomas *et al.* (2003) and this paper.

Wet Periods:													
White Paintings Shelter “A” Horizon Ages ^a	2a 2.5	3a 5–7.5		4a 15	5a 25–26	6a 31	7a 36	8a 47–51	9a 58–60	10a 65–73	11a 97		115
Makgadikgadi Pan Lake Events ^b		8.5		17.1	27		39		64		92	105	
Tsodilo Hills Lake Events ^c	Shore ages: Shell ages:		12–13	18 14–17	23	32	36						
Antarctic/Heinrich Events ^d			H0 12	H1 17.5	H2 24	H3 30	H4/A 1 38	H5- A2/A3 45/52	H6/A 4 58	A5/A 6 68/73			
Dry Periods:													
PS Events ^e					PS1 19–22	PS2 26–29	PS3 33–37	PS4 42	PS5 53	PS6(?) 65–71			
Submerged Speleothems ^f	7.5–11		13–15		28–31			62			107–112		
Tsodilo Hills Linear Dunes ^g					28–30	34–35		50–54		63	78/88	98	

2001; Steig and Alley, 2002). Little *et al.* (1997) note that upwelling events PS1–PS6 in marine core GeoB 1711 correlate with Heinrich events H1–H6 in the North Atlantic with a consistent 3 ka phase lead in the Southern Hemisphere while Vidal *et al.* (1999) found that warming trends in the South Atlantic were about 1.5 ka earlier than in the North Atlantic. Blunier and Brook (2001) point out that over the last 90 ka the onset of seven major millennial scale warmings in Antarctica preceded the onset of Greenland warmings by 1.5–3 ka. The thermal antiphasing between the southern and northern surface Atlantic is thought to result from the freshwater-induced collapse of the Atlantic thermohaline circulation. NADW is associated with a considerable inter-hemispheric northward heat transport in the Atlantic. Reducing this transport results in immediate cooling in the (high latitude) Northern Hemisphere that is accompanied by a warming at least in some parts of the Southern Hemisphere.

During Heinrich events, the North Atlantic Ocean cooled due to slowing or cessation of the NADW flow while at the same time the South Atlantic and Indian oceans warmed (e.g. Sicre *et al.*, 2005). Colder conditions in the Northern Hemisphere caused a southward shift in the Inter Tropical Convergence Zone (ITCZ) while the warmer oceans in the Southern Hemisphere weakened the South Atlantic and South African anticyclones and associated SE trade and Westerly winds, and increased moisture in air masses moving onto southern Africa. These changes brought generally warmer and wetter conditions to the subcontinent. In contrast, the ITCZ migrated northwards in the intervals between Heinrich events and the colder southern oceans led to a strengthening of anticyclones. As a result, air masses coming off the oceans were drier and the African subcontinent became generally more arid and windier.

4.6 CONCLUSIONS

White Paintings shelter is a rich source of evidence for understanding human and environmental history in the Kalahari. Seven meters of aeolian sediment have accumulated in the shelter over the past 100 ka, augmented by locally derived colluvial material from the adjacent hill and by detrital material spalled from the rock shelter wall and ceiling. Relative contributions from these sources have varied through time as a result of climate and environmental changes to produce differentiable strata. Periods of greater aridity are represented by strata with finer and better sorted sands, lower gravel amounts, more rapid depositional rates, and a lower density of artifacts. Periods of greater moisture availability are represented by strata with slightly coarser and more poorly sorted sands, more gravel, a stable to slowly accreting land surface, a higher occupational intensity, the presence of fish bones, and enhanced pedogenesis with the resulting geochemical indicators. The presence of the palaeolake immediately west of the shelter would also have restricted aeolian contributions to the site during wetter intervals.

Nine new OSL ages help to refine the site chronology and provide a more robust temporal framework for interpreting the palaeoenvironmental data than was previously available. The OSL ages are in proper stratigraphic order, are consistent with age constraints associated with the cultural zones for the region, and confirm the more reliable of the previously determined age estimates. Ages of fish bones in the Lower Fish deposit and of the associated LSA microlithic assemblages were previously uncertain. Radiocarbon ages on the fish bones, along with sedimentological evidence, suggest that these are Early Holocene materials that were intruded downward in portions of the site into older underlying sediments. The consistency of the OSL chronology suggests that the sediment column represents an intact sequence on the edge of the site, and is therefore a suitable record of local palaeoenvironment.

The data suggest a trend towards more available moisture in the Pleistocene and Early to Middle Holocene, with a shift toward more arid conditions in the Late Holocene. Superimposed on this general trend are short-term, millennial scale oscillations in climate. Somewhat wetter and possibly cooler conditions, reduced aeolian sedimentation, and enhanced pedogenesis seem to have occurred at intervals during MSA and ELSA times. The evidence presented here indicates that buried soil A horizons, which mark periods of increased surface stability due to increased moisture and reduced aeolian activity, formed at ca. 2.5, 5–7.5, 15, 25–26, 31, 36, 47–51, 58–60, 65–73, 97, and 115 ka. Soil development occurred preferentially during Heinrich events in the North Atlantic and synchronous Antarctic warmings in the Southern Hemisphere. At these times there was a southward shift in the Inter Tropical Convergence Zone (ITCZ) and a warming of the Southern Hemisphere oceans that weakened the South Atlantic and South African anticyclones and associated SE trade and West-erly winds. This increased the transport of moisture from oceans to land and brought generally warmer and wetter conditions to the subcontinent.

ACKNOWLEDGEMENTS

This research was funded by National Geographic Society grant 7201–02 and by National Science Foundation grants 9108549, 9520982, and 0313826 to Robbins and Brook and grants 0002193 and 0725090 to Brook. We are grateful to the authorities and staff of the National Museum, Monuments and Art Gallery of Botswana for facilitating this research. Permission to work at Tsodilo was granted by the Office of the President, Republic of Botswana. We are particularly grateful to Alison S. Brooks for collecting new OSL samples for us when she re-opened the White Paintings excavation in 2003 to retrieve dosimeters installed the previous year.

REFERENCES

- Blunier, T. and Brook, E.J., 2001, Timing of millennial-scale climate change in Antarctica and Greenland during the last glacial period. *Science*, **291**, pp. 109–112.
- Blunier, T., Chappellaz, J., Schwander, J., Dällenbach, A., Stauffer, B., Stocker, T.F., Raynaud, D., Jouzel, J., Clausen, H.B., Hammer, C.U. and Johnsen, S.J., 1998, Asynchrony of Antarctic and Greenland climate change during the last glacial period. *Nature*, **394**, pp. 739–743.
- Brook, G.A., Cowart, J.B. and Brandt, S.A., 1998, Comparison of Quaternary environmental change in eastern and southern Africa using cave speleothem, tufa and rock shelter sediment data. In: *Quaternary Deserts and Climatic Change* (eds. A.S. Alsharhan, K.W. Glennie, G.L. Whittle and C.G. St. C. Kendall), A.A. Balkema, Rotterdam, pp. 239–249.
- Brook, G.A., Marais, E., Srivastava, P. and Jordan, T., 2007, Timing of lake-level changes in Etosha Pan, Namibia, since the Middle Holocene from OSL ages of relict shorelines in the Okondeka region. *Quaternary International*, **175**(1), pp. 29–40.
- Burrough, S.L., Thomas, D.S.G. and Bailey, R.M., 2009, Mega-Lake in the Kalahari: A Late Pleistocene record of the Palaeolake Makgadikgadi system. *Quaternary Science Reviews*, **28**, pp. 1392–1411.
- Duller, G.A.T., 1999, *Luminescence Analyst computer programme V2.18*. Department of Geography and Environmental Sciences, University of Wales, Aberystwyth.

- Ivester, A.H., 1995, *A Late Quaternary palaeoenvironmental record from sediments at White Paintings Rock Shelter, Tsodilo Hills, Botswana*. MA thesis, University of Georgia, Athens.
- Janitzky, P., 1986, Field and Laboratory Methods used in a Soil Chronosequence Study. In: Singer, M.S. and Peter Janitzky (1986), *USGS Bulletin*, **1648**.
- Kabata-Pendias and Pendias, Henryk, 1984, Trace Elements in Soils and Plants. *CRC Press*, 315 p.
- Little, I.G., Schneider, R.R., Kroon, D., Price, B., Summerhayes, C.P. and Segl, M., 1997, Trade wind forcing of upwelling, seasonality, and Heinrich events as a response to sub-Milankovitch climate variability. *Palaeoceanography*, **12**(4), pp. 568–576.
- McCormac, F.G., Hogg, A.G., Blackwell, P.G., Buck, C.E., Higham, T.F.G. and Reimer, P.J., 2004, SHCal04 Southern Hemisphere Calibration 0–11,0 cal kyr BP. *Radiocarbon*, **46**, pp. 1087–1092.
- Murray A.S. and Wintle, A.G., 2000, Luminescence dating of quartz using an improved single-aliquot regenerative-dose protocol. *Radiation Measurements*, **32**, pp. 57–73
- Prescott, J.R. and Hutton, J.T., 1994, Cosmic ray contributions to dose rates for luminescence and ESR dating: large depths and long-term time variations. *Radiation Measurements*, **23**, pp. 497–500.
- Reimer, P.J., Baillie, M.G.L., Bard, E., Bayliss, A., Beck, J.W., Blackwell, P.G., Bronk Ramsey, C., Buck, C.E., Burr, G.S., Edwards, R.L., Friedrich, M., Grootes, P.M., Guilderson, T.P., Hajdas, I., Heaton, T.J., Hogg, A.G., Hughen, K.A., Kaiser, K.F., Kromer, B., McCormac, F.G., Manning, S.W., Reimer, R.W., Richards, D.A., Southon, J.R., Talamo, S., Turney, C.S.M., van der Plicht, J. and Weyhenmeyer, C.E., 2009, IntCal09 and Marine09 radiocarbon age calibration curves, 0–50,000 years cal BP. *Radiocarbon*, **51**, pp. 1111–1150.
- Robbins, L.H., Murphy, M.L., Brook, G.A., Ivester, A.H., Campbell, A.C., Klein, R.G., Milo, R.G., Stewart, K.M., Downey, W.S. and Stevens, N.J., 2000, Archaeology, Palaeoenvironment, and Chronology of the Tsodilo Hills White Paintings Rock Shelter, Northwest Kalahari Desert, Botswana. *Journal of Archaeological Science*, **27**, pp. 1085–1113.
- Schaetzl, R.J. and Anderson, S., 2005, Soils: Genesis and Geomorphology. *Cambridge University Press*, 817 p.
- Sicre, M.A., Labeyrie, L., Ezat, U., Duprat, J., Turon, J.L., Schmidt, S., Michel, E. and Mazaud, A. 2005. Mid-latitude southern Indian Ocean response to Northern Hemisphere Heinrich events. *Earth and Planetary Science Letters*, **240**, pp. 724–731.
- Steig, E.J. and Alley, R.B., 2002, Phase relationships between the Antarctic and Greenland climate records. *Annals of Glaciology*, **35**, pp. 451–456.
- Stuiver, M. and Reimer, P.J., 1993, Extended ¹⁴C database and revised CALIB radiocarbon calibration program, *Radiocarbon*, **35**, pp. 215–230.
- Thomas, D.S.G., Brook, G., Shaw, P., Bateman, M., Haberyan, K., Appleton, C., Nash, D., McLaren, S. and Davies, F., 2003, Late Pleistocene wetting and drying in the NW Kalahari: an integrated study from the Tsodilo Hills, Botswana. *Quaternary International*, **104**(1), pp. 53–67.
- Tite, M.S., 1972, Methods of Physical Examination in Archaeology. *Seminar Press*, 389 p.
- van Loon, J.C. and Barefoot, R.R., 1989, Analytical methods for geochemical exploration. *Academic Press: London*, 344 p.
- Verosub, K.L., Fine, P., Singer, M.J. and Tenpa, J., 1993, Pedogenesis and palaeoclimate: interpretation of the magnetic susceptibility record of Chinese loess-palaeosol sequences. *Geology*, **21**, pp. 1011–1014.
- Vidal, L., Schneider, R.R., Marchal, O., Bickert, T., Stocker, T.F. and Wefer, G., 1999, Link between the North and South Atlantic during the Heinrich events of the last glacial period. *Climate Dynamics*, **15**, pp. 909–919.

CHAPTER 5

Ecosystem change during MIS 4 and early MIS 3: Evidence from Middle Stone Age sites in South Africa

Grant Hall

*ACACIA Programme, School of Geography, Archaeology and Environmental Studies, University of the Witwatersrand, South Africa
Environmental Processes and Dynamics (EPD), Pretoria, South Africa*

Stephan Woodborne

Environmental Processes and Dynamics (EPD), Pretoria, South Africa

ABSTRACT: Several Middle Stone Age (MSA) site in Southern Africa present evidence of environmental changes during Marine Isotope Stages (MIS) 4 and 3 between 70 ka and 50 ka. Of these, Sibudu Cave, KwaZulu-Natal, has yielded a detailed record of how global-scale climate change events manifest locally. During MIS 4 (70 ka to 60 ka) conditions were similar to those during the Last Glacial Maximum. During the transition between MIS 4 and MIS 3 at around 60 ka the Sibudu environment changed from a predominantly forested community to more open grass/woodland mosaic. Other MSA sites from across South Africa provide complementary palaeoenvironmental proxy data but imprecise dating presents a cross-correlation challenge. Archaeological sites on the western portion of South Africa appear to have been abandoned earlier and for longer than sites in the East, most likely as a result of adverse climatic conditions. Regional scale climate events in southern Africa are driven by ocean/atmosphere interactions, and at this time weakening of the palaeo-Agulhas Current and an eastward shift of the Agulhas Retroflexion resulted in lower sea surface temperatures and a corresponding decrease in humidity and rainfall.

5.1 INTRODUCTION

The planet is currently warming (Trenberth *et al.*, 2007) and climate change modelling is the means by which the impact of this warming is determined. The high level of complexity in ecosystems reduces the skill of models to forecast the future impact of these changes. An alternative approach is to examine past records of global climates where the associated ecosystem responses are documented. Evidence for past global warming change is derived from isotope analysis of marine cores and polar ice cores. The most recent of these global-scale events took place at the end of the last glaciation commencing approximately 20 ka ago and is known as Marine Isotope Stage 2 (MIS 2). The penultimate warming was between MIS 4 (70 ka to 60 ka) and early MIS 3 (60 ka to 50 ka), and is the subject of this analysis. While the warming is known to have taken place, little evidence has been presented for the associated terrestrial ecosystem response to this change.

Through multi-disciplinary analysis of cultural, biological and geological material from middle and lower latitude terrestrial sites it is possible to reconstruct local environmental conditions through time. Seven South African Middle Stone Age (MSA) archaeological sites (Figure 1) provide environmental evidence for MIS 4/early MIS 3. These are Sibudu Cave, Border Cave, Rose Cottage Cave, Klasies River Mouth, Boomplaas Cave, Blombos Cave, Diepkloof Rockshelter and Wonderwerk Cave. Between ~75 ka–55 ka there was a fundamental change in technological and cultural features compared with earlier and later MSA assemblages (Mellars, 2006; Mitchell, 2002). The stone tool industries of this time include the distinctive Still Bay and Howiesons Poort assemblages. Although the Still Bay has ages of ~75 ka–70 ka (Jacobs *et al.*, 2008a, b; Tribolo *et al.*, 2005) and the Howiesons Poort dates to between 65 ka–60 ka (Jacobs *et al.*, 2008a, b; Tribolo *et al.*, 2005) depending on the site and dating methods, the Still Bay is the older of the assemblages and always underlies the Howiesons Poort. There is associated evidence for modern human behaviour such as the use of composite stone tools, sophisticated hunting techniques and symbolic expressions (Mellars, 2006; Mitchell, 2002). The appearance of the Still Bay and Howiesons Poort in various MSA sites across South Africa is thought to be a response to sharply oscillating climatic conditions during MIS 4 and early MIS 3 (Mellars, 2006; Mitchell, 2002).

The ecosystem responses that took place at the archaeological sites in southern Africa are proxied in several lines of evidence including the macro-faunal, micro-faunal, botanical and sedimentological evidence that is preserved. It is possible that the environmental proxies themselves may be biased. Anthropogenic influences (e.g. choice of firewood), excavation, sampling methods and the differential preservation of material may complicate the situation (Allott, 2005). Nevertheless where distinctive environmental shifts are shown to occur, they should have regional manifestations, and they should be recorded in the other sites.

In this analysis the local and regional records are compared with palaeoclimatic data from a number of sites around the world to obtain a global perspective of climate

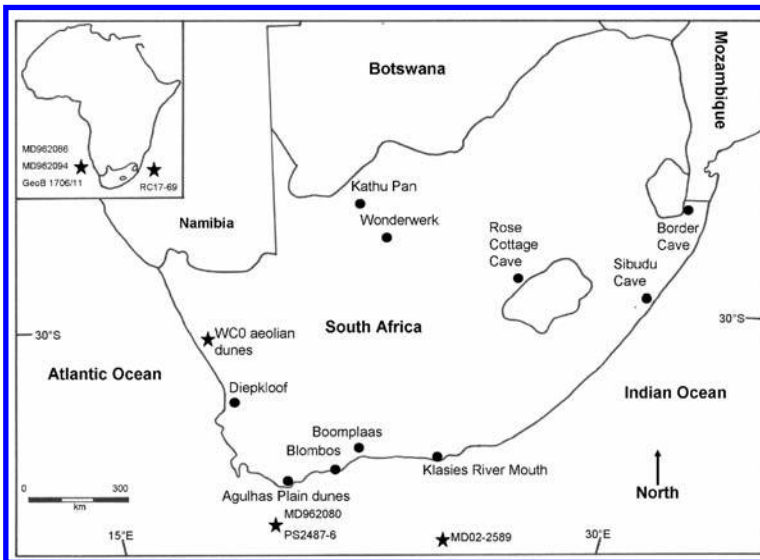


Figure 1. Map of Southern Africa showing the locations of Middle Stone Age archaeological sites, deep sea cores and aeolian sediments mentioned in the text.

change at this time. Lake sediments, speleothems, aeolian deposits and archaeological sites have become a source of palaeoenvironmental proxies at a local terrestrial scale. This paper compares records of climate change for the period 70 ka to 50 ka (MIS 4 and early MIS 3) from a number of ocean cores as well as archaeological, geological and other types of research sites from Southern Africa.

5.2 SIBUDU CAVE

Sibudu Cave, located in KwaZulu-Natal, was the most recent of the MSA sites to be excavated in Southern Africa, and has the advantages of being well-dated and the subject of multi-disciplinary studies. It has an MSA cultural sequence that contains pre-Still Bay, Still Bay, Howiesons Poort, post-Howiesons Poort, late and final MSA stone tool assemblages (Cochrane, 2006; Delagnes *et al.*, 2006; Villa *et al.*, 2005; Villa and Lenoir, 2006; Wadley, 2005, 2007, 2008). Optically Stimulated Luminescence (OSL) ages for 14 sediment samples (Table 1) from the three youngest lithic phases

Table 1. Optically Stimulated Luminescence dates for the pre-Still Bay, Still Bay, Howiesons Poort, post-Howiesons Poort, late and final Middle Stone Age levels from Sibudu Cave (Jacobs and Roberts, 2008; Jacobs *et al.*, 2008a, b).

final MSA	Location	Level	Sample	Age (ka)
SIB11	East	Co	Sediment	34,7 ± 1,7
SIB10	East	Bu	Sediment	35,6 ± 2,0
SIB22	East	LBMOD	Sediment	48,9 ± 2,8
late MSA				
SIB14	North	MOD	Sediment	48,3 ± 2,0
SIB8	North	OMOD	Sediment	48,3 ± 1,8
SIB13	North	OMOD-BL	Sediment	47,0 ± 1,8
SIB7	North	RSp	Sediment	46,6 ± 1,9
SIB12	East	RD	Sediment	49,0 ± 2,0
post-HP				
SIB6	North	BSp	Sediment	58,0 ± 2,1
SIB4	North	SS	Sediment	53,6 ± 2,0
SIB9	North	P	Sediment	59,1 ± 2,2
SIB3	North	Ch2	Sediment	58,6 ± 1,9
SIB2	North	Y1	Sediment	58,2 ± 2,5
SIB1	North	B/Gmix	Sediment	57,8 ± 2,3
Howiesons Poort				
SIB15		GR2	Sediment	61,6 ± 1,5
SIB17		GS2	Sediment	63,8 ± 2,5
SIB19		PGS	Sediment	64,7 ± 1,9
Still Bay				
SIB20		RGS	Sediment	70,5 ± 2,0
Pre-Still Bay				
SIB21		LBG	Sediment	72,5 ± 2,0
SIB24		LBG2	Sediment	73,2 ± 2,3
SIB23		BS	Sediment	77,3 ± 2,2

are available (Jacobs, 2004; Jacobs *et al.*, 2008a, b; Wadley and Jacobs, 2004, 2006); these have weighted mean ages of $57,5 \pm 1,4$ ka (post-Howiesons Poort), $47,6 \pm 1,2$ ka (late MSA) and $35,1 \pm 1,4$ ka (final MSA) (Jacobs *et al.*, 2008a). Ages for the Pre-Still Bay, Still Bay and Howiesons Poort layers are based on seven OSL dates derived from additional sediment samples (Jacobs *et al.*, 2008a, b; Jacobs and Roberts, 2008). Based on these results, the Howiesons Poort occupation falls between 65 ka–62 ka, the Still Bay dates to 70 ka and the Pre-Still Bay to between 75 ka–72 ka (Jacobs *et al.*, 2008a, b; Jacobs and Roberts, 2008). The three broad age clusters, ~58 ka, ~48 ka and ~35 ka and the Howiesons Poort are distinguished by differences in lithic assemblages, environmental characteristics and long hiatuses of $9,8 \pm 1,3$ ka and $12,6 \pm 2,1$ ka (Jacobs *et al.*, 2008a, b; Wadley and Jacobs, 2006). A third hiatus occurred after ~35 ka occupation, lasting until about 1.000 BP.

5.2.1 Sibudu environment during MIS 4

Sedimentological and mineralogical analyses of the Still Bay and Howiesons Poort layers show relatively high percentages of calcite and this suggests higher humidity (Pickering, 2006; Schiegl and Conard, 2006; Wadley, 2006). Magnetic susceptibility data from layers deposited at the end of MIS 4 (~58 ka) imply a cold, glacial climate (Herries, 2006). The cold ~58 ka layers contain gypsum growth within the sediments. However, the magnetic susceptibility data should be viewed with caution, as sedimentological analysis of the deposits indicate that the majority of the sediment is anthropogenic in origin and this may complicate interpretation (Goldberg *et al.*, 2009; Pickering, 2006).

Tree species richness is well correlated with evapotranspiration across a wide range of ecosystems. Changes in evapotranspiration will thus have an influence on trees species composition and distribution on localised site level, as well as on a broad community level (Stephenson, 1998). Local levels of moisture availability at a site are dependent on effective evapotranspiration which is not only affected by precipitation, but a number of factors including aspect, slope, temperature, humidity, wind speed and direction, soil moisture content, depth and type and the presence of rivers (McDowell *et al.*, 2008; Verstraeten *et al.*, 2008). The carbonised seed assemblage prior to 58 ka from Sibudu Cave is predominantly composed of evergreen taxa, implying the presence of closed forested environments (Sievers, 2006; Wadley, 2004). This interpretation is supported by the composition of woody taxa identified in the charcoal assemblage. Taxa such as *Podocarpus*, *Buxus* and *Curtisia*, evergreen forest species are noted. The presence of these species suggests that available moisture was high during this period, but not necessarily higher than present (Allott, 2006). Although the assemblage at this time is dominated by *Podocarpus* species (Allott, 2004, 2005) and the area appears to have been predominantly a forested one, there is evidence for a woodland/savanna community in the vicinity (Allott, 2006). Throughout the MSA occupations at Sibudu there is evidence that a mosaic environment existed around the site, partly due to the location of the site and the continual presence of the Tongati River (Wadley, 2006). Carbonised Cyperaceae (sedges) are present throughout the MSA sequence. Sedges grow in moist conditions and the occurrence of *Schoenoplectus* spp. seeds indicates open water, demonstrating that the Tongati River, that flows in front of the site was perennial during site occupations. Carbon isotope analyses of *Podocarpus* and *Celtis* charcoal from Howiesons Poort layers (65 ka–62 ka) indicate conditions of elevated levels of water availability and humidity (Hall *et al.*, 2006, 2008).

The extensive faunal assemblage provides further evidence of environmental change through time in the Sibudu area. The Howiesons Poort faunal assemblage is dominated (91,4%) by small species preferring semi-closed or closed habitats, such as blue duiker, bushbuck, bush pig and vervet monkey (Clark and Plug, 2008). This supports the botanical evidence for the presence of an evergreen forested environment. In addition, a small suite of species (8,6%), including buffalo and blue wildebeest show the occurrence of open savanna/woodland near the site (Clark and Plug, 2008), supporting the charcoal data (Allott, 2006). This provides further evidence for a mosaic of vegetation types in the area. A large variety of aquatic species including mammals, reptiles, water birds, fish, amphibians and molluscs have been identified (Plug, 2004, 2006) and these, together with the presence of *Schoenoplectus* spp. seeds, demonstrate that the Tongati River was perennial, even in the past.

The micromammal species composition provides further evidence for a cooler, humid forested environment. Two key species, *Cricetomys gambianus* (Giant rat) and *Rhinolophus clivosus* (Geoffroy's horseshoe bat) both require humid conditions. In addition *C. gambianus* cannot tolerate high overall temperatures (Glenny, 2006).

5.2.2 Sibudu environment during MIS 3

Palaeoenvironmental evidence from the post-Howiesons Poort layers ($58,5 \pm 1,4$ ka) indicates a general trend of oscillating warm/cool phases and drier conditions than seen during the Howiesons Poort. Magnetic susceptibility data suggest an initial (~58 ka) very cold environment which became progressively warmer through MIS 4, alternating with brief cool phases (Herries, 2006). Sedimentological and mineralogical analyses reveal a high proportion of gypsum nodules in many of the layers (Pickering, 2006; Schiegl and Conard, 2006; Wadley, 2006). Such gypsum accumulations may be considered an indicator of arid conditions (Goldberg and MacPhail, 2006).

The vegetation patterns show a reduction of forested areas and an increase in more open woodland and grassland communities, reflecting the previous trend of a mosaic environment around the site. Pollen and phytolith data, although limited, reveal the presence of a grass-dominated community and the presence of savanna taxa such as *Acacia* (Renaut and Bamford, 2006; Schiegl and Conard, 2006; Schiegl *et al.*, 2004). The seed assemblage is still dominated by evergreen forest taxa, but it also reveals an increase in the number of deciduous savanna/woodland taxa (Sievers, 2006; Wadley, 2004). The composition of the charcoal assemblage shows a similar trend with the presence of dry-adapted genera such as *Acacia*, *Celtis* and *Ziziphus* and cooler climate indicators such as *Erica* spp. (Allott, 2005, 2006). The presence of riverine forest taxa attest to the continued presence of a mosaic of vegetation communities around the site. A substantial change in the local environment is suggested by the occurrence of a pioneer shrub species, *Leucosidia sericea* (which at present does not occur near the coast) (Allott, 2006).

Micromammal evidence for a significant environmental shift at the same time is derived from the identification of another habitat specific pioneer species, *Mastomys natalensis* (Natal multimammate mouse) which does not inhabit forested areas (Glenny, 2006). Carbon isotope values from *Podocarpus* and *Celtis* charcoal from ~58 ka layers are less negative than those from the earlier Howiesons Poort layers, suggesting that both species were responding to more arid conditions at ~58 ka (Hall *et al.*, 2006, 2008).

The faunal species composition of the ~58 ka layers (post-Howiesons Poort) shows a dramatic shift in response to the changing environment. At this time the

highest proportion of large grazing species are recorded indicating an open environment with increased grass cover (Wadley *et al.*, 2008). Small bovid species are less frequent and larger savanna/woodland species such as giraffe, zebra, blue wildebeest and red hartebeest dominate the assemblage (Cain, 2005, 2006; Clark and Plug, 2008; Plug, 2004; Wadley *et al.*, 2008; Wells, 2006). A recent analysis of the fauna (Clark and Plug, 2008) shows that during the youngest post-Howiesons Poort layers there was predominantly open savanna/woodland with large grazers. Prior to this, there was still a riverine forest community, along with the savanna/woodlands. The occurrence of a riverine forest faunal community during the early phase of the post-Howiesons Poort suggests that the transition between forest and grassland during MIS 4 and MIS 3 was gradual, rather than abrupt.

5.3 ARCHAEOLOGICAL EVIDENCE OF ENVIRONMENTAL CHANGE FROM OTHER MSA SITES IN SOUTH AFRICA

Improvements in OSL, Electron Spin Resonance (ESR) and uranium-series (U-Th) dating should allow correlations between available environmental proxies from Sibudu and other MSA sites. However there are complications. When comparing the chronologies for the distinctive stone tool technical complexes between sites, it is clear that there are some discrepancies. An underlying assumption is that these stone tool assemblages would be ubiquitous and autochthonous, and that the timing of their rise and demise should be well matched. The transition from Still Bay to Howiesons Poort is not synchronous across MSA sites, and the assemblage that precedes the Howiesons Poort is not always designated Still Bay. This may be because the Still Bay is of very short duration and does not always occur in all sequences. However, it is likely that the problem lies with the precision and accuracy of the dating techniques. The dating conundrum complicates attempts to fine-tune palaeoenvironmental evidence across space or through time. For consistency in this study, the most recently published luminescence ages are used (where available), but earlier published dates based on other methods have been noted (Table 2).

A summary of palaeoenvironmental evidence from Sibudu Cave and these sites is presented in Figure 2 and Table 2. The majority of these sites are located on or near to the coast, particularly in the southern Cape. Exceptions are Rose Cottage Cave, Border Cave and Wonderwerk Cave which are located in the South African interior.

5.3.1 Palaeoenvironmental evidence from archaeological sites during MIS 4

Evidence from Border Cave, northern KwaZulu-Natal, suggests fluctuating environmental conditions between 80 ka and 60 ka. Proxy data from cave sediments (Butzer *et al.*, 1978), microfauna (Avery, 1982, 1992) and macrofauna (Deacon and Lancaster, 1988; Klein, 1977) indicate that conditions were cooler and moister than present. Local vegetation communities comprised extensive *Podocarpus* dominated forest and thick bush towards the end of MIS 4. As with Sibudu Cave there is evidence for a hiatus from about 58 ka. Evidence of spring activity and rock spalling from the Howiesons Poort sediments of Rose Cottage Cave, eastern Free State Province, suggest that conditions in this area were also colder and moister than present (Deacon and Lancaster, 1988). Charcoal and pollen analyses indicate that there were complex changes in the vegetation. Prior to the Howiesons Poort occupation the local vegetation comprised riverine and other well-watered communities. Vegetation diversity decreased during

Table 2. Summary table for Sibudu Cave and other Middle Stone Age sites cited. The age range, dating techniques and dating references is provided for each site.

Site	Age range	Dating techniques	Dating references
Sibudu Cave	Iron Age: ~1.000 BP	Radiocarbon (¹⁴ C)	Wadley and Jacobs, 2004
	final MSA: ~35 ka	OSL	Jacobs, 2004
	late MSA: ~48 ka	OSL	Jacobs and Wadley, 2006
	post-HP: ~58 ka	OSL	Jacobs et al., 2008a, b
	HP: 65 ka–62 ka	OSL	Jacobs and Roberts, 2008
	Still Bay: 70,5 ka	OSL	
	Pre-Still Bay: 77 ka–72 ka	OSL	
Border Cave	Iron Age	Radiocarbon (¹⁴ C)	Butzer <i>et al.</i> , 1978; Beaumont <i>et al.</i> , 1978
	ELSA: ~38 ka	AAR	Miller <i>et al.</i> , 1993
	Howiesons Poort: ~55–75 ka MSA II	ESR	Grün et al., 1990a Grün and Beaumont, 2001
Rose Cottage Cave	LSA	Radiocarbon (¹⁴ C)	Wadley and Vogel, 1991
	ELSA: ~29–40 ka	OSL	Jacobs, 2004; Pienaar <i>et al.</i> , 2008
	post-HP: 56 ka	TL	Tribolo <i>et al.</i> , 2005; Woodborne and Vogel, 1993
	Howiesons Poort: 65 ka–63 ka		Jacobs and Roberts, 2008
Klasies River	MSA III: ~>45–50 ka	Radiocarbon (¹⁴ C)	Vogel, 2001
	Howiesons Poort: 65 ka–63 ka	AAR	Bada and Deems, 1975
	Pre-HP: 72 ka–71 ka	OIS correlation	Deacon and Geleijnse, 1988; Shackleton, 1982
	MSA II: ~75–94 ka	Palaeoenviro-proxies	Butzer, 1978; Deacon, 1989
	MSA I: ~90–115 ka	Uranium series OSL ESR	Vogel, 2001 Feathers, 2002; Tribolo <i>et al.</i> , 2005 Grün <i>et al.</i> , 1990b Jacobs and Roberts, 2008

(Continued)

Table 2. (Continued).

Site	Age range	Dating techniques	Dating references
Boomplaas Cave	LSA	Radiocarbon (^{14}C)	Fairhall <i>et al.</i> , 1976
	ELSA: ~21 ka post-HP: >40 ka Howiesons Poort: ~55–65 ka	Palaeoenviro-proxies U-Th AAR	Deacon <i>et al.</i> , 1984 Vogel, 2001 Brooks <i>et al.</i>, 1993; Miller <i>et al.</i>, 1999
Blombos Cave	LSA: ~2 ka 3 MSA phases, including	Radiocarbon (^{14}C)	d'Errico <i>et al.</i> , 2001
		OSL	Henshilwood <i>et al.</i> , 2001; Vogel <i>et al.</i> , 1999
	Still Bay: 85 ka–76 ka, 73 ka MSA 2: ~99–143 ka	ESR TL	Jacobs, 2004, 2005; Jacobs <i>et al.</i>, 2003a, 2003b, 2006 Jones, 2001 Tribolo <i>et al.</i>, 2005, 2006
Diepkloof	LSA: ~1800 BP	Radiocarbon (^{14}C)	Parkington and Poggenpoel, 1987; Parkington, 1990
	Howiesons Poort: 63 ka–58 ka	Radiocarbon (AMS)	
	Still Bay: 73 ka–71 ka	OSL TL	Parkington, 1999 Parkington <i>et al.</i> , 2005 Tribolo, 2003, Tribolo <i>et al.</i> , 2005 Jacobs and Roberts, 2008
Wonderwerk Cave	MSA (incl'd Howiesons Poort): ~70–220 ka	U-Th	Johnson <i>et al.</i> , 1997
		AAR	Johnson <i>et al.</i> , 1997 Beaumont and Vogel, 2006

the Howiesons Poort suggesting a drying trend (Wadley *et al.*, 1992). Wonderwerk Cave, in the Northern Cape Province, has yielded non-archaeological evidence from sedimentary (Beaumont and Vogel, 2006; Butzer, 1984a, b; Butzer *et al.*, 1979) and faunal (Avery, 2006; Beaumont, 1990) analyses of the cave deposits. The site was not occupied from 70 ka until 12,5 ka, but sediment layers were formed by natural processes. These non-archaeological data suggest that prior to 30 ka the local environment was drier and colder than present, with grazers present throughout the sequence. This is thought to be due to very low rainfall conditions in the interior of South Africa between MIS 4 and MIS 2, when it has been estimated that rainfall was about 60% lower than present values (Johnson *et al.*, 1997).

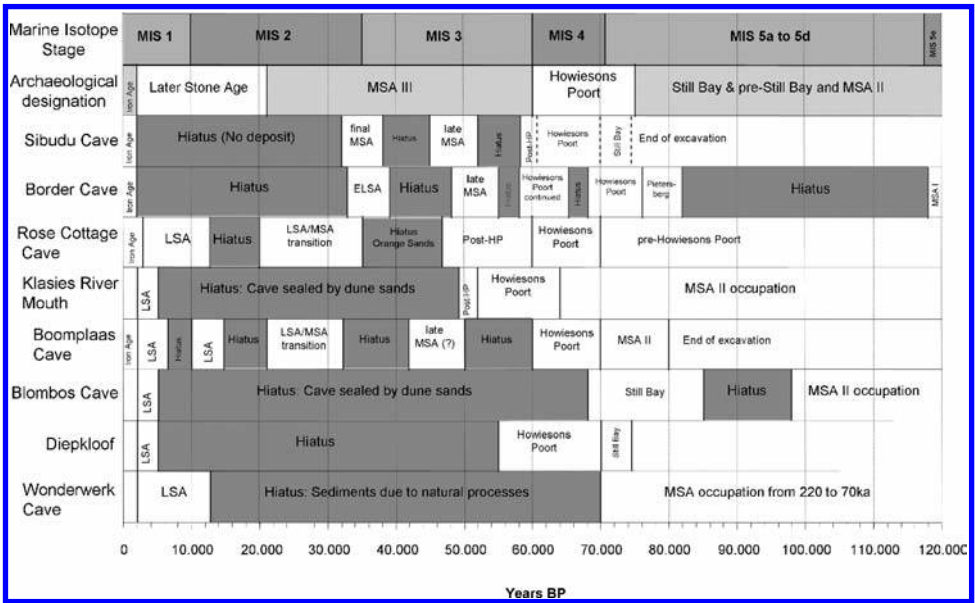


Figure 2. Summary graph of Marine Isotope Stages 1 to 5, archaeological designations and occupation/hiatus periods for Sibudu Cave and other Middle Stone Age sites from South Africa during the last 120 ka.

Klasies River Mouth, a complex of caves and overhangs on the southern Cape coast has provided faunal, botanical and geological evidence from the MSA II, Howiesons Poort and post-Howiesons Poort levels, suggesting a shift from cooler in MSA II to more moderate conditions in the post-Howiesons Poort. Environmental interpretations from this site are complicated by rising and falling sea levels under interstadial and stadial conditions, respectively, and there are some inconsistencies amongst the ages and cultural designations of the various levels, so interpretations should be made with care. The MSA II faunal assemblage is dominated by browsers (86%) indicating a bushy/wooded terrestrial environment. The presence of Antarctic/sub-Antarctic marine mammals suggests a colder marine environment than seen during the Holocene (Deacon and Lancaster, 1988). During the Howiesons Poort there is an increase in grazing species suggesting the presence of grasslands (Deacon, 1989, 1995; Deacon and Lancaster, 1988; Singer and Wymer, 1982) and cooler, possibly drier conditions than recorded for the MSA II levels (Avery, 1992, Klein, 1976, 1983; Thackeray, 1992, Thackeray and Avery, 1990). The $\delta^{18}\text{O}$ values of shell samples from MSA I through the Howiesons Poort and MSA III deposits also suggest a cooling trend (Deacon and Lancaster, 1988) through MIS 4. Palaeoenvironmental reconstructions from the Howiesons Poort levels of Boomplaas Cave, southern Cape, are based on faunal assemblages (Avery, 1982; Deacon *et al.*, 1984) and charcoal and pollen analyses (Scholtz, 1986). During MIS 4 environmental conditions were extremely harsh, being much colder and drier than present. The site of Blombos Cave on the southern Cape coast has no Howiesons Poort occupation, only evidence of the earlier Still Bay and MSA II phases. The site was sealed by dune sands from ~70 ka until 2000 BP (Jacobs *et al.*, 2006). Proxy data from marine fauna and shellfish assemblages and geological analyses indicate a transition between warm conditions during MIS 5a to colder conditions during MIS 4 (Henshilwood *et al.*, 2001). Faunal (Parkington *et al.*, 2005), charcoal (Cartwright and

Parkington, 1997) and sedimentological (Butzer, 1979) analyses from Diepkloof rock shelter in the north-western Cape indicate that during the Howiesons Poort occupations the climate was cooler and moister than present. Charcoal assemblages from this period contain afro-montane species such as *Podocarpus* and *Kiggelaria* which require year-round moisture (Cartwright and Parkington, 1997).

5.3.2 Palaeoenvironmental evidence from archaeological sites during early MIS 3

Evidence from sites in the interior of South Africa is presented first again, followed by evidence from the coastal sites. Based on proxy data from Border Cave, the local vegetation shifted from dense woodland communities to more open woodland savanna with variations in the amount of grass versus bush at the beginning of MIS 3 (Avery, 1982; Butzer *et al.*, 1978; Klein, 1977). These shifts are in-line with the Sibudu environmental records. At Rose Cottage Cave the environment appears to have become colder than in MIS 4 and there is evidence of more mesic conditions (Wadley *et al.*, 1992). There is a hiatus after the post-Howiesons Poort occupation indicated by a layer of almost culturally sterile orange sand that lasted from ~48 ka–~35 ka (Harper, 1997). Although no archaeological evidence is available from Wonderwerk Cave during this time, sedimentary evidence (Beaumont and Vogel, 2006; Butzer, 1984a, b) indicates that the environment was generally dry.

At Klasies River Mouth, faunal evidence from post-Howiesons Poort levels shows a further increase in grazing species compared with the Howiesons Poort levels. This indicates a continuation in the shift to more open grasslands and cooler conditions in early MIS 3. After 50 ka the sites were sealed by dune sands (Butzer, 1978; Deacon and Lancaster, 1988; Singer and Wymer, 1982). Oxygen isotope data from shell samples from this period confirm the cooling trend (Deacon and Lancaster, 1988). At Boomplaas Cave charcoal studies indicate that during early MIS 3 (60 ka–50 ka) a cold, very dry harsh climate prevailed, based on the range of woody species reflected (Scholtz, 1986). From ~55 ka to 40 ka conditions began to ameliorate (Deacon and Lancaster, 1988). In general, evidence from Boomplaas suggests that MIS 3 was cooler and moister than the subsequent Last Glacial Maximum (Deacon *et al.*, 1984). A series of occupational hiatuses occurred after the Howiesons Poort (Deacon, 1979). No environmental evidence is available from Blombos Cave because the site was sealed by dune sands during this time (Henshilwood *et al.*, 2001). Charcoal data from Diepkloof indicates a change in the selection of firewood species composition at this time suggesting a shift to drier conditions (Cartwright and Parkington, 1997; Parkington *et al.*, 2005). This shift to drier conditions is supported by the dominance of larger grazing species in the faunal assemblage (Parkington *et al.*, 2005).

During MIS 4 and early MIS 3, climatic conditions were extremely variable and resulted in the majority of the sites being abandoned for prolonged periods when conditions were unsuitable for human occupation (Figure 2). Assuming that the landscape was abandoned by people due to environmental conditions, it is interesting that occupation at sites in the eastern summer-rainfall region of South Africa (Sibudu Cave, Border Cave and Rose Cottage) persisted after the western (including the winter-rainfall zone) sites were abandoned. Environmental evidence from the various sites suggests that the eastern regions experienced greater precipitation than the more arid western regions. Towards the end of MIS 3 and through MIS 2 the environment over much of central South Africa was extremely harsh and sites in this area were unoccupied for periods of up to 60,000 years. During MIS 2 western South Africa appears to have been wetter than present conditions (Chase and Meadows, 2007). Climatic

conditions in the eastern regions were more favourable for longer periods, but during MIS 2, most sites show intermittent occupations or an absence of occupation.

5.4 OTHER TERRESTRIAL RECORDS OF PALAEO-CLIMATE CHANGE

In South Africa terrestrial palaeoclimatic records from numerous caves, lacustrine, spring, fluvial and coastal systems provide proxy data from different climate zones across the country. Butzer (1984a, b) compiled a series of proxy records based on sedimentological and lithostratigraphic analyses from a number of such sites. During MIS 4 and early MIS 3, the southern Cape region experienced humid to sub-humid conditions, the south-western Cape was semi-arid, south-central and eastern South Africa was initially cold and humid during MIS 4, becoming warmer and humid during MIS 3 and the northern portions of the country were cold and arid. Palynological and sedimentological evidence from Agulhas Plain lunette dune accretion from two pans in the southern Cape region (Figure 1) suggest that from the end of MIS 4 and early MIS 3 conditions became slightly drier or similar to present conditions (Carr *et al.*, 2006). Indications of arid and cold conditions in the northern regions are supported by a range of pollen data from the sites of Florisbad, Wonderwerk Cave and Kathu Pan, located in the northern and north-central parts of South Africa (Figure 1). The pollen data suggests that between ~75 ka–64 ka this area was extremely arid and cold (van Zinderen Bakker, 1995).

The Pretoria Saltpan (Tswaing Crater), a meteorite impact north-east of Tshwane in the Gauteng Province, provides a rainfall record for the last 200 ka (Partridge, 1999; Partridge *et al.*, 1997; 1999). The rainfall data show a decrease between 70 and 60 ka associated with decreasing insolation (Figure 3), however the interpretations should be made cautiously as relative dating methods were used at the site. The data show that the eastern summer rainfall area of South Africa was becoming drier at this time. This would have affected the vegetation communities around Sibudu Cave and Border Cave. The forested environments would have been reduced to river/stream margins and an expansion of woodland and grassland savanna communities would have occurred.

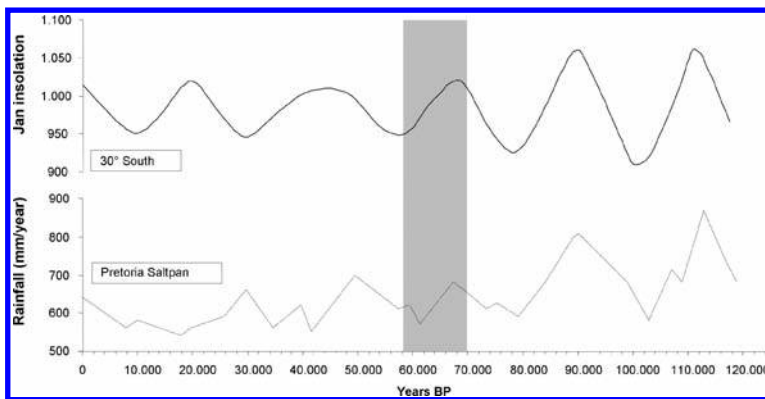


Figure 3. Southern African January insolation, 30° south (Partridge *et al.*, 1997) and Pretoria Saltpan (Tswaing Crater) tuned rainfall (mm/year) time series (Partridge *et al.*, 1997). The shaded area indicates the period of interest for this study.

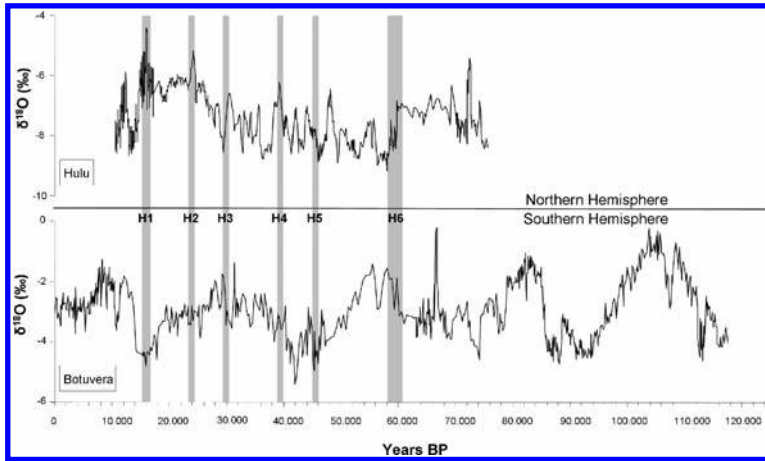


Figure 4. High-resolution $\delta^{18}\text{O}$ time series from northern and southern hemisphere speleothems for the last 120 ka. Dansgaard/Oeschger events 20–17 (numbered) and Heinrich events 1–6 (shaded areas) are presented. Top: Combined oxygen isotope ratios from five speleothems from Hulu Cave, China (Wang *et al.*, 2004). Bottom: Oxygen isotope ratios from speleothems from Botuvera Cave, southeastern Brazil (Cruz *et al.*, 2005).

Oxygen isotope time series from U-Th dated speleothems from two sites in South America, Bahia State (NE Brazil) and Botuvera Cave (SE Brazil) provide a record of oscillating temperatures and aridity (Figure 4). During MIS 4, conditions were cool and wet followed by warmer and drier environments during early MIS 3 (Cruz *et al.*, 2005; Wang *et al.*, 2004).

The Botuvera speleothem $\delta^{18}\text{O}$ record shows a notable spike at ~70 ka indicating a very wet period and then an abrupt shift to an arid period, suggesting a shift to glacial conditions in MIS 4. This is in contrast to results from the $\delta^{18}\text{O}$ records (Figure 4) from the northern hemisphere Hulu Cave speleothems, which show that between 70 ka and 55 ka conditions were warm and dry before abruptly becoming cool and wet (Wang *et al.*, 2001).

The long term variability of East African climates has been reconstructed using a series of drill cores from Lake Malawi and Lake Tanganyika (Cohen *et al.* 2007, Scholz *et al.*, 2007). Between 135 ka–70 ka these regions experienced episodic periods of extremely arid conditions. After 70 ka the climate seems less variable and overall conditions became more humid and general moisture availability increased. This is thought to be due to diminished precessional scale variability (Cohen *et al.*, 2007). These post 70 ka conditions are similar to those indicated by the Hulu speleothems and suggest that the East African climate was more likely influenced by changes occurring in the northern hemisphere.

5.5 PALAEOENVIRONMENTAL EVIDENCE FROM SOUTHERN AFRICAN DEEP SEA CORES

Deep sea cores along the western, southern and eastern coasts of southern Africa provide evidence of the local manifestation of global climatic changes during MIS 4 and early MIS 3. Cores from the Walvis Ridge and Namibian continental slope along the western coast of southern Africa (Figure 1) provide a record of climatic variability

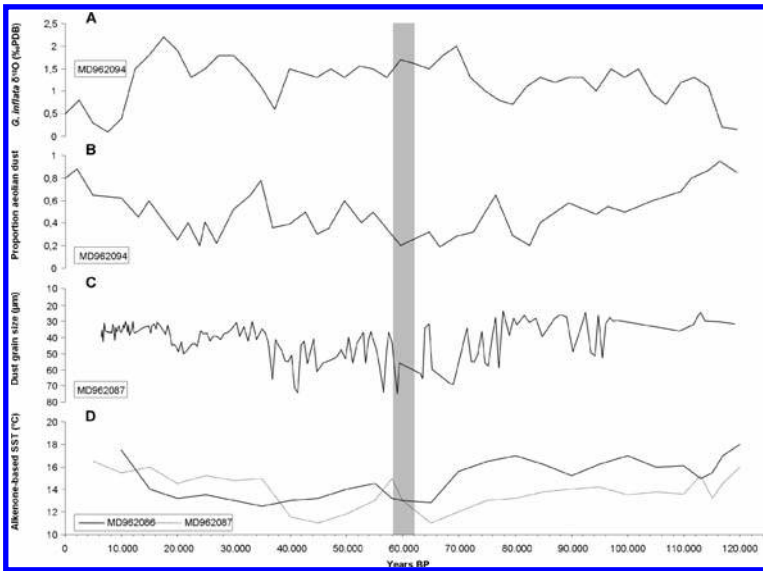


Figure 5. Palaeoenvironmental proxy data sets from deep sea cores of the western coast of southern Africa for the last 120 ka. Age models and stratigraphy of the cores are mostly created by correlating $\delta^{18}\text{O}$ records of selected planktonic and/or benthic foraminifera with the SPECMAP record developed by Imbrie *et al.* in 1984. The shaded area indicates the period of interest for this study. A: $\delta^{18}\text{O}$ record for *Globorotalia inflata* from deep sea core MD962094 (Stuut *et al.*, 2002). B: The proportion of aeolian dust from deep sea core MD962094 (Stuut *et al.*, 2002). C: Time series of dust grain size (μm) from deep sea core MD962087 (Pichevin *et al.*, 2005). D: Alkenone-based sea surface temperatures (SST) for deep sea cores MD962086 and 87 (Pichevin *et al.*, 2005).

regulated by shifting climatic fronts during glacial and interglacial periods (Little *et al.*, 1997; Pichevin *et al.*, 2005; Stuut *et al.*, 2002). The $\delta^{18}\text{O}$ records of *Globorotalia inflata*, a pelagic foram (Figure 5A) and the proportion of aeolian dust (Figure 5B) from MD962094 indicate intensified south-east trade winds and enhanced winter rainfall during MIS 4 and relatively arid conditions during MIS 3 (Stuut *et al.*, 2002, 2004). Several cores, MD962094, GeoB1706, 1711, and MD962086/87 provide records of variation in upwelling events of the cold Benguela Current that flows northwards along the western coast of southern Africa. Upwelling is controlled by the relative position of the Subtropical Convergence Zone which affects the heat flux into the southern Atlantic Ocean from rings of warm water spawned from the Agulhas Current Retroflexion (Little *et al.*, 1997). Geochemical, micropalaeontological and isotope records from GeoB1706 and 1711 show that during MIS 4-3 increased upwelling of cold nutrient-rich water occurred (Little *et al.*, 1997). Weaker trade winds during MIS 3 resulted in warmer water from the Agulhas Current to move into the colder Benguela region (Pichevin *et al.*, 2005). South-east trade winds show increased intensity during glacial periods resulting in increased upwelling (Pichevin *et al.*, 2005; Stuut *et al.*, 2002). Dust grain-size (Figure 5C) data from MD962087 and alkenone-based sea surface temperatures from MD962086/87 (Figure 5D) indicate a similar pattern. Evidence for humid conditions during glacial periods and drier conditions during interglacials is derived from OSL dated cores (WC03-1, 2, 5, 10, 11 and 18) taken from aeolian dune sands along the west coast of South Africa (Figure 1) (Chase and Thomas, 2006, 2007). Changes in the sediments were related to variations in moisture, wind strength and

sediment supply. There were periods of increased activity/deposition of aeolian sands during MIS 4 associated with increased humidity (Chase and Thomas, 2006, 2007). The study area is within the winter rainfall zone of South Africa. Rainfall in this area is influenced by westerly temperate frontal systems and these are thought to be more vigorous during glacial periods, resulting in wetter conditions (Barrable *et al.*, 2002).

Cores PS2487-6 from the Agulhas Retroflexion and MD962080 from the Western Agulhas Bank (Figure 1) provide records of variation in the frequency and intensity of Agulhas warm water leakages, responses to shifts in the STCZ and global changes (Flores *et al.*, 1999, Rau *et al.*, 2002). $\delta^{18}\text{O}$ and $\delta^{13}\text{C}$ records, foraminifera species assemblages and sediment composition and texture show that during glacial periods (MIS 2, 3, 4) there was a northwards displacement of the STCZ and an eastward movement of the Agulhas Retroflexion (Flores *et al.*, 1999; Rau *et al.*, 2002). Further evidence for changes in ocean current circulation patterns comes from core MD02-2589 on the southern Agulhas Plateau, where isotopic and grain-size data indicate a northward shift of the Antarctic Circumpolar Current (Molyneux *et al.*, 2007) which would have had an impact on the Agulhas Current. An eastward shift of the Agulhas Retroflexion would have an impact on environmental conditions along the eastern coast of southern Africa and may be a factor determining the environmental changes seen in the local Sibudu environment at around 60 ka. It has been demonstrated that the Agulhas Current has a significant influence on the summer rainfall patterns of the eastern coast at a variety of timescales (Cook *et al.*, 2004).

Core RC17-69, off the eastern coast of KwaZulu-Natal (Figure 1) was influenced by the warm Agulhas Current. Foraminifera assemblages from this core suggest that during glacials, the Agulhas Current was weakly developed in summer months and may have been replaced by cooler subtropical waters during winter months (Hutson, 1980). During the LGM the current was seasonably variable and heat transport from tropical latitudes was reduced (Prell and Hutson, 1979; Prell *et al.*, 1980a, b). The cooling or reduction of the Agulhas Current during MIS 4 (~60 ka), coupled with glacial conditions, would have had a significant impact on the environment of the east coast of southern Africa (Reason and Mulenga, 1999). Oxygen isotope records from core MD 73-025, south of Madagascar, and RC17-69 do indicate a cooler period during MIS 4 (Prell and Hutson, 1979; Shackleton, 1977; Tyson, 1991).

5.6 DISCUSSION AND CONCLUSION

Oxygen and deuterium isotope sequences from Greenland (GRIP, N-GRIP, GISP2) and Antarctic (Vostok, Epica, Byrd) ice cores (Figure 6) show that MIS 4 was a period during which the earth emerged from near glacial conditions (the ice core data for 65 ka are almost analogous to those of 22 ka, which is considered to be the height of the last glacial). The problem of mid-latitude ecosystem responses is complicated by differences between the northern and southern hemisphere records, particularly regarding the timing of major events (e.g. Blunier *et al.*, 1998; Blunier and Brook, 2001; Jansen *et al.*, 2007; Leuschner and Sirocko, 2000; Petit *et al.*, 1999; Schmittner *et al.*, 2003). This makes it difficult to determine whether ecosystem changes are responding to Northern or Southern Hemisphere forcing, or whether low- to mid-latitude forcing of climate change took place. Earlier studies (e.g. Blunier *et al.*, 1998; Blunier and Brook, 2001, Leuschner and Sirocko, 2000, Petit *et al.*, 1999) suggested that the timing of large southern hemisphere climate events lead the northern hemisphere by 1500–3000 years. More recent research suggests that the south leads the north by approximately 400–500 years (Schmittner *et al.*, 2003).

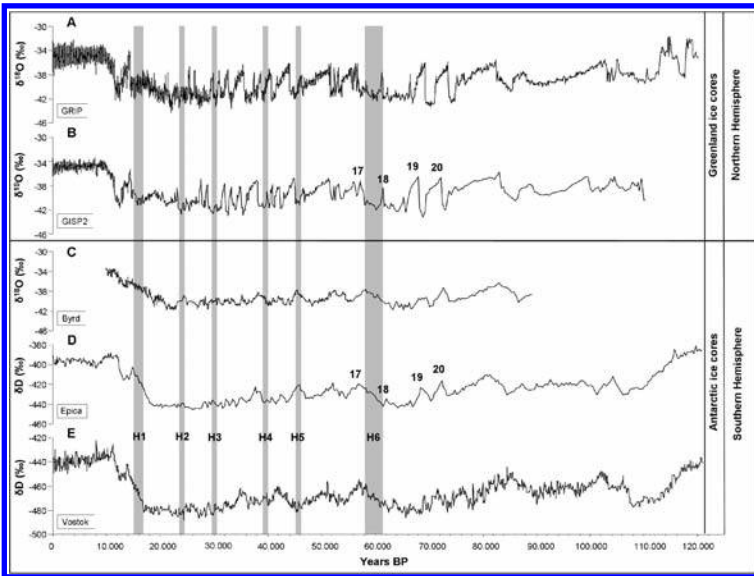


Figure 6. High-resolution $\delta^{18}\text{O}$ and δD time series from northern and southern hemisphere ice cores for the last 120 ka. Dansgaard/Oeschger events 20–17 (numbered) and Heinrich events 1–6 (shaded areas) are presented. A: Oxygen isotope ratios from GRIP, Greenland (Blunier and Brook, 2001). B: Oxygen isotope ratios from GISP2, Greenland (Blunier and Brook, 2001). C: Oxygen isotope ratios from the Byrd ice core, Antarctica (Blunier and Brook, 2001). D: Deuterium isotope ratios from the Epica ice core, Antarctica (Jouzel *et al.*, 2004). E: Deuterium isotope ratios from the Vostok ice core, Antarctica (Petit *et al.*, 2001).

Where global climatic changes are synchronous in the northern and southern high latitude records, they should manifest in low latitude regional and local palaeoenvironmental records. In both Greenland and Antarctic ice cores, rapid increases in air temperatures of 5–10°C (Landais *et al.*, 2007; Rahmstorf, 2002) are followed by a rapid return to cold (stadial) conditions. Notable cold phases called Dansgaard/Oeschger (DO) events (Dansgaard *et al.*, 1984; Oeschger *et al.*, 1984) occur with 1000, 1450 and 3.000 year cyclicities (Leuschner and Sirocko, 2000). Twenty-two DO events have been identified in the Greenland ice cores and nine corresponding DO events have been identified in the Antarctic cores (Bender *et al.*, 1994). Antarctic DO events are characterised by slower warming and cooling than Greenland events (Bender *et al.*, 1994).

Significant DO events are followed by massive episodic discharges of icebergs from the Laurentide and Scandinavian ice-sheets and are called Heinrich events (Bond *et al.*, 1993; Heinrich, 1988; Leuschner and Sirocko, 2000; Rahmstorf, 2002). Heinrich events always occur during cold stadials and are followed by an abrupt shift to warmer climatic conditions (Bond *et al.*, 1993; Rahmstorf, 2002). Between ~70 ka and 50 ka (MIS 4 and 3) Greenland oxygen and deuterium isotope records (Figure 6 A and B) from the GRIP (Blunier and Brook, 2001; Grootes *et al.*, 1993), GISP2 (Blunier and Brook, 2001) and N-GRIP (Landais *et al.*, 2007; Jouzel *et al.*, 2005, 2007) ice cores, and Antarctic records from the Byrd (Blunier and Brook, 2001), Epica (Jouzel *et al.*, 2005) and Vostok (Petit *et al.*, 1999) ice cores (Figure 6 C, D and E) show that DO events 20–17 and H6 are documented in both the Northern Hemisphere and Southern Hemisphere. The isotopic excursions are not as great in Antarctica and the changes are not as abrupt as those in Greenland (Bender *et al.*, 1994). This can be clearly seen during H6, between DO 18 and DO 17 in Antarctica where $\delta^{18}\text{O}$ and δD values

gradually become less negative indicating a slower warming trend than that seen in the Greenland records. The changes should therefore have an environmental impact at low latitudes.

Linking the terrestrial ecosystem and environmental proxies to climate change proxies requires consideration of the Earth System, and in particular the role of ocean currents in heat distribution. The difference in the rate of change in the Northern and Southern Hemispheres is possibly due to changes in the global thermo-haline circulation (Schmittner *et al.*, 2003). A change in the northward circulation of warmer water from the southern oceans (reduction of the warm Agulhas Current eddies) into the Atlantic Ocean would result in a cooling of the northern latitudes and warming in the southern latitudes (Blunier *et al.*, 1998; Blunier and Brook, 2001; Rahmstorf, 2002; Schmittner *et al.*, 2003; Stocker, 2000, 2002). The Agulhas Current plays a significant role in determining the weather patterns over southern Africa, and hence DO events should be recognisable in the palaeoenvironmental records of the region. However the correlation may not be as simple as a teleconnection. Palaeoclimatic data from core MD97-2120, east of New Zealand, suggests that southern hemisphere mid and low latitude climates were more variable than can be inferred from the Antarctic ice core data (Pahnke *et al.*, 2003; Pahnke and Zahn, 2005). This highlights the need to examine a range of proxy data sets derived from both marine and terrestrial sites to improve understanding of regional and local climatic variability through time.

Focussing on the Southern Hemisphere, an important observation in the Antarctic data sets is the similarity between the climatic conditions during MIS 4 and MIS 2, the Last Glacial Maximum (LGM). This is not limited to the $\delta^{18}\text{O}$ and δD records. The dust, Fe, Ca and other chemical flux records from the Vostok and Epica ice cores (Figure 7) are proxies for sea ice extent (sodium (Na) flux); marine biological productivity (sulphate (SO_4) flux); aridity of surrounding continents (Iron (Fe), calcium (Ca), dust, methane (CH_4)); aerosol fluxes of marine, volcanic, terrestrial, cosmogenic and anthropogenic origin and direct records of changes in atmospheric gas (CO_2) composition (Petit *et al.*, 1999; Wolff *et al.*, 2006). The data all suggest that during MIS 4 conditions were as severe as those during the cold and dry MIS 2, but not as prolonged. By gathering more evidence for the environmental manifestations this may contribute to a better understanding of why a shift to interglacial conditions occurred at the end of MIS 2, but did not occur at the end of MIS 4 despite the apparent similarity in precursive conditions.

The local manifestation of the global-scale climate events has been reviewed in this paper. Sibudu Cave has yielded the most comprehensive record for the region. Faunal and botanical assemblages, cave sediments, magnetic susceptibility of sediments, geology and carbon isotope analysis of charcoal show that at the end of MIS 4 the environment around Sibudu Cave was humid and cooler than present, supporting a substantial evergreen forest with patches of drier, open woodland/savanna (Table 2). The shifts seen in the plant and animal communities preserved in the ~58 ka layers provide evidence for oscillating climatic conditions into MIS 3. Evidence from more recent layers implies alternating cooler and warmer conditions with an overall warming trend, although temperatures remained lower than present (Herries, 2006). The forested area that existed in the pre-60 ka period may have been reduced by ~58 ka, allowing more open woodland and grassland communities to develop during the cooler and drier phase.

During the warmer phases of MIS 3, grasslands decreased and woodland savanna predominated. Indirect evidence for a dramatic climate change between the ~58 ka and ~48 ka occupations is suggested by a hiatus of 9.8 ± 1.3 ka between these two occupational phases (Jacobs *et al.*, 2008a, b; Jacobs and Roberts, 2008). This hiatus coincides with a period of colluviation between 56 ka–52 ka, an indication of

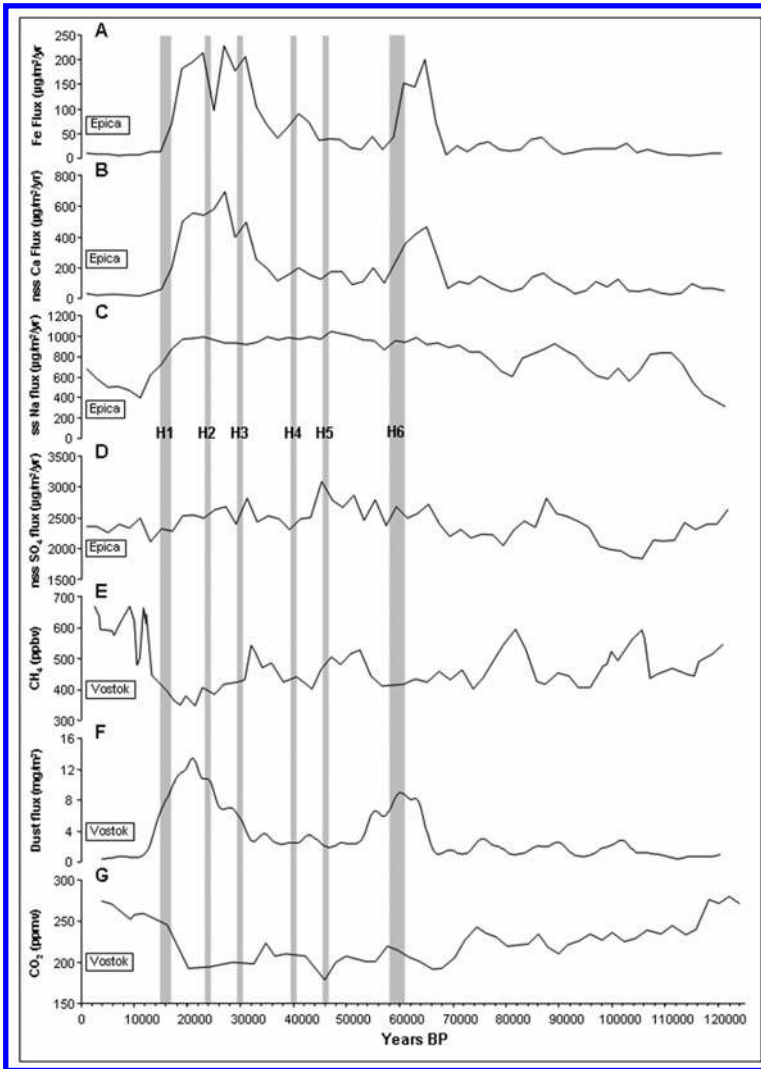


Figure 7. Chemistry data time series from the Epica and Vostok ice cores, Antarctica for the last 120 ka. The shaded areas indicate Heinrich events 1–6. A: Iron (Fe) flux from Epica (Wolff *et al.*, 2006). B: Non sea salt calcium (nssCa) flux from Epica (Wolff *et al.*, 2006). C: Sea salt sodium (ssNa) flux from Epica (Wolff *et al.*, 2006). D: Non sea salt sulphate (nssSO₄) flux from Epica (Wolff *et al.*, 2006). E: Methane (CH₄) variability from the Vostok ice core (Chappellaz *et al.*, 1990). F: Dust flux record from the Vostok ice core (Petit *et al.*, 1990). G: Carbon dioxide (CO₂) concentrations from the Vostok ice core (Barnola *et al.*, 1987).

arid conditions or transitional climates with reduced vegetation cover, recorded from a series of well-dated stratigraphic sequences from erosion gullies in KwaZulu-Natal (Botha, 1996, Botha and Partridge, 2000, Botha *et al.*, 1992, Clarke *et al.*, 2003, Wintle *et al.*, 1995). Environmental conditions were likely unsuitable for the use of the shelter as a permanent dwelling during hiatus periods, perhaps because of a particularly arid phase (Jacobs *et al.*, 2008a, b).

The predominant forest type in KwaZulu-Natal is classified as part of the Indian Ocean coastal belt biome (Mucina *et al.*, 2006) and it requires high moisture levels

(rainfall, humidity). Forested communities are also constrained by the local substrate and therefore migration over time to more suitable areas is not a viable option (Eeley *et al.*, 1999). During colder and drier periods such as during early MIS 3 the forested areas would have been reduced.

Evidence for glacial conditions in the southern hemisphere during MIS 4 and a shift to an ameliorating climate in MIS 3 has been recovered from Antarctic ice cores, deep sea cores and speleothems. These are similar to the harsh cold conditions seen in the LGM (MIS 2). The proxy environmental data from deep sea cores and other sites from the eastern region of South Africa indicate that between 70 ka and 60 ka the prevailing climatic conditions were colder and wetter than present. However, during MIS 3 temperatures began to slowly rise. Rainfall data from the Tswaing Crater indicate that rainfall began to decrease during this time, in response to decreasing insolation. On the western portion, proxy data from deep sea cores and aeolian dune sand deposits indicate colder and humid conditions with increasing wind strengths associated with lower Sea Surface Temperatures (SST) and increased cold water upwelling along the western coast during MIS 4 and MIS 3. Prior to 70 ka, the south-western proxy data suggests that relatively arid conditions persisted. Records of local and regional climate changes from southern Africa show that during the period 70 ka–50 ka, conditions were overall colder and drier in the eastern regions and colder and wetter in the western regions. Western, south-western MSA sites abandoned earlier and for longer than MSA sites on the eastern region of South Africa as the local environments were less suitable for human occupation than in the east. Studies utilising a range of palaeoenvironmental proxies (e.g. pollen sequences and speleothems) and modern meteorological records combined with various Global Circulation Models have indicated that the eastern portion of South Africa responds differently to climate change from that of the western regions (Barrable *et al.*, 2002; Cook *et al.*, 2004; Scott *et al.*, 2008). The eastern portions are influenced by moisture circulation patterns from the South West and tropical Western Indian Ocean affected by the position of the ITCZ and sea surface temperatures of the Agulhas Current (Cook *et al.*, 2004). The western regions are affected by the degree of upwelling of the Benguela Current (Reason and Mulenga, 1999) and the northward movement of anticyclonic high-pressure systems which bring in moisture-rich westerly winds (Barrable *et al.*, 2002).

Such a profound change was possibly due to a change in the strength or temperature of the Agulhas Current or an eastward shift of the Agulhas Retroflexion. Summer rainfall along the south eastern coast of KwaZulu-Natal is influenced by the proximity and temperature of the Agulhas Current. Alongshore variations in the rainfall gradient are related to the distance between the coast and the current at the continental shelf edge and this influence extends up to 50 km inland (Jury *et al.*, 1993), and includes the Sibudu region. A weaker/cooler Agulhas Current and an eastward shift of the Agulhas Retroflexion would lower SST's along the eastern coast, resulting in a decrease in summer rainfall and also lower humidity levels (Jury *et al.*, 1993; Reason, 2002; Reason and Mulenga, 1999; Tyson, 1999). If SST's are cool in the western southern Indian Ocean (along the southeast coast of South Africa) and warmer in the eastern areas, the air over south-eastern Africa is drier and rainfall decreases (Reason, 2002; Reason and Mulenga, 1999). Proxy evidence from core RC17-69 suggests that a weakening of the Agulhas Current occurred towards the end of MIS 4 and that there was a corresponding decrease in rainfall as indicated by the Tswaing record.

This study highlights the necessity to examine multiple strands of palaeoenvironmental evidence and the connections between global climate change events and the impact of these changes on local environments and human populations during this time. It also indicates the need to ensure that dating of sites is secure before these strands of palaeoenvironmental evidence can be convincingly linked.

ACKNOWLEDGEMENTS

The following individuals provided invaluable assistance: Prof. Lyn Wadley and Prof. Mary Scholes for constructive suggestions and comments. Financial assistance for the project is gratefully acknowledged from the Palaeo-Anthropological Scientific Trust (PAST), the National Research Foundation (NRF) and the University of the Witwatersrand. Environmental Processes and Dynamics (EPD), CSIR is to be thanked for the use of its equipment. Opinions expressed here are not necessarily shared by any of the funding agencies or institutions.

REFERENCES

- Allott, L.F., 2004, Changing environments in Oxygen Isotope Stage 3: reconstructions using archaeological charcoal from Sibudu Cave. *South African Journal of Science* **100**(3), pp. 179–184.
- Allott, L.F., 2005, *Palaeoenvironments of the Middle Stone Age at Sibudu Cave, KwaZulu-Natal, South Africa: An analysis of archaeological charcoal*. PhD thesis, University of the Witwatersrand, Johannesburg.
- Allott, L.F., 2006, Archaeological charcoal as a window on palaeovegetation and wood use during the Middle Stone Age at Sibudu Cave. *Southern African Humanities* **18**(1), pp. 173–201.
- Avery, D.M., 1982, The micromammalian fauna from Border Cave, KwaZulu, South Africa. *Journal of Archaeological Science* **9**, pp. 187–204.
- Avery, D.M., 1992, The environment of early modern humans at Border Cave, South Africa: micromammalian evidence. *Palaeogeography, Palaeoclimatology, Palaeoecology* **91**, pp. 71–87.
- Avery, D.M., 2006, Pleistocene micromammals from Wonderwerk Cave, South Africa: practical issues. *Journal of Archaeological Science* **33**, pp. 1–13.
- Bada, J.L. and Deems, L., 1975, Accuracy of data beyond the 14-C dating limit using the aspartic acid racemisation reaction. *Nature* **255**, pp. 218–219.
- Barrable, A., Meadows, M.E. and Hewitson, B.C., 2002, Environmental reconstruction and climate modelling of the Late Quaternary in the winter rainfall region of the Western Cape, South Africa. *South African Journal of Science* **98**, pp. 611–616.
- Beaumont, P.B., 1990, Wonderwerk Cave. In: Beaumont, P.B. and Morris, D. (Eds.) *Guide to the archaeological sites in the Northern Cape*. McGregor Museum, Kimberley, pp. 101–134.
- Beaumont, P.B., De Villiers, H. and Vogel, J.C., 1978, Modern man in sub-Saharan Africa prior to 49,000 years BP: a review and evaluation with particular reference to Border Cave. *South African Journal of Science* **74**, pp. 409–419.
- Beaumont, P.B. and Vogel, J.C., 2006, On a timescale for the past million years of human history in central South Africa. *South African Journal of Science* **102**, pp. 217–228.
- Bender, M., Sowers, T., Dickson, M.-L., Orcharado, J., Grootes, P., Mayewski, P.A. and Meese, D.A., 1994, Climate correlations between Greenland and Antarctica during the past 100 000 years. *Nature* **372**, pp. 663–666.
- Blunier, T. and Brook, E.J., 2001, Timing of millennial-scale climate change in Antarctica and Greenland during the Last Glacial Period. *Science* **291**, pp. 109–112.
- Blunier, T., Chappelaz, J., Schwander, J., Dällenbach, A., Stauffer, B., Stocker, T.F., Raynaud, D., Jouzel, J., Clausens, H.B., Hammers, C.U. and Johnson, S.J., 1998, Asynchrony of Antarctic and Greenland climate change during the last glacial period. *Nature* **394**, pp. 739–743.

- Bond, G., Broecker, W., Johnson, S., McManus, J., Labeyrie, L., Jouzel, J. and Bonani, G., 1993, Correlations between climate records from North Atlantic sediments and Greenland ice. *Nature* **365**, pp. 143–147.
- Botha, G.A., 1996, The geology and palaeopedology of Late Quaternary colluvial sediments in northern KwaZulu-Natal/Natal. *Council for Geoscience Memoirs* **83**, pp. 1–165.
- Botha, G.A. and Partridge, T.C., 2000, Colluvial deposits. In: Partridge, T.C and Maud, R.R (Eds.), *The Cenozoic of southern Africa*. New York: Oxford University Press, pp. 88–99.
- Botha, G.A., Scott, L., Vogel, C. and von Brunn, V., 1992, Palaeosols and palaeoenvironments during the Late Pleistocene Hypothermal in northern Natal. *South African Journal of Science* **88**, pp. 508–512.
- Brooks, A.S., Hare, P.E. and Kokis, J.E., 1993, *Age of anatomically modern human fossils from the cave of Klasies River Mouth, South Africa*. Carnegie Institute of Washington, Year Book **92**, pp. 95–96.
- Butzer, K.W., 1978, Sediment stratigraphy of the Middle Stone Age sequence at Klasies River Mouth, Tsitsikama coast, South Africa. *South African Archaeological Bulletin* **33**, pp. 1–15.
- Butzer, K.W., 1984a, Late Quaternary environments in South Africa. In: Vogel, J.C. (Ed.) *Late Cainozoic Palaeoclimates of the Southern Hemisphere*. A.A. Balkema, Rotterdam.
- Butzer, K.W., 1984b, Archaeology and Quaternary environment in the interior of Southern Africa. In: Klein, R.G. (Ed) *Southern African Prehistory and Palaeoenvironments*. A.A. Balkema, Rotterdam, pp. 1–64.
- Butzer, K.W., Beaumont, P.B. and Vogel, J.C., 1978, Lithostratigraphy of Border Cave, KwaZulu, South Africa: A Middle Stone Age sequence beginning c. 195,000 B.P. *Journal of Archaeological Science* **5**, pp. 317–341.
- Butzer, K.W. Stuckenrath, R. and Vogel, J.C., 1979, The geo-archaeological sequence of Wonderwerk Cave, South Africa. *Abstracts from the Society of Africanist Archaeologists American Meeting*, Calgary.
- Cain, C.R., 2005, Using burnt bone to look at Middle Stone Age occupation and behaviour. *Journal of Archaeological Science* **32**, pp. 873–884.
- Cain, C.R., 2006, Human activity suggested by the taphonomy of 60 ka and 50 ka faunal remains from Sibudu Cave. *Southern African Humanities* **18**(1), pp. 241–260.
- Carr, A.S., Thomas, D.S.G., Bateman, M.D., Meadows, M.E. and Chase, B., 2006, Late Quaternary palaeoenvironments of the winter-rainfall zone of southern Africa: Palynological and sedimentological evidence from the Agulhas Plain. *Palaeogeography, Palaeoclimatology, Palaeoecology* **239**, pp. 147–165.
- Cartwright, C. and Parkington, J.E., 1997, The wood charcoal assemblages from Elands Bay Cave, South-western Cape: principles, procedures and preliminary interpretation. *South African Archaeological Bulletin* **52**, pp. 59–72.
- Chase, B.M. and Thomas, D.S.G., 2006, Late Quaternary dune accumulation along the western margin of South Africa: distinguishing forcing mechanisms through the analysis of migratory dune forms. *Earth and Planetary Science Letters* **251**, pp. 318–333.
- Chase, B.M. and Meadows, M.E., 2007, Late Quaternary dynamics of southern Africa's winter rainfall zone. *Earth-Science Reviews* **84**, pp. 103–138.
- Chase, B.M. and Thomas, D.S.G., 2007, Multiphase Late Quaternary aeolian sediment accumulation in western South Africa: Timing and relationship to palaeoclimatic changes inferred from the marine record. *Quaternary International* **166**, pp. 29–41.

- Chappellaz, J., Barnda, J.M., Raynaud, D., Korotkevich, Y.S. and Larius, C., 1990, Ice core record of atmospheric methane over the past 160,000 years. *Nature* **345**, pp. 127–131.
- Clark, J.L. and Plug, I., 2008, Animal exploitation strategies during the South Africa Middle Stone Age: Howiesons Poort and post-Howiesons Poort fauna from Sibudu Cave. *Journal of Human Evolution* **54**, pp. 886–898.
- Clarke, M.L., Vogel, J.C., Botha, G.A. and Wintle, A.G., 2003, Late Quaternary hillslope evolution recorded in eastern South African colluvial badlands. *Palaeogeography, Palaeoclimatology, Palaeoecology* **197**, pp. 199–212.
- Cochrane, G.W.G., 2006, An analysis of the lithic artefacts from the ~60 ka layers of Sibudu Cave. *Southern African Humanities* **18**(1), pp. 69–88.
- Cohen, A.S., Stone, J.R., Beuning, K.R.M., Park, L.E., Reinthal, P.N., Dettman, D., Scholz, C.A., Johnson, T.C., King, J.W., Talbot, M.R., Brown, E.R. and Ivory, S.J., 2007, Ecological consequences of early Late Pleistocene megadroughts in tropical Africa. *Proceedings of the National Academy of Science USA* **104**, pp. 16422–16427.
- Cook, C., Reason, C.J.C. and Hewitson, B.C., 2004, Wet and dry spells with particularly wet and dry summers in the South African summer rainfall region. *Climate Research* **26**, pp. 17–31.
- Cruz Jr., F.W., Burns, S.J., Karmann, I., Sharp, W.D., Vuille, M., Cardoso, A.O., Ferrari, J.A., Silva Dias, P.L. and Viana Jr, O., 2005, Insolation-driven changes in atmospheric circulation over the past 116,000 years in subtropical Brazil. *Nature* **434**, pp. 63–66.
- Dansgaard, W., Johnsen, S.J., Clausen, H.B., Dahl-Jensen, P., Gundestrup, N., Hammer, C.U. and Oeschger, H., 1984, North Atlantic climatic oscillations revealed by deep Greenland ice cores. In: Hansen, J.E. and Takahasi, T. (Eds.), *Climate Processes and Climate Sensitivity, Geophysical Monograph Series 29*, American Geophysical Union (AGU), Washington DC, pp. 288–298.
- Deacon, H.J., Deacon, J., Scholtz, A., Thackeray, J.F., Brink, J.S. and Vogel, J.C., 1984, Correlation of palaeoenvironmental data from the Late Pleistocene and Holocene deposits at Boomplaas Cave, southern Cape. In: Vogel, J.C. (Ed.) *Late Cainozoic palaeoclimates of the Southern Hemisphere*. A.A. Balkema, Rotterdam, pp. 330–352.
- Deacon, H.J. and Geleijnse, V.B., 1988, The stratigraphy and sedimentology of the main site sequence, Klasies River, South Africa. *South African Archaeological Bulletin* **43**, pp. 5–14.
- Deacon, H.J. and Lancaster, N., 1988, *Late Quaternary palaeoclimates of southern Africa*. Clarendon Press: Oxford.
- Deacon, H.J., Talma, A.S. and Vogel, J.C., 1988, Biological and cultural development of Pleistocene people in an Old World southern continent. In: Prescott, J.R. (Ed.), *Early man in the southern Hemisphere*. University of Adelaide, Adelaide, pp. 523–531.
- Deacon, H.J., 1979, Excavations at Boomplaas Cave—a sequence through the Upper Pleistocene and Holocene in South Africa. *World Archaeology* **10**(3), pp. 241–256.
- Deacon, H.J., 1989, Late Pleistocene palaeoecology and archaeology in the southern Cape. In: Mellars, P.A. and Stringer, C.B. (Eds.), *The human revolution: behavioural and biological perspectives on the origins of modern humans*. Edinburgh University Press, Edinburgh.
- Deacon, H.J., 1995, Two Late Pleistocene-Holocene archaeological depositories from the southern Cape, South Africa. *South African Archaeological Bulletin* **50**, pp. 121–131.
- Delagnes, A., Wadley, L., Lombard, M. and Villa, P., 2006, Crystal quartz backed tools from the Howiesons Poort at Sibudu Cave. *Southern African Humanities* **18**(1), pp. 43–56.

- Eeley, H.A.C., Lawes, M.J. and Piper, S.E., 1999, The influence of climate change on the distribution of indigenous forest in KwaZulu-Natal, South Africa. *Journal of Biogeography* **26**, pp. 595–617.
- Fairhall, A.W., Young, A.W. and Erickson, L.J., 1976, University of Washington date IV. *Radiocarbon* **18**, pp. 221–239.
- Feathers, J.K., 2002, Luminescence dating in less than ideal conditions: case studies from Klasies River Main site and Duinefontein, South Africa. *Journal of Archaeological Science* **29**, pp. 177–194.
- Flores, J.-A., Gersonde, R. and Sierro, F.J., 1999, Pleistocene fluctuations in the Agulhas Current Retroflexion based on the calcareous plankton record. *Marine Micropalaeontology*, pp. 1–22.
- Glenny, W., 2006, An analysis of the micromammal assemblage from Sibudu Cave, KwaZulu-Natal. *Southern African Humanities* **18**(1), pp. 279–288.
- Goldberg, P. and MacPhail, R.I., 2006, *Practical and theoretical geoarchaeology*. Blackwell, Oxford.
- Goldberg, P., Miller, C.E., Schiegl, S., Ligouis, B., Berna, F., Conard, N.J. and Wadley, L., 2009, Bedding, hearths, and site maintenance in the Middle Stone Age of Sibudu Cave, KwaZulu-Natal, South Africa. *Archaeol Anthropol Science* DOI 10.1007/s12520-009-0008-1, pp. 1–28.
- Grootes, P.M., Stuiver, M., White, J.W.C., Johnson, S. and Jouzel, J., 1993, Comparison of oxygen isotope records from the GISP2 and GRIP Greenland ice cores. *Nature* **366**, 552–554.
- Grün, R., Beaumont, P.B. and Stringer, C.B., 1990a, ESR dating evidence for early modern humans at Border Cave in South Africa. *Nature* **344**, pp. 537–539.
- Grün, R., Shackleton, N.J. and Deacon, H.J., 1990b, Electron spin resonance dating of tooth enamel from Klasies River Mouth Cave. *Current Anthropology* **31**, 427–432.
- Grün, R. and Beaumont, P.B., 2001, Border Cave revisited: a revised ESR chronology. *Journal of Human Evolution* **40**, pp. 467–482.
- Hall, G., Woodborne, S. and Scholes, M., 2006, *Woodland ecosystems response to past climatic change; stable carbon isotope analysis of archaeological charcoal: the 60 ka event at Sibudu Cave, KwaZulu-Natal, South Africa*. Poster presented at the ESSP Open Science Conference on Global Environmental Change: Regional Challenges, Beijing, China, November 2006.
- Hall, G., Woodborne, S. and Scholes, M., 2008, Stable carbon isotope ratios from archaeological charcoal as palaeoenvironmental indicators. *Chemical Geology* **247**, pp. 384–400.
- Harper, P.T.N., 1997, The Middle Stone Age sequence at Rose Cottage Cave: a search for continuity and discontinuity. *South African Journal of Science* **93**, pp. 470–475.
- Heinrich, H., 1988, Origin and consequences of cyclic ice rafting in the North-east Atlantic Ocean during the past 130,000 years. *Quaternary Research* **29**, pp. 142–152.
- Henshilwood, C.S., Sealy, J.C., Yates, R., Cruz-Uribe, K., Goldberg, P., Grine, F., Poggenpoel, C., van Niekerk, K. and Watts, I., 2001, Blombos Cave, Southern Cape, South Africa: Preliminary report on the 1992–1999 excavations of the Middle Stone Age levels. *Journal of Archaeological Science* **28**, pp. 421–448.
- Herries, A.I.R., 2006, Archaeomagnetic evidence for climate change at Sibudu Cave. *Southern African Humanities* **18**(1), pp. 131–147.
- Hutson, W.H., 1980, The Agulhas Current during the Late Pleistocene, analysis of modern faunal analogues. *Science* **207**, pp. 64–66.
- Jacobs, Z., Wintle, A. and Duller, G.A.T., 2003a, Optical dating of dune sand from Blombos Cave, South Africa: I – multiple grain data. *Journal of Human Evolution* **44**, pp. 599–612.

- Jacobs, Z., Wintle, A. and Duller, G.A.T., 2003b, Optical dating of dune sand from Blombos Cave, South Africa: II – single grain data. *Journal of Human Evolution* **44**, pp. 613–625.
- Jacobs, Z., 2004, *Development of luminescence dating techniques for dating Middle Stone Age sites in South Africa*. PhD thesis, University of Wales, Aberystwyth.
- Jacobs, Z., 2005, Testing and demonstrating the stratigraphic integrity of artefacts from MSA deposits at Blombos Cave, South Africa. In d’Errico, F. and Backwell, L. (Eds.), *From Tools to Symbols. From Early Hominids to Modern Humans*. Johannesburg: Wits University Press, pp. 459–474.
- Jacobs, Z., Duller, G.A.T., Wintle, A. and Henshilwood, C.S., 2006, Extending the chronology of deposits at Blombos Cave, South Africa, back to 140 ka using optical dating of single and multiple grains of quartz. *Journal of Human Evolution* **51**, pp. 255–273.
- Jacobs, Z., Wintle, A., Duller, G.A.T., Roberts, R.G. and Wadley, L., 2008a, New ages for the post-Howiesons Poort, late and final Middle Stone Age of Sibudu, South Africa. *Journal of Archaeological Science* **35**(7), pp. 1790–1807.
- Jacobs, Z., Roberts, R.G., Galbraith, R.F., Deacon, H.J., Grün, R., Mackay, A., Mitchell, P., Vogelsang, R. and Wadley, L., 2008b, Ages for the Middle Stone Age of Southern Africa: Implications for human behaviour and dispersal. *Science* **322**, pp. 733–735.
- Jacobs, Z. and Roberts, R.G., 2008, Testing times: Old and new chronologies in the Howiesons Poort and Still Bay industries in environmental context. *South African Archaeological Society Goodwin Series* **10**, pp. 9–34.
- Jansen, E.J., Overpeck, K.R., Briffa, J.-C., Duplessy, F.J., Masson-Delmotte, D., Olago, B., Otto-Bliesner, W.R., Peltier, S., Rahmstorf, R., Ramesh, D., Raynaud, D., Rind, O., Solomina, R., Villalba, R. and Zhang, D., 2007, Palaeoclimate. In: Solomon, S., Qin, D., Manning, M., Chan, Z., Marquis, M., Averyt, K.B., Tignor, M. and Miller, H.L. (Eds.), *Climate Change 2007: The Physical Science Basis*. Contributions of Working Group I to the Fourth Assessment Report of the Intergovernmental Panel on Climate Change. Cambridge University Press, Cambridge and New York.
- Johnson, B.J., Miller, G.H., Fogel, M.L. and Beaumont, P.B., 1997, The determination of late Quaternary palaeoenvironments at Equus Cave, South Africa, using stable isotopes and amino acid racemisation in ostrich eggshell. *Palaeogeography, Palaeoclimatology, Palaeoecology* **136**, pp. 121–137.
- Jones, H.L., 2001, *Electron spin resonance dating of tooth enamel at three Palaeolithic sites*. Unpublished M.Sc. thesis, McMaster University.
- Jouzel, J., et al., 2004, EPICA Dome C Ice Cores Deuterium Data. IGBP PAGES/World Data Center for Paleoclimatology. Data Contribution Series # 2004-038. NOAA/NGDC Paleoclimatology Program, Boulder CO, USA.
- Jouzel, J., Masson-Delmotte, V., Stievenard, M., Landais, A., Vimeux, F., Johnsen, S., Sveinbjörnsdóttir, A., and White, J.W.C., 2005, Rapid deuterium-excess changes in Greenland ice cores: a link between the ocean and the atmosphere. *Comptes Rendus Geoscience* **337**, pp. 957–969.
- Jouzel, J., Stievenard, M., Johnsen, S., Landais, A., Masson-Delmotte, V., Sveinbjörnsdóttir, A., Vimeux, F., von Grafenstein, U. and White, J.W.C., 2007, The GRIP deuterium-excess record. *Quaternary Science Reviews* **26**, pp. 1–17.
- Jury, M.R., Valentine, H.R. and Lutjeharms, J.R.E., 1993, Influence of the Agulhas Current on summer rainfall along the southeast coast of South Africa. *Journal of Applied Meteorology* **32**, pp. 1282–1287.
- Klein, R.G., 1976, The mammalian fauna of the Klasies River Mouth sites, southern Cape Province, South Africa. *South African Archaeological Bulletin* **32**, pp. 14–27.

- Klein, R.G., 1977, The mammalian fauna from the Middle and Later Stone Age (Late Pleistocene) levels of Border Cave, Natal Province, South Africa. *South African Archaeological Bulletin* **32**, pp. 14–27.
- Klein, R.G., 1983, Palaeoenvironmental implications of Quaternary large mammals in the fynbos region. In: Deacon, H.J., Hendey, Q.B. and Lambrechts, J.J.N. (Eds.), *Fynbos palaeoecology: a preliminary synthesis*. South African National Scientific Progress Report **75**, pp. 116–138. CSIR, Pretoria.
- Landais, A., Masson-Delmotte, V., Combourieu Nebout, N., Jouzel, J., Blunier, T., Leuenberger, M., Dahl-Jensen, D. and Johnsen, S., 2007, Millennial scale variations of the isotopic composition of atmospheric oxygen over Marine Isotope Stage 4. *Earth and Planetary Science Letters* **258**, pp. 101–113.
- Leuschner, D.C. and Sirocko, F., 2000, The low-latitude monsoon climate during Dansgaard-Oeschger cycles and Heinrich Events. *Quaternary Science Reviews* **19**, pp. 243–254.
- Little, M.G., Schneider, R.R., Kroon, D., Price, B., Bickert, T. and Wefer, G., 1997, Rapid palaeoceanographic changes in the Benguela Upwelling System for the last 160,000 years as indicated by abundances of planktonic foraminifera. *Palaeogeography, Palaeoclimatology, Palaeoecology* **130**, pp. 135–161.
- McDowell, N., Pockman, W.T., Allen, C.D., Breshears, D.D., Cobb, N., Kolb, T., Plaut, J., Sperry, J., West, A., Williams, D.G. and Yepez, E.A., 2008, Mechanisms of plant survival and mortality during drought: why do some plants survive while others succumb to drought? *New Phytologist* **178**, pp. 719–739.
- Mellars, P., 2006, Why did modern human populations disperse from Africa ca. 60,000 years ago? A new model. *Proceedings of the National Academy of Science USA* **103**(25), pp. 9381–9386.
- Miller, G.H., Beaumont, P.B., Jull, A.J.T. and Johnson, B., 1993, Pleistocene geochronology and palaeothermometry from protein diagenesis in ostrich eggshells: Implications for the evolution of modern humans. In: Aitken, M.J., Stringer, C.B. and Mellars, P.A. (Eds.), *The origin of modern humans and the impact of chronometric dating*. Princeton University Press: Princeton.
- Miller, G.H., Beaumont, P.B., Deacon, H.J., Brooks, A.S., Hare, P.E. and Jull, A.J.T., 1999, Earliest modern humans in southern Africa dated by isoleucine epimerization in ostrich eggshell. *Quaternary Science Review* **18**, pp. 1537–1548.
- Mitchell, P., 2002, *The archaeology of southern Africa*. Cambridge University Press, Cambridge.
- Molyneux, E.G., Hall, I.R., Zahn, R. and Diz, P., 2007, Deep water variability on the southern Agulhas Plateau: Interhemispheric links over the past 170 ka. *Palaeoceanography* **22**, PA4209, doi: 10.1029/2006PA001407.
- Mucina, L., Scott-Shaw, C.R., Rutherford, M.C., Camp, K.G.T., Matthews, W.S., Powrie, L.W. and Hoare, D.B., 2006, Indian Ocean Coastal Belt. In: Mucina, L. and Rutherford, M.C. (Eds.), *The vegetation of South Africa, Lesotho and Swaziland*. Stelitzia 19, South African National Biodiversity Institute, Pretoria, pp. 569–580.
- Oeschger, H., Beer, J., Siegenthaler, U., Stauffer, B., Dansgaard, W. and Langway, C.C., 1984, Late glacial climate history from ice cores. In: Hansen, J.E. and Takahasi, T. (Eds.), *Climate Processes and Climate Sensitivity*, Geophysical Monograph Series **29**, American Geophysical Union (AGU), Washington DC, pp. 299–306.
- Pahnke, K., Zahn, R., Elderfield, H. and Schulz, M., 2003, 340,000-year centennial-scale marine record of Southern Hemisphere climate oscillation. *Science* **301**, pp. 948–952.
- Pahnke, K. and Zahn, R., 2005, Southern Hemisphere water mass conversion linked with North Atlantic climate variability. *Science* **307**, pp. 1741–1746.

- Parkington, J.E., 1990, A critique on the consensus view on the age of the Howiesons Poort assemblages in South Africa. In: Mellars, P. (Ed.), *The Emergence of Modern Humans: An archaeological perspective*. University of Edinburgh Press, Edinburgh, pp. 34–55.
- Parkington, J.E., 1999, Western Cape landscapes. *Proceedings of the British Academy* **99**, pp. 25–35.
- Parkington, J.E. and Poggenpoel, C., 1987, Diepkloof Rock Shelter. Papers in the prehistory of the Western Cape, South Africa. *BAR International Series* **332**, pp. 269–293.
- Parkington, J.E., Poggenpoel, C., Rigaud, J.-P. and Texier, P.J., 2005, From tool to symbol: the behavioural context of intentionally marked ostrich eggshell from Diepkloof, Western Cape. In: d'Errico, F. and Backwell, L. (Eds.), *From Tools to Symbols: From early hominids to modern humans*. Witwatersrand University Press, Johannesburg, pp. 475–492.
- Partridge, T.C., 1999, The sedimentary record and its implications for rainfall fluctuations in the past. In: Partridge, T.C. (Ed.), *Tswaing—investigations into the origin, age and palaeoenvironments of the Pretoria Saltpan*. Council for Geosciences, Pretoria, pp. 127–142.
- Partridge, T.C., Demenocal, P.B., Lorentz, S.A., Paiker, M.J. and Vogel, J.C., 1997, Orbital forcing of climate over South Africa: A 200,000-year rainfall record from the Pretoria Saltpan. *Quaternary Science Reviews* **16**, pp. 1125–1133.
- Partridge, T.C., Metcalfe, S.E. and Scott, L., 1999, Conclusions and implications for a model of regional palaeoclimates during the last two glacials. In: Partridge, T.C. (Ed.), *Tswaing—investigations into the origin, age and palaeoenvironments of the Pretoria Saltpan*. Council for Geosciences, Pretoria, pp. 193–198.
- Pienaar, M., Woodborne, S. and Wadley, L., 2008, Optically Stimulated Luminescence Dating at Rose Cottage Cave. *South African Journal of Science* **104**, pp. 65–70.
- Petit, J.R., Mounier, L., Jouzel, J., Korotkevich, Y.S., Kotlyakov, V.I. and Larius, C., 1990, Palaeoclimatological and chronological implications of the Vostok core dust record. *Nature* **343**, pp. 56–58.
- Petit, J.R., Jouzel, J., Raynaud, D., Barkov, N.F., Barnolo, J.M., Basik, I., Bender, M., Chappellaz, J., Davis, M., Delaygue, G., Delmotte, M., Kotlyakov, V.M., Legrand, M., Lipenkov, V.Y., Larius, C., Pépin, L., Ritz, C., Saltzman, E. and Stievenard, M., 1999, Climate and atmospheric history of the past 420 000 years from the Vostok ice core, Antarctica. *Nature* **399**, pp. 429–431.
- Petit, J.R., *et al.*, 2001, Vostok Ice Core Data for 420,000 Years, IGBP PAGES/World Data Center for Paleoclimatology Data Contribution Series #2001-076. NOAA/NGDC Paleoclimatology Program, Boulder CO, USA.
- Pichevin, L., Cremer, M., Giraudeau, J. and Bertrand, P., 2005, A 190 ky record of lithogenic grain-size on the Namibian slope: Forging a tight link between past wind-strength and coastal upwelling dynamics. *Marine Geology* **218**, pp. 81–96.
- Pickering, R., 2006, Regional geology, setting and sedimentology of Sibudu Cave. *South African Humanities* **18**(1), pp. 123–129.
- Plug, I., 2004, Resource exploitation: animal use during the Middle Stone Age at Sibudu Cave, KwaZulu-Natal. *South African Journal of Science* **100**, pp. 151–158.
- Plug, I., 2006, Aquatic animals and their associates from the Middle Stone Age levels at Sibudu. *Southern African Humanities* **18**(1), pp. 289–299.
- Prell, W.L. and Hutson, W.H., 1979, Zonal temperature-anomaly maps of Indian Ocean surface waters: Modern and ice age patterns. *Science* **206**, pp. 454–456.
- Prell, W.L., Hutson, W.H. and Williams, D.F., 1980a, The subtropical convergence and Late Quaternary circulation in the Southern Indian Ocean. *Marine Micropalaeontology* **4**, pp. 225–234.

- Prell, W.L., Hutson, W.H. and Williams, D.F., 1980b, Surface circulations of the Indian Ocean during the Last Glacial Maximum approximately 18,000-years BP. *Quaternary Research* **14**, pp. 309–336.
- Rahmstorf, S., 2002, Ocean circulation and climate during the past 120,000 years. *Nature* **419**, pp. 207–214.
- Rau, A.J., Rogers, J., Lutjeharms, J.R.E., Giraudeau, J., Lee-Thorp, J.A., Chen, M.-T. and Waelbroeck, C., 2002, A 450-kyr record of hydrological conditions on the western Agulhas Bank Slope, south of Africa. *Marine Geology* **180**, pp. 183–201.
- Reason, C.J.C., 2002, Sensitivity of the southern African circulation to dipole sea-surface temperature patterns in the South Indian Ocean. *International Journal of Climatology* **22**, pp. 377–393.
- Reason, C.J.C. and Mulenga, H., 1999, Relationships between South African rainfall and SST anomalies in the Southwest Indian Ocean. *International Journal of Climatology* **19**, pp. 1651–1673.
- Renaut, R. and Bamford, M.K., 2006, Results of preliminary palynological analysis at Sibudu Cave. *Southern African Humanities* **18**(1), pp. 235–240.
- Schiegl, S., Stockhammer, P., Scott, C. and Wadley, L., 2004, A mineralogical and phytoliths study of the Middle Stone Age hearths in Sibudu Cave, KwaZulu-Natal, South Africa. *South African Journal of Science* **100**(3), pp. 185–194.
- Schiegl, S. and Conard, N.J., 2006, The Middle Stone Age sediments at Sibudu: results from FTIR spectroscopy and microscopic analyses. *Southern African Humanities* **18**(1), pp. 149–172.
- Schmittner, A., Saenko, O.A. and Weaver, A.J., 2003, Coupling of the hemispheres in observations and simulations of glacial climate change. *Quaternary Science Reviews* **22**, pp. 659–671.
- Scholtz, A., 1986, *Palynological and palaeobotanical studies in the southern Cape*. Unpublished M.A. thesis, University of Stellenbosch, South Africa.
- Scholz, C.A., Johnson, T.C., Cohen, A.C., King, J.W., Peck, J.A., Overpeck, J.T., Talbot, M.R., Brown, E.T., Kalindekaffe, L., Amoako, P.Y.O., Lyons, R.P., Shanahan, T.M., Castañeda, I.S., Heil, C.W., Forman, S.L., McHargue, L.R., Beuning, K.R., Gomez, J. and Pierson, J., 2007, East African megadrought between 135 and 75 thousand years ago and bearing on early-modern human origins. *Proceedings of the National Academy of Science USA* **104**, pp. 16416–16421.
- Scott, L., Holmgren, K. and Partridge, T.C., 2008, Reconciliation of vegetation and climatic interpretations of pollen profiles and other regional records from the last 60 thousand years in the Savanna Biome of southern Africa. *Palaeogeography, Palaeoclimatology, Palaeoecology* **257**, pp. 198–206.
- Shackleton, N.J., 1977, The oxygen isotope stratigraphy record of the Late Pleistocene. *Philosophical Transactions of the Royal Society, London* **280**, pp. 169–182.
- Shackleton, N.J., 1982, Stratigraphy and chronology of the Klasies River Mouth deposits: oxygen isotope evidence. In: Singer, R. and Wymer, J. (Eds.) *The Middle Stone Age at Klasies River Mouth in South Africa*. University of Chicago Press, Chicago, pp. 194–199.
- Sievers, C., 2006, Seeds from the Middle Stone Age layers at Sibudu Cave. *Southern African Humanities* **18**(1), pp. 203–222.
- Singer, R. and Wymer, J., 1982, *The Middle Stone Age at Klasies River Mouth in South Africa*. University of Chicago Press, Chicago.
- Stephenson, N.L., 1998, Actual evapotranspiration and deficit: biologically meaningful correlates of vegetation distribution across spatial scales. *Journal of Biogeography* **25**, pp. 855–870.
- Stocker, T.F., 2000, Past and future reorganizations in the climate system. *Quaternary Science Reviews* **19**, pp. 301–319.

- Stocker, T.F., 2002, North-South connections. *Science* **297**, pp. 1814–1815.
- Stuut, J.-B.W., Prins, M.A., Schneider, R.R., Weltje, G.J., Jansen, J.H.F. and Postma, G., 2002, A 300-kyr record of aridity and wind strength in south-western Africa: inferences from grain-size distributions of sediments on Walvis Ridge, SE Atlantic. *Marine Geology* **180**, pp. 221–233.
- Stuut, J.-B.W., Crosta, X., van der Borg, K. and Schneider, R., 2004, Relationships between Antarctic sea ice and southwest African climate during the Late Quaternary. *Geology* **32**, pp. 203–213.
- Thackeray, J.F., 1992, Chronology of Late Pleistocene deposits associated with *Homo sapiens* at Klasies River Mouth, South Africa. *Palaeoecology of Africa and the Surrounding Islands* **23**, pp. 177–191.
- Thackeray, J.F. and Avery, D.M., 1990, A comparison between temperature indices for Late Pleistocene sequences at Klasies River and Border Cave, South Africa. *Palaeoecology of Africa and the Surrounding Islands* **21**, pp. 311–316.
- Trenberth, K.E., Jones, P.D., Ambenje, P., Bojariu, R., Easterling, D., Klein Tank, A., Parker, D., Rahimzadeh, F., Renwick, J.A., Rusticucci, M., Soden, B. and Zhai, P., 2007, Observations: Surface and Atmospheric Climate Change. In: Solomon, S., Qin, D., Manning, M., Chen, Z., Marquis, M., Averyt, K.B., Tignor, M. and Miller, H.L. (Eds.), *Climate Change 2007: The Physical Science Basis*. Contribution of Working Group I to the Fourth Assessment Report of the Intergovernmental Panel on Climate Change. Cambridge University Press, Cambridge, United Kingdom and New York, NY, USA.
- Tribolo, C., 2003, *Apport des méthodes de la luminescence à la chronologie de technofaciés du Middle Stone Age associés aux premiers Hommes Modernes du Sud l'Afrique*. Unpublished PhD thesis, Bordeaux University.
- Tribolo, C., Mercier, N. and Valladas, H., 2005, Chronology of the Howiesons Poort and Still Bay techno-complexes: assessment and new dates from luminescence. In: d'Errico, F. and Backwell, L. (Eds.), *From Tools to Symbols: From early hominids to modern humans*. Witwatersrand University Press, Johannesburg, pp. 493–511.
- Tribolo, C., Mercier, N., Selo, M., Valladas, H., Joron, J.-L., Reyss, J.-L., Henshilwood, C.S., Sealy, J. and Yates, R., 2006, TL dating of burnt lithics from Blombos Cave (South Africa): further evidence for the antiquity of modern human behaviour. *Archaeometry* **48**, pp. 341–357.
- Tyson, P.D., 1991, Climatic change in southern Africa: Past and present conditions and possible future scenarios. *Climate Change* **18**, pp. 241–258.
- Tyson, P.D., 1999, Atmospheric circulation changes and palaeoclimates of southern Africa. *South African Journal of Science* **95**, pp. 194–201.
- van Zinderen Bakker, E.M., 1995, Archaeology and palynology. *South African Journal of Science* **50**, pp. 98–105.
- Verstraeten, W.W., Veroustraete, F. and Feyen, J., 2008, Assessment of evapotranspiration and soil moisture content across different scales of observation. *Sensors* **8**, pp. 70–117.
- Villa, P., Delagnes, A. and Wadley, L., 2005, A late Middle Stone Age artefact assemblage from Sibudu (KwaZulu-Natal): comparisons with the European Middle Palaeolithic. *Journal of Archaeological Science* **32**, pp. 399–422.
- Villa, P. and Lenoir, M., 2006, Hunting weapons of the Middle Stone Age and Middle Palaeolithic: spear points from Sibudu, Rose Cottage and Bouheben. *Southern African Humanities* **18**(1), pp. 89–122.
- Vogel, J.C., 2001, Radiometric dates for the Middle Stone Age in South Africa. In: Tobias, P.V., Raath, M.A., Moggi-Cecchi, J. and Doyle, G.A. (Eds.) *Humanity—From African naissance to coming Millennia*. Witwatersrand University Press, Johannesburg, pp. 261–268.

- Vogel, J.C., Wintle, A.G. and Woodborne, S., 1999, Focus; luminescence dating of coastal sands: overcoming changes in environmental dose rate. *Journal of Archaeological Science* **26**, pp. 729–733.
- Wadley, L., 1997, Rose Cottage Cave: Archaeological work 1987 to 1997. *South African Journal of Science* **93**, pp. 439–444.
- Wadley, L., 2004, Vegetation changes between 61 500 and 26 000 years ago: the evidence from seeds in Sibudu Cave, Kwazulu-Natal. *South African Journal of Science* **100**(3), pp. 167–173.
- Wadley, L., 2005, A typological study of the final Middle Stone Age stone tools from Sibudu Cave, KwaZulu-Natal. *South African Archaeological Bulletin* **60**, pp. 51–63.
- Wadley, L., 2006, Partners in grime: results of multi-disciplinary archaeology at Sibudu Cave. *Southern African Humanities* **18**(1), pp. 315–341.
- Wadley, L., 2007, Announcing a Still Bay industry at Sibudu Cave, South Africa. *Journal of Human Evolution* **52**(6), pp. 681–689.
- Wadley, L., 2008, The Howiesons Poort Industry of Sibudu Cave. *South African Archaeological Society Goodwin Series* **10**, pp. 122–132.
- Wadley, L. and Vogel, J.C., 1991, New dates from Rose Cottage Cave, Ladybrand, eastern Orange Free State. *South African Journal of Science* **87**, pp. 605–607.
- Wadley, L., Esterhuysen, A. and Jennerat, C., 1992, Vegetation changes in the eastern Orange Free State: the Holocene and later Pleistocene evidence from charcoal studies at Rose Cottage Cave. *South African Journal of Science* **88**, pp. 558–563.
- Wadley, L. and Jacobs, Z., 2004, Sibudu Cave, Kwazulu-Natal: Background to the excavations of Middle Stone Age and Iron Age occupations. *South African Journal of Science* **100**(3), pp. 145–151.
- Wadley, L. and Jacobs, Z., 2006, Sibudu Cave: background to the excavations, Stratigraphy and dating. *Southern African Humanities* **18**(1), pp. 1–26.
- Wadley, L., Plug, I. and Clark, J.L., 2008, The contribution of Sibudu fauna to an understanding of KwaZulu-Natal environments at ~58 ka, ~48 ka and ~35 ka. *Festschrift for I. Plug, BAR publications*, Oxford.
- Wang, Y.J., Cheng, H., Edwards, R.L., An, Z.N., Wu, J.Y., Shen, C.-C. and Dorale, J.A., 2001, A high-resolution absolute-dated Late Pleistocene monsoon record from Hulu Cave, China. *Science* **294**, pp. 2345–2348.
- Wang, X., Auler, A.S., Edwards, R.L., Cheng, H., Cristalli, P.S., Smart, P.L., Richards, D.A. and Shen, C.-C., 2004, Wet periods in northeastern Brazil over the past 210 kyr linked to distant climate anomalies. *Nature* **432**, pp. 740–743.
- Wells, C.R., 2006, A sample integrity analysis of faunal remains from the RSp layer at Sibudu Cave. *Southern African Humanities* **18**(1), pp. 261–277.
- Wintle, A.G., Botha, G.A., Li, S.-H. and Vogel, J.C., 1995, A chronological framework for colluviation during the last 110 kyr in KwaZulu-Natal. *South African Journal of Science* **91**, pp. 134–139.
- Woodborne, S. and Vogel, J.C., 1993, Luminescence dating at Rose Cottage Cave: a progress report. *South African Journal of Science* **93**, pp. 476–478.
- Wolff, E.W., Fischer, H., Fundel, F., Ruth, U., Twarloh, B., Littot, G.C., Mulvaney, R., Röthlisberger, R., de Angelis, M., Boutron, C.F., Hansson, M., Jonsell, U., Hutterli, M.A., Lambert, F., Kaufmann, P., Stauffer, B., Stocker, T.F., Steffensen, J.P., Bigler, M., Siggard-Andersen, M.L., Udisti, R., Becagli, S., Castellano, E., Severi, M., Wagenbach, D., Barbante, C., Gabrielli, P. and Gaspari, V., 2006, Southern Ocean sea-ice extent, productivity and iron flux over the past eight glacial cycles. *Nature* **440**, pp. 491–496.

CHAPTER 6

The potential of Poaceae, Cyperaceae and Restionaceae phytoliths to reflect past environmental conditions in South Africa

Carlos E. Cordova

Department of Geography, Oklahoma State University, Stillwater, Oklahoma, United States of America

Louis Scott

Department of Plant Sciences, University of the Free State, Bloemfontein, South Africa

ABSTRACT: This paper explores the potential of diagnostic phytoliths in the Poaceae, Cyperaceae and Restionaceae of South Africa to define their bioclimatic indicator value for palaeoecological reconstructions. It includes an assessment of the morphological aspects of the grass silica short cells (GSSC) in C₃ grass subfamilies (Pooideae, Danthoioideae, and Ehrhartoideae) and C₄ grass subfamilies (Panicoideae, Chloridoideae and Aristidoideae) stressing their biogeographic distribution and diagnostic advantages and limitations. This initial assessment shows that selected GSSC as well as sedge and restio phytoliths are potential indicators of climatic variables such as total annual precipitation, rainfall seasonality, rainfall variability and summer temperatures. Further, we propose that a regionally based protocol for graminoid phytolith interpretation can potentially assess the expansion of the winter rainfall zone during the cold stages of the Pleistocene.

6.1 INTRODUCTION

Studies of African grass phytoliths have provided a useful tool for palaeoclimatic reconstructions, particularly in tropical latitudes and summer rainfall areas of the continent (e.g., Alexandre *et al.*, 1997; Bremond *et al.*, 2005, 2008; Barboni *et al.*, 2007). South Africa and parts of Namibia, however, do not follow most of the taxonomic and biogeographic patterns of grasses commonly found elsewhere in Africa. The unique biogeographic and taxonomic patterns of graminoids in this region are the result of a winter rainfall season (Vogel *et al.*, 1978), subtropical dry lands with winter, summer and bimodal rainfall seasons (Mulder and Ellis, 2000), and the presence of distinct flora irradiated from the Cape Floral Kingdom (Linder, 2003; Galley *et al.*, 2007).

The distribution of Poaceae (grasses) in South Africa is strongly linked to annual rainfall, rainfall seasonality and elevation (Figure 1). Thus, C₃ grasses are concentrated in the winter rainfall zone and at high elevations in the all-year and summer rainfall zones (Vogel *et al.*, 1978; Gibbs-Russell, 1988). The most widespread C₃ grasses belong to the more locally diverse and endemic Ehrhartoideae and Danthoioideae

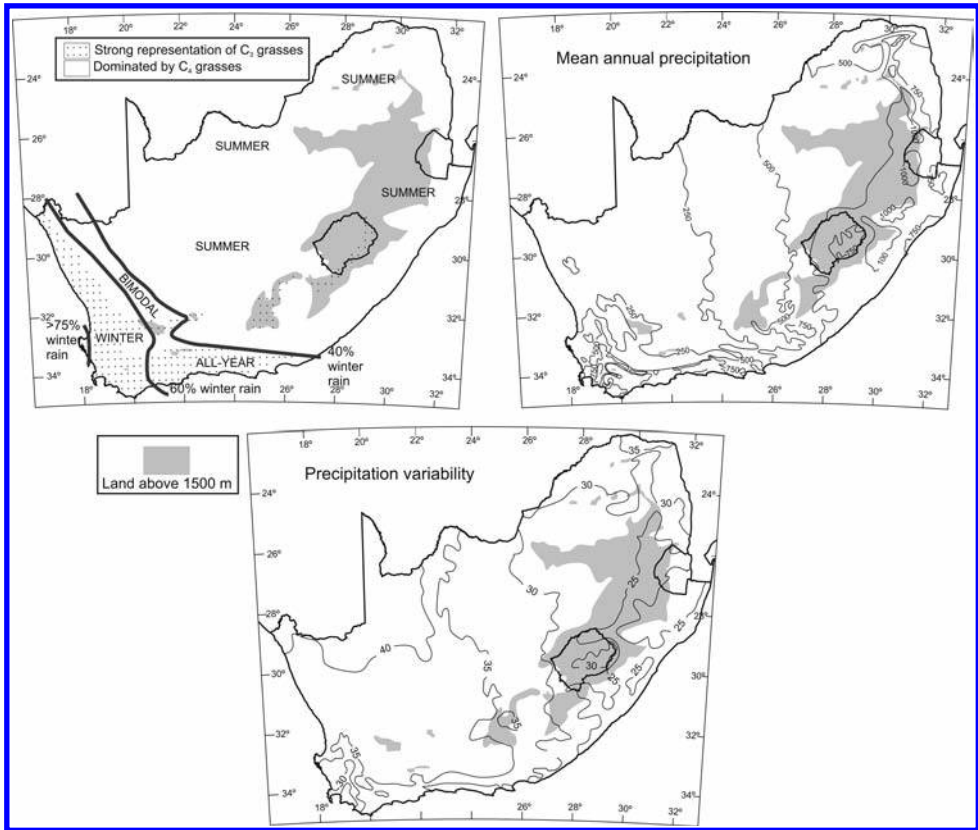


Figure 1. Distribution of grasses and rainfall seasonality, annual rainfall (mm), and rainfall variability (mm).

subfamilies, and the more cosmopolitan Pooideae subfamily. The C_4 grasses belong to the Panicoideae and Chloridoideae subfamilies, which are widespread in all of the country, particularly in the summer rainfall region, and the Aristidoideae subfamily, which has a more restricted distribution (Gibbs-Russell, 1988). The winter rainfall zone has a peculiar biogeographic distribution of Poaceae and other graminoids. For example, the Restionaceae (restios or Cape reeds) and Cyperaceae (sedges) dominate over the Poaceae in most vegetation types of the fynbos, the typical biome of the winter rainfall zone (Rebello *et al.*, 2006). Both, the Restionaceae and Cyperaceae produce diagnostic phytoliths (Piperno, 2006), which is an advantage for the identifying fynbos biome characteristics in fossil phytolith assemblages.

Rossouw (2009) provided an insight to the complexity of the taxonomic and biogeographic distribution of leaf Grass Silica Short Cell (GSSC) morphotypes across 309 native grass species for palaeoclimatic reconstruction. The present study, on the other hand, provides an independent summary of GSSC morphotypes and restio and sedge phytoliths and an alternative protocol to interpret graminoid phytolith assemblages. Furthermore, this study attempts to provide an additional tool to pollen and carbon stable isotopes for reconstructing the fluctuations of the winter rainfall zone.

The research presented here is a preliminary characterization of diagnostic phytoliths of Poaceae, Cyperaceae and Restionaceae and their geographic variability in relation to biomes, vegetation units, and rainfall patterns in central and western South Africa. Thus, this research has four specific objectives: (1) create a basic classification of grass silica short cell morphotypes at the subfamily level based on a compilation of morphotypes from identified plant specimens; (2) establish a general classification of diagnostic Restionaceae and Cyperaceae phytoliths from identified plant specimens; (3) evaluate the potential of GSSC morphotypes in phytolith assemblages from soil surface samples across a transect straddling the winter and summer rainfall regions; and (4) evaluate the potential of diagnostic Restionaceae and Cyperaceae phytoliths across various biomes in the winter, summer, all-year and bimodal rainfall regions of South Africa.

The modern surface samples along transects is an ongoing study that looks at representative phytolith morphotypes characteristic of each biomes in areas winter and summer rainfall zones the Southern and western parts of South Africa including transitional zone (i.e., the bimodal and all-year rainfall areas) (Figure 1). The protocol presented here is provisional, and subject to further testing.

6.2 METHODS

6.2.1 Reference collection

The plant specimens used as reference for the classification of GSSC morphotypes and Cyperaceae and Restionaceae phytoliths were collected at the sampling areas of the transects and identified by taxonomists at the University of the Free State and the University of Cape Town. The collections include 30 species of grasses, 5 species of Cyperaceae and 20 species of Restionaceae. Phytoliths were obtained from inflorescence, leaf, culm, and in most cases from roots. Photographs of GSSC from leaf phytoliths of 309 grass species published by Rossouw (2009) were used as additional reference.

6.2.2 The transects

The collection of samples along transects had the objective of identifying the most common Grass Silica Short Cell (GSSC) morphotypes across the biomes of west, south and central South Africa. Two transects run along rainfall gradients and across the winter, bimodal, all-year and summer rainfall zones (Figure 2B). The sample localities were spaced based on the distribution of bioregions, vegetation types, and vegetation units of the classification by Mucina and Rutherford (2006). The total number of surface soil samples collected is 118, of which only a selection of 43 have been analyzed and their data presented here. The additional 75 samples are still being processed and analyzed.

The locality of each sample was selected in areas with less apparent disturbance away from roads and fields or areas with noticeable exotic vegetation. At each sample locality a 2 × 2 meter quadrat was laid and the cover vegetation was described and the percent coverage of grasses, restios, sedges, forbs, and woody plants were estimated. In areas with trees, the quadrats were 5 × 5 meters. After describing the vegetation and taking the GPS reading, 5 pinches of surface soil were collected at random spots within the quadrat. At least two samples were taken in each vegetation unit crossed by the transect.

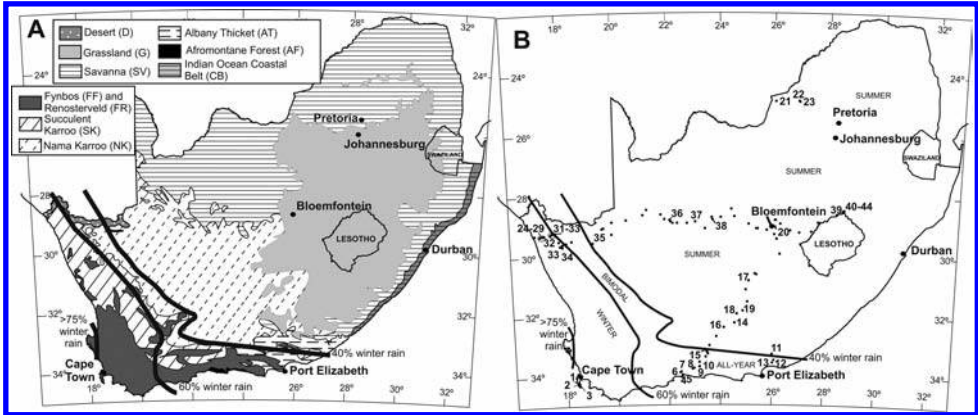


Figure 2. Biomes of South Africa, Lesotho and Swaziland (A) and surface sample transect (B). Samples used in this study are numbered.

6.2.3 Processing, identification and counting

Phytoliths from surface soil samples collected along the transects were extracted by a modified version of the POW method (see Lentfer and Boyd, 1999). This method involves the removal of carbonates using 35% hydrochloric acid and the removal of organics by ignition at 500°C for 2 1/2 hours. The samples were mounted on slides using Entellan as a medium. Identification and counting were done at 400x under a refraction microscope and each sample involved at least 300 counts.

The processing was done separately for inflorescence, leaves, and culm, and in some cases roots. Extraction of phytoliths from plant specimens was carried out by ignition at 500°C for 2 1/2 hours. After cooling the carbonates were removed in 35% hydrochloric acid, neutralized and mounted on slides using Entellan as a medium.

Identification and counting of GSSC morphotypes and Cyperaceae and Restionaceae phytoliths were accomplished using the classification described below. Photographs as references were used, as opposed than the morphotype renderings presented here. The counts included 500–700 phytoliths including dicots. The percentages for Poaceae, Cyperaceae, and Restionaceae were based on the total number of phytolith of the three families. The percentages of each GSSC morphotypes were based on the total number of diagnostic GSSC morphotypes. The grouping of percentages into subfamilies is explained in section 6.4.1

6.2.4 Maps as sampling background

This research strategy involved the construction of general maps to show the distribution of grass subfamilies and the areas of relatively high diversity. The maps were created using lists of important taxa provided for each vegetation unit in Mucina and Rutherford (2006), which contains a paper and electronic version of the vegetation map of South Africa, Lesotho and Swaziland. A layer with dots spaced every 15 degrees was laid over the map of vegetation units. Each dot pointed to a particular

vegetation type, from which a record of graminoid species was obtained from the list of important taxa. Then the number of native species was selected and isolines were traced to enclose areas with more than 5 species. The outer borders of the distribution of grasses were defined using the species maps in Gibbs-Russell *et al.* (1990). The species counted for the maps include only native ones. This methodology is based on maps of grass subfamilies for the Great Plains of North America published by Brown (1993) who compiled information from lists of grasses published in county surveys.

The maps of grass subfamilies distribution presented in this paper include the Pooideae, Ehrhartoideae, and Danthonioideae, and Aristidoideae (Figures 3 and 4) and distribution of Cyperaceae and Restionaceae families (Figure 5). The maps are based on the distribution of native species of each taxonomic group. These maps are not intended to be an accurate distribution of graminoid families and subfamilies, but an indication of their broad geographic distribution, areas of concentration, and genus-level diversity. Maps for Panicoideae and Chloridoideae are not presented here because of space limitations in this paper. The Panicoideae and Chloridoideae subfamilies are present in the entire territory of South Africa, but dominate in the summer rainfall area (see Figure 1).

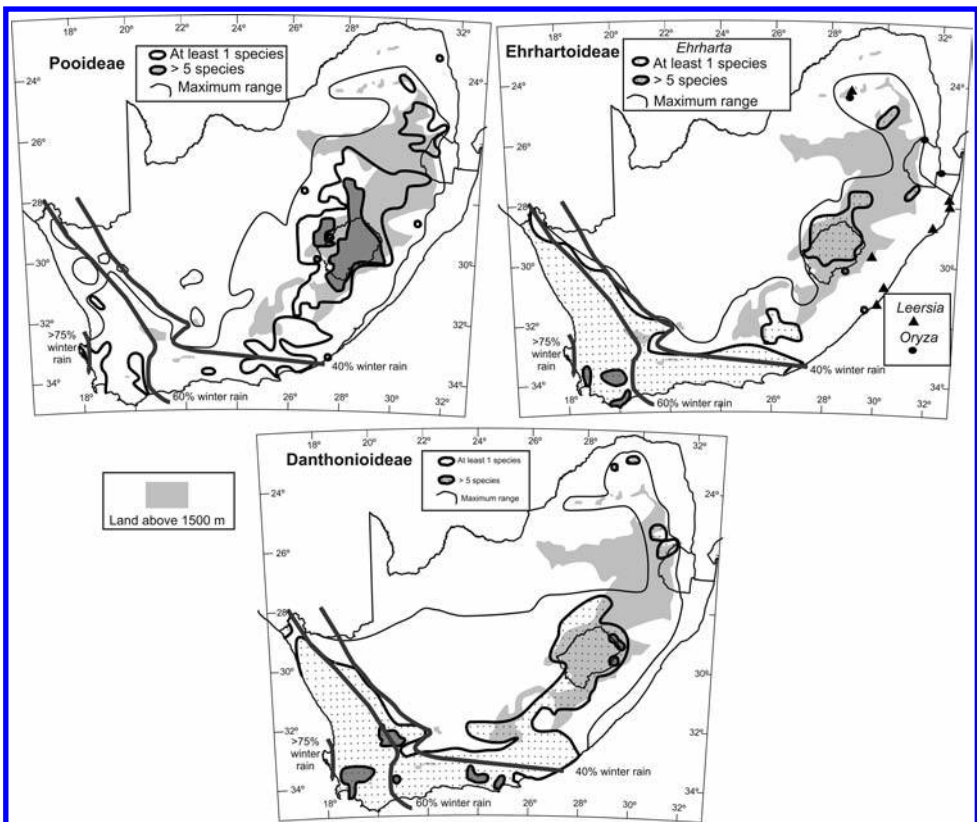


Figure 3. Distribution of Pooideae, Danthonioideae and Ehrhartoideae.

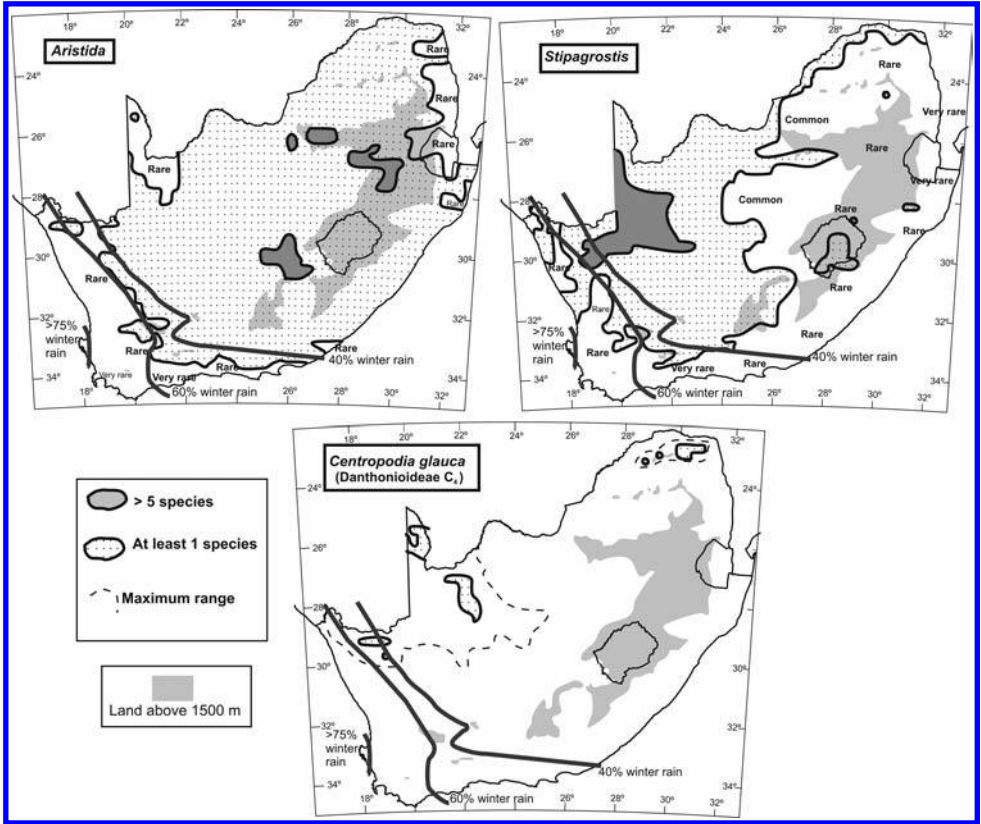


Figure 4. Distribution of Aristidoideae (*Aristida* and *Stipagrostis*) and *Centropodia glauca* (C₄ Danthioioideae).

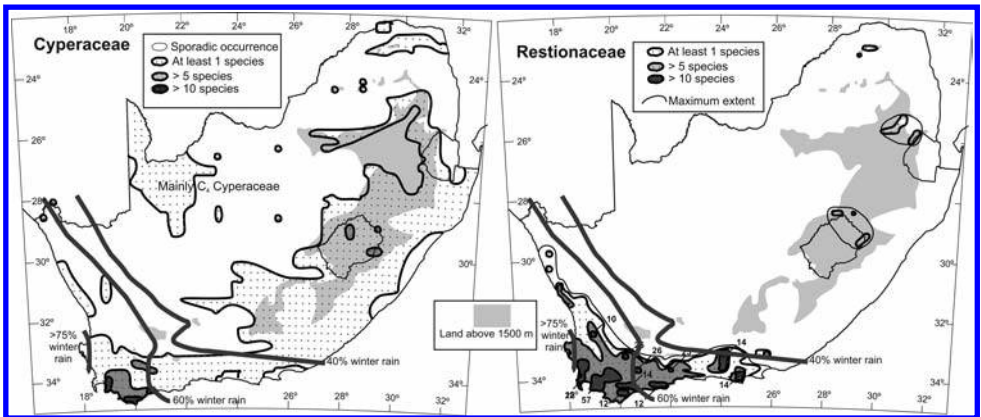


Figure 5. Distribution of Cyperaceae and Restionaceae.

6.3 BIOGEOGRAPHIC ASPECTS OF SOUTH AFRICAN GRAMINOIDS

6.3.1 C₃ and C₄ grasses

The maps of grass species distribution based on the PRECIS database (Gibbs-Russell *et al.*, 1990) provide a picture of the diversity and geographic distribution of species in Southern Africa that is difficult to appreciate given the high complexity at low taxonomic levels. But when seen at the subfamily level, some interesting biogeographic patterns emerge (Vogel *et al.*, 1978; Gibbs-Russell, 1988; Gibbs-Russell *et al.*, 1990). But more useful for phytolith research for palaeoclimatic reconstruction is the focus on the distribution C₃ and C₄ subfamilies (Scott, 2002; Rossouw, 2009).

The C₃ grass subfamilies include the Pooideae, Ehrhartoideae and Danthonioideae (Figure 3). The Pooideae in South Africa are represented by 4 tribes (Poodeae, Triticaeae, Avenae, and Stipaeae), 36 genera, and 125 species, of which 62 species are native (Gibbs-Russell *et al.*, 1990). The introduced species, most of which are from the Mediterranean region are widespread in many areas of the Cape region where they have been naturalized (Gibbs-Russell *et al.*, 1990; van Wyk and van Oudtshoorn, 2004). Although the Pooideae are widespread in the winter rainfall zone, the subfamily has its largest diversity in the mountains within the summer rainfall area.

The dominant genus of Ehrhartoideae in Southern Africa is the genus *Ehrharta*, which evolved in the Cape Region and has phylogenetic ties with Australia (Verboom *et al.*, 2003). Other Ehrhartoideae in South Africa belong to the Oryzaceae tribe (the rice tribe), with *Leersia* (2 species) and *Oryza* (3 species) as two common genera in aquatic environments (Gibbs-Russell *et al.*, 1990). The genus *Ehrharta* dominates in the Cape Region, but it is widely found in the mountains and along the south coast to central Kwazulu-Natal. The highest species diversity of the *Ehrharta* world-wide is found in the Cape Region of South Africa, where 22 species out of 56 exist (Verboom *et al.*, 2003).

The Danthonioideae was previously assigned to the Danthoniae tribe within the subfamily (Danthoniae in Gibbs-Russell *et al.*, 1990). Its status as a separate subfamily is confirmed in by the Grass Phylogeny Working Group (2003). The Danthonioideae subfamily includes one tribe and it is found in all continents. However, the highest taxonomic diversity is found in the South Africa, where 9 genera and 125 species have been identified (Linder and Barker, 2000). Within South Africa the highest diversity occurs in the Cape Region (Figure 3). *Centropodia glauca* is a C₄ species in the C₃-dominated Danthonioideae. This species is treated here separately because it is widely distributed in the Kalahari region (Figure 4).

The C₄ grasses dominate in the summer rainfall season, but they are widely distributed in the other rainfall regions as well. Overall, their dominant families are the Panicoideae and Chloridoideae. According to Gibbs-Russell (1988) the Panicoideae dominate in the eastern third of the country and the Chloridoideae in the western part of the summer rain region. Therefore, the Chloridoideae are more drought tolerant and more apt for areas of higher rain variability (Figure 1).

The Aristidoideae have a more localized distribution (Figure 4) and are poorly known in terms of GSSC morphotypes. The two representative genera in South Africa are *Aristida* and *Stipagrostis*, which concentrate in different regions. While *Aristida* occupies the central part of the country sharing territory similar with the Chloridoideae, *Stipagrostis* dominates in the Kalahari and the Bushmanland Karroo (Figure 4). However, in the same subfamily, *Aristida* and *Stipagrostis* present remarkable differences in GSSC morphology. Therefore, because of their differences in their biogeographic distribution and phytolith morphology they are treated separately in this study.

6.3.2 Cyperaceae and Restionaceae

The Cyperaceae and Restionaceae families in South Africa present different distribution patterns. The Cyperaceae have a widespread distribution, particularly because of their photosynthetic duality (Figure 5). However, in terms of diversity and representation they tend to concentrate in the winter-rainfall region and at high elevations. Cyperaceae are also relatively abundant at high elevations and in wet grounds. Other areas with large number of them include the Drakensberg grasslands (Mucina *et al.* 2006).

The Restionaceae, a C_3 family, are concentrated in the winter-rainfall region (Figure 5), where they are the dominant graminoid in the fynbos biome, except in the Renosterveld (Rebello *et al.*, 2006). During the transect collection it was also observed that in some fynbos vegetation types, grasses tend to dominate in disturbed areas, particularly where fire is a factor, although at the end of the succession they are outnumbered again by the restios and sedges.

6.3.3 Bioclimatic framework of graminoid distribution

Characterization of grass phytoliths using multivariate statistics has shown a complex mesh of crossover areas involving annual precipitation and rainfall seasonality (Mulder and Ellis, 2001; Rossouw, 2009) as well as geographic aspects such as shade, topography, and a number of microclimatic factors (Rossouw, 2009). But overall the general aspect of bioclimatic distribution of phytoliths at the grass subfamily level has yet to be explored by downplaying the lesser known grass subfamilies (Ehrhartoideae, Danthonioideae and Aristidoideae). Additionally, no study has yet evaluated the bioclimatic significance of the Cyperaceae and Restionaceae families. Therefore, a bioclimatic characterization of grass subfamilies and graminoid families is one of the initial objectives of this study. The main variables explored here are total annual rainfall, temperature of the growing season, rainfall variability, and rainfall seasonality (Figure 6).

The C_3 grass subfamilies have strong concentration in the winter region, particularly the Cape grasses (Danthonioideae and Ehrhartoideae). Although these two subfamilies share a similar territory, the Danthonioideae seem to be more common in the mountains of the summer-rainfall region, while the Ehrhartoideae are more widespread along the south coast (Figure 3). The Pooideae are more common at high elevations in the summer region than the other two C_3 subfamilies and less abundant in the winter-rainfall region. The Danthonioideae and Ehrhartoideae extend their territory farther north along the west coast towards the drier areas of the northwest where rainfall variability is higher. Records obtained during the transect show that the majority of Pooideae observed in the Cape Region are non-native species (e.g., the genera *Avena*, *Briza*, *Bromus*, *Hordeum*) most of which occupy mainly disturbed areas, and a large number naturalized (Gibbs-Russell *et al.*, 1990). This situation raises the question: What was the distribution of native Pooideae in pre-European times? The answer may be difficult to find, although a detailed phytolith study in high resolution sedimentary records could provide an idea at least at a subfamily level.

The C_4 grass subfamilies present a more diverse distribution both geographically and bioclimatically (Figure 6). The Panicoideae have predominance in areas of the summer-rainfall region where rain is abundant and less variable. The more drought-resistant Chloridoideae and Aristidoideae extend into the drier parts of the country,

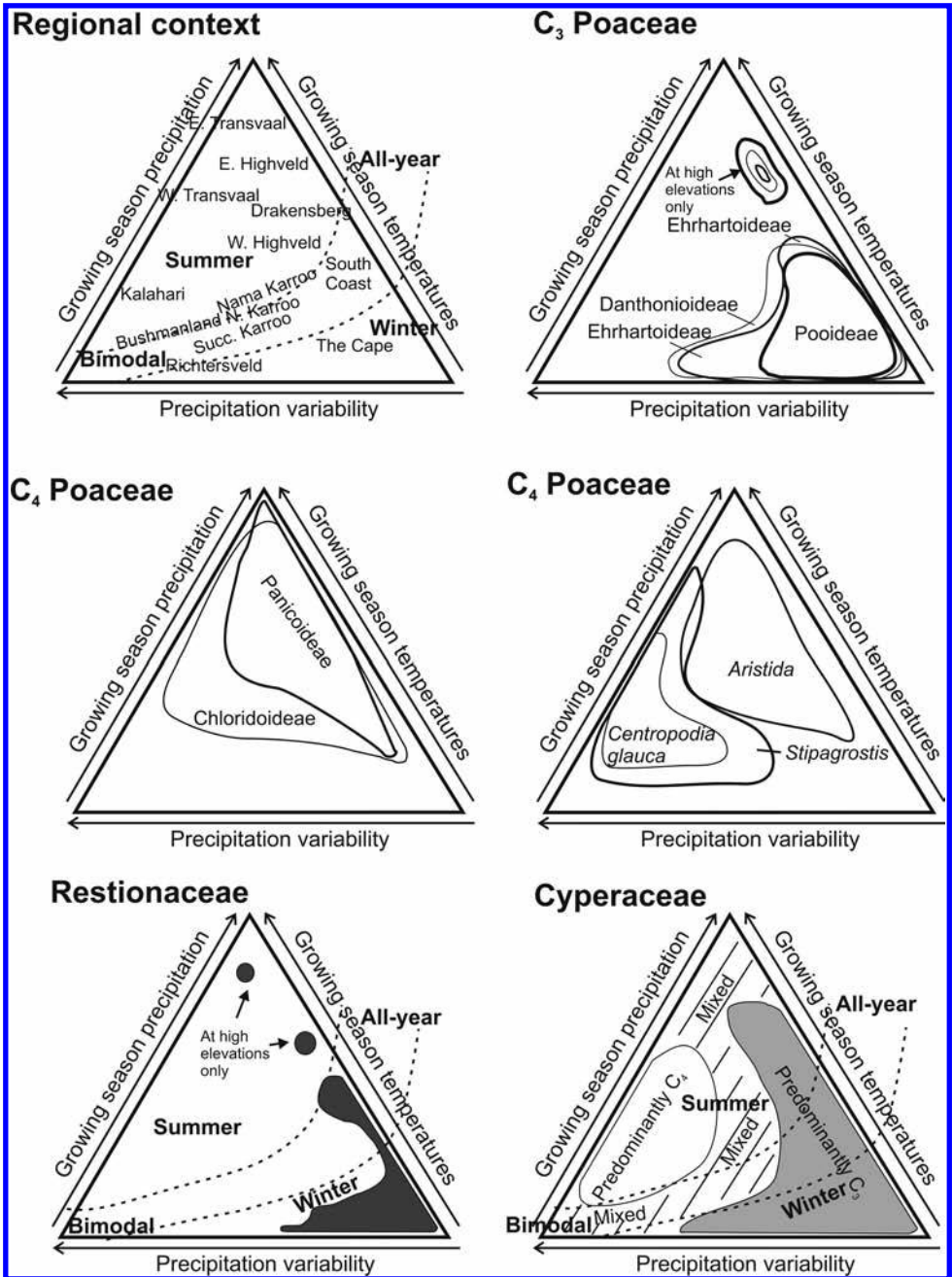


Figure 6. Conceptual bioclimatic framework of graminoid distribution in South Africa. Each taxonomic group is represented as areas where they are strongly present. The models are based on distribution of native species.

particularly the north and west. *Aristida* and the Chloridoideae seem to occupy similar territories, in the subhumid, semi-arid parts of the Grassland and Nama-Karoo biomes. The Chloridoideae, however, extend into areas of the bi-modal, all-year, and winter rainfall regions. During the recording of species in the quadrats along the transect, the Chloridoideae appear sometimes to dominate or co-dominate with the C_3 grass subfamilies in the less humid parts of the winter-rain region. The number of Chloridoideae declines in areas of higher precipitation in the mountains on all zones. *Stipagrostis* dominates in areas of lowest annual precipitation and highest variability in the northwestern end of the summer-rainfall regions and the northern part of the bimodal rainfall region.

The Cyperaceae are widespread, but with stronger presence in the Southern part of the winter-rain region, particularly in some fynbos ecotypes, and at high elevations. But its diversity, cosmopolitan nature, and aquatic affinity are not indicative of particular climatic aspects (Kotze and O'Connor, 2000). C_3 and C_4 Cyperaceae are found in most biomes of South Africa, with the marked abundance of C_4 Cyperaceae in the Kalahari sands. However, the fynbos presents a high species diversity and strong representation in the landscape (Rebello *et al.*, 2006). Therefore, a large number of Cyperaceae diagnostic phytoliths may be indicative of winter rain or overall cool and wet conditions. The Restionaceae, which are strongly concentrated in the winter rainfall zone appear also in limited numbers at high elevations elsewhere (Figure 5).

6.4 OPAL PHYTYOLITH MORPHOTYPES

6.4.1 Classification of phytolith morphotypes

The classification of GSSC morphotypes singled out from identified grass specimens resulted in 111 morphotypes, which were divided into 12 shape-based groups (Figures 7, 8 and 9). The designation of these groups is based on names selected from previous classifications proposed by Twiss *et al.* (1969), Mulholland and Rapp (1992), Brown (1984), Fredlund and Tieszen (1994, 1997) and Madella *et al.* (2005). The 12 shape-based groups however, have no taxonomic affinity or value, they are used here as means of facilitating the handling of a large number of morphotypes.

Each GSSC morphotype is labelled with a capital letter (e.g., A, B, C) within each group (Tables 1–9). The individual GSSC morphotypes were used here define diagnostic morphotypes to each taxonomic group of grasses. Therefore, the most abundant morphotypes in each group were selected and classified by their uniqueness, distinctiveness and share in each taxonomic group.

Cyperaceae and Restionaceae phytoliths were treated here separately and their division was purely based on the most common shapes found in the reference collections (Figure 10). The Cyperaceae phytoliths (Figure 10-A) include several hat forms (1), papillae (2 and 3), long keeled (4 and 5), silicified hairs (7), wavy and anticlinal cells (6, 8, 9, 10) as well as composites and long (10, 11, and 12). The most common and diagnostic found in soil samples are numbers 1, 2, 3, 6, 9 and 10.

The Restionaceae phytoliths (Figure 10-B) are dominated by discoidal forms, some of which are keeled, papilated, or resemble a volcano, have concentric lines, keeled surfaces and pitted surfaces (1–14). Other groups include tracheal shapes (19), hairs (16), and paddle shape elongated shapes (15, 18, 20, 21, and 22). The most distinctive and more abundant in soil samples where restios grow are the discoidal and paddle shapes.

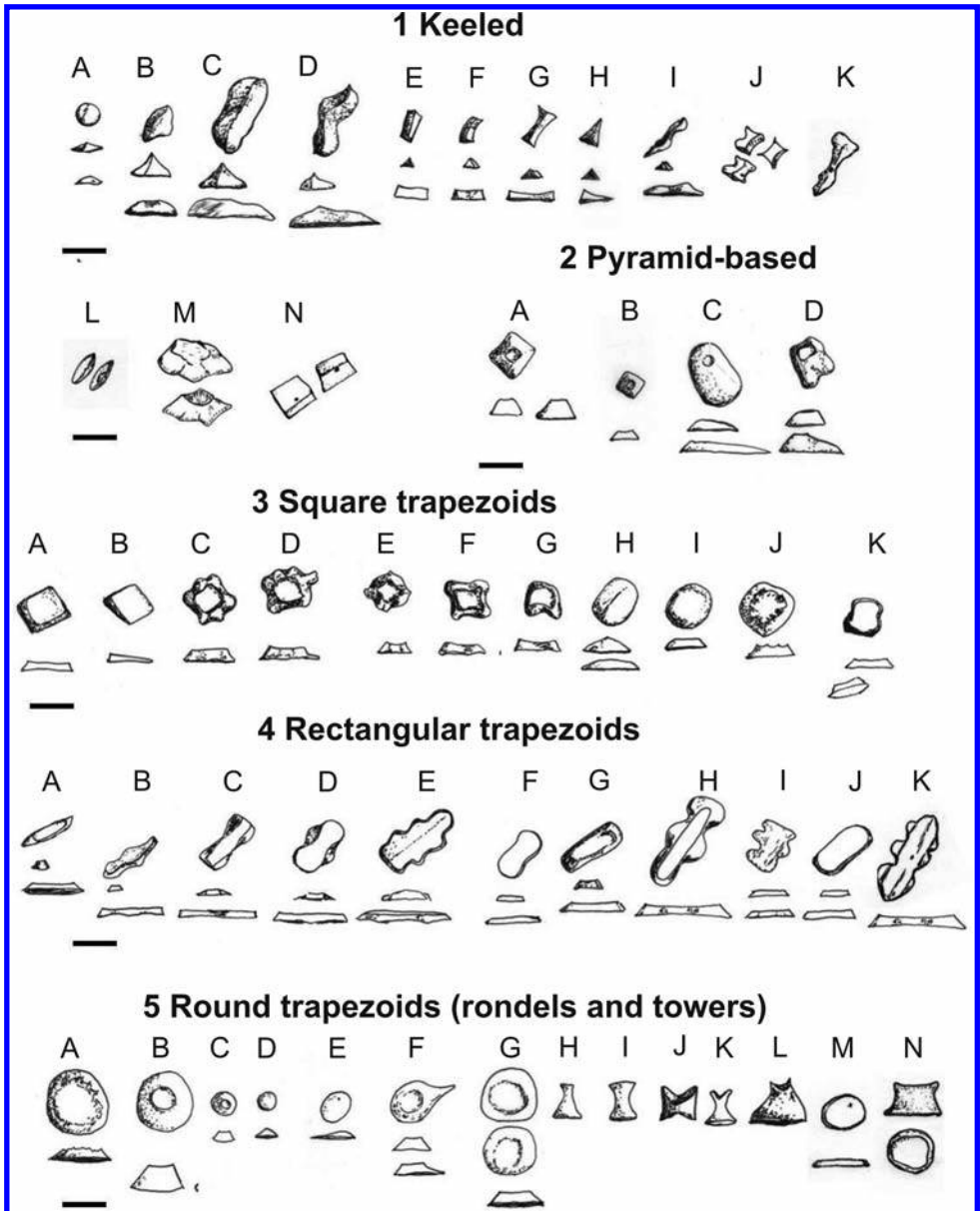


Figure 7. Short-cell morphotypes Groups 1–5. Scale bars are 20 µm long.

6.4.2 Distinctive and shared GSSC morphotypes

The distribution GSSC morphotypes among Poaceae taxonomic groups (subfamily, tribe, genera and species) represents a problem because of morphotype share among subfamily. In this study, the approach taken for solving this problem encompasses first an assessment of the relative abundance of each GSSC-morphotype in each taxonomic

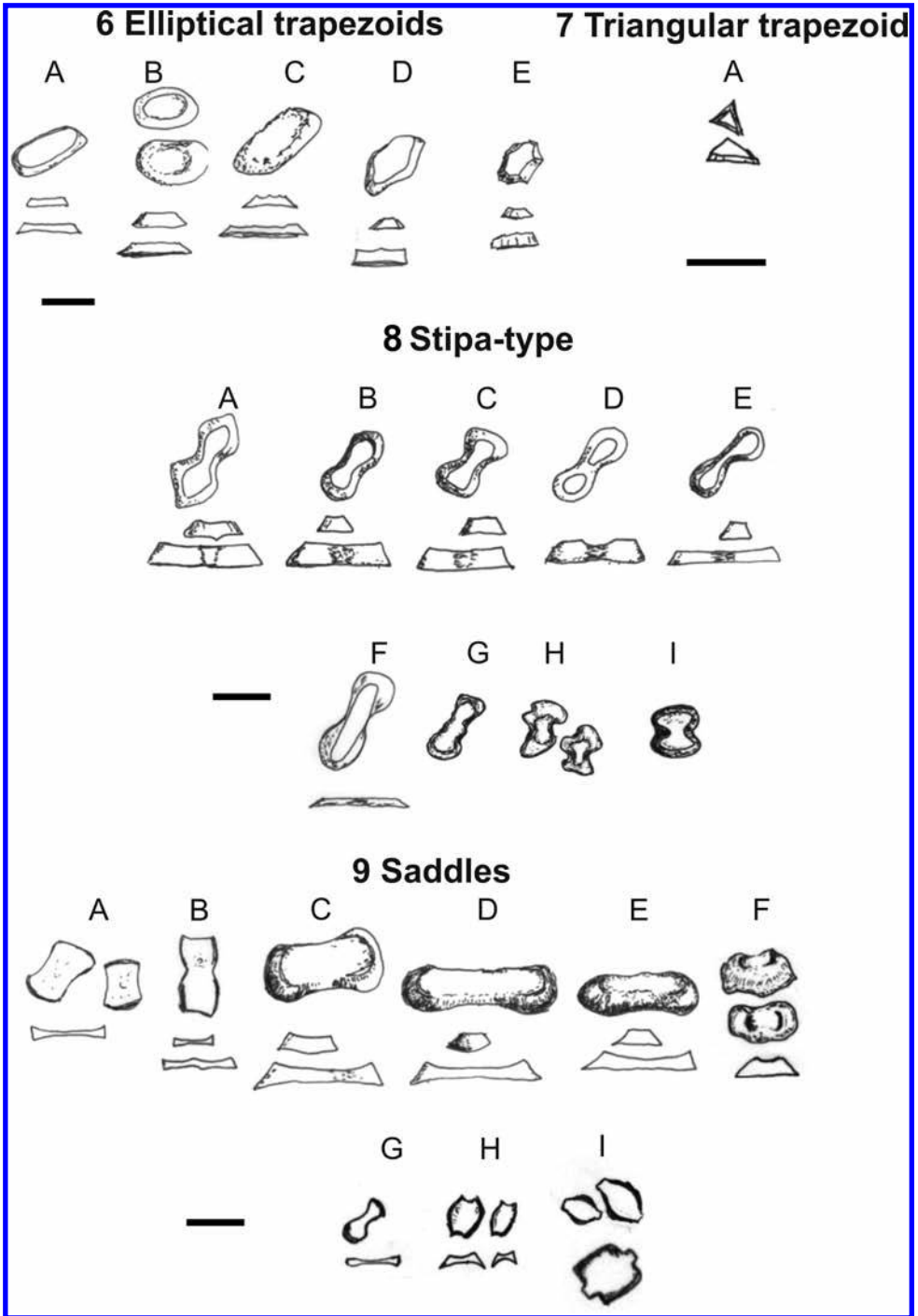


Figure 8. Short-cell morphotypes Groups 6–9. Scale bars are 20 μm long.

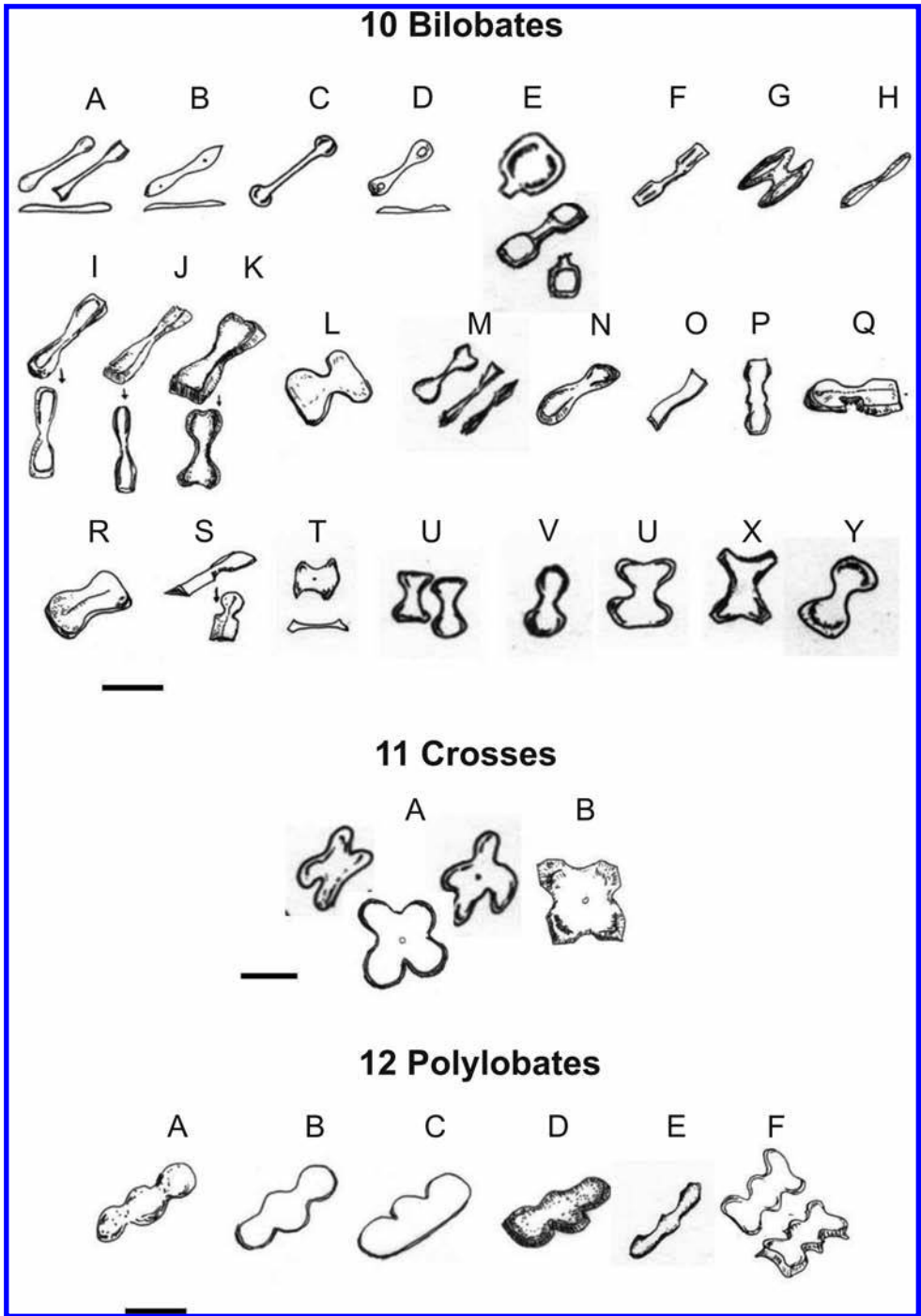


Figure 9. Short-cell morphotypes Groups 10–12. Scale bars are 20 μm long.

Table 1. Subfamily Pooideae. Relative abundance of GSSC morphotypes.

	Very abundant	Abundant	Common	Rare	Very rare
1 Keeled	B	C	A D	E	E
2 Pyramid-based trapezoids			A C		
3 Square-based trapezoids	A	I K	H C ¹		B
4 Rectangle-based trapezoids		F	A G H K	E	J
5 Round-based trapezoids		BC	D G N	E J K L	H
6 Elliptical trapezoids			A B C		
7 Triangular trapezoids					
8 Stipa-type		B	A C G H I	E F	
9 Saddles					
10 Bilobates					L U
11 Crosses					
12 Polylobates			D E ²		

¹ Found only in *Koeleria lachnantha*.² Only found in several *Stipa*.**Table 2.** Subfamily Ehrhartoideae. Relative abundance of GSSC morphotypes.

	Very abundant	Abundant	Common	Rare	Very rare
1 Keeled	A B	H	C D	K	E F G
2 Pyramid-based trapezoids			A	C	
3 Square-based trapezoids		B	A		C D E F
4 Rectangle-based trapezoids			C G J	H	
5 Round-based trapezoids			C D H M ¹	M	E I K N
6 Elliptical trapezoids					
7 Triangular trapezoids			A		
8 Stipa-type		C			
9 Saddles			D E		
10 Bilobates		T ²	F Q R S T W	L M N U W	E G K X
11 Crosses		B ³			
12 Polylobates					

¹ Abundant in *Ehrharta longiflora*, otherwise rare.² Abundant in *Leersia hexandra*, common to rare in *Ehrharta*.³ observed in *L. hexandra* only.

Table 3. Subfamily Danthonioideae, C₃ species. Relative abundance of GSSC morphotypes.

	Very abundant	Abundant	Common	Rare	Very rare
1 Keeled	A B	G	C I K L N ¹	M	
2 Pyramid-based trapezoids		D	C	A	
3 Square-based trapezoids		B G	C D F	A I K	
4 Rectangle-based trapezoids		E I F G J	C D H I	A	
5 Round-based trapezoids	C D		B F	G J	H I N
6 Elliptical trapezoids			B I	A D	
7 Triangular trapezoids					A
8 Stipa-type		B	E F	C I	
9 Saddles		C	F		
10 Bilobates		Q ² R ²	G O R S	Q	B D
11 Crosses					
12 Polylobates			B		

¹ Found in several species of *Pentameris*.

² Found in *Schismus* species only.

Table 4. Subfamily Danthonioideae, *Centropodia glauca*. Relative abundance of GSSC morphotypes.

	Very abundant	Abundant	Common	Rare	Very rare
1 Keeled		A	B		
2 Pyramid-based trapezoids					D
3 Square-based trapezoids			A E I J		G
4 Rectangle-based trapezoids					
5 Round-based trapezoids			C	B G	
6 Elliptical trapezoids		B		C D	
7 Triangular trapezoids					A
8 Stipa-type			E H	C	B
9 Saddles			C		F
10 Bilobates					
11 Crosses					
12 Polylobates					

Table 5. Subfamily Arundinoideae. Relative abundance of GSSC morphotypes.

	Very abundant	Abundant	Common	Rare	Very rare
1 Keeled		G	B	A	
2 Pyramid-based trapezoids	D				
3 Square-based trapezoids			A ¹	I	
4 Rectangle-based trapezoids			C D F	E	J
5 Round-based trapezoids		B C	N	K ¹	H I L
6 Elliptical trapezoids				B	A
7 Triangular trapezoids			A		
8 Stipa-type					
9 Saddles	C		E F		D
10 Bilobates		A ²	C U		
11 Crosses			A ²		
12 Polylobates			B C	R	

¹ *Phragmites australis* only.² *Arundo donax* only.**Table 6.** Subfamily Aristidoideae, genus *Aristida*. Relative abundance of GSSC morphotypes.

	Very abundant	Abundant	Common	Rare	Very rare
1 Keeled			G	A	
2 Pyramid-based trapezoids					
3 Square-based trapezoids					K
4 Rectangle-based trapezoids				F	
5 Round-based trapezoids		B			K
6 Elliptical trapezoids					E
7 Triangular trapezoids					A
8 Stipa-type					D
9 Saddles			I		
10 Bilobates	B	A C D	H		U
11 Crosses					
12 Polylobates					

Table 7. Subfamily Aristidoideae, genus *Stipagrostis*. Relative abundance of GSSC morphotypes.

	Very abundant	Abundant	Common	Rare	Very rare
1 Keeled		H	A E M	B D J	G
2 Pyramid-based trapezoids			C	D	
3 Square-based trapezoids	B C	A	D E I J		F
4 Rectangle-based trapezoids		F	G J		C
5 Round-based trapezoids	D	C E	F J	G	
6 Elliptical trapezoids		B	C	D	E
7 Triangular trapezoids			A		
8 Stipa-type					
9 Saddles			C F	D E	
10 Bilobates			E	D U	
11 Crosses					
12 Polylobates					

Table 8. Subfamily Chloridoideae. Relative abundance of GSSC morphotypes.

	Very abundant	Abundant	Common	Rare	Very rare
1 Keeled			J	H	
2 Pyramid-based trapezoids					
3 Square-based trapezoids					B
4 Rectangle-based trapezoids					
5 Round-based trapezoids			H I J K	L	N
6 Elliptical trapezoids				D E ¹	
7 Triangular trapezoids					
8 Stipa-type					
9 Saddles	A B	G H			
10 Bilobates		M ² U			
11 Crosses					
12 Polylobates					

¹ Known also as *Spartina*-type (Lu and Liu, 2003).

² Common only in *Schmidtia*.

Table 9. Subfamily Panicoideae. Relative abundance of GSSC morphotypes.

	Very abundant	Abundant	Common	Rare	Very rare
1 Keeled			J		
2 Pyramid-based trapezoids					
3 Square-based trapezoids				K	
4 Rectangle-based trapezoids			F		
5 Round-based trapezoids			M	H	J L
6 Elliptical trapezoids					
7 Triangular trapezoids					
8 Stipa-type					C
9 Saddles				G H	
10 Bilobates	K V W X	I J	P U	Y	M
11 Crosses		A			
12 Polylobates			A F	D	

group and the division of morphotypes between shared and distinctive to each family. Abundance here has been divided as follows:

- Very abundant, morphotype constitutes more than 80% in at least 50% of all the species in the taxon.
- Abundant, morphotype constitutes 60–80% in at least 50% of all species in the taxon.
- Common, morphotype constitutes 30–60% in at least 50% of all species in the taxon.
- Rare, morphotype constitutes 10–30% in at least 50% of all species in the taxon.
- Very rare, morphotype constitutes less than 10% in at least 50% of all species in the taxon.

The taxonomic groups included in Poaceae in this study are the most abundant sub-families in South Africa (Pooideae, Ehrhartoideae, Danthonioideae, Arundinoideae, Aristidoideae, Panicoideae and Chloridoideae). The Aristidoideae family was split into its main genera, *Aristida* and *Stipagrostis*, given that these two taxa dominate in different parts of the country and that their GSSC morphotypes are remarkably different. *Centropodia glauca* was separated from the Danthonioideae given its widespread distribution in the northwest and that its C₄ photosynthetic pathway is different from the rest of the subfamily. The matrices in Tables 1 to 9 represent the abundance of each GSSC morphotype arranged by group (left column) found in all the grass specimens collected and analyzed directly or referenced in Rossouw (2009). Find the corresponding GSSC morphotype, by group and letter in Figures 7, 9 and 9. For example a B in the row of '1 Keeled' (left column) corresponds to morphotype B in the Keeled group.

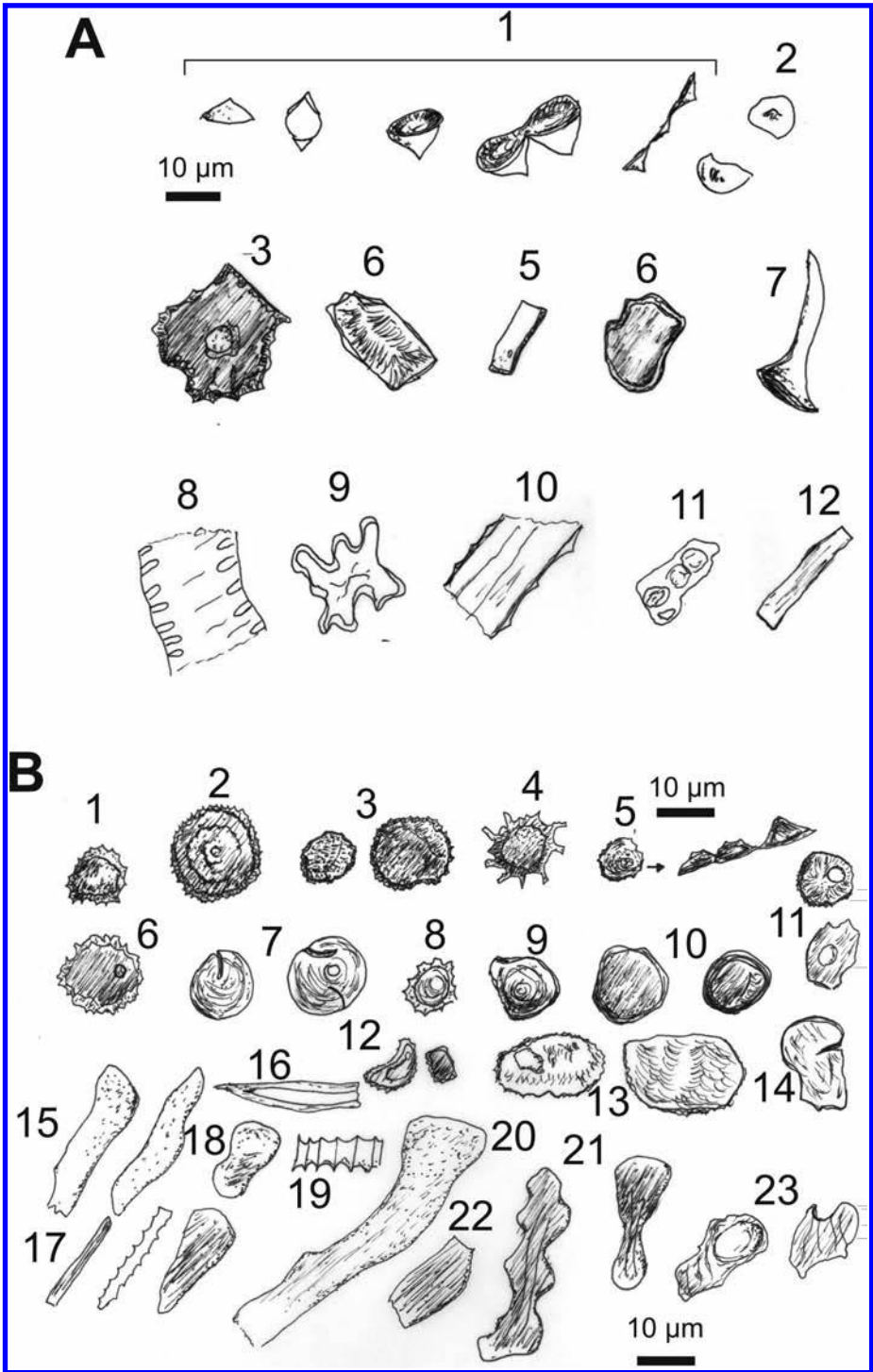


Figure 10. Cyperaceae and Restionaceae phytoliths

To reduce the number of shared morphotypes, the Rare and Very Rare categories were eliminated. Nevertheless, the resulting number of shared morphotypes is still high among some taxonomic groups (Table 10). By far the highest share occurs between Pooideae and Danthonioideae (12), Pooideae and Ehrhartoideae (12), Pooideae and Stipagrostis (12), Ehrhartoideae and Danthonioideae (13), and Danthonioideae and *Stipagrostis* (14). On the other hand, it is possible to view the shared and distinctive GSSC morphotypes overall by each taxonomic group (Table 11). The distinctive GSSC morphotypes encompass the ones that are exclusive (i.e., not found in any other group) to each taxonomic group, and those that are present in other taxonomic group as Rare or Very Rare.

The Pooideae have the largest number of distinctive GSSC morphotypes (12); Arundinoideae has the lowest (2), and *Centropodia glauca* has no distinctive morphotypes (Table 11). On the other hand, the Danthonioideae, Ehrhartoideae and Arundinoideae have the largest number of shared GSSC morphotypes, with 33, 26 and 26, respectively. *Aristida* has the lowest number of shared morphotypes (2), followed by Panicoideae (6) and Chloridoideae (7) (Table 11).

The meaning of these numbers is that in soil and sediment samples, a taxonomic group with high number of distinctive GSSC morphotypes is likely to be overrepresented (e.g. Pooideae). Conversely, a taxonomic group with a low number of distinctive morphotypes is likely to be misrepresented or invisible in the assemblages (e.g. Arundinoideae and *Centropodia glauca*). On the other hand, taxonomic groups with

Table 10. Number of shared GSSC morphotypes between taxonomic groups.

Taxonomic group	Po	Eh	Dan	Cg	Aru	Ari	Sti	Pa	Chl
Pooideae		12	12	8	7	1	12	2	0
Ehrhartoideae			13	3	6	1	6	2	1
Danthonioideae				4	7	2	14	3	0
<i>Centropodia glauca</i>					5	1	7	1	1
Arundinoideae						1	4	2	1
<i>Aristida</i>							1	0	0
<i>Stipagrostis</i>								2	0
Panicoideae									1
Chloridoideae									

Table 11. Number of morphotypes in each taxonomic group, divided by distinctive, unique and shared.

Subfamilies	Total	Distinctive (unique)	Shared
Pooideae	35	12 (5)	23
Ehrhartoideae	31	5 (4)	26
Danthonioideae	41	8 (4)	33
<i>Centropodia glauca</i>	11	0	11
Arundinoideae	28	2 (1)	26
<i>Aristida</i>	8	6 (4)	2
<i>Stipagrostis</i>	27	4 (0)	23
Panicoideae	13	7 (5)	6
Chloridoideae	13	5 (2)	8

a high number of shared GSSC morphotypes are likely to be misrepresented. Those with the lowest number of shared morphotypes (Aristida, Panicoideae, and Chloridoideae) are likely to represent the group with more fidelity. However, the assessment of the distinctive-shared GSSC morphotypes can only be assessed with soil samples in the context of the distribution of each taxonomic group in the modern landscape.

6.5 RESULTS

The geographic distribution of GSSC morphotypes resulted from the general classification created in this study was tested from selected modern surface samples along two transects straddling the winter and summer rainfall region (Figure 2). The GSSC morphotypes were grouped by distinctive and shared morphotypes for each of the main grass subfamilies (Figures 11 and 12). The assumption is that the real frequency of diagnostic GSSC morphotypes for each group should lie somewhere between the distinctive value (top of dark bar) and the shared value (top of open bar).

The samples have been positioned in a spatial sequence from the winter to the summer rainfall zone. The graphs were arranged separating the C₃ from the C₄ dominated taxa. The Arundinoideae were excluded because its species are predominantly aquatic. *Centropodia glauca* was also excluded because it has no distinctive GSSC morphotypes (Table 11).

The distribution of all Poaceae phytoliths (short-cell, long-cell, pointy and bulbiforms) in relation to the distinctive Cyperaceae and Restionaceae phytoliths in each soil surface sample were plotted as a way of representing the three most important graminoid groups in the landscape (Figure 13).

6.6 DISCUSSION

The distribution of GSSC morphotypes by taxonomic group across the selected surface samples of the two transects shows interesting patterns when viewed in relation to vegetation type and rainfall seasonality and variability. The GSSC assigned to Pooideae are abundant in the winter rainfall zone, but appear still in high numbers elsewhere. The highest numbers of both shared and distinctive types for Pooideae are found in the fynbos samples of the Cape Peninsula (FFs9) and Renosterveld vegetation types (FR). This may be the result of high incidence of naturalized Pooideae, which today are found widespread (See section 1.3.1)

The GSSC morphotypes assigned to the Cape grasses (Ehrhartoideae and Danthonioideae) do show their highest frequencies in the soil surface samples from the winter rainfall zone, particularly the fynbos (FF). In the samples from the winter-rainfall succulent karroo (SK vegetation units) Danthonioideae show larger frequencies of morphotypes at high elevations, while the Ehrhartoideae shows larger frequencies in samples at low elevations. In the highest parts of the Drakensberg grassland (Gd) none of the diagnostic GSSC morphotypes of three C₃ subfamilies predominate, but their numbers are lower than the winter-rainfall region. The highest frequencies of GSSC morphotypes in the Drakensberg grassland samples is in the Panicoideae, followed by the Chloridoideae (Figure 12), which suggests that despite high elevation the C₄ grasses are still the dominant group.

The GSSC morphotypes assigned to the Panicoideae and Chloridoideae appear in relatively moderate and high amount in all samples, but they concentrated in those from summer rainfall zone, showing a parallel with their actual distribution in the landscape.

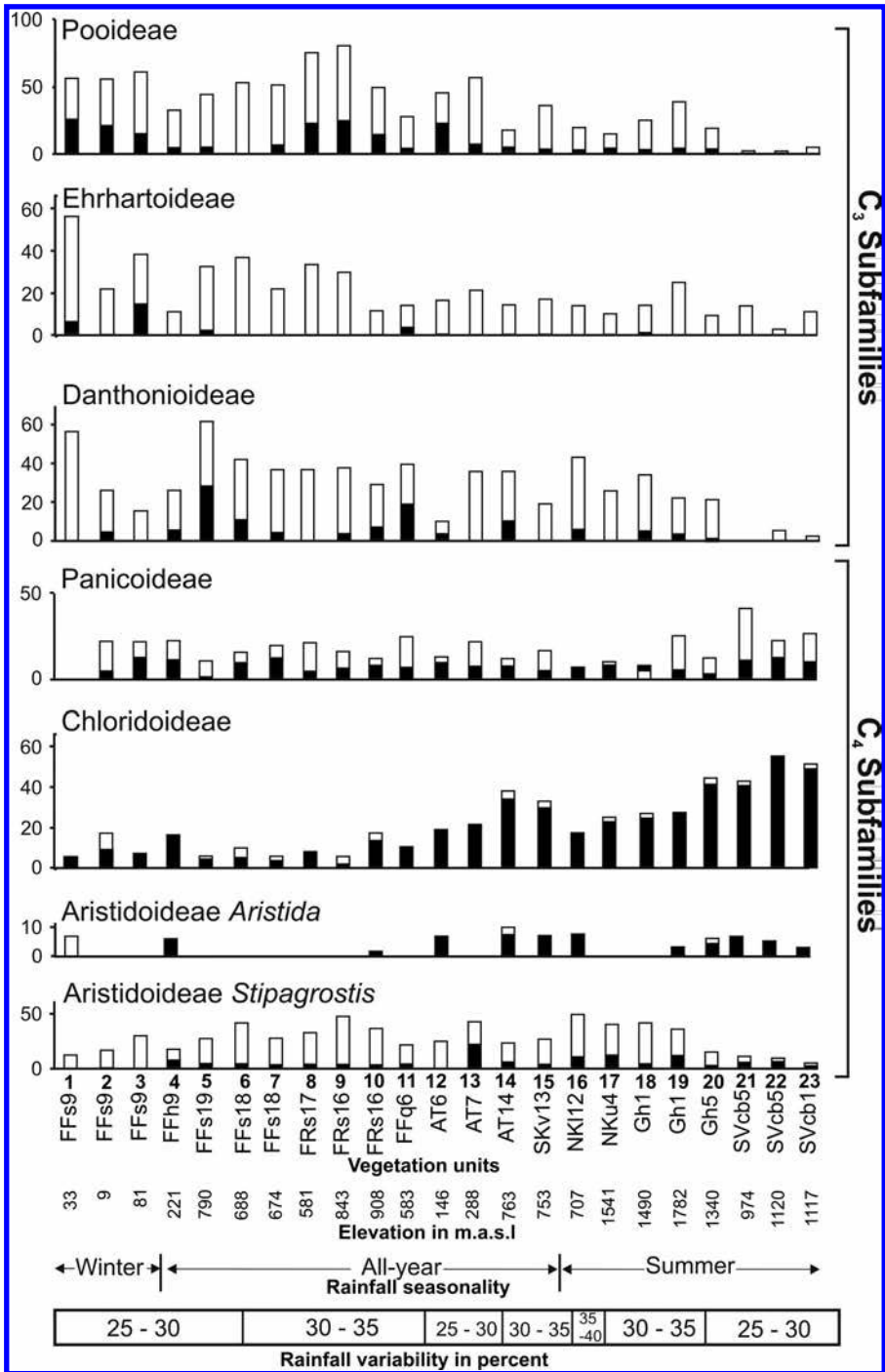


Figure 11. Results of surface soil samples along the west–east transect (Figure 2). The black bar corresponds to the percent of distinctive (including unique) GSSC morphotypes. The white bar is the percentage of shared GSSC morphotypes.

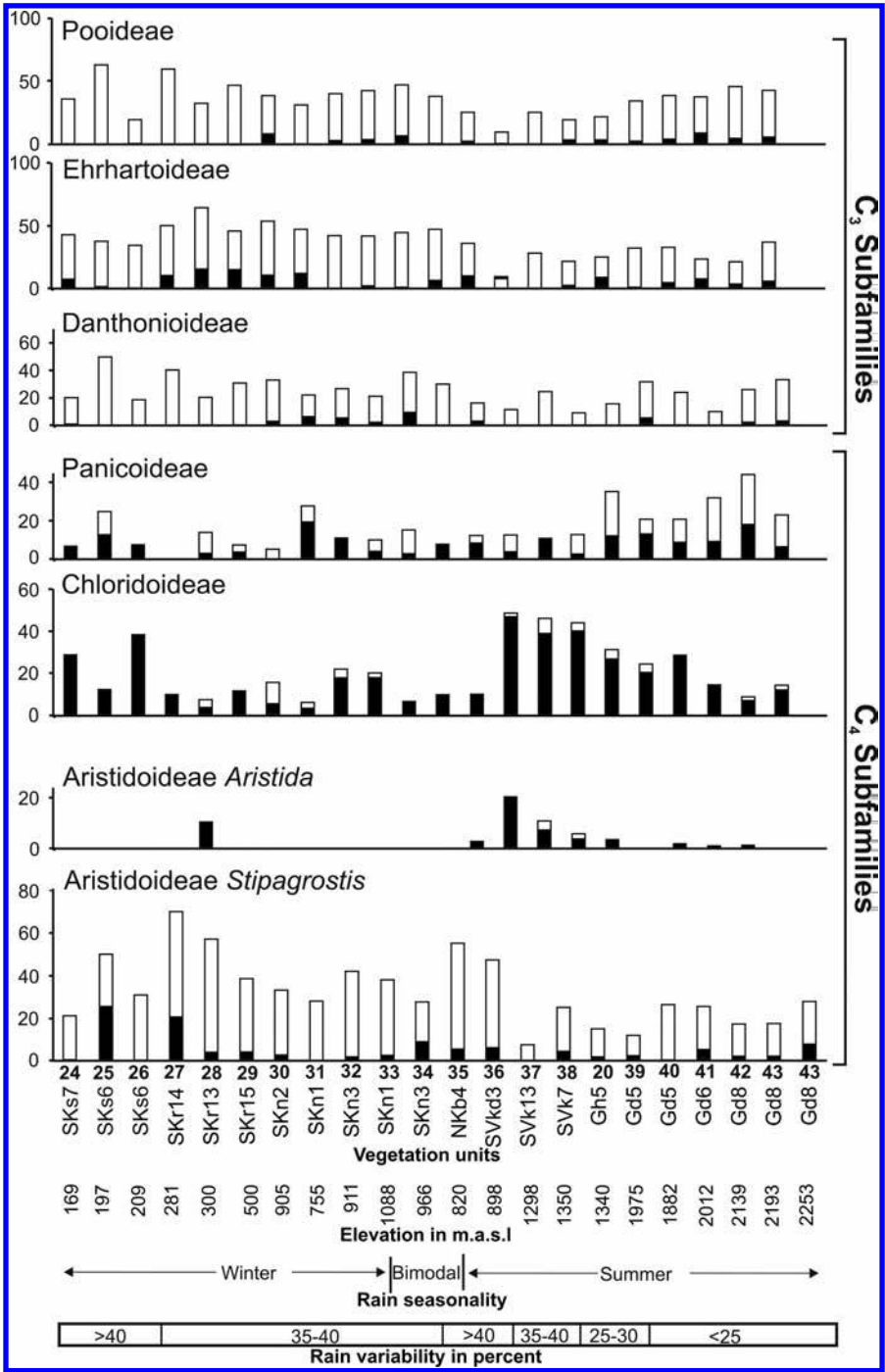


Figure 12. Results of surface soil samples south–north transect (Figure 2). The black bar corresponds to the percent of distinctive (including unique) GSSC morphotypes. The white bar is the percentage of shared GSSC morphotypes.

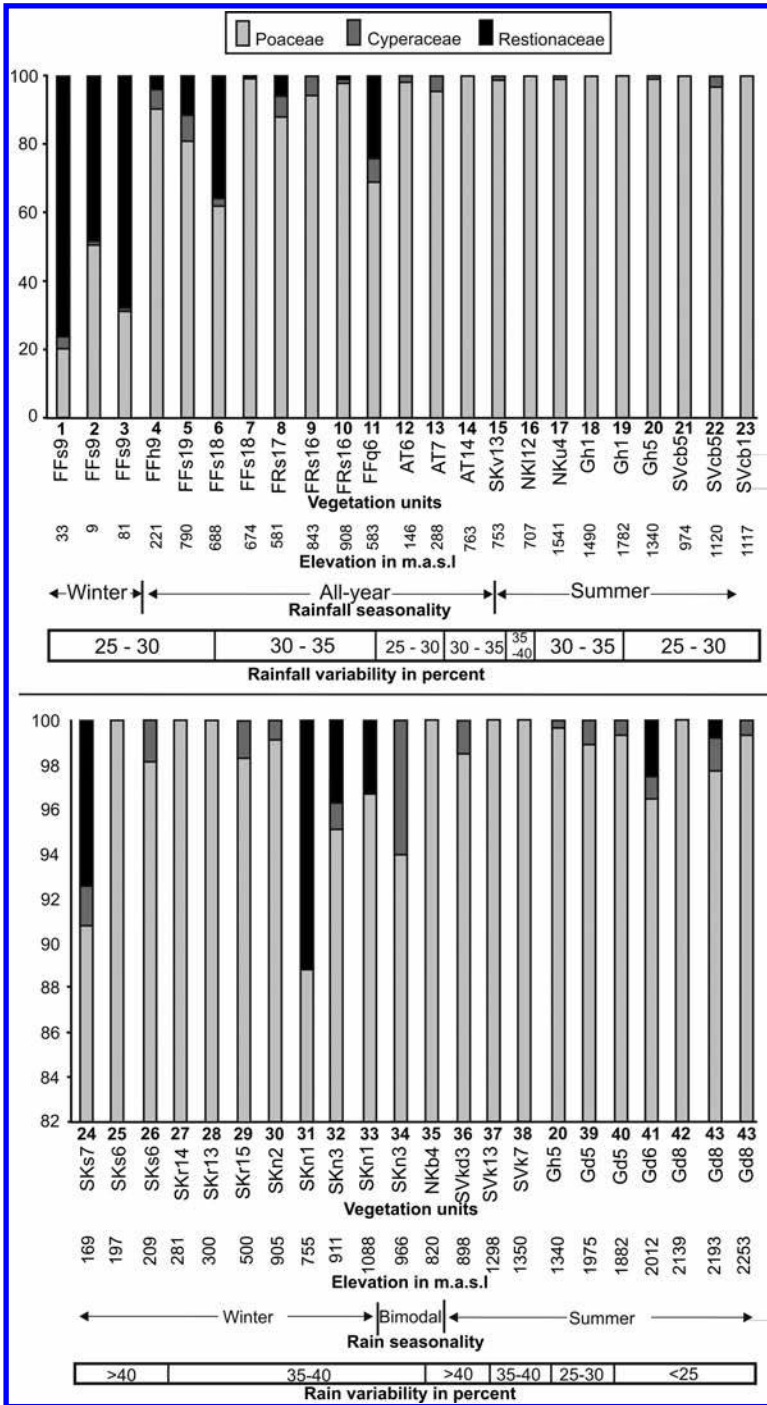


Figure 13. Percent of phytoliths diagnostic of Poaceae, Cyperaceae and Restionaceae in soil surface samples. Percent calculated from the total diagnostic graminoid phytoliths. A) West-East transect, B) South-North transect.

The distribution of *Aristida* GSSC morphotypes in the samples transect parallels those of the Chloridoideae morphotypes. *Stipagrostis* GSSC morphotypes do not reflect the distribution of this genus in the landscape. Their frequencies in samples where the genus is abundant (samples 25, 27, 35 and 36) are not considerably high to denote abundance. On the other hand, samples outside the actual range of *Stipagrostis* grasses contain noticeable frequencies (samples 13, 19, 41, 43).

The Restionaceae diagnostic phytoliths are almost exclusively confined to the winter rainfall zone. The Cyperaceae phytoliths are present in almost all the assemblages, but appear in higher numbers in the samples from the winter rainfall zone and at elevations above 1.500 m elsewhere. Overall, the distribution of Restionaceae in relation to the other two families suggests high potential as indicator of winter rain and fynbos vegetation in fossil phytolith assemblages.

6.7 CONCLUSIONS

The preliminary results of this study point to the potentials and limitations of GSSC morphotypes for defining grass subfamilies. These problems are addressed in the study by Rossouw (2009) where the significant diagnostic features are assessed. In the present study, matrices of GSSC-morphotype abundance for each subfamily (Tables 1–9) show that morphotype sharing among subfamilies is one of the main problems for taxonomic resolution in grass phytolith assemblages. The major problems encountered in this analysis are the excessive abundance of Pooideae morphotypes and the poor regional definition of *Stipagrostis* morphotypes. Additionally, the definition of diagnostic GSSC morphotypes Ehrhartoideae and Danthonioideae, although thus far have shown geographic affinity to the winter rainfall zone, seem to require more resolution to separate them from the Arundinoideae and *Stipagrostis*.

This study also showed that despite the problems mentioned above, there is a regional characterization of GSSC morphotypes when analyzed in modern surface samples along transects across the summer and winter rainfall zones and from lower to higher elevations (Figures 11 and 12). The best regional definition of GSSC morphotypes is shown by *Aristida*, and the Panicoideae and Chloridoideae subfamilies. Danthonioideae and Ehrhartoideae present relative high frequencies in the winter rainfall zone.

The conceptual models proposed by van Zinderen Bakker (1967, 1976), Heine (1981) and Cockroft *et al.* (1987) to explain the rainfall distribution and seasonality during glacial periods and the interpolations using proxy data (Chase and Meadows, 2007) suggest a complex and often contradictory movement of the winter and summer rainfall boundaries. Diagnostic phytoliths of Restionaceae and Cyperaceae and the GSSC of Cape grasses (Danthonioideae and Ehrhartoideae) are the most promising tool to identify the extent of the winter rainfall zone in the past. The Restionaceae, in particular, should be used to define the expansion of the fynbos biome and fynbos vegetation types into other parts of Southern Africa. However, the study presented here is only a preliminary assessment of the potential that graminoid phytoliths have for palaeoclimatic and overall palaeoecological conditions in South Africa.

ACKNOWLEDGEMENTS

We thank Lloyd Rossouw for the use of his kiln in the University of the Free State palynology laboratory. We thank Dr. Johan Venter and Dr. Andor Venter of the Geo

Potts Herbarium, Department of Plant Sciences, University of the Free State, and Dr. Anthony Verboom and Jasper Slingsby for assistance in specimen identification. The College of Arts and Sciences at Oklahoma State University, the National Endowment for the Humanities (NEH) via the American Center of Oriental Research (ACOR) in Amman, Jordan supported C. Cordova. The National Research Foundation (NRF, GUN 2053236) supported L. Scott. Any opinions, findings, and conclusions are those of the authors and the NEH and NRF do not accept any liability in regard thereto.

REFERENCES

- Alexandre, A., Meunier, J.-D., Lézine, A.M., Vincens, A. and Schwartz, D., 1997, Phytoliths: indicators of grassland dynamics during the Late Holocene in intertropical Africa. *Palaeogeography, Palaeoclimatology, Palaeoecology*, **136**, pp. 213–229.
- Barboni, D., Bremond, L. and Bonnefille, R., 2007, Comparative study of modern phytolith assemblages from intertropical Africa. *Palaeogeography, Palaeoclimatology, Palaeoecology*, **246**, pp. 454–470.
- Bremond, L., Alexandre, A., Peyron, O. and Guiot, J., 2005, Grass water stress estimated from phytoliths in West Africa. *Journal of Biogeography*, **32**, pp. 311–327.
- Bremond, L., Alexandre, A., Wooller, M.J., Hely, C., Williamson, D., Schafer, P.A., Majule, A. and Guiot, J., 2008, Phytolith indices as proxies of grass subfamilies on East African tropical mountains. *Global and Planetary Change*, **61**, pp. 209–224.
- Brown, D.I., 1984, Prospects and limits of a phytolith key for grasses in the central United States. *Journal of Archaeological Science*, **11**, pp. 345–368.
- Brown, D.I., 1993, Early nineteenth century grasslands of the Midcontinent Plains. *Annals of the Association of American Geographers*, **83**, pp. 589–612.
- Chase, B. and Meadows, M., 2007, Late Quaternary Dynamics of Southern Africa's winter rainfall zone. *Earth Science Reviews*, **84**, pp. 103–138.
- Cockroft, M.J. Wilkinson, M.J. and Tyson, P.D., 1987, The application of present-day climatic model to the Late Quaternary in Southern Africa. *Climatic Change*, **10**, pp. 161–181.
- Fredlund, G.G. and Tieszen, L.T., 1994, Modern phytolith assemblages from the North American Great Plains. *Journal of Biogeography*, **21**, pp. 321–335.
- Fredlund, G.G. and Tieszen, L.L., 1997, Calibrating grass phytolith assemblages in climatic terms: Application to Late Pleistocene assemblages from Kansas and Nebraska. *Palaeogeography, Palaeoclimatology, Palaeoecology*, **136**, pp. 199–211.
- Galley, C., Bytebier, B., Bellstedt, D.U. and Linder, H.P., 2007, The Cape element in the Afrotropical flora. *Proceedings of the Royal Society B*, **274**, pp. 535–543.
- Gibbs-Russell, G.E., 1988, Distribution of subfamilies and tribes of Poaceae in Southern Africa. *Monographs in Systematic Botany, Missouri Botanical Gardens*, **25**, pp. 555–566.
- Gibbs-Russell, G.E., Watson, L., Koekemoer, M., Smook, L., Barker, N.P., Anderson, H.M. and Dallwitz, M.J., 1990, *Grasses of Southern Africa. Memoirs of the Botanical Survey of South Africa* **58**, (Pretoria: National Botanical Institute).
- Grass Phylogeny Working Group, 2003, GPWP Current Cladogram. Available at <http://www.virtualherbarium.org/grass/gpwg/default.htm>
- Heine, K., 1982, The main stages of the Late Quaternary evolution of the Kalahari region, Southern Africa. *Palaeoecology of Africa*, **15**, pp. 53–76.
- Kotze, D.C. and O'Connor, T.G., 2000, Vegetation variation within and among palustrine wetlands along an altitudinal gradient in KwaZulu-Natal, South Africa. *Plant Ecology*, **146**, pp. 77–96.

- Lentfer C.J. and Boyd, W.E., 1999, A comparison of three methods for the extraction of phytoliths from sediments. *Journal of Archaeological Science*, **25**, pp. 1159–1183.
- Linder, H.P., 2003, The radiation of the Cape flora, Southern Africa. *Biological Reviews* **78**, pp. 597–638.
- Linder, H.P. and Barker, N.P., 2000, Biogeography of the Danthonieae. In *Grasses: Systematics and Evolution*, edited by Jacobs, S.W.L. and Everett, J., (Melbourne: CSIRO), pp. 231–238.
- Lu, H. and Liu K.B., 2003, Phytoliths of common grasses in the coastal environments of southeastern USA. Estuarine, *Coastal and Shelf Science*, **58**, pp. 587–600.
- Madella, M., Alexandre, A. and Ball, T., 2005, International Code for Phytolith Nomenclature 1.0. *Annals of Botany*, **96**, pp. 253–260.
- Mulder, C. and Ellis, R.P., 2000, Ecological significance of south-west African leaf phytoliths: a climatic response of vegetation biomes to modern aridification trends. In *Grasses: Systematics and Evolution*, edited by Jacobs, S.W.L. and Everett, J., (Melbourne: CSIRO), pp. 248–258.
- Mulholland, S.C. and Rapp, G.J., 1992, A morphological classification of grass silica bodies. In *Phytolith Systematics: Emerging Issues*, edited by Rapp, G.J. and Mulholland, S.C., (New York: Plenum), pp. 65–81.
- Piperno, D.R., 2006, *Phytoliths: A comprehensive guide for archaeologists and palaeoecologists*, (Lanham, Maryland: Altamira Press).
- Rebelo, A.G., Boucher, C., Helme, N., Mucina, L. and Rutherford, M.C., 2006, Fynbos Biome. In *The Vegetation of South Africa, Lesotho, and Swaziland*, *Strelitzia* 19, edited by Mucina, L. and Rutherford, M.C., (Pretoria: South African National Biodiversity Institute), pp. 53–219.
- Rossouw, L., 2009, *The application of fossil grass-phytolith analysis in the reconstruction of Cainozoic environments in the South African interior*, PhD dissertation, (Faculty of Natural and Agricultural Sciences, University of the Free State, Bloemfontein).
- Scott, L., 2002, Grassland development under glacial and interglacial conditions in Southern Africa: review of pollen, phytoliths, and isotope evidence. *Palaeogeography, Palaeoclimatology, Palaeoecology*, **177**, pp. 47–57.
- van Wyk, E. and van Oudtshoorn, F., 2004, *Guide to Grasses of Southern Africa*, 2nd edition, (Pretoria: Briza).
- van Zinderen Bakker, E.M., 1967, Upper Pleistocene stratigraphy and Holocene ecology on the basis of vegetation changes in Sub-Saharan Africa. In *Background to Evolution in Africa*, edited by Bishop, W.W. and Clark, J.D., (Chicago, University of Chicago Press), pp. 125–147.
- van Zinderen Bakker, E.M., 1976, The evolution of Late Quaternary palaeoclimates of Southern Africa. *Palaeoecology of Africa*, **9**, pp. 160–202.
- Vogel, J.C., Fuls, A. and Ellis, R.P., 1978, The geographical distribution of Kranz grasses in South Africa. *South African Journal of Science* **74**, pp. 209–215.
- Verboom, G.A., Linder, H.P. and Stock, W.D., 2003, Phylogenetics of the grass genus *Ehrharta*: evidence for radiation in the summer-arid zone of the South African Cape. *Evolution*, **57**, pp. 2008–2010.

CHAPTER 7

Topographic and hydrologic control of gully erosion phenomena in palaeolandscapes of Swaziland, Southern Africa

Samanta Pelacani

Department of Soil Science and Plant Nutrition, University of Florence, Florence, Italy

Michael Märker

Heidelberger Akademie der Wissenschaften, Universität Tübingen, Tübingen, Germany

ABSTRACT: A *meso-scale* approach is used to assess gully evolution and relative sediment production, in the Mbothoma area, Swaziland, by comparing gully morphology using Digital Terrain Models (DTMs). Time series of aerial photos, taken from 1961 to 1990, were used to derive high resolution DTMs. Particular attention was focused on three gully systems. Two are evolving dynamically whereas the third is in a stable context. One of the dynamic gully systems developed on a convex slope along a cattle path, while the other dynamic gully formed on a heavily overgrazed, concave slope, along a small creek, which drains the wetland area situated in the middle part of its catchment. On a concave slope the gully is directly connected to the stream since the beginning of its evolution. For the Mbothoma area a linear headcut retreated at a rate between $8,8 \text{ m y}^{-1}$ and $12,4 \text{ m y}^{-1}$ was calculated. Sediment loss ranged between $0,7 \text{ t ha}^{-1} \text{ y}^{-1}$ and $1,5 \text{ t ha}^{-1} \text{ y}^{-1}$. The results show that the gully evolution was influenced by bedrock control, structural lineations and riverbed erosion. The growth of dynamic gullies is strictly dependent on the deepening of the gully bottom at the mouth (local erosion base level) that is in turn is influenced by the temporary base level (regional erosion base level). Quartzite dykes exert structural control on the local base levels in longitudinal profile and hence determine the river behaviour in the upstream areas. Furthermore a topographic analysis of gully position revealed the there is no critical topographic threshold value for gully initiation.

7.1 INTRODUCTION

Swaziland is severely affected by gully erosion, features known in the Bantu Swazi language as *dongas*. Gully erosion has been recognized since the 1930s and according to the WMS Associates (1988) it contributes up to $250.000 \text{ m}^3 \text{ y}^{-1}$ to the sediment budget of Swaziland's rivers. Gully erosion is more important than inter-rill and rill erosion (Märker *et al.*, 2001). This type of erosion is very frequent in the Middleveld region, especially on highly populated, communal land ($43,65$ inhabitants per km^2) with high livestock concentrations. Here, the calculated carrying capacity is $0,27 \text{ LSU ha}^{-1}$

(Live Stock Units) while the actual stocking rate is 0,87 LSU per ha. Numerous studies report that landscape degradation in Southern Africa was started in the nineteenth century when first Europeans arrived (Showers, 1996; Keay-Bright and Boardman, 2009). Generally, there is a tendency to attribute gully erosion phenomena to recent human impacts. However gullies have been identified during the Late Quaternary in response to a long-term adjustment of the landscape (Botha *et al.*, 1994; Meadows, 2001). In Southern Africa most of the currently donga formation could be considered as Quaternary manifestations.

Numerous researchers have made use of aerial photos and Geographical Information Systems (GIS) to assess the factors and conditions that favour gulling (e.g. Bocco *et al.*, 1990; Desmet *et al.*, 1999; Nachtergaele and Poesen, 1999; Betts *et al.*, 2003; Daba *et al.*, 2003), and to measure erosion rates (e.g. Derose *et al.*, 1998; Martínez-Casasnovas *et al.*, 2003). In Swaziland, WMS Associates (1988) used a time series of aerial photos taken between 1947 and 1987 to determine gully erosion rates. The volume of material that has eroded from a 5,0 km² catchment located in the upper Middelveld in 40 years is about 15.000 m³ y⁻¹; calculated from linear growth rates and changes in gully morphology. Subsequently, Mushala *et al.* (1994) analyzed the gully distribution and their relationship to land systems and to land tenure in the same study area. It appears that erosion rates from arable lands are not high as a result of excellent soil conservation work in the past (Murdoch and Andriese, 1964), but erosion is more severe in grazing lands, particularly in areas near watering points and dip-tanks (Manyatsi, 1997). On the other hand, the influences of the livestock owners through stocking rates and grazing management practices are strongly related to land tenure. Using the ERU approach for the Upper Middelveld, Märker *et al.* (2001) found that the distribution of the different erosional processes and their intensities were strongly influenced by the North to South trending system of amphibolite/serpentine and dolerite/granophyre dykes. To identify critical conditions for gully initiation, Morgan and Mngomezulu (2003) studied gullied and ungullied catchments in the Middelveld of Swaziland. Using the topographic threshold approach they have found a negative relationship between the contributing area and its slope. These findings imply that gullies developed by subsurface processes although no evidence exists for soil piping processes. Similarly, Egboka and Nwankwor (1985) observed in the Agulu-Nanka gully complex, Anambra, Nigeria, that groundwater seepage contributes to the gullyng process. Furthermore, Whitlow (1989) reported that in Zimbabwe gullies are especially associated with wetland areas, a process termed *dambo* gullyng. These wetlands, characteristic of granitic substrate, occur at the headwaters of river system draining plateau surface and are responsible to maintain base flows during the dry season (Mäckel, 1974). Traditionally, these areas are used for cattle grazing, promoting gullyng (Whitlow, 1989). The same situation is recognized in areas underlain by granodioritic saprolite in Swaziland. Here, the wetlands are associated with Mineral Hydromorphic soils (I soil set; Murdoch, 1968) are characterized by poor drainage, because the infiltration is prevented by the presence of less permeable, stone line layers or a plugging layer. In these areas vertical percolation is only possible if soil cracking occurs. Hence, in the study area soils have a significant effect on the runoff generation characteristics.

Studying the gully network incised into quartzitic sandstone bed rock in the Saddleback Pass area, Barberton, South Africa, Dardis and Beckedahl (1988) observed that the development of gullies is a result of changes of the base level. In the Mbotoma area the gully erosion seems to be induced by an abrupt lowering of the erosion base level, initiated in the 1960s (Sidorchuk, 2006). Results from micromorphology, stable carbon isotope analysis and Optical Stimulated Luminescence dating (OSL) of Masotcheni Formation colluvia (KwaZulu Natal, South Africa) show that current gully

erosion is due to a lack of erodible material upslope, leaving downslope deposits as the only sediment source for fluvial redistribution (Temme *et al.*, 2008). In the Drakenberg foothills, for the Masotcheni Formation colluvia the following deposition phases span from before 42 ka to 0,17 ka. In details from 42 ka to 29 ka are recognized slope processes, mainly solifluction, and fluvial redistribution under cold climate. During the Last Glacial Maximum no deposits have been found; from 11 ka to 0,17 ka were recorded a fluvial redistribution of upstream material and older deposits. Using radiocarbon and infrared stimulated luminescence dating methods, Clarke *et al.* (2003), at Voordrag site in South Africa, have found that the colluvium is formed when the climate in southern Africa is most arid. Correlating these data to the marine Oxygen Isotope Stages (OIS), they estimated that colluviation started 100 ka and it continued through OIS 4 and 2. Furthermore, in late OIS 4 and in OIS 3 are recognized the periods of hillslope stability. Sediments similar to those studied by Clarke *et al.* (2003) are regionally distributed and also occur in Swaziland where the Bovu and Mphunga colluvium are linked to successive phases of Southern Africa Stone Age archaeology (Price Williams, 1981; Price Williams *et al.*, 1982; Dardis, 1990; Rienks *et al.*, 2000). Using radiocarbon dates, Dardis (1990), at Mkhondvo sites in Swaziland, has estimated a denudation rates of 70 B (Bubnoff units; 1B = 1 mm ka⁻¹ or 1,6 t km⁻² y⁻¹) from 30.000 to 870 B.P, a denudation rate of 1.000 B from 870 to 360 B.P. with an increases to 4.000 B from 360 B.P. to the present. This corresponds to 20 kB for the past 100 yrs. The authors are aware of the limitations of the radiocarbon dating, as pointed out by Botha *et al.* (1994). However as far as we know, these were the only data available for Swaziland. Dardis (1990) also reported that the accelerated erosion rates are similar to other badland areas in the world. The results found at Mkhondvo, suggest that colluviation, climatically controlled, is particularly sensitive to other factors probably related to human activity (Dardis, 1990). In fact, gullying occurs mainly on footslope position where colluvial material is available (Keay-Bright and Boardman, 2006; Kakembo *et al.*, 2009).

Considering the Mbothoma valley developed under same climatic and lithologic conditions and land use, a *meso-scale* approach was used, hence only intrinsic changes are considered (Faulkner, 2008). Our objectives are: i) to examine the dynamics of gully development and to quantify sediment yield, and ii) to highlight the factors influencing the occurrence of gullies. For these purposes Digital Terrain Models (DTMs) were derived from aerial photos from the period between 1960 and 1990. Particular attention was focused on two gully systems located in the Middleveld of Swaziland. These gullies were developed in the middle part of the slope that we assume belongs to the Bovu colluvium formation.

7.2 MATERIALS AND METHODS

7.2.1 Study area

The study area is the Mhalambanjeni Stream basin, a right bank tributary of the Mbuluzi River, located 20 km north of Manzini, Swaziland (Figure 1). The catchment area of the Mhalambanjeni is ca. 42 km² while the catchment area of the Mbuluzi River is 3.320 km². Before crossing into Mozambique the Mbuluzi River yields an average of 372 Mm³ of runoff per year (Matondo and Dlamini, 2000). This investigation was conducted in the Mbothoma area which is considered representative for the Upper Middleveld. Here, three gullies systems were studied (Figure 1). Previous studies of gully erosion phenomena in the area were conducted by Mushala *et al.* (1994),

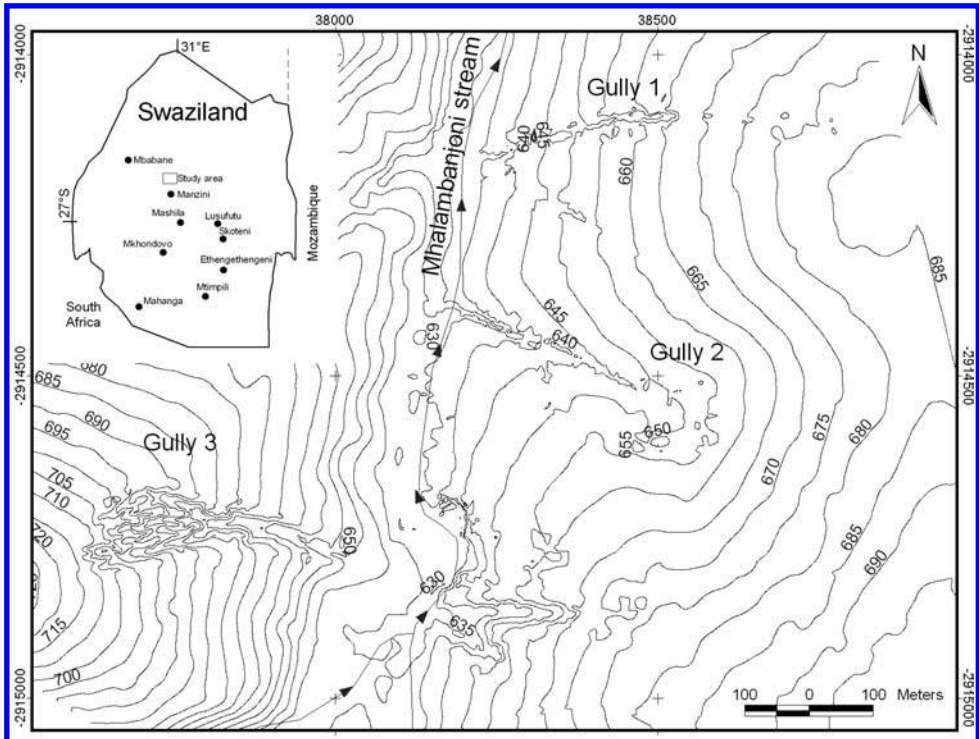


Figure 1. Locations of radiocarbon-dated colluvium sites in Swaziland after Dardis (1990) and the Mbothoma study area. The topographic map with a 5 m contour interval shows the three gully systems investigated. The gullies n. 1 and n. 2 are in a dynamic phase while the n. 3 is in a static phase.

Märker *et al.* (2001), Pelacani (2001), Sidorchuk *et al.* (2003), Hochschild *et al.* (2003) and Pelacani *et al.* (2009). One of the gully systems (site 1, [Figure 1](#); [Figure 2](#)) evolved on a convex slope along a cattle path, whereas the other (site 2, [Figure 1](#); [Figure 2](#)) is a *dambo* type gully incising a heavily overgrazed wetland area that covers approximately 1,5% of the 41,8 ha gully catchment. It evolved on a concave slope along a small creek which drains the wetland area situated centrally on the slope. The third gully (site 3; [Figure 1](#)) is a stable, vegetated gully with Guava shrub encroachment and thorny shrubs (*Caesalpinia decapetala*). The side walls, steeper than 45°, incise a convex slope. The altitudes of the study area range from 610 to 760 m asl, with an average slope of 12%. The climate is subtropical with a marked seasonal variation in temperature and prevailing summer rains (October to March) which accounts for 75% of the 900 mm annual rainfall. Convective storms with intensities of 200 mm hr⁻¹, with storm duration of 15 minutes and return periods of 20 years deliver much of the rainfall. The country is vulnerable to tropical cyclones and droughts that contribute to high erosion rates from highly erodible soils and granodioritic saprolites substrates, by desiccation cracking during droughts and from extreme rainfall events. The climate is strongly influenced by air masses from different origins; i) air masses from the equatorial convergence zone; ii) moist maritime air masses from subtropical eastern continental India responsible for occasional cyclones, and iii) dry continental tropical and marine masses coming from western South Africa that bring winter rains

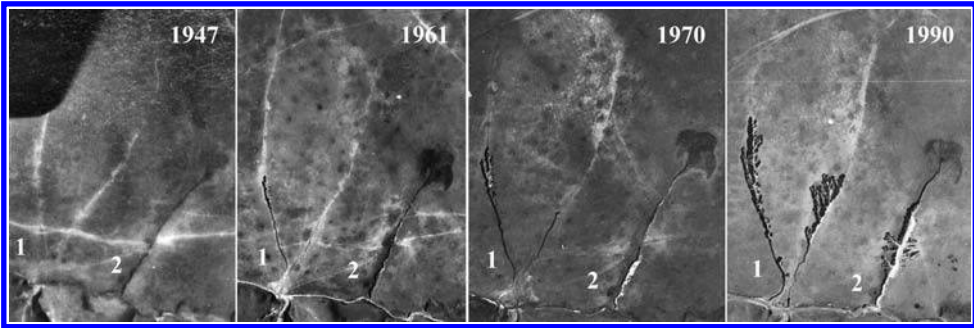


Figure 2. Time series of aerial photos from 1947 to 1990. The gully 1 developed on a convex slope along cattle paths, while the gully 2 is a dambo type gully, developed on a concave slope in a heavily overgrazed area. The aerial photos have different original scales. Permission to publish courtesy of Chief Director of Surveys and Mapping, Department of Land Affairs, Republic of South Africa.

with occasional snow. The mean annual rainfall erosivity is $4.500 \text{ MJ mm ha}^{-1} \text{ h}^{-1}$ with a mean rainfall energy of 180 MJ ha^{-1} (Kiggundu, 1986; Schulze, 1997). Hence, the 25-year recurrence interval shows a mean rainfall erosivity of $9.500 \text{ MJ mm ha}^{-1} \text{ h}^{-1}$ having a mean rainfall energy of 260 MJ ha^{-1} . Mean annual temperature is about 19°C and minimum daily temperatures is 5°C in winter.

The bedrock comprises rocks of the Archean Usutu Intrusive Suite; biotite, granodiorites and diorites, dating from about 3.350 Ma. Moreover, there are occurrences of amphibolites and serpentinites of the older Dwalile Metamorphic Suite (Hunter *et al.*, 1984) as well as younger, Late Jurassic dolerite dykes. The soils are polygenetic since they have developed from the thick soil-saprolite complex derived from igneous and metamorphic rocks weathered under tropical humid climates during the Cretaceous and Early Tertiary (Fränze, 1984). Subsequently, soils were partly denudated in phases of morphodynamic activity and eventually they “redeveloped” in humid phases during the late Neogene (Partridge, 1997). The occurrence of stone-lines could be indicating an erosion surface and the extent of redeposited sediments or could be associated with archaeological assemblages (Price Williams *et al.*, 1982). According to FAO (1989) classification, the soils consist of Rhodic Ferralsols underlain by saprolite (Scholten *et al.*, 1997). These soils show little vertical or lateral variation in texture. Locally, quartz veins are exposed in the gully walls and near the mouth. Furthermore, the exposure of markedly red soil or sediment usually indicates the presence of doleritic dykes (WMS Associates, 1988). The soils have very low to low CEC (Cation Exchange Capacity), with values ranging from 2 to 15 cmol kg^{-1} , while the pH values (KCl) for the topsoil range from 3,5 to 4,5 tending to increase with depth (Mushala *et al.*, 1994). The soils have high clay contents varying with topographic position; 36% at the summit and backslope positions, 51% at midslope position and 75% at footslope position (Mushala *et al.*, 1994). The clay fraction is dominated by kaolinite.

The calculated erodibility factor (K-factor; Wishmeier and Smith, 1978) ranges from 0,014 to $0,053 \text{ t ha h MJ}^{-1} \text{ ha}^{-1} \text{ mm}^{-1}$. The topsoil shows low erosion risk while the transitional zone between the soil and saprolite is characterized by highest K-factor values (Mushala *et al.*, 1994).

Vegetation is predominantly tall grassland with associated trees and shrubs, in the new classification of vegetation types, this area falls into the Swaziland Sour Bushveld (Dobson and Lotter, 2004). However, much of this natural vegetation has been replaced by cultivated species and as a result of overgrazing by unpalatable grass and

species less nutritious to livestock. The dominant grasses species are *Eragrostis biflora*, *Eragrostis cilianensis*, *Sporobolus africana* and *Hypparhenia filipendula*. There are also poisonous species such as *Asclepias spp.*, *Lantana camara*, *Solanum spp.* and *Pteridium aquilinum*.

7.2.2 Implementation and evaluation criteria

To assess the historical development of gullies we analysed a time series of different aerial photo jobs taken from 1947 to 1990 (Figure 2). In addition, a high precision geodetic survey in 1998, $\pm 0,3$ m, yields up to date information on the gully morphology. The methodology used to obtain the DTMs is reported in previously published paper by Sidorchuk *et al.* (2003) and Pelacani *et al.* (2009). By comparing the DTMs it was possible to obtain morphometric information at time steps in the gully development process and to estimate the volume of eroded sediment. The volume of eroded from soil-saprolite layers was achieved by computing elevation differences between the different time steps following the method of Derose *et al.* (1998). Soil and saprolite losses were calculated using soil bulk density values ranging from $1,13$ – $1,50$ g cm⁻³ (Mushala *et al.*, 1994). The lower value was used for topsoil while the higher value represented the saprolite. Furthermore, the gullies were examined for their area-slope characteristics. The area-slope relationship quantifies the local topographic gradient as a function of drainage area, following the relationship:

$$A^\alpha S = \text{constant} \quad (1)$$

A is the contributing area and S is the slope gradient. For a natural catchment the exponent α ranges between 0,4 and 0,7 (Montgomery and Dietrich, 1988, 1989; Tarboton *et al.*, 1992; Willgoose *et al.*, 1991; Desmet *et al.*, 1999). Two alternatives were considered:

- i. The gully is directly connected to the stream network from the beginning of its evolution. The dominant processes are seepage erosion and concentrated overland flow.
- ii. The gully is initially disconnected to the permanent drainage network. The prevailing process is concentrated overland flow.

To identify the location of the gully initiation point during the first phase of the study, a Stream Power Index (SPI; Moore *et al.*, 1988) and Topographic Wetness Index (TWI; Moore *et al.*, 1988) were used. Predicted locations of gullies were compared with the locations identified by field observation and photo aerial interpretation. The TWI is commonly used for assessing the spatial distribution of saturated areas while the SPI is used as a measure of the power of concentrated surface runoff, and thus, the potential for channel incision. This approach was chosen because gully erosion in this area is caused either by Hortonian runoff or by Dunne runoff (Horton, 1945; Dunne *et al.*, 1975). In fact, some gully heads developed from concentration of rills into a leading rill that, in turn, leads to gully network development. Conversely, some gully heads are associated with wetland areas. For areas affected by footpaths and tracks a procedure that takes into account the concentrated flow path was applied to predict gulling expansion. To represent this linear features a binary mask was created using the same method reported in Pelacani *et al.* (2008). If these features are not considered during the computation of the topographic indices, high prediction errors in the estimation of the head-cut location and the subsequent morphology of the gully may

result. In fact, the pathways strongly influence the overland flow and hence determine the alignment of the gullies. The local slope gradients were derived using the method proposed by Zevenbergen and Thorne (1987). The unit contributing area was calculated with a multiple flow algorithm (Desmet and Govers, 1996). At this point, gully head position was plotted in relation to its slope and drainage area. During this computation the slope and drainage area of the middle slope position was measured for the convex slope. Conversely, we applied the procedure for the gully developed on the concave slope at the lower slope position. A log-normal distribution was used to fit the contributing area-slope relationship.

7.3 RESULTS

7.3.1 Stage of gully development and sediment production

We performed a quantitative assessment of gully dynamics by comparing the morphology of the gullies using DTMs. Particular attention was focused on two gullies in a dynamic stage of development. The concept of four phases in gully growth was introduced by Kosov *et al.* (1978, cited in Sidorchuk, 1999). He defined the following stages; i) rapid growth rate of gully maximum length, ii) deepening, iii) increasing area, and iv) increasing volume. The same phases were recognised in the Mbothoma area (Figure 4). Following Sidorchuk (1999; 2003; 2006) the studied gullies, sites 1 and 2, are in a dynamic stage, the first development phase. Following the experiment of Kosov *et al.* (1978) the first stage extends over about 5% of the gully lifespan, although more than >90% of the gully length, 60% of the gully area and 35% of the gully volume develops during this phase. Considering the evolution of *dambo* gullying (Figure 3) after 51 years the length is still increasing while the maximum depth of the main trunk tends to level off after 35 years (60% of the gully's lifetime). The length curve can be subdivided in two parts, a steep initial part for the first 15 years followed by a tapering of the slope to acquire almost a straight line thereafter. The curves of the area and volume show an inverse trend. Aerial photo interpretation revealed that the gully was a creek in 1947 (Figure 2). In 1961 the “*dambo* gully” was linear and V-shaped. Since then the gully has retained the linear form but evolved into U-shaped cross sections with the maximum deepening in the middle part of the gully system.

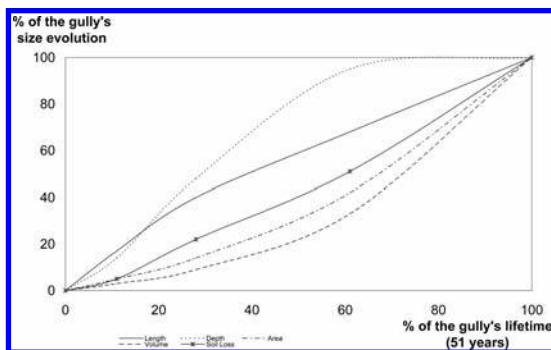


Figure 3. Morphodynamics of Mbothoma *dambo* type gully growth during the first 51 years.

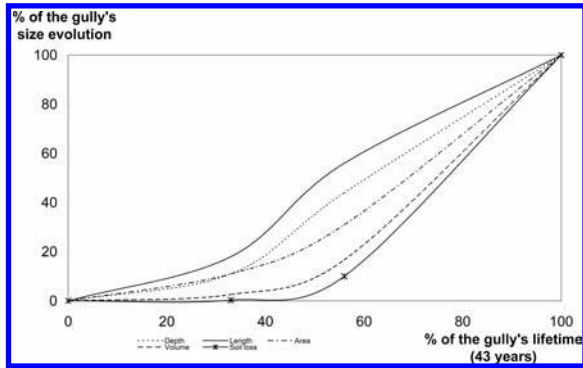


Figure 4. Morphodynamics of Mbothoma gully growth during the first 43 years.

From 1947 to 1998 the gully length increased at a rate of $8,8 \text{ m y}^{-1}$; its depth increased at $0,35 \text{ m y}^{-1}$ while the width rate was $0,4 \text{ m y}^{-1}$.

Considering the gully development on a convex slope, in the first 14 years the average growth rate was $15,7 \text{ m y}^{-1}$ along the axial part with a deepening of $0,21 \text{ m y}^{-1}$. During this stage the linear gully topography shows a number of knick points and is disconnected from the stream network. From 1947 to 1998 the gully length increased at a rate of $12,4 \text{ m y}^{-1}$ whereas its depth increased at $0,35 \text{ m y}^{-1}$. The morphodynamics of gully growth on the convex slope during the first 43 years is reported in Figure 4.

These results are comparable with previous studies in the same study area and other monitoring gully sites in Swaziland. For the Mbothoma site, WMS Associates (1988), found a headwall retreat at a rate of $1,2$ to 10 m y^{-1} , with a maximum head gully retreat of 2 to 6 between 1961 and 1980.

The gully head retreat reported in the present study, $8,8 \text{ m y}^{-1}$ and $12,4 \text{ m y}^{-1}$, is comparable to those reported for other areas in the world: $8,4 \text{ m y}^{-1}$ in the black soil region of north eastern China; 0 to 15 m y^{-1} in the alluvio-lacustrine sedimentary basin of the Njemps Flats, Kenya; and $9,85 \text{ m y}^{-1}$ in the clayey-loamy sediments of the Western Africa Sahel zone of Burkina Faso (Wu *et al.*, 2008; Oostwoud Wijdenes and Bryan, 2001; Marzloff and Ries, 2007).

In the study area it was found that on a concave hillslope the gully is directly connected to the stream from the beginning of its evolution (Figure 2). In the case of a convex hillslope, the evolution of the gully occurs in the context of the gully outlet which is disconnected from the stream network. Here, small gullies, apparently disconnected, are formed along the slope. Under these conditions the future gully displays a number of knick points that represent the upstream boundary of the disconnected gully-basins. The evolution stages from a discontinuous into a continuous, linear, arroyo type gully were described earlier by Leopold *et al.* (1964) and more recently by Bull (1997). Furthermore, the dominant process in gullies connected to the stream network is seepage erosion and concentrated overland flow, whereas the principal process for gullies disconnected to permanent drainage network is concentrated overland flow. Similar evolution has been reported by Oliveira (1990) for the gully developed in the Bananal area of Brazil. In the Mbothoma area, the presence of gullies is influenced by the dip direction of bedrock controlling the seepage of ground water from the gully walls and/or from the side slope. Furthermore, the location of the wetland area is influenced by the presence of quartz veins that are more resistant to weathering.

Considering an active gully area of 0,11 km², the volume of eroded sediment by *dambo* gulling from 1961 to 1971 was equivalent to 1 t ha⁻¹ y⁻¹, totalling 8,9 t ha⁻¹. Subsequently, from 1970 to 1990, the soil loss was 0,5 t ha⁻¹ y⁻¹, representing a decrease in the soil loss rate. From 1990 to 1998 there was an increase and the soil loss reached 1,7 t ha⁻¹ y⁻¹, totalling 14,3 t ha⁻¹. In the first 51 years the gully has eroded 0,7 t ha⁻¹ y⁻¹, amounting to 37,2 t ha⁻¹.

The linear gully with an active gully area of 0,16 km², developed on a convex slope along the cattle path a rate of 1,5 t ha⁻¹ y⁻¹ over the first 43 years, amounting to 64 t ha⁻¹. The soil loss rates reported in the present study were comparable to those reported from other tropical grazing lands; 1,5 t ha⁻¹ y⁻¹ was calculated for the Nlwa River Basins containing intensive agriculture (RBCIA) in Australia, considering an average gully age of 100 years (Hughes *et al.*, 2001). Table 1 reports the phases of gully development, the associated soil loss and the relative stream dynamic in Mhalambanjonjoni catchment, which will be discussed below.

7.3.2 Assessment of gulying susceptibility using the hillslope area relation

The value of the exponent α (Equation 1) for the log-normal section of the gully area-slope relation is 0,24. This value fits within the range reported in other studies where ephemeral gullies on grazing area or cropland were investigated (Vandekerckhove *et al.*, 1998). Hancock and Evans (2006) found a threshold value of α in an undisturbed catchment in Northern Australia explaining topographic gully initiation. However, for the Mbothoma area it appears that no single, critical value can describe gully initiation. In fact, the results show that the whole drainage network of the Mhalambanjonjoni catchment is potentially subject to gulying.

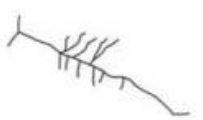
Furthermore, for the Mbothoma conditions, a significant linear expansion of gullies takes place for *SPI* values within the range of 3 to 5,5. Therefore, the *SPI* value that range from 5,5 to 7,3 correspond to the main channel of the gullies. This result agrees to those reported by Kakembo *et al.* (2009) in the communal areas of Eastern Cape (South Africa). However, in the Mbothoma area, gulying occurs in the middle and upper hillslope positions on convex slope and not mostly on concave and lower parts of the slope, contradicting the observations of Poesen *et al.* (2003) and Kakembo *et al.* (2009). They affirm that as slope steepness, the critical drainage area for gully initiation decreases and vice versa. In the Mbothoma area the presence of cattle paths induces gully initiation in small drainage areas.

For the TWI the value range from 5 to 11,5, and the mean value is 7, this corresponds to the minimum value associated with the wetland area.

7.3.3 Factors influencing the occurrence of gullies

To understand which factors are influencing the occurrence of gullies the study was extended to an ungullied catchment including a right bank tributary of the Mhalambanjonjoni stream which is draining the westerly aspect slopes of the Mbothoma highland. These slopes are characterized by the presence of cattle paths and two small stable gullies but no active gully systems. Because the valleys have developed under the same climatic, lithologic and stratigraphic conditions, the research was focused on two key questions: i) is there a structural constraint or control? and, ii) what are the characteristics of the longitudinal profile of the Mhalambanjonjoni stream and its tributary? A geological map shows the dip direction of the bedrock. It is hypothesised that

Table 1. Phases of dambo type gully development and associated soil loss, considering an active gully area of 0.11 km², as well as the relative stream dynamics in the Mhalambanjoni catchment, Swaziland.

Time steps	Soil loss		Base level [m/y]	Length		Depth		Width		Gully shape 
	[t/ha/y]	[t/ha]		[m]	[m/y]	[m]	[m/y]	[m]	[m/y]	
1947–1961	0,3	3,8		250	17,8	5	0,4	14	1,0	
1961–1970	1,0	8,9	0,25	380	11,5	12	1,1	19	0,5	
1970–1990 (Tropical Cyclone Domoina, 1984)	0,5	9,0	0,93	400	1,0	18	0,3	28	0,5	
1990–1998 (collapsed amphibolite dyke, observed in field, 1999)	1,7	14,3		490	10,0	18	0,0	30	0,3	
1961–1990			0,68							
1947–1998	0,7	37,2			9,6		0,3		0,6	

the presence of gullies is influenced by the dip direction of the bedrock controlling the seepage of ground water from the gully walls and/or from the side slopes, especially for *dambo* type gullying. In fact, ground water sapping was observed at the head of the gully and locally at the side walls due to seepage that emerges from the saprolite just above the contact with the palaeosols showing hydromorphic characteristics. The sites of ground water seepage are commonly marked by cavities in the gully wall that range in size from centimetres to a few meters due to sapping erosion.

The longitudinal profiles of the Mhalambanjoni stream and its tributary are shown in Figure 5. The longitudinal profile of the tributary shows greater steepening in the upstream direction than the Mhalambanjoni stream for the same segment distance. This shape is controlled by the presence of a knickpoint downstream and by a headwater reservoir. On the other hand the longitudinal profile of the Mhalambanjoni stream is characterized by step-pool patterns, with pools developed in granodiorite saprolite and steps created by amphibolite dykes. Field observation in 1999 revealed the collapse of an amphibolite dyke crossing the Mhalambanjoni stream downstream the gully study site. It is hypothesized that Tropical Cyclone “Domoina” during January 1984 which delivered 242 mm d⁻¹ storm rainfall in Mbothoma area, caused the removal of the blocking dykes and consequently the erosional base was lowered. The significant erosion of the river bed revealed the dykes that were shown on early DTMs from the seventies. Sidorchuk *et al.* (2003) have calculated that between 1961 and 1970 the lowering of stream base level was of 0,25 m y⁻¹, increasing to 0,93 m y⁻¹. Generally, the erosion of granodioritic saprolite

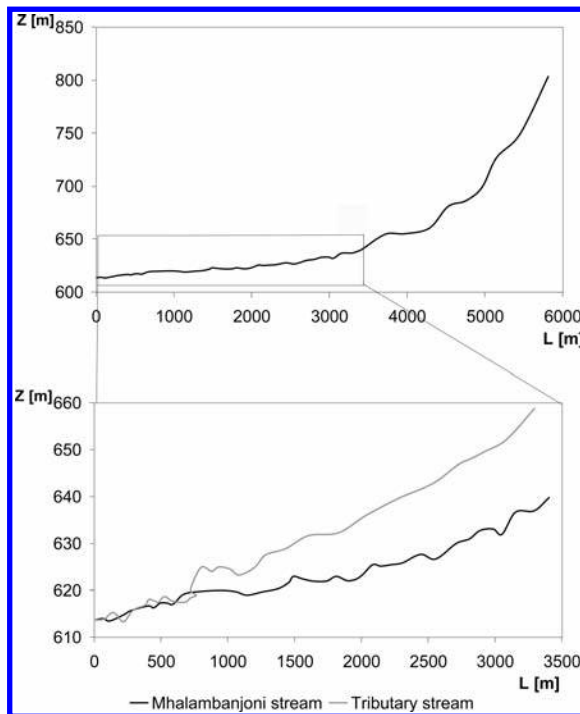


Figure 5. Evolution of the longitudinal profile for the Mhalambanjoni Stream and its tributary. The longitudinal profile of the tributary was compared to the same section of the Mhalambanjoni Stream that runs parallel to it.

was more intense than the resistant amphibolite. Moreover, the stream is laterally planing (eroding) the bedrock creating meanders. The presence of the amphibolite dykes has determined headwater knick point migration which in turn has led to incision into granodiorite causing the abandonment and desiccation of the floodplains at the mouth of the stable gully, while the incision of the valley forms new gullies. Rapid lowering of the amphibolite and its removal induces a drop in local base level, hence generating a knick point that migrates upstream into the granodiorite saprolite. Knick point migration results in channel incision in the upstream valley, retarding lateral migration. Consequently, we observe a channel straightening through increased cut-off that may also lead to a lowering of the groundwater table. Reconstruction of the longitudinal gully profiles during their evolution shows the progressive upstream migration of the knick point. The migration is connected to the lowering of the base level. The evolution of gully growth is strictly dependent on the deepening of the gully bottom at the mouth. The phases of gully development, the volume of eroded sediment and the relative stream dynamic are reported in Table 1. The net result of these processes is to produce a complex drainage network, with local base-levels forming within sub-basins.

Returning to the previous discussion, it appears that the base level of the Malhambanjoni controls the development of the connected gullies system. This scenario represents a case where the flow is constant leading to an equilibrium phase. On the other hand, in the presence of catastrophic events such as the Cyclone Domoina, the system becomes dynamic again. This interpretation is evident in Figure 4 where the curve that shows the lengthening of the gully is proportional to the time increment. Here, contrary to the findings by other researchers, the area and the volume grow exponentially with time. The sequence of gully development from the initiation to the ultimate stabilisation can be seen as the result of interactions between erosional and stabilization events. The associated events of stabilization lead to meandering with the formation of terraces. This, in turn, leads to a reduction of the contributing area and finally the colonization by the vegetation starting from the mouth.

7.4 CONCLUSIONS

The Mbothoma gullies are developed on a concave slope, in the wetland context of a *dambo* type gully, and on a convex slope along a cattle path. On the concave slope, the gully has been directly connected to the stream network since initiation. Conversely, on the convex slope the evolution of the gully occurs in a condition where the outlet of the gully is disconnected from the stream network. The comparison for the same period reveals that the gully developed on convex slope has eroded at twice the rate of the gully developed on a concave slope, respectively $1,5 \text{ t ha}^{-1} \text{ y}^{-1}$ and $0,7 \text{ t ha}^{-1} \text{ y}^{-1}$. Furthermore, the soil loss rates of $1,5 \text{ t ha}^{-1} \text{ y}^{-1}$, and the gully head retreat of $8,8 \text{ m y}^{-1}$ and $12,4 \text{ m y}^{-1}$, is comparable to those reported for other areas in the world. There is no evidence for a critical slope or drainage area for gully initiation. However, although the majority of gullies occur in the upper reaches of the catchment (i.e. diffusive region at areas approximately less than 2.000 m^2), gullies can occur throughout the entire drainage network. Consequently the whole catchment is at risk. The findings demonstrate that, in the study catchment using a *meso-scale* approach, the slope-area relationship cannot explain gully characteristics and hence their development. To understand which factors are influencing the occurrence of gullies it is necessary to extend the study area into ungullied catchments and to consider the evolution of the entire stream network.

ACKNOWLEDGMENTS

We sincerely thank Dr. Greg A. Botha as a reviewer for comments that improved the manuscript. This work was supported by the European Union, INCO-DC, contract nr. IC 18-CT97-0144. Samanta Pelacani was funded by a University of Florence Ph.D. studentship.

REFERENCES

- Betts, H.D., Trustrum, N.A., and Derose, R.C., 2003, Geomorphic changes in a complex gully system measured from sequential digital elevation models, and implications for management. *Earth Surface Processes and Landforms*, **28**, pp. 1043–1058.
- Bocco, G., Palacio, J., and Valenzuela, C.R., 1990, Gully erosion monitoring using GIS and geomorphologic knowledge. *ITC Journal*, **3**, pp. 253–261.
- Botha, A.B., Wintle, A.G., and Vogel, J.C., 1994, Episodic Late Quaternary palaeogully erosion in northern KwaZulu-Natal, South Africa. *Catena*, **23**, pp. 327–340.
- Bull, W.B., 1997, Discontinuous ephemeral streams. *Geomorphology*, **19**, pp. 227–276.
- Clarke, M.L., Vogel, J.C., Botha, G.A. and Wintle, A.G., 2003, Late Quaternary hillslope evolution recorded in eastern South African colluvial badlands. *Palaeogeography, Palaeoclimatology, Palaeoecology*, **197**, pp. 199–212.
- Daba, S., Rieger, W. and Strauss, P., 2003, Assessment of gully erosion in eastern Ethiopia using photogrammetric techniques. *Catena*, **50**, pp. 273–291.
- Dardis, G.F., 1990, Late Holocene erosion and colluvium deposition in Swaziland. *Geology*, **18**, 934–937.
- Dardis G.F. and Beckedahl H.R., 1988, Gully formation in Archaean Rocks at Saddleback Pass, Barberton Mountain Land, South Africa. In *Geomorphological Studies in Southern Africa*; edited by Dardis, G.F. and Moon, B.P. (Balkema, Rotterdam, NL), pp. 285–296.
- Derose, R.C., Gomez, B., Marden, M. and Trustrum, N.A., 1998, Gully erosion in Mangatu Forest, New Zealand, estimated from digital elevation models. *Earth Surface Processes and Landforms*, **23**, pp. 1055–1053.
- Desmet, P.J.J. and Govers, G., 1996, Comparison of Routing Algorithms for Digital Elevation Models and Their Implications for Predicting Ephemeral Gullies. *International Journal of Geographical Information Science*, **10**, pp. 311–331.
- Desmet, P.J.J., Poesen, J., Govers, G. and Vandaele, K., 1999, Importance of slope gradient and contributing area for optimal prediction of the initiation and trajectory of ephemeral gullies. *Catena*, **37**, pp. 377–392.
- Dobson, L. and Lotter, M., 2004, Vegetation Map of Swaziland. In: Mucina, L. and Rutherford, M.C. (eds.), *Vegetation Map of South Africa, Lesotho and Swaziland: Shapefiles of basic mapping units*. Beta version 4.0, February 2004, National Botanical Institute, Cape Town.
- Dunne, T., Moore, T.R. and Taylor, C.H., 1975, Recognition and prediction of runoff producing zones in humid regions. *Hydrological Science Bulletin*, **20**, pp. 305–327.
- Egboka, B.C.E. and Nwankwor, G.I., 1985, The hydrological and geotechnical parameters as agents for gully-type erosion in the Rain-Forest Belt of Nigeria. *Journal of African Earth Science*, **3**, pp. 417–425
- FAO, 1989, Soil map of the world—revised legend. Reprint of World Soil Resources Report 60, FAO, Rome, 1988. ISRIC, Technical Paper 20, Wageningen, Netherlands.
- Faulkner, H., 2008, Connectivity as crucial determinant of badland morphology and evolution. *Geomorphology*, **100**, pp. 91–103.

- Fränze, O., 1984, *Bodenkunde—Südafrika*. Beiheft zu Blatt 4. Serie S, *Afrika-Kartenwerk*. Gebrüder Bornträger, Berlin und Stuttgart.
- Hancock, G.R. and Evans, K.G., 2006, Gully position, characteristics and geomorphic thresholds in an undisturbed catchment in northern Australia. *Hydrological Processes* **20**, pp. 2935–2951.
- Horton, R.E., 1945, Erosional development of streams and their drainage basins; hydrophysical approach to quantitative morphology. *Geol Soc Am Bull.*, **56**, pp. 275–370.
- Hochschild, V., Märker, M., Rodolfi, G. and Staudenrausch, H., 2003, Delineation of erosion classes in semi-arid southern African grassland using vegetation indices from optical remote sensing data. *Hydrological Processes*, **17**, pp. 917–928.
- Hughes, A.O., Prosser, I.P., Stevenson, J., Scott, A., Lu, H., Gallant, J. and Moran, C.J., 2001, Gully erosion mapping for the national land and water resources audit. Technical Report 26/01, CSIRO Land and Water, Canberra.
- Hunter, D.R., Baker, F. and Millard, H.T., 1984, Geochemical investigation of Archean bimodal and Dwalidle Metamorphic Suites, Ancient Gneiss Complex, Swaziland. *Precambrian Research*, **24**, pp. 131–155.
- Kakembo, V., Xanga, W.W. and Rowntree, K., 2009, Topographic thresholds in gully development on the hillslopes of communal areas in Ngqushwa Local Municipality, Eastern Cape, South Africa. *Geomorphology*, **110**, pp. 188–194.
- Kiggundu, L., 1986, Distribution of rainfall erosivity in Swaziland. *Research paper*, **22**. Kwaluzeni Campus, University of Swaziland.
- Kosov, B.F., Nikol'skaya, I.I. and Zorina, Y.F., 1978, Eksperimental'nyye issledovaniya ovragoobrazovaniya. In *Eksperimental'naya Geomorphologiya*, Makkaveev NI (eds.). Izd. Mosk. Univ. **3**, Moskva, pp. 113–140.
- Keay-Bright, J. and Boardman, J., 2006, Changes in the distribution of degraded land over time in the central Karoo, South Africa. *Catena*, **67**, pp. 1–14.
- Keay-Bright, J. and Boardman, J., 2009, Evidence from field-based studies of rates of soil erosion on degraded land in the central Karoo, South Africa. *Geomorphology*, **103**, pp. 455–465.
- Leopold, L.B., Wolman, M.G. and Miller, J.P., 1964, *Fluvial processes in geomorphology*. Freeman, San Francisco. 522 p.
- Mäckel, R., 1974, Dambos: a study in morphodynamic activity on the plateau regions of Zambia. *Catena*, **1**, pp. 327–365.
- Manyatsi, A.M., 1997, Procedure for assessing land degradation status in Swaziland using remotely sensed data. *UNISWA Journal of Agriculture*, **6**, pp. 21–35.
- Märker, M., Moretti, S. and Rodolfi, G., 2001, Assessment of water erosion processes and dynamics in semi-arid regions of Southern Africa (Kwazulu/Natal, RSA and Swaziland) using the Erosion Response Units concept (ERU). *Geografia Fisica e Dinamica Quaternaria*, **24**, pp. 71–83.
- Martínez-Casasnovas, J.A., Antón-Fernández, C. and Ramos, M.C., 2003, Sediment production in large gullies of the Mediterranean area (NE Spain) from high-resolution digital elevation models and geographical information systems analysis. *Earth Surface Processes and Landforms*, **28**(5), pp. 443–456.
- Marzloff, I. and Ries, J.B., 2007, Gully erosion monitoring in semi-arid landscapes. *Zeitschrift für Geomorphologie*, N.F. **51**, pp. 405–425.
- Matondo, J. and Dlamini, T., 2000, Water resources development in the Mbuluzi River Basin. *UNISWA Research Journal of Agriculture, Science and Technology*, **4**(1), pp. 27–33.
- Meadows, M.E., 2001, The role of Quaternary environmental change in the evolution of landscapes: case studies from southern Africa. *Catena*, **42**, pp. 39–57.

- Montgomery, D.R. and Dietrich, W.E., 1988, Where do channels begin? *Nature*, **336**, pp. 232–234.
- Montgomery, D.R. and Dietrich, W.E., 1989, Source areas, drainage density and channel initiation. *Water Resources Research*, **25**, pp. 1907–1918.
- Morgan, R.P.C. and Mngomezulu, D., 2003, Threshold conditions for initiation of valley-side gullies in the Middle Veld of Swaziland. *Catena*, **50**, pp. 401–414.
- Moore, I.D., Burch, G.I. and MacKenzie, D.H., 1988, Topographic effects on the distribution of surface soil water and the location of ephemeral gullies. *Transactions of the American Society of Agricultural Engineers*, **31**, pp. 1098–1107.
- Murdoch, G., 1968, *Soils and Land Capability in Swaziland*. Ministry of Agriculture; Publisher: Mbabane, SW, pp. 360.
- Murdoch, G. and Andriessie, J.P., 1964, Soil and Irrigability Survey of the Lower Usuthu Basin (South) in the Swaziland Lowveld. *Department of Technical Cooperation, Overseas Research Publication*, **3**, London.
- Mushala, H.M., Scholten, T., Felix-Henningsen, P., Morgan, R.C.P. and Rickson, R.J., 1994, *Soil erosion and river sedimentation in Swaziland*. Final report to the EU, Contract number TS2-CT90-0324.
- Nachtergaele, J. and Poesen, J., 1999, Assessment of soil loss by ephemeral gully erosion using high-altitude (stereo) aerial photographs. *Earth Surface Processes and Landforms*, **24**, pp. 693–706.
- Oliveira, M.A.T., 1990, Slope geometry and gully erosion development: Bananal, São Paulo, Brazil. *Zeitschrift für Geomorphologie*, **34**, pp. 423–434.
- Oostwoud Wijdenes, D.J. and Bryan, R.B., 2001, Gully-head erosion processes on a semi-arid valley floor in Kenya: a case study into temporal variation and sediment budgeting. *Earth Surface Processes and Landforms*, **26**, pp. 911–933.
- Partridge, T.C., 1997, Late Neogene uplift in eastern and Southern Africa and its palaeoclimatic implications. *Tectonic Uplift and Climate Change*. Editor Ruddiman, W.F. pp. 63–85, Plenum, New York.
- Pelacani, S., 2001, *Evolution of gullied landforms in a catchment of Swaziland, Southern Africa, by means of photo interpretation techniques and hydro-erosive models*. University of Florence, Unpublished BSc. Thesis.
- Pelacani, S., Märker, M. and Rodolfi, G., 2008, Simulation of soil erosion and deposition in a changing land use: a modelling approach to implement the support practice factor. *Geomorphology*, **99**, pp. 329–340.
- Pelacani, S., Märker, M. and Rodolfi, G., 2009, Modelling the potential impact of groundwater dynamics on gully erosion and drainage basin evolution. In: *Geomorphology and Plate Tectonics*. Edited by Ferrari, D.M. and Guiseppi, A.R., pp. 141–158, Nova Science Publishers, Inc. ISBN 978-1-60741-003-4.
- Poesen, J., Nachtergaele, J., Verstraeten, G. and Valentin, C., 2003, Gully erosion and environmental change: importance and research needs. *Catena*, **50**, pp. 91–133.
- Price-Williams, D., 1981, A preliminary report on recent excavation of Middle and Late Stone Age levels at Sibebe Shelter, North-West Swaziland. *South African Archaeological Bulletin*, **36**, pp. 22–28.
- Price-Williams, D., Watson, A. and Goudie, A.S., 1982, Quaternary colluvial stratigraphy, archeological sequences and paleoenvironment in Swaziland, Southern Africa. *The Geographical Journal*, **148**(1), pp. 50–67.
- Rienks, S.M., Botha, G.A. and Hughes, J.C., 2000, Some physical and chemical properties of sediments exposed in a gully (donga) in northern KwaZulu-Natal, South Africa and their relationship to the erodibility of the colluvial layers. *Catena*, **39**, pp. 11–31.
- Scholten, T., Felix-Henningsen, P. and Schotte, M., 1997, Geology, soils and saprolites of the Swaziland Middleveld. *Soil Technology*, **11**, pp. 229–246.

- Schulze, R.E., 1997, *South African atlas of agrohydrology and climatology*. Report TT82/96, Water Resources Commission, Pretoria, 276 p.
- Showers, K.B., 1996, Soil Erosion in the Kingdom of Lesotho and Development of Historical Environmental Impact Assessment. *Ecological Applications*, **6**(2), pp. 653–664.
- Sidorchuk, A., 1999, Dynamic and static models of gully erosion. *Catena*, **37**, pp. 401–414.
- Sidorchuk, A., 2006, Stages in gully evolution and self-organized criticality. *Earth Surface Processes and Landforms*, **31**, pp. 1329–1344.
- Sidorchuk, A., Märker, M., Moretti, S. and Rodolfi, G., 2003, Gully erosion modelling and landscape response in the Mbuluzi River catchment of Swaziland. *Catena*, **50**, pp. 507–525.
- Tarboton, D.G., Bras, R.L. and Rodriguez-Iturbe, I., 1992, A physical basis for drainage density. *Geomorphology*, **5**, pp. 59–76.
- Temme, A.J.A.M., Baartman, J.E.M., Botha, G.A., Veldkamp, A., Jongmans, A.G. and Wallinga, J., 2008, Climate controls on Late Pleistocene landscape evolution of the Okhombe Valley, KwaZulu-Natal, South Africa. *Geomorphology*, **99**, pp. 280–295.
- Vandekerckhove, L., Poesen, J., Oostwoud Wijdenes, D. and de Figueiredo, T., 1998, topographical threshold for ephemeral gully initiation in intensively cultivated areas of the Mediterranean. *Catena*, **33**, pp. 271–292.
- Willgoose, G.R., Bras, R.L. and Rodriguez-Iturbe, I., 1991, A physical explanation of an observed link area-slope relationship. *Water Resources Research*, **27**(7), pp. 1697–1702.
- WMS Associates, 1988, *Gully erosion in Swaziland*. Final report. Project Number 851039 Fredericton, New Brunswick., Canada. http://www.idrc.ca/en/ev-83068-201_851039-1-IDRC_ADM_INFO.html
- Wishmeier, W.H. and Smith, D.D., 1978, Predicting rainfall erosion losses a guide to conservation planning. *Agricultural handbook*, **537**. USDA, Washington DC.
- Whitlow, R., 1989, A review of dambo gullying in South-Central Africa. *Zambezia*, **16**, pp. 123–150.
- Wu, Y., Zheng, Q., Zhang, Y., Liu, B., Cheng, H. and Wang, Y., 2008, Development of gullies and sediment production in the black soil region of Northeastern China. *Geomorphology*, **10**, pp. 683–691.
- Zeuberger, L.W. and Thorne, C.R., 1987, Quantitative analysis of land surface topography. *Earth Surface Processes and Landforms*, **12**, pp. 47–56.

CHAPTER 8

Gypsum in desert soils, subsurface crusts and host sediments (Western Desert of Egypt)

Ashraf Mohamed & Konrad Rögner

*Department of Geography, Ludwig-Maximilians-Universität,
München, Germany*

Sixten Bussemer

*Institute of Geography and Geology, Ernst-Moritz-Arndt-Universität,
Greifswald, Germany*

ABSTRACT: The enrichment of gypsum in desert soils, subsurface crusts and host sediments—forming powder or solid, consolidated gypcretes—is related to an interaction of the following processes: 1) eolian transport from source areas, 2) temporary sedimentation at the land surface, 3) solution and displacement of gypsum by descending percolating water, 4) evaporation of water and precipitation of gypsum. These processes cannot be related to the environment of today, especially to the recent climatic conditions. There is a need of a more humid climate during the development of the gypcretes.

8.1 INTRODUCTION

8.1.1 Objectives and aims of the study

The area of Egypt and especially the margins of the Nile valley as well as of the Faiyum depression are confronted with a notable pressure by reclamation projects a result of the high population growth ratio (?). In a lot of these areas—foreseen for landuse projects—gypsum is outcropping in enriched or concentrated form at (surficial) or near to the surface (subsurficial). Usually the gypsum is hardened as a surface or subsurface duricrust, forming consolidated horizons, which are handicaps for the cultivation in land use projects. Especially the agricultural projects need urgently geomorphological studies with the aim of a detailed knowledge (i.e. distribution, thickness, matter) of the crusts.

The aims of our studies were: 1) Mapping and description of gypcretes und petrogypsic horizons with a geomorphological and sedimentological point of view, 2) laboratory analyses, 3) considerations concerning the kind of development and the environment during the formation of the crusts, 4) an attempt to reconstruct paleoclimatic conditions and their changes in a rough outline.

8.1.2 Previous work

Gypcretes and petrogypsic horizons (powder gypsum) are characteristic features in the area of our field studies (Figure 1). But these have been studied rarely in Egypt. Since

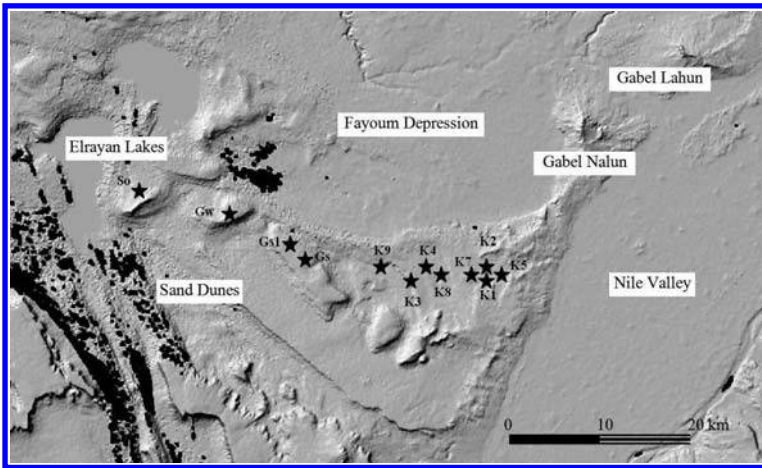


Figure 1. Location of the profiles (stars) and the Digital Elevation Model (DEM after SRTM data) of the study area (in black: sand dunes).

the early works of Beadnell (1905) and Blanckenhorn (1921) there exist only few studies concerning the formation and/or the distribution of gypcretes. And if studies have been carried out, they have dealt with the semiarid area of the Mediterranean Egypt (Ali and West, 1983). In the recent book of Embabi (2004) the description of crusts (“Surface crusts”) reflects only on “calcretes, duricrust, caliche and ferricrete”.

During the last few years studies of gypcretes in the hyperarid regions of Egypt have been published, dealing with the Gebel el Naalun area (Aref, 2003; Rögner *et al.*, 2006; Bussemer *et al.* 2009). The continuation of our studies as well as the presentation of the following paper has to be regarded as a continuation of our own work in a more extended area (the Gebel el Na'alun area is only a spot in the huge desert of Egypt).

8.1.3 Location

The area of field studies is situated close to the southern part of the oasis of Faiyum (Figure 1). The TPC-map (Tactical Pilot Chart, no. H-5 A, scale 1:500.000) showed for at least 20 years a small blue signature in this region, which was named ‘aqueduct’. The construction of this irrigation channel (water source is the river Nil) started in 1946, but the “real” work has begun in 2004. Therefore the aqueduct has been a dry ditch for a period of more than 60 years.

In that dry channel we have carried out a major part of our field studies (profiles “Kanal” 1–9), because the deep outcrops enable to identify the crusts and the solid rocks over long distances under comfortable conditions. Therefore, the results presented below are representative ones, in no case they mirror singularities.

8.1.4 Methods

The different profiles were examined in the field by means of the normal spectrum (i.e. observation, drawing, photos, measurements, status of consolidation, sampling,

etc.). During field work at the isolated hills and mesas some parts of sampling were executed by drilling.

The laboratory analyses (chapter 8.3) reflect merely a small part of the carried out investigations. The following paper is focused only on results concerning the ratios between Calcite (CaCO_3), Gypsum (CaSO_4), salts soluble in water (e.g. NaCl) and the left over (residual/remaining material, mostly called “rest”), which consists predominantly out of Quartz (SiO_2).

The calcite-content was measured by the SCHEIBLER-method (see Schlichting *et al.*, 1995), gypsum was detected by means of the sulphur content (CS-analyzer, Fa. Eltra), the dissolved salts by weight (Reeuwijk, 1995). Quartz was measured by RFA (PW 2404). The total amount of the left over/the remaining material/the “rest” was determined by weight after calcite, gypsum and soluble salts had been removed by solution.

8.2 PHYSICAL SETTING

8.2.1 Climate

From the matter and distribution of the gypcretes it can be concluded, that their formation must have occurred under climatic conditions differing significantly from the climate of today. That is the reason for the presentation of a few climatic data (Table 1). A short evaluation of meteorological and climatological conditions reveals that precipitation is very low. These very small amounts (Table 1) are confronted with very high values of transpiration (>3.000 mm) and evapotranspiration (>5.000 mm). According to the definition of the UNESCO (MAB, Technical Notes 7, 1977) the climate is “hyperarid”, in an extraordinary manner.

The amounts of maximum rainfall during 24 h indicate that the annual mean can be reached or even exceeded during one single rainfall event with an extraordinary intensity. Some phenomena observed in the region—like erosion processes or the moving of soluble salts over distances of tens of centimeters—can be explained only by these high maximum rainfall values (with a high intensity, too) during 24 h.

8.2.2 Geomorphology and geology

The study area is a relative gentle landscape, which is interrupted by some escarpments and hills (see Figure 1). The differences in relative and absolute heights are moderate.

More in detail, the study area is characterized by the following different geomorphic landforms:

1. A gravelly plain which reaches a height of 75 m in the east and slopes gently down to the west to a height of approx. 30 m.
2. An area with mesas in the middle part of the study area, with a maximum height of ca. 100 m asl. These mesas surround the Fayoum depression as an escarpment (especially in the northern part they form cuestas, but this is out of focus in this study).
3. The isolated hills at the western part of the study area, reaching heights between 40 m and 80 m (and sometimes more).

A lot of outcrops show an enrichment of gypsum at or near to the surface. The possible source areas are in a rough outline: (1) Veins or horizons of gypsum in the

Table 1. The mean annual precipitation of the Faiyum Region in mm and the maximum rainfall during 24 h. Data from Mohamed (2003) and Rögner (1998).

Station	Fayoum	Shakshuk	Kom Oshim	Beni Suef	Baharia
mm/year:	10,7	9,2	13,2	8,2	3,6
max. 24 h:	44	16	49,3	16,6	11,6

solid rock below or near the crusts (i.e. more or less autochthonous), (2) other sources more far away from the crusts (i.e. allochthonous).

Therefore it is vital to present a short outline of geology to decide, whether the gypsum can be derived from the outcropping rock or not. The outcropping solid rocks are marine in origin, carbonaceous and from Eocene (and Oligocene) age, sometimes superposed by Pliocene and often by Quaternary material.

The Eocene limestones of Egypt have been described as Mokattam Formation (lower and upper) by Zittel (1883) at first. According to the results of Swedan, (1986: 39) the Mokattam Formation is (again) subdivided in two members: (1) El Breig member (TemMb = Tertiary, Eocene, middle, Mokattam, Breig) and (2) Ravine member (TemMr, = Tertiary, Eocene, middle, Mokattam, Ravine).

Both members contain gypsum in very small amounts as small nodules and/or thin bands or veins. Both members could be a possible source for parts of the gypsum. But predominantly (in an overwhelming manner) they consist of limestone without any gypsum content.

For a colored version of the geological map of Swedan (1986) see Mohamed (2003) (<http://edoc.ub.uni-muenchen.de/1012/>), Rögner *et al.*, (2006), Bussemer *et al.*, (2006) (www.desertnet.de/proceedings/start.htm).

8.3 GYPSUM AND GYPCRETES

8.3.1 Gypsum crusts—a definition

Gypcretes are rarely studied compared to calcretes. Therefore, a common, obligatory, ‘fixed’ and accepted definition is lacking. In some papers scientists follow the definition of Watson, which is given below as a citation.

“Gypsum crusts have been defined as ‘accumulations at or within 10 m of the land surface from 0,10 m to 5,0 m thick containing more than 15% by weight gypsum ... and at least 5,0% by weight more gypsum than the underlying bedrock“ (Watson, 1989, p. 28).

This definition is generally valid, even if the gypsum does not form consolidated crusts, e.g. if it appears as a nodule or as a powdery enrichment. We accept this definition and use it in its whole content. The Encyclopedia of Geomorphology (Vol. 1, pp. 507–509, author: Eckardt, G.) follows the above quoted definition.

Regarding the environment Watson (1989) states that the development of gypsum crusts takes place between 250 and 25 mm of annual precipitation. Gypsum crusts will be dissolved above the value of 250 mm, while below 25 mm only the solution of “common” salts like NaCl (Halite) is possible.

8.3.2 Profiles, distribution and description

12 different profiles were recorded in the study area (Figure 1) in detail. Profiles “Kanal” 1 to 9 are located in the gravelly desert plain south of the Faiyum depression.

The profiles “El Garaq S” and “El Garaq S1” represent a transition area between the gravelly plain and the mesas, which surround the Faiyum depression. Profile “El Garaq W” was taken at a mesa and profile “See O” at the top of a limestone hill in the Wadi El Raiyan depression.

All profiles named “Kanal” (numbers 1 to 9, taken in the long ditch, the “aqueeduct” of the TPC map) show macroscopically nearly the same successions of horizons or sequences (from top to bottom):

- desert pavement (in most cases disturbed by human influence),
- gypcrete (usually developed as duricrust, with a higher sand content (e.g. the “rest”) in the uppermost part and a lower or nearly missing sand content in deeper situations,
- gypcrete (usually developed as duricrust),
- solid rock “swimming” in gypsum,
- limestone/shale penetrated by small bands or veins of gypsum,
- solid rock without cracks and fissures, no traces resp. very small traces of gypsum.

The other profiles seem to be not so well developed. The sequence of horizons is reduced (from top to bottom):

- desert pavement (undisturbed),
- gypcrete (usually developed as blister or scattered gypsum, with a higher sand content in the uppermost part),
- gypcrete (usually developed as duricrust),
- solid rock (no traces resp. very small traces of gypsum).

The description of the investigated profiles is given in Figure 2. A short comparison allows the following statements: 1) There is an increase in thickness of the gypsum crusts from East to West in the “Kanal-sections”. This could be related to a decrease in elevation above sea level (landscape dips gentle to the West). Deep positions in relief seem to promote the accumulation of gypsum. 2) The exposed positions “El Garaq S” to “See O” (top of mesas or hills) result in relatively thin gypcreted. Exposed positions do not favour the accumulation of gypsum.

1. Only in profiles “Kanal 5” and “Kanal 1” ascending groundwater could be the triggering factor in crust-formation. But the gypsum veins in the named profiles found in the shales—could be also regarded as a result of diagenetic processes (as in the other shale-profiles).
2. The gypsum veins in the profile “Kanal” 8, “Kanal” 4 and “El Garaq S1” are the result of descending water. This assumption could also explain the gypsum veins in the limestone sequence of “Kanal” 1.
3. The solid rock influences at most the lower part of the crusts. But in a lot of cases the crusts are superposed to the solid rock like a carpet.

Result: There exist good indications for a descending percolation-model of water (“per descensum”) enriched with gypsum, the evaporation of this water and the precipitation of gypsum. An ascending model does not fit with the field observations!

The top of the profiles consists normally of a desert pavement; therefore the profiles are truncated by processes of deflation (and sometimes by fluvial erosion). The thickness of the recent profiles is reduced compared to that of the time of formation. The fact that the desert pavement consists of hard and very resistant components like flint, petrified wood, quartz pebbles (sometimes nummulites) enables to think on distinct weathering processes. But horizons or materials indicating intensive chemical weathering cannot be proven by field and laboratory data.

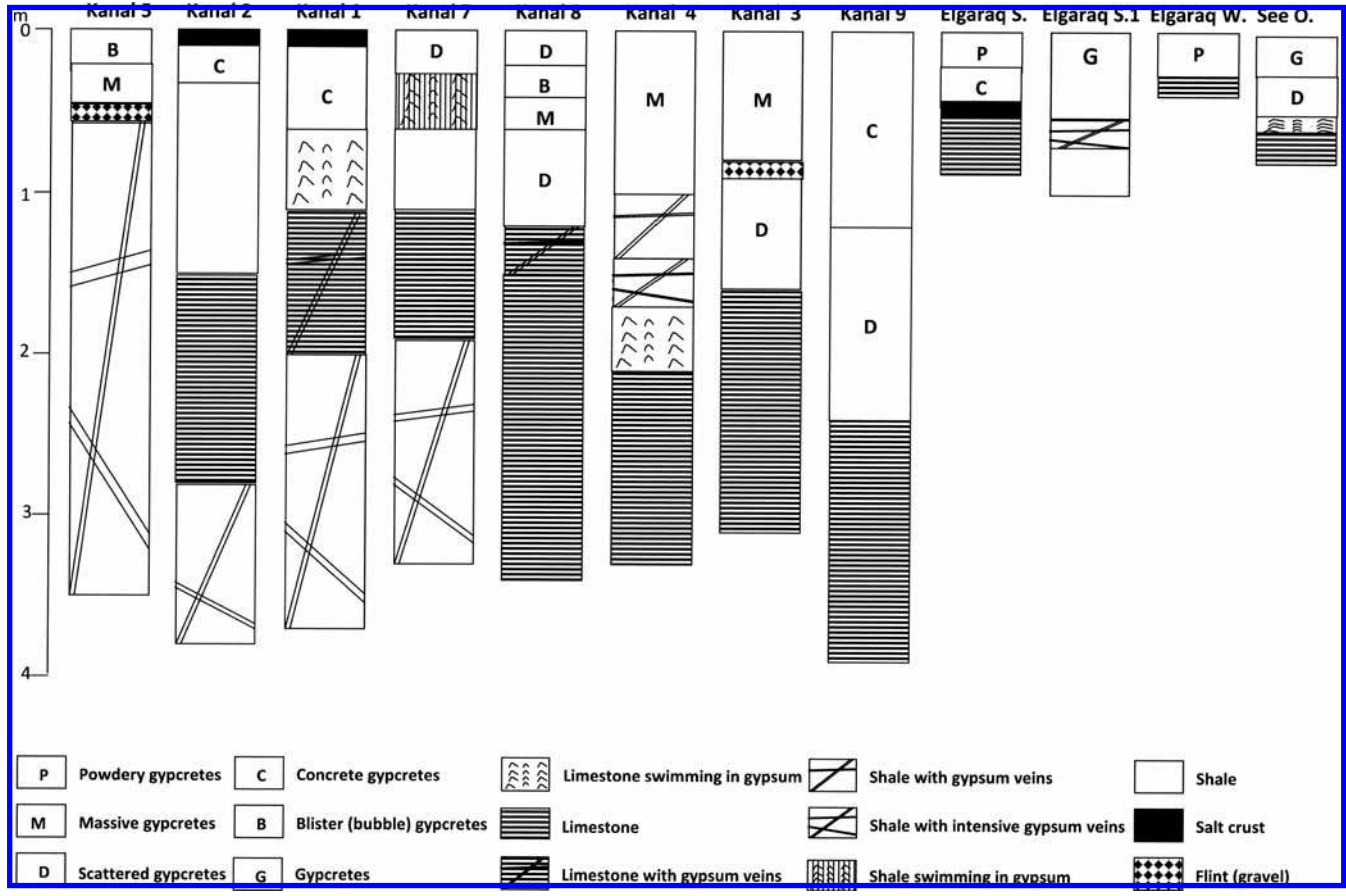


Figure 2. The 12 profiles according to the results of the field studies. Profile “Kanal 5” is situated in the East, “See O” in the West of the study area. Differentiation of the types of crusts according to Mohamed (2003).

8.3.3 Analyses, interpretation and classification

Gypsum is outcropping in enriched or concentrated form at or near to the surface of most of the studied landforms and in all studied profiles.

In previous studies dealing with the Gebel El Naalun Region (Rögner *et al.*, 2006) all profiles have displayed gypsum crusts/gypcretes according to the definition of Watson (1985, 1988, 1989, see chapter 8.2.1). Exceptions of that kind of distribution demonstrate only the recent wadi-sediments and the shoreline deposits of the historical Lake Moeris (mentioned by Herodotus 500 B.C.). These both geomorphological positions reveal no gypsum in the profiles, while the subrecent wadi sediments indicate the beginning of gypsum enrichment. In the region of the present study all landforms are proved by gypcretes, independent of the type of the underlying rocks.

In a previous work Mohamed (2003) differentiated 5 types of gypcretes based on a textural description: powdery, massive, concreted, scattered and bubbly. This classification is used in Table 2.

The thickness of the gypcretes reaches up to 120 cm (profile "Kanal" 9), with an average of 40 cm. Related to textural types the thickness varies widely, but it is lower at the top of the mesas and isolated hills than in the gravelly plains.

The laboratory analyses (Table 3) confirm the results of the field studies in distinct manner. All profiles show an enrichment of gypsum in the surficial and subsurficial parts, while in most cases the underlying bedrock is free or nearly free of gypsum: Profile El Garaq W exposes a thin crust (25 cm) with a gypsum content of 20% while the solid rock below is free of gypsum (0,4%). In that small profile the crust is influenced by the solid rocks (high content of calcite) and even the desert pavement consists of nummulites gizehensis.

Location Kanal 7 shows an evident decrease in gypsum from the surface to deeper horizons (gypcrete: 83,6%; the transition zone: 33,0%; shale 6,6%; the solid limestone below: only 1,0%). In this profile a change between shale, limestone and shale (again) can be noticed. This superposition does not influence the gypsum content, but that of the other components.

The dissolved salts are enriched especially in a depth of 20–60 cm (samples 8–2 and 8–3), which could be caused by the infiltration of extraordinary rainfall amounts during 24 h (Table 1) to a depth, where water evaporates and the salts are precipitated. Distinct indicators for descending water are the described gypsum horizons (samples 8–1, 8–2

Table 2. Statistical data of the gypcretes. The number of the investigated crusts differs from the number of profiles, because most of the profiles show more than one type of gypsum crust.

type of gypcretes	number of gypcretes	in%	average thickness in cm	maximum thickness in cm	minimum thickness in cm
surface	11	44	36,4	120	5
subsurface	14	56	43,8	120	8
in sediments	21	84	36,45	120	5
in solid rocks	4	16	68,3	120	35
powdery	5	20	15	25	5
massive	6	24	53,7	100	22
concreted	5	20	48,8	120	10
scattered	7	28	38,5	120	8
blister/bubbly	2	8	15	20	10

Table 3. Geochemical data of the different profiles.

	“rest” (weight %)	calcite (weight %)	gypsum (weight %)	salts (weight %)
Kanal-1				
1-1	44,9	0,7	41,9	12,5
1-2	19,6	76,5	0,8	3,0
1-3	69,6	17,4	1,0	12,0
1-4	4,5	0,0	93,0	2,5
1-5	56,6	10,6	10,9	21,9
Kanal-2				
2-1	62,4	2,9	31,3	3,4
2-1a	76,5	11,3	5,9	6,3
2-2	81,8	14,3	0,8	3,1
2-3	10,8	84,2	0,6	4,4
2-4	59,5	39,5	0,9	0,0
Kanal-3				
3-1	44,0	5,8	47,5	2,7
3-2	17,0	5,5	74,3	3,1
3-3	6,6	26,2	66,2	1,0
3-4	9,2	27,8	61,8	1,2
3-5	5,3	50,9	42,3	1,4
3-6	1,5	95,2	2,3	1,1
Kanal-4				
4-1	18,6	3,3	77,2	0,8
4-4	62,6	6,9	12,9	17,5
4-3	22,6	2,2	62,0	13,2
4-4	37,9	2,5	44,6	15,0
4-5	7,2	89,8	1,2	1,8
4-6	2,7	93,4	3,3	0,6
Kanal-5				
5-1	50,8	1,2	46,0	1,9
5-2	68,0	0,5	24,4	7,2
5-3	4,7	0,0	85,9	9,4
5-5	71,9	0,0	3,6	24,6
5-6	89,2	0,0	0,7	10,1
Kanal-7				
7-1	14,5	0,2	83,6	1,7
7-2	56,7	2,0	33,0	8,3
7-3	46,6	29,2	6,6	17,7
7-4	8,0	88,5	1,1	2,4
7-5	8,2	30,4	1,0	10,3

(Continued)

Table 3. (Continued).

	“rest” (weight %)	calcite (weight %)	gypsum (weight %)	salts (weight %)
Kanal-8				
8-1	19,2	1,3	78,9	0,6
8-2	8,0	3,2	80,2	8,6
8-3	4,9	20,2	69,7	5,1
8-4	4,6	37,2	57,8	0,4
8-5	2,5	34,5	62,3	0,7
8-6	0,4z	98,9	0,1	0,6
Kanal-9				
9-1	13,6	3,2	74,3	9,0
9-2	5,5	34,1	56,0	4,5
9-3	1,4	96,2	0,5	1,8
9-4	8,6	60,8	2,3	28,3
(“salt-curtain”)				
El-Garaq-S				
S-1	17,2	47,2	35,5	0,1
S-2	3,8	49,2	25,3	21,7
S-3	3,4	51,0	3,6	42,1
S-4	4,9	91,9	1,8	1,3
(salt-crust)				
El-Garaq-S1				
S1-1	67,2	15,8	16,4	0,6
S1-2	26,2	8,8	64,2	0,8
S1-3	32,4	5,0	61,2	1,4
S1-4	50,0	9,7	31,2	9,1
S1-5	57,3	14,1	23,6	5,0
S1-6	66,3	10,7	15,4	7,7
S1-7	62,6	12,7	14,9	9,8
El-Garaq-W				
W-1	7,8	71,4	20,4	0,5
W-2	2,3	96,4	0,4	0,8
See-O				
1-1	37,3	44,9	17,2	0,6
1-2	22,1	47,6	29,4	0,9
1-3	22,7	52,5	19,4	5,4
1-4	20,5	78,2	0,2	1,1

and 8–3), as well as the fact that gypsum penetrates into the top of the solid rocks (sample 8–4). As a result of this strong penetration of gypsum, the limestone particles seem to swim. The same information (of descending water with dissolved material) is given by the small bands of gypsum crystals (sample 8–5). These veins of gypsum crystals run down through the solid limestone (sample 8–5) and are ending after a few decimeters.

This evaluation of the laboratory analyses (result: descending water with dissolved gypsum) is supported by other field observations in the area of Gebel el

Na⁺alun, where bands/veins of gypsum crystals penetrate the solid limestone as well as the superposed gypcretes (Rögner *et al.*, 2006, Abb. 7, p. 98).

The results of laboratory analyses of another profile (“Kanal” 9) give answer to questions concerning the recent solution and precipitation processes. The gypcrete is forming a horizon with a thickness of 120 cm (Table 3, sample 9–1). At a depth of 120–240 cm, small veins of gypsum penetrate the solid limestone (sample 9–2) and between 240 and 390 cm the solid rock contains only 0,5% of gypsum (no veins!) and 1,8% of salts. But at some specific parts of the wall of the ditch the solid rock (below 240 cm depth) is covered by a curtain of material which consists to a high amount of salts (sample 9–4). The development of this curtain could have started not before 1946 (= beginning of the digging of the ditch) and is related to the (before mentioned) extraordinary rainfall during 24 h. This type of rainfall is able to infiltrate, to descend into the gypcretes and into the limestone. But the water is only able to solve salts and not gypsum or carbonates. The “rest”, calcite and gypsum were transported as normal “bedload” of small particles while water was running along the wall of the ditch. The deep infiltration at this location is supported by fissures and desiccation cracks. By means of the “salt curtain” the recent processes of solution and precipitation can be limited to the solution of salts like NaCl (Halite), the solution of gypsum needs higher amounts of rainfall.

The recent enrichment of salt is also documented by the results of profile El Garaq S, which is situated in the center of a small and flat endorheic basin. In horizon S-3 the salt content culminates in 42,1% (Table 3), which is the highest value in all studied profiles. The salts are concentrated in a small horizon beneath the gypcrete. This coincides with the possibility of salt solution, movement by descending processes and precipitation under recent conditions, while today’s rainfall is not able to solve and to move the gypsum.

Result: The formation of the gypcretes at the southern rim of the Faiyum depression took place under a more humid environment.

8.4 DISCUSSION

Other studies concerning the gypsum crusts/gypcretes (e.g. Goudie, 1973, p. 121; Eckardt, 2006) describe different possibilities for the sources of gypsum and different models of gypcrete formation. It is possible to group them as follows:

(1) Evaporation model from water bodies like marine environments, lakes, lagoons, saline pans, playas or sabkhas, and accumulation of gypsum as gypcretes. (2) In situ model: During the wet season the dissolution by percolating rain water takes place, during the dry season there is re-precipitation from water descending over a very limited distance towards the surface. (3) Fluvial model: The deposition of suitable materials and their precipitation in valleys or channels and those which involve the deposition or alteration of materials by sheet-flood action. (4) Groundwater model: The crust is a result of the upward capillary flow of gypsiferous water induced by constant and rapid evaporation at the surface in a comparatively rainless region (“per ascensum” model). (5) The “per descensum” model: The solutions containing gypsum might be leached from the upper soil horizons to accumulate at depth.

The models 1 to 4 can be excluded. In the area of field studies the gypcrete outcroppings are found in geomorphological positions which do not allow a reconstruction of evaporation basins (model 1). Model 2 cannot be proved because it needs gypsiferous rocks at the surface; they don’t exist. The geomorphological position of the crusts denies the model 3. It is impossible, that ascending and evaporating groundwater (model 4) is responsible for the enrichment of gypsum at or near the surface,

because in most cases the underlying rock is free or nearly free of gypsum. This is proven by means of the described sequences, analyses and the conclusions.

It is proved by field observations that gypsum—in some special situations—occurs in the solid shale as veins. But the volume of these veins is very small, compared to the mighty crusts. And it is also a result of our previous studies (Rögner *et al.*, 2006), that veins of gypsum penetrate not only the solid limestone or shale but the superposed gypcretes too. In this special case the veins are younger than the formation of the massive gypsum crusts! Vice versa, the massive crusts are the sources of the gypsum veins.

Desiccation cracks, filled with gypsum (and other eolian material), indicate, that ascending groundwater was not responsible for the enrichment of gypsum in the cracks; ascending water would destroy the cracks. Normally the formation of the crust is older than the genesis of the desiccation cracks and the filling of the cracks is the youngest element.

Based on the own studies we are able to propose the following model (Figure 3), which has clear relationship with the above described model 5. The arguments are given by field and laboratory analyses (chapter 8.3).

The main sources of the gypsum are situated in the marine surroundings (Mediterranean Sea, about 250 km to the North; the Gulf of Suez and the Red Sea, 130 km to the East) and especially the Qattara depression (–134 m below sea level and situated in the Northwest), in which gypsum is outcropping as gypsum dykes at the bottom of the depression (related to ascending groundwater).

The gypsum is deflated by wind action and is transported together with the (eolian) dust and sand to the sedimentation areas. Precipitation (rainfall, fog, dew) leads to a wash out and a temporary deposition at the surface (Figure 3a). Dry deposition (fall out) is also a possibility. The dust material is trapped by sparse vegetation and/or a wet surface. The precipitation events, especially the rainfall, cause infiltration, a solution of gypsum and soluble salts, followed by descending percolation (Figure 3b)

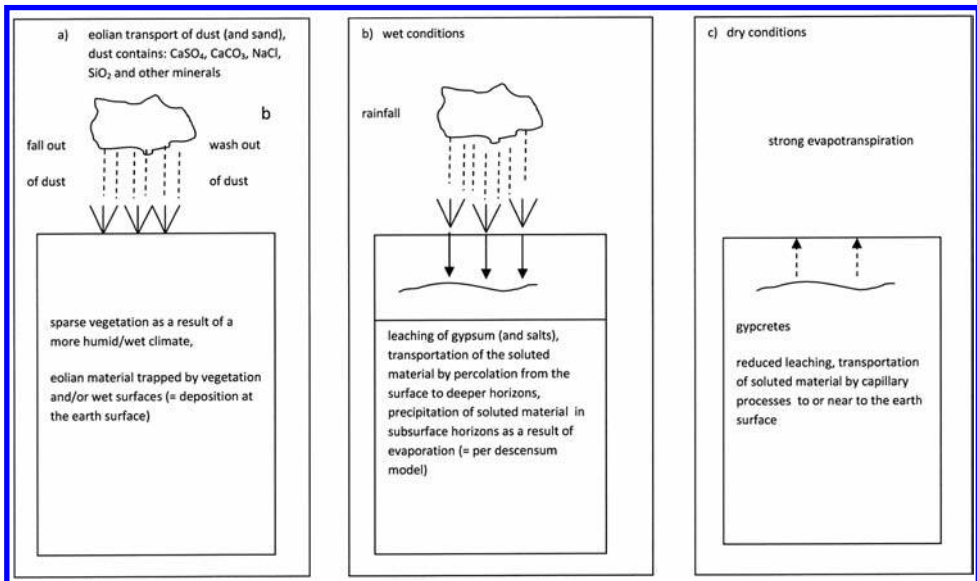


Figure 3. Suggested model for the development of the gypcretes in the study area.

and by precipitation of gypsum. The “rest”, which could not be dissolved, is concentrated in the uppermost horizons, sometimes forming a vesicular layer. Dry conditions lead generally to evaporation and/or to the ascending percolation of water (caused by capillarity) to or near to the surface, resulting in deposition of gypsum by evaporation and other processes (Figure 3c).

Result: The development of the gypcretes has been caused by infiltrating and descending rainwater. The gypsum is of allochthonous origin, has been transported by winds (atmospherically), was washed out and/or accumulated in a relative dry (but not hyperarid!) environment as dust (or it is the product of chemical reactions). A descending water system led to the enrichment of the gypsum at or near the surface.

The age of the crust formation is young but not recent, a fact which is proven by the existence of gypcretes at all land surfaces, besides the recent wadi sediments and the shoreline sediments of the historical Lake Moeris.

The development of the crusts calls for a definitely moist climate compared with the hyperarid climate of today. According to the statement of Watson (1985, 1989) the annual rainfall must have been in the order of 250 mm as maximum and at least 50 mm in the minimum. The last threshold is derived from the interpretation of location “Kanal 9”, because there was no mobilization of gypsum during rainfall events with a value of ca. 50 mm in 24 h.

During the time of the enrichment of gypsum and the formation of the crusts, the rainfall must have exceeded the values of today with a factor of 5 to 25. But the climate stayed arid; otherwise the crusts would have been destroyed by solution.

There has been no exact age dating of the crusts so far, but the time of formation could be assumed with young Pleistocene to Holocene (but not recent!). This assumption—derived from geomorphological results—is supported by the data of Said (1981), who reported an age of “early Late Pleistocene” for gypsum crusts in the area of the Nile valley. That is a contradiction to the papers, which have dealt with gypcretes in the Faiyum area: A Pliocene age for crust formation proposed by Beadnell (1905) is too old, a recent age proposed by Blanckenhorn (1921) is too young.

REFERENCES

- Ali, Y.A. and West, I., 1983, Relationships of modern gypsum nodules in sabkhas of loess to compositions of brines and sediments in northern Egypt. *Journal of Sedimentary Petrology*, **53**, pp. 1151–1168.
- Aref, M.A.M., 2003, Classification and depositional environments of Quaternary pedogenic gypsum crusts (gypcrete) from east of the Fayoum Depression, Egypt. *Sedimentary Geology*, **155**, pp. 87–108.
- Ball, J., 1939, *Contributions to the Geography of Egypt*. Survey of Egypt, Cairo. (reprinted 1952).
- Beadnell, H.J., 1905, *The topography and geology of the Fayoum Province of Egypt*. Survey Department, Cairo, Egypt.
- Blanckenhorn, M., 1921, *Ägypten. Handbuch der Regionalen Geologie*, **VII**, **23**, Heidelberg.
- Bussemer, S., Rögner, K., Mayer, Th. and Michel, J., 2009, Gypsum and gypsum crusts (Gypcretes) at the rims of the Faiyoum-Depression (Egypt). *Zentralblatt für Geologie und Paläontologie, Teil I*, **3** and **4**, pp. 169–179.
- Embabi, N.S., 2004, *The geomorphology of Egypt. Volume I – The Nile Valley and the Western Desert*.

- Goudie, A., 1973, *Duricrusts in tropical and subtropical landscapes*. Clarendon Press Oxford.
- Mohamed, A.Y.A.H., 2003, Die Krusten der Ränder der Fayoum Depression—Geomorphologische Untersuchungen. *Ph.D. Thesis Faculty of Geosciences. LMU München*, <http://edoc.ub.uni-muenchen.de/1012/>. Unpublished.
- Pfannenstiel, M., 1953, Das Quartär der Levante. Teil II: Die Entstehung der ägyptischen Oasendepressionen. In: *Abhandlungen der mathematisch-naturwissenschaftlichen Klasse*, **7**, Wiesbaden, pp. 337–411.
- Rögner, K. and Müller-Koch, K., 1998, Rezente morphodynamische Prozesse in der Wadi Raiyan Region, Ägypten. *Paderborner Geographische Studien*, **11**, pp. 37–56.
- Rögner, K., Bussemer, S., Meier, K., Mayer, Th., and Mohamed, A.Y.A.H., 2006, Die Gipskrusten der Gebel el Na'alun Region (Ägypten). *Mitteilungen der Geographischen Gesellschaft in München*, München, **88**, pp. 79–111.
- Said, R., 1981, *The geological evolution of the river Nile*. Springer Verlag, New York.
- Sandford, K.S. and Arkell, W.J. 1929, The origin of the Fayoum Depression. *Geographical Journal*, **24**, pp. 578–584.
- Schlichting, E., Blume, HP. and Stahr, K., 1995, *Bodenkundliches Praktikum*. Berlin/Wien.
- Swedan, A.H., 1986, Contributions to the Geology of Fayoum area. *Ph.D. Thesis, Faculty of Sciences, Cairo Univ., Egypt*. Unpublished.
- UNESCO, 1977, Map of the world distribution of arid regions (MAB Technical Notes 7, eplanatory note), Paris.
- van Reeuwijk, L.P., 1995, Procedures for Soil Analysis, fifth edition, *ISRIC Technical Paper*, 9, (Wageningen, The Netherlands).
- Watson, A., 1979, Gypsum crusts in deserts. *Journal of arid Environments*, **2**, pp. 3–20.
- Watson, A., 1983, Gypsum crusts. In *Chemical sediments and Geomorphology*, edited by Goudie, A.S. and Pye, K. (Academic Press), pp. 133–161.
- Watson, A., 1985, Structure, chemistry and origin of gypsum crusts in southern Tunisia and the central Namibia desert. *Sedimentology*, **32**, pp. 855–875.
- Watson, A., 1988, Desert gypsum crusts as palaeoenvironmental indicators, a micro-petrographic study of crusts from southern Tunisia and the central Namib desert. *Journal of arid Environments*, **15**, pp. 19–42.
- Watson, A., 1989, Desert crusts and rock varnish. In *Arid Zone Geomorphology*, edited. by Thomas, D.S.G., (Belhaven Press, London), pp. 25–55.
- Zittel, K.A., 1883, Beiträge zur Geologie und Paläontologie der Libyschen Wüste. *Paläontographica*, **8X**, Kassel.

CHAPTER 9

New findings from geological, geomorphological and sedimentological studies on the palaeoenvironmental conditions in Southern Cameroon

Mark Sangen, Joachim Eisenberg & Jürgen Runge
Department of Physical Geography, University Frankfurt, Frankfurt am Main, Germany
CIAS, Centre for Interdisciplinary African Studies, Frankfurt am Main, Germany

Boniface Kankeu
Ministry of Scientific Research and Innovation/Institute of Geological and Mining Research (MINRESI/IRGM), Cameroun

Mesmin Tchindjang
Département de Géographie, Université de Yaoundé I, Cameroun

ABSTRACT: Proxy data on palaeoenvironmental conditions in equatorial Central Africa were compiled during the first phase of the DFG-funded ReSaKo-project (2004–2006) from the alluvial sedimentary basin of the Ntem interior delta and sites across river sections of the middle and lower catchment of the Nyong River in SW Cameroon. The focus of the second project-phase (2007–2009) was laid on the exploration of identical sites in the upper catchment areas of the Nyong and Sanaga Rivers, close to the recent rain forest-savanna margin (2007). Additional reconnaissance corings were carried out across the Boumba, Dja and Ngoko Rivers, which drain into the Congo Basin (2008). Here we present results from selected areas across the upper Sanaga (Bélabo region), Nyong (Akonolinga region), Boumba (Lomié region) and Ngoko catchments (Moloundou region), which show striking correlations with our earlier findings on palaeoenvironmental conditions since the late *Maluékien* (OIS 3). Additional hand-corings, geomorphological, sedimentological and partially geological investigations and alluvial sediment analysis as well as ^{14}C - and $\delta^{13}\text{C}$ -data provide further insights into Late Pleistocene history of equatorial Central Africa and substantiate formulated hypotheses.

9.1 INTRODUCTION

9.1.1 State of the art

The ReSaKo-project has proved the significance of Central African, tropical alluvial sediments for palaeoenvironmental and palaeohydrological studies (Runge *et al.*, 2006; Sangen 2008). Across selected reaches of anastomosing, anabranching, and meandering

river sections valuable sediment archives with embedded palaeosurfaces were uncovered, yielding maximum ages around 50 ka BP. Significant grain-size fluctuations as well as pedological and sedimentological characteristics of alluvial deposits indicate major modifications of run-off and sedimentation behaviour, most likely related to climatic fluctuations and internal fluvial reorganizations. First results from the Ntem and Nyong catchments (Runge *et al.*, 2006; Sangen, 2009) show high correlation with findings from hemi-pelagic (e.g. Schneider *et al.*, 1997; Zabel *et al.*, 2001; Adegbe *et al.*, 2003; Weldeab *et al.*, 2007) and lacustrine (e.g. Street-Perrott and Perrott, 1990; Maley and Brenac, 1998; Nguetsop *et al.*, 2004; Gasse *et al.*, 2008; Giresse *et al.*, 2008) data archives covering various sediment-stratigraphic periods. Fluvial-morphological response is highly dependent on monsoonal, hydrological and ecological feedbacks to climatic changes. The latter are basically determined by orbital parameters (Imbrie *et al.*, 1984; Berger and Loutre, 1991) and global boundary conditions as well as inherited teleconnections (Blunier and Brook, 2001; Vidal and Arz, 2004). Various proxy data recovered from hemi-pelagic archives (Congo, Niger, Nyong and Sanaga deep-sea fans) manifest variations in the intensity of terrestrial erosion, weathering and fluvial-morphological activity, which are linked to climatic and monsoon-intensity fluctuations (Schneider *et al.*, 1997; Zabel *et al.*, 2001; Adegbe *et al.*, 2003; Holtvoeth *et al.*, 2005; Weldeab *et al.*, 2007). These findings have been corroborated by various studies on marine pollen (e.g. Marret *et al.*, 1999; Dupont *et al.*, 2000; Lézine and Cazet, 2005), phytoliths (Abrantes *et al.*, 2003) and diatoms (Pokras, 1987; Jansen and van Iperen, 1991). The climatic oscillations in western and central monsoonal Africa show high correlation with periodic orbital and insolation cycle changes (Rossignol-Strick, 1983; Pokras and Mix, 1987; Prell and Kutzbach, 1987; DeMenocal *et al.*, 2000; Lézine *et al.*, 2005). Extraterrestrial forced climate variability induces major global modifications of the atmospheric, oceanic, hydrological and ecological cycles, which in turn imply far reaching, complex feedbacks and impacts on global circulation processes (Barker *et al.*, 2004; Vidal and Arz, 2004). As a consequence, the western tropical African region experienced major environmental changes which are linked to ITCZ displacements and variations of the monsoon/harmattan forcing (Rossignol-Strick, 1983; Pokras and Mix, 1987; Chiang *et al.*, 2003; Broccoli *et al.*, 2006). These climatic and environmental oscillations are known as hypothermal (cool and semi-arid to arid; *Maluékien* ~70–40 ka BP, *Léopoldvillien* ~27–14 ka BP) and hyperthermal (humid and moist; *Njilien* ~40–27 ka BP, *Kibangien A* ~12–5 ka BP) phases following early climatic stratigraphies postulated by van Zinderen Bakker (1962; 1967) and De Ploey (1964; 1965) based on sedimentary records from Angola and the Malebo (Stanley) Pool in Congo. Thus striking climatic and environmental changes in western Central Africa occurred during the *Maluékien/Njilien* transition (OIS 3), Last Glacial Maximum (LGM) and the Pleistocene/Holocene transition. Shorter climatic fluctuations occurred during several stages of the Holocene (e.g. 8.2 ka event, *First Millennium BC Crisis*, Little Ice Age; Mayewski *et al.*, 2004; Wanner *et al.*, 2008). Most of these modifications have been verified by palynological (Dupont *et al.*, 2000; Maley, 2001; Lézine and Cazet, 2005) and lacustrine sediment archives (Barker *et al.*, 2004; Elenga *et al.*, 2004; Gasse *et al.*, 2008). Nevertheless, the impact of Late Quaternary climate change on tropical African fluvial systems is still not well understood, although a lot of progress has been made (Neumer, 2007; Gasse *et al.*, 2008; Lespez *et al.*, 2008; Sangen, 2008, 2009; Thomas, 2008). In spite of increasing contributions palaeoenvironmentally evaluable sediment archives from alluvial rivers in Africa are very limited. Most of the palaeoenvironmental and palaeoclimatic proxy data from Southern Cameroon originate from lacustrine (e.g. Servant and Servant-Vildary, 2000; Elenga *et al.*, 2004; Gasse *et al.*, 2008), hemi-pelagic (Schneider *et al.*, 1997; Zabel *et al.*, 2001; Schefuß *et al.*, 2005; Adegbe *et al.*,

2003; Weldeab *et al.*, 2005, 2007) and other terrestrial (Kadomura, 1995; 2000; Thomas, 2000, 2004, 2008; Thomas and Thorp, 2003; Runge, 2008) sediment archives.

The ReSaKo-project provides the first detailed alluvial sedimentary record for the in this context unexplored Southern Cameroonian region. This record includes valuable information concerning the climatic and environmental changes of the last 50 ka BP. Besides river catchment evolution studies (geomorphological, geological and neotectonic investigations), sediment-stratigraphic and fluvial-morphological analysis of the alluvia delivered supplementary information for the reconstruction of palaeoenvironmental conditions in Central Africa. During the first ReSaKo-project phase selected sites in the lower catchments of the Ntem and Nyong Rivers (Runge *et al.*, 2005, 2006; Sangen, 2008, 2009), which drain into the Atlantic Ocean, were intensively studied. These sites are located in the south-western coastal hinterland and covered by dense Guinean-Congolian tropical rain forest. While study sites along the middle to lower catchment areas (transition zone “*surface intérieure/surface côtière*”, Segalen, 1967) of the Nyong and Ntem are characterized by structural dominated river shapes with limited and young sedimentary basins, the Ntem interior delta with its anastomosing river section and the coastal plains comprise of thick alluvial sediment archives. These contain embedded palaeosurfaces, covering multiple chronostratigraphic periods, and distinguishable sedimentary units, which document several shifting fluvial-morphological phases. Besides coarse-grained sandy (48 to 45 ka BP), also palustrine (swampy gyttja) Pleistocene (30 and 18–14 ka BP) as well as thick Holocene deposits were sampled in the alluvial plain of the interior delta, while across the coastal plain Late Holocene to recent sediments were uncovered. Almost 100 corings, including multiple channels transgressing transects, manifest the complex fluvial-morphological evolution of the interior delta. The sediment archives indicate frequent avulsion, channel migration and floodplain reformation with most striking reorganizations of the fluvial systems centred around the *Maluékien/Njilien*- as well as Pleistocene/Holocene-transition and the LGM. Several shorter and smaller scale perturbations can be postulated for different periods of the Holocene (around 8, 5, 3,8, 1,5 and 0,8 ka BP), which may result from climatic fluctuations but also increasing anthropogenic impacts, especially since the Neolithic and the inauguration of metallurgy around 2,6 ka BP (e.g. Schwartz, 1992; Eggert *et al.*, 2006; Höhn *et al.*, 2008; Meister, 2008; Ngomanda *et al.*, 2009). Subsequently, erosional and aggradation processes have been intensified by anthropogenic activities (industrial logging, shifting cultivation, dam construction, etc.). To obtain additional information from more continental fluvial system sections, located close to the recent rain forest-savanna margin, in the second project-phase (subproject J. Runge, Ru 555/14-2) fieldwork concentrated on eastern (upper catchment areas of the Nyong and Sanaga Rivers) and south-eastern regions (Boumba and Ngoko Rivers) of the Southern Cameroonian study region (Figure 1). With regard to the neotectonic evolution of those river basins (Eisenberg, 2008, 2009), suitable locations for the sampling of palaeoenvironmental proxy data (alluvia) were thoroughly prospected using geomorphological and pedological methods. This paper presents results from the fieldwork carried out around Bélabo (4°55'N, 13°17'E; 623 m asl), Akonolinga (3°46'N, 12°15'E; 671 m asl), Ayos (03°54'N, 12°31'E; 693 m asl), Mankako (3°18'N, 14°04'E; 590 m asl), Ouesso (3°24'N, 14°32'E; 582 m asl) and Mokounounou (1°56'N, 15°20'E; 367 m asl).

9.1.2 Study area

The Southern Cameroonian region comprises of two large geomorphological units: the *Plateau sud-Camerounaise* or *surface intérieure* (African I, Eocene) and the *surface*

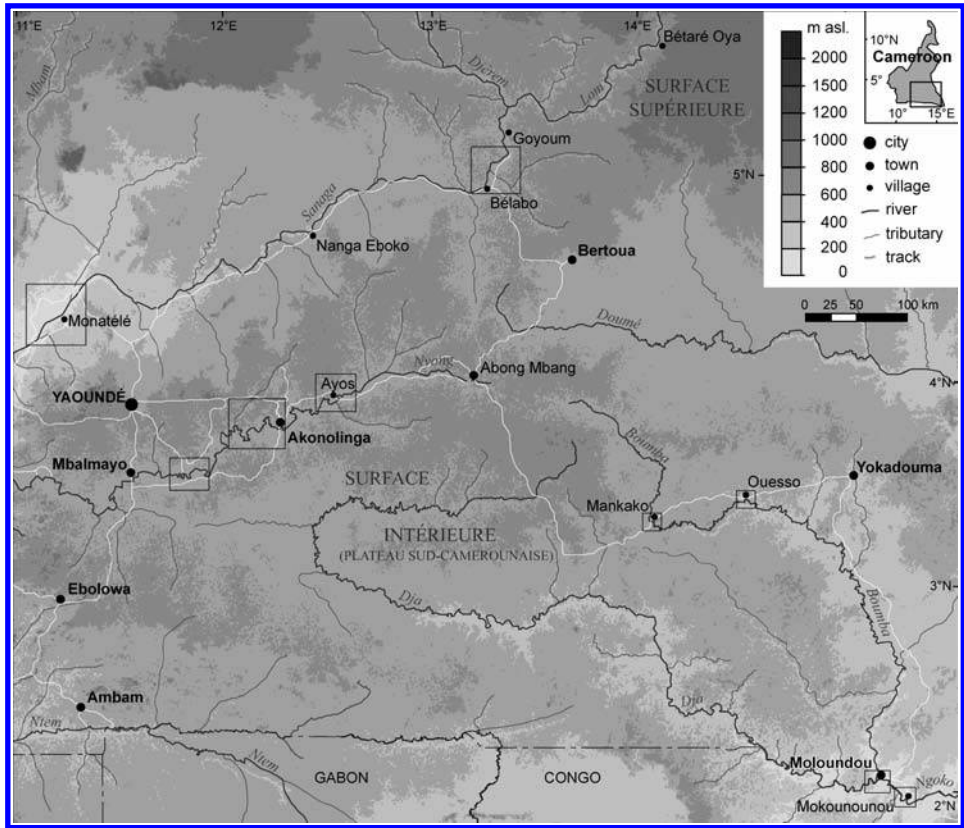


Figure 1. Map of the eastern part of the Southern Cameroonian study area based on Shuttle Radar Topographic Mission-data (2000), showing fieldwork sites (boxes) across the upper Sanaga and Nyong as well as Boumba and Ngoko Rivers during the second ReSaKo-project phase (2007–2008).

côtière with appending peneplain step as well as ridge and swell landscape with typical inselbergs and mature valley systems (cf. Segalen, 1967). In Cameroon the north-western rise of the Congo Basin corresponds to the catchment areas of the Sanaga, Nyong and Ntem Rivers, draining across the peneplain step to the Atlantic Ocean, and those of the Boumba, Dja and Ngoko, tributaries of the Sangha, which drains into the Congo River basin (Olivry, 1986; Runge, 2008).

The basement rocks of the middle and upper catchments of the Nyong and Sanaga River belong to the Pan-African Central Africa Fold Belt (CAFB). The CAFB resulted from the collision between the stable Archean craton to the south and one or two palaeoproterozoic blocks to the north ca. 600 Ma ago, juvenile crustal rock formations, and the intensive reworking of the pre-Pan-African basement (Castaing *et al.*, 1994). The heterogeneous, generally crystalline basement rocks of the middle and upper catchments of the Nyong and Sanaga cover the boundary zone between the southernmost part of the belt represented by a regional E–W external nappe, thrust southward onto the stable Archean (2.900–3.000 Ma) Congo craton and extending from Cameroon to the Central African Republic (CAR). The more internal domains of the Pan-African orogen are dominated by a large volume of magmas often spatially associated with major shear zones. The nappe in Cameroon includes the

neoproterozoic Yaoundé Group, which overthrusts both Congo craton and Nyong Group, and the assumed palaeo-proterozoic Bafia Group thrust onto the Yaoundé group to the north (Ball *et al.*, 1984; Nédelec *et al.*, 1993; Toteu *et al.*, 2004). In the more internal domain of the Pan-African orogen, the large-scale Adamaoua shear zone is a corridor of high strain rocks that extends across Central Cameroon in a NE–SW direction (Dumont, 1986; Ngako *et al.*, 2003). To the south, the Sanaga shear zone extends without discontinuity from the Gulf of Guinea in southwestern Cameroon to Central Sudan. From recent studies (Kankeu and Greiling, 2006) it is suggested that the Sanaga shear zone represents a transitional zone between the marginal orogenic, low-angle fold and thrust belt with general compression, and an internal belt dominated by high angle faults and transpressions. As important part of the Pan-African evolution, these structures also influenced the subsequent processes of formation. Large-scale reactivation led to the formation of Mesozoic-Cenozoic rifts and basins, which reach from Central Cameroon (Cretaceous Djerem and Mbéré) towards the NE rift basins of the Sudan (Ngangom, 1983; Dumont, 1986; Giraud *et al.*, 2005). Furthermore, recent earthquakes appear to be spatially related to the pre-existing Pan-African shear zones, which may thus be in a state of continuing reactivation.

While more northern regions (Nyong and Sanaga catchments) experience tropical climate with monsoonal rainfalls during boreal summer, the southern study region is marked by equatorial (“Guinean”) climate with two dry and wet seasons (short and long rainy/dry season) in consequence of the seasonal migration of the ITCZ and emerging African monsoon. Rainfall varies between 3.000 mm across the Atlantic coast (Gulf of Guinea) and 1.500 mm towards the eastern to south-eastern country border (Yokadouma, 1.607 mm; Moloundou, 1.455 mm; cf. Olivry, 1986), including several specific regional climatic types (cf. Tsalefac, 2006). This has favoured the development of perennial meandering to anabranching fluvial systems in densely forested environments. The upper catchment areas of the Nyong and Sanaga mark the recent rain forest-savanna border. Accordingly, floodplains and alluvial ridges are seasonally flooded and subsequently reshaped and reorganized by frequent avulsions and additional fluvial-morphological processes.

The slightly undulated peneplain is characterized by narrow floodplains with primarily less valuable proxy data archives, i.e. sandy sediments with multiple stratigraphy-shifts. However, by detailed survey of small-scale fluvial forms using LANDSAT scenes, abandoned channels were identified which are cut off from defined structural river networks. The sediments of these up-silted channels are nearly lacustrine. The combination of ‘demi-oranges’ and ‘bas-fonds’ with polyconvex inselbergs and wide, partly hydromorphic floodplains are characterized by thick sediments which allow conclusions on their fluvial-morphologic evolution and the palaeoclimate in the region (Eisenberg, 2009).

9.1.3 Methods

In approach to fieldwork campaigns, satellite imagery (LANDSAT ETM+, ASTER) and DEM (Digital Elevation Model by SRTM) were extensively evaluated to locate suitable sampling sites. According to physio-geographical parameters like relief, hydrology, soils and vegetation, geomorphological forms were differentiated which allow a simplified identification of sediment archives (Eisenberg, 2009). During physio-geographical, geomorphological and sedimentological as well as geological oriented fieldwork, closer survey, observation and sampling was realized across several alluvial ridges of the Sanaga (Dizangué/Lac Ossa, Monatélé, Mbargue, Bélabo, Sakoudi) and Nyong

(Abong Mbang, Ayos, Akonolinga, Mengba) Rivers. In the vicinity of Akonolinga and Ayos extended fieldwork was carried out in the floodplain of the Nyong River with colleagues from the *Departement de Géographie de l'Université Yaoundé I* (M. Tchindjang) and B. Kankeu from MINRESI/IRGM, who provided geological expertise and analysis. In the upper catchment area of the Boumba River two sites near Mankako and Ouesso and near Mokounounou (Moloundou) an abandoned meander loop of the Ngoko River were sampled. In total, 63 hand-corings up to 550 cm depth and 3 exposure sites (pits) yielded sandy to clayey alluvial sediments containing supplemental sediment archives with valuable proxy data on past fluvial, ecological and environmental conditions. The sediments were sampled with EIJKELKAMP EDELMAN-corer in 20 cm layers. At some locations, a thin percussion-probe (3 cm diameter, 50 cm length) was used when ground water level was reached and recovery with EDELMAN-corer was not possible. The sampling of these undisturbed sediment cores additionally allowed a more detailed sediment-stratigraphic analysis.

After texture and soil colour were determined in the field, the samples were analysed at the laboratory of the Institute of Physical Geography in Frankfurt. Here pH (solved in 0,1 n KCl, after Meiwes *et al.*, 1984), grain sizes (after Köhn; DIN 19683, 1973), soil colour (wet and dry, Munsell Color Charts), organic material (OM) and carbon (C_{tot}) contents (with LECO EC-12), nitrogen (N_{tot} , after Kjeldahl; DIN ISO 10694, 1996) and dithionite (Fe_d) as well as oxalate solvable quantum of iron (Fe_o) and manganese (after Mehra and Jackson, 1960; with AAS Perkin Elmer Analyst 300) were determined. During coring, macro-rests and organic sediment from sedimentary units, fossil organic horizons and palaeosurfaces were collected for ^{14}C (AMS) radiocarbon dating and determination of stable carbon isotopic composition values ($\delta^{13}C$). These data provide preliminary (maximum) ages of the alluvial sediments as well as conclusions on former vegetation composition (C_3/C_4 species; cf. Schwartz, 1991; Giresse *et al.*, 1994; Runge, 2002). In total 32 samples from different locations and depths were extracted and analysed by the “*Centro di DATazione e Diagnostica (CEDAD)*” of Salento University in Lecce, Italy. From geological rock samples thin-sections were prepared for microscopic analysis. GPS data was recorded and integrated into an ArcGIS-project database.

9.2 RESULTS

9.2.1 Bélabo and Sakoudi region, upper Sanaga catchment

The Sanaga is Cameroon's major river with a catchment area of about 133.000 km² and a length of 976 km. From their source on the *surface de Meiganga* (Cretaceous, Post-Gondwana; Segalen, 1967) at 1.050 m asl the major tributaries Djerem and Lom, draining the Adamaoua-Plateau (*surface supérieure*; Segalen, 1967), unify near the village of Goyoum (15°12'N, 13°22'E; 640 m asl) to continue as the Sanaga River which flows south-westwards. On the *surface intérieure* it changes its flow direction to the west along the Pan-African Sanaga shear zone (Dumont, 1986). The drainage network is characterized by the Pan-African structures of the heterogeneous, generally crystalline granitiferous micaschists and gneisses of the Yaoundé Group (Nédelec *et al.*, 1986; Nzenti *et al.*, 1988). The existence of recent tectonic movements along the Sanaga shear zone is shown by the present seismicity with recent earthquakes epicentres along the zone, which may thus be in a state of continuing reactivation. These include the 1986 Garoua Boulai earthquake and the 2005 Monatélé earthquake (Nangue, 2007). The latter was widely felt in Central Cameroon and was perceptible at distances up to

150 km from the instrumental epicentre. Beneath the structural oriented river course the Sanaga shows partially a sinuous, slightly meandering river system and regularly splits up its main channel into a braided to anabranching, multi-channel pattern, which is divided by sandy, vegetated islands. Such fan-like fluvial physiognomies can easily be detected around B elabo (Figure 2) and Monat el e, where also the rain forest-savanna border stretches approximately N of the course of the Sanaga River. South of Goyoum, near the village of Sakoudi, a small tributary of the Sanaga, separated from the main stream by a distinctive sandy levee, was sampled in swampy environment. Fine-grained, sandy to clayey sediments at the base (215–200 cm) are covered by sandy alluvial sediments and lithofacies (90% sand with up to 15–30% coarse sand and 20–40% medium sand fractions; Figure 3). The profile shows a coarsening-upward sequence until 100 cm depth and then a fining upward sequence towards the top (70–80% fine-grained sediments, with up to 30% clay). Macro-rests from 213 cm depth gave a ^{14}C -age of 3.894 ± 50 yrs. BP and a $\delta^{13}\text{C}$ of $-29,2 \pm 0,2\text{‰}$ (Figure 4). Here, high organic material (2,40%) content and low pH (3,70) were measured.

Near the city of B elabo ($4^{\circ}55'\text{N}$, $13^{\circ}17'\text{E}$; 623 m asl) a ~350 m long transect was laid through an area where an abandoned (cut-off) channel on a large island between two Sanaga channels was identified prior to the fieldwork campaign. The transect consists of 4 hand-corings (C12–15) and one exposure site on the S-bench of the Sanaga (Figure 4).

While on the S (exposure-site and C15) and N-bench (C14) predominantly sandy to silty alluvial sediments (20–40% fine-grained sand, 30–40% silt and 25–30% clay) were sampled, towards the middle of the island and the location of the abandoned channel more fine-grained sediments were discovered. In C13 the alluvial sediments show up to 95% fine-grained textures (30–70% clay).

The contents of total carbon and OM are high in the lower layers of C15 and C14 (1,05–3%) and very low in C12 and C13 (around 0,20%). Also pH-values are slightly

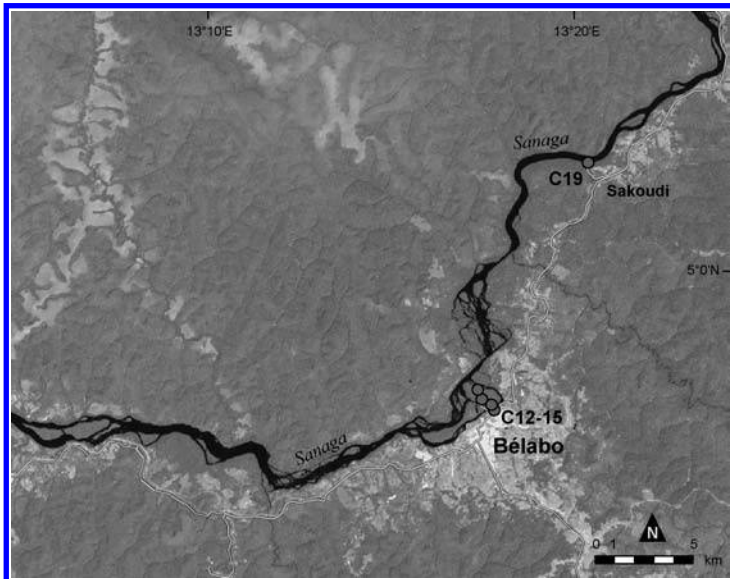


Figure 2. Map of the B elabo research area based on LANDSAT-ETM+ satellite images, showing the reconnaissance routes, coring sites and major settlements/villages.

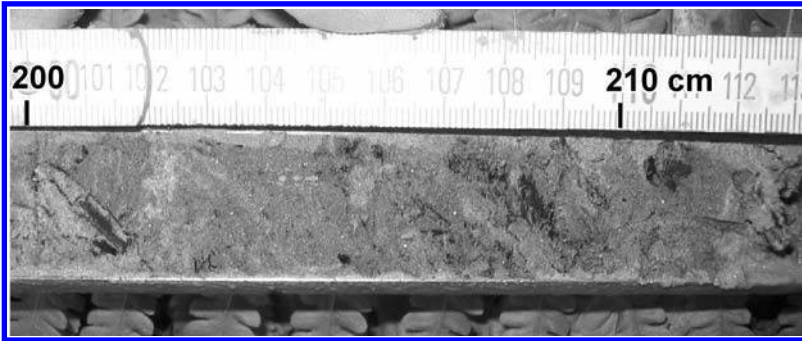


Figure 3. Sandy organic alluvial sediments and macro-rests found at the base of core C19 (5°2'N, 13°20'E) at the location Sakoudi, yielding a ¹⁴C-age of 3.894 ± 50 yrs. BP (photo: M. Sangen 2007).

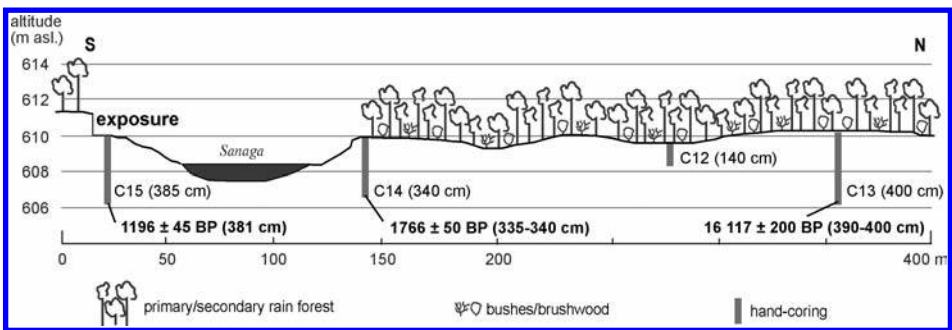


Figure 4. Transect with hand-corings carried out near Bélabo and corresponding ¹⁴C-data.

higher in the profiles located on the island (4,5–5 as opposed to 3,5–4). ¹⁴C-data from macro-rests found in C15 and C14 give relative young ages (C15, 381 cm: 1.196 ± 45 yrs. BP and C14, 335–340 cm: 1.766 ± 50 yrs. BP), whereas organic sediment from C13 (390–400 cm) gave a surprisingly old age of 16.117 ± 200 yrs. BP (Figure 6). The appending isotopic composition values indicate rain forest (C₃) dominated vegetation (–23,6 and –24,3‰), whereas unfortunately the δ¹³C-value for C13 was not provided.

9.2.2 Akonolinga and Ayos region, upper Nyong catchment

The upper Nyong catchment is characterized by broad (~1–3 km), swampy and regularly inundated valleys with swampy vegetation draining the tertiary peneplain surface “Plateau sud-Camerounaise” in 600–700 m asl (Africaine I, Segalen, 1967). The Yaoundé Group forms the basement rock of the middle and upper catchments of the Nyong and Sanaga Rivers. The lithology comprises of low-grade Mbalmayo schist, interpreted as the sole of the nappe (Nédelec *et al.*, 1986), the medium-grade micaschists and the Yaoundé high-grade gneisses. From previous geochemical studies, the meta-sediments of the Yaoundé region were interpreted as a shallow water greywacke and shale sequence deposited in an extensional environment related to the Congo craton (Nzenti *et al.*, 1988). Alternative interpretations suggest that the Yaoundé Group

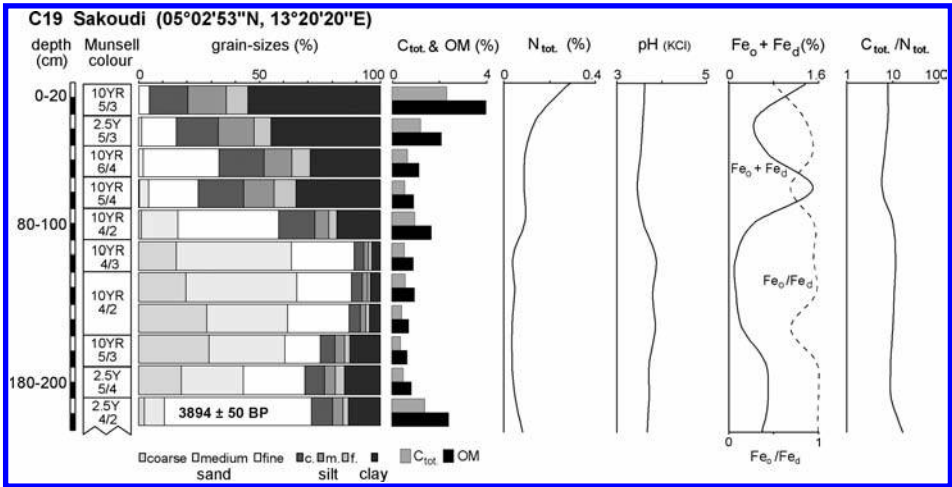


Figure 5. Sediment characteristics of core C19 across the Sanaga near Sakoudi with increasingly coarse-grained sandy sediments from around 3,8 ka BP.

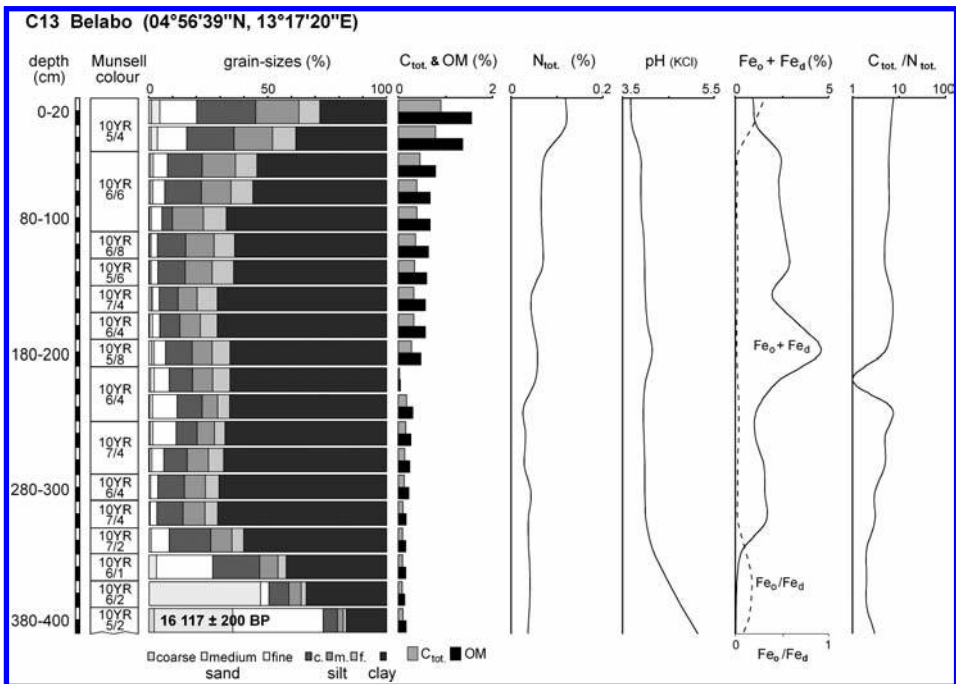


Figure 6. Sediment characteristics of alluvia found in C13. Coarse sandy sediments are covered by fine-grained clayey overbank sediments (fining upward sequence) and topped by a coarsening upward profile above 100 cm.

is an allochthonous unit emplaced onto the Congo craton (Penaye *et al.*, 1993; Toteu *et al.*, 2001). The basement rock is made up of the medium grade micaschists of the Yaoundé Group thrust onto the Congo craton. Continuing reactivation of pre-existing Pan-African structures associated with the geophysical northern margin of the Congo craton is shown by spatially related recent earthquakes. Between Ayos and Akonolinga, the Nyong has developed a slight meandering river course in wide valleys covered by aquatic grasses, bushes and trees (e.g. *Uapaca paludosa*, *Uapaca guineensis*, *Uapaca heudelotti*, *Iringia grandifolia*, *Detarium macrocarpum*, *Duboscia viridiflora*, *Wildemaniodoxa laurentii*, *Garcinia spp.*, *Raphia hookeri*, *Halopegia azurea*, *Caloncoba brevipe*, *Echinochloa purpurea*) and herbaceous vegetation (e.g. *Festuca arundinacea*, *Halopegia azurea*, *Caloncoba brevipe*). The landscape physiognomy is identical at both locations and inclination between Ayos and Akonolinga is extremely low with 0,05‰. The river system has created a sinuous to meandering pattern (sinuosity is 1,4 between Ayos and the confluence with the Mfoumou River downstream Akonolinga). At Ayos the catchment surface of the Nyong amounts 5.300 km² and at Akonolinga 8.350 km². This area lies in the transitional zone between tropical and equatorial climate. Mean annual precipitation values around 1.600 mm and mean annual discharge 90 m³/s.

Near Akonolinga, a transect was laid through the seasonally inundated floodplain, stretching some 1.500 m (Figure 7). The transect contains 10 hand-corings (C23–C26, C28 and NY11–13, NY16–17) and an exposure-site on the S-bench of the Nyong. Laboratory analysis of sediments from cores C23, 26 and 28 document generally low (<1%) total carbon and OM content at the bottom of the deposits, except for the base (420–400 cm) of core C28, where it is slightly higher (OM: 1,71%). With the exception of basal deposits in cores C23 and C26 (420–400 cm: 4,10 and 220–200 cm: 4,02), no pH exceeding 4 has been determined in the samples. Sediment textures are sandy (5–15% coarse sand and 5–38% medium sand) at the base (420–380 cm) of C23, which was sampled at the foot of a slope where cacao (*Theobroma cacao*) was cultivated under secondary rain forest. The location of C23, around 1.400 m from the recent river channel, marks the transition from forest into the open vegetation (reed, grasses) across the Nyong's floodplain, here associated with bushes and isolated small trees. From 380–280 cm depth, the profile's textures show fining upward sequences with clay reaching 70–80% and silt around 15%. From 280 to 180 cm depth, sandy (5–35%) and silty (15–35%) sediment textures increase, whereas clay reduces to 38%. Towards the top, clayey textures dominate (up to 64%), with decreasing silty and less variable sandy fractions. Groundwater level was found in around 90 cm and ferralitic sediments complicated coring from 400 cm onward. Leaf fragments were found in 420–400 cm depth during preparation of the samples for laboratory analysis. Clayey organic sediments sampled during fieldwork in 160–150 cm yielded a ¹⁴C-age of 28.358 ± 300 yrs. BP and corresponding δ¹³C-value –20,1‰ (Figure 8).

Some 100–150 m further N, towards the recent river bench, C28 was sampled close to a small gallery forest, which stretches E to W along the small periodical rivulet Tetar (tributary of the Nyong). The coring reached 470 cm, whereas sediments until 420 cm were sampled. Here samples were also taken by the *Département de Géographie of Université de Yaoundé I* under supervision of M. Tchindjang. Groundwater level was found in 280 cm depth and a clayey, fossil organic sediment layer between 420–360 cm. Sediments from the base to 340 cm are sandy (up to 50%) to clayey (40%), with very low silt content (6–7%). The profile then shows a fining-upward sequence with high clayey (up to 87%) and increasing silty (up to 20%) fractions. In 420–400 cm total carbon (0,99%) and OM content (1,71%) are relatively enhanced compared to the rest of the profile (decreasing rapidly to 0,31% in 180 cm and then slightly increasing towards the top). Maxima were found in 20–0 cm (7,71%) and 40–20 cm (1,95%). pH fluctuates

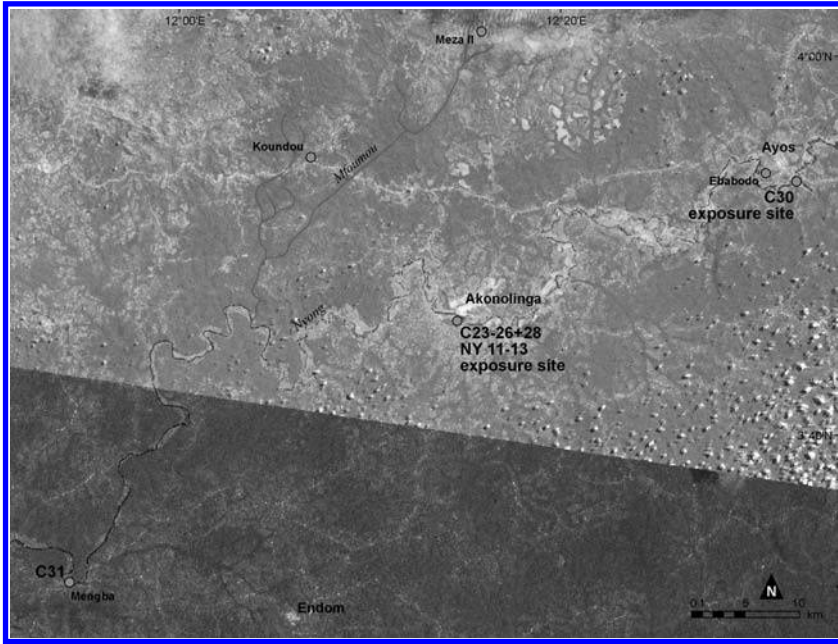


Figure 7. Map (LANDSAT ETM+) of the upper Nyong study area in the vicinity of Akonolinga and Ayos, showing channel physiognomy and coring sites.

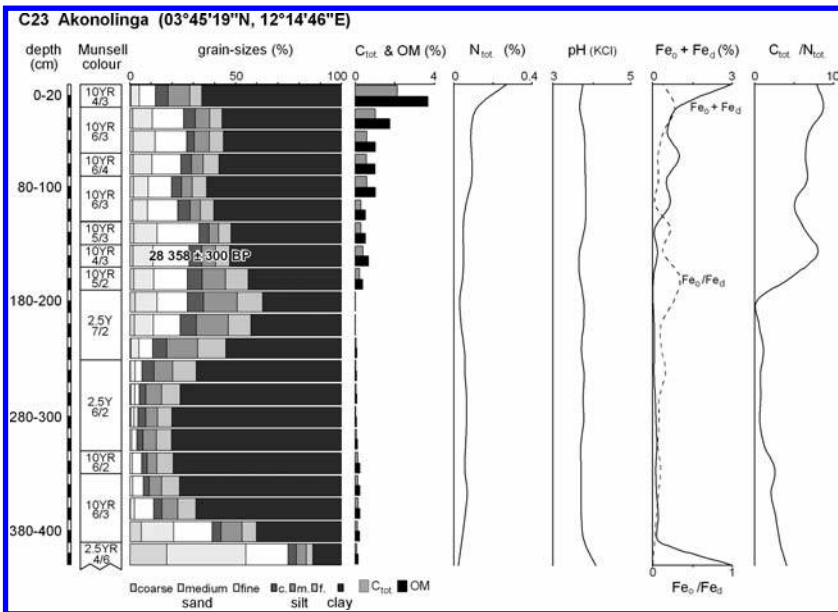


Figure 8. Sedimentological and pedological characteristics of alluvial sediments found in C23 of the Akonolinga transect. Coarse-grained sandy Pleistocene-age sediments are covered by fine-grained clayey to silty sediments in a fining upward profile interrupted by a slight coarsening upward between 240–140 cm depth.

between 3,45 and 3,78. Macro-rests sampled from 420–400 cm yielded a ^{14}C -age of 42.940 ± 1.500 yrs. BP and a corresponding $\delta^{13}\text{C}$ -value of $-19,6\text{‰}$. Three further hand-corings (C24, 360 cm depth; C25, 300 cm and C26, 220 cm) confirmed the previous findings. Sandy sediments near the bases were again covered by very clayey and sometimes silty fine-grained sediments, although no dateable organic sediments were found. Finally an exposure site on the S-bench of the Nyong River was carefully examined. Here alternating sandy and clayey, organic layers were found. Organic macro-rests from the deepest organic sediment layer were dated to a ^{14}C -age of 902 ± 45 yrs. BP with a corresponding $\delta^{13}\text{C}$ -value of $-24,2\text{‰}$.

In 2008, fieldwork around Akonolinga concentrated on sampling sediments from the rivulet Tetar, which only during the rainy season periodically drains the floodplain. Three cores (NY11–13, see Figure 7) yielded very clayey laminated sediments underlain by sandy to silty deposits from ~4–2 m depth. Coarse basal (sandy) sediments gave a maximum ^{14}C -age of 31.904 ± 300 yrs. BP ($\delta^{13}\text{C}$: $-33,5 \pm 0,4\text{‰}$) in 380 cm depth and fine-grained clayey deposits a minimal ^{14}C -age of 18.858 ± 100 yrs. BP ($\delta^{13}\text{C}$: $-18,1 \pm 0,2\text{‰}$) in 180 cm depth (transition layer sandy/clayey sediments, Figure 9).

Additional corings across the Mfoumou River, a tributary which drains into the Nyong west of Akonolinga from the north-east, uncovered palaeoenvironmentally invaluable sandy sediments without dateable material. The Mfoumou River drains a recently by savanna islands covered undulated landscape with inselbergs. From geomorphological and pedological studies at this site, additional information on the genesis and persistence of savanna habitats inside forested areas and the rain forest-savanna dynamics over time in general could be obtained. The study of Tchomga (1996) concluded that savannas in the Mfoumou region are of palaeoclimatic origin. This is further confirmed by field evidence of the river Nyong sediments (silt with micaceous paillets and without galets) which testifies the palaeoclimatic origin of savannas. At Meza II however, the topographic sequence presents conglomeratic hardpans with a

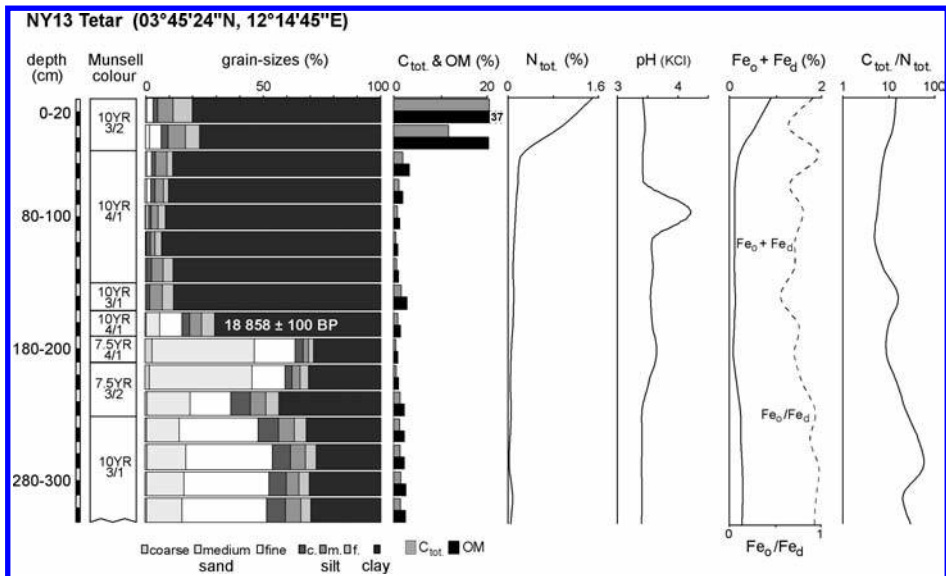


Figure 9. Sediment characteristics of alluvial sediments found in the Tetar rivulet (NY13). Coarse-grained sandy (Pleistocene-age) sediments are covered by fine-grained clayey sediments above 180 cm depth.

conserved lithostructure which built up from the base rock in place and which retook granules and grains of quartz that ascertains neo-formation. Quartz granules result from a quartz reef of N 51°E orientation. According to this effect the edaphic origin of savanna can be confirmed. This was further sustained by anthropogenic actions thus effectively justifying the name of the village Koudou which means savanna. Furthermore the hills of the area are characterized by savanna on the summits and forest at the slopes. This process seems to have been facilitated by bush fires which have greatly contributed to the destruction of the initial vegetation from 3,000 BP to the present (charcoal collected at the banks of river Nyong). Terraces at the banks of river Nyong can be linked to this destruction. Today forest is re-conquering its lost space. However, the confusion generated by annual pluviometric totals leads Tchomga (1996) to the conclusion that the savanna was of palaeoclimatic origin without considering the monthly distribution of precipitation.

Near Ayos, an abandoned channel and an exposure site across the N-bench of the Nyong were sampled. Alluvial sediments at this site indicate relative younger deposition ages. Macro-rests from the base (280 cm) of an abandoned channel (C30) yielded a ^{14}C -age of 724 ± 45 yrs. BP with corresponding $\delta^{13}\text{C}$ -value $-25,8\text{‰}$. The whole profile consists of very clayey, organic deposits with abundant macro-rests. Values for total carbon and OM content vary between 2,09 to 23,58% and 3,60 to 40,65%, respectively, with highest values close to the base. pH fluctuates between 3,73 and 4,36 and is higher in the deeper layers. Identical deposits were found in additional periodical anabranches across the Nyong floodplain at Ayos and Ebabodo (Figure 7). Also here the sandy basal sediment layers yielded ^{14}C -ages around 700 years BP. The exposure site, which revealed mixed layers of sandy and organic, clay-rich deposits, indicates shifting depositional processes and discharge episodes. A clayey fine-grained strata-layer in 180 cm was dated to a ^{14}C -age of 1.508 ± 50 yrs. BP (corresponding $\delta^{13}\text{C}$ -value: $-18,0\text{‰}$).

Alongside the external limits of the floodplain at Akonolinga and Ayos locally laterit crust crops out of neighbouring slopes and outer levees. Outcrops of basement rocks are scarce and when available deeply weathered. Geologically, the region is part of the Neoproterozoic Yaoundé nappe, overlying the Archean Congo craton since the Pan-African orogeny (Nedelec *et al.*, 1986). South of Ayos a medium grade micaschist basement rock of the Yaoundé Group showing heavy weathering was geologically studied and sampled. The two main Pan-African shortening phases, D1 and D2 reported by pioneering workers in the Yaoundé Group (i.e. Ball *et al.*, 1984; Nedelec *et al.*, 1986; Nzenti *et al.*, 1988) were identified.

Finally further fieldwork across the upper Nyong catchment was carried out near Edjom to the SW of Akonolinga. Core C31 ($03^{\circ}31'56''\text{N}$, $11^{\circ}53'51''\text{E}$; 280 cm) was sampled in the Nyong floodplain near Mengba. At this location very dark (10YR 2/1), sandy (60–80% fS) deposits are covered by brownish-greyish (10YR 5/2, 6/2) fine-grained, clayey (70–80%) sediments, which rapidly increase from 220–200 cm and yielded relative low values for C_{tot} (<1%), OM (<2%), N_{tot} (<0,2%), pH (~3,5) and C/N (<10). Iron content increases from around 0,2 to 3% in 80–60 cm. Lower (base, 280–260 cm) and upper (220–200 cm) limit of the sandy sedimentary unit were dated to ^{14}C -ages of 13.357 ± 60 BP ($\delta^{13}\text{C}$ not diagnosable) and 11.107 ± 90 yrs. BP ($\delta^{13}\text{C}$: $-28,9 \pm 0,1\text{‰}$).

9.2.3 Mankako and Ouesso region, upper Boumba catchment

Between Lomié ($3^{\circ}10'\text{N}$, $13^{\circ}37'\text{E}$; 640 m asl) and Yokadouma ($3^{\circ}31'\text{N}$, $15^{\circ}06'\text{E}$; 640 m asl), two sites across the upper Boumba River were sampled. Here the Boumba drains the SE towards the Sangha River and Congo basin orientated peneplain of the

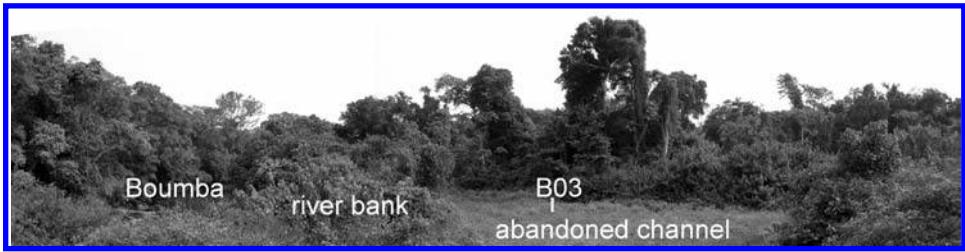


Figure 10. Sampling location near Mankako (photo: M. Sangen 2008).

“Plateau Sud-Camerounaise” in altitudes around 500–600 m asl (Africaine I, Segalen, 1967). Basement rocks are composed of the Yaoundé Group in the NW and the Palaeozoic *Groupe de Mangbaï* in the SE. Climate is tropical to equatorial and to the E and SE increasingly continental with precipitation decreasing from 1.643 (Lomié) to 1607 (Yokadouma) and 1.485 mm (Moloundou, 2°03'N, 15°13'E; 500 m asl). Mean annual discharges (1966–1981) at Biwala (3°09'N, 14°57'E; 485 m asl; catchment area: 10.340 km²), 180 (Mankako) and 90 km (Ouesso) downstream, averaged 104 m³/s. Physio-geographic settings are highly comparable to the upper Nyong and Ntem catchments.

At Ouesso (03°24'N, 14°32'E), a seasonally inundated river bench some 10 m from the river channel (dry season) was sampled. In core B02 (376 cm) dark (10YR 3/2, 4/1 and (4/2) sandy (47–73% fS, 15–31% mS) sediments from 376–300 cm with elevated C_{tot} (0,60–2,28%), OM (1,03–4,97%) and N_{tot} (0,045–0,176%) contents and C/N-values (10–16) as well as pH (4,4–4,7) are covered by fine-grained textures with abruptly increasing clayey and silty (~50% clay and ~30% silt) textures. These are overlain by a sandy coarsening-upward sequence from 120 cm. C_{tot} (0,30–0,40%), OM (0,50–0,80%), N_{tot} (0,070–0,090%) and C/N (3–6) decreases, while pH initially shows increasing tendency (4,9) before dropping to 4,1. The brighter fine-grained deposits (10YR 6/4 and 7/1) yielded maximum iron contents (2,2–3,4%) with 90% Fe_d , indicating sophisticated pedogenesis. Sandy, organic sediment from 376–360 cm depth was dated (¹⁴C-AMS) to 2.728 ± 60 yrs. BP ($\delta^{13}C$: -35,5 ± 0,2‰).

Near Mankako (3°18'N, 14°04'E), B03 (320 cm) was sampled in an abandoned, seasonally flooded branch, which is separated from the main channel by a marked river bank.

Also at this location from the base (320–280 cm) dark (10YR 3/1) sandy (65–75% fS) textures with increased C_{tot} (0,66–0,93%), OM (1,14–1,60%), N_{tot} (0,027–0,046%) contents and high C/N (20–25) were found. In a distinct fining-upward sequence (20–46% clay), pH falls from 5,5 to 4,1, while iron content generally increases (0,11–3,4%). These brighter (10YR 5/4, 5/6, 6/1) deposits show reduced analytic values (C_{tot} : 0,08–0,56%; OM: 0,14–0,97%; N_{tot} : 0,029–0,101% and C/N: 2–7) and maxima of iron in 220–200 and 160–140 cm (10YR 5/8). High Fe_d (>90%) repeatedly indicates an advanced age of the deposits. This was confirmed by a ¹⁴C-age of >45.000 yrs. BP ($\delta^{13}C$: -29,6 ± 0,1‰) for basal sandy sediment.

9.2.4 Mokounounou region, upper Ngoko catchment

The Ngoko catchment (76,000 km²) includes the catchment areas of the Boumba (27,400 km²) and Dja River (38,600 km²). Major geologic formations are the *Ntem Complex* and the *Dja Series* in the W, the *Groupe de Yaoundé* in the N and the *Groupe*

de Mangbaï in the SE. Boumba and Dja join near Moloundou (2°03'N, 15°13'E; 500 m asl) to continue as Ngoko River. From 1989–1992 discharge averaged 687 m³/s. To the SE of Moloundou, an abandoned meander loop of the Ngoko was intensely investigated and sampled. In this abandoned meander the Lake Mokounounou has developed. Three corings on the inlet and outlet of the former meander loop were carried out to acquire information on the fluvial-morphological evolution of this river section.

Across the inlet, cores N02 (393 cm), 03 (400 cm) and 05 (470 cm) were collected. At these sites, all located within the former, seasonally flooded meander channel, sandy deposits were found at the base of the corings. They are covered by fining-upward sequences with successively increasing (5–70%) clayey and silty (10–40%) textures. Within and above the sandy units, dark (10YR 3/2) organic layers with high macro-rest content (leaf and wood fragments) occur. C_{tot.} reaches values around 2%, OM ~6%, N_{tot.} 0.2% and pH fluctuates around 4. Iron content is very high (~5%) and even reaches 16% in N05 (440–420 cm; 86% Fe_d). Macro-rests from the basal sandy units yielded ¹⁴C-ages of 1.041 ± 45 (N02, 393 cm; δ¹³C: -28,4 ± 0,2‰) and 1.228 ± 35 years BP (N05, 470 cm; δ¹³C: -28,1 ± 0,3‰).

Sediments from the sealed outlet of the abandoned meander are distinctly finer (50–60% clay, 30–40% silt) and more consistently sorted/bedded. Dark (10YR 3/1, 3/2 and 4/1), high organic (C_{tot.}: 2–6%, OM: 4–12%, N_{tot.}: 0,25–0,5%) sediments containing macro-rests and vivianite, are covered by more brighter and reddish coloured deposits with decreasing contents. While pH fluctuates around 4 and C/N-values around 20, iron content reaches 2,5–3%. The palustrine to lacustrine deposits indicate temporarily swampy and stillwater conditions. The sediments, which are highly suitable for palynological studies, yielded minimum ¹⁴C-ages of 892 ± 40 (N04, 470–460 cm; δ¹³C: -26,0 ± 0,3‰) and 938 ± 45 years BP (N01, 550–540 cm; δ¹³C: -28,0 ± 0,2‰).

9.3 INTERPRETATION AND DISCUSSION

The detected coarse sandy layers in the Nyong floodplain near Akonolinga, with high ages at the bases of several hand-corings (C23, C28 and NY11), indicate braiding and sand-transporting fluvial systems of the proto-Nyong, which prevailed since the *Maluëkien* and through the *Njilien* (OIS 3, ~50–27 ka BP), Last Glacial Maximum (LGM, OIS 2) until the Pleistocene/Holocene transition. This is evidenced by a coarse sandy sediment unit in the deepest layers of the corings, which is overlying basement (schists of the Yaoundé Series) and ferralitic crusts. The findings of this coring transect manifest phases of increased aggradation and fluvial activity between 43 and 32 ka BP. This is consistent with insolation maxima (Berger and Loutre, 1991) in tropical regions (0–15°N) and enhanced monsoon intensity as well as fresh-water input to the Gulf of Guinea (Weldeab *et al.*, 2007). Discharge pulses presumably occurred during warming events over Antarctica (Blunier *et al.*, 1998; Blunier and Brook, 2001; Jouzel *et al.*, 2007) and asynchronous warming events during major Dansgaard-Oeschger cycles on the northern hemisphere (NGRIP Members 2004). Additional evidence for enhanced fluvial-morphological activity during this Late Pleistocene phase has been gathered from the Boumba catchment (Mankako) and the interior delta of the Ntem (Abong and Meyo Ntem; cf. Sangen, 2008, 2009). The overlying fine-grained (mostly clayey) overbank sediments (fining-upward sequences) represent more stable conditions in probably densely vegetated gallery-forest habitats. These have been deposited after the more arid and less active phase of the LGM (*Léopoldvillien*) and the turbulent Pleistocene/Holocene transition. Nevertheless, at Mengba and around Bélabo in

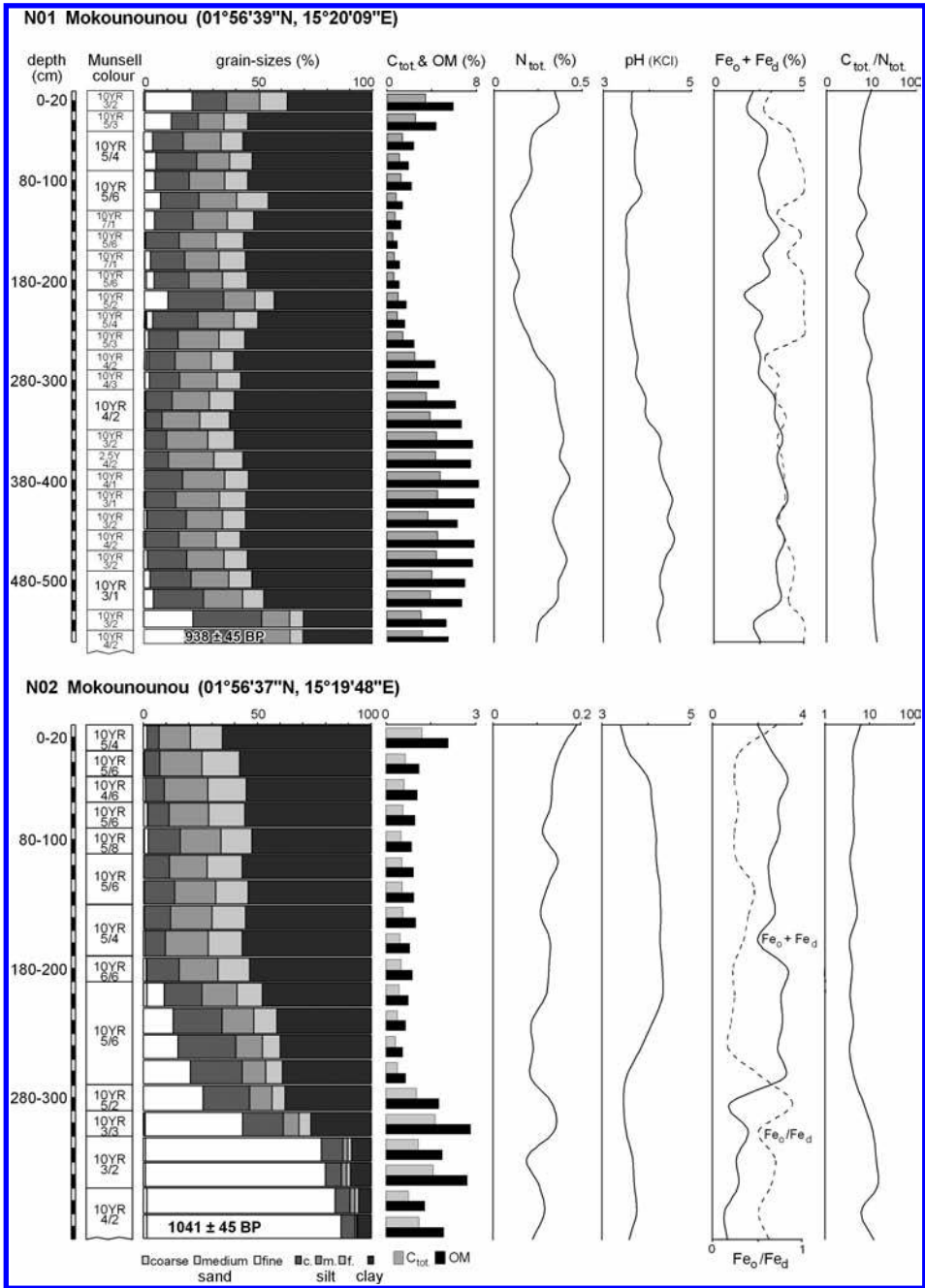


Figure 11. Coring profiles from the abandoned meander loop at Mokounounou. The upper profile was taken from the outlet and the lower profile from the inlet section.

the upper Sanaga catchment, this transition stage is archived as additional turbulent fluvial-morphological phase with coarse sandy deposits. In combination with in the course of the LGM largely fragmented landscape and vegetation units, especially close to the recent rain forest-savanna border, rapidly increasing humidity might have caused extensive reorganizations (channel migrations, cut and fill sequences) across the investigated river sections. The sedimentary record and ^{14}C -data indicate a most turbulent episode between around 16–14 ka BP, conform to earlier findings from the Congo and Niger Rivers (e.g. Marret *et al.*, 2001; Lézine *et al.*, 2005).

The Early and Middle Holocene have not been recorded by ^{14}C -analysis in the deposits of the upper Nyong and Sanaga as well as Boumba and Ngoko Rivers. However, this period is represented by thick (2–4 m) loamy to clayey sediment units across several coring sites. In correlation with numerous earlier results (e.g. Elenga *et al.*, 2004; Gasse *et al.*, 2008 and references therein), the sedimentary record substantiates an increasing stable episode with deposition and shaping of recent floodplain physiognomy. Enhanced humidity (maximum during African Humid Period from 9–4 ka BP, DeMenocal *et al.*, 2000) and maximum rain forest expansion (Maley, 2001) as well as seasonal climatic and hydrological conditions promoted the metamorphosis of braiding to anabranching into more sinuous and meandering fluvial systems. Seasonal flooding and overbank sedimentation generated stable (vegetated) river banks and alluvial ridges, which might only have been slightly modified during extreme events. Anyhow, towards the Late Holocene the alluvial record locally shows abrupt changes in sediment delivery. At Sakoudi, increasing coarse-grained sandy sediments indicate modified run-off and sedimentation dynamics (abrupt and rapidly increasing coarse sandy deposits). Comparable findings were also found at sites across the lower Nyong (B6, Donenda) and interior delta (C13 Meyos, L22 Nyabessan) as well as many undated sedimentary profiles, substantiating the assumption of a general supra-regional climatic trigger (Sangen, 2009). The period after 4 ka BP is known as including a pronounced environmental shift throughout tropical Africa and even South America (Vincens *et al.*, 1999; Marchant and Hooghiemstra, 2004; Marret *et al.*, 2006), with changing seasonality (longer dry season), recurring forest regression, savannization and decreasing landscape stability. The summation of these processes and modifications together with more irregular and unstable fluvial-morphological activity might be responsible for these marked shifts in the sedimentary record.

Another comparable striking shift is documented for the period around 2,8–2 ka BP, including the sites Ouesso (B02, Boumba), Njok (B01, Nyong) and Anguiridjang (L40) as well as Nyabessan (L18, L19) in the Ntem's interior delta (Sangen, 2008, 2009). At Nyabessan this environmental shift has been verified by palynological studies (cf. Ngomanda *et al.*, 2009). Finally, most recent perturbations of the Late Holocene can be postulated for the periods around 1,7–1 ka BP (C14 and 15, Bélabo; N01 and 05, Mokounounou), also registered across earlier study areas (L02 and 05, Meyo Ntem and L30, Tom, in the Ntem's interior delta; Sangen, 2008, 2009), and a phase around 0,7–0,4 ka BP. The latter is evident by several channel aggradations and abandonments in the Ayos study area (exposure site, C30, NY05) as well as additional texture shifts in alluvial archives across the Nyong (B05, Lipombe II) and interior delta (L18, Nyabessan; L24 Nnémepong; L27, Akom; L34 Nkongmeyos; cf. Sangen, 2008, 2009). These last oscillations seem to correlate with northern hemisphere climatic fluctuations of the Medieval Warm Period and the Little Ice Age (e.g. Mayewski *et al.*, 2004; Verschuren, 2004; Wanner *et al.*, 2008).

While Late Pleistocene oscillations of the climatic, hydrological and ecological systems correspond very well to Milankovitch-scale fluctuations and especially the precession cycle, Late Holocene climate changes seem to be triggered by much more

complex feedbacks and teleconnections. As possible triggers solar activity oscillations (Van Geel *et al.*, 1999), modified ocean circulation (Denton and Broecker, 2008), increased (tropical) volcanic activity (Wanner *et al.*, 2008) and enhanced ENSO amplitude (Rodbell *et al.*, 1999; Chang *et al.*, 2006) have been suggested. As a consequence, ITCZ position migration and seasonality changes occurred in the western African monsoon domain, which induced far-reaching environmental impacts. Nevertheless, our alluvial record most significantly documents Late Pleistocene to Early Holocene fluvial-morphological modifications. Concerning vegetation dynamics, our findings indicate that C₃-dominated ecosystems ($\delta^{13}\text{C}$ between -35 and -23‰) have prevailed across the fluvial systems, even during most cool and arid (e.g. LGM) episodes. This confirms the assumption of “fluvial rain forest refugees” (Colyn *et al.*, 1991; Maley, 2001). Only at sites located across the recent rain forest-savanna margin (e.g. B elabo, Akonolinga, Ayos and Mengba) more transitional vegetation communities ($\delta^{13}\text{C}$ around -20‰) persisted. To conclude, the Late Holocene findings on palaeoenvironmental conditions in the study area remain somewhat speculative and may be altered by increasing anthropogenic activity inside the tropical African rain forest domain since around 3 ka BP and especially with the adoption of metallurgy around 2.6 ka BP (Schwartz, 1992; Eggert *et al.*, 2006; H ohn *et al.*, 2008; Meister, 2008; Ngomanda *et al.*, 2009). Therefore, additional studies should follow, integrating new methods and technologies on the one hand and additional regions on the other.

ACKNOWLEDGEMENTS

We gratefully thank the German Research Association (DFG) for the funding of these studies and all colleagues involved in this research, especially colleagues from Cameroon. Also we thank our laboratory team for data analysis and Dr. G. Quarta from CEDAD for providing ^{14}C - and $\delta^{13}\text{C}$ -data. Particular we would like to thank all people from IRD (especially R. Oslisly), GTZ and MINRESI who were very helpful with information and services, which were most fundamental during a political crisis and riots in Cameroonian begin 2008. Last but not least we thank all friendly and helpful Cameroonian natives in the study areas, with whose dedication the fieldwork became a great success.

REFERENCES

- Abrantes, F., 2003, A 340,000 year continental climate record from tropical Africa—news from opal phytoliths from the equatorial Atlantic. *Earth and Planetary Science Letters*, **209** (1–2), pp. 165–179.
- Adegbie, A.T., Schneider, R.R., R ohl, U. and Wefer, G., 2003, Glacial millennial-scale fluctuations in Central African precipitation recorded in terrigenous sediment supply and freshwater signals offshore Cameroon. *Palaeogeography, Palaeoclimatology, Palaeoecology*, **197**, pp. 323–333.
- Ball, E., Bard, J.P. and Soba, D., 1984, Tectonique tangentielle dans la catazone Pan-africaine du Cameroun: les gneiss de Yaound e. *Journal of African Earth Sciences*, **2**, pp. 91–95.
- Barker, P.A., Talbot, M.R., Sreet-Perrott, F.A., Marret, F., Scourse, J. and Odada, E.O., 2004, Late Quaternary climate variability in Intertropical Africa. In *Past Climate Variability through Europe and Africa*, edited by Battarbee, R.W., Gasse, F. and Stickley, C.E., (Dordrecht: Springer), pp. 117–138.

- Berger, A. and Loutre, M.F., 1991, Insolation values for the climate of the last 10 million years. *Quaternary Science Reviews*, **10**, pp. 297–317.
- Blunier, T., Chappellaz, J., Schwander, J., Dällenbach, A., Stauffer, B., Stocker, T.F., Raynaud, D., Jouzel, J., Clausen, H.B., Hammer, C.U. and Johnsen, S.J., 1998, Asynchrony of Antarctic and Greenland climate change during the last glacial period. *Nature*, **394**, pp. 739–743.
- Blunier, T. and Brook, E.J., 2001, Timing of millennial-scale climate change in Antarctica and Greenland during the last glacial period. *Science*, **109**, pp. 109–112.
- Broccoli, A.J., Dahl, K.A. and Stouffer, R.J., 2006, Response of the ITCZ to Northern hemisphere cooling. *Geophysical Research Letters*, **33**, L01702, doi:10.1029/2005GL024546.
- Castaing, C., Feybesse, J.L., Thieblemont, D., Triboule, C. and Chevremont, P., 1994, Palaeogeographical reconstructions of the Pan-African/Brasiliano-orogen: closure of oceanic domain or intracontinental convergence between major blocks. *Precambrian Research*, **69**, pp. 327–344.
- Chang, P., Fang, Y., Saravanan, R., Ji, L. and Seidel, H., 2006, The cause of the fragile relationship between the Pacific El Niño and the Atlantic Niño. *Nature*, **443**, pp. 324–328.
- Chiang, J.C.H., Biasutti, M. and Battisti, D.S., 2003, Sensitivity of the Atlantic Inter-tropical Convergence Zone to last glacial maximum boundary conditions. *Palaeoceanography*, **18/4**, 1094, doi: 10.1029/2003PA000916.
- Colyn, M., Gauthier-Hion, A. and Verheyen, W., 1991, A re-appraisal of palaeoenvironmental history in Central Africa: evidence for a major fluvial refuge in the Zaïre basin. *Journal of Biogeography*, **18**, pp. 403–407.
- DeMenocal, P., Ortiz, J., Guilderson, T., Adkins, J., Sarnthein, M., Baker, L. and Yarusinsky, M., 2000, Abrupt onset and termination of the African Humid Period: rapid climate responses to gradual insolation forcing. *Quaternary Science Reviews*, **19**, pp. 347–361.
- Denton, G.H. and Broecker, W.S., 2008, Wobbly ocean conveyor circulation during the Holocene? *Quaternary Science Reviews*, **27**, pp. 1939–1950.
- De Ploey, J., 1964, Cartographie géomorphologique et morphogénese aux environs du Stanley-Pool (Congo). *Acta Geographica Lovaniensia*, **3**, pp. 431–441.
- De Ploey, J., 1965, Position géomorphologique, gènesè et chronologie de certains dépôts superficiels du Congo occidental. *Quaternaria*, **7**, pp. 131–154.
- DIN 19683, 1973, Bestimmung der Korngrößenzusammensetzung nach Vorbehandlung mit Natriumpyrophosphat, Teil 1 und 2. (Berlin: Beuth-Verlag).
- DIN 19684, 1977, Bodenuntersuchungsverfahren in landwirtschaftlichen Wasserbau, Chemische Laboruntersuchungen, Teil 2 (Berlin: Beuth-Verlag).
- DIN ISO 10694, 1996, Bodenbeschaffenheit—Bestimmung von organischem Kohlenstoff und Gesamtkohlenstoff nach trockener Verbrennung (Elementaranalyse), (Berlin: Beuth-Verlag).
- Dumont, J.F., 1986, Identification par télédétection de l'accident de la Sanaga (Cameroun). Sa position dans le contexte des grands accidents d'Afrique Centrale et de la limite nord du craton concolais. *Géodynamique*, **1**, pp. 13–19.
- Dupont, L.M., Jahns, S., Marret, F. and Ning, S., 2000, Vegetation changes in equatorial West Africa: time slices for the last 150 ka. *Palaeogeography, Palaeoclimatology, Palaeoecology*, **155**, pp. 95–122.
- Eggert, M.K.H., Höhn, A., Kahlheber, S., Meister, C., Neumann, K., and Schweizer, A., 2006, Pits, Graves and Grains: Archaeological and Archaeobotanical Research in Southern Cameroon. *Journal of African Archaeology*, **4**(2), pp. 273–298.

- Eisenberg, J., 2008, A palaeoecological approach to neotectonics: the geomorphic evolution of the Ntem River in and below its interior delta, SW Cameroon. *Palaeoecology of Africa*, **28**, pp. 259–272.
- Eisenberg, J., 2009, *Morphogenese der Flusseinzugsgebiete von Nyong und Ntem in Süd-Kamerun unter Berücksichtigung neotektonischer Vorgänge*. PhD-thesis, Goethe-University Frankfurt, pp. 1–219.
- Elena, H., Maley, J., Vincens, A. and Farrera, I., 2004, Palaeoenvironments, palaeoclimates and landscape development in Atlantic equatorial Africa: A review of key sites covering the last 25 kyrs. In *Past climate variability through Europe and Africa*, edited by Battarbee, R.W., Gasse, F. and Stickley, C.E., (Dordrecht: Springer), pp. 181–198.
- Gasse, F., Chalié, F., Vincens, A., Williams, M.A.J. and Williamson, D., 2008, Climatic patterns in equatorial and Southern Africa from 30,000 to 10,000 years ago reconstructed from terrestrial and near-shore proxy data. *Quaternary Science Reviews*, **27** (25–26), pp. 2316–2340.
- Gersonde, R., Crosta, X., Abelmann, A. and Armand, L., 2005, Sea-surface temperature and sea ice distribution of the Southern Ocean at the EPILOG Last Glacial Maximum—a circum-Antarctic view based on siliceous microfossil records. *Quaternary Science Reviews*, **24**, pp. 869–896.
- Guirand, R., Bosworth, W., Thierry, J. and Delplaque, A., 2005, Phanerozoic geological evolution of Northern and Central Africa: an overview. *Journal of African Earth Sciences*, **43**, pp. 83–143.
- Giresse, P., Mvoubou, M., Maley, J. and Ngomanda, A., 2008, Late-Holocene equatorial environments inferred from deposition processes, carbon isotopes of organic matter, and pollen in three shallow lakes of Gabon, west-central Africa. *Journal of Palaeolimnology*, doi: 10.1007/s10933-008-9231-5.
- Höhn, A., Kahlheber, S., Neumann, K. and Schweizer, A., 2008, Settling the rain forest: The environment of farming communities in Southern Cameroon during the First Millennium BC. *Palaeoecology of Africa*, **28**, pp. 29–41.
- Holtvoeth, J., Kolonic, S. and Wagner, T., 2005, Soil organic matter as an important contributor to late Quaternary sediments of the tropical West African continental margin. *Geochimica et Cosmochimica Acta*, **69**, pp. 2031–2041.
- Imbrie, J., Hays, J.D., Martinson, D.G., McIntyre, A., Mix, A.C., Morley, J.J., Pisias, N.G., Prell, W.L. and Shackleton, N.J., 1984, The orbital theory of Pleistocene climate: Support from a revised chronology of the marine $\delta^{18}\text{O}$ record. In *Milankovitch and Climate. Understanding the response to astronomical forcing*, edited by Berger, A., Imbrie, J., Hays, J., Kukla, G. and Saltzman, B. (NATO ASI Series, Series C: Mathematical and Physical Sciences), **126**, I, pp. 269–305.
- Jansen J.H.F. and Van Iperen, J.M., 1991, A 220 000-year climatic record for the east equatorial Atlantic Ocean and equatorial Africa: evidence from diatoms and opal phytoliths in the Zaire (Congo) deep-sea fan. *Palaeoceanography*, **6**, pp. 573–591.
- Jouzel, J., Masson-Delmotte, V., Cattani, O., Dreyfus, G., Falourd, S., Hoffmann, G., Minster, B., Nouet, J., Barnola, J.M., Chappellaz, J., Fischer, H., Gallet, J.C., Johnsen, S., Leuenberger, M., Loulergue, L., Luethi, D., Oerter, H., Parrenin, F., Raisbeck, G., Raynaud, D., Schilt, A., Schwander, J., Selmo, E., Souchez, R., Spahni, R., Stauffer, B., Steffensen, J.P., Stenni, B., Stocker, T.F., Tison, J.L., Werner, M. and Wolff, E.W., 2007, Orbital and millennial Antarctic climate variability over the past 800,000 years. *Science*, **317/5839**, pp. 793–797.
- Kadomura, H., 1995, Palaeoecological and palaeohydrological changes in the humid tropics during the last 20,000 years, with reference to Equatorial Africa. In *Global Continental Palaeohydrology*, edited by Gregory, K.J. and Starkel, L.V., (Chichester: Wiley and Sons), pp. 177–202.

- Kadomura, H., 2000, Late Holocene and historical forest degradation and savannization in Equatorial Africa. *Regensburger Geographische Schriften*, **33**, pp. 76–98.
- Kankeu, B., 2008, *Anisotropie de la Susceptibilité Magnétique (ASM) et fabriques des roches Néoprotérozoïques des régions de Garga-Sarali et Bétaré-Oya à l'Est Cameroun: implications géodynamiques pour l'évolution de la chaîne pan-africaine d'Afrique Centrale*. Thèse de doctorat, Université de Yaoundé I, Faculté des Sciences, Yaoundé, pp. 232.
- Kankeu, B. and Greling, R.O., 2006, Magnetic fabrics (AMS) and Transpression in the Neoproterozoic basement of eastern Cameroon (Garga-Sarali area). *Neues Jahrbuch für Geologie und Paläontologie*, **239**, pp. 263–287.
- Lespez, L., Rasse, M., le Drezen, Y., Tribolo, C., Huyssecom, E. and Ballouche, A., 2008, L'évolution hydrogéomorphologique de la vallée du Yamé (Pays Dogon, Mali): signal climatique et hydrosystème continental en Afrique de l'Ouest entre 50 et 4 ka. *Géomorphologie: relief, processus, environnement*, **3**, pp. 169–185.
- Lézine, A.-M. and Cazet, J.P., 2005, High-resolution pollen record from core KW31, Gulf of Guinea, documents the history of the lowland forests of West Equatorial Africa since 40,000 yr ago. *Quaternary Research*, **64**, pp. 432–443.
- Lézine, A.-M., Duplessy, J.C. and Cazet, J.P., 2005, West African monsoon variability during the last deglaciation and the Holocene: Evidence from fresh water algae, pollen and isotope data from core KW31, Gulf of Guinea. *Palaeogeography, Palaeoclimatology, Palaeoecology*, **219**, pp. 225–237.
- Maley, J., 2001, The Impact of Arid Phases on the African Rain Forest Through Geological History. In *African Rain Forest Ecology and Conservation*, edited by Weber, W., White, L., Vedder, A. and Naughton-Treves, L., (London: Yale University Press), pp. 68–87.
- Maley, J. and Brenac, P., 1998, Vegetation dynamics, Palaeoenvironments and Climatic changes in the Forests of West Cameroon during the last 28,000 years BP. *Review of Palaeobotany and Palynology*, **99**, pp. 157–187.
- Marchant, R. and Hooghiemstra, H., 2004, Rapid environmental change in African and South American tropics around 4000 years before present: a review. *Earth-Science Reviews*, **66**, pp. 217–260.
- Marret, F., Scourse, J.D., Jansen, F.J.H. and Schneider, R., 1999, Changements climatiques et paléocéanographiques en Afrique centrale atlantique au cours de la dernière déglaciation: contribution palynologique. *Comptes rendus de l'Académie des Sciences Serie II Fasc. A—Sciences de la Terre et des planètes*, **329**, pp. 721–726.
- Marret, F., Scourse, J.D., Versteegh, G., Jansen, F.J.H. and Schneider, R., 2001, Integrated marine and terrestrial evidence for abrupt Congo River palaeodischarge fluctuations during the last deglaciation. *Journal of Quaternary Science*, **16**, pp. 761–766.
- Marret, F., Maley, J. and Scourse, J., 2006, Climatic instability in west equatorial Africa during the Mid- and Late Holocene. *Quaternary International*, **150**, pp. 71–81.
- Mayewski, P.A., Rohling, E.E., Stager, J.C., Karlén, W., Maasch, K.A., Meeker, L.D., Meyerson, E.A., Gasse, F., van Kreveld, S., Holmgren, K., Lee-Thorp, J., Rosqvist, G., Rack, F., Staubwasser, M., Schneider, R.R. and Steigl, E.J., 2004, Holocene Climate Variability. *Quaternary Research*, **62**, pp. 243–255.
- Mehra, O.P. and Jackson, M.L., 1960, Iron oxide removal from soils and clays by dithionite-citrate system buffered with sodium bicarbonate. *Clays and Clay Minerals Proceedings*, **7**, pp. 317–377.
- Meister, C., 2008, Recent archaeological investigations in the tropical rain forest of south-west Cameroon. *Palaeoecology of Africa*, **28**, pp. 43–57.
- Nange, M.J., 2007, The seismicity of Cameroon. *Sciences et Développement*, **5**, pp. 24–25.

- Nedelec, A., Myniem, D. and Barbey, P., 1993, High-P–high-T anatexis of Archaean tonalitic grey gneisses: the Eseka migmatites, Cameroon. *Precambrian Research*, **62**, pp. 191–205.
- Nedelec, A., Macaudiere, J., Nzenti, J.P. and Barbey, P., 1986, Evolution structurale et métamorphique des schistes de Mbalmayo (Cameroun). Implications pour la structure de la zone mobile panafricaine d’Afrique Centrale, au contact du craton du Congo. *Comptes Rendus de l’Académie des Sciences*, **303**, pp. 75–80.
- Neumer, M., 2007, *Reliefformen, fluviale Morphodynamik und Sedimente in den wechselfeuchten Tropen Zentralafrikas: Indikatoren für die subrezente und rezente Landschaftsentwicklung*. PhD-thesis, Goethe-University, Frankfurt a. M., pp. 1–304.
- Ngako, V., Affaton, P., Nange, J.M. and Njanko, T., 2003, Pan-African tectonic evolution in Central and Southern Cameroon: transpression and transtension during sinistral shear movements. *Journal of African Earth Sciences*, **36**, pp. 207–214.
- Ngangom, E., 1983, Etude tectonique du fossé crétacé de la Mbéré et du Djérem, Sud Adamaoua, Cameroun. *Bulletin de Centres Recherches Exploration-Production Elf Aquitaine*, **7**, pp. 339–347.
- Ngomanda, A., Neumann, K., Schweizer, A. and Maley, J., 2009, Seasonality change and the third millennium BP rainforest crisis in Central Africa: a high resolution pollen profile from Nyabessan, Southern Cameroon. *Quaternary Research*, **71/3**, pp. 307–318.
- Nguetsop, V.F., Servant-Vildary, S. and Servant, M., 2004, Late Holocene climatic changes in West Africa, a high resolution diatom record from equatorial Cameroon. *Quaternary Science Reviews*, **23**, pp. 591–609.
- North Greenland Ice Core Project (NGRIP) Members, 2004, High-resolution record of Northern Hemisphere climate extending into the last interglacial period. *Nature*, **431**, pp. 147–151.
- Nzenti, J.P., Barbey, P., Macaudiere, J. and Sob, D., 1988, Origin and evolution of the Late Precambrian high-grade Yaoundé gneisses (Cameroon). *Precambrian Research*, **38**, pp. 91–109.
- Olivry, J.C., 1986, *Fleuves et rivières du Cameroun*. (Paris: ORSTOM), pp. 1–733.
- Penaye, J., Toteu, S.F., Van Schmus, W.R. and Nzenti, J.-P., 1993, U-Pb and Sm-Nd preliminary geochronologic data on the Yaoundé’ series, Cameroon: signification of the granulitic rocks in the ‘Centrafrican’ belt. *Comptes Rendus de l’Académie des Sciences Paris*, **317**, pp. 782–794.
- Pokras, E.M., 1987, Diatom record of Late Quaternary climatic change in the eastern equatorial Atlantic and tropical Africa. *Palaeoceanography*, **2/3**, pp. 273–286.
- Pokras, E.M. and Mix, A.C., 1987, Earth’s precession cycle and Quaternary climatic change in tropical Africa. *Nature*, **326**, pp. 486–487.
- Prell, W.L. and Kutzbach, J.E., 1987, Monsoon variability over the past 150,000 years. *Journal of Geophysical Research*, **92**, pp. 8411–8425.
- Rodbell, D.T., Seltzer, G.O., Anderson, D.M., Abbott, M.B., Enfield, D.B. and Newman, J.H., 1999, An ~15,000-year record of El Niño-driven alluviation in southwestern Ecuador. *Science*, **283**, pp. 516–520.
- Rosignol-Strick, M., 1983, African monsoons, an immediate climate response to orbital insolation. *Nature*, **304**, pp. 46–49.
- Runge, J., 2008, Of deserts and forests: insights into Central African palaeoenvironments since the Last Glacial Maximum. *Palaeoecology of Africa*, **28**, pp. 15–27.
- Runge, J., Eisenberg, J. and Sangen, M., 2005, Ökologischer Wandel und kulturelle Umbrüche in West- und Zentralafrika—Prospektionsreise nach Südwestkamerun vom 05.03.–03.04.2004 im Rahmen der DFG-Forschergruppe 510: Teilprojekt “Regenwald-Savannen-Kontakt (ReSaKo)”. *Geoökodynamik*, **26**, pp. 135–154.

- Runge, J., Eisenberg, J. and Sangen, M., 2006, Geomorphic evolution of the Ntem alluvial basin and physiogeographic evidence for Holocene environmental changes in the rain forest of SW Cameroon (Central Africa)—preliminary results. *Zeitschrift für Geomorphologie, N.F., Supplement-Band*, **145**, pp. 63–79.
- Runge, J., Sangen, M., Neumer, M., Eisenberg, J. and Becker, E., in press, Late Quaternary valley and slope deposits in the environs of the Congo basin and their palaeoenvironmental significance. *Palaeogeography, Palaeoclimatology, Palaeoecology*.
- Sangen, M., 2008, New evidence on palaeoenvironmental conditions in SW Cameroon since the Late Pleistocene derived from alluvial sediments of the Ntem River. *Palaeoecology of Africa*, **28**, pp. 79–101.
- Sangen, M., 2009, *Physiogeographische Untersuchungen zur pleistozänen und holozänen Umweltgeschichte an Alluvionen des Ntem-Binnendeltas und alluvialer Sedimente der Flüsse Boumba, Ngoko, Nyong und Sanaga in Süd-Kamerun*. Unpublished PhD-thesis, Goethe-University, Frankfurt a. M., pp. 1–343.
- Sangen, M., in review, New results on palaeoenvironmental conditions in Equatorial Africa derived from alluvial sediments of Cameroonian rivers. *Proceedings of the Geological Association*.
- Schefuß, E., Schouten, S. and Schneider, R.R., 2005, Climatic controls on Central African hydrology during the past 20,000 years. *Nature*, **437**, pp. 1003–1006.
- Schneider, R.R., Müller, P.J. and Wefer, G., 1994, Late Quaternary palaeoproductivity changes off the Congo deduced from stable carbon isotopes of planktonic foraminifera. *Palaeogeography, Palaeoclimatology, Palaeoecology*, **110**, pp. 255–274.
- Schneider, R.R., Price, B., Müller, P.J., Kroon, D. and Alexander, I., 1997, Monsoon related variations in Zaire (Congo) sediment load and influence of fluvial silicate supply on marine productivity in the east equatorial Atlantic during the last 200,000 years. *Palaeoceanography*, **12/3**, pp. 463–481.
- Schwartz, D., 1992, Assèchement climatique vers 3000 B.P. et expansion Bantu en Afrique Centrale atlantique: quelques réflexions. *Bulletin de la Société géologique de France*, **3**, pp. 353–361.
- Segalen, P., 1967, Les sols et géomorphologie du Cameroun. *Cahiers ORSTOM*, **1/7**, pp. 137–187.
- Servant, M. and Servant-Vildary, S., 2000, *Dynamique à long terme des écosystèmes forestiers intertropicaux. Publications issues du Symposium international « Dynamique à long terme des écosystèmes forestiers intertropicaux », Paris, 20–22 mars 1996.* (Paris: UNESCO), pp. 1–434.
- Street-Perrott, F.A. and Perrott, R.A., 1990, Abrupt climatic fluctuations in the tropics: the influence of Atlantic Ocean Circulation. *Nature*, **343**, pp. 607–612.
- Thomas, M.F., 2000, Late Quaternary environmental changes and the alluvial record in humid tropical environments. *Quaternary International*, **72**, pp. 23–36.
- Thomas, M.F., 2004, Landscape sensitivity to rapid environmental change—a Quaternary perspective with examples from tropical areas. *Catena*, **55**, pp. 107–124.
- Thomas, M.F., 2008, Understanding the impacts of Late Quaternary climate change in the tropical and sub-tropical regions. *Geomorphology*, **101**, pp. 146–158.
- Thomas, M.F. and Thorp, M.B., 2003, Palaeohydrological reconstruction for tropical Africa since the Last Glacial Maximum—evidence and problems. In *Palaeohydrology: Understanding Global Change*, edited by Benito, G. and Gregory, K.J., (Chichester: Wiley and Sons), pp. 167–192.
- Toteu, S.F., Van Schmus, W.R., Penaye, J. and Michard, A., 2001, New U-Pb and Sm-Nd data from north-central Cameroon and its bearing on the pre-Pan African history of Central Africa. *Precambrian Research*, **108**, pp. 45–73.

- Toteu, S.F., Penaye, J. and Poudjourn Djomeni, Y., 2004, Geodynamic evolution of the Pan-African belt in Central Africa with special reference to Cameroon. *Canadian Journal of Earth Sciences*, **41**, pp. 73–85.
- Tsalefac, M., 2006, Carte du Climat. In *Atlas du Cameroun*, edited by Yahmed, D.B., (Paris: Les Éditions Jeune Afrique), pp. 60–61.
- van Geel, B., Raspopov, O.M., Renssen, H., van der Plicht, J., Dergachev, V.A. and Meijer, H.A.J., 1999, The role of solar forcing upon climate change. *Quaternary Science Reviews*, **18**, pp. 331–338.
- van Zinderen Bakker, E.M. and Clark, J.D., 1962, Pleistocene climates and cultures in north-eastern Angola. *Nature*, **196**, pp. 639–642.
- van Zinderen Bakker, E.M., 1967, Upper Pleistocene and Holocene stratigraphy and ecology on the basis of vegetation changes in sub-Saharan Africa. In *Background to Evolution in Africa*, edited by Bishop, W.W. and Eas, D.C., (Chicago: University Press), pp. 125–147.
- Verschuren, D., 2004, Decadal and century-scale climate variability in tropical Africa during the past 2000 years. In *Past climate variability through Europe and Africa*, edited by Battarbee, R.W., Gasse, F. and Stickley, C.E., (Dordrecht: Springer), pp. 139–158.
- Vidal, L. and Arz, H., 2004, Oceanic climate variability at millennial time-scales: Models of climate connections. In *Past climate variability through Europe and Africa*, edited by Battarbee, R.W., Gasse, F. and Stickley, C.E., (Dordrecht: Springer), pp. 31–44.
- Vincens, A., Schwartz, D., Elenga, H., Reynaud-Farrera, I., Alexandre, A., Bertaux, J., Mariotti, A., Martin, L., Meunier, J.-D., Nguetsop, F., Servant, M., Servant-Vildary, S. and Wirmann, D., 1999, Forest response to climate changes in Atlantic Equatorial Africa during the last 4000 years BP and inheritance on the modern landscapes. *Journal of Biogeography*, **26**, pp. 879–885.
- Wanner, H., Beer, J., Bütikofer, J., Crowley, T.J., Cubasch, U., Flückiger, J., Goosse, H., Grosjean, M., Joos, F., Kaplan, J.O., Küttel, M., Müller, S.A., Prentice, I.C., Solomina, O., Stocker, T.F., Tarasov, P., Wagner, M. and Widmann, M., 2008, Mid-to Late Holocene climate change: an overview. *Quaternary Science Reviews*, **27**, pp. 1791–1828.
- Weldeab, S., Schneider, R.R., Kölling, M. and Wefer, G., 2005, Holocene African droughts relate to eastern equatorial Atlantic cooling. *Geology*, **33/12**, pp. 981–984.
- Weldeab, S., Lea, D.W., Schneider, R.R. and Andersen, N., 2007, 155,000 years of West African monsoon ocean thermal evolution. *Science*, **316**, pp. 1303–1307.
- Youta Happi, J., 1998, *Arbres contre graminées: la lente invasion de la savane par la forêt au Centre-Cameroun*. Thèse de Doctorat d'Etat, Université de Paris-Sorbonne, pp. 1–238.
- Zabel, M., Schneider, R., Wagner, T., Adegbe, A.T., de Vries, U. and Kolonic, S., 2001, Late Quaternary Climate Changes in Central Africa as inferred from Terrigenous Input in the Niger Fan. *Quaternary Research*, **56**, pp. 207–217.

CHAPTER 10

Palaeoclimate of Ondiri Swamp, Kikuyu, Kenya, from 1.350 to 1.810 AD

Julian A. Ogondo

*National Museums of Kenya, Kenya
University of Nairobi, Nairobi, Kenya*

Daniel O. Olago & Eric O. Odada

University of Nairobi, Nairobi, Kenya

ABSTRACT: Ondiri Swamp is located at longitude 36°40'E and latitude 1°15'S in Kikuyu Division, Kiambu District, Central Province. Ondiri Swamp has an area of approximately 0,468 km², and is situated about 10 km west from the centre of Nairobi City. It lies at 2,200 m asl and 10 m below the general topography. It is a major source of Nairobi River. The area is influenced by the Asian and Indian Ocean monsoonal systems with rainfall ranging from 800 mm–1,200 mm yr⁻¹. The vegetative cover comprise of species of Cyperaceae, reeds (Plagmites), *Typha* (Cattails) and water grass (*Vossia*) which are aquatic plants. The area is underlain by the Limuru trachytes and associated pyroclastic rocks which were the final outpours of the Rift volcanic lava during the Miocene–Pleistocene times. In this paper a 600 yr BP (1.350 to 1.810 AD), 50 cm core was recovered at the centre of the swamp in May 2007 for palaeoclimate reconstruction based on diatoms assemblages and sediment geochemistry. The major diatoms at Ondiri Swamp were *Amphipleura pellucida*, *Navicula gawaniensis*, *Pinularia tropica*, *Eunotia tenella*, *Melosira ambigua*, *Nitzschia subrostrata*, *Surirella* sp., *Eunotia pectinalis*, *Cyctotella iris*, *Nitzschia latens* and *Strauroneis phoenicenteron* which are mainly associated with larger and more open wetland. The younger level was dominated by *Navicula tenella*, *Navicula el Kab*, *Nitzschia linearis*, *Navicula halophila*, *Gomphonema gracile*, *Navicula salinicola*, *Frustulia rhomboides* *Eunotia pectinalis* and *Hantzschia amphioxys* which are associated with smaller wetlands. The Ondiri Swamp record has a high coherency with the Lake Naivasha record, particularly from 1,500 to 1,850 AD when the hydrological variability signal was particularly strong in Lake Naivasha, notwithstanding the fact that Ondiri Swamp is primarily maintained by groundwater and Lake Naivasha by surface water.

10.1 INTRODUCTION

Wetlands including lakes and swamps sediments are natural archives that provide long-term records of past changes in climate-catchment processes as well as changes in biological communities. Diatomaceous sediment deposits are natural archives of palaeoclimate and their analyses have provided a wealth of interesting and important information about palaeoenvironmental investigations and climate change (Owen, 2002; Owen and Renaut, 2000; Barker *et al.*, 1990; Feibel *et al.*, 1991). A lot of palaeoclimatic data (in Kenya and Eastern Africa) have been gathered from large lakes (Lake Victoria, Lake Turkana, Lake Naivasha, Lake Malawi, Lake Tanganyika), small lakes primarily in the Rift Valley system, and from maars and tarns at high altitude sites such as Mount Kenya. This paper aims to study the palaeoclimate of the last

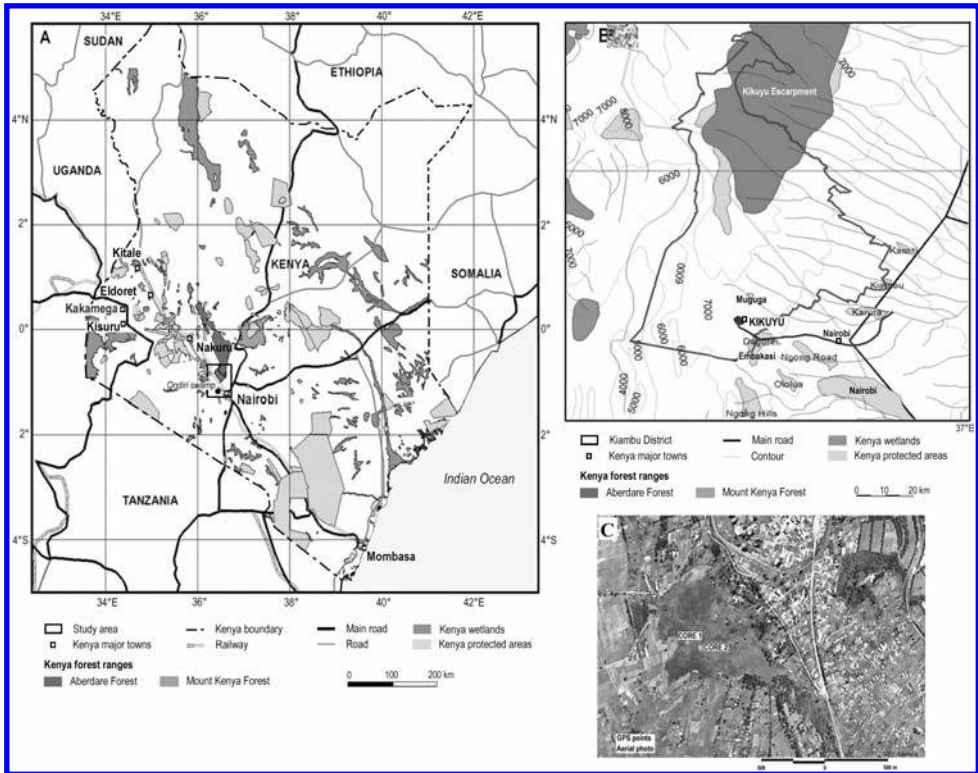


Figure 1. (A) Location of Ondiri Swamp with respect to Kenya and East African region (Redrawn from Afri cover ILRI-UNEP, 2000); (B) Detailed topography of Ondiri Swamp (as a major source of Nairobi River) with respect to Kikuyu escarpment and other major Highlands (Redrawn from Afri cover ILRI-UNEP); (C) location of Ondiri Swamp, Kikuyu and major roads (Landsat Images, 1980) Google Earth.

1,000 years for the Nairobi area on the western flank of the Kenya Rift Valley, based on analysis of the lithology, diatom assemblages and sediment geochemistry of Ondiri Swamp. Ondiri Swamp is located at latitude $36^{\circ}40'$ and longitude $1^{\circ}15'$ in Kikuyu Division of Kiambu District approximately 10 km west of Central Nairobi in Central Province, Kenya (Figure 1). The swamp is a major source of Nairobi River that drains to the Athi River which eventually empties into the Indian Ocean.

10.2 BACKGROUND

Ondiri swamp is situated within that part of Eastern Africa that is influenced by the Asian and Indian Ocean monsoonal systems. The seasonal migration of the Intertropical Convergence Zone (ITCZ) results in northern and southern subtropical belts of monsoonal climates with summer rains and winter drought (Gasse, 2000), bracketing a large humid equatorial zone with two rainy seasons that peak in April and November. The rainfall at Ondiri Swamp ranges from 800 to 1,200 mm yr⁻¹, while higher altitude sites surrounding it have rainfall that reaches up to 2,000 to 2,400 mm yr⁻¹ (Morgan, 1967). The area is generally sub-humid to semi-humid (Figure 2).

Ondiri Swamp has numerous species of Cyperaceae, reeds (Plagmites), *Typha* (Cattails) and water grass (Vossia) which are aquatic plants that grow all year round

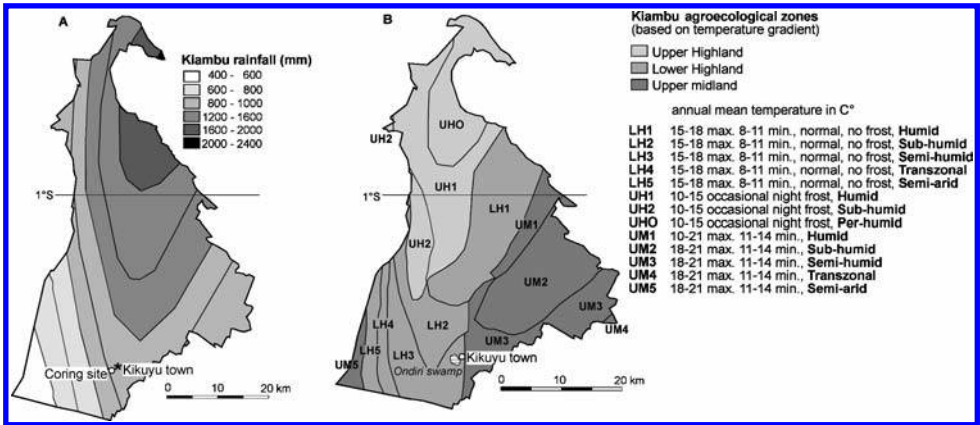


Figure 2. (A) Rainfall distribution of Ondiri Swamp and surrounding areas. (B) Temperatures and humidity of Ondiri swamp and surrounding areas (Redrawn from Afri cover ILRI-UNEP, 2000).

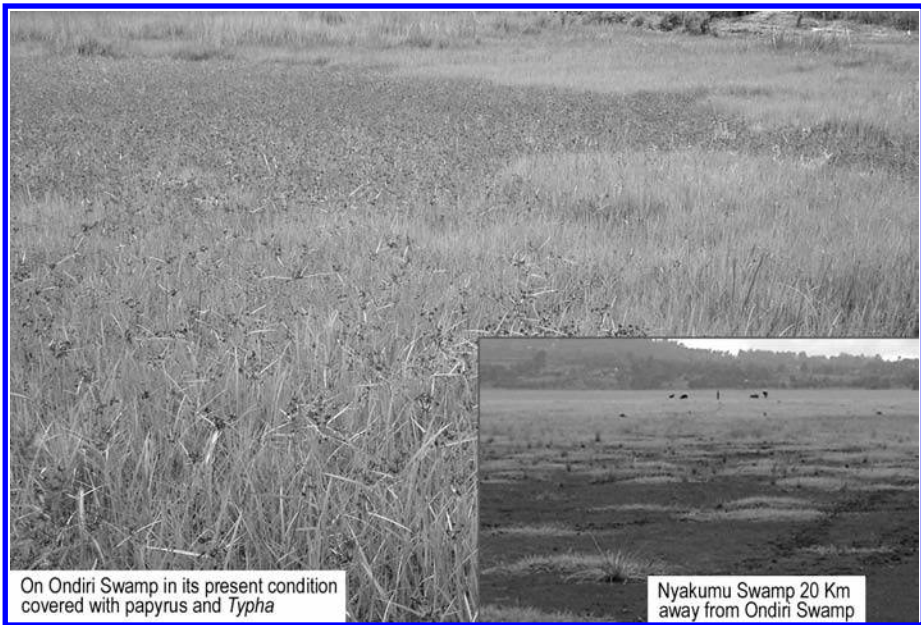


Figure 3. Area of study (Ondiri) with *Typha* and adjacent swamps (Nyakumu Swamp).

and produce large amounts of organic matter (Figure 3) that decompose and accumulate to form a thick mat (50 cm thick) on top of the water (Kinyanjui, 2003).

The areas around the Ondiri Swamp comprise plateau sloping up to its edge and its step-faulted flank. The main faults in the region form part of a complex North-South fracture pattern associated with the Rift Valley system. The rocks mainly found at Ondiri Swamp are the Limuru trachyte and associated pyroclastic rocks which were the final outpours of the Rift volcanic lava. The underlying lava in the down thrown blocks or strips are responsible for the local perched water tables,

and hence development of internal drainage and swamps or lakes (Saggerson, 1991). Ondiri Swamp is a major source of Nairobi River and joins other minor streams from the Kikuyu escarpment (Figure 1) and drains into the Athi River which is one of the two major Kenyan rivers that drain into the Indian Ocean. Olago and Opiyo (2000) suggested that the sediments of Ondiri Swamp are partly derived from erosion, transportation and accumulation of sediments derived from the local geological succession (trachytes). Swamps such as Ondiri are common within the Rift fault zones of West Nairobi (Saggerson, 1991; Gregory, 1921), varying in size from a few square metres (like Ondiri Swamp) to the largest Nyakumu Swamp (Figure 3) depression which is believed to have formed through volcanic vent deflation.

10.3 MATERIALS AND METHODS

Two short (50 cm) sediment cores were collected from Ondiri swamps using a Russian corer during fieldwork in May 2007. Core 1 was located at 1°15'0,79"S and 36°39'22,93"E and Core 2 at 1°15'2,16"S and 36°39'26,24"E (Figure 1). Sediments lying at or near the sediment water interface could not be retrieved by the Russian Corer due to their 'soupy' unconsolidated nature. The cores had similar lithology, and thus only core 1 was subjected to further analysis as outlined below.

The core was sub-sampled at 5 cm intervals giving 10 samples, with an additional four sub-samples at higher resolution in levels of stratigraphic interest, hence a total of fourteen samples for each of the analyses described below. Analysis of moisture content, total organic matter (TOM), sediment geochemistry and diatom assemblages was undertaken. In order to measure variations in moisture content, wet samples of approximately of 0,5–1 grams were weighed from each sampled level. The samples were dried for 12 hours at 105°C in an oven and later cooled to room temperature. The moisture content was determined by the difference in weight between the freshly extruded samples and the dried samples and results presented as a percentage of the wet over dried weights. For the determination of total organic matter (TOM), samples of approximately of 0,8–1.5 grams were ignited in a muffled furnace for 12 hours at 550°C, cooled in a desiccator and re-weighed. The TOM was determined by the difference in weight between the freshly extruded samples and the dried samples and results presented as a percentage of the wet over dried weights. Sediment samples were analysed for the major oxides as well as Zn, Pb, Cu, Cr and Ni using XRF and atomic absorption, respectively, at the Mines and Geology Department of the Ministry of Environment and Mineral Resources, Kenya. The technique employed for diatom processing is outlined in Leng and Baker (2006). Samples of about one cubic centimetre each were cleaned by treatment with 5% hydrochloric acid and 30% hydrogen peroxide to remove contents of carbonates and organic matter. The prepared diatom samples were mounted on glass slides with Naphrax and examined under oil immersion Leitz Dialux 20EB light microscope. The diatoms were counted under x400 magnification; detailed features were examined under x1000 magnification.

10.4 RESULTS

10.4.1 Lithology

When first extruded the upper ten centimeter of the core was highly variable in color and texture. The upper most sediment was light brown and fluid, becoming slightly

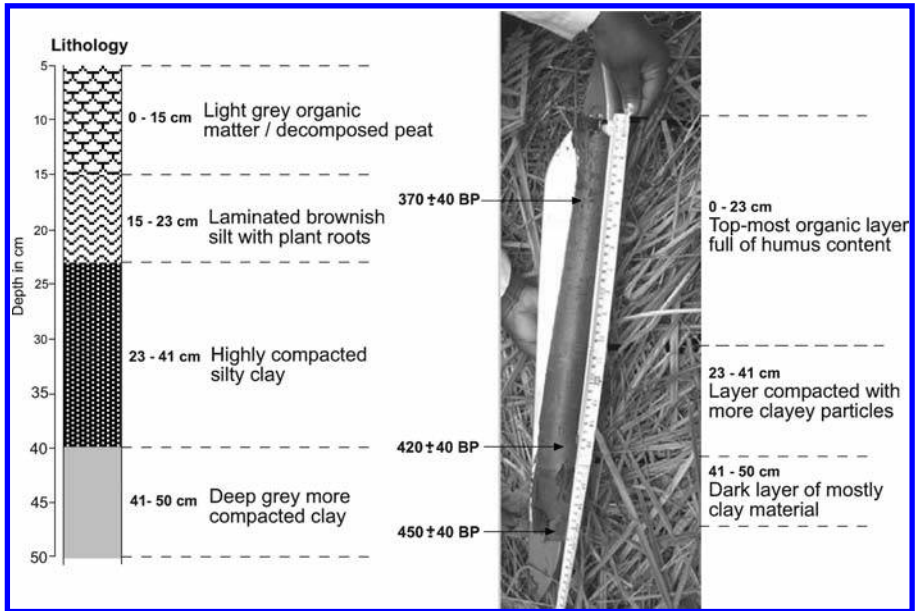


Figure 4. Lithology of the Ondiri Swamp core.

gelatinous after partial drying (Figure 4). The upper one through to ten centimeters were generally moist, with the exception of the hard layer following twenty centimeters which was very dry and composed of layered sand, beneath which was finer sediment partially weathered into soil. Colorful bands and zones characterized many parts of the core from the top through to forty centimeter, these included flecks of white CaCO_3 , several regions of very smooth grey-brown or grey-black sediment and a number of whitish flocculent zones. In the lower forty through to fifty centimeters the sediment was very dark and fine but included very thin bands of clay (Figure 4).

10.4.2 Moisture content (MC), TOM and sediment geochemistry

There is a general increase in moisture content from the bottom (33%) to the top (50%), with two positive excursions between 35–40 cm (up to 62%) and at 10–15 cm (68%), which reflect changes in the sediment lithology, from clayey to silty and silty to clayey, respectively (Figure 5).

The Total Organic Matter (TOM) is relatively low in the bottom 10 cm of the core within the deep grey clay unit (38–40%), with a peak at level 43–45 cm (52,44%). From 40 cm to the top of the core the TOM is relatively invariant (from 50–56%), with a decrease to about 47% between 20 and 30 cm (Figure 5). The stable carbon isotope values of the radiocarbon dated samples are close to -20‰ (Table 1), suggesting that the organic materials are derived primarily from aquatic macrophytes and/or mixed C_3 and C_4 and humic organic materials derived from the catchment (Olago *et al.*, 2000).

There is not much significant variation in the major sediment geochemistry, save for relatively high P_2O_5 content in the bottom deep grey clay unit, and an increase in P_2O_5 , Fe_2O_3 and Al_2O_3 in the top 5–10 cm of the core. Relatively high Cr and Ni concentrations

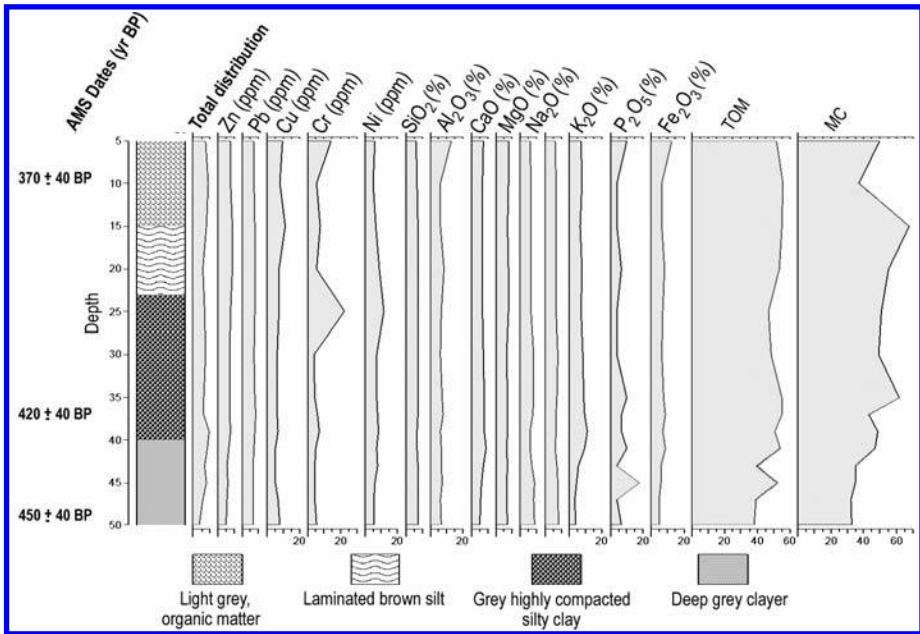


Figure 5. Geochemistry of Ondiri Swamp showing different chemical content at various levels.

Table 1. Radiocarbon ages and associated organic matter content and stable carbon isotope value for the dated sediment.

Core interval (cm below mud surface)	Age (¹⁴ C yr. BP)	Age (cal. yr. AD)	Average organic matter (%)	δ ¹³ C (‰)
10	370 ± 40	1.536 ± 68	53,83	-20,0
37	420 ± 40	1.505 ± 65	52,04	-19,9
47	7.410 ± 40		44,58	-17,5

are recorded at 25 cm, close to the transition from silty clay to laminated silt, and high Cr concentration at 5 cm in the organic sediments.

10.4.3 The diatom assemblages

Zone Ondiri 1 (50–41 cm)

This zone is dominated by: *Amphipleura pellucida* (12,5–22,1%), *Navicula gawaniensis* (0–22,1%), *Pinularia tropica* (0–21,1%), *Eunotia tenella* (0–15,7%), *Melosira ambigua* (0–11,5%), *Nitzschia subrostrata* (0–12,3), *Surirella* sp. (0–10,2%), and *Eunotia pectinalis* (2,2–8,4%) (Figure 6). The dominant assemblage reflects low to medium alkalinity (0,2–50 meq l⁻¹), neutral to slightly alkaline and low conductivity (300–1.000 μS cm⁻¹) aquatic environment. *Amphipleura pellucida* is characteristic of disturbed habitat, it is eurythermal while others are either eurythermal, periphyton or planktonic.

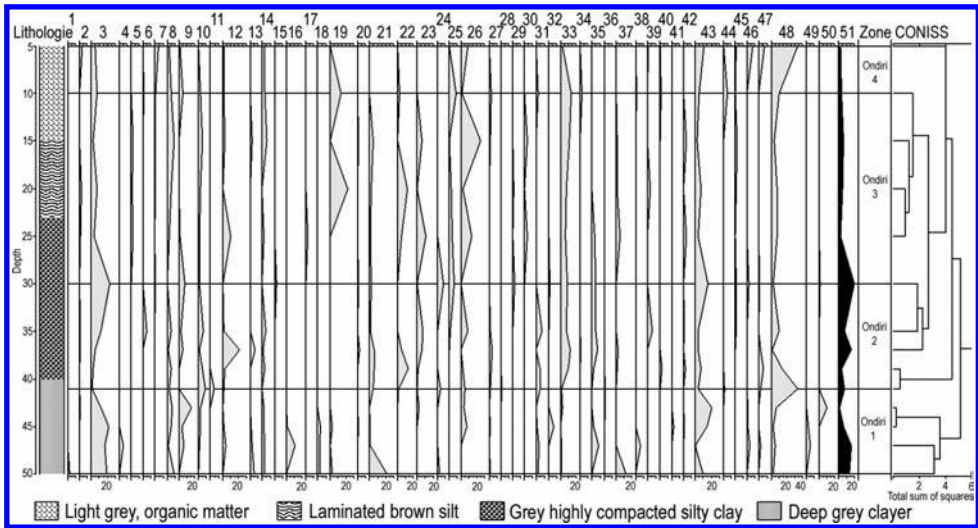


Figure 6. The fifty four species clustered for final analysis, the four diatoms zones recognized within the diatoms assemblages of Ondiri Swamp: Ondiri 1, Ondiri 2, Ondiri 3 and Ondiri 4 from the oldest to the youngest.

Zone Ondiri 2 (30–41 cm)

The dominant diatoms in this zone are: *Amphipleura pellucida* (0,8–23,2%), *Gomphonema gracile* (0,6–21,3) and *Stauroneis phoenicenteron* (1,4–33,6%), *Navicula halophila* (0–13,4%), *Nitzschia linearis* (2–12,8%) and *Pinularia tropica* (2,8–15,2%). The dominant species reflect slightly higher alkalinity (≥ 2 –100 meq l⁻¹), slightly alkaline and high conductivity waters of ≥ 300 –10.000 $\mu\text{S cm}^{-1}$. There are more periphyton and plankton species in this zone with a few eurytopic or epipellic, epilithic-subaerial, oligothermal or eurythermal types.

Zone Ondiri 3 (30–10 cm)

The dominant diatoms are: *Navicula sp. 3 af. tenella* (2,2–24,5%) and *Navicula el Kab* (0–22,0%), *Nitzschia linearis* (6,4–14,3%), *Navicula halophila* (0–13,0%), *Gomphonema gracile* (0,4–10,1) and *Stauroneis phoenicenteron* (4–10,1%). The species assemblages reflects medium alkalinity (2–50 meq l⁻¹), slightly alkaline and low conductivity (300–1.000 $\mu\text{S cm}^{-1}$) aquatic environment. This zone is very interesting because the two dominant species i.e., the *Navicula el Kab*, a phytoplankton and *Navicula sp. 3 af. Tenella* which is plankton living in bottom mud alternated in response to different water conditions.

Zone Ondiri 4 (10–0 cm)

The zone had relatively fewer species, the most dominant being *Stauroneis phoenicenteron* (34,2%), *Navicula sp. 3 af. tenella* (8,0%), *Pinularia tropica* (11,2%) and *Rhopalodia gibberula* (6,6%). In this zone there is the introduction of *Rhopalodia gibberula* which is an indicator of strong alkaline waters in East Africa, while other species are either planktonic or periphytic.

10.4.4 Age model

For radiocarbon age determination, three samples of organic sediment of about 3 grams each, packaged in aluminium foil in a well wrapped spongy box, were sent to Beta Analytic Inc., Miami, Florida (USA) for analysis by AMS dating techniques. Three radiocarbon dates were obtained for the core (Figure 4). While the dates are consistent down core, the date obtained near the bottom of the core (450 yrs BP) is likely to reflect contamination with old terrestrial carbon eroded from the surrounding catchment area and deposited in the swamp. The age of 370 yr BP at 10 cm is likewise too old, as it yields an unlikely sedimentation rate of 0,2 mm per year. The age of the sediment core has therefore been calculated by simple regression, omitting the basal date of 7,410 yr BP. The regression is defined by the equation $y = 9,3676x + 116,57$ and has an r^2 value of 0,611. The age of the core top is given by the regression as 117 yr BP, which is reasonable, given the lack of recovery of the very soft “soupy” sediment at/ near the sediment-water interface.

10.5 DISCUSSION

Zone 1 (Table 2) coincides with a compacted clay horizon, and has a diatom assemblage that reflects a slightly wet episode, but the presence of diatoms such as *Amphipleura pellucida* which is characteristic of disturbed habitat, indicates that episodic terrigenous sediment input (traced by the relatively high P_2O_5 content) was an important characteristic of this period and signifies fairly low water levels. Low organic matter contents also suggest low aquatic macrophyte productivity and may also reflect a catchment with sparse vegetation and reduced inputs of terrestrial organic matter.

Table 2. Radiocarbon and calendar ages for the diatom zones in Ondiri Swamp and palaeoclimate compared with the Lake Naivasha record.

Diatom Zone	Age (^{14}C yr. BP)	Age (cal. yr. AD)	Palaeoclimate	
			Ondiri Swamp	Lake Naivasha (Verschuren <i>et al.</i> , 2000)
Zone 4	210–117	1761–1810	Drier	Drying from 1760, Drought ca. 1800–1850
Zone 3	398–210	1523–1761	Progressive wetness with a drier interval centred at 1553 AD	Wet ca. 1600–1760 AD Dry ca. 1520–1600 AD
Zone 2	501–398	1415–1523	Drier than in Zone 1, shallower water in Swamp maintained by groundwater inputs	Wet ca. 1430–1520
Zone 1	585–501	1354–1415	Dry catchment with sparse vegetation, shallow water in Swamp maintained by groundwater inputs	Drought ca. 1370–1400 AD

The data suggests a slightly arid period with water in Ondiri Swamp being sustained largely by groundwater inputs from the faulted terrain of the eastern shoulder of the Kenya Rift.

In Zone 2 (Table 2), conditions become dryer, with the *Amphipleura pellucida*, reflecting disturbed habitat, becoming the dominant diatom species. Increase in the silt content of the terrigenous material as well as in alkalinity and conductivity as indicated by the diatom assemblage indicates that the water level was lower than in Zone 1.

In Zone 3 (Table 2), conditions became wetter than in Zone 2, but the dominant diatom assemblage here is different from that in Zone 1, with *Navicula* strongly dominant. This zone has three major lithological changes, from compacted silty clay at the bottom, through to laminated silt in the middle, and terminating with decomposed peat at the top. This zone marks a time of progressive increase in water level from the dryer period in Zone 2 with *Navicula el Kab* (a phytoplankton) dominant, followed by a short-lived decline in water level with rooted macrophytes encroaching deeper into the swamp environment and *Navicula sp. 3 af. Tenella* (a benthic diatom) dominant. This is accompanied by a peak in Ni and Cr levels, which suggest increased terrigenous input of sediment through catchment erosion and development of an immature palaeosol. Ni can be precipitated mainly with Fe oxides and organic compounds (Eaton, 1979). Following this, an eventual modest increase in water level accompanied by establishment of floating macrophytes and dominance of *Navicula el Kab*, is inferred.

In Zone 4 (Table 2), the dominant species changes to *Stauroneis phoenicenteron*, which is pH indifferent and has a wide range of ecological tolerance. Coupled with the appearance of *Rhopalodia gibberula* which is an indicator of strong alkaline waters, and a low species diversity compared to the other zones, this diatom assemblage reflects a relatively dry, unstable and disturbed environment, consistent both with natural aridity and human/animal disturbance. The lithology of this zone is characterized by decomposed peat, reflecting a significant amount of macrophytes occupying the swamp. The Cr enrichment at 5 cm probably relates to trivalent chromium that readily substitutes for Fe³⁺ in minerals, and co-precipitates with Fe³⁺ as insoluble Cr(OH)₃ at high pH values.

The Ondiri Swamp record has a high coherency with the Lake Naivasha record (Table 2), particularly from 1500 to 1850 AD when the hydrological variability signal was particularly strong in Lake Naivasha. The apparent asynchrony with the Naivasha record in Zone 2 can be related to the fact that the Ondiri Swamp is primarily ground water fed from the faulted flanks of the eastern shoulder of the Kenya Rift, while Lake Naivasha is primarily fed by surface water, so that low amplitude variability of surface waters is modulated by the temporally slower and more muted response of groundwater. The high resolution, 1.000 yr hydrological record of droughts and wet periods for Lake Naivasha has been shown to be broadly coeval with solar insolation: arid periods or drought events were broadly coeval with phases of high solar radiation, and intervening periods of increased moisture were coeval with phases of low solar radiation (Verschuren *et al.*, 2000). This relationship has also been intimated for the Kilimanjaro ice cores, where ¹⁸O minima are related to solar minima (Thompson *et al.*, 2002).

ACKNOWLEDGMENTS

University of Nairobi, Department of Geology, National Museums of Kenya: The Director General; Director Research and Scientific Collections; Head of Earth Sciences Department; the entire Earth Sciences Staff. British Institute of Eastern Africa: Dr. Justin Willis for radiocarbon dating grant.

REFERENCES

- Barker, P., F. Gasse, F., Roberts, N. and Taieb, M., 1990, Taphonomy and diagenesis in diatom assemblages: A Late Pleistocene palaeoecological study from Lake Magadi, Kenya. *Hydrobiologia*, **214**, pp. 267–272.
- Eaton, A., 1979, Leachable trace elements in San Francisco Bay sediments, indicators of sources and estuarine processes. *Environmental Geology and Water Sciences*, **2**, pp. 333–339.
- Feibel, C.S., Harris J.M., and Brown F.H., 1991, In: Koobi Fora Research project: The Fossil Ungulates: Geology, Fossil Artiodactyls and Palaeoenvironments, edited by J.M. Harris. *Clarendon Press*, **3**, Oxford, pp. 321–370.
- Gasse, F., 2000, Hydrological changes in the African tropics since the Last Glacial Maximum. *Quaternary Science Reviews*, **19**, pp. 189–211.
- Gregory, J.W., 1921, *The Rift Valleys and Geology of East Africa*. London.
- Kinyanjui, D.M., 2003, *Palynology and heavy metals in the sediments and waters of the Ondiri Swamp, Kikuyu, Kenya: Past influences, present practices, future needs*. MSc. Thesis, University of Nairobi, Kenya. 72 p.
- Leng, M.J. and Barker, P.A., 2006, A review of the oxygen isotope composition of lacustrine diatom silica for Palaeoclimate reconstruction. *Earth Science Reviews*, **75**, pp. 5–27
- Morgan, W.T., 1967, Nairobi City and Region. *Oxford University Press*, London, 154 p.
- Olago, D.O. and Opiyo, N.A., 2001, Pollution assessment in Nairobi River Basin. In: *Pollution assessment Report of the Nairobi River Basin Project*, edited by P.F. Okoth and P. Otieno. UNEP/Africa Water Network.
- Olago, D.O., Street-Perrott, F.A., Perrott, R.A., Ivanovich, M., Harkness, D.D., Odada, E.O., 2000, Long-term temporal characteristics of palaeomonsoon dynamics in equatorial Africa. *Global and Planetary Change*, **26**, pp. 159–171.
- Owen, R.B. and Renaut, R.W., 2000, Spatial and temporal facies variations in the Pleistocene Ologesailie Formation, southern Kenya Rift Valley. In: *Lake Basins through Space and Time*, edited by Gierlowski-Kordesch E.H. and Kelts, K.K. *American Association Petroleum Geologists*, pp. 553–559.
- Owen, R.B., 2002, Sedimentological characteristics and origins of diatomaceous deposits in the East African Rift System. In: *Sedimentation in Continental Rifts*, edited by Renaut, R.W. and Ashley, G.M. *SEPM Special Publication*, **73**, pp. 233–246.
- Saggerson, E.P., 1991, *Geology of the Nairobi Area*, **98**. Ministry of Environment and Natural Resources, Mines and Geology Department, Nairobi, 65 p.
- Thompson, L.G., Mosley-Thompson, E., Davis, M.E., Henderson, K.A., Brecher, H.H., Zagarodnov, V.S., Mashiotto, T.A., Lin, P.N., Mikhalenko, V.N., Hardy, D.R., Beer, J., 2002, Kilimanjaro ice core records: evidence of Holocene climate change in tropical Africa. *Science*, **298**, pp. 589–593.
- Verschuren, D., Kathleen, R.L. and Cumming, B.F., 2000, Rainfall and drought in equatorial East Africa during the past 1.100 years. *Nature*, **403**, pp. 410–413.

CHAPTER 11

A cluster-analysis-based climate classification for NE Africa

Brigitta Schütt, Katharina Ducke & Jan Krause

Department of Earth Sciences, Physical Geography, Freie Universität, Berlin, Germany

ABSTRACT: A cluster-based climate classification using data sets on monthly temperature and monthly precipitation is presented for NE Africa. Results show close agreements with the established climate classifications of Köppen-Geiger, Troll-Paffen and Lauer-Frankenberg. Spatial analysis of the rainfall variability coefficient confirms the high variability of the regional climate. Complementary time series analysis of annual temperature and precipitation data for climate stations along a N–S transect covering the zonal and altitudinal variations of NE Africa validates the reliability of the database and the high capacity of the cluster-analysis-based climate classification. Clear relationships of climate variations with irregularly occurring events such as ENSO, NAO or volcanic eruptions cannot be confirmed.

11.1 INTRODUCTION

11.1.1 Objective

Effective global climate classifications are mostly based on complex evaluation of climate records, sometimes supplemented by phytological information. Owing to the insufficient data bases, including the number of climate stations and the length of time series available for the different climatic elements in different areas, these climate classifications have varying degrees of weakness. Moreover, classifications impose sharply drawn borders on natural climatic transition zones. In addition, the climate types often credibly describe only the centre of the region, and the reliability of this typification decreases with increasing distance from this centre. Furthermore, effective climate classifications are static systems that do not consider climatic fluctuations (Buckle, 1996).

This paper aims to develop a climate classification of NE Africa based on cluster analysis of climatological records of the area's climate stations. Based on the climatic elements of precipitation and temperature for the area of interest, a climate classification will be developed and the climatic types will be defined. The quality of the cluster-analysis-based climate classification will be controlled by a complementary analysis of climate dynamics, including regional rainfall variability, and by a time series analysis of annual climate data for climate stations along a zonal transect reaching from the Mediterranean into the Sahel and covering the major climate zones as well as the different characters of the altitudinal gradient.

11.1.2 State of the art

Climate classifications are used to define and classify climatic areas and their characteristics. They reflect the relation between climatic elements and climatic factors, including their effect on the Earth's surface (Scherhag and Lauer, 1982). Global climate classifications are already available in several versions that build on different data sets and origins. For example, the classifications of Köppen-Geiger (Köppen, 1936) are based on quantitative threshold values of temperature and precipitation that are chosen according to their effect on dispersion and development of vegetation (Heyer, 1988). The classification of Troll-Paffen (Troll and Paffen, 1964) similarly depends on global limits of vegetation; its basis consists of seasonal changes of the elements radiation, temperature, precipitation and humidity, closely linked with vegetation zones (Heyer, 1988). By contrast, the classification of Lauer-Frankenberg (Lauer *et al.*, 1996) shows a purely climatic structuring. It is not oriented towards vegetation limits and only uses measured data of the 1901–1960 period. The factors included are radiation, humidity, aridity, continentality, and frost occurrence (Frankenberg, 1995).

Cluster analysis is a common method to describe climatological relations and causes. Several researchers (e.g., Unal *et al.*, 2003; Mimmack *et al.*, 2001; Domroes *et al.*, 1998; Fovell and Fovell, 1993) applied the method of cluster analysis to define different climatic types within a large area on the basis of climatic elements such as temperature and precipitation. Gong and Richman (1995) give an overview of sundry clustering applications. For selected regions of NE Africa, various climate elements such as precipitation and temperature were investigated by time series analysis (e.g., Gianini *et al.*, 2008; Hafez and Robaa, 2008; Domroes and El-Tantawi, 2005; Elagib and Mansell, 2000; Hafez and Hasanean, 2000; Gießner, 1989; Gläser *et al.*, 1989; Flohn, 1987; Trilsbach and Hulme, 1984; Klaus, 1981; El Tom, 1972), but a systematic spatial analysis of climate data applying the approach of cluster analysis is still lacking.

11.1.3 Study site

Geographical setting

The area of interest comprises the territories of Egypt and Sudan as well as adjacent areas of Chad, Libya, and the Central African Republic (Figure 1). The study area has a low relief (Figure 2) consisting of an extended tableland with Nubian Sandstone as parent material (Klitzsch and Wycisk, 1999). This tableland relief is interrupted by some orographic elements such as the Red Sea Hills, which run parallel to the Red Sea, and several other mountainous areas such as Jebel Uweinat in the area of the Egyptian-Libyan-Sudanese border, Jebel Marra in Northwestern Chad and Ennedi Plateau in Eastern Sudan. In addition, the Tibesti Mountains, the Air Mountains and the Ahaggar Mountains in central Sahara extend into the area of interest (Goudie, 2002; Herz, 1970). To the South, the study area includes part of the Yadé Massif and the Bongo Massif in the northern Central African Republic (Woodfork, 2006) (Figure 2). Along this N–S transect, seven climate stations have been selected for ongoing time series analysis of climate data.

Wide parts of the area described are covered by deserts. West of the Nile, the Libyan Desert extends from the Mediterranean Sea in the north southward to the northern Sudan. East of the Nile is the Eastern Desert; southward of it, the Nubian Desert (Goudie, 2002). Towards the south, the vast desert region merges into the savannah areas. While the River Nile is a perennial stream, fed by the frontal flows of the Blue Nile from the Ethiopian Highlands and the White Nile outflowing from Lake Victoria,

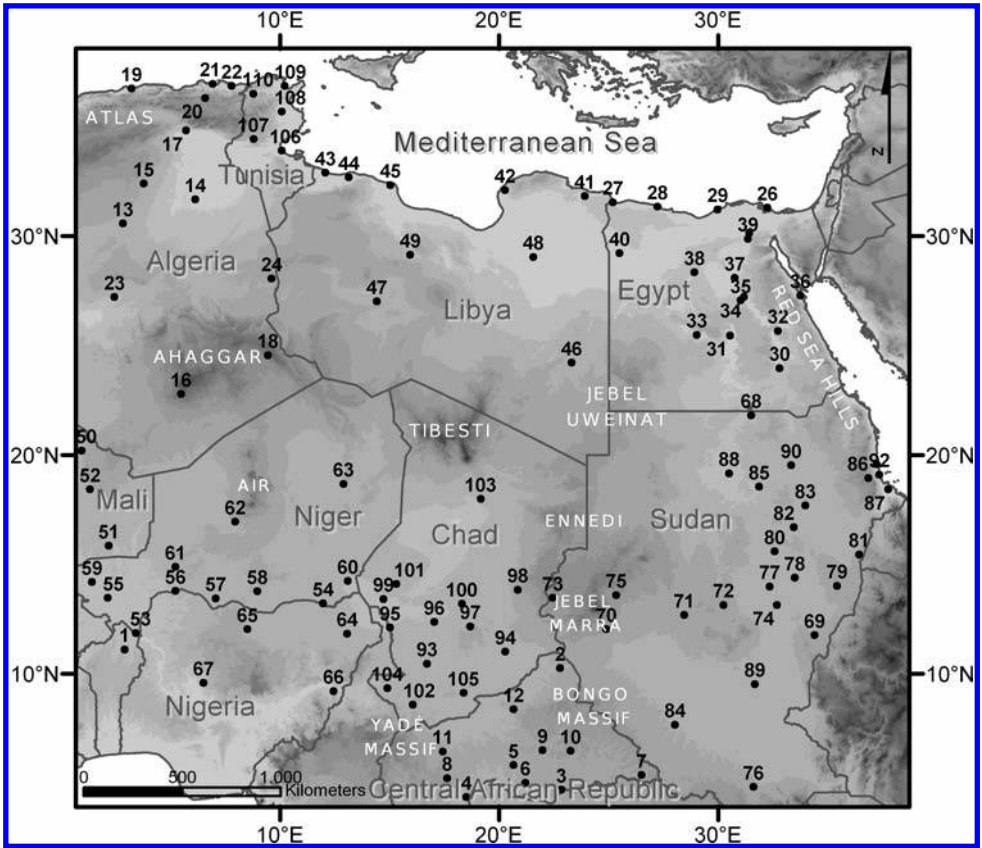


Figure 1. Map of Northern Africa with international boundaries. Black dots mark locations of the climate stations included in this research (cf. Table 1) (map source: GTOPO30).

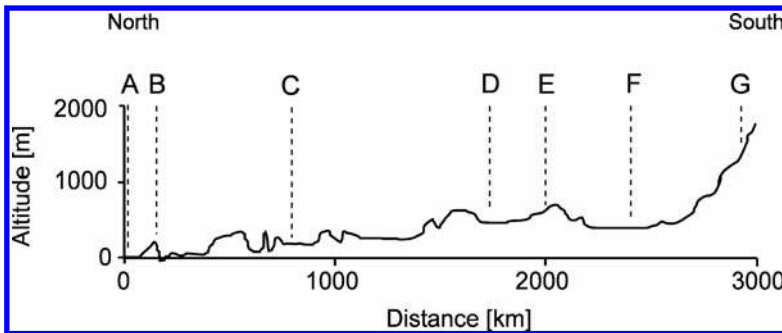


Figure 2. Schematic topographic profile of the N-S-transect running parallel to the Nile valley with spatial arrangement of the selected climate stations (A–G). For location of climate stations A–G see Figure 3 and Table 1.

most of its tributaries are ephemeral, at present only with erratic runoff (Schiffers, 1971). The perennial Chari and Logone rivers feed Lake Chad from the south, where the more humid conditions of the Sahelian-Saharan and Sudanian-Guinean zones occur (Schiffers, 1971).

Climate characters

The climate in NE Africa primarily depends on the location of the subtropical high pressure belt and the seasonal shift of the Intertropical Convergence Zone (ITCZ) (Edgell, 2006; Goudie, 1997). The spatial distribution of rainfall and its seasonality are determined by the general circulation pattern: in the northern hemisphere summer, the ITCZ and an associated low pressure cell over the Sahara lie between the moist SW monsoon in the south and the dry NE trade wind in the north. In NE Africa, these NE trade winds are locally called “Etesians” if they have a strong northerly component. On average, rainfall brought by the summer SW monsoon is recorded up to 17°N (Ruddiman, 2008; Herz, 1970). In the northern hemisphere winter months, the ITCZ shifts south of the Equator, parallel to the dynamic high-pressure cell forming over the Sahara. In consequence, wide areas of the southern Mediterranean coast are affected by the rainbearing mid-latitude westerlies, whereas the dry NE trade wind influences the southern Sahara desert and the sub-Saharan Sahel. Hence, the area of interest separates into a winter and a summer rainfall regime, with the Sahara in between (Weischet and Endlicher, 2000; Goudie, 1997).

Existing effective global climate classifications characterize the area of interest as follows. On the basis of simple algorithms, including monthly temperature and precipitation, the phytogenetically based climate zone classification after Köppen-Geiger (e.g., Köppen, 1936; updated map by Kottek *et al.*, 2006) defines wide parts of the study area as hot and dry desert climates (Bwh climate) (Figure 8). To the north, these desert climates extend as far as the Mediterranean. Only where the coastal region is mountainous (Atlas Mountains, Jebel Akdhar) does a dry-subhumid climate with dry, hot summers and rainfall brought by the westerlies during winter occur (Csa climate). To the south, the subtropical Bwh climate shades into the tropical Bsh climate, characterised by high average temperatures and summer rainfall. From North to South, the number of humid months as defined by Köppen-Geiger ($T > 2P$) increases to two months (Müller-Hohenstein, 1981). The tropical savannah follows to the South, with summer rainfall and up to nine humid months (Aw climate). In the area of interest, this Aw climate occurs in a zone reaching from the Southern Sudan to the west and covering the North of the Central African Republic and Cameroon, the South of Chad, and most of Nigeria.

By contrast, the climate zone classification introduced by Troll-Paffen (Troll and Paffen, 1964) is based on seasonal changes of temperature and precipitation and focuses on ecological nonconformities (Figure 8). The Troll-Paffen climate classification shows an explicit strip of dry-summer steppe climate with humid winters, the so-called ‘Mediterranean Climate’ (IV 1,2 climate). Southward, the subtropical semi-desert and desert climates (IV5 climate) follow. South of the Tropic of Cancer, amidst the hyperarid zone, they are succeeded by the zones of tropical semi-desert and desert climate (V5 climate) and tropical dry climate (V4 climate). These three zones—IV 1,2, IV 5, V 5 climates—cover the main part of the eastern Sahara. Corresponding to the increasing rainfall due to the seasonal shift of the ITCZ, the climate zones of the south represent the transition from the wet-and-dry tropical climate (V3 climate) to the tropical humid-summer climate (V2 climate) and subsequently the tropical rainy climate (V1 climate).

The climate zone classification introduced by Lauer-Frankenberg (Lauer *et al.*, 1996; Figure 8) is an integrative climate zone classification, merging genetic and effective climate elements and focusing on solar nonconformities. The eco-physiologically based climate zone classification integrates solar components, measured climate station data and real vegetation-cover information to capture the natural and anthropogenic interdependency of the climate-vegetation-soil system. This climate zone classification also shows a distinct strip of subtropical winter rain (B2 sa, B2a climates) along the African Mediterranean. Depending on the latitude, the number of annual humid months varies between 0 and 5. The area of the Sahara immediately to the south is defined as a subtropical continental arid climate in the north (B1a climate) and a warm-tropical arid climate in the south (A2a climate). In the Sahel, a zone with a warm-tropical semi-arid climate type follows, with about 3–5 humid months (A2 sa climate). Towards the south this zone is succeeded by a zone of warm-tropical semi-arid climate, with annually 6–9 humid months (A2 sh climate). The zonal structure evident in the Köppen-Geiger and Troll-Paffen climate classifications is less clear in the Lauer-Frankenberg system owing to its integrated effects of altitude and continentality (distance to the sea).

11.2. DATA SOURCE AND ANALYSIS

11.2.1 Data source

The study is based on monthly climate data predominantly on temperature and precipitation. The main data are the databases provided by the Food and Agriculture Organization of the United Nations (FAO, 2009, Gomme *et al.*, 2004). In part this data set is supplemented by monthly climate data provided by the Global Historical Climatology Network of the National Climate Data Center (NOAA NCDC GHCN, 2002; Peterson *et al.*, 1998; Vose *et al.*, 1992). Within the area of interest and its further vicinity, 110 climate stations with data records longer than 30 years are provided in the databases of FAO and the Global Historical Climatology Network (Table 1). Both databases were merged to reduce the number of missing values. For error control, time series of both databases were compared; missing values were only supplemented a) for precipitation if data sets run parallel with $\Delta < 0,05$, b) for temperature if the monthly averaged deviation totaled less than $2,5^{\circ}\text{C}$. If this procedure was not successful, gaps within the monthly time series of the 110 climate stations were filled by interpolation: temperature time series are completed by linear interpolation using the previous two and successive two values (years) of the respective month (Rapp, 2000). Unfortunately, gaps at the beginning and the end of the temperature time series were not filled. Gaps in monthly rainfall time series are not filled because of the high rainfall variability in the area of interest.

Stationarity and homogeneity of the climate data are tested for selected stations. The stationarity is verified by using a simple estimating formula (e.g., Bernhofer *et al.*, 2003; Schönwiese, 2000):

$$st = \pm s \cdot \sqrt{\frac{n}{m \cdot (m-1)}} \quad (1)$$

where st = stationary, s = standard deviation, n = sample size and m = number of data included in each subinterval. As a result, two st -lines are constructed. Subsequent

Table 1. List of the climate stations used for the cluster-analysis-based climate classification. Geographical localisation includes geographical coordinates and altitude (in metres) (* stations that are used within the N–S transect; CAR = Central African Republic). For location of the climate stations also see Figure 1.

	Station	Country	Longitude	Latitude	Altitude (m asl)
1	Kandi	Benin	2,93	11,13	292
2	Birao	CAR	22,78	10,28	464
3	Bangassou	CAR	22,83	4,73	500
4	Bangui	CAR	18,51	4,4	366
5	Bambari	CAR	20,65	5,85	475
6	Alindao	CAR	21,2	5,05	449
7	Obo	CAR	26,5	5,4	651
8	Bossembele	CAR	17,63	5,26	674
9	Bria	CAR	21,98	6,53	584
10	Yalinga	CAR	23,26	6,5	602
11	Bossangoa	CAR	17,43	6,48	465
12	N'Dele	CAR	20,65	8,4	511
13	El Golea	Algeria	2,86	30,56	397
14	Hassi Messaoud	Algeria	6,15	31,66	142
15	Ghardaia	Algeria	3,81	32,38	450
16	Tamanrasset	Algeria	5,51	22,78	1378
17	Biskra	Algeria	5,73	34,8	87
18	Djanet	Algeria	9,46	24,55	1054
19	Dar El Beida	Algeria	3,25	36,71	25
20	Constantine	Algeria	6,61	36,28	694
21	Skikda	Algeria	6,95	36,93	7
22	Annaba	Algeria	7,81	36,83	4
23	In Salah	Algeria	2,46	27,2	293
24	In Aménas	Algeria	9,63	28,05	562
25	Cairo	Egypt	31,4	30,13	74
26	Port Said	Egypt	32,23	31,28	6
27	Salloum	Egypt	25,18	31,53	6
28	Mersa Matruh*	Egypt	27,21	31,33	30
29	Alexandria/E.N.	Egypt	29,95	31,2	7
30	Aswan*	Egypt	32,78	23,96	194
31	Kharga	Egypt	30,53	25,45	73
32	Luxor	Egypt	32,7	25,66	88
33	Dakhla	Egypt	29	25,48	111
34	Asyut	Egypt	31,16	27,2	52
35	Asyut – Airport	Egypt	31,01	27,05	70
36	Hurghada	Egypt	33,73	27,28	7
37	Minya	Egypt	30,73	28,08	40
38	Baharia	Egypt	28,9	28,33	130
39	Helwan*	Egypt	31,33	29,86	141
40	Siwa	Egypt	25,48	29,2	13
41	El Adem	Libya	23,9	31,81	155
42	Benina	Libya	20,26	32,08	132
43	Zuara	Libya	12,08	32,88	3
44	Tripoli Internat.	Libya	13,15	32,66	81

(Continued)

Table 1. (Continued).

	Station	Country	Longitude	Latitude	Altitude (m asl)
45	Misurata	Libya	15,05	32,31	32
46	Kufra	Libya	23,3	24,21	435
47	Sebha	Libya	14,43	27,01	432
48	Gialo	Libya	21,56	29,03	60
49	Hon	Libya	15,95	29,13	267
50	Tessalit	Mali	0,98	20,2	491
51	Menaka	Mali	2,21	15,86	278
52	Kidal	Mali	1,35	18,43	459
53	Gaya	Niger	3,45	11,88	203
54	Maine-Soroa	Niger	11,98	13,23	337
55	Niamey Airp.	Niger	2,16	13,48	227
56	Birni-N'Konni	Niger	5,25	13,80	273
57	Maradi	Niger	7,08	13,46	373
58	Zinder	Niger	8,98	13,78	453
59	Tillaberry	Niger	1,45	14,20	210
60	N'guigmi	Niger	13,11	14,25	286
61	Tahoua	Niger	5,25	14,90	391
62	Agadez	Niger	7,98	16,96	502
63	Bilma	Niger	12,91	18,68	357
64	Maiduguri	Nigeria	13,08	11,85	35
65	Kano	Nigeria	8,53	12,05	481
66	Yola	Nigeria	12,46	9,23	174
67	Minna	Nigeria	6,53	9,61	260
68	Wadi Halfa	Sudan	31,48	21,81	183
69	Damazine	Sudan	34,38	11,78	470
70	Nyala	Sudan	24,88	12,05	674
71	En Nahud	Sudan	28,43	12,70	564
72	El Obeid *	Sudan	30,23	13,16	574
73	Geneina	Sudan	22,45	13,48	805
74	Kosti	Sudan	32,66	13,16	381
75	El Fasher	Sudan	25,33	13,61	730
76	Juba *	Sudan	31,60	4,86	457
77	Ed Dueim	Sudan	32,33	14,00	378
78	Wad Medani	Sudan	33,48	14,4	408
79	Gedaref	Sudan	35,4	14,03	599
80	Khartoum *	Sudan	32,55	15,6	380
81	Kassala	Sudan	36,40	15,46	500
82	Shendi	Sudan	33,43	16,70	360
83	Atbara	Sudan	33,96	17,70	345
84	Wau	Sudan	28,01	7,70	438
85	Karima	Sudan	31,85	18,55	249
86	Gebeit	Sudan	36,83	18,95	796
87	Tokar	Sudan	37,73	18,43	19
88	Dongola	Sudan	30,48	19,16	226
89	Malakal *	Sudan	31,65	9,55	388
90	Abu Hamad	Sudan	33,31	19,53	312

(Continued)

Table 1. (Continued).

	Station	Country	Longitude	Latitude	Altitude (m asl)
91	Port Sudan	Sudan	37,21	19,58	2
92	Suakin	Sudan	37,33	19,10	3
93	Bouso	Chad	16,71	10,48	336
94	Am Timan	Chad	20,28	11,03	436
95	N'Djamena	Chad	15,03	12,13	295
96	Bokoro	Chad	17,05	12,38	301
97	Mongo	Chad	18,68	12,18	428
98	Abeche	Chad	20,85	13,85	549
99	Bol-Berim	Chad	14,73	13,43	292
100	Ati	Chad	18,31	13,21	334
101	Mao	Chad	15,31	14,11	355
102	Moundou	Chad	16,06	8,61	422
103	Faya	Chad	19,16	18,00	234
104	Pala	Chad	14,91	9,36	455
105	Sarh	Chad	18,38	9,15	365
106	Gabes	Tunisia	10,10	33,88	5
107	Gafsa	Tunisia	8,81	34,41	314
108	Kairouan	Tunisia	10,10	35,66	68
109	Tunis/Carthage	Tunisia	10,23	36,83	4
110	Jendouba	Tunisia	8,80	36,48	144

stationarity can be expected if the arithmetic means of the chosen subintervals lie completely within this span.

The homogeneity is identified by the Abbe test (Equation 2) and with the help of the double mass curves (Dyck, 1980):

$$1 - \frac{1}{\sqrt{n-1}} \leq \frac{2 \cdot A}{B} \leq 1 + \frac{1}{\sqrt{n-1}}$$

$$A = (x_1 - x)^2 + (x_2 - x)^2 + \dots + (x_n - x)^2 - \frac{1}{2} [(x_1 - x)^2 - (x_n - x)^2] \tag{2}$$

$$B = [(x_1 - x) - (x_2 - x)]^2 + [(x_2 - x) - (x_3 - x)]^2 + \dots + [(x_{n-1} - x) - (x_n - x)]^2$$

where n = sample size, x = arithmetic mean and x_i = value of the time series at a specific time i .

Owing to the high climate variability in the investigated arid to dry-subhumid climates, outliers within the time series are expected, but detailed time-series analysis for seven climate stations along the N-S transects shows that distinct outliers do not occur. In view of the methods we plan to apply, the monthly data set are transformed into annual values. The annual temperature results from the arithmetic mean of the respective 12 monthly values. Several missing values are included in the calculation. Because of the low variability within the temperature time series the possible resultant error is marginal. By contrast, the annual precipitation amount that results from the sum of monthly values is only calculated for years in which all 12 monthly values are available. Years with at least one missing monthly value are classified as a default value.

11.2.2 Methods

Climate classification

For climatic classification a cluster analysis is applied. The hierarchical clustering method is based on monthly precipitation and temperature data (24 variables) of the 110 climate stations of the clino-period of 1961–1990. These 110 climate stations are located in the area of interest (52 stations) as well as in adjoining regions in northern Africa according to the supra-regional characters of the atmospheric circulation (58 stations) (cf. Table 1). The clustering algorithm used is Ward's method in combination with the Squared Euclidean Distance (Fovell and Fovell, 1993; Kalkstein *et al.*, 1987). The input variables are identified by applying a principal component analysis to generate a reduced number of factors out of many potential relevant variables still explaining almost the whole variance of the original data set (Bahrenberg *et al.*, 2003; Fovell and Fovell, 1993).

Rainfall variability

Rainfall variability is analysed for the 1961–1990 period. It is described by the coefficient of variation which corresponds to the ratio of the standard deviation to the mean. The coefficient of variation is expressed as a percentage (Schönwiese, 2000; Linacre, 1992).

Time series analysis

Climatic variations and long-term trends within the time series of precipitation and temperature are analysed by a trend analysis of annual data for seven climate stations along a N–S transect running parallel to the River Nile, representing different climatic regions. The trends of both the annually averaged (temperature) and annually accumulated (precipitation) climate parameters are represented by absolute and relative values, calculated under specification of the coefficient of determination (R^2) and trend-to-noise ratio (Tr/N) (Rapp, 2000). According to Schönwiese (2000) a trend-to-noise ratio of about 2 implies a level of significance of 95%. Calculation of trend-to-noise ratio requires normal variables (Schönwiese, 2000).

Additionally to the trend analysis, the time series is smoothed with a five-year moving average (Schlittgen and Streitberg, 1989). Gaps in the middle of the time series are incorporated into the trend analysis, and time series are cut when a gap of more than three years appears at the beginning or end of the time series. To characterise the long-term precipitation behaviour, precipitation values are z-standardised (referring to the 1961–1990 period) in terms of mean and standard deviation (SD) (Trilsbach and Hulme, 1984). On this basis two matrices are produced which contrast wet sequences (+1 SD) with dry sequences (–1 SD).

11.3 RESULTS

11.3.1 Classification

A harmonic and steady climate description of the area of interest is generated by applying Ward's method for cluster analysis and seven as the chosen number of clusters. Based on the mean monthly temperature and precipitation data (in total: 24 variables), three new variables are designed using the principal component analysis to explain the

bulk of the variance. The resulting variables, subsequently taken as input variables for the cluster analysis, are: mean annual temperature, mean added precipitation of the May–October period, and mean added precipitation of the November–April period. In the resulting cluster-analysis-based climate classification, zonal structure is clearly displayed and climate stations are clearly assignable (Figure 3).

Cluster 1 and cluster 7 represent mountainous regions and comprise climate stations located in parts of the Atlas Mountains (cluster 1) and the highlands of the Central African Republic (cluster 7). Cluster 2 describes a small zone along the NE African Mediterranean coast. Towards the south, the two clusters 3 and 4 follow, both predominantly characterised by arid conditions (Figure 3). Clusters 3 and 4 differ with regard to the duration and arrival of the rainy season; the boundary between both clusters is located between 22 and 25°N. Between 11 and 14°N cluster 5 affiliates to cluster 4. Compared to the broad zones of clusters 3 and 4, cluster 5 is only small

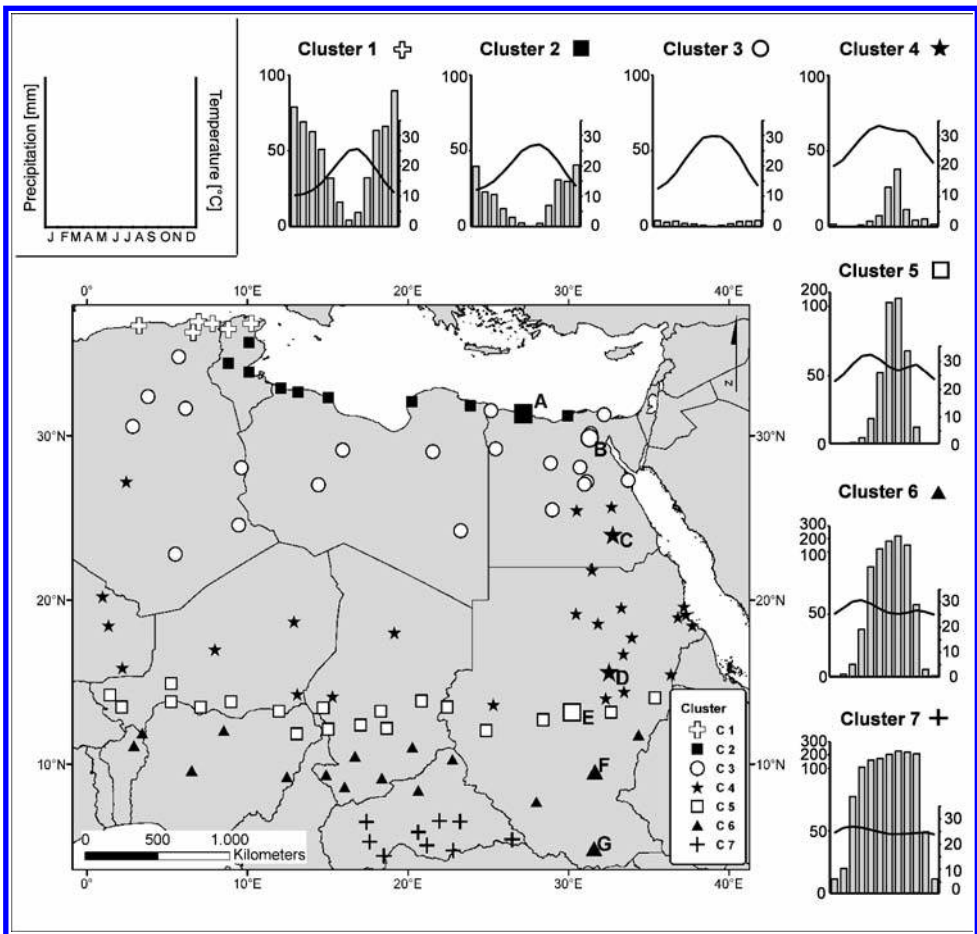


Figure 3. Climate classification of NE Africa and adjacent areas based on the results of the cluster analyses using Ward’s method. Climate charts represent mean monthly values of precipitation and temperature of all stations within a cluster of the reference period 1961–1990. Symbols mark locations of climate stations listed in Table 1. A–G mark the climate stations along the N–S transect that were chosen for time series analysis (Figure 2).

in size. The southward adjoining cluster 6 has less zonal character and encompasses primarily climate stations which are located in the area between 12°N and 7°N in the north of Nigeria and south of Chad and Sudan. Clusters 1–3 show rainfall prevailing during the winter season, between November and April. The annual amount of rainfall is highest in cluster 1 and decreases towards cluster 3, where winter rainfall is erratic. Clusters 4–7 display an increase of rainfall from north to south with a general occurrence of summer rainfall. The annual temperature also increases from north to south. This is accompanied by a change of the seasonal cycle of annual temperature from one distinct peak in July and August in the northern clusters (clusters 3 and 4) to two weaker peaks in April/May and October in the southern clusters (cluster 5–7).

11.3.2 Rainfall variability

Rainfall variability coefficients are given in percentages for 1961–1990 as reference period (Figure 4). A calculated maximum rainfall variation coefficient of about 360% is detected for the climate station at Dakhla (Egypt). Corresponding values for the neighbouring climate stations at Luxor and Aswan total 290% and 270%. In general, the rainfall variation coefficients total more than 150% in central and southern Egypt, in northern Sudan and eastern Libya (Figure 4). This concentration of high rainfall

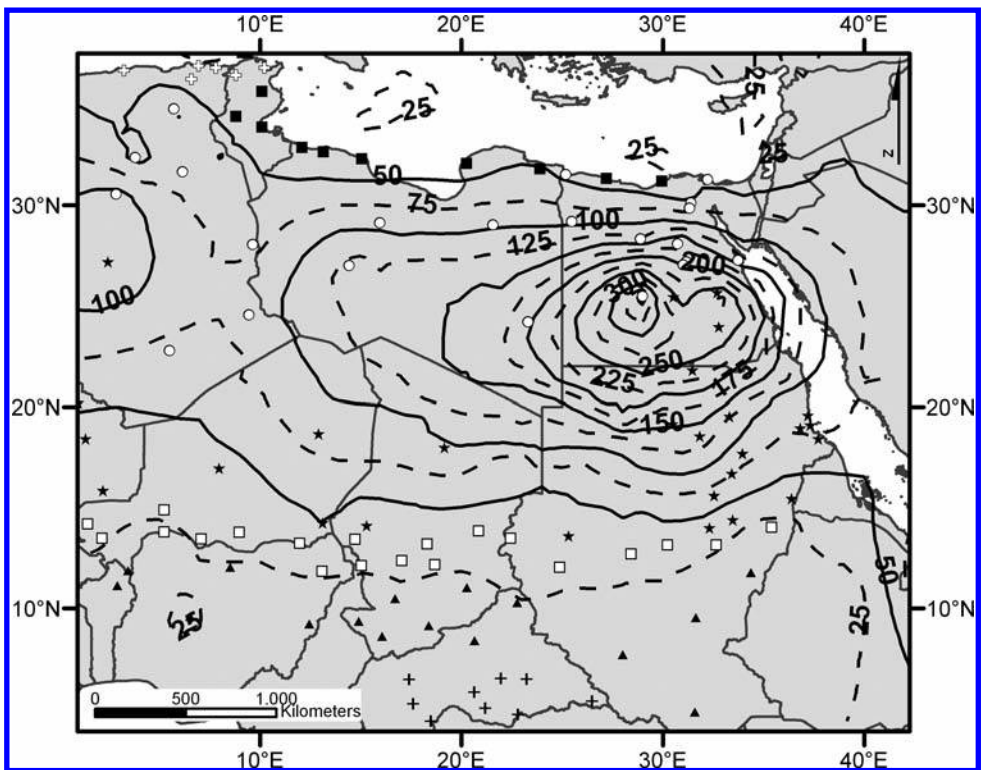


Figure 4. Rainfall variability coefficients given in percentage to the clino-period 1961–1990 as reference period. For symbols of clusters 1–7 see legend Figure 3.

variation coefficients in the central Libyan Desert shows a radial decrease of rainfall variability: to the north, along the Mediterranean coast, rainfall variation coefficients total 30–50%. To the west, in the central and western Sahara, another maximum, slightly smaller than in the Libyan Desert, occurs with 110–120% rainfall variability coefficients at the climate stations of In Salah and El Golea. To the south, towards the equator, rainfall variability decreases to values of 10–25%.

11.3.3 Time series analysis

For quality control of the cluster-analysis-based climate classification, seven climate stations were selected along a N–S transect reaching from the Mediterranean to the Sahel and covering the major zonal and altitudinal units. Annual average temperature and annual accumulated precipitation data were subjected to a time series analysis to verify resilience of the climate data because of their high variability and to identify superordinate elements of climate dynamics.

Mean annual temperatures

To accentuate variations of the mean annual temperature, data are plotted as the difference to the average of the clino-period 1961–1990. Analysis of the linear trend of this annual mean temperature deviation of the seven selected climate stations reveals strong oscillations and different developments.

The short time series of Mersa Matruh climate station (Figure 5A; cluster 2) shows a distinct negative trend of mean annual temperatures since the 1950s, superimposed by increasing mean annual temperatures since the 1980s. The climate station at Helwan (Figure 5B), assigned to cluster 3, provides climate data for the entire 20th century. The mean annual temperatures show a slight overall increase since the early 20th century.

An extended warm period between 1920 and 1940 is conspicuous, whereas mean annual temperature deviation and corresponding mean annual temperature have decreased since the early 1940s and reached a low point in the early 1960s. Since the early 1960s, mean annual temperatures have constantly increased while continuously subject to strong oscillations. The climate stations at Aswan (Figure 5C) and Khartoum (Figure 5D) are both located in cluster 4. A negative trend of annual mean temperature deviations is visible. For Aswan climate station, distinct above-average mean annual temperature deviations between 1920 and 1975 result from the low reference value averaged for the clino-period 1961–1990, affected by the continuously decreasing mean annual temperatures since 1975. In Khartoum the warm period in the early 20th century lasted only until 1940, followed by a cool phase lasting for 10 years and slightly but continuously increasing mean annual temperatures since 1955. The climate station at El Obeid (Figure 5E) is allocated to cluster 5, with the available time series covering the period from 1940 to 1990. Whereas during the 1940s and 1950s mean annual temperatures oscillate around the average, they reach minimum values during the 1960s. Since the early 1970s, mean annual temperatures have been subject to an ongoing increase with persisting strong oscillations. The climate stations at Malakal (Figure 5F) and Juba (Figure 5G) are both allocated to cluster 6. Both data series cover the period since 1940 and end in the 1990s. Data of mean annual temperature deviations of Malakal climate station are subject to strong oscillations without a clear trend. By contrast, data of mean annual temperature deviations at Juba climate station show a clear positive trend for the 1950–1985 period. Furthermore, the time series

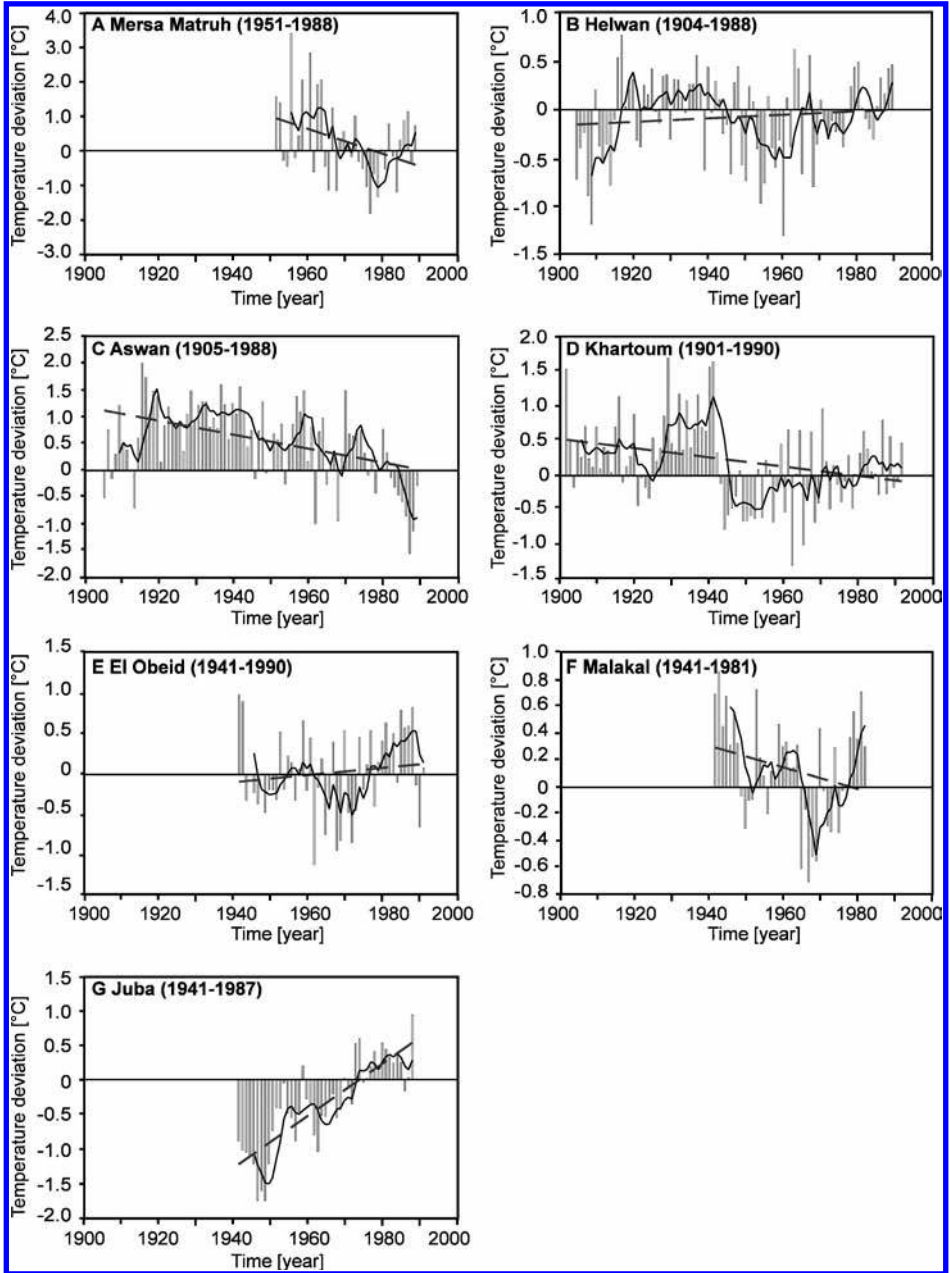


Figure 5. Mean annual temperature plotted as the difference to the average of the clino-period 1961–1990 of the selected stations along the N–S transect (A–G); grey columns: deviation of annual temperature from the long-term mean (reference value: 1961–1990); dashed grey line—specification of linear trend; black curve—five-year moving average.

Table 2. Results of the temperature trend analysis; indication of coefficient of determination (R^2), trend-to-noise ratio (Tr/N) and absolute trend value (Tr-abs).

Station	Period	R^2	Tr/N	Tr-abs
A Mersa Matruh	1951–1988	0,12	-1,14	-0,45
B Helwan	1904–1988	0,01	0,34	0,15
C Aswan	1905–1988	0,19	-1,50	-1,09
D Khartoum	1900–1990	0,09	-1,05	-0,63
E El Obeid	1941–1990	0,02	0,43	0,22
F Malakal	1941–1981	0,06	-0,84	-0,33
G Juba	1941–1987	0,68	2,77	1,76

of mean annual temperature deviations of Juba climate station shows a trend-to-noise ratio (Tr/N) of 2,77, confirming the statistical significance of the described trend. By contrast, the mean annual temperature time series of the other climate stations under discussion do not document significant trend developments, neither for the coefficient of determination nor for the trend-to-noise ratio (Table 2).

Annual precipitation

The comparative trend analysis of the mean annual temperature deviations shows that long-term temperature development is highly regional in character. Compared to the mean temperature deviation time series, the rainfall time series have rather weakly pronounced periods. By contrast, trend analysis of the precipitation time series indicates some supraregional features. Time series show the difference between the annual precipitation and the average annual precipitation of the clino-period 1961–1990, displayed as annual precipitation deviation (Figure 6). All time series indicate a negative trend of annual precipitation for the available measurement periods. However, coefficients of determination are not significant ($\Delta > 0,05$), and trend-to-noise ratio values remain low (Table 3). In summary, none of the rainfall trend developments shown in Figure 6 is statistically significant.

In general, an intermittent decrease of annual rainfall coincides with a decrease in the length and intensity of humid periods. Wet and dry phases alternate regularly, comparable to oscillations (Figure 6). Repeatedly pronounced wet years are followed by pronounced dry years (Figure 7). In addition, all time series analysed (Figure 6) show almost constantly higher positive anomalies than negative anomalies related to the reference values of the clino-period.

At Mersa Matruh climate station (Figure 6A; cluster 2), several wet periods were recorded during the first half of the 20th century. Above-average wet years occurred mainly in the 1920s and 1930s. Dry periods were also repeatedly recorded, increasingly during the second half of the 20th century. Wet and dry years vary in the range of the reference values. At Helwan climate station (Figure 6B; cluster 3), a decline of wet years is also visible, especially when the first and the second half of the 20th century are compared (Figure 7). On the whole, the first half of the 20th century was much wetter than the present, briefly interrupted by a dry phase in the late 1930s. From the 1950s to the end of the time series, the frequency of drier years increased, in conjunction with a balanced fluctuation around the reference value. At Aswan climate station (Figure 6C; cluster 4), a distinct wet period was recorded in the 1940s. From the 1950s onwards, wetter and drier periods alternate; however, the most recent wet periods

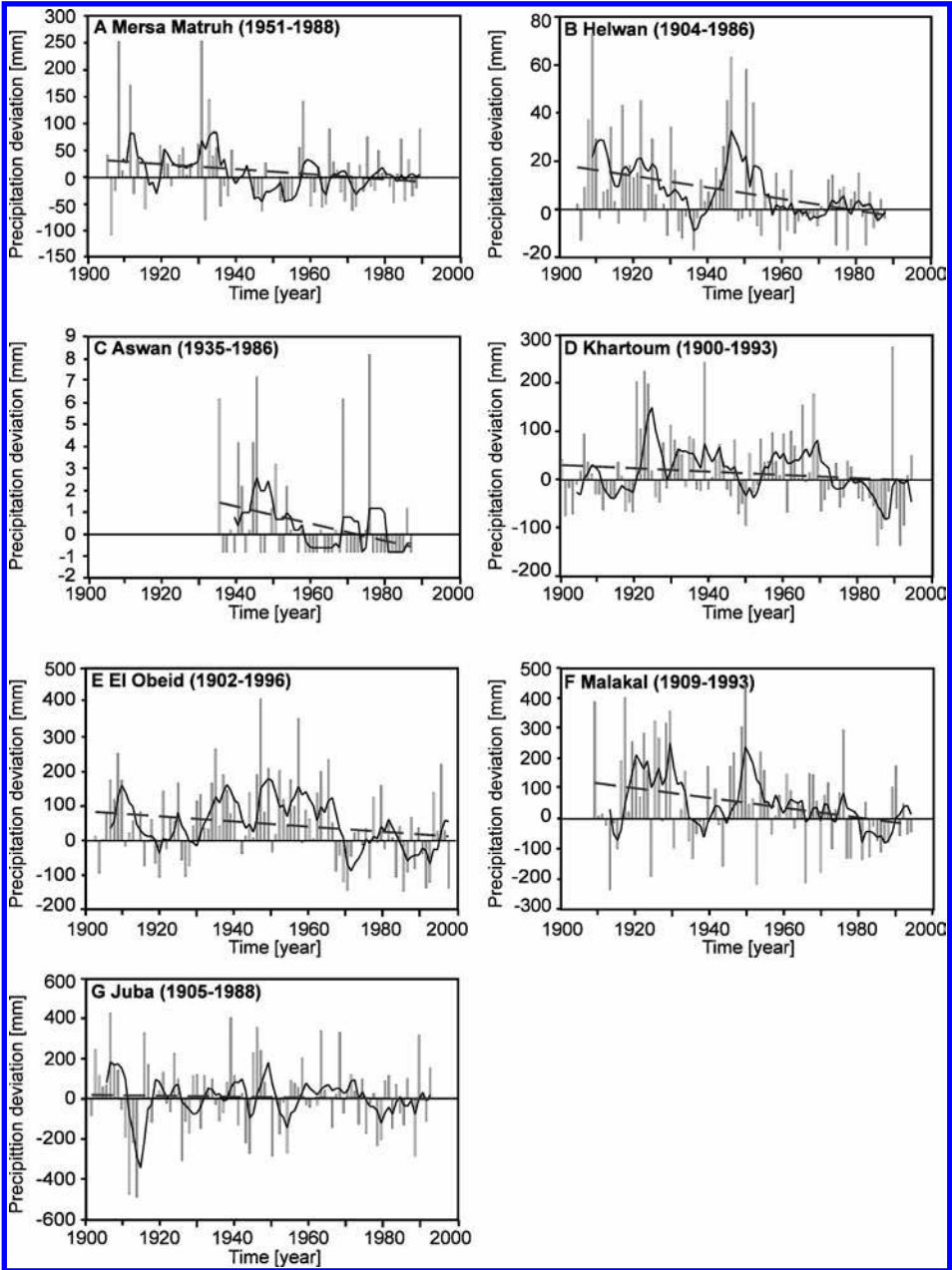


Figure 6. Annual precipitation time series plotted as the difference to the average annual precipitation of the 1961–1990 clino-period of the selected stations along the N–S transect (A–G); (grey columns: deviation of annual temperature from the long-term mean (reference value: 1961–1990); dashed grey line—specification of linear trend; black curve—five-year moving average).

Table 3. Results of the precipitation trend analysis; indication of coefficient of determination (R^2), trend-to-noise ratio (Tr/N), absolute trend value (Tr-abs), relative trend value (Tr-rel) and rainfall variability (r_v ; reference period: 1961–1990).

Station	Period	R^2	Tr/N	Tr-abs	Tr-rel	r_v (%)
A Mersa Matruh	1905–1988	0,0330	–0,013	0,87	–0,0060	34,7
B Helwan	1904–1986	0,0990	–0,115	–2,13	–0,0800	52,0
C Aswan	1935–1986	0,0670	–0,390	–0,92	–0,7400	271,3
D Khartoum	1900–1993	0,0140	–0,005	–0,36	–0,0020	63,8
E El Obeid	1902–1996	0,0350	–0,006	–0,70	–0,0020	33,0
F Malakal	1909–1993	0,0700	–0,008	–1,17	–0,0020	16,3
G Juba	1901–1991	0,0010	–0,001	–0,14	–0,0001	16,1

did not reach the intensity recorded during the 1940s. At Khartoum climate station (Figure 6D; cluster 4) and El Obeid climate station (Figure 6E; cluster 5), the period of relatively increased rainfall at Aswan climate station observed in the 1940s can be confirmed. However, a subsequent markedly dry period as observed for the northward located climate stations (Figure 6A–C) cannot be confirmed. Compared to the present, the 1950s and 1960s at Khartoum and El Obeid climate station showed above-average humidity, repeatedly interrupted by short dry phases. Since the late 1960s, the climate at both stations has become distinctly drier, evidenced by the decreasing annual rainfall (Figure 6) as well as by the increasing frequency of dry years (Figure 7). At Malakal climate station (Figure 6F; cluster 6), rainfall records show above-average values for the 1916–1931 and 1946–1953 time spans, whereas during the 1930s annual rainfall oscillates around the average of the 1961–1990 clino-period. Since the late 1950s, however, annual rainfall has again fluctuated around the clino-period average, indicating a period of distinctly lower annual precipitation and an increasing number of dry years in the 1980s. In contrast to the development of annual rainfall as described for the climate stations in Egypt and central Sudan, a significant decrease of annual precipitation at Juba climate station (cluster 6) cannot be confirmed. High variability of annual rainfall is documented by a smooth run of the values with a balanced fluctuation around the reference value of the clino-period (Figure 6G) and the repeated occurrence of dry and wet years (Figure 7).

11.4 DISCUSSION

11.4.1 Cluster-analysis-based climate classification

The climate classification achieved by cluster analysis of mean monthly temperature and precipitation data (Figure 3) also differentiates the overall temperature regimes as reflected by the temperature and precipitation regimes. The winter rainfall characterising clusters 1–3 results from the Westerlies and is brought by cyclones shifting from west to east across the Mediterranean Sea. Locally mountainous coastal zones form a natural barrier to these cyclones and thus receive particularly high amounts of winter rainfall (cluster 1). By contrast, climate stations assigned to cluster 2 are located along the coastal areas of Libya and Egypt without any direct connection to orographic barriers. These stations obtain distinctly less precipitation than those attributed to cluster 1 because of their lack of orographic exposure (Mensching and

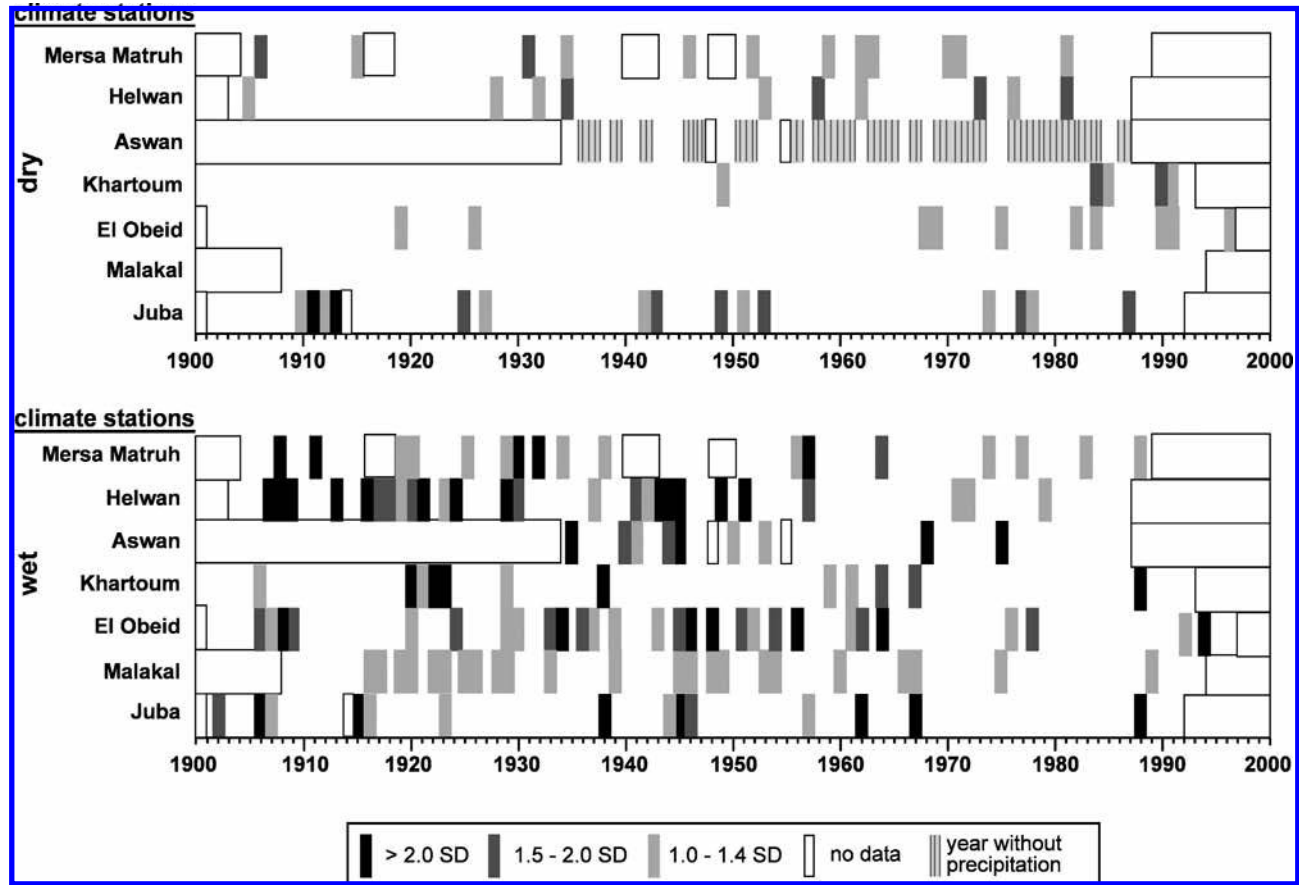


Figure 7. Wet (+) and dry (-) years referring to z-standardised standard deviation SD (reference period: 1961–1990). Years without symbols represent ‘normal’ years, not characterised by excessive dryness or wetness.

Wirth, 1989; Herz, 1970). The West–East alignment of the northeast African coastline causes coastal divergence effects and thus downward-moving air masses and cloud dissolution (Weischet and Endlicher, 2000). Inland of the Mediterranean coast, a rapid and pronounced decrease of precipitation occurs (Figure 3; climate charts of cluster 2 and cluster 3), indicating a small-scale change from a semi-arid to an arid climate. The annual temperature in clusters 1–3 increases in the same manner. Climate charts of clusters 1–3 uniformly show a single temperature peak during summer, caused by maximum insolation due to the high position of the sun and a lack of cloud cover (Tschierschke, 1998).

In contrast to clusters 1–3, clusters 4–7 show distinct summer rainfall. Precipitation of climate stations subsumed in clusters 4–7 is brought by the African SW monsoon, whose easterly extension reaches Khartoum (Scherhag and Lauer, 1982). The magnitude and duration of the summer rainy season and, correspondingly, the amount of annual precipitation increase from north to south as a result of the longer influence of the moist monsoonal air masses which is directly linked to the duration of the rainy period (Herz, 1970). The lack of orographic barriers results in a wide-ranging zonal classification, describing the seasonal shift and magnitude of the African SW monsoon. Finally, climate charts of clusters 4–7 clearly display the seasonal cycle of solar position, as a result of which the annual temperature curve tends to form two peaks. From the Mediterranean Sea to the Equator, the temperature graphs of the climate charts of clusters 1–7 clearly show that the climate changes from a distinct seasonal climate with one maximum (clusters 1–3) to a balanced seasonal cycle with low fluctuations and two smaller temperature maxima (cluster 4–7). In climate charts of clusters 4–7, temperatures also reflect the seasonal influence of the SW monsoon, effecting a reduced insolation due to precipitation and cloud cover (Blüthgen and Weischet, 1980; Elagib and Mansell, 2000; Klaus, 1981).

In the cluster-analysis-based climate classification, differentiation of the hyper-arid areas of the central and eastern Sahara into cluster 3 and cluster 4 is ambiguous. Modelled climate charts (Figure 3) show marked differences in seasonality of rainfall with a faint winter rainy season for cluster 3 and a distinct summer rainy season for cluster 4. However, climate stations considered in the cluster analysis show no evident rainy season at all, as their data records include several years without any rainfall. According to Shahin (1985), rainfall in the area of Lower Egypt and along the Libyan and west Egyptian Mediterranean coast is theoretically always possible from September to May. Comparable statements exist for the central part of the Sahara according to cluster 4, where Grunert (1979) states that rainfall is possible during all seasons but cannot be expected. Altogether, differences between the climate stations in the transition zone between cluster 3 and 4 are too small to allow a distinct differentiation exclusively based on the precipitation data. The cluster-analysis-based classification for this transition zone is mainly based on the annual temperature data. To improve the classification results within the hyperarid regions, integration of additional variables such as daily rainfall data and monthly air pressure data is required. However, the quality of cluster-analysis-based climate classification is heavily dependent on the number and allocation of climate stations and the quality of available data.

A comparison of the results of the cluster-analysis-based climate classification with the global climate classifications after Köppen-Geiger, Troll-Paffen and Lauer-Frankenberg (Figure 8) reveals congruences as well as divergences: all the climate classifications mentioned have an almost zonal arrangement in common, while several mountainous areas appear as insular areas. The climate classification after Köppen-Geiger shows the fewest matches with the cluster-analysis-based climate classification.

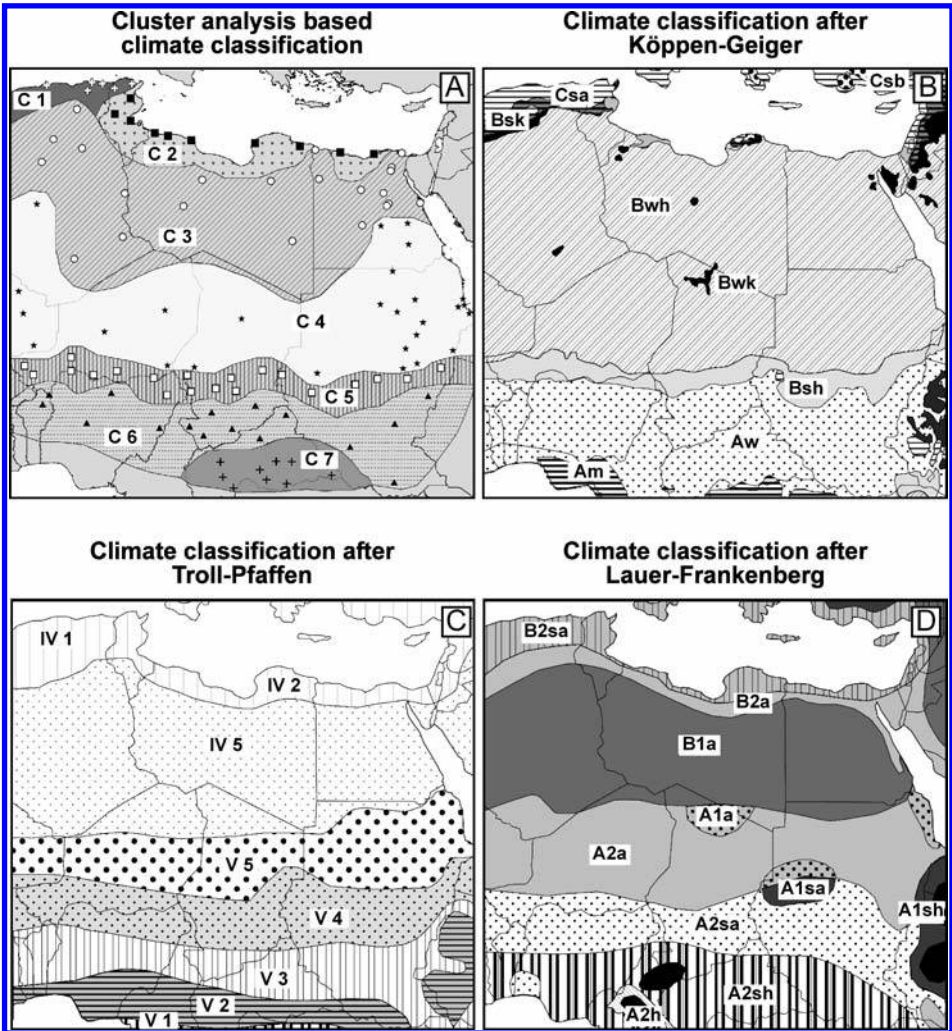


Figure 8. Comparison of the climatic classifications for NE Africa based on cluster analysis (A), after Köppen-Geiger (B; map source: Kottek *et al.*, 2006), after Troll-Paffen (C; map source: Scherhag and Lauer, 1982) and after Lauer-Frankenberg (D; map source: Frankenberg, 1995).

The Köppen-Geiger system's strong reference to vegetation dissemination and distribution limits does not allow the differentiation of the Sahara into the northern part, predominantly influenced by the seasonal change between trade winds and Westerlies, and the southern part, to a greater extent influenced by the seasonal change between trade winds and SW monsoon.

The cluster-analysis-based differentiation of arid climates along the Mediterranean coast and in the Sahara desert shows multiple analogies to the climate classifications after Troll-Paffen and Lauer-Frankenberg. However, delimitations between areas under greater subtropical or tropical influence apparently cannot be drawn reliably due to the low density of available climate stations (differentiation between a) cluster 3 and 4, b) Troll-Paffen's climate zones IV5 and VI, c) Lauer-Frankenberg's climate zones

B1a and A2a). South of the Sahara, the increasing annual rainfall amount as well as the increasing reliability of the occurrence of the rainy season is displayed in all four climate classifications (Figure 8). This is documented by the transition from the semi-arid to the dry-subhumid and semi-humid conditions as well as by the increase of the length of rainy seasons of the respective climate zones and the corresponding clusters.

The climate classification after Troll-Paffen features the most similarities with the results of the cluster-analysis-based climate classification. This agreement includes the differentiation between tropical and subtropical arid climates of the Sahara as well as the depiction of the Sahel (Figure 8; (A) cluster 5 and (C) V4 climate). By contrast, the Sahel zone is not clearly distinguished from the southern fringe of the Sahara in the climate classification after Lauer-Frankenberg (Figure 8).

11.4.2 Rainfall variability

The rainfall variability data in the databases of FAO and the Global Historical Climatology Network match well with those of Elagib and Mansell (2000), Gießner (1989) or El Tom (1972). Comparable analyses exist predominantly for climate stations in Sudan. For El Fasher/Sudan, Gießner (1989) specifies a rainfall variability of 29,5%, which fits in with the data calculated by this study, totalling 32,7%. The increasing rainfall variability coefficient from the equator northward to the Egyptian Libyan desert (Figure 4) corresponds to the observations of Elagib and Mansell (2000). For the climate stations at Ed Damazin and Dongola they quote rainfall variabilities of 13,85% (calculated value of this study: 13,0%) and 122,9% (calculated value of this study: 148%) referring to the 1940–1996 period (Elagib and Mansell, 2000). Differences of data can be explained by unequally long data records. A rainfall variability gradient for the Sudan presented by El Tom (1972) for the 1931–1960 clino-period nicely reflects the situation as displayed in Figure 4 (1961–1990 clino-period). The highest rainfall variability coefficients of about 246% are documented by El Tom (1972) for the northern border of Sudan. In comparison, for the climate station of Wadi Halfa the rainfall variability coefficient totals 248,5% for the 1961–1990 clino-period (cf. Table 3).

In summary, it can be pointed out that climate stations within the dry areas (Figure 3, cluster 3 and 4) show highest rainfall variabilities (Figure 4). This relation between increasing rainfall variability and increasing aridity has been pointed out by Dahamsheh and Aksoy (2007) and by Elagib and Addin Abdu (1997), among others. The highest rainfall variability coefficients can be found in areas with permanent arid conditions where rainfall appears erratic but might occur more or less throughout the year. This area is located in the transition zone between the influence of the Westerlies and the SW monsoon. The uncertainty of allocating rainfall to its origin in this region reflects the results of the cluster analysis.

11.4.3 Time series analysis

An increase of global temperature during the 20th century according to IPCC (2002) is specified by Ruddiman (2008) and Burroughs (2003), whose studies show a global warming with two warm phases from 1901–1944 and 1977–1999 that are interrupted by a cooling-off period. For the climate stations along the N–S-transect, the shortness of the measurement period means that this warming phase stated for the early 20th century can only be confirmed for Helwan, Aswan and Khartoum climate stations, as measurement periods did not start until the 1940s at the Mersa Matruh, El Obeid,

Malakal and Juba climate stations. By contrast, the cooling phase in the middle of the 20th century can be confirmed for all the climate stations, even when the magnitude of cooling is highly variable. The warming phase in the late 20th century is monitored along the entire N–S-transect; only at Aswan climate station have annual average temperatures decreased since the late 1970s (Figure 5C). A slight cooling-off at Aswan climate station at the beginning of the 1980s is also confirmed by Domroes and El-Tantawi (2005). However, they confirm an increase of annual average temperature from 1971 to 2000 for Egyptian climate stations. Sudanese climate stations are analysed by Elagib and Mansell (2000), who detect a temperature increase in the period of 1941–1996 especially in the central and southern regions (also compare Figure 5D–G).

Temperature anomalies observed within the time series may be affected by the North Atlantic Oscillation (NAO). Analyses of the NAO's influence on winter temperature in Egypt were performed by Hafez and Robaa (2008), Hasanean (2004) and Hasanean (2001), who confirm significant correlations between the occurrence of NAO and negative temperature anomalies, predominantly confirmed for the western and central parts of Egypt. Comparable interrelations are also proved for the adjacent territory of Israel (Hasanean, 2001; Ben-Gai *et al.*, 1999). Checking the accordance of NAO events and temperature anomalies of the climate data available for the climate stations along the N–S transect reveals only weak interrelations. At Helwan climate station, for example, an accumulation of warm years in the 1930s coincides with a number of years with a negative NAO index. However, unlike during the 1950s, distinct negative temperature anomalies do not show any correlations to NAO index (Climatic Research Unit, 2004). In contrast to NAO events, El Niño-Southern Oscillation (ENSO) events do not seem to have any influence on the annual average temperatures at the climate stations examined. This is also confirmed by Hasanean (2004), who confirms the lack of significant statistical correlation between ENSO events and measured temperatures at Egyptian climate stations. By contrast, Hafez and Robaa (2008) confirm a significant relation between anomalies of autumn temperatures and the occurrence of El Niño events in the southwest of Egypt.

As well as ENSO and NAO events, volcanic eruptions may also have an effect on short-term temperature fluctuations. Within the observation period two big volcanic eruptions took place: Mount Agung in 1963 and El Chichón in 1982. For the Middle East and NE Africa, a cooling during the first and second winters after the Mount Agung eruption was detected (Graf, 2002; Robock and Mao, 1995). Also the climate stations examined along the N–S transect (Figure 2) uniformly show a negative temperature anomaly for the year 1964 as a possible consequence of the Mount Agung eruption. By contrast, a short cooling following the El Chichón eruption appears quite heterogeneous: at Helwan and Aswan climate stations cooling tendencies already began in 1981, before the El Chichón eruption, whereas at Khartoum climate station a negative temperature anomaly is first indicated in 1984. Only Mersa Matruh and El Obeid climate stations show a short-time cooling in the years 1982 and 1983. However, the assignment remains uncertain owing to a possible distortion of the volcanic signal by concurrent El Niño/ENSO events in 1963/64 and 1982/83 (Kelly *et al.*, 1996, Robock and Mao, 1995).

Evaluation of the time series of rainfall anomalies at the climate stations along the N–S transect discloses a lack of zonal connectivity as demonstrated by the analysis of the temperature anomalies (Figure 6). Differences in the development of wet and dry periods, which are also visible at climate stations located in the respective cluster, are mainly attributed to the high rainfall variability (Figure 4). This relation is in particular valid for the arid and semiarid areas. Already Trilsbach and Hulme (1984) proved that rainfall in NE Africa has a high spatial and temporal variability that may cause the coeval incidence of a dry year and a wet year at neighbouring areas at the regional scale. At the climate stations analysed along the N–S transect, dry and wet phases alternate

during almost each decade. However, supra-regional, concurrent periods of average annual precipitation, as mentioned above, cannot be clearly accounted for (Figure 7). In general, the beginning of a wet phase—as marked by increasing positive annual precipitation anomalies—as well as its duration and peak can temporarily shift between the different climate stations by 1–4 years. Also Buckle (1996) and Mainguet (1994) observe alternating wet and dry phases for the Sahel. The dry periods are partly marked as droughts and lasted from 1912–1915, 1925–1928, 1940–1944, 1947–1949, 1968–1973, and 1977–1985 (Buckle, 1996; Mainguet, 1994). In the available data sets for the climate stations along the N–S–transect these dry phases are only partially confirmed (Figure 6, Figure 7). In addition, a decrease of frequency of wet phases during the 20th century is generally indicated (Figure 7) and is confirmed by various authors (Burroughs, 2003; IPCC, 2002; Elagib and Mansell, 2000; Davies and Alredaisy, 1995; Hulme, 1992; Gläser *et al.*, 1989). Giannini *et al.* (2003) and Paeth and Friedrichs (2004) point out the connection between dry and wet sequences in Sahelian and tropical Atlantic Sea Surface Temperature (SST), in which increasing SST means an increased occurrence of dry periods and droughts. According to Giannini *et al.* (2003), this caused the negative trend of rainfall from the late sixties to the eighties.

Closely linked with the effects of SST, the influence of ENSO on rainfall fluctuations has to be discussed. In the Mediterranean area, ENSO generates an equatorward (El Niño) and poleward (El Niña) dislocation of the winter subtropical jet stream associated with a dislocation of meridional transport of moisture and heat (Price *et al.*, 1998). Correlations for NE Africa's neighbouring areas are shown for Israel and Turkey by Ziv *et al.* (2006), Cullen and deMenocal (2000) and Price *et al.* (1998). An effect of ENSO on climate south of the Sahara has also been considered. Camberlin *et al.* (2001) document a weakening of the SW monsoon as a result of El Niño events and increasing SST. By contrast, Nicholson and Kim (1997) do not identify a primary ENSO signal in Sahelian-Sudanese rainfall time series, although a connection between El Niño and SST as well as SST and Sahelian-Sudanese rainfall has been noticed. Because of missing evidence about ENSO signals in the time series of the northern transect's climate stations, only a few statements can be made (ENSO events after Schönwiese, 2008; Kahya and Karabörk, 2001; Price *et al.*, 1998): at Mersa Matruh and Helwan climate stations, the wet years of 1977 and 1988 as well as 1977–1979 and 1982 coincide with El Niño events, whereas the dry years of 1970–71, 1973 and 1975 can be explained by La Niña events. In the time series of the climate stations south of Sahara, El Niño events cannot be reliably and explicitly identified. For instance, the El Niño event of 1976/67 can be clearly identified in the rainfall records of Malakal and Juba climate stations. Moreover, the El Niño event of 1979 can be clearly identified for Khartoum and Malakal climate stations. The El Niño event of 1989/90 might have triggered the below-average dry years in 1990 and 1991 as detected for Khartoum and El Obeid climate stations. The El Niño events of 1982/83 and 1987/88 are overlapped by the extended dry periods of the 1980s. Nor can effects of La Niña events be identified in the climate records of the climate stations south of the Sahara.

As well as the effects of ENSO events, the influence of NAO on rainfall anomalies has to be assessed. According to Hafez and Hasanean (2000), a positive NAO index during the winter influences wet anomalies at northern Africa extending eastward into the Arabian Sea. This is confirmed by the significant correlations between NAO index and winter rainfall for the data records at Mersa Matruh climate station (Hafez and Hasanean, 2000). Furthermore, positive NAO indices as stated by the Climatic Research Unit (2004) coincide with wet sequences of the climate stations Mersa Matruh and Helwan, both characterised by winter rain in the years 1907–1909, 1918–1923, 1929–1930, 1956–1957. On the other hand, there are wet anomalies that

cannot be assigned to positive NAO indices. For the climate stations Mersa Matruh and Helwan, too, coinciding negative NAO indices and dry anomalies can be identified for the years 1980 and 1981. NAO has no effect on the precipitation records of the climate stations of the N–S transect south of Aswan owing to the unusual weak influence of the Westerlies in these regions (Ben-Gai *et al.*, 1998; Cullen and deMenocal, 2000; Hafez and Hasanean, 2000).

11.5 CONCLUSIONS

Evaluation of the results of the cluster-analysis-based climate classification by comparison with the well-established climate classifications after Köppen-Geiger (Köppen, 1936), Troll-Paffen (Troll and Paffen, 1964) and Lauer-Frankenberg (Lauer *et al.*, 1996) clearly demonstrates the high capacity of the cluster-analysis-based climate classification at least on a supraregional or global scale. Advantages of the cluster-analysis-based climate classification are the very simple input parameters and therefore its general applicability, the input parameters used being monthly temperature and precipitation data—data sets that are in general available for each climate station. The approach presented and evaluated here is applied to subtropical and tropical climates; to confirm general applicability, application of the approach needs to be spatially extended.

The capacity of the cluster-analysis-based climate classification is highly dependent on the reliability of the available data records. In respect of the results of the time series analysis of temperature and precipitation data, it should be mentioned that climate and weather conditions are generally subject to high variability in the area studied. Testing of correlations between temperature and precipitation anomalies and possibly triggering event (ENSO, NAO, volcanic eruption) confirm the high variability of climate data. Furthermore, significant correlations describing the relation between temperature and rainfall anomalies are altogether weak in the present study. In consequence, single parameters cannot explain the whole variance of the fluctuations. In many cases ENSO, NAO or volcanic eruption events do not have a recognisable effect on the climate.

However, the widespread availability of data sets on monthly temperature and precipitation makes the cluster-analysis-based climate classification a powerful tool, worth further pursuit.

ACKNOWLEDGEMENTS

This study was facilitated by the Cluster of Excellence Exc264 TOPOI and was supported as part of the project AI-15 Climate in global change—climate in local perception, pursuing investigations of the ‘Limnosahara’ research project (Schu 949/9) funded by the German Research Foundation (DFG). We thank Ellen Leipner for assistance in drawing the figures and Anne Beck for English-language editing.

REFERENCES

- Bahrenberg, G., Giese, E. and Nipper, J., 2003. *Statistische Methoden in der Geographie. Band 2. Multivariate Statistik*. Berlin, Stuttgart: Borntraeger (Studienbücher der Geographie).
- Ben-Gai, T., Bitan, A., Manes, A., Alpert, P. and Rubin, S., 1998, Spatial and Temporal Changes in Rainfall Frequency Distribution Patterns in Israel. *Theoretical and Applied Climatology*, **61**, 3, pp. 177–190.

- Ben-Gai, T., Bitan, A., Manes, A., Alpert, P. and Rubin, S., 1999, Temporal and Spatial Trends of Temperature Patterns in Israel. *Theoretical and Applied Climatology*, **64**, 3–4, pp. 163–177.
- Blüthgen, J. and Weischet, W., 1980, *Allgemeine Klimageographie*, (Berlin: Walter de Gruyter & Co.).
- Buckle, C., 1996, *Weather and Climate in Africa*, (Harlow: Addison Wesley Longman).
- Burroughs, W.H., 2003, *Climate Into the 21st Century*, (Cambridge: Cambridge University Press).
- Camberlin, P., Janicot, S. and Pocard, I., 2001, Seasonality and atmospheric dynamics of the teleconnection between African rainfall and tropical sea-surface temperature: Atlantic vs. ENSO. *International Journal of Climatology*, **21**, pp. 973–1005.
- Climatic Research Unit, 2004, North Atlantic Oscillation (NAO) – <http://www.cru.uea.ac.uk/cru/data/nao.htm> (01.05.2009)
- Cullen, H.M. and deMenocal, P.B., 2000, North Atlantic influence on Tigris-Euphrates Streamflow. *International Journal of Climatology*, **20**, pp. 853–863.
- Dahamsheh, A. and Aksoy, H., 2007, Structural characteristics of annual precipitation data in Jordan. *Theoretical and Applied Climatology*, **88**, 3, pp. 201–212.
- Davies, H.R.J. and Alredaisy, S.M.A.H., 1995, Desertification: or perhaps not? White Nile, Sudan, 1980–92. *GeoJournal*, **37**, 4, pp. 479–482.
- Domroes, M. and El-Tantawi, A., 2005, Recent Temporal and Spatial Temperature Changes in Egypt. *International Journal of Climatology*, **25**, pp. 51–63.
- Domroes, M., Kaviani, M. and Schaefer, D., 1998, An Analysis of Regional and Intra-annual Precipitation Variability over Iran using Multivariate Statistical Methods. *Theoretical and Applied Climatology*, **61**, 3, pp. 151–159.
- Dyck, S., 1980, *Angewandte Hydrologie—Teil 1: Berechnung und Regelung des Durchflusses der Flüsse*, (Berlin, München: Verlag von Wilhelm Ernst & Sohn).
- Edgell, H.S., 2006, *Arabian Deserts: Nature, Origin and Evolution*, (Dordrecht: Springer).
- El Tom, M.A., 1972, The Reliability of Rainfall over the Sudan. *Geografiska Annaler A*, **54**, 1, pp. 28–31.
- Elagib, N.A. and Addin Abdu, A.S., 1997, Climate variability and aridity in Bahrain. *Journal of Arid Environments*, **36**, 3, pp. 405–419.
- Elagib, N.A. and Mansell, M.G., 2000, Recent trends and anomalies in mean seasonal and annual temperatures over Sudan. *Journal of Arid Environments*, **45**, 3, pp. 263–288.
- Flohn, H., 1987, Rainfall teleconnections in northern and northeastern Africa. *Theoretical and Applied Climatology*, **38**, 4, pp. 191–197.
- Food and Agriculture Organization of the United Nations [FAO], 2009, *Climate data*. http://www.fao.org/nr/climpag/data_2_en.asp (27.05.2008)
- Fovell, R.G. and Fovell, M.-Y.C., 1993, Climate Zones of the Conterminous United States Defined Using Cluster Analysis. *Journal of Climate*, **6**, 11, pp. 2103–2135.
- Frankenberg, L., 1995, *Moderne Klimakunde: Grundwissen von Advektion bis Treibhausklima*, (Braunschweig: Westermann Schulbuchverlag).
- Giannini, A., Biasutti, M., Held, I. and Sobel, A., 2008, A global perspective on African climate. *Climate Change*, **90**, 4, pp. 1573–1480.
- Giannini, A., Saravanan, R. and Chang, P., 2003, Oceanic Forcing of Sahel Rainfall on Interannual to Interdecadal Time Scales. *Science*, **302**, pp. 1027–1030.
- Gießner, K., 1989, Die räumlich-zeitliche Niederschlagsstruktur im westlichen Jebel-Marra-Vorland und deren hydrologische Auswirkungen. In *Aktuelle morphodynamische Prozesse im Einzugsbereich des unteren Atbara (Nile Province, Rep. Sudan) und im westlichen Vorland des Jebel Marra (Darfur, Rep. Sudan)*, edited by Mensching, H.G., (Hamburg: Akademie der Wissenschaften, Göttingen), pp. 79–125.

- Gläser, B., Mensching, H.G. and Pörtge, K.-H., 1989, Die Zerstörung des Ökosystems am unteren Atbara (Republik Sudan). Auswirkungen anthropogener Eingriffe und klimatischer Veränderungen auf einen nordsahelischen Lebensraum. In *Aktuelle morphodynamische Prozesse im Einzugsbereich des unteren Atbara (Nile Province, Rep. Sudan) und im westlichen Vorland des Jebel Marra (Darfur, Rep. Sudan)*, edited by Mensching, H.G., (Hamburg: Akademie der Wissenschaften in Göttingen), pp. 15–77.
- Gommes, R., Grieser, J. and Bernardi, M., 2004, FAO agroclimatic databases and mapping tools. *European Society For Agronomy-Newsletter*, **26**, pp. 1–5.
- Gong, X. and Richman, M.B., 1995, On the Application of Cluster Analysis to Growing Season Precipitation Data in North America East of the Rockies. *Journal of Climate*, **8**, 4, pp. 897–931.
- Goudie, A.S., 1997, Weathering Processes. In *Arid Zone Geomorphology: Process, Form and Change in Drylands*, edited by Thomas, D.S.G., (Chichester: John Wiley & Sons), pp. 25–39.
- Goudie, A.S., 2002, *Great Warm Deserts of the World: Landscapes and Evolution*, (New York: Oxford University Press).
- Graf, H. 2002, Klimänderungen durch Vulkane. *Promet*, **28**, 3–4, pp. 133–138.
- Grunert, J., 1979, Wetter und Witterung in der zentralen Sahara 1977 und 1978. *Würzburger Geographische Arbeiten*, **49**, pp. 1–65.
- Hafez, Y.Y. and Hasanean, H.M., 2000, The variability of wintertime precipitation in the northern coast of Egypt and its relationship with the North Atlantic Oscillation, *ICEHM2000, Cairo University*, pp. 175–186.
- Hafez, Y.Y. and Robaa, S.M., 2008, The Relationship between the Mean Surface Air Temperature in Egypt and NAO Index and ENSO. *The Open Atmospheric Science Journal*, **2**, pp. 8–17.
- Hasanean, H.M., 2001, Fluctuations of surface air temperature in the Eastern Mediterranean. *Theoretical and Applied Climatology*, **68**, pp. 75–87.
- Hasanean, H.M., 2004, Wintertime surface temperature in Egypt in relation to the associated atmospheric circulation. *International Journal of Climatology*, **24**, pp. 985–999.
- Herz, K., 1970, Afrika. In *Das Gesicht der Erde—Band 1*, edited by Neef, E., (Leipzig: Brockhaus Verlag), pp. 307–354.
- Heyer, E., 1988, *Witterung und Klima: Eine allgemeine Klimatologie*, (Leipzig: Teubner Verlag).
- Hulme, M., 1992, Rainfall Changes in Africa: 1931–1960 to 1961–1990. *International Journal of Climatology*, **12**, pp. 685–699.
- Intergovernmental Panel on Climate Change [IPCC] (2002): *Klimaänderung 2001; Synthesebericht/Zwischenstaatlicher Ausschuss für Klimaänderung*, (Bonn: Dt. IPPC Koordinierungsstelle des BMBF und des BMU) Deutsche IPCC Koordinierungsstelle des BMBF und des BMU. Bonn.
- Kahya, E. and Karabörk, M.C., 2001, The analysis of El Niño and La Niña signals in streamflows of Turkey. *International Journal of Climatology*, **21**, pp. 1231–1250.
- Kalkstein, L.S., Tan, G. and Skindlov, J.A., 1987, An Evaluation of Three Clustering Procedures for Use in Synoptic Climatological Classification. *Journal of Applied Meteorology*, **26**, 6, pp. 717–730.
- Kelly, P.M., Jones, P.D. and Pengqun, J., 1996, The spatial response of the climate system to explosive volcanic eruptions. *International Journal of Climatology*, **16**, pp. 537–550.
- Klaus, D., 1981, Klimatologische und klima-ökologische Aspekte der Dürre im Sahel. *Erdwissenschaftliche Forschung*, **16**.
- Klitzsch, E. and Wycisk, P., 1999: Beckenentwicklung und Sedimentationsprozesse in kratonalen Bereichen Nordost-Afrikas im Phanerozoikum. In *Sonderforschungsbereich*

- Geowissenschaftlicher Probleme in Ariden und Semiariden Gebieten. Nordost-Afrika Strukturen und Ressourcen*, edited by Klitzsch, E. and Thorweihe, U., (Weinheim: Wiley-VCH), pp. 61–108.
- Köppen, W., 1936, Das geographische System der Klimate. In *Handbuch der Klimatologie*, edited by Köppen, W. and Geiger, G., (Berlin: Borntraeger), pp. 1–44.
- Kottek, M., Grieser, J., Beck, C., Rudolf, B. and Rubel, F., 2006, World Map of the Köppen-Geiger climate classification updated. *Meteorologische Zeitschrift*, **15**, 3, pp. 259–263.
- Lauer, W., Rafiqpoor, M.D. and Frankenberg, P., 1996, Die Klimate der Erde—Eine Klassifikation auf ökophysiologischer Grundlage der realen Vegetation. *Erdkunde*, **50**, 4, pp. 275–300.
- Linacre, E., 1992, *Climate data and resources: a reference and guide*, (New York: Routledge).
- Mainquet, M., 1994, *Desertification: natural background and human mismanagement*, (Berlin: Springer).
- Mensching, H. and Wirth, E., 1989, *Nordafrika und Vorderasien—Der Orient*, (Frankfurt a. Main: Fischer Taschenbuch Verlag).
- Mimmack, G.M., Mason, S.J. and Galpin, J.S., 2001, Choice of Distance Matrices in Cluster Analysis: Defining Regions. *Journal of Climate*, **14**, 12, pp. 2790–2797.
- Müller-Hohenstein, K., 1981, *Die Landschaftsgürtel der Erde*. Stuttgart.
- Nicholson, S.E. and Kim, J., 1997, The relationship of the El Niño-Southern Oscillation to African rainfall. *International Journal of Climatology*, **17**, pp. 117–135.
- NOAA NCDC GHCN, 2002, Global Historical Climatology Network: monthly weather station temperature and precipitation—[http://iridl.ldeo.columbia.edu/SOURCES/.NOAA/.NCDC/.GHCN/\(02.06.2008\)](http://iridl.ldeo.columbia.edu/SOURCES/.NOAA/.NCDC/.GHCN/(02.06.2008))
- Paeth, H. and Friedrichs, P., 2004, Seasonality and time scales in the relationship between global SST and African rainfall. *Climate Dynamics*, **23**, 7–8, pp. 815–837.
- Peterson, T.C., Vose, R.S., Schmoyer, R.L. and Razuvaev, V., 1998, Global Historical Climatology Network (GHCN) quality control of monthly temperature data. *International Journal of Climatology*, **18**, pp. 1169–1179.
- Price, C., Stone, L., Huppert, A., Rajagopalan, B. and Alpert, P., 1998, A possible link between El Niño and precipitation in Israel. *Geophysical Research Letters*, **35**, 21, pp. 3963–1966.
- Rapp, J., 2000, *Konzeption, Problematik und Ergebnisse klimatologischer Trendanalysen für Europa und Deutschland*, (Offenbach a. Main: Selbstverlag des Deutschen Wetterdienstes).
- Robock, A. and Mao, J., 1995, The Volcanic Signal in Surface Temperature Observations. *Journal of Climate*, **8**, pp. 1086–1103.
- Ruddiman, W.F., 2008, *Earth's Climate: Past and Future*, (New York: W.H. Freeman and Company).
- Scherhag, R. and Lauer, W., 1982, *Klimatologie*, (Braunschweig: Georg Westermann Verlag).
- Schiffers, H. (1971): Das Wasser in der Sahara. In *Die Sahara und ihre Randgebiete: Darstellung eines Naturgroßraumes*, edited by Schiffers, H., (München: Weltforum-Verlag), pp. 405–428.
- Schlittgen, R. and Streitberg, B.H.J., 1989, *Zeitreihenanalyse*, (München: R. Oldenbourg Verlag).
- Schönwiese, C.D., 2000, *Praktische Statistik für Meteorologen und Geowissenschaftler*, (Berlin, Stuttgart: Gebrüder Borntraeger).
- Schönwiese, C.D., 2008, *Klimatologie*, (Stuttgart: Verlag Eugen Ulmer).
- Shahin, M., 1985, *Hydrology of the Nile Basin*, (Amsterdam: Elsevier).

- Trilsbach, A. and Hulme, M., 1984, Recent rainfall changes in central Sudan and their physical and human implications. *Transactions of the Institute of British Geographers*, **9**, pp. 280–298.
- Troll, C. and Paffen, K.H., 1964, Karte der Jahreszeiten—Klimate der Erde. *Erdkunde*, **18**, 1, pp. 5–28.
- Tschierschke, K. (1998): Statistische Analyse und Interpretation langjähriger Niederschlags- und Temperaturdaten von Klimastationen im Tschadseegebiet. *Berichte des Sonderforschungsbereiches 268*, **10**, pp. 11–140.
- Unal, Y., Kindap, T. and Karaca, M., 2003, Redefining the climate zones of Turkey using cluster analysis. *International Journal of Climatology*, **23**, 9, pp. 1045–1055.
- Vose, R.S., Schmoyer, R.L., Steurer, P.M., Peterson, T.C., Heim, R., Karl, T.R. and Eischeid, J., 1992, *The global historical climatology network: Long-term monthly temperature, precipitation, sea level pressure, and station pressure data*. ORNL/CDIAC-53, NDP-041. Carbon Dioxide Information Analysis Center, Oak Ridge National Laboratory, Oak Ridge, Tennessee.
- Weischet, W. and Endlicher, W., 2000, *Regionale Klimatologie—Teil 2: Die Alte Welt. Europa, Afrika, Asien*, (Stuttgart: Teubner Verlag).
- Woodfork, J.C., 2006, *Culture and customs of The Central African Republic* (Culture and Customs of Africa), (Westport: Greenwood Pub Group Inc).
- Ziv, B., Dayan, U., Kushnir, Y., Roth, C. and Enzel, Y., 2006, Regional and global atmospheric patterns governing rainfall in the southern Levant. *International Journal of Climatology*, **26**, pp. 55–73.

CHAPTER 12

Climate and palaeoenvironment evolution in north tropical Africa from the end of the Tertiary to the Upper Quaternary

Jean Maley

*Département Paléoenvironnements and Paléoclimatologie,
ISEM-CNRS, Université de Montpellier-2, Montpellier, France*

ABSTRACT: Desert conditions appeared in the Sahara between 10 and 7 million years ago (Ma) following a long savanna environment phase that lasted from the beginning of the Oligocene to the end of the Miocene. Starting at about 7 My and up until the Late Quaternary, environmental conditions varied in a cyclical manner, wherein humid milieus succeeded semi-arid and finally desertic ones. This succession presented a periodicity between 20.000 and 24.000 years, which allows a link to an orbital forcing. The oldest prehistoric industries found in the Sahara belong to the Late Acheulean, between 600.000 and 300.000 years. These were succeeded by Middle Stone Age industries until about 70.000 years, then they evolved towards the Late Stone Age before the Last Great Arid phase synchronous with the Last Glacial Maximum (LGM). The last great humid phase of the Late Quaternary, which is described in detail, occurred after the LGM between ca. 15.000 and 4.500 years cal BP. This phase was not homogeneously humid, as it was interrupted by arid periods sometimes accompanied by eolian reactivation. In the Chad Basin, the humid conditions led to the formation of an immense Mega-Chad Lake during the Middle Holocene. A distinctly less important, final lacustrine phase intervened at the beginning of the Late Holocene. There was also an important erosive phase between ca. 2.400 and 1.900 cal BP; this phase is worth mentioning because it is found up to the equatorial zone where it was associated with a strong contraction of the forest, and in particular with the formation of a savanna corridor through the Congolian Forest area. The last two Millennia are studied in detail and using, in particular, diverse historical data, a relatively precise reconstruction of the variation in Lake Chad levels during the last Millennium is provided. For the latter period, there are quite good correlations between variation curves of solar activity and of Lake Chad levels. In the second part of this paper various palaeoclimatic interpretations are presented to try to explain the humid phases, in particular. Indeed these phases seem to result not only from the reinforcement of the annual Monsoon, but also, during the cooler inter-seasons, from Extratropical Cyclonic Depressions known as “Saharan Depressions”. Precise quite monthly isotopic data obtained from gastropod shell dated to the Middle Holocene clearly show two rainy seasons during the course of a year—one relatively long, tied to the annual Monsoon and a second shorter one, which might be referred to Saharan Depressions.

12.1 INTRODUCTION

7 million years ago climatic aridification was underway in north tropical Africa, marked by the development of desert conditions in the Chad Basin (Schuster *et al.*, 2006, 2009). This aridity phase corresponded to the end of a great climatic cycle that might have

begun at about the beginning of the Tertiary. Indeed, a thermic maximum was reached during the Paleocene–Eocene boundary, around 55 million years ago, which was followed by a general cooling trend (Zachos *et al.* 2001) (Figure 1). Various studies have shown that during this warm period, there was a major diversification of mammals (Jaeger, 2001; Gingerich, 2006) and Angiosperms (Schrire *et al.*, 2005). In a world without polar ice, (Nunes and Norris, 2006), this warm climate favored the emergence of a “boreo-tropical” flora in the Northern Hemisphere composed of tropical and temperate taxa (Janis, 1993, Figure 2); this flora has been well documented by pollen (Cavagnetto and Anadon, 1996) and molecular genetical studies, in particular by Schrire *et al.* (2005) based on Leguminosae (Caesalpinaceae, Mimosaceae, Papilionaceae). During the Eocene, numerous tropical taxa evolved associated with climates having a marked annual dry season; this occurred particularly around the Tethys (Schrire *et al.*, 2005), an ancient ocean that extended in a zonal manner from central America, to the south of Laurasia and up to Asia (Meulenkamp and Sissingh, 2003).

The cooling trend that continued during the Middle and Late Eocene was associated with the extension of tropical taxa into North Africa (Janis, 1993, Figure 3), which at this time was closer to the equator (Guiraud *et al.*, 2005). Pollen analyses reveal that starting at about 45 Ma, the forest vegetation near the Gulf of Guinea presented numerous similarities with the modern tropical flora (Salard-Cheboldaeff, 1981; Maley, 1996). Recent molecular genetical studies have clearly shown that part of the equatorial forest arboreal vegetation is derived from the drier “boreo-tropical” flora which migrated towards the equator at the end of the Eocene (Schrire *et al.*, 2005; Burgoyne *et al.*, 2005). Conversely, other equatorial forest species appear to have evolved around the beginning of the Tertiary from an archaic Gondwanan flora (Maley, 1996; Couvreur *et al.*, 2008).

The first growth of ice sheets in the Antarctic about 34 Ma led to a dramatic cooling during the Eocene-Oligocene transition (Zachos *et al.*, 2001) (Figure 1). This cooling provoked global climatic shocks, marked by aridifications (Retallack, 2001), which led to major modifications of the Fauna and Flora; this event is commonly known as the “Grande Coupure” (Hartenberger, 1983, 2001). In the North of Africa, a major sedimentological change, characterized by the deposition of principally detritical Formations of the “Continental Terminal”, has been dated to the beginning of the Oligocene and persisted until the end of the Miocene (Maley, 1980; Boudouresque *et al.*, 1982). In the Chad Basin (Eastern Niger and Bodelé), the base of the Continental Terminal has been associated with ferruginized oolite deposits (Faure, 1966). These deposits are explained by the domination of distinctly contrasted tropical climates, having a humid season alternating with a long dry one, similar to the Sudanian climate of today. Given this, we can conclude that during the Oligocene and Miocene, savannas largely dominated the land presently occupied by the Sahara.

This interpretation is, notwithstanding, somewhat problematic because numerous isotopic studies have shown that the development of herbaceous plants having C₄ photosynthesis, essentially grasses (*Graminae*—dominates of present day tropical savannas), were not present until towards the end of the Miocene (7–8 Ma), and that prior to this only C₃ photosynthetic plants existed (Zazo *et al.*, 2000; Retallack, 2001; Ségalen *et al.*, 2007). However, palynological studies from Cameroon (Salard-Cheboldaeff, 1981) to Egypt (Kedves, 1971, 1983) provide evidence that *Graminae* pollen appeared during the Eocene, followed by a dramatic upsurge in Northeast Africa at the time of the “Grande Coupure”, about 34 Ma, which, logically, would correspond to an expansion of grass-rich savanna environment (Maley, 1996). Additionally, at Fort Ternan, Kenya, a fossil flora rich in *Graminae* was found in Middle Miocene strata dated about 15 Ma (Retallack, 1992), this discovery was confirmed by isotopic data indicating the presence of C₄ plants as well as fossils of herbivores adapted to savanna ecosystems

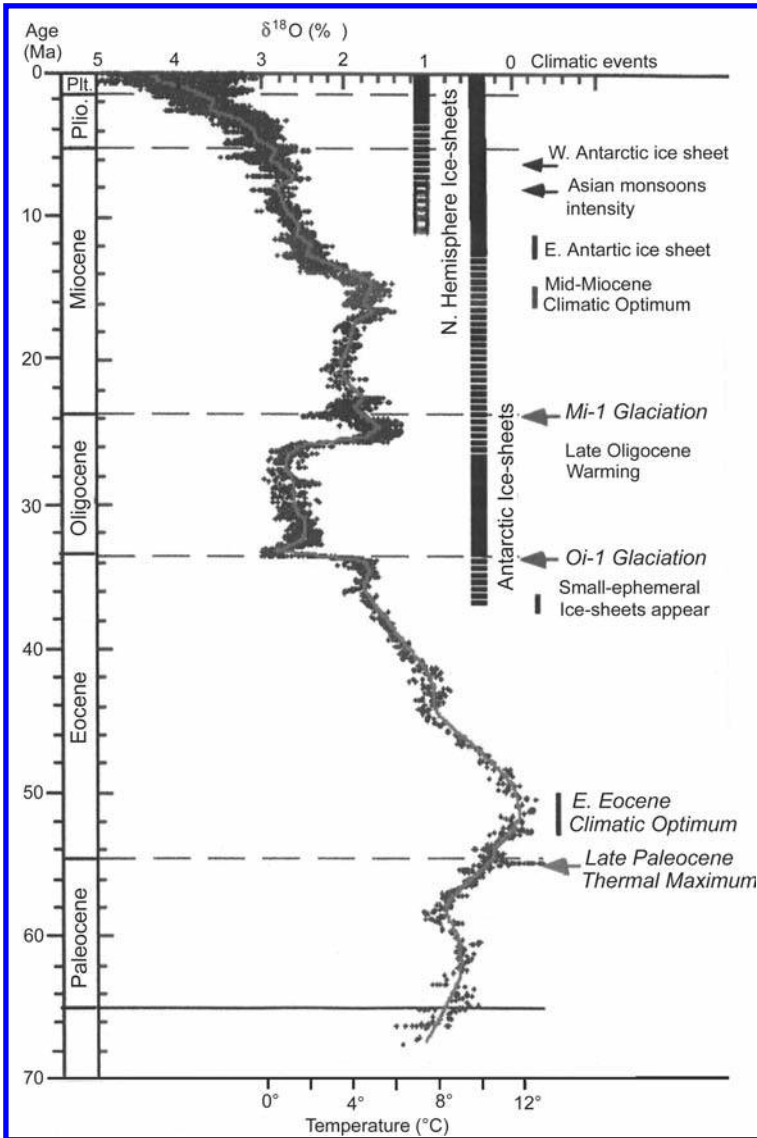


Figure 1. Long-term variation of $\delta^{18}\text{O}$ in deep sea waters (scale at top), compiled from more than 40 sampling sites around the world (sites DSDP and ODP) (left curve). This curve, which essentially expresses variation in the total mass of continental ice, correlates also with variation in the temperature of deep sea waters (scale at bottom). In this way, this curve illustrates the global variation in temperatures during the Tertiary. In the center, the major fluctuations of the icecaps in the Antarctic and, later, in the Northern Hemisphere. At right are presented the major climatic events, in particular the principal glacial phase in the Antarctic (adapted from Figure 2 in Zachos *et al.*, 2001).

(Morgan *et al.*, 1994). This savanna expansion occurred at the beginning of a global cooling phase, which characterized the last part of the Cenozoic (Figure 1). These data from diverse sources demonstrate that Graminae-dominated savanna biotopes developed progressively in tropical milieus during the Neogene, leading to near domination of these environments towards the end of the Miocene (Janis, 1993).

12.2 THE APPEARANCE OF DESERT CONDITIONS IN THE SAHARA

Eolian transport of large quantities of sand and dust is the principal characteristic of desert conditions. Based on this fact, analyses of long cores taken offshore, from the Gulf of Guinea to Western Africa, has proven to be a reliable method for long-term study of the appearance and development of the Sahara (Sarnthein *et al.*, 1982; Stein and Sarnthein, 1984). The aforementioned authors demonstrated that at the beginning of the Late Miocene, about 11 Ma, eolian particles became numerically important offshore of West Africa, and that there have been more or less cyclic recrudescence episodes up until the recent Quaternary (Chamley, 1988). Indeed, this age is close to that recorded for the first glaciations in the Northern Hemisphere (ca. 10 Ma; Maslin and Christensen, 2007). Pollen data obtained from the Niger delta indicate that near the Gulf of Guinea, the first episode of savanna expansion occurred about 10 Ma followed by a second more pronounced episode around 7 Ma; this last expansion, albeit with numerous fluctuations, has continued until the present (Morley, 2000, [Figures 7–11](#)).

Palaeontological and geological studies undertaken in the northeast of the Chad Basin between Koro-Toro and Toros-Ménalla, led to the discovery in 1995 of an Australopithecine aged about 3,5 Ma (Brunet *et al.*, 1995) followed in 2001, of an Anthropoid named “Toumai” (Brunet *et al.*, 2002) for which the associated fauna provided an age of about 7 Ma (Vignaud *et al.*, 2002); both ages have recently been confirmed by ^{10}Be dating (Lebatard *et al.*, 2008). The demonstration that at the base of the deposits where Toumai was discovered there was a dune formation, confirms that in the north of Chad, typical desert conditions have existed since the end of the Miocene (Schuster, 2002; Schuster *et al.*, 2006). Moreover, detailed study of deposits for this region ranging

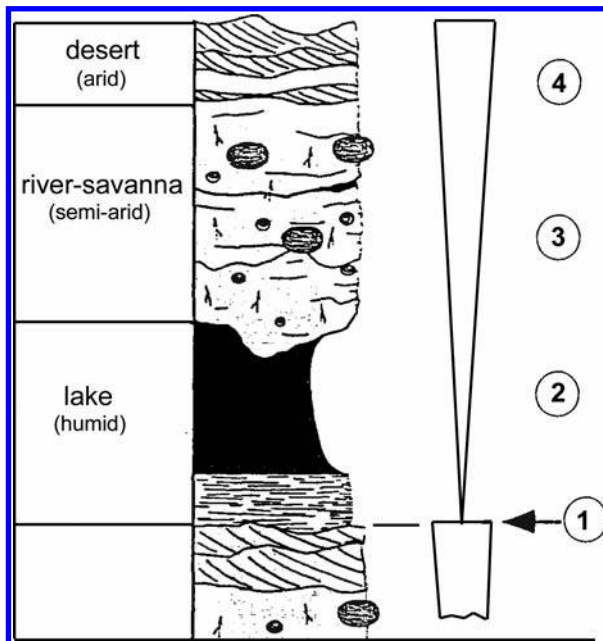


Figure 2. Sedimentary *Type sequence* of Mio-Pliocene deposits from Northern Chad (Düringer *et al.*, 2000). The base of this sequence rests on a discontinuity (1). The sequence is composed of: (2) Firstly, diatomites then clays (transgressive lacustrine deposits). (3) followed by a thick sandstone series (seasonal fluvial facies), (4) ending with eolian desert sands.

from the end of the Miocene to the end of the Pliocene, have demonstrated cyclic sedimentary successions, relatively similar to each other, which have led to the description of a *Type sequence* (Düringer *et al.*, 2000; Schuster, 2002) (Figure 2).

The sequence is composed first (2) of accumulated eolian sand (desert phase), then (3), transgressive on this sand, deposition of a diatomite and clay which was formed in a lacustrine environment (humid phase), finally (4) the end of the sequence is represented by a thick sandstone horizon corresponding to a fluvial facies (contrasting climate phase). The majority of fossils have been found in this sandstone horizon.

12.3 PERIODIC CLIMATE CHANGES

The demonstration of a cyclic sedimentary sequence going from desert to humid to contrasting conditions, between 7 and 1,8 Ma (end of the Pliocene), means that during this interval there must have been periodic climate variations of considerable magnitude, with the possibility of development, in particular during the humid phase, of a large Palaeo-Chad comparable to Lake Mega-Chad, or simply “Mega-Chad”, of the Middle Holocene (Schuster, 2002; Ghienne *et al.*, 2002; Leblanc *et al.*, 2006) (chapter 12.5.2). During the Quaternary, similar cyclic deposits continued in the center and south of the Chad Basin (Servant, 1973; Servant-Vildary, 1973; Servant and Servant-Vildary, 1980; Matheis, 1976). Examination of recent deposits from Kanem, in the center of the basin, shows that a similar sedimentary sequence continued to be laid down during the Late Pleistocene and Holocene (Table 2) (chapter 12.5.1), from which it can be established that this sequence lasted about 22,000 years (Maley, 2004a; Table 2). This timescale is important because it allows us to associate the evolution of this sequence to an orbital forcing (Maley, 2004a) which, at low latitudes, is determined by the precession of the equinoxes, the dominant rhythm of which is between 19,000–23,000 years (Rognon, 1989; Gasse, 2006). However recently, statistical studies on dust records from marine cores, going back to 5 Ma, and taken from the West, East and North of the Sahara, have shown the existence of complex periodicities related to orbital forcings (Trauth *et al.*, 2009). These studies have shown that the fluxes of dust from the Sahara followed these three directions, had relatively similar rhythms and, particularly, that the amplitude of the precession phases were strongly modulated and accentuated by variations in eccentricity of the Earth’s orbit. Superposed upon a basic cyclicity of about 22,000 years, the eccentricity cycle of 41,000 years led to supercycles, of greatest intensity, of 400,000 years, and also to other cycles of 100,000 years (Trauth *et al.*, 2009, Figure 7). These authors also tried to correlate major steps of hominization with certain phases of eccentricity maxima, such as the appearance of the genus *Homo* and the emergence of the Oldoway Industrial Complex around 2,5 Ma, as well as the debut of Acheulean technology about 1,7 Ma (Trauth *et al.*, 2009).

Not only is the aforementioned Type sequence important to understanding climate change, it is significant because of its seeming universality. In terms of sedimentology and palaeoenvironment, it is very similar to a sequence type from the end of the Triassic period known as the “Van Houten Cycle”, which was observed in a geological Formation deposited in the tropical zone during about 22 Ma (Olsen *et al.*, 1978). These authors were able to show that the periodicities recorded in this Formation were controlled by Milankovitch orbital cycles and that the elementary sequence of Van Houten has a periodicity of about 20,000 years (Olsen and Kent, 1996), that is, the length of time corresponding to that here estimated for the Chad.

The fauna that lived in the regions north of Chad between 7 and 1,8 Ma, during the phases characterized by the deposition of sandstone sediments, appeared to have

always been adapted to savanna environments (Schuster, 2002; Vignaud *et al.*, 2002). During the two other parts of these sedimentary sequences, the absence of fossils implies that this fauna wasn't present. In any case, during the development of large lakes of the Mega-Chad type, this fauna should have lived close to the banks and towards the edges of the Chad Basin. Conversely, during the third part of each sequence, during which desert conditions developed, lasting for about 10.000 years, when it is referenced to a chronology obtained by the most recent sedimentary sequence (Maley, 2004a), it appears that this entire fauna should have migrated to the far-flung edges of the Sahara, either towards the north, possibly close to the shores of the palaeo-Mediterranean, or considering its tropical character, more likely to the south towards the equator. Indeed, during the last great arid episode that occurred between 24.000 and 15.000 calendar years BP (cal BP, Before Present), contemporaneous with the Last Glacial Maximum (LGM), various studies have shown that desert conditions extended towards the south to about 10°N at the level of Chad and North Cameroon, (Sieffermann, 1970) that is, an extension of nearly 700 km with respect to its mean meridional limit situated at about 16°N during the 20th century (Maley, 2004a). It becomes apparent from other studies that during this very arid period, the great majority of tropical biodiversity persisted in a series of "refugia" close to the equator, along the periphery of the Gulf of Guinea and in the Congo Basin (Maley, 1987, 1996, 2004b; Fontaine *et al.*, 2004). It is worthy of mention that in Nigeria, certain dense forest islands, known locally as *Kurmi*, develop in savannas at about 9°–8°N, far north of the main actual forest (Jones, 1963); these islands represent possible examples of composite refuges, wherein towards the center grow species of dense forest surrounded at the periphery by Sudanian arboreal species. From a biogeographical point of view, Linder *et al.* (2005) showed that a continuity existed between the "phytochoria" of the Guineo-Congolian forests and the Sudanian savannas. This characteristic is well illustrated by frequent vicariant events within diverse genera linking these two assemblages (Letouzey, 1985; Satabié, 1994).

In this way, it is possible to conclude that since at least 7 Ma, and maybe even as early as the beginning of eolian activity, 11 Ma (see above), great climatic changes followed a first order rhythm of about 22.000 years, during which there were periodic phases of contraction and isolation of tropical milieus, followed by expansion, particularly of savanna environments in West Africa. Given the central position in Africa of the most humid environments, these phenomena probably also effected all savanna biotopes situated towards the periphery, that is, those of East Africa and South Africa—with respect to the latter, stretching from Angola to Tanzania. These great shifts, ultimately originating from orbital forcing and characterized by phases of expansion then contraction of vital areas, were accompanied by cyclic isolation, a condition susceptible to the induction of evolutionary processes (Jansson and Dynesius, 2002; Maslin and Christensen, 2007; see also the "species pump" as explained by Stebbins, 1974). In this way, it is possible that these dramatic climatic oscillations may have played a role in the evolution and development of the *Hominidae* lineage (Brunet and Picq, 2001) and for the great apes (Thomas and Picq, 2001); similarly, this theory has been evoked for numerous animal and plant species of present day central African forest, because, as presented above, (chapter 12.1) since the end of the Eocene many existent forest species evolved from savanna plants (Schrire *et al.*, 2005; Burgoyne *et al.*, 2005).

12.4 MAN AND CLIMATE DURING THE QUATERNARY

In the North of Africa, remains of prehistoric industries, spanning principally from the Middle Palaeolithic to the Neolithic, are relatively frequent across Saharan environments

and their periphery. Numerous studies have been concerned with their associated deposits, such that a body of significant evidence exists related to the palaeoenvironment. Based on a general schema, succession of the different industries provides a rough chronology. This method was used until the early 1960's, when it was replaced by radiocarbon dating, a technique that gives a relatively precise chronology of upper Quaternary deposits. Over the last 20 years, however, refinement of new dating techniques have brought to light a weakness of radiocarbon dating towards its technical limits, before 25–30.000 years BP, attributable to various forms of contamination, especially when the dated specimen is a carbonate (Fontugne, 1997). Presently, the two most commonly used dating techniques for the Quaternary are based on thermoluminescence techniques (TL, OSL) and Uranium series (Fontugne, 1997; Causse *et al.*, 1988).

The oldest industrial complex made by Man appears about 2,5 Ma represented by the earliest Oldowayan. The sites are principally found in East and South Africa, and characterized by cut pebbles (choppers) (Berthelet *et al.*, 2001). In the North of Africa, sites going back to the Oldowayan are quite rare and principally situated in Northern Maghreb (Raynal *et al.*, 2001; Sahnouni, 2005). Thus far, no site has been found in the Sahara. In the Maghreb, Ain el-Hanech in Algeria, near Setif, is the oldest and best-studied site. Discovered by C. Arambourg, it was recently dated to be 1,8 Ma, and is the proof that the first representatives of the genus *Homo* (*H. erectus* and *H. ergaster*) rapidly spread throughout Africa (Sahnouni, 2005). The following palaeontological assemblage has been associated with the site: elephant, rhinoceros, horse, hippopotamus, giraffe, suids, diverse antelopes and buffalos—animals characteristic of a rich tropical savanna biotope (Sahnouni, 2005).

The Acheulean constituted the next cultural step. It is characterized by the importance of bifaces and hand-axes, the latter made on large flakes. Acheulean industries have been found throughout Africa, however, the earliest stages, dated to 1,7 to 1 Ma have been mostly found in East and South Africa (Berthelet *et al.*, 2001), but also in the Maghreb (Morocco, Algeria) (Raynal *et al.*, 2001; Sahnouni, 2005). Only lithic industries referred to the Late Acheulean have been found in the Sahara and of those, few evince precise, well-established stratigraphies. From East to West, the best studied sites having the Late Acheulean in stratigraphy, have been principally found in the eastern Egyptian Sahara (Hill, 2001) and in the Nile valley (Vermeersch *et al.*, 2006; van Peer, 1998; van Peer and Vermeersch, 2007), in the West of the Chad Basin at Bilma (Baumhauer *et al.*, 1997) and at Adrar Bous (Williams *et al.*, 1987), in the Southwest of Libya, at Tradart Acacus (Cremaschi and Di Lernia, 1998), North of Hoggar, at Tihodaine (Rognon, 1967; Thomas, 1977), in the North of Mali, in the region of Taoudenni (Petit-Maire *et al.*, 1991) and near Adrar in Mauritania (Vernet, 1993). The most detailed studies have been conducted in the Egyptian Sahara where specialists have shown among other things that the Late Acheulean developed between 600.000 and 150.000 years ago (Hill, 2001; Wendorf and Schild, 2005; van Peer and Vermeersch, 2007) (Table 1).

Transition into the Middle Palaeolithic (Middle Stone Age, MSA) occurred gradually between around 250.000 and 150.000 years, marked by the decline in bifaces and the rise of tools produced by more specialized flint knapping methods, prepared mostly by the “Levallois” technique. This technique is more advanced and characterized by an intentional preparation of the core. It is thought that this transition was associated with the appearance of “Modern Man”, *Homo sapiens sapiens* (Wendorf and Schild, 2005; van Peer and Vermeersch, 2007). Many studies have been conducted in the eastern Sahara at the Daklah (Churcher *et al.*, 1999) and Kharga oases (Smith *et al.*, 2007) and especially at the two neighboring sites of Bir Tarfawi and Bir Sahara located in Southern Egypt, in a region now completely deserts (Wendorf *et al.*, 1990, 1993; Szabo *et al.*, 1995; Wendorf and Schild, 2005). These studies have shown that

the periods during which Man could have lived there, correspond to relatively humid phases, characterized by the spread of more or less large lacustrine extensions associated with a tropical savanna fauna and flora. With respect to the Bir Tarfawi and Bir Sahara sites, the detailed stratigraphy and numerous datings of the various levels has revealed that there were 7 to 8 humid phases alternating with dry phases between about 300,000 and 70,000 years. In particular, researchers concluded that during the largest lacustrine phase, (Gray Lake 2, [Table 1](#))—which would have occurred during the warmest phase of the last Interglacial (Isotopic Stage 5e) (chapter 12.6.1)—the rains were estimated to have been nearly 500 mm per year.

Between about 150,000 and 70,000 years, the diverse industries of the Middle Palaeolithic that developed in these regions and in the Nile valley, have been referred to several Mousterian variants, principally the Nubian and Aterian (Wendorf *et al.*, 1993, Wendorf and Schild, 2005; Van Peer and Vermeesch, 2007). These authors have shown that the Nubian must have been limited to Egypt and Sudan and that, from a technological point of view, it might have been the origin of the Aterian (Van Peer and Vermeesch, 2007). The last mentioned industry, typical of North Africa, developed across the entire Sahara, except in montane zones (Tillet, 1989; Débenath, 1992). Some authors think the Aterian must have disappeared during the hyper-arid phase dated between 70,000 and 60,000 years (Cremaschi *et al.*, 1998), however, it appears that this disappearance applied only to certain regions of the Northern Sahara, as it is clear that in the Maghreb this industry only disappeared after 35,000 years (Wrinn and Rink, 2003); moreover, precise geological data show that in the southern Sahara, the Aterian must have survived until the beginning of the LGM, in particular in the western part of Chad Basin (Baumhauer *et al.*, 1997) and also in the west of Mali (Morel *et al.*, 1997). Research at several different Saharan sites have allowed the dating of two relatively humid intervals between 60,000 years and the beginning of the LGM around 23,000 years ([Table 1](#)), the first of minor magnitude between ca. 50,000 and 40,000 years, and a second of relatively greater importance between ca. 30,000 and 23,000 years (Petit-Maire, 1992; Szabo *et al.*, 1995; Rasse *et al.*, 2004), which corresponded with a major aquifer recharging phase in Northern (Sonntag *et al.*, 1980) and Meridional Sahara (Edmunds *et al.*, 1999, 2004; Edmunds, 2008); there developed in this latter area a large Palaeo-Chad lake having poorly defined limits (Servant, 1973). Archeologists have demonstrated that it was during this final phase, posterior to 70,000 years that the Aterian acquired characteristics of the Late Palaeolithic (Late Stone Age), such as blade manufacturing technology (van Peer and Vermeesch, 2007; Garcea, 2009).

The dozens of documented humid/arid sequences from about 300,000 years shows the continuity of a climatic cyclicity. Given that traces of certain humid phases could have been erased by erosion, it is reasonable to conclude that this cyclicity was close to about 20–25,000 years, similar to the cycle for earlier periods mentioned above.

Up until now, all of the humid phases that have been described essentially concerned low altitude sites. However, in the high mountains of the central Sahara an important humid phase was shown to have occurred between ca. 24,000 and 15,000 cal years BP, that is, in synchrony with the LGM and at the same time as aridity and eolian activity reached a maximum at low altitudes in the north and south Saharan plains (Rognon, 1996; Maley, 2000). This particular humid phase, confined to the Saharan mountains, was responsible on the one hand for the construction of an intermediate sequence of the “Middle Terrace” at Hoggar and Tibesti (Messerli *et al.*, 1980), and on the other hand, an important lacustrine phase, especially well developed at Tibesti, particularly in the “Trou au Natron”, a vast volcanic crater about 5 km in diameter, the upper lip of which is between 2,300 and 2,600 m altitude, and a maximum depth of 1,000 m (Faure, 1969; Maley *et al.*, 1970). Numerous diatomite outcrops testify that a lake having a depth of around 500 m existed in this large crater during the LGM (Maley, 2000).

Table 1. Synthetic representation of the succession of humid and arid phases and the principal prehistoric cultures in the Egyptian Sahara and the Nile Valley from ca. 330.000 to 60.000 years (after Wendorf *et al.*, 1990, 1993, 2005; van Peer and Vermeesch, 2007), and in the eastern and central Sahara from ca. 50.000 to 15.000 years cal BP (after Petit-Maire, 1992; Baumhauer *et al.*, 1997).

Egyptian Sahara and Nile Valley (Wendorf <i>et al.</i> , 1990,1993, 2005; Van Peer and Vermeesch, 2007)				
Estimated datations	Isotopic stages	Climate	Phases	Prehistory
ca. 330.000–300.000 years	9	Humid		Late Acheulean
ca. 300.000–250.000 years	8	Hyper-arid		
ca. 250.000–240.000 years	7e	Semi-Arid	Sebkra	Late Acheulean
ca. 230.000–220.000 years	7d	Arid		
ca. 220.000–210.000 years	7c	Humid	White Lake 1	Late Acheulean & MSA
ca. 200.000 years	7b	Arid		
ca. 190.000 years	7a	Semi-Arid	Sebkra	Late Acheulean & MSA
ca. 180.000–150.000 years	6 g-d	Hyper-arid		
ca. 150.000–140.000 years	6c	Humid	Grey Lake 1	Mousterian & Nubian
ca. 140.000–130.000 years	6b	Arid		
ca. 130.000–115.000 years	5e	Humid	Grey Lake 2	Mousterian & Nubian
ca. 115.000–110.000 years	5d	Arid		
ca. 105.000–95.000 years	5c	Humid	Grey Lake 3	Mousterian & Nubian
ca.90.000–80.000 years	5b	Arid		
ca. 80.000–70.000 years	5a	Humid	Green Lake	Nubian & Aterian
ca. 70.000–60.000 years	4b-a	Hyper-arid		
Eastern and central Sahara (Petit-Maire, 1992; Szabo <i>et al.</i> , 1995; Baumhauer <i>et al.</i> , 1997)				
ca.50.000–40.000 years	3c	Semi-Arid	Sebkra	Aterian
ca.40.000–30.000 years	3b	Hyper-arid		
ca. 27.000–22.000 years	3a	Humid	Lacustrine	Aterian?
ca. 22.000–15.000 years	2b/DMG	Hyper-arid		

12.5 THE LAST GREAT HUMID PERIOD DURING THE LATE PLEISTOCENE AND HOLOCENE

12.5.1 Lacustrine deposits (Table 2 and Table 3)

The study and dating of successive lacustrine deposits have been critical to the characterization of the different humid phases at the end of the Quaternary. This said, it is not always easy to distinguish with respect to the source of the lacustrine deposits,

the part attributable to local or regional rain and that to the rising of the water table, a phenomenon that can result in influxes from more or less far away. Inputs from the water table can also sometimes locally delay or neutralize an arid phase manifestation. It has been noted, however, that rises in the water table are frequently associated with favorable regional climatic conditions (Gasse, 2002).

In the Saharan plains, the last great interval of aridity, which was accompanied by strong eolian activity, occurred between about 24,000 and 15,000 cal years BP. This phase, contemporaneous with the LGM at high latitudes in both hemispheres (Rogon, 1996), corresponded in the Sahara to a lowering of temperatures by between 5 °C and 7 °C—as deduced from several concordant measurements (Noble gases content) conducted on fossil waters dated from this epoch (Beyerle *et al.*, 2003; Edmunds *et al.*, 2004; Edmunds, 2008). The first well characterized lacustrine phase occurred later between ca. 15,200 and 13,900 cal BP (12,900–12,000 ¹⁴C BP) (Humid I) in the Southern Sahara, particularly at certain places in the Chad Basin (Maley, 1981, 2004a; Gasse *et al.*, 1990, Gasse, 2002) (Figure 3). This generalized humid phase occurred from tropical Sahara to the equator (Maley and Brenac, 1998a) and was responsible for the highest recorded flood levels of the Nile (“Wild Nile” stage) up until the end of the Holocene. The two great African lakes, Lake Victoria in Uganda and Lake Tana in Ethiopia which were close to the sources of the two branches of the Nile, White Nile (Johnson *et al.*, 1996) and Blue Nile, respectively, completely dried out around 17,000 cal BP, at the height of the LGM. These two lakes were suddenly refilled towards the beginning of the humid phase as a result of intense monsoon reactivation (Williams *et al.*, 2000; Lamb *et al.*, 2007). More to the North, in middle Egypt, recent research in the Nile loops near Qena suggests that large dunes close to the river could be the remains of eolian sandy “dams” across the Nile which, at this time, could have reinforced these very high fluvial levels (Vermeersch, 2006). Aridity returned to all of the Sahara (Arid I), especially during the last great glacial

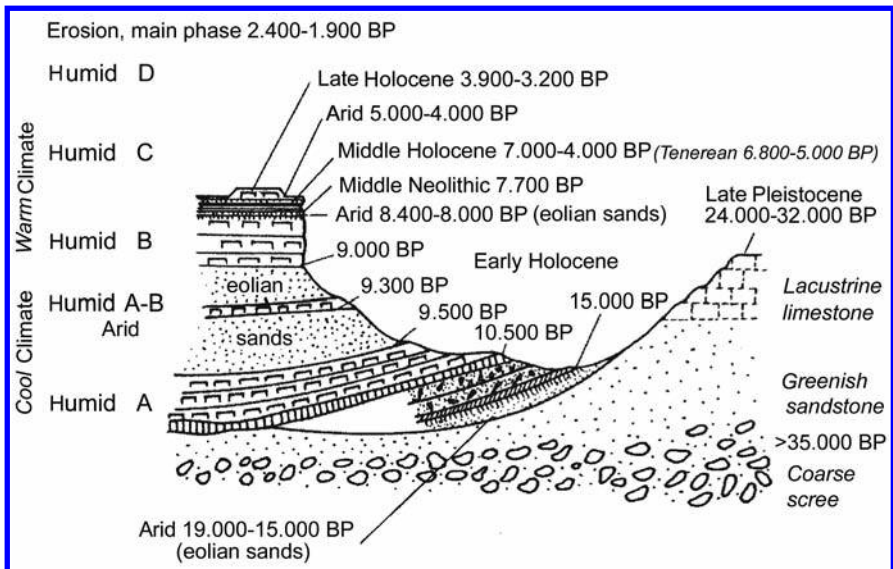


Figure 3. Recent Quaternary deposits from the southern Sahara near Fachi, in the isolated depression of Dogomboulo (Eastern Niger), Chad Basin, western sector. The Holocene was subdivided into six Members, from A to E. (adapted from Maley, 1981 and 2004a). Calibrated radiocarbon datings after Reimer *et al.* (2004).

expansion in the Northern Hemisphere known as the “Younger Dryas”, between ca. 12.900 and 12.000 cal BP (11.000–10.200 ^{14}C BP). Even though the aridity continued in the Northern Sahara, a relatively brief humid phase occurred at various places in meridional Sahara, especially the Chad Basin (Humide II), between ca. 11.700 and 11.200 cal BP (10.100–9.800 ^{14}C BP) (Maley, 1981, 2004a; Gasse, 2002). In these regions, a brief arid phase occurred between ca. 11.200 and 10.700 cal BP (9.800–9.500 ^{14}C BP) (Arid II), just before the first great humid phase that touched all of the Sahara (Humid III), between ca. 10.700/10.500 and 9.500 cal BP (9.500/9.300–8.500 ^{14}C BP). This phase was responsible for considerable lacustrine deposits, often with diatomites, across western and central Sahara (Servant and Servant-Vildary, 1980; Gasse *et al.*, 1987), up to the Eastern Sahara (Schild and Wendorf, 2001; Hoelzmann *et al.*, 2004; Kuper and Kröpelin, 2006). In meridional Libya between Murzuq and Shati, an enormous lake developed in the vast Fezzan depression. Known as the “Mega-Fezzan” it attained a size of about 76.000 km², from ca. 11.000 to 9.000 cal BP (OSL datings) (Armitage *et al.*, 2007).

Thereafter a regressive phase intervened between ca. 9.500 and 9.000 cal BP (8.500–8.100 ^{14}C BP). This phase is well defined in the Chad Basin (Arid III) where it was interrupted by a brief lacustrine transgression around 9.300 cal. BP (8.300 ^{14}C BP) (Maley, 1981) (Figure 3).

According to various previously cited authors, a new important lacustrine phase (Humid IV) occurred between ca. 9.000 and 8.400 cal BP (8.100–7.600 ^{14}C BP). It bears mentioning that in septentrional Sahara, especially at Sebkh Mellala, the preceding regressive phase was not evident, possibly resulting from phreatic water influxes, and only a long humid phase was observed between ca. 10.500 and 8.400 cal BP (9.300–7.600 ^{14}C BP) (Gibert *et al.*, 1990).

An arid phase, brief but intense (Arid IV), has been described for ca. 8.400 to 8.000 cal BP (7.600–7.400 ^{14}C BP), both in the North of the Sahara (Sebkh Mellala) and the South, which, among other things, was accompanied by the resumption of eolian activity in the Chad Basin (Baumhauer *et al.*, 1997; Gasse, 2002), up to the Manga (13°N) (Holmes *et al.*, 1999). Notwithstanding, at the Acacus (Cremaschi *et al.*, 1999) a single long arid phase was recorded between ca. 9.000 and 8.050 cal BP (8.100–7.300 ^{14}C BP).

A new generalized humid phase (Humid V) in the North and South of the Sahara began around 8.000 cal BP (7.300–7.200 ^{14}C BP), often highlighted by an erosive discontinuity; in the South, this humid phase ended at about 7.650–7.400 cal BP (6.800–6.500 ^{14}C BP), whereas in the North (Sebkh Mellala) it continued until about 5.700 cal BP (5.000 ^{14}C BP) (Gibert *et al.*, 1990). In Southern Sahara, this particular humid phase (H. V), corresponded sometimes with low, marshy type, lacustrine deposits or, often with palaeosols on slopes or tops of interfluves (Felix-Henningsen, 2000).

In the south of the Sahara, an intercalated arid phase (Arid V) linked with eolian reactivation occurred between ca. 7.400 and 6.800 cal BP (6.500–6.000 ^{14}C BP). Thereafter, between ca. 6.900 and 4.900 cal BP (6.000–4.300 ^{14}C BP) there developed anew a generalized humid phase (Humid VI) which, however, was not characterized by high lacustrine levels in southern Sahara, but by finely stratified sand facies (Fachi) corresponding to seasonal drying of ponds either by the development of ferruginous soil types, frequently in the form of ferruginous crusts, or sometimes by vertisols (Air valleys) (Maley, 1981, 2004a) (Figure 3). As becomes evident further on these diverse deposits were formed in a warm and evaporative “tropical” setting, distinctly different from the “cool” ambiance which accompanied phases Humid I to IV (Beyerle *et al.*, 2003).

After 5.000 cal BP (4.400 ^{14}C BP) an aridification phase began which culminated in a very arid period (Arid VI) between 4.200 and 4.000 cal BP (3.800–3.700 ^{14}C BP). The ouadi east of Tibesti stopped flowing around 4.300 cal BP (Ounianga site: Kröpelin

et al., 2008). Eolian reactivations have been dated to this period, such as in the Manga (west of Lake Chad) (TL datation of ca. 4.100 cal BP: Holmes *et al.*, 1999), or in the eastern Sahara (Said, 1993).

Rapidly following this, in the North (Gasse *et al.*, 1987) as well as in the South of the Sahara (Chad Basin), a new humid phase of relatively important magnitude intervened as evinced, for example, by a lake over 20 m deep at Agadem, in Eastern Niger (Servant, 1973) and also, the last Palaeo-Chad at an altitude of about 286 m (Maley, 2004a) (Humid VII) between ca. 3.900 and 3.200 cal BP (3.600–3.000 ¹⁴C BP). Palaeosols have also been referred to this period (Felix-Henningsen, 2000).

A generalized arid phase followed between ca. 3.000 and 2.700 cal BP (2.900–2.500 ¹⁴C BP) (Arid VII), accompanied by strong eolian reactivation, as in Ounianga (Kröpelin *et al.*, 2008).

In certain sectors of the southern Sahara, such as in northern Chad at Borkou, low lacustrine levels or marsh facies, have been recorded between ca. 2.600 and 2.300 cal BP (2.450–2.200 ¹⁴C BP) (Humid VIII), probably here mostly related to fluvial discharge from Bahr el Ghazal (Maley, 1981, 2004a), but also with some return of rain, attested by a transitory lowering of salinity in Ounianga (Kröpelin *et al.*, 2008). The last part of this humid phase evolved in a major erosive period, between ca. 2.400 to 1.900 cal BP.

12.5.2 The Mega-Chad (Figure 4a and 4b)

Before concluding this discussion about the oscillations of humid and arid phases recorded near the end of the Holocene, it is necessary to return to the Middle Holocene because during this epoch, the Mega-Chad lake developed. This immense Palaeo-Chad lake once occupied the entire central endoreic depression of the Chad Basin (Tilho, 1925; Schneider, 1969; Ghienne *et al.*, 2002; Leblanc *et al.*, 2006) (Figures 4a and 4b). The Mega-Chad had a size of about 340.000 km², similar to that of the Caspian Sea. Its level was stabilized by a threshold having an overflow channel situated in its south-west angle, near Bongor, at an altitude of 320/325 m (Schuster *et al.*, 2003). This channel evacuated the overflow waters towards the Niger river *via* the Mayo Kebi, a tributary of the Bénoué (Figures 4a and 4b).

The Mega-Chad was fed by various sources, partly from direct precipitation onto its surface, partly from streams and rivers draining the majority of the Chad Basin from the sudano-guinean savannas in the South, to the Tibesti mountains in the North (Maley, 1981, 2004a; Sépulchre *et al.*, 2008). The diminution of evaporation, largely related to the annual persistence of cloud cover, a phenomenon associated with probably two annual rainy seasons, also played a significant positive role. With respect to fluvial inputs, the major part flowed into the Mega-Chad by two large deltas (Figures 4a and 4b), one on the southeast flank where the palaeo rivers Chari and Logone converged (Torrent, 1966), and one on the north, the Angamma situated at the foot of the Tibesti (Servant *et al.*, 1969; Servant, 1973). As observed by Pias (1964, 1967, 1970: research done without radiocarbon dating), the large southern delta, which was mostly constituted of coarse sandy deposits, was linked to a sandy fluvial Formation, qualified as being “recent” by this author—in contrast to an “early” sandy Series, which had been reworked during the eolian phase of the Kanemian, during the LGM, thus before ca. 15.000 cal BP. This recent sandy fluvial Series, often covered by a red ferruginous type soil (Pias, 1970), is transgressive on a clay Formation characterized by the frequency of calcareous nodules of vertisolic origin. Various studies have shown that this clay Formation developed in most of Southern Chad during the Early Holocene, and ended about 8.500 cal BP (Bouteyre *et al.*, 1964; Cabot, 1967; Dupont

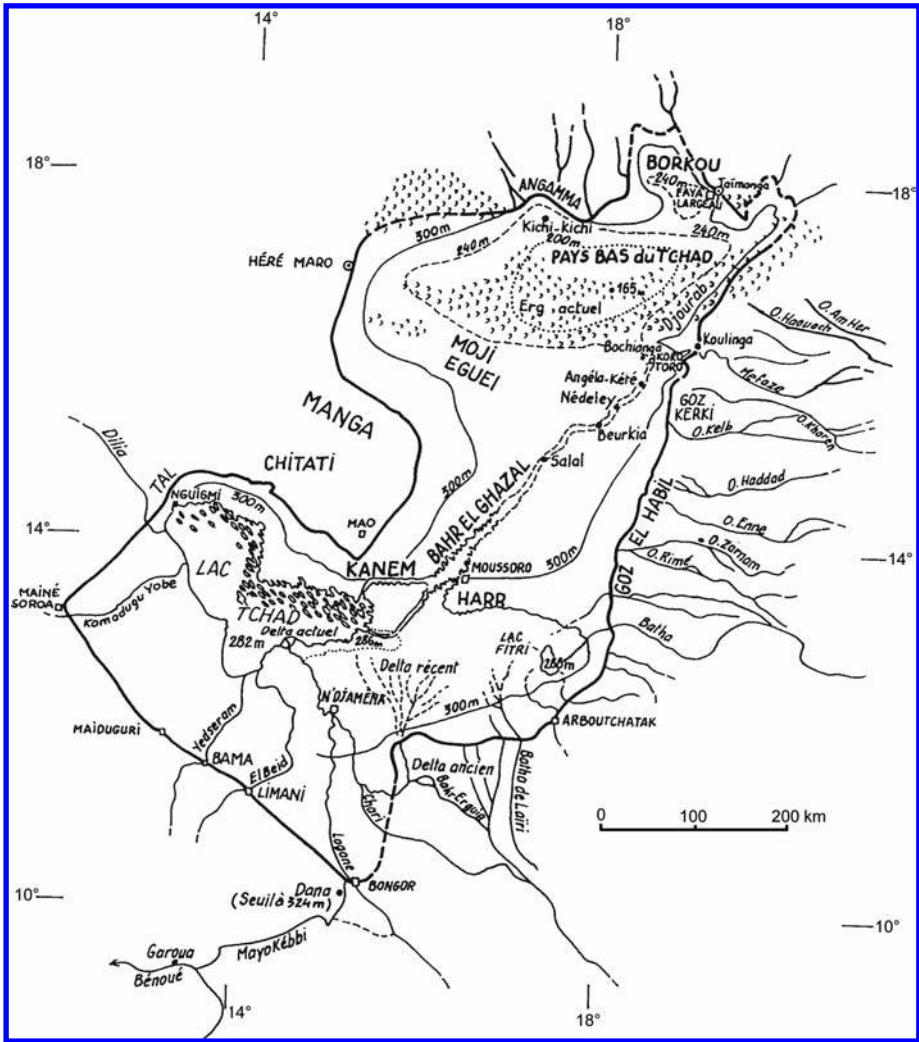


Figure 4a. Map of the Mega-Chad at about 320 m based on the position of the sandy perilacustrine barrier (Schneider, 1969); toponymy completed from Maley (1981).

and Delaune, 1970), confirming that the Mega-Chad, which was associated with this great delta, was functional beginning ca. 8.500 cal BP (7.700 ¹⁴C BP), that is, during the Middle Holocene (Maley, 2004a).

The study of diverse sections taken from the interior of the Mega-Chad perimeter (Servant, 1973) as well as the detailed analysis of the Tjeri section (Figure 5) from its center (about 10 km north of Moussorro, Figure 4a), have introduced greater precision, showing that the Mega-Chad was functional between ca. 8.500 and 6.300 cal. BP (7.700–5.500 ¹⁴C BP), with 3 relatively well characterized sub-phases from 8.500 to 8.200 (MC-1), 7.900 to 7.500 (MC-2) and 6.900 to 6.300 (MC-3) cal BP (7.700–7.400; 7.100–6.600; 6.000–5.500 ¹⁴C BP) (Maley, 2004a; Leblanc *et al.*, 2006).

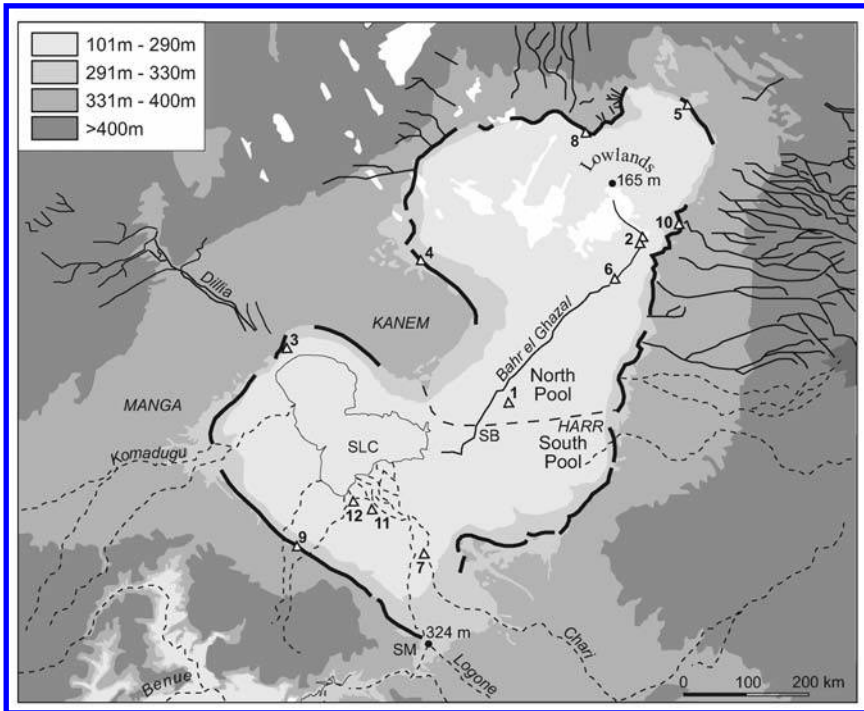


Figure 4b. Map of the Mega-Chad at about 320–325 m: Black and White image of the Central Basin produced from Shuttle Radar Topographic Mission (SRTM) data, clearly delineating the Mega-Chad in the regional geomorphology (from Leblanc *et al.*, 2006, [Figure 1](#)). Each half-tone corresponds to an altitude defined in the legend at upper left. The bold lines correspond to the remains of the Sandy Perilacustrine Barrier (Ghienne *et al.*, 2002), the black lines to rivers inactive during the 20th century, the dotted line to actual water courses, and the fine dotted line divides the Mega-Chad into a northern and southern basin, determining a threshold about 286 m at the level of the Bahr el Ghazal (12.5, 4). SLC: middle limit of Lake Chad during the 20th century for an altitude of 282 m. SB: fossil valley of Bahr el Ghazal. SM: Mayo-Kebbi valley which corresponds to the traces of the ancient Mega-Chad overflow towards the Bénoué. The open triangles mark the position of the principal dated samples ([Table 1](#) in Leblanc *et al.*, 2006).

During its functional existence, the Mega-Chad was surrounded by a large, sandy offshore bar complex formed mostly by fluvial alluvia, which were redistributed along its shores by regular currents. These currents were produced by prevailing and seasonal winds, the monsoon in the summer and the harmattan during the other seasons (Ghienne *et al.*, 2002; Schuster *et al.*, 2005; Bouchette *et al.*, 2010). Information obtained on the amounts of fluvial discharge and precipitation feeding the Mega-Chad, deduced mostly from pollen markers in the Tjeri's log ([Figure 5](#)), has shown that these different influxes were not always synchronized from one side of the Basin to the other, (chapter 12.6.4). It appears that the decrease or disappearance of certain water inputs, for example those from river discharge and rain in the northern half of the basin, could be compensated for by greater influx coming from the south. For this reason, it is difficult to directly compare certain humid phases in the southern Sahara with the extension phases of the Mega-Chad. This is the case for the MC-1 phase, however, phases MC-2 and MC-3 were synchronized to important humid phases in southern Sahara ([Table 3](#)).

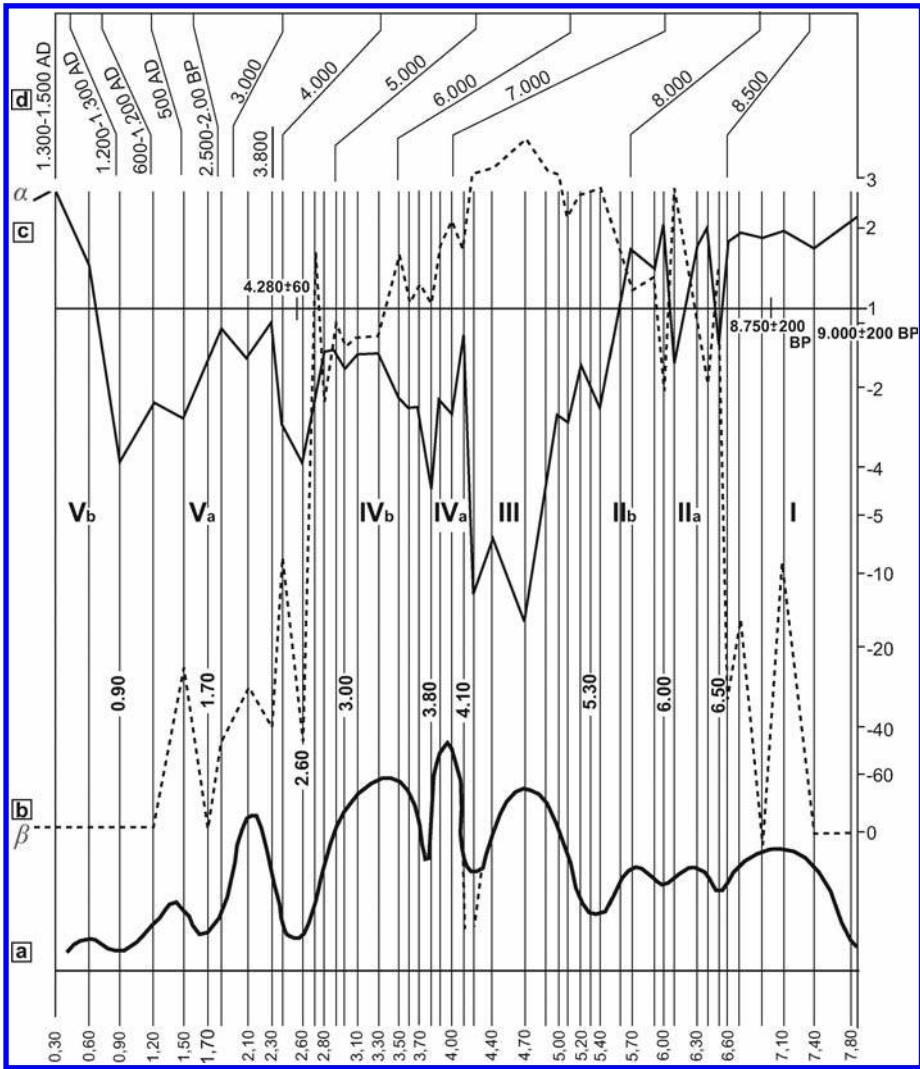


Figure 5. Holocene vegetation and lacustrine level variation in the central portion of the Chad Basin. Section of Tjéri, close to Moussoro (Figure adapted from Maley, 1981, 2004a). Pollen study by Maley (1981) and diatoms by Servant-Vildary (1978). a) at the base, levels in meters. Bold Curve: relative variation of the lacustrine levels based on diatomites and other geological data. b) Pollen variations (relative %) of the Sudano-Guinean element (dotted line); β present day percentages. Pollen curves b and c were calculated based on the average recorded in all levels, using a logarithmic scale (0 is arbitrarily fixed at -80). The Sudano-Guinean element developed under pluviocities greater than 1.000 mm/year, in the southern part of the Chad Basin. Studies conducted on present-day Lake Chad have shown that the pollen referred to this element were carried to the Lake by the Chari river: their variation over time can therefore serve as an indicator of the variation in the relative importance of fluvialite inputs at the study site (Maley, 1972, 1981). c) Pollen variation (relative %) of the Sahelian element (continuous line); α present day percentages. The Sahelian element constitutes the principal regional vegetation of Kanem, around Lake Chad (Maley, 1972, 1981). d) Chronology based on 3 radiocarbon datings (7,75 m: 9.000 ± 200 BP; 7,0 m: 8.750 ± 200 BP; 2,50 m: 4.280 ± 60 BP) and on regional correlations with various notable events (Maley, 1981, 2004a).

Table 3. Synthetic representation of the succession of humid and arid phases in the Sahara since ca. 22.000 years until the first Millennium AD after numerous references cited in the text. The data are presented from left to right and from South to North: Sahara (Mali, Chad Basin, eastern Sahara); Tibesti (central Saharan mountain); Fezzan (southern Libya); North of western Sahara (Sebkhra Mellala). Wavy line, approximate limit (+/- 300 years). The chronology is presented with calendar datings in the last column on left (calibration after Reimer *et al.*, 2004) and with radiocarbon datings in the last column on right.

years BP	Southern Sahara (Mali, Chad basin, Eastern Sahara)	TIBESTI	FEZZAN	Northern Sahara (S. Mellala)	¹⁴ C years BP
0					0
1.000					1.100
2.000	Erosion				2.050
	Humid 8		Arid	Arid	
3.000	Arid 7				2.900
	Humid 7	Fluvial deposits	Fluvial deposits	Humid	
4.000	Arid 6				3.700
5.000		Erosion	Arid	Arid	4.400
6.000	Humid 6				5.300
7.000	Arid 5	Conglomerat	Humid	Humid	6.100
	Humid 5	Lacustrine			
8.000	Arid 4	Calcrete		Arid	7.200
	Humid 4	Lacustrine	Arid		
9.000	Arid 3	Arid		Humid	8.100
	Humid 3	Lacustrine	Lake Mega Fezzan		8.900
11.000	Arid 2	Arid			9.550
	Humid 2				
12.000	ARID 1				10.200
	Younger Dryas (Maximum of Aridity)	Lacustrine			11.100
14.000		?			12.100
	Humid 1	Regression Calcrete	?		12.700
16.000		Lacustrine			13.400
17.000					14.200
18.000	Strong Aridity	Regression			14.800
19.000	LGM (Last Glacial Maximum)				15.800
20.000		Lacustrine			16.900
21.000					17.800
22.000					18.400

At the debut of the recent Holocene, contemporaneous with Humid VII described above, between ca. 3.900 and 3.200 cal BP, the last large Palaeo-Chad was formed, which, however, never attained the Mega-Chad stage. Its level was probably somewhere between 285 and 288 m. The little lacustrine offshore bar that culminates at these altitudes at the periphery of the present day lake, particularly in the south-east (Figure 4a), probably correspond to this lacustrine stage, as does the terrace that is exposed on the western flank of the interdune of Tjéri (Maley, 2004a, Figure 2). The formation of the “recent delta” described by Schneider (1969) in the north of the Chari-Baguirmi plain and to the south of Bahr el Ghazal (Figure 4a) also likely intervened at this epoch. The southern apex of this fossil delta is situated at about 300 m altitude and its frontal zone at about 286 m. When this great Palaeo-Chad regressed, considerable fluvial flows were continued into the Bahr el Ghazal, as supported by a dating of ca. 3.200 cal BP of fluvial oysters in living position at Koro-Toro, at about 25 m above the present day thalweg. The discharges were probably greatly reduced during Arid VII (ca. 3.000–2.700 cal BP) but they restarted between ca. 2.600 and 2.300 cal BP (Humid VIII) to, in particular, feed the thin residual lacustrine deposits at Borkou (Chad lowlands), which have been dated to this epoch (Maley, 1981). Now these marshes and this river flowing from south-east to north-east were succinctly described by the historian Herodotus, who died about 2.450 cal BP. In his celebrated historical work he reports that an expedition of Nasamons, a tribe that lived in Syrte north of Libya, left for the south and, after a long journey, apparently reached the Borkou (Carpenter, 1956). Herodotus tells that “the Nasamons were captured by small men of less than average size... who conducted them across extensive marshes and beyond that, to a city where everyone was of a similar size and black in color. Along the city, a large river flowed from sunset towards sunrise: they saw crocodiles” (Maley, 2004a).

12.5.3 The fluvial deposits

Sedimentology of fluvial deposits as well as their variation over time provide important information on palaeoenvironments and palaeoclimates. This is illustrated in the Chad Basin, for example, by the “Middle Terrasse” of central and meridional Sahara (Table 3), or by the fluvial terraces of North Cameroon, which were referred by Hervieu (1967, 1970) to two climatic-sedimentary cycles. The first cycle known as “Douroumian”, corresponds to deposits formed towards the end of the Pleistocene, before the great arid phase of the Kanemian, and is characterized by coarse sediments laid down by violent floods under semi-arid dry conditions. The end of this cycle is characterized by a relatively humid, stable phase, which was marked by a pedogenesis phase called the “Peskeborian”, with the formation of red soils, different from Holocene soils (Hervieu, 1967, 1970). This particular humid phase, which must have intervened between ca. 27 and 22.000 cal BP, would have been associated with a large Palaeo-Chad, the geomorphology of which is poorly defined and which developed in Kanem at the end of the Kamala Formation (Servant, 1973; Maley, 2004a). The second cycle, called “Bossumian”, corresponds to the clay formation having calcareous nodules of the southern Chad plains that extended up to the flanks of the Mandara Mountains and the Adamaoua Plateau. This formation forms a fluvial terrace that can attain in places a thickness of more than 30 m (Hervieu, 1970; Marliac, 1973; Gavaud *et al.*, 1975). The terrace was begun about 20–21.000 cal BP (ca. 18.000 ¹⁴C BP) and finished about 8.500 cal BP (ca. 7.700 ¹⁴C BP) (Maley, 1981, 1982). The first phase of the Bossumian, until about 18.000 cal BP (ca. 15.000 ¹⁴C BP), corresponded to relatively coarse levels. Clay deposits, mostly of loess origin, corresponded to the second phase, which has been

associated with the generalized development of vertisols (in which calcareous nodules developed) in the interfluvies and which continued until about 8.500 cal BP (Maley, 1981). These clay deposits were the result of significant and regular dust inputs carried from the Sahara (Maley, 1982). Further West, in the Senegal River basin, Michel (1973) described clayey fluvial deposits (Remblai 1), which would have been contemporaneous to Bossumian. A sandy fluvial Formation (Remblai 2) would have been deposited during the Middle Holocene (Michel, 1973; Maley, 1981).

The large Angamma delta developed to the north of the Mega-Chad (Figure 4a) is constituted by three sequences, from Early to Middle Holocene (Servant, 1973; Ergenzinger, 1978). These three sequences are found again upstream on the uphill slopes of Tibesti, in the upper part (Member 2) of the "Middle Terrace" (Table 3), which is a very characteristic fluvial formation throughout central Sahara (Messerli *et al.*, 1980; Maley, 1977, 1981, 2000).

South of the Niger loop, an important archaeological site was recently discovered at Ounjougou, in the Yamé valley. This valley cuts across the north flank of the Bandiagara Plateau in Dogon Country (Huysecom *et al.*, 2004; Rasse *et al.*, 2004, 2006; Mayor *et al.*, 2005). The thick fluvial deposits, currently under study, have contributed important information about the palaeoclimate and prehistory of the southern Sahel zone of Mali. The Ounjougou sequence is of interest firstly because of its length, and numerous OSL datings show that it must have begun before Isotopic Stage 5 (ca. 130.000 years) (Rasse *et al.*, 2004). Various prehistoric industries using the Levallois technique have been found in many levels. The Holocene, which has been studied in detail (Rasse *et al.*, 2006), constitutes a distinct thick sequence. It is embanked in that of the Pleistocene, probably during an arid phase that appears to have been contemporaneous with the "Younger Dryas" (ca. 12.000–13.000 cal. BP). The Early Holocene forms a subsequence made of more or less coarse sediments with finer levels, ranging from ca. 11.200 to 9.000 cal BP (ca. 9.800–8.100 ¹⁴C BP), which have been associated, in part, with an Early Neolithic phase characterized by the presence of pottery (Huysecom *et al.*, 2009). A long sedimentary hiatus intervenes in the Middle Holocene, from ca. 9.000 to ca. 6.500 cal BP (ca. 8.000–5.700 ¹⁴C BP); this hiatus seems to have been contemporaneous with the erosive phase that ended the construction of the Bossumian terrace in the Chad Basin. Following this, a more regular sedimentation intervenes in the Yamé valley. This sediment is associated with a rich savanna vegetation (Ballouche, work in progress). Another sedimentary hiatus situated about 4.500–4.000 cal BP separates these deposits from an original fluvial Formation characterized by varves, the expression of seasonal deposits. This Formation, which began about 3.800 cal BP and ended about 3.000 cal BP (Mayor *et al.*, 2005), is contemporaneous with the last large Palaeo-Chad, (chapter 12.5.2). Breunig and Neumann (2002) showed that the generalized arid phase (Aride VI), which followed and lasted until about 2.500 cal. BP, appears to have corresponded to the transition from the Neolithic to the 1st Iron Age across the Sahel of Western Africa. This last appears to have flowered during Humid VIII (ca. 2.600 and 2.300 cal BP).

Then a relatively important and generalized erosive phase intervened between ca. 2.400 to 1.900 cal. BP, across the southern Sahara (Maley, 1981, 2004b) up to the equatorial Forest Domain, frequently associated with the laying down of coarse, sometimes conglomerate, deposits (Maley and Brenac, 1998b). In the southern Chad Basin, this particular climatic phase was associated to the final expansion of savannas on the Adamaoua Plateau (Vincens *et al.*, 2009). This phase of considerable perturbation of Central Africa forest was also expressed by savanna expansion in many parts of the present forested area (Maley, 2001, 2002), as from north of Mount Cameroon up to around Barombi-Mbo lake (Maley and Brenac, 1998a). An ancient savanna corridor

running from the southeast extremity of Cameroon up to the Plateau Batéké in North Congo was first hypothesized by Letouzey (1968, 1985), based on phytogeographical data, and later Maley (2001, 2002) and Maley and Willis (2010) provided precisions and datations linking this savanna corridor to this phase.

Around Central Chad, the erosive phase mentioned above, which ended towards ca. 2,000–1,900 cal BP, was responsible for a profound erosion of the Bahr el Ghazal, in particular for about 15 m in its middle course at Salal (Figure 4a) and probably more than 40 m in its lower course at Koro-Toro. This last value is obtained based on the following: fluviatile oysters in living position dated of ca. 3,200 cal. BP are located at about 25 m above the present day thalweg (chapter 12.5.2), added to sedimentary filling until present, which could amount to ca. 15 m, as referenced by the filling at Salal. Thereafter, in this last place, a thick sedimentary Series rapidly filled in the new thalweg. The filling begins by a blackish clay sequence 4.5 m thick, which has been dated towards the base to about 1,700 cal BP (Servant, 1973). This is followed by a second sequence of sandy alluvia deposited for 7.5 m that terminated about the 12th century AD, (cf. below). The series finishes with a 3 m sequence of eolian sand reworked from earlier neighboring dunes. The size of the first 2 sequences and especially the sedimentology of the first, can only be explained by direct fluviatile inputs, which must have passed by certain still functional branches of the “recent delta”. A similar grey-blue clay is also found in the lower part of deposits making-up the small Chari delta of today (section of Adidé; Mathieu, 1978). Thus, it appears that the clay sequence of Bahr is the result of sedimentary inputs coming from upstream basins of the Chari and Logone Rivers (Adamaoua: Central Africa and Cameroon) where, beginning from 1,850 cal. BP (1,900 ¹⁴C BP), a 2–3 m thick clay sequence was laid down (Maley, 1981; Maley and Brenac, 1998b).

Starting at the conglomerate level, mentioned above, this clay sequence constitutes the lowest part of a “Low Terrace”, which has been found across the Sudanian and Sudano-Guinean zones of West Africa (Maley, 1981) as well as throughout the equatorial forest domain (Maley and Brenac, 1998b; Maley, 2004b), from the central part of the Congo Basin to Ghana and Sierra Leone (Thomas and Thorp, 1992). The construction of this Low Terrace was continued by a sandier middle sequence, which could be dated between 700 and 1,200 AD. This dating correlates well with the second sandy-alluvial sequence of Bahr el Ghazal, of which—the principal flowing ended in the 12th century AD—this last point was confirmed by the fact that the earliest archeological sites found at the bottom of the Bahr have been dated to century AD (“Haddadian”: Treinen-Claustre, 1982). The upper sequence, which is mostly sandy, was probably largely laid down during the last phase of flow in the 17th century. In the south of the Chad Basin, erosion of the Low Terrace and formation of its relief began in the 19th century, and accelerated during the 20th (Maley, 1981; Maley and Brenac, 1998b). Hence, the first clay sequence of this terrace implies the existence of considerable and regular fluviatile flows between ca. 300 and 700 AD (1,700 and 1,300 cal BP). In contrast, the second sandy-loamy sequence corresponded to lesser and more seasonal flows between ca. 700 and 1,200 AD.

12.5.4 Lake Chad over the last two Millennia

The diverse sedimentological data reported above for the Lake Chad region provide palaeoenvironmental information on the last two Millennia. Notwithstanding, other data, largely archeological and historical, sometimes provide very precise information on climatic conditions of certain epochs at various places in the Sahara and

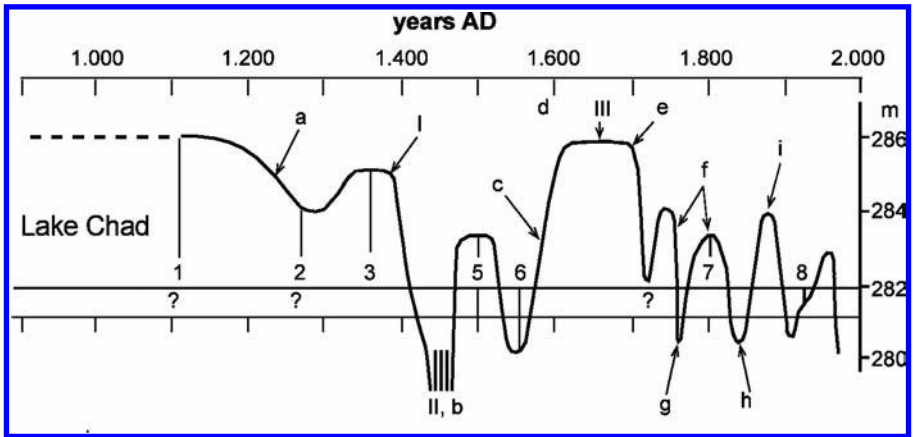


Figure 6. Variation in Lake Chad levels (a,b,c) during the last Millennium, in calendar years AD (Maley, 1981, 1993, 2004a). Numbers 1 to 8 correspond to the position of the palynological samples, roman numbers I, II and III, to the radiocarbon dated levels (average calibrated values) and the letters a to i, to various dated historical data (adapted from Maley, 1981, 1993, 2004a).

its meridional margin (Maley, 1981; Mayor *et al.*, 2005). With respect to the last Millennium, a reconstruction of Lake Chad's levels was accomplished (Figure 6) by studying a sedimentary core (60 cm) sampled close to Baga-Sola, in the lake's central sector, towards the north of the "Great Barrier" (high bottom frequently covered with aquatic vegetation separating the south and north basin). The reconstruction involved the following 3 steps (Maley, 1981, 1993):

a. Geological step: A first curve was traced based on sedimentological variations:

- (1) peat, organic matter or sandy-clay layers, linked to low lake levels;
- (2) layers with retraction fissures containing wood charcoal of a burnt vegetation, linked to low lake levels and drying phase;
- (3) compact clay layers, linked to relatively high lake levels.

Three calibrated radiocarbon datings (I, II, III) allowed the establishment of a relatively rough (± 100 years) chronological control.

- b. Palynological step: Analysis of pollen from the different sedimentary levels allowed refinement of the variation relative to the high and low lacustrine layers, principally using hygrophilous plants as proxies, as these pollen grains increase—or decrease—in proportion to the development—or diminution—of marshy conditions and hence to lower—or higher lacustrine levels.
- c. Historical step: Certain historical data referred directly or indirectly to the levels of Lake Chad or other data coming from oral traditions and dated by reference to historical events. Together this information allowed the further refinement of this curve and also to chronologically pin it down thanks to precise dating of some remarkable points. For detailed information on these data, the reader is referred to the following publications: Maley 1981, 1993, 2004a.

The variety and precision of certain historical data are due to the fact that for a little over 2,000 years, Lake Chad hasn't extended to the lowest part of the basin, which is located about 165 m at Borkou (Lowlands of Chad), but has been positioned between altitudes of 281 and 282 m (average altitude during the 20th century) on the south flank of the basin and below a threshold located at Kanem, close to its eastern

shore (Leblanc *et al.*, 2006) (Figure 4b). The hydrologists of ORSTOM, (now IRD) calculated that the crossing of this threshold and the establishment of a permanent flow into the Bahr el Ghazal could only have occurred when the lake attained an altitude close to 286 m (cf. Maley, 1981; Olivry *et al.* 1996). Given that historical data combined with information from oral traditions clearly indicate a permanent flow of Bahr el Ghazal during all of the 17th century, therefore, it can be concluded that the level of Lake Chad must have been about 286 m (Maley, 1981, 1993).

Given that the Chad Basin is quite extensive, going from central Sahara in the North towards the tropical humid savannas in the South (sudano-guinean zone), the climatic tendencies of these two distant regions could either be in or out of phase. During the 17th century at the peak of the Little Ice Age, the tendencies were completely out of phase. During the previous centuries, the nomadic Kreda tribe wandered across the Borkou, towards the south of the Sahara; however, after a new phase of aridity closely tied to a strong increase in eolian activity, the Kreda were forced in the 17th century to migrate towards the Kanem, further south, where they live today. According to Kreda oral tradition, when they emigrated from Borkou, the Bahr el Ghazal flowed (Maley, 1981, 2004a). This important fact is confirmed by other precise historical testimony (Maley, 1981). Physical data confirm that there was strong eolian activity at this epoch in the center of the Chad Basin, at Manga (Holmes *et al.*, 1999). Given, therefore, the great aridity that developed in the south of the Sahara, the waters that overflowed from Lake Chad at this epoch, feeding the Bahr, could only have come from the Chari and Logone Rivers, and particularly from rains that fell on the savannas of their upper catchments. From this it is clear that in the 17th century, on the one hand rains of the Sudano-Guinean zone must have been greater than today and on the other the harmattan of southern Sahara was considerably reinforced. This particular climatic behavior, practically unknown during the 20th century, appears to have been general during this epoch across north tropical Africa (Maley, 1981, 2004a) because very strong floods were reported in the Niger bend, often cutting the city of Timbuktu in two (Péfontan, 1922), and at the same time, there was intense regional aridity (Cissoko, 1968) associated with strong eolian reactivation (Stokes *et al.*, 2004; Rendell *et al.*, 2003). Nearby in Mauritania, a recent dune phase was also dated to approximately the 17th century (Sarnthein, 1978), but could have begun in the second half of the 15th century forward (cf. below) (Hanebuth and Henrich, 2008). During this epoch, the strong floods of the Niger must have been fed by intense and prolonged rains on the upper part of its catchment, which is also situated in the Sudano-guinean zone. From a geographical and climatic point of view, the basin of the Niger River (for its upper and middle courses) is rather similar to that of the Chad. Further to the East, voyagers reported that in the 17th century, certain lakes of the Ethiopian Plateau overflowed (Grove *et al.*, 1975), this agrees well with the very strong floods in the Nile's lower course indicated for this epoch. In particular, Fayoum Lake, which is fed by a branch of the Nile, experienced a transgressive phase registered by historical testimony (Maley, 1981). It will become evident further on that similar out of phase climates occurred in other Holocene epochs such as between ca. 300 and 700 AD and about 8.300–8.100 cal BP.

It is worth mentioning that the out of phase climate of the 17th century was so unusual, it has rarely been well interpreted by historians. The reports of great floods and overflowing of lakes fed by these large rivers across the Sahel, led them to conclude that there was a humid phase in this climatic zone, without taking into account the many proofs of aridity and, above all, eolian reactivation in the Sahel and the southern Sahara. Historians also neglected the fact that over 85% of floods depend even today on fluvial influxes originating in the south of the great river basins (Niger, Chari and Logone, Nile) which are in the Sudano-guinean zone.

By contrast, around the middle of the 15th century, climatic phenomena were very different because at this epoch, the Chari and Logone flows were so reduced that the meridional part of Lake Chad had completely dried out. Several precise geologic data can be referred to this phenomenon, in particular desiccation fissures filled with carbonized debris and formation of a calcareous crust in the archipelago near Bol (Maley, 1981). This drought phase was confirmed by detailed data from oral traditions collected by Seignobos (1993) from certain Fellata tribes (Peuls), who today live in the south of Lake Chad. By matching historical facts, this author was able to date the drought to the middle of the 15th century, something that corresponds well to the average value of the two radiocarbon datings mentioned above (Maley, 1981). The oral histories report that at this epoch a very strong regional drought forced the Fellata to move their villages to the dried out part of southern Lake Chad where there was still pasture and water in hollowed out wells at the bottom of the dried out lake! The precision of the testimonies allow us to conclude that the drought lasted about one generation, that is 20–25 years, so that it must have occurred from ca. 1.440 to 1.470 AD (Maley, 1993, 2004a). The sudden return of the river floods drowned all of the villages, which is why the Fellata memorized this catastrophic event. At this epoch, therefore, the considerable diminution in rain extended from the Sahel to the Sudano-guinean zone (Maley, 2004a). Recent study of a marine core sampled offshore of Mauritania, the base of which spans back ca. 5.000 years BP (Hanebuth and Henrich, 2008), demonstrates that the most intense eolian activity peaked about 1.470 AD, providing additional evidence of the very dry conditions during this short period—which can be compared with Arid VI (ca. 4.200–4.000 cal BP) and certain, albeit much less intense, arid phases of the 20th century.

Incidentally, this intense drought phase that intervened during the middle of the 15th century can also provide an explanation of some dry stone structures found at certain summits of the Mandara mountains at about 1.000–1.200 m, in the Sudanian zone of northwest Cameroon (ca. 10°55'N–13°45'E). These massive structures, built by local people, probably ancestors of today's Mafa, are called by archeologists "DGB", an abbreviation of the original Mafa name. These local people consider the DGB to be "ancient fortified chiefs houses", whereas archeologists thought they were look-out towers, in view of their position on ridge tops of dominating hills (David, 2004; David *et al.*, 2008). However, after archaeological excavations, no human remains were found, so they could not have been tombs, nor were there signs of human habitation, leading archeologists to wonder what the real function of these stone-built structures was. Furthermore, it appears that these structures had only been constructed and used in the 15th century, as clearly indicated by radiocarbon datings (David *et al.*, 2008). The fact that these dry stone structures must have been contemporaneous with the severe drought phase in the middle of the 15th century and that there are sometimes found the remains of large funnel-mouthed narrow-necked ceramic vessels has led to the hypothesis that these particular structures must have served to collect water. When it was foggy, water would have condensed in abundance on the cold walls of the numerous cavities laid out in the "DGB" (Maley and David, 2008). During this long drought, the quasi absence of rain clouds, especially of cumuliform type, could have been compensated by the presence of non-rainy stratiform clouds, which when clinging to hill tops, would have generated abundant fog (Maley, 1982). Hence, water could condense on the cold walls of the cavities and been collected by large ceramic vessels. This particular method of collecting water is used by various peoples around the world, such as in the Cape Verde islands and the Andes (Gioda *et al.*, 1994). In nature, this phenomenon is exploited by vegetation that develops in "cloud forests" (Cavalier and Goldstein, 1989). It is significant that the only relictual cloud forest

of the Mandara mountains, dominated by *Olea capensis* (Letouzey, 1985), is found at Hosséré Oupay (ca. 1.300 m), a neighboring summit of the “DGB’s” (Maley and David, 2008).

The base of the core sampled at Baga-Sola has been dated around the 11th to 12th centuries AD; however, information on Lake Chad during the 1st Millennium AD can be deduced from other data coming first from the Tjéri section, which ended about the beginning of last Millennium when the Bahr el Ghazal ceased its principal phase of flow around the 12th century AD (Figure 5) (Maley, 1981), and from the “Low Terrace” discussed above. Indeed, the section of Adidé in the delta of present day Lake Chad (Mathieu, 1978) presents a compact clay sequence under the last Millennium layers, which are dated in their lower part. This clay sequence, because of its stratigraphic context, can be referred to the lower part of the “Low Terrace”. Thus, it is evident that considerable and regular fluvial influxes fed Lake Chad between ca. 300 and 700 AD, followed by a phase having more seasonal flows between ca. 700 and 1.200 AD. As noted above, Lake Chad’s levels were controlled by an overflow channel by which excess water was discharged into the Bahr el Ghazal, so it can be concluded that during the 1st Millennium AD the lake’s level was always between about 286–287 m, but under different climatic conditions. Our data demonstrate that between ca. 300 and 700 AD practically all inputs came from fluvial influxes because an upsurge in eolian activity has been noted for this epoch in Central Chad (at Manga; Holmes *et al.*, 1999), in the Niger loop (Mayor *et al.*, 2005) and in Mauritania (Hanebuth and Henrich, 2008). Conversely, for the period ca. 800 to 1.200 AD which corresponds to the maximum of the “Middle-Age Warm Period” (Keigwin, 1996; Mann *et al.*, 2008), data are more diverse. First, the pollen spectrum obtained from the Baga-Sola core shows that in the 12th century, the Sahelian vegetation surrounding Lake Chad was distinctly more developed than it is today, suggesting that regional rainfall must have been greater. As certain historical information explained further on, the rainfall probably corresponded to two successive rainy seasons. This relatively high lacustrine level can therefore be explained by a longer rainy and cloudy period during the year and decreased evaporation thereafter. At this epoch, fluvial influxes (marked by Sudano-guinean pollen types, the percentage of which diminished to half that found presently, Maley, 1981) played a secondary role in feeding the lake, whereas today 80 to 85% of inputs are fluvial (Olivry *et al.*, 1996; Maley, 2004a). At this epoch, the Sahelian zone must have been in its ensemble distinctly more humid, something which favored the development of regional populations, as attested, for example, by the fact that the Capital of the Kanem Empire, Manam, was at that time at Bodelé, towards the present southern limit of the Sahara (Zeltner, 1980), and that the Capital of the Ancient Ghana Empire was in a similar position in the south of present day Mauritania (Mayor *et al.*, 2005; Maley, 1981, 2004a).

12.6 PALAEOCLIMATIC INTERPRETATIONS

12.6.1 Introduction

In a departure from the detailed descriptions of the humid/arid phases in previous sections, here, an attempt is made to characterize the various rain systems that could be responsible for the different humid phases.

Interpretations are only possible for the phases having datings or relatively precise estimations, such as those presented in Table 1 for the last 330.000 years and in Tables 2 and 3 for details of the last 20.000 years. Table 1 shows that the principal humid phases

correlate relatively well with major warm phases and also with certain relatively warm interstades, which intervened globally and are represented by “Isotopic Stages” determined in marine environments (Martinson, 1987) (Table 1, column 2). It can also be seen that intermediate arid periods correlate with relatively cold phases (Table 1). Most researchers studying the sequences of the eastern Sahara have arrived at these same conclusions (Wendorf *et al.*, 1993; Szabo *et al.*, 1995), as well as specialists studying central (Libya: Gaven *et al.*, 1981) and western Saharan sequences (Mali: Petit-Maire, 1992; Sénégal: Lézine and Casanova, 1991). The approximate correlation between the humid phases and interglacial periods or certain relatively warm interstades, has been interpreted to be the result of intensification of the African monsoon, which would have extended over all of the Sahara (Prell and Kutzbach, 1987; McKenzie, 1993). This interpretation is based on the fact that in the middle of the boreal summer today, at the hottest moment of the year in the Northern Hemisphere, the monsoon has its most northward extension. Such an interpretation is readily understandable for the warmest phases, i.e. Isotopic Stage 5 (5e, 5c and 5a; from 13.000 to 75.000 years), however, it is less evident for certain humid phases synchronous to “temperate” interstades, which intervened during the long cold periods of isotopic stage 6 (6c) or stage 3 (3c, 3a), when important volumes of ice subsisted in the high latitudes of the Northern Hemisphere. Wendorf *et al.* (1993, p. 566) have already remarked that the “traditional model” that only includes the monsoon is not applicable to all humid phases of the central Sahara. Moreover, estimations of annual pluviosity, based on diverse precise geological data, appear too great at this latitude to be explained only by monsoon rains, as for example for the presently totally desertic site of Bir Terfawi in Southern Egypt. During the greatest lacustrine phase, the “Gray Lake 2” stage (Table 1), which would have intervened during the warmest phase of the last Interglacial (Isotopic Stage 5e, chapter 12.6.1), the estimated rains would have been close to 500 mm per year. Later, during the Holocene, there is no evidence of a permanent lake for this site, the estimated rains would have been distinctly less and comprised between 200 and 50 mm. In particular, the role of the monsoon during the Last Glacial Maximum (LGM), between ca. 24.000 and 15.000 years cal BP, appears totally inadequate to explain the important humid phase, which has been demonstrated for this epoch. In the high mountains of central Sahara, in the crater of Tibesti, there existed a large lake having a depth of 500 m (Maley, 2000). And all the more so, as the end of this lacustrine phase, which intervened about 15.000 cal BP, coincided with the beginning of the first great and well-characterized extension of the monsoon into the low latitudes of tropical Africa (see above Humid I phase, between ca. 15.200 and 13.900 cal BP).

12.6.2 The Saharan cyclonic depressions

Isotopic geochemical studies of oxygen conducted on sediments of ancient lacustrine sequences can provide important data for reconstructing some climate components at the time these sediments were formed (McKenzie, 1993; Sultan *et al.*, 1997; Smith *et al.*, 2004). However, to properly interpret these results, it is important to first consider the isotopic studies (oxygen and hydrogen, in particular the measure of the relative importance of the heavy isotopes $\delta^{18}\text{O}$ and δD , the deuterium, characterizing the extent of evaporation) done on fossil waters coming from phreatic tables at sites across the Sahara (Sonntag *et al.*, 1980; Edmunds *et al.*, 2004), and also of present day rain water, which for each sampling station, have been revealed to be similar to water in the upper part of the phreatic table (Joseph *et al.*, 1992). Oxygen isotopic study of lacustrine carbonates has shown their isotopic value ($\delta^{18}\text{O}$) to be close to that of

rainwater recharging the water table, which fed the different lakes (Smith *et al.* 2004). In an important synthetic study, Sultan *et al.* (1997) demonstrated that there exists a fundamental difference between the entire north of the Sahara, north of ca. 20°N, called the “Saharan Zone”, and the southern part of the Sahara, between latitudes 20° and 10°N, known as the “Sahelian Zone” (Figure 7).

In the Sahelian zone, present day rains result, for the most part, from squall lines (Leroux, 1996, 2001). These are more or less North–South alignments of large cumulus clouds that form in the monsoon and move from East to West in an eastern flux generated, in the low levels, by the East African Jet (Cook, 1999), and, in the upper levels, by the Tropical Easterly Jet, which is generated by the thermal contrast produced between the equatorial zone and the eurasiatic continental regions (Flohn, 1971; Leroux, 1996, 2001). In a sub-Saharan transect about 4.000 km long, the isotopic composition of rains issuing from squall lines show an enrichment from west to east in $\delta^{18}\text{O}$ and δD ; this has been attributed to a strong contribution of evaporated waters from the Indian Ocean and advected by the eastern flux (Joseph *et al.*, 1992). However, a mixing is produced in these clouds with water vapor coming from the atlantic monsoon and which is aspirated to the base of large cumulus clouds during their westward travels (Cadet and Nnoli, 1987). Based on these different data, Sultan *et al.* (1997) concluded that if the ancient humid periods in the “Saharan Zone” were the consequence of the extension of the monsoon towards the north, roughly similar isotopic compositions should be observed between groundwaters of the “Saharan Zone” and those in the present day “Sahelian Zone”, characterized, in particular, by a

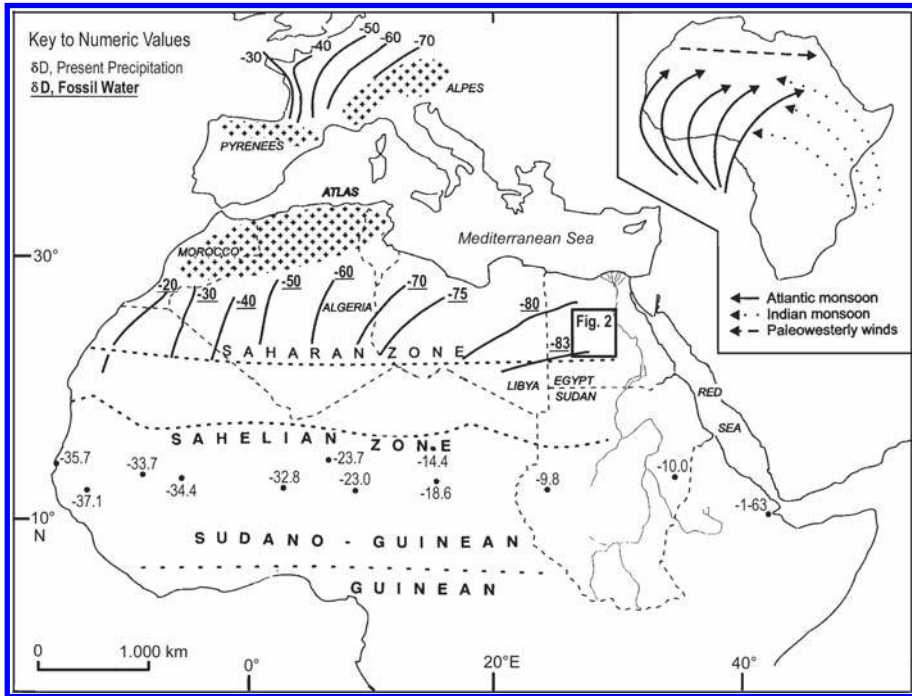


Figure 7. Regional variations in δD , from South to North, of the upper part of phreatic tables in the Sahelo-Sudanian zone, of fossil waters from the north Saharan zone, and present day water from western European phreatic tables. (Figure adapted from Sultan *et al.*, 1997).

gain from West to East. However analyses by Sonntag *et al.* (1980) and Edmunds *et al.* (2004) on fossil waters of the “Saharan Zone”, show the contrary, that is, a net loss of $\delta^{18}\text{O}$ and δD from West to East (Figure 7). The authors attribute this phenomenon to a “continental effect” dependent on rains associated to a circulation from the west, in a manner similar to what is observed nowadays in Western Europe. Thus, the rains that fed the ancient phreatic tables weren’t the result of the monsoon, but of cyclonic depressions circulating in a western flux, as is presently the case in the Maghreb and the Mediterranean zone.

However, new modeling of the African monsoon by Patricola and Cook (2007) have led them to conclude that in the Middle Holocene, in the south of the Sahara during the summer (July and August), rain systems moved from West to East in a cyclonic circulation. In their models these authors explain this reversed circulation in comparison to the present, by the absence of the African Easterly Jet in low levels of atmosphere. Indeed in their modelizations of the Middle Holocene, the estimated surface temperatures of the Sahara appear to be lower than today by 2 °C to 4 °C, strongly neutralizing the south-north thermic contrast on which this jet depends (Cook, 1999). Patricola and Cook (2007) explain this temperature decrease by a greater development of vegetation and also by an increase in cloud cover. However, for the South–North thermic contrast not to have existed, it is necessary that the temperature decrease affected the greater part of the year, not just the summer, which implies, not only the persistence of the vegetation—which plays an important role—but that of cloud cover throughout most of the year. It is evident that such climatic conditions could not have been the simple product of increased summer rains nor, in particular, could a longer annual cloud cover have resulted without the development in the months preceding and succeeding summer other climatic systems generating cloud cover and rains.

Throughout the world, such systems commonly occur in subtropical regions of both Hemispheres and are known as “Extratropical Depressions” (Flohn, 1971; Nicholson and Flohn, 1980). Recently, new detailed studies have been done on these climatic systems by Knippertz (2005; Knippertz and Martin, 2005) who called them “Tropical Plumes”, an expression which aptly describes the expulsion of tropical humid air in the subtropics, to the north of the Inter-Tropical Convergence Zone (ITCZ). These Tropical Plumes appear as long transverse cloudy bands, mostly oriented SW to NE, intersecting the subtropical anticyclone belt—a phenomenon that occurs on both sides of the equator—and periodically links, in space and time, the large equatorial humid belt with subtropical and temperate latitudes, where these cloudy bands carry gusts of humid air, major sources of rain in these regions. It is in this way that the majority of rains in the Mediterranean region, which belongs to the subtropical Domain, are generated by these cyclonic Extratropical Depressions (Arz *et al.*, 2003; Knippertz *et al.*, 2003). In the Sahara, these depressions have been often called Saharan Depressions (Dubief, 1963, 1999).

The formation of these depressions occurs throughout the cool season, from autumn to the following spring, when deep meanders are produced in the upper westerly circulation (Rossby waves), corresponding at these latitudes to the Subtropical Jet Stream, and when these meanders spread towards the equator (Figure 8) (see also the schemas presented by Knippertz, 2005, Figure 10). The cold air that often infiltrates at high altitude in these depressionary corridors provokes rapid undulations of the ITCZ, in this way favoring brief invasions of equatorial humid air (Nicholson and Flohn, 1980), hence the expression Tropical Plumes (Knippertz, 2005). The humid air that feeds these pluvial systems, therefore, does not come from the northern sector, as was once mistakenly thought, but mostly from marine sectors of southwest or

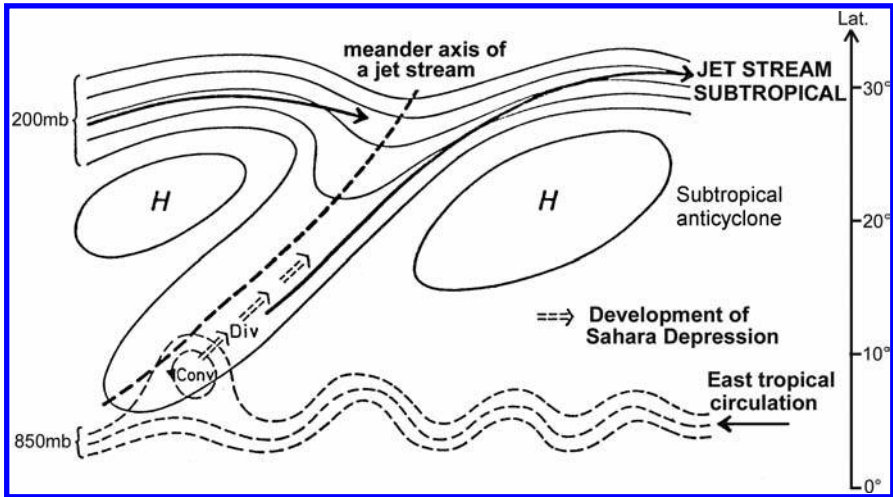


Figure 8. Schematic diagram of the formation and travel of “Saharan Depressions” (Extratropical Depressions). Interaction between a high-tropospheric polar flow (200 mb) in a meander of the Subtropical Jet Stream, and tropical humid air circulating in low level tropical Easterlies (850 mb), induce the genesis (convergence) of a cyclonic Depression which is dragged into (divergence) a westerly flux (Figure adapted from Nicholson and Flohn, 1980).

west tropical Africa. Such cyclonic pluvial systems that form in this way at the north of the InterTropical Front (ITF; ground trace of monsoon front) are carried by the western flux, generated by the Subtropical Jet, and discharge their rain throughout the Sahara (Dubief, 1963, 1999), when climatic conditions are favorable (Drochon, 1971; Nicholson and Flohn, 1980; Thépenier and Cruette, 1981; Knippertz, 2005). Hence, one speaks frequently of “winter rains”, or cool season rains, or “mango rains” near the Sahelian fringe, or even, around Mali and Senegal, of “Heug rains” (Dubief, 1963, 1999; Charre, 1974; Maley, 1981). Exceptionally in the heart of the boreal winter when the ITF is close to the equator, these pluvial systems can even today affect north tropical savannas (Knippertz and Fink, 2006a).

To conclude, the thermic conditions described by Patricola and Cook (2007) to explain the cyclonic circulation of the monsoon during the Middle Holocene, also appear to be favorable to the formation of extratropical Depressions (Knippertz, 2005)—which, in this way, every year could have preceded and followed rains generated by the monsoon, (chapter 12.6.3).

12.6.3 Seasonal contribution of monsoon rains and cyclonic rains in meridional Sahara

In view of this hypothesis, it is interesting to observe that relatively elevated $\delta^{18}\text{O}$ values of -12 to -5‰ , obtained for certain lacustrine carbonates from the Egyptian Sahara and formed during the humid periods of Isotopic Stage 5, led Smith *et al.* (2004) to conclude that such values can be explained by lacustrine environments fed by both the monsoon and cyclonic Saharan Depressions. Such a double origin of rain is an important climatic phenomenon and had been earlier proposed to explain certain lacustrine phases of the Saharan Holocene (Maley, 1977, 1981). For the Early Holocene, Arz *et al.* (2003) had also demonstrated the importance of “Mediterranean” cyclonic rains in the northern

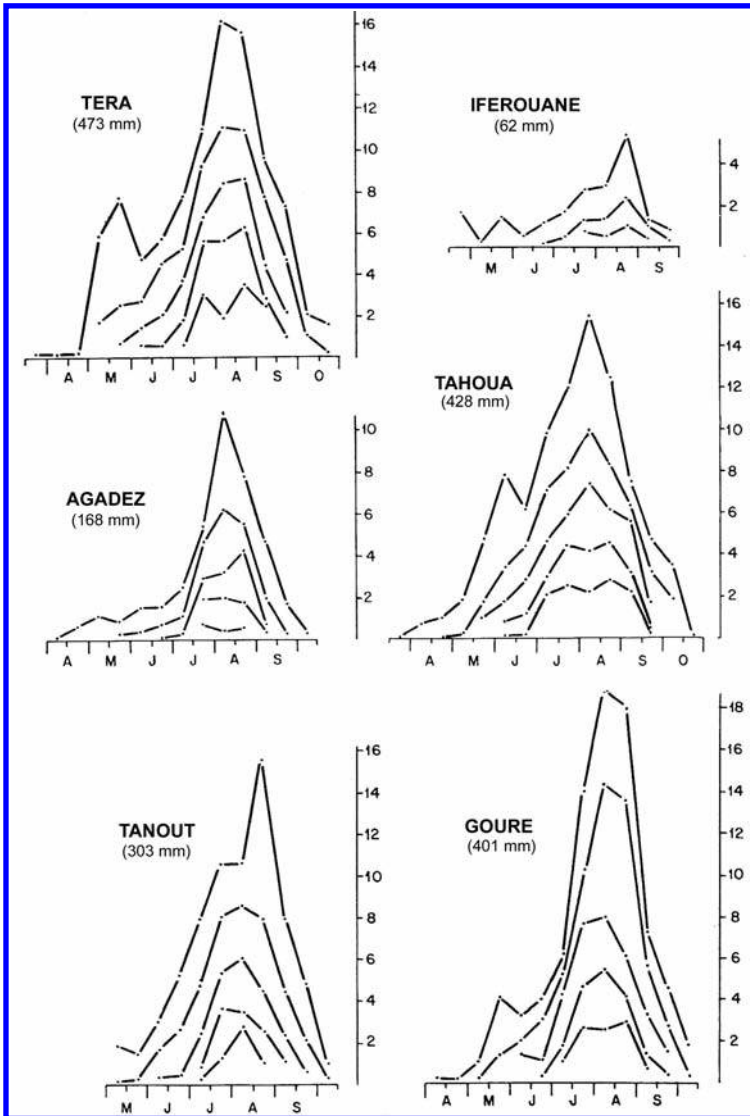


Figure 9. Present day examples of Spring rains linked to extratropical Depressions. Annual evolution of bimonthly pluviometry for several stations in Niger (characterized by their annual total), expressed by quintiles calculated over 30 years (1941 to 1970): Q5, Q4, Q3, Q2, Q1 from external curves to internal curves (from Charre, 1974).

Sahara, in particular, north of the Red Sea. With respect to the 20th century, examination of available data for the south and center of the Sahara show that the annual association of monsoon rains and cyclonic rains, linked to the Saharan Depressions, was a frequent phenomenon (Figure 9). For certain Saharan stations, these depressions played a major role, as, for example, at the Tamanrasset station near Hoggar, which, between 1925 and 1970, received annually an average of nearly 50 mm; the rains linked to the northern extension of the summer monsoon (July, August) only represented about 30%

of this total, the remaining 70% were the result of cyclonic rains falling north of the ITF (Dubief, 1963, 1999; Maley, 1981, p. 480, [Table 1](#)). However, when the vast literature treating palaeoclimates of the Sahara is examined, especially with respect to modeling Holocene climates, it is evident that the great majority of authors almost always attributed ancient humid periods solely to phases of expansion of the monsoon, neglecting rains of cyclonic origin generated by Extratropical Depressions.

Several historians studying the last Millennium in these regions have reported examples of rains which must have resulted from these two separate origins. At the beginning of the 16th century, a traveler, Valentin Fernandès, observed in Senegal that local people plant and harvest twice a year, in April and September (Daveau, 1969), probably related to cyclonic rains falling during the first months of the year (i.e. Heug rains chapter 12.6.2), and after, during the summer, to rains from the monsoon. A similar situation probably also existed for the medieval Ghana Empire, which developed in present day southern Mauritanian Sahara beginning in the 7th century until its demise in the 13th century (Mayor *et al.*, 2005). The famous Wagadou legend, which recounts the conditions of the establishment and end of medieval Ghana, explains that each year rains began to fall during the Spring festival and were followed later by summer rains; the legend also tells that the end of Ghana was directly related to the disappearance of the Spring rains (Monteil, 1953; Maley, 1981).

Concerning the humid phases of the Saharan Holocene, this double origin of rains had already been proposed based upon both pollen analyses and characteristics of fluvial sediments, which can provide information about the character of the flows (Maley, 1977, 1981; Baumhauer *et al.*, 1997). In this way it is possible to link relatively coarse sandy levels to stormy monsoon, and the more regular, fine levels to cyclonic rains of the Saharan Depressions (Maley, 1981, 2000). In South America, for the subtropics of the Southern Hemisphere, Servant and Servant-Vildary (2003) used the same sedimentological criteria to distinguish monsoon rains from extra-tropical rains generated by the austral equivalent of extratropical Depressions. Additionally, in the numerous lacustrine sequences of the Chad Basin, especially the Late Pleistocene and Early Holocene, from ca. 11.700 to 8.400 cal BP (Humids 2, 3 and 4) (i.e. 10.100–7.600 ¹⁴C BP) but also more punctually during the Middle Holocene and finally with a certain upsurge in the Late Holocene (Humid 7), there have been found diatom assemblages having both tropical species, which lived in eutrophic and generally warm waters, and psychrophilic species, which lived in oligotrophic, usually cool, waters (Servant-Vildary, 1978). In an effort to reconcile the existence of these composite diatom assemblages, the hypothesis of a double origin of rains was proposed (Maley, 1981; Baumhauer *et al.*, 1997).

Notwithstanding, the best data allowing confirmation of this hypothesis come from isotopic studies. Such studies can reveal the seasonality of rains and thermic conditions associated with them, which have led to the formation of lacustrine deposits and diverse associated fossils (e.g. shells). With respect to the Saharan Holocene, $\delta^{18}\text{O}$ values were measured in lacustrine carbonates from sections sampled at twenty sites situated between the Taoudenni region (4°W) and west of Lake Chad (13°E) (Williams *et al.*, 1987; Dubar, 1988; Gasse, 2002). One result of these studies was that the apparent increase in $\delta^{18}\text{O}$, which is observed today from West to East in the monsoon rains across the Sahel and southern Sahara (as reported above, see Joseph *et al.*, 1992), didn't exist during the Holocene humid phases, but that, in contrast, isotopic values decreased with distance from the sea, that is, from West to East (Gasse, 2002). This important conclusion shows that the tendency of isotopic values was similar to the Saharan Zone (Northern Sahara: [Figure 7](#)) and, hence, the majority of rains apparently must have depended upon cyclonic rains linked to the Saharan Depressions and

that probably there was another part associated to the monsoon (as described by Patricola and Cook's model, 2007). Moreover, the development in the Middle Holocene, particularly in ca. 6.900 to 4.900 cal BP (Humid phase 6), of red ferruginous tropical soils and also of coarse sediments (Tables 2 and 3), clearly indicate that at this epoch a large proportion of the monsoon rains were stormy, hence, formed in a warm evaporating environment, (chapter 12.6.4). These important geological data strongly suggest that some of Patricola and Cook's (2007; chapter 12.6.2) results might correspond better to extratropical Depressions, which are characterized by a cyclonic circulation and form under relatively cool conditions (Knippertz, 2005).

To try to determine the relative importance of these two rain types, it is necessary to reconstruct the seasonal succession of rains during the year. Results related to this question have been obtained by analyzing gastropod shell incremental growth layers. Studies on how gastropods construct their shells have demonstrated that they develop in isotopic equilibrium with the aquatic milieu in which they live (Abell *et al.*, 1996a). Given this, studies of the shells of the oyster (*Etheria elliptica*) that lives in Lake Victoria have demonstrated that the ring layers formed relatively regularly and that the variation in the isotopic ($\delta^{18}\text{O}$) values of each layer did indeed reproduce the double seasonality of the rains that occur annually in this equatorial region (Abell *et al.*, 1996a). A similar study was conducted on fossil shells of the same oyster, *Etheria elliptica*, collected from the lower reaches of Wadi Howar in Sudan, southern Sahara (site K113; ca. 18°N–30°30'E) and dated to ca. 7.500 cal BP (Rodrigues *et al.*, 2000). These authors were able to conclude that during approximately each year of its growth, there had also been in this region two rainy seasons, one relatively long about 4–5 months, and, after a drier season, a second shorter rainy season that lasted about 2 months. The isotopic values varied between –10 and –12 ‰, which corresponds to much less evaporated water than found in free water from these regions today (Rodrigues *et al.*, 2000). The authors advanced the hypothesis that this double seasonality would have been similar to that which exists today close to the equator in East Africa, as is also the case, e.g., for forest regions near the Gulf of Guinea (south of Cameroon, Nigeria, Ghana, Ivory Coast, etc.) (Leroux, 1996, 2001). However, in light of the latitude 18°N of the station K-113, it appears physically impossible that the two annual seasons demonstrated by this study intervened in the monsoon south of the ITF. Given the presence of an intercalated season without rain, this would imply that the ITF, the ground level trace of the monsoon front, had shifted very far to the north of the Sahara for several months. But, as is well recognized, each year, at the longitude of the Sudan, the ITCZ also redescends relatively far to the south of the equator; such an amplitude of annual oscillation is physically impossible, in particular to allow a rainy season of 4–5 months in the southern Sahara. The only possible explanation is that the two rainy seasons had different origins, one formed in the monsoon and the second was related to Saharan Depressions. Additionally, highly depleted isotopic values of other shells collected in a nearby sector at the same latitude (site P. 195) (Abell *et al.*, 1996b) might be explained by the mixing at high altitudes of humid tropical air with cold polar air, which is canalized in undulations of the Subtropical Jet Stream (Figure 8), and as mentioned above, this phenomenon is a driving force for the formation of pluvial systems.

These different data clearly demonstrate that during a large part of the Holocene the Saharan Depressions have played a large role in the feeding of lacustrine environments in the south and central Sahara, seasonally adding to monsoon rains. As already indicated above, the simultaneous presence of tropical and psychrophilic diatoms in the different lacustrine phases that succeeded over the course of the Holocene, tends to reinforce this interpretation. Nonetheless, these preliminary conclusions need to be confirmed by future isotopic studies of the numerous gastropod fossils distributed

across levels at diverse Saharan stations, and also, whenever possible, of fossil mammal teeth, the growth layers of which can also be a source of similar information (Koch, 1998). The implications of these results must be considered when constructing future models of the Saharan Holocene. Therefore, it will be necessary to demonstrate the seasonal activity leading both to the Saharan Depressions and the monsoon rains—and for this, variations in the four major annual seasons must be taken into account. With respect to the Holocene, Knippertz's work (2005) might be taken as a starting point and eventually the model Patricola and Cook (2007) could be adapted using certain data furnished for this period by Lorenz *et al.* (2006). These last authors have provided reconstructions of seasonal variations in marine and continental surface temperatures based on monthly and seasonal insolation variation deduced from orbital parameters.

12.6.4 The monsoon rains

As described in the preceding paragraphs, there have been attempts based on different criteria, either biological (pollen and vegetation, diatoms) or sedimentological, to separate, monsoon rains, which are mostly stormy, from rains of the Saharan Depressions, which are relatively more fine. It is also possible to use pedological criteria when palaeosols are found. In this fashion, it was previously shown that in southern Sahara and especially during Humid VI (ca. 6.800 and 5.000 cal BP), red ferruginous soils were formed as well as ferruginous crusts. Given that soils of this type exist mostly today in the Sahelo-sudanian savanna belt, it can therefore be deduced that there existed during this epoch a warm and evaporative ambiance, characterized by a well marked dry season and, above all, a relatively strong rainy season tied to the monsoon. The importance of monsoon rains during this humid phase is also confirmed by the laying down of coarse often conglomeratic sediments (Tables 2 and 3) as is found towards the summit of the upper sequence of the Angamma delta, as well as the summit of the “Middle Terrace” of Tibesti and of Air (Maley, 1981; Baumhauer *et al.*, 1997), which were deposited starting ca. 7.000 cal. BP, synchronous with the last phase of the Mega-Chad (MC3; 6.900–6.300 cal BP). It is worth mentioning that these conglomeratic levels, which express a very strong erosion, are, however, deposited in an apparently systematic manner at the summit of fluvial sedimentary series and that the erosion of these formations up to the bottom of the talwegs, didn't occur until much later between ca. 5.000 and 4.000 cal BP. The reason for this “partial” erosion between ca. 7.000 and 5.000 cal BP can be attributed firstly to the development of a relatively thick vegetation, mostly along the water courses—that stabilized the banks—as the palaeobotanical data (pollen and wood charcoal) (Maley, 1981; Ritchie and Haynes, 1987; Neumann, 1992) demonstrates well for this phase; this corresponded to a large expansion of the Sahelian vegetation into the meridional and central Sahara (Figure 5) (Jolly *et al.*, 1998). However, this partial erosion could also have been determined by the seasonal importance of rains tied to the Saharan Depressions—something which recalls the hypotheses presented above. Only future studies can resolve this question.

It is useful to examine other periods when the monsoon exhibited unusual behavior otherwise unknown or rare during the 20th century. During certain periods of the Holocene for which the palaeoenvironmental data is relatively precise, a strongly marked, out of phase pluviometric tendency was shown, corresponding to a large decrease in rain in the Sahel and tropical Sahara (southern part of the Sahara), and a very large increase in rains in the Sudano-guinean zone. The Sudanian zone occupies a hinge-like

position with respect to this special climatic configuration. This particular situation has been well described above under studies of the last two Millennia, particularly for the 17th century, but it also characterized the period spanning from ca. 300 to 700 AD and the end of the Early Holocene, between ca. 8.400 and 8.100 cal BP. Even so, the most precise information exists for the 17th century, which corresponded with the Little Ice Age maximum. This reference to a sudden cooling phase appears to be a primary characteristic, and probably one of the keys to this climatic out of phase, as the period 300 to 700 AD also corresponded to a well characterized cooling phase in the Northern Hemisphere (Lamb, 1977, 1982). This is also the case for the short period centered about 8.200 cal BP, which has been the subject of numerous publications showing, among other things, its tight association with a very marked, albeit brief, cooling in Greenland (Von Grafenstein *et al.*, 1998; Alley and Agustsdottir, 2005) and which also has been compared to the Little Ice Age (Rohling and Palike, 2005).

The relatively sudden marked cooling phases of the Northern Hemisphere explain the acceleration of the harmattan in the Sahara and the reinforcement of the eolian activity that ensued. This reinforced eolian activity was responsible for the transport, in particular towards the south, of large quantities of dust; it has been shown that the loess type deposits played an important sedimentological and pedological role in the entire tropical zone, up to the equatorial forest belt (Maley, 1982). Concerning the period 300 to 700 AD, these loess inputs were largely responsible for the generalized clay deposits making up the lower sequence of the previously described Low Terrace. Conversely, as it is not easy to explain the considerable, synchronous, increase in rains further south in the Sudano-guinean zone, it might be useful to consider the possible role these dust particles might have played in the aforementioned climatic out of phase, as potential “condensation nuclei” in clouds (see Maley, 1982). In fact, this inquiry can be broadened to include the entire Early Holocene and the question of whether the large clay deposits found throughout the south of the Chad Basin at this epoch (upper part of Bossumian) were also related to a particular seasonal eolian activity in the southern Sahara? This is a relationship that the present author has previously tried to show (Maley, 1982). The fact, as demonstrated above that the Saharan Depressions have played a large role during this epoch, could also possibly explain the reinforcement of eolian activity. The triggering of these depressions, at its origin, was determined by descents of polar air above the Sahara (Nicholson and Flohn, 1980), this last phenomenon, especially when the pluvial system doesn't form because of the punctual absence of humid air, is, by contrast, the cause of intense sand storms (Jalu *et al.*, 1965; Knippertz and Fink, 2006b).

The climatologist Leroux (1996, 2001), who stresses the role of the “Mobile Polar Highs”, presented a scheme of what, in his view, are the three major types of precipitation variations in West and Central Africa (Figure 10), with respect to the activity of the subtropical anticyclones which frame the tropical zone. These schemas do not directly take into account variations in Sea Surface Temperature (SST); even so, this factor is, nonetheless, induced in part by the activity of these anticyclones, which play a major role in dynamic climatology (Janicot *et al.*, 1998; Mahé *et al.*, 2001; Janicot, 2009; Sepulchre *et al.* 2009). The first two schematized types (Figure 10), correspond well to the two major rain variation types that strongly dominated the 20th century, and which are characterized by opposing and alternating tendencies according to the years or periods, between approximately the equatorial forest belt and the north tropical sector (Bigot *et al.*, 1997; Mahé *et al.*, 2001; Mounier and Janicot, 2004). Studies conducted on the Holocene have shown that these opposing tendencies well characterize the climatic functioning of the major part of the Holocene, which can be illustrated by the oscillation of a North to South Dipole (Maley, 1997, 2004b). However, some

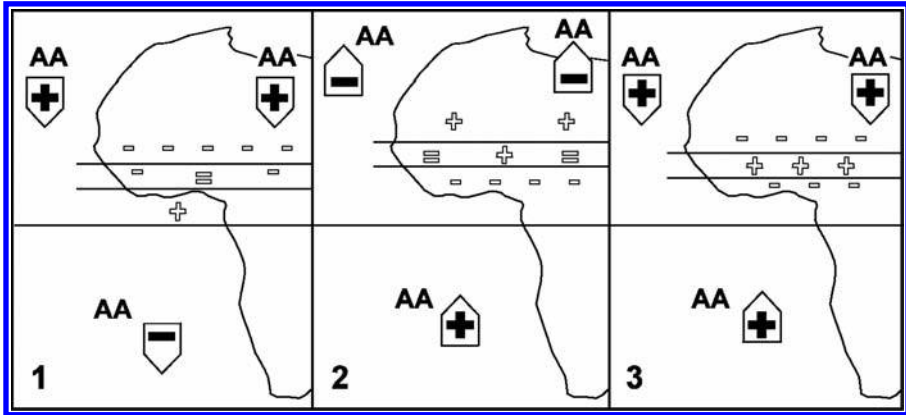


Figure 10. Schematic diagram of precipitation variability in West Africa based on the alternate reinforcement and weakening of subtropical anticyclones (AA) in the North and South, with three principal modes (after Leroux, 1996, Figure 84): the first 2 illustrate a classic alternating Dipole during the contemporary period which opposes (1) either lowering of precipitation in north tropical regions, from the Sahel to the Sudano-guinean zone, and with increases in the Guinean forest zone, (2) or the inverse, i.e., increasing precipitation from the Sahel to the Sudano-guinean zone and with decreases in the Guinean forest zone. The third mode (3) is marked by a reinforcement of rains in a central belt corresponding approximately to the Sudano-guinean zone; this last situation is atypical for the 20th century but appears to illustrate well the situation that dominated during the 17th century, at the time of the Little Ice Age maximum phase, which indeed strongly reinforced the north and south subtropical anticyclones.

climatologists studying on the 20th century have provided evidence of certain rare situations wherein there are three belts presenting different tendencies (Moron, 1994). Mode 3 described by Leroux (Figure 10) consists of, from North to South, three belts having mutually opposing tendencies. The passage of the positive belt centered in the Sudano-guinean zone, to the negative belt centered on the Sahel and southern Sahara, is produced at the level of the Sudanian climatic zone. It is at this level that the monsoon “jump” intervenes each year (Janicot and Sultan, 2001). It is possible to advance the hypothesis that, under certain circumstances, yet to be determined, (e.g., possibly related to strong variations in the activity of the African Easterly Jet), the “jump” isn’t produced, something that might possibly lead to the development of mode 3, with the rains concentrating on the central belt. Under another hypothesis, it is possible to envision that there were interactions between the monsoon and extratropical Depressions—these last might have been more numerous as a result of increases in polar descents favored by this cold period. Whichever of these hypotheses is most likely, this third belt type described by Leroux (1996, 2001) appears to be realistic. It corresponds well to the climatic out of phase described above, all the more so as the 3rd belt, which is situated on the Guinean zone and, hence, concerns the northern part of the forest domain, is characterized by a decrease in rains. This last phenomenon is confirmed by certain data for the Little Ice Age, such as the considerable lowering of Bosumtwi Lake, Ghana (Shanahan *et al.*, 2009), as well as that of Kamalété Lake, found further south in the center of Gabon (Ngomanda *et al.*, 2007).

From a more general point of view, the functioning of the African monsoon is quite complex. For example, certain phases of Northern Hemisphere cooling (Bradley *et al.*, 2003; Mann *et al.*, 2008), can be associated either to a great reduction of monsoon activity, as around the middle of the 15th century (drying out of Lake

Chad), or the contrary, by an increase in monsoon activity in a part its range (overflowing of Lake Chad), as happened during the 17th century. Moreover, within the annual oscillation zone of the African ITCZ, the correlation with temperature variations in the Northern Hemisphere is inconsistent, considering that in eastern Africa during the last Millennium, variations in two neighboring lakes situated on the equator, Naivasha (Verschuren *et al.*, 2000) and Victoria, were synchronous with each other (Stager *et al.*, 2005), but with completely opposing tendencies with respect to Lake Chad. It is evident that these different phenomena can only be interpreted at a more global scale.

In an effort to understand the complex mechanisms that govern climate functioning of north tropical Africa, it is indispensable to know the mechanisms controlling interannual variability of the West African Monsoon (WAM). Many recent studies (Vizy and Cook, 2002; Giannini *et al.*, 2008; Zhang and Delworth, 2005; Janicot, 2009) have shown, firstly, that at the seasonal level the WAM exhibits several modes of functioning, some of which have been presented above (Figure 10). These different modes appear to be mostly forced by large-scale anomalies of the Sea Surface Temperature (SST). Hence, there exist remote teleconnections between the WAM (in particular the different “belts” presented in Figure 10) and the large interannual variations of the SST over the Pacific and Indian Oceans (see phenomena tied to the ENSO) (Mann *et al.*, 2009) by the development close to the equator of Kelvin waves propagating towards the East (influencing Sahel rains), and Rossby waves, propagating towards the West (influencing rains in the Guinean zone) (Mounier and Janicot, 2004). Another important mode is influenced by the contrast or opposition between extratropical SST’s in Southern Hemisphere oceans and those of the Northern Hemisphere. With respect to the latter, the North Atlantic Ocean plays a dominant role, in particular by the intermediary of the Atlantic Multidecadal Oscillations (AMO), with “warmer” and other “cooler” SST phases. Several specialists have associated the AMO with variations of the Atlantic arm of the Thermo-Haline Circulation (THC) (e.g. Knight *et al.*, 2005); this phenomenon has been the subject of numerous studies, as much for the contemporary (20th century) as the recent Quaternary periods (Clark *et al.*, 2002; Gray *et al.*, 2004; Kuhlbrodt *et al.*, 2007).

The last Millennium has often been the framework for studies of mechanisms governing global climates. This is largely because data for this period is the most precise and abundant, and because the temperature variations were relatively large, particularly between the “Thermic Medieval Optimum” (TMO, ca. 800 to 1.400 AD) and the “Little Ice Age” (LIA, ca. 1.400–1.850 AD); moreover, this occurred without the strong anthropic influences which affected the 20th century (Bradley *et al.*, 2003; Mann *et al.*, 2008, 2009). For example, Seager *et al.* (2007) were able to show that during the TMO, tropical regions of South America and Africa were affected by more humid climates in the North, such as in the Sahel and in Central America, and by drier climates in the South, such as in Amazonia and in East Africa (as was illustrated above, after Stager *et al.*, 2005), but with moderate to strong Nile floods, i.e., with a rather humid climate in Ethiopia (situated more to the North) in phase with the source zones of the other great north-tropical African rivers (Chari and Logone, Niger), and finally, with a strong monsoon in India (Janicot, 2009). These different tendencies correlate best with, on the one hand, a “warm” phase of the AMO in the Atlantic and, on the other, a La Niña type phase in the Pacific (low relative SST) (Seager *et al.*, 2007; Mann *et al.*, 2009). Generally, the climate of north tropical Africa shows a positive correlation with the AMO, and in particular a “warm” phase with a relatively humid Sahel (Dahl *et al.*, 2005; Giannini *et al.*, 2008), something which corresponds well with the previously presented data for the region around Lake Chad during the 12th century.

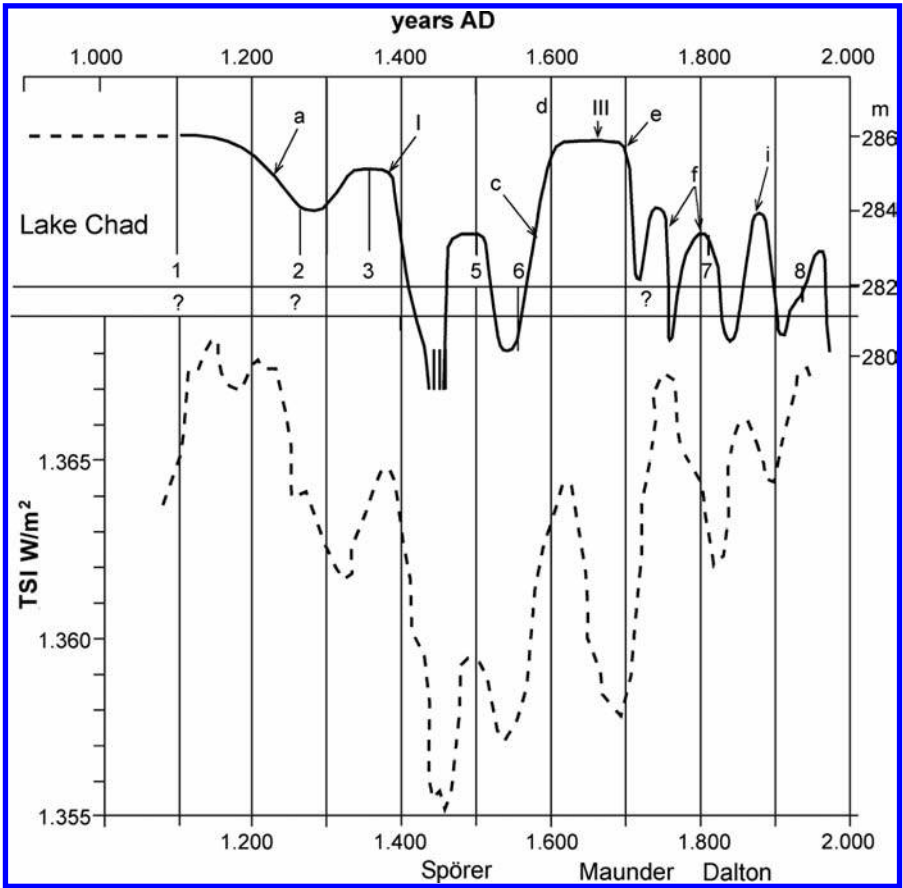


Figure 11. Comparison of the variation of solar activity (TSI, Total Solar Irradiance, in Watt per m^2) and Lake Chad levels during the last Millennium. The solar activity curve (TSI) is from Bard *et al.* (2007).

12.6.5 Monsoon and solar activity

Before ending this last part devoted to climatic interpretations, it is interesting to mention that the curve of variation in Lake Chad levels during the last Millennium, in particular during the strongest oscillations, compares quite well (Figure 11) with a curve of the variation in solar activity (Bard *et al.*, 2000; Bard and Frank, 2007). The correlation is particularly apparent at the level of the cyclicity of the variations, but less so with respect to the level of the amplitude of the variations. As remarked by Bard and Frank (2007), solar activity was at a minimum during the “Spörer” phase (15th–16th century)—while in Chad, this minimum appears to correlate with a drying out of the Lake in the middle of the 15th century. This phenomenon corresponded to minimal activity of the monsoon and also a relatively sudden cooling phase in the Northern Hemisphere, which corresponded with the beginning of the LIA (Bradley *et al.*, 2003; Mann *et al.*, 2008). In contrast, during the 17th century, the heightened intensity of the monsoon in the Sudano-guinean zone (on the central belt of Type 3

of Leroux; Figure 10) occurred at the time of the LIA cooling maximum and about the same time that solar activity lowered in a continuous manner during the “Maunder” phase. In addition, it should be recalled that the sudden cooling that intervened around ca. 8.200 BP was also compared to the LIA and attributed to a solar minimum (Rohling and Palike, 2005).

In a more general manner, numerous explanations and hypotheses have been proposed to account for certain observed correlations between solar activity and various terrestrial climates, but without any real consensus among the scientific community (e.g. see Bard *et al.*, 2000, 2007; Shindell *et al.*, 2006; Chase *et al.*, 2010). Among them, certain hypotheses are of interest with respect to the study of north tropical Africa. For example, in connection with the notable influence of the AMO on tropical climates, as presented above, numerous studies have shown a good correlation between the AMO and variations in atmospheric pressure in the North Atlantic, a phenomenon known as “North Atlantic Oscillation” (NAO) (Latif *et al.*, 2006; Kim *et al.*, 2007). A relatively strong and regular correlation has been demonstrated between the NAO and solar activity—something that might be explained by the weakness of the terrestrial magnetic field near the poles, and in this way solar activity is able to exercise a greater effect (Kodera, 2003). In addition, the ENSO, which is a major atmospheric phenomenon in tropical regions (Stott *et al.*, 2002), also would be an important “mediator” between solar activity and this large climatic oscillation (Emile-Geay *et al.*, 2007).

12.7 CONCLUSIONS

At the close of this detailed study of the climatic variations over the Sahara and the Sahel (*sensu lato*), particularly for the Late Pleistocene and the Holocene, relatively complex climatic systems have been highlighted, in which the Monsoon was not the sole actor—contrary to what many modelers have tried to demonstrate. It appears evident that during the humid periods, Saharan Depressions also intervened frequently and seasonally, and that these are regional expressions of the more general phenomenon of Extratropical Depressions or Tropical Plumes, which future models will have to take into account. In addition, to determine the relative importance of these two climatic systems, it was shown that only highly refined isotopic studies, conducted on properly dated fossils—either the incremental growth layers of certain gastropod shells or layers of mammalian teeth—will be able to provide convincing results concerning the seasonality of these different rains. Moreover, future models should also take into account the correlations emphasized in the previous section, not only with respect to the SST observed across the world’s oceans, but also, particularly for explaining abrupt climatic changes, with respect to certain major components of atmospheric circulation, such as the trade winds and middle latitude westerlies (Clark *et al.*, 2002; Seager *et al.*, 2007).

ACKNOWLEDGEMENTS

P. Knippertz, M. Schuster, P.M. Vermeersch, R. Vernet, M.A.J. Williams are thanked for their critical comments. A large part of the materials presented in this synthesis was obtained with support from several programs funded by ORSTOM, now IRD. The author is very grateful to Dawn Frame for the quality of her English translation, and to Claudine Dieulin (IRD) for drawing the Tables 2 and 3. This work was done in the framework of Département Paléoenvironnements and Paléoclimatologie, ISEM-CNRS UMR 5554, University of Montpellier-2.

REFERENCES

- Abell, P.I., Amegashitsi, L. and Ochumba, P.B., 1996a, The shells of *Etheria elliptica* as records of environmental change in Lake Victoria. *Palaeogeogr., Palaeoclimato., Palaeoeco.*, **119**, pp. 215–219.
- Abell, P.I., Hoelzmann, P. and Pachur, H.J., 1996b, Stable isotope ratios of gasteropod shells and carbonate sediments of NW Sudan as palaeoclimatic indicators. *Palaeoecology of Africa*, **24**, pp. 33–52.
- Alley, R.B. and Agustsdottir, A.M., 2005, The 8k event: cause and consequences of a major Holocene abrupt climate change. *Quat. Sc. Rev.*, **24**, pp. 1123–1149.
- Armitage, S.J., Drake, N.A., Stokes, S., El-Hawat, A., Salem, M.J., White, K., Turner, P. and McLaren, S.J., 2007, Multiple phases of north African humidity recorded in lacustrine sediments from the Fazzan Basin, Libyan Sahara. *Quat. Geochrono.*, **2**, pp. 181–186.
- Arz, H.W., Lamy, F., Patzold, J., Muller, P.J. and Prins, M., 2003, Mediterranean moisture source for an Early Holocene humid period in the northern Red Sea. *Science*, **300**, pp. 118–121.
- Bard, E., Menot-Combes, G. and Delaygue, G., 2004, Des dates fiables pour les 50.000 dernières années. *Pour la Science*, **42**, pp. 54–59.
- Bard, E., Raisbeck, G.M., Yiou, F. and Jouzel, J., 2001, Solar irradiance during the last 1.200 years based on cosmogenic nuclides. *Tellus*, **52B**, pp. 985–992.
- Bard, E. and Frank, M., 2007, Climate change and solar variability: What's new under the sun? *Earth and Plan. Change Lett.* **248**, pp. 1–14.
- Baumhauer, R., Morel, A. and Tillet, T., 1997, Palaeomilieus et peuplement préhistorique dans l'Aïr, le Ténéré, le Djado et le Kowar. In *Sahara, paléomilieus et peuplement préhistorique au Pléistocène supérieur*. T. Tillet ed., pp. 229–265. Publ. L'Harmattan, Paris.
- Berthelet, A., Chavaillon, J. and Picq, P., 2001, Des Hominidés et des outils. Les débuts de la préhistoire. Habitats et cultures chez les Australopithèques et les Hommes. In: *Aux origines de l'humanité. I-De l'apparition de la vie à l'homme moderne*, edited by Coppens, Y., Picq, P. Publ. Fayard, Paris, pp. 300–347.
- Beyerle, U., Ruedi, J., Leuenberg, M., Aeschbach-Hertig, W., Peeters, F., Kipfer, R. and Dodo, A., 2003, Evidence for periods of wetter and cooler climate in the Sahel between 6 and 40 kyr BP derived from groundwater. *Geophys. Res. Lett.*, **30**, pp. 1173–1177.
- Bigot, S., Camberlin, P., Moron, V. and Richard, Y., 1997, Structures spatiales de la variabilité des précipitations en Afrique: une transition climatique à la fin des années 1960? *C.R. Acad. Sc., Paris*, sér. 2 A, **324**, pp. 181–188.
- Bouchette, F., Schuster, M., Ghienne, J.F., Denamiel, C., Roquin, C., Moussa, A., Marsaleix, P. and Düringer, P., 2010, Hydrodynamics in Holocene Lake Mega-Chad. *Quat. Res.*, **74**, pp. 36–45.
- Boudouresque, L., Dubois, D., Lang, J. and Trichet, J., 1982, Contribution à la stratigraphie et à la paléogéographie de la bordure occidentale du bassin des Iullemméden au Crétacé supérieur et au Cénozoïque (Niger et Mali, Afrique de l'ouest). *Bull. Soc. Géol. France*, **24**(7), pp. 685–695.
- Bouteyre, G., Cabot, J. and Dresch, J., 1964, Observations sur les formations du Continental terminal et du Quaternaire dans le bassin du Logone (Tchad). *Bull. Soc. Géol. France*, (7) **6**, pp. 23–27.
- Bradley, R.S., Briffa, K.R., Cole, J.E., Hughes, M.K. and Osborn, T.J., 2003, The climate of the Last Millennium. In: Alverson, K., Bradley, R.S., Pedersen, T.F. eds.: *Palaeoclimate, Global change and the Future*. Springer Verlag, Berlin, pp. 105–141.

- Breunig, P. and Neumann, K., 2002, Continuity or Discontinuity? The 1st. Millennium BC-Crisis in West African prehistory. In *Tides of the Desert*, edited by T. Lenssen-Erz. *Africa Praehistorica*, **14**, pp. 491–505.
- Brunet, M., Beauvilain, A., Coppens, Y., Heintz, E., Moutaye, A. and Pilbeam, D., 1995, The first australopithecine 2.500 kilometres west of the Rift valley (Chad). *Nature*, **378**, pp. 273–275.
- Brunet, M. and Picq, P., 2001, La grande expansion des Australopithèques. Des Hominidés aux marges des forêts africaines. In: Coppens, Y., Picq, P., *Aux origines de l'humanité. I—De l'apparition de la vie à l'homme moderne*. Publ. Fayard, Paris, pp. 200–261.
- Brunet, M., Guy, F., Pilbeam, D. Mackaye, H.T., Likius, A., Ahounta, D., Beauvilain, A., Blondel, C., Bocherens, H., Boisserie, J.R., de Bonis, L., Coppens, Y., Dejax, J., Denys, C., Douring, P., Eisenmann, V., Fanone, G., Fronty, P., Geraads, D., Lehmann, T., Lihoreau, F., Louchart, A., Mahamat, A., Merceron, G., Mouchelin, G., Otero, O., Pelaez, P.C., Ponce, M., Rage, J.-C., Sapanet, M., Schuster, M., Sudre, J., Tassy, P., Valentin, X., Vignaud, P., Viriot, L., Zazzo, A. and Zollikofer, C., 2002, A new hominid from the Upper Miocene of Chad, Central Africa. *Nature*, **418**, pp. 145–151.
- Burgoyne, P.M., van Wyk, A.E., Anderson, J.M. and Schrire, B.D., 2005, Phanerozoic evolution of plants on the African plate. *J. Afr. Earth Sc.*, **43**, pp. 13–52.
- Cabot, J., 1967, Les lits du Logone. Etudes géomorphologiques. *Soc. Edit. Enseignement Sup.*, Paris, 120 p.
- Cadet, D.L. and Nnoli, N.O., 1987, Water vapour transport over Africa and the Atlantic ocean during summer 1979. *Quart. J.R. Meteor. Soc.*, **113**, pp. 581–602.
- Carpenter, R., 1956, A trans-saharan caravan route in Herodotus. *American J. Archaeology*, **60**, pp. 231–242.
- Causse, C., Conrad, G., Fontes, J.C., Gasse, F., Gibert, E. and Kassir, A., 1988, Le dernier Humide pléistocène du Sahara nord-occidental daterait de 80–100.000 ans. *C.R. Acad. Sc., Paris*, (sér.2) **306**, pp. 1459–1464.
- Cavagnetto, C. and Anadon, P., 1996, Preliminary palynological data on floristic and climatic changes during the Middle Eocene–Early Oligocene of the eastern Ebro basin, NE Spain. *Rev. Palaeobot. and Palyno.*, **92**, pp. 281–305.
- Cavelier, J. and Goldstein, G., 1989, Mist and fog interception in elfin cloud forests in Colombia and Venezuela. *J. Trop. Ecology*, **5**, pp. 309–322.
- Chamley, H., 1988, Contribution éolienne à la sédimentation marine au large du Sahara. *Bull. Soc. Géol. France* (sér.8), **4**, pp. 1091–1100.
- Charre, J., 1974, Le climat du Niger. *Thèse Géographie*, Université de Grenoble, 188 p.
- Chase, B.M., Meadows, M.E., Carr, A.S. and Reimer, P.J., 2010, Evidence for progressive Holocene aridification in Southern Africa recorded in Namibian hyrax middens: Implications for African Monsoon dynamics and the “African Humid Period”. *Quaternary Research*, **74**, pp. 36–45.
- Churcher, C.S., Kleindienst, M.R. and Schwarcz, H.P., 1999, Faunal remains from a Middle Pleistocene lacustrine marl in Dakhleh Oasis, Egypt: palaeoenvironmental reconstructions. *Palaeogeogr., Palaeoclimato., Palaeoeco.*, **154**, pp. 301–312.
- Cissoko, S.M., 1968, Famines et épidémies à Tombouctou et dans la boucle du Niger du XVIème au XVIIIème s. *Bull. Inst. Fr. Afrique Noire*, sér. B, **30**, pp. 806–821.
- Clark, P.U., Pisias, N.G., Stocker, T.F. and Weaver, A.J., 2002, The role of the thermohaline circulation in abrupt climate change. *Nature*, **415**, pp. 863–869.
- Cook, K.H., 1999, Generation of the African Easterly Jet and its role in determining West African precipitation. *J. Climate*, **12**, pp. 1165–1184.

- Couvreur, T.L., Chatrou, L.W., Sosef, M.S. and Richardson, J.E., 2008, Molecular phylogenetics reveal multiple Tertiary vicariance origins of the African rain forest trees. *BioMedCentral Biology*, **6**, pp. 54–88.
- Cremaschi, M. and di Lernia, S., 1998, The geoarchaeological survey in central Tadrart Acacus and surroundings (Libyan Sahara). Environment and cultures. In: Cremaschi, M., di Lernia, S., *Wadi Teshuinat. Palaeoenvironment and Prehistory in SW Fezzan (Libyan Sahara)*. Publ. All’Insegna del Giclio, Milano, pp. 243–296.
- Cremaschi, M., di Lernia, S. and Garcea, E.A., 1998, Some insights on the Aterian in the Libyan Sahara: chronology, environment and archaeology. *African Archaeo. Rev.*, **15**, pp. 261–286.
- Cremaschi, M. and di Lernia, S., 1999, Holocene climatic changes and cultural dynamics in the Libyan Sahara. *Afr. Archaeo. Rev.*, **16**, pp. 211–238.
- Dahl, K.A., Broccoli, A.J. and Stouffer, R.J., 2005, Assessing the role of North Atlantic freshwater forcing in millennial scale climate variability: a tropical Atlantic perspective. *Climate Dyn.*, **24**, pp. 325–346.
- Daveau, S., 1969, La découverte du climat au cours des navigations portugaises (XV^e et début XVI^e siècle). *Bull. Inst. Fr. Afrique Noire, sér. B*, **31**, pp. 953–988.
- David, N., 2004, Watch or water towers? Stone-built sites in N. Cameroon’s Mandara mountains and their functions. *Univ. Pennsylvania, Publ. Expedition*, **46**, pp. 30–35. www.museum.upenn.edu/publications/
- David, N., Klassen, J., Maceachern, S., Maley, J., Muller-Kosack, G., Richardson, A. and Sterner, J., 2008, Performance and agency: the DGB sites of Northern Cameroon. *BAR Intern. Series, Oxford, British Archaeo. Report*, **1830**, 155 p.
- Debenath, A., 1992, Hommes et cultures matérielles de l’Atérien marocain. *L’Anthropologie*, **96**, pp. 711–720.
- Drochon, A., 1971, La saison sèche au Sénégal. *Publ. ASECNA, Dakar*, 43 p.
- Dubar, C., 1988, *Eléments de paléohydrologie de l’Afrique saharienne: les dépôts quaternaires d’origine aquatique du nord-est de l’Air (Niger, programme PALHYDAF)*. Thèse Univ. Paris-Sud, 184 p.
- Dubief, J., 1963, Le climat du Sahara. L’eau atmosphérique au Sahara. *Mém. hors série. Inst. Rech. Sahar. Univ. Alger*, **2**(1), 275 p.
- Dubief, J., 1999, L’Ajjer, Sahara central. *Ed. Karthala, Paris*.
- Dupont, B. and Delaune, M., 1970, Etude de quelques coupes dans le Quaternaire récent du sud du lac Tchad. *Cahier ORSTOM, série Géologie*, **2**, pp. 49–60.
- Duringer, P., Ghienne, J.F., Schuster, M., Brunet, M. and Vignaud, P., 2000, Les séquences climatiques “arides-humides” des sites pliocènes à Australopithèques du Tchad: influences de la balance climatique équatoriale sur les oscillations du paléo-lac Tchad. In *Les Hominidés et leurs environnements. Histoire et Interactions*, Congrès, Univ. Poitiers, Résumé, p. 41.
- Edmunds, W.M., Fellman, E. and Goni, I.B., 1999, Lakes, groundwater and palaeohydrology in the Sahel of NE Nigeria: evidence from hydrogeochemistry. *J. Geological Society, London*, **156**, pp. 345–355.
- Edmunds, W.M., Dodo, A., Djoret, D., Gasse, F., Gaye, C.B., Goni, I.B., Travi, Y., Zouari, K. and Zuppi, G.M., 2004, Groundwater as an archive of climatic and environmental change: Europe to Africa. In Battarbee, R.W. *et al.*: *Past Climate variability through Europe and Africa*. Springer, Dordrecht, pp. 279–306.
- Edmunds, W.M., 2008, Groundwater in Africa—palaeowater, climate change and modern recharge. In *Applied groundwater studies in Africa*. Edited by Adelana, S. *et al.*, Taylor and Francis Publ. The Netherlands, pp. 305–322.
- Emile-Geay, J., Cane, M., Seager, R., Kaplan, A. and Almasi, P., 2007, ENSO as a mediator of the solar influence on climate. *Palaeoceanography*, **666**, pp. 10–29.

- Ergenzinger, P.J., 1978, Das Gebiet des Enneri Misky im Tibesti Gebirge, Rep. Tchad. Erläuterungen zu einer geomorphologischen Karte 1/200.000. *Berliner Geographische Abhandlungen*, **23**, 58 p.
- Faure, H., 1966, Reconnaissance géologique des formations sédimentaires post-paléozoïques du Niger oriental. *Mém. Bur. Rech. Géol. Min.* **47**, 630 p.
- Faure, H., 1969, Lacs quaternaires du Sahara. *Mittel. Intern. Verein. Limnologisch.*, Stuttgart, **17**, pp. 131–146.
- Felix-Henningsen, P., 2000, Palaeosols on Pleistocene dunes as indicators of palaeomonsoon events in the Sahara of East Niger. *Catena*, **41**, pp. 43–60.
- Flohn, H., 1971, Tropical circulation pattern. *Bonner Meteo. Abhandl.*, **4**, 83 p.
- Fontaine, C., Lovett, P., Sanou, H., Maley, J. and Bouvet, J.M., 2004, Genetic diversity of the Shea tree (Karité, *Vitellaria paradoxa*), detected by RAPD and chloroplast microsatellite markers. *Heredity*, **93**, pp. 639–648.
- Fontugne, M., 1997, Fiabilité des datations “absolues” pour le Pléistocène supérieur des milieux désertiques ou semi-arides. In: Tillet, T.: *Sahara, paléomilieux et peuplement préhistorique au Pléistocène supérieur*. Publ. L’Harmattan, Paris, pp. 393–408.
- Garcea, E., 2009, The evolutions and revolutions of the Late Middle Stone Age and Lower Later Stone Age in Northwest Africa. In *The Mediterranean from 50.000 to 25.000 BP: Turning points and new directions*. Edited by Camps, M., Szmídt, C., pp. 51–66.
- Gasse, F., Fontes, J.C., Plaziat, J.C., Carbonel, P., Kaczmarek, I., de Deckker, P., Soulie-Marsche, I., Callot, Y. and Dupeuble, P.A., 1987, Biological remains, geochemistry and stable isotopes for the reconstruction of environmental and hydrological changes in the Holocene lakes from north Sahara. *Palaeogeogr., Palaeoclimatol., Palaeoecol.*, **60**, pp. 1–46.
- Gasse, F., Tehet, R., Durand, A., Gibert, E. and Fontes, J.C., 1990, The arid-humid transition in the Sahara and the Sahel during the last deglaciation. *Nature*, **346**, pp. 141–146.
- Gasse, F., 2000, Hydrological changes in the African tropics since the Last Glacial Maximum. *Quat. Sc. Rev.*, **19**, pp. 189–211.
- Gasse, F., 2002, Diatom-inferred salinity and carbonate oxygen isotopes in Holocene waterbodies of the western Sahara and Sahel (Africa). *Quat. Sc. Rev.*, **21**, pp. 737–767.
- Gasse, F., 2006, Climate and hydrological changes in tropical Africa during the past million years. *C.R. Palevol.*, **5**, pp. 35–43.
- Gavaud, M., Rieffel, J.M. and Muller, J.P., 1975, Les sols de la vallée de la Bénoué, de Lagdo au confluent du Faro. Vol. I-Facteurs de l’environnement. *Rapport ORSTOM, Yaoundé*, 82 p.
- Gaven, C., Hillaire-Marcel, C. and Petit-Maire, N., 1981, A Pleistocene lacustrine episode in Southeastern Libya. *Nature*, **290**, pp. 131–135.
- Ghienne, J.F., Schuster, M., Bernard, A., Düringer, P. and Brunet, M., 2002, The Holocene giant Lake Chad revealed by digital elevation models. *Quat. Intern.*, **87**, pp. 81–85.
- Giannini, A., Biasutti, M. and Verstraete, M., 2008, A climate model-based review of drought in the Sahel: Desertification, the re-greening and climate change. *Glob. and Plan. Ch.*, **64**, pp. 119–128.
- Gibert, E., Arnold, M., Conrad, G., de Deckker, P., Fontes, J.C., Gasse, F. and Kassir, A., 1990, Retour des conditions humides au Tardiglaciaire au Sahara septentrional (Sebkha Mellala, Algérie). *Bull. Soc. Géol. Fr. (sér.8)*, **6**, pp. 497–504.
- Gingerich, P.D., 2006, Environment and evolution through the Palaeocene–Eocene thermal maximum. *Trends Ecol. and Evol.*, **21**, pp. 246–253.
- Gioda, A., Espejo, R., Blot, J. and Neuvy, O., 1994, Arbres fontaines, eau de brouillard et forêts de nuages. *Sécheresse*, **5**, pp. 237–243.

- Gray, S.T., Graumlich, L.J., Betancourt, J.L. and Pederson, G.T., 2004, A tree-ring based reconstruction of the Atlantic Multidecadal Oscillation since 1567 A.D. *Geophys. Res. Lett.*, **31**, pp. L12205.
- Grove, A.T., Street, F.A. and Goudie, A.S., 1975, Former lake levels and climatic change in the Rift Valley of Southern Ethiopia. *Geogr. J.*, **141**, pp. 177–202.
- Guiraud, R., Bosworth, W., Thierry, J. and Delplanque, A., 2005, Phanerozoic geological evolution of Northern and Central Africa: an overview. *J. Afr. Earth Sc.*, **43**, pp. 83–143.
- Hanebuth, T.J. and Henrich, R., 2008, Recurrent decadal-scale dust events over Holocene Western Africa and their control on canyon turbidite activity (Mauritania). *Quat. Sc. Rev.*, **28**, pp. 261–270.
- Hartenberger, J.L., 1983, “La Grande Coupure”. *Pour la Science*, pp. 26–38.
- Hartenberger, J.L., 2001, Une brève histoire des Mammifères. *Publ. Belin*, Paris, 288 p.
- Hervieu, J., 1967, Sur l’existence de deux cycles climato-sédimentaires quaternaires dans les monts Mandara et leurs abords (Nord-Cameroun). Conséquences morphologiques et pédogénétiques. *C.R. Acad. Sc., Paris*, (sér. D), **264**, pp. 2624–2627.
- Hervieu, J., 1970, Le Quaternaire du Nord-Cameroun. Schéma d’évolution géomorphologique et relations avec la pédogenèse. *Cah. ORSTOM, série Pédologie*, **8**, pp. 295–317.
- Hill, C.L., 2001, Geologic contexts of the Acheulian (Middle Pleistocene) in the eastern Sahara. *Geoarchaeology*, **16**, pp. 65–94.
- Hoelzmann, P., Gasse, F., Dupont, L.M., Salzmann, U., Staubwasser, M., Leuschner, D.C. and Sirocko, F., 2004, Palaeoenvironmental changes in the arid and subarid belt (Sahara-Sahel-Arabian Peninsula) from 150 kyr to Present. In Battarbee, R.W. *et al.* eds: *Past Climate variability through Europe and Africa*. Springer, Dordrecht, pp. 219–256.
- Holmes, J.A., Street-Perrott, F.A., Perrott, R.A., Stokes, S., Waller, M.P., Huang, Y., Eglinton, G. and Ivanovich, M., 1999, Holocene landscape evolution of the Manga Grasslands, NE Nigeria: evidence from palaeolimnology and dune chronology. *J. Geol. Society, London*, **156**, pp. 357–368.
- Huysecom, E., Ozainne, S., Raeli, F., Ballouche, A., Rasse, M. and Stokes, S., 2004, Ounjougou (Mali): a history of Holocene settlement at the southern edge of the Sahara. *Antiquity*, **78**, pp. 602–616.
- Huysecom, E., Rasse, M., Lespez, L., Neumann, K., Fahmy, A., Ballouche, A., Ozainne, S., Maggetti, M., Tribolo, C. and Soriano, S., 2009, The emergence of pottery in Africa during the tenth millennium cal BC: new evidence from Ounjougou (Mali). *Antiquity*, **83**, pp. 905–917.
- Jaeger, J.J., 2001, La Terre avant les Hommes. In: Coppens, Y., Picq, P.: *Aux origines de l’humanité. I-De l’apparition de la vie à l’homme moderne*. Publ. Fayard, Paris, pp. 26–71.
- Jalu, R., Bocquillon, M. and Bonnefous, M., 1965, Tempête de sable sur le Sahara. *La Météorologie*, **78**, pp. 105–112.
- Janicot, S., Harzallah, A., Fontaine, B. and Moron, V., 1998, West African monsoon dynamics and eastern equatorial Atlantic and Pacific SST anomalies (1970–88). *J. Climate*, **11**, pp. 1874–1882.
- Janicot, S. and Sultan, B., 2001, Intra-seasonal modulation of convection in the West African monsoon. *Geophys. Res. Lett.*, **28**, pp. 523–526.
- Janicot, S., 2009, A comparison of Indian and African monsoon variability at different time scales. *C.R. Geoscience*, **341**, pp. 575–590.
- Janis, C.M., 1993, Tertiary mammal evolution in the context of changing climates, vegetation, and tectonic events. *Ann. Rev. Ecol. Syst.*, **24**, pp. 467–500.

- Jansson, R. and Dynesius, M., 2002, The fate of clades in a world of recurrent climatic change: Milankovitch oscillations and evolution. *Ann. Rev. Ecol. Syst.*, **33**, pp. 741–777.
- Johnson, T.C., Scholz, C.A., Talbot, M.R., Kelts, K., Rickettsi, R.D., Ngobi, G., Beuning, K., Ssemmanda, I. and McGill, J.W., 1996, Late Pleistocene dessication of Lake Victoria and rapid evolution of Cichlid fishes. *Science*, **273**, pp. 1091–1093.
- Jolly, D., Prentice, C., Bonnefille, R., Maley, J. and 32 co-auteurs, 1998, Biome reconstruction from pollen and plant macrofossil data for Africa and the Arabian peninsula at 0 and 6.000 years. *J. Biogeography*, **25**, pp. 1007–1027.
- Jones, E.W., 1963, The forest outliers in the Guinea zone of Northern Nigeria. *J. Ecology*, **51**, pp. 415–434.
- Joseph, A., 1992, Isotope characteristics of meteoric water and groundwater in the Sahelo-Sudanese zone. *J. Geophys. Res.*, **97**, pp. 7543–7551.
- Kedves, M., 1971, Présence de types sporomorphes importants dans les sédiments pré-quadernaires égyptiens. *Acta. Bota. Acad. Sc. Hungaricae*, **17**, pp. 371–378.
- Kedves, M., 1981, Etudes palynologiques sur les sédiments pré-quadernaires de l’Egypte. Néogène-1. *Grana*, **20**, pp. 119–130.
- Kedves, M., 1983, Etudes palynologiques sur les sédiments pré-quadernaires de l’Egypte. Néogène-2. *Grana*, **22**, pp. 39–49.
- Keigwin, L.D., 1996, The Little Ice Ages and Medieval Warm Period in the Sargasso Sea. *Science*, **274**, pp. 1504–1508.
- Kim, J.H., Meggers, H., Rimbu, N., Lohmann, G., Freudenthal, T., Müller, P.J. and Schneider, R.R., 2007, Impacts of the North Atlantic gyre circulation on Holocene climate off Northwest Africa. *Geology*, **35**, pp. 387–390.
- Knight, J.R., Allan, R.J., Folland, C.K., Vellinga, M. and Mann, M.E., 2005, A signature of persistent natural thermohaline circulation cycles in observed climate. *Geophys. Res. Lett.*, **32**, pp. L20708.
- Knippertz, P., 2005, Tropical–extratropical interactions associated with an Atlantic Tropical Plume and Subtropical Jet streak. *Mon. Weather Rev.*, **133**, pp. 2759–2776.
- Knippertz, P., Fink, A.H., Reiner, A. and Speth, P., 2003, Three late summer/early autumn cases of tropical–extratropical interactions causing precipitation in Northwest Africa. *Mon. Weather Rev.*, **131**, pp. 116–135.
- Knippertz, P. and Martin, J.E., 2005, Tropical Plumes and extreme precipitation in subtropical and tropical Africa. *Quart. J. Roy. Meteor. Soc.*, **131**, pp. 2337–2365.
- Knippertz, P. and Fink, A.H., 2006a, An unusual dry-season precipitation event over West Africa: the role of an extratropical upper-level disturbance for the heat low and a surge in the monsoonal southwesterlies. *27th Conf. On Hurricanes and Trop. Meteor.*, **6D.6**, 4 p.
- Knippertz, P. and Fink, A.H., 2006b, Synoptic and dynamic aspects of an extreme springtime Saharan dust outbreak. *Quart. J. Roy. Meteor. Soc.*, **132**, pp. 1153–1177.
- Koch, P.L., 1998, Isotopic reconstruction of past continental environments. *Ann. Rev. Earth and Planet. Sc. Lett.*, **26**, pp. 573–613.
- Kodera, K., 2003, Solar influence on the spatial structure of the NAO during the winter 1900–1999. *Geophys. Res. Lett.*, **30**, pp. 4, 1175.
- Kröpelin, S., Verschuren, D., Lézine, A.M., Eggermont, H., Cocquyt, C., Francus, P., Cazet, J.P., Fagot, M., Rumes, B., Russell, J.M., Darius, F., Conley, D.J., Schuster, M., von Suchodoletz, H. and Engstrom, D.R., 2008, Climate-driven ecosystem succession in the Sahara: the past 6.000 years. *Science*, **320**, pp. 765–768.
- Kuhlbrodt, T., Griesel, A., Montoya, M., Levermann, A., Hofman, M. and Rahmstorf, S., 2007, On the driving processes of the Atlantic meridional overturning circulation. *Rev. Geophys.*, **45**, pp. 1–32.

- Kuper, R. and Kröpelin, S., 2006, Climate-controlled Holocene occupation in the Sahara: motor of Africa's evolution. *Science*, **313**, pp. 803–807.
- Lamb, H.F., Bates, C.R., Coombes, P.V., Marshall, M.H., Umer, M., Davies, S.J. and Dejen, E., 2007, Late Pleistocene desiccation of Lake Tana, source of the Blue Nile. *Quat. Sc. Rev.*, **26**, pp. 287–299.
- Lamb, H.H., 1977, Climate: Present and Future II, Climatic history and the future. *Methuen Publ.*, London, 835 p.
- Lamb, H.H., 1982, Climate, history and the modern world. *Methuen Publ.*, London, 387 p.
- Latif, M., Boning, C., Willebrand, J., Biastoch, A., Dengg, J., Keenlyside, N. and Schweckendiek, U., 2006, Is the thermohaline circulation changing between 1951–1989? *J. Climate*, **19**, pp. 4631–4637.
- Lebatard, A.E., Bourles, D.L., Düringer, P., Jolivet, M., Braucher, R., Carcaillet, J., Schuster, M., Arnaud, N., Monie, P., Lihoreau, F., Likius, A., Mackaye, H.T., Vignaud, P. and Brunet, M., 2008, Cosmogenic nuclide dating of *Sahelanthropus tchadensis* and *Australopithecus bahrelghazali*: Mio-Pliocene hominids from Chad. *Proceed. Nat. Acad. Sc.*, **105**, pp. 3226–3231.
- Leblanc, M., Favreau, G., Maley, J., Nazoumou, Y., Leduc, C., Stagnitti, F., van Oevelen, P.J., Delclaux, F. and Lemoalle, J., 2006, Reconstruction of Megalake Chad using February 2000 Shuttle Radar Topographic Mission data. *Palaeogeogr., Palaeoclimatol., Palaeoecol.*, **239**, pp. 16–27.
- Leroux, M., 1996, La dynamique du temps et du climat. *Masson édit.*, 310 p.
- Leroux, M., 2001, The meteorology and climate of tropical Africa. *Springer*, London, 548 p.
- Letouzey, R., 1968, Etude phytogéographique du Cameroun. *Encyclopédie Biol.*, **69**, 508 p.
- Letouzey, R., 1985, *Notice de la carte phytogéographique du Cameroun au 1/500.000*. Inst. Carte Intern. Végétation, Toulouse and Inst. Rech. Agron., Yaoundé.
- Lezine, A.M. and Casanova, J., 1991, Correlated oceanic and continental records demonstrate past climate and hydrology of North Africa (0–140 ka). *Geology*, **19**, pp. 307–310.
- Linder, P.H., Lovett, J., Mutke, J.M., Barthlott, W., Jurgens, N., Rebelo, T. and Kuper, W., 2005, A numerical re-evaluation of the sub-Saharan phytochoria of mainland Africa. *Biol. Skr.* **55**, pp. 229–252.
- Lorenz, S.J., Kim, J.H., Rumbu, N., Schneider, R.R. and Lohmann, G., 2006, Orbitally driven insolation forcing on Holocene climate trends: evidence from alkenone data and climate modelling. *Palaeoceanography*, **21**, PA1002, 14 p.
- Mahe, G., L'Hôte, Y., Olivry, J.C. and Wotling, G., 2001, Trends and discontinuities in regional rainfall of West and Central Africa, between 1951–1989. *Hydro. Sc. J.*, **46**, pp. 211–226.
- Maley, J., 1972, La sédimentation pollinique actuelle dans la zone du lac Tchad. *Pollen and Spores*, **14**, pp. 263–307.
- Maley, J., 1977, Palaeoclimates of Central Sahara during the Early Holocene. *Nature*, **269**, pp. 573–577.
- Maley, J., 1980, Les changements climatiques de la fin du Tertiaire en Afrique: leur conséquence sur l'apparition du Sahara et de sa végétation. In: *The Sahara and the Nile. Quaternary environments and prehistoric occupation in Northern Africa*. Edited by M.A.J. Williams, H. Faure, Balkema Publ., Rotterdam, pp. 63–86.
- Maley, J., 1981, Etudes palynologiques dans le bassin du Tchad et paléoclimatologie de l'Afrique nord-tropicale de 30.000 ans à l'époque actuelle. Thèse Sc., Montpellier, *Travaux et Documents ORSTOM, Paris*, **129**, 586 p.

- Maley, J., 1982, Dust, Clouds, Rain types, and climatic variations in Tropical North Africa. *Quaternary Research*, **18**, pp. 1–16.
- Maley, J., 1987, Fragmentation de la Forêt Dense Humide Africaine et extension des biotopes montagnards au Quaternaire récent: nouvelles données polliniques et chronologiques. Implications paléoclimatiques et biogéographiques. *Palaeoecology of Africa*, **18**, pp. 307–334.
- Maley, J., 1993, Chronologie calendaire des principales fluctuations du lac Tchad au cours du dernier millénaire. Le rôle des données historiques et de la tradition orale. In: *Datation et Chronologie dans le Bassin du lac Tchad*. Séminaire du Réseau Méga-Tchad, Sept. 1989, edited by D. Barreteau, C. von Graffenried, *Colloques et Séminaires ORSTOM*, pp. 161–163.
- Maley, J., 1996, The African rainforest: main characteristics of changes in vegetation and climate from the Upper Cretaceous to the Quaternary. *Proceed. R. Soc. Edinburgh, Biol. Sc.*, **104B**, pp. 31–73.
- Maley, J., 1997, Middle to Late Holocene changes in tropical Africa and other continents: Palaeomonsoon and sea surface temperature variations. In *Third Millennium BC climate change and Old World collapse*. Edited by H.N. Dalfes, G. Kukla, H. Weiss, pp. 611–640, NATO ASI Series, *Global Environmental Change*, Springer-Verlag, Berlin.
- Maley, J., 2000, Last Glacial Maximum lacustrine and fluvial formations in the Tibesti and other Saharan Mountains, and large scale climatic teleconnections linked to the activity of the Subtropical Jet Stream. *Global and Planetary Change*, **26**, pp. 121–136.
- Maley, J., 2001, La destruction catastrophique des forêts d'Afrique centrale survenue il y a environ 2.500 ans exerce encore une influence majeure sur la répartition actuelle des formations végétales. *Systematic and Geography of Plants*, **71**, pp. 777–796.
- Maley, J., 2002, A catastrophic destruction of African forests about 2.500 years ago still exerts a major influence on present vegetation formations. *Bulletin Inst. Development Studies*, **33**, pp. 13–30.
- Maley, J., 2004a., Le bassin du Tchad au Quaternaire récent: formations sédimentaires, paléoenvironnements et préhistoire. La question des Paléotchads. In *L'évolution de la Végétation depuis deux millions d'années*. Edited by J. Renault-Miskovsky and A.M. Semah, Publ. Artcom-Errance, Paris, pp. 179–217.
- Maley, J., 2004b, Les variations de la végétation et des paléoenvironnements du Domaine forestier africain au cours du Quaternaire récent. In *L'évolution de la Végétation depuis deux millions d'années*. Edited by J. Renault-Miskovsky and A.M. Semah, Publ. Artcom-Errance, Paris, pp. 143–178.
- Maley, J., Cohen, J., Faure, H., Rognon, P. and Vincent, P.M., 1970, Quelques Formations lacustres et fluviales associées à différentes phases du volcanisme au Tibesti (nord du Tchad). *Cahier ORSTOM, série Géologie*, **2**, pp. 127–152.
- Maley, J. and Brenac, P., 1998a, Vegetation dynamics, Palaeoenvironments and Climatic changes in the forests of Western Cameroon during the last 28.000 years BP. *Rev. Palaeobot. and Palynology*, **99**, pp. 157–187.
- Maley, J. and Brenac, P., 1998b, Les variations de la végétation et des paléoenvironnements du Sud Cameroun au cours des derniers millénaires. Etude de l'expansion du Palmier à huile. In *Géosciences au Cameroun*. Edited by J.P. Vicat and P. Bilong. *Collection GéoCam*, **1**, Presses Univ. Yaoundé-1, pp. 85–97.
- Maley, J. and David, N., 2008, Climate in DGB times. In *Performance and agency: the DGB sites of Northern Cameroon*. Edited by N. David. BAR, Intern. Series, Oxford, British Archaeo. Report. **1830**, pp. 112–113.

- Maley, J. and Willis, K., 2010, Did a savanna corridor open up across the Central African forests 2.500 years ago? *CoForChange European Progr.*, Letter **2**, 5 p.
- Mann, M.E., Zhang, Z., Hughes, M.K., Bradley, R.S., Miller, S.K., Rutherford, S. and Ni, F., 2008, Proxy-based reconstructions of hemispheric and global surface temperature variations over the past two millennia. *Proc.Nat. Acad. Sc.* **105**, 36, pp. 13252–13257.
- Mann, M.E., Zhang, Z., Rutherford, S., Bradley, R.S., Hughes, M.K., Shindell, D., Ammann, C., Faluvegi, G. and Ni, F., 2009, Global signatures and dynamical origins of the Little Ice Age and Medieval Climate Anomaly. *Science*, **326**, pp. 1256–1260.
- Marliac, A., 1973, Prospection archéologique au Cameroun. 2-L'industrie de la Basse Terrasse du Mayo Louti. *Cah. ORSTOM, série Sc. Hum., Paris*, **10**, pp. 47–114.
- Martinson, D.G., Pisias, N.G., Hays, J.D., Imbrie, J., Moore, T.C. and Shackleton, N.J., 1987, Age dating and the orbital theory of the Ice Ages: development of a high-resolution 0 to 300.000-year chronostratigraphy. *Quat. Res.*, **27**, pp. 1–29.
- Maslin, M.A. and Christensen, B., 2007, Tectonics, orbital forcing, global climate change, and human evolution in Africa: introduction to the African palaeoclimate special volume. *J. Human Evol.*, **53**, pp. 443–464.
- Matheis, G., 1976, Short review of the geology of the Chad Basin in Nigeria. In *Geology of Nigeria*. Edited by Kogbe, C.A.. Elizabethan Publ., Nigeria, pp. 289–294.
- Mathieu, P., 1978, Découverte d'oolithes ferrugineuses en stratigraphie sous le delta actuel du Chari (Tchad). *Cah. ORSTOM, série Géologie*, **10**, pp. 203–208.
- Mayor, A., Huyssecom, E., Gallay, A., Rasse, M. and Ballouche, A., 2005, Population dynamics and palaeoclimate over the past 3.000 years in the Dogon country, Mali. *J. Anthropol. Archaeol.*, **24**, pp. 25–61.
- McKenzie, J.A., 1993, Pluvial conditions in the eastern Sahara following the penultimate deglaciation: implications for changes in atmospheric circulation patterns with global warming. *Palaeogeogr., Palaeoclimatol., Palaeoecol.*, **103**, pp. 95–105.
- Messerli, B., Winiger, M. and Rognon, P., 1980, The Saharan and East African uplands during the Quaternary. In *The Sahara and the Nile. Quaternary environments and prehistoric occupation in northern Africa*. Edited by Williams, M.A.J. and Faure, H., Balkema Publ., Rotterdam, pp. 87–132
- Meulenkamp, J.E. and Sissingh, W., 2003, Tertiary palaeogeography and tectonostratigraphic evolution of the northern and southern peri-Tethys platforms and the intermediate domains of the African-Eurasian convergent plate boundary zone. *Palaeogeogr., Palaeoclimatol., Palaeoecol.*, **196**, pp. 209–228.
- Michel, P., 1973, Les bassins des fleuves Sénégal et Gambie. Etude géomorphologique. *Mémoire ORSTOM, Paris*, **63**, 2 p.
- Monteil, C., 1953, La légende du Ouagadou et l'origine des Soninké. *Mém. Inst. Fr. Afr. Noire*, **23**, pp. 361–408.
- Morel, A., Tillet, T., Poupeau, G. and Raimbault, M., 1997, Bassin de Taoudenni. In *Sahara, paléomilieux et peuplement préhistorique au Pléistocène supérieur*. Edited by Tillet, T., Publ. L'Harmattan, Paris, pp. 101–123.
- Morgan, M.E., Kingston, J.D. and Marino, B.D., 1994, Carbon isotopic evidence for the emergence of C₄ plants in the Neogene from Pakistan and Kenya. *Nature*, **367**, pp. 162–165.
- Morley, R.J., 2000, Origin and evolution of tropical rain forests. J. Wiley, Chichester.
- Moron, V. 1994, Guinean and Sahelian rainfall anomaly indices at annual and monthly time scales (1933–1990). *Int. J. Climatol.*, **14**, pp. 325–341.
- Mounier, F. and Janicot, S., 2004, Evidence of two independent modes of convection at intraseasonal timescale in the West African summer monsoon. *Geophys. Res. Lett.*, **31**, pp. L16116.

- Neumann, K., 1992, Une flore soudanienne au Sahara central vers 7.000 BP: les charbons de bois de Fachi, Niger. *Bull. Soc. Bota. France*, **139**, pp. 565–569.
- Nicholson, S.E. and Flohn, H., 1980, African environmental and climatic changes and the General Atmospheric Circulation in Late Pleistocene and Holocene. *Climatic Change*, **2**, pp. 313–348.
- Ngomanda, A., Jolly, D., Bentaleb, I., Chepstow-Lusty, A., Makaya, M., Maley, J., Fontugne, M., Oslisly, R. and Rabenkogo, N., 2007, Lowland rainforest response to hydrological changes during the last 1.500 years in Gabon, western equatorial Africa. *Quat. Res.*, **67**, pp. 411–425.
- Ngomanda, A., Neumann, K., Schweizer, A. and Maley, J., 2009, Seasonality change and the third Millennium BP rainforest crisis in Southern Cameroon (Central Africa). *Quat. Res.* **71**, pp. 307–318.
- Nunes, F. and Norris, R.D., 2006, Abrupt reversal in ocean overturning during the Paleocene/Eocene warm period. *Nature*, **439**, pp. 60–63.
- Olivry, J.C., Chouret, A., Vuillaume, G., Lemoalle, J. and Bricquet, J.P., 1996, Hydrologie du lac Tchad. *Monographie Hydrologique ORSTOM*, **12**, 266 p.
- Olsen, P.E., Remington, C.L., Cornet, B. and Thomson, K.S., 1978, Cyclic change in Late Triassic lacustrine communities. *Science*, **201**, pp. 729–733.
- Olsen, P.E. and Kent, D.V., 1996, Milankovitch climate forcing in the tropics of Pangaea during the Late Triassic. *Palaeogeogr., Palaeoclim., Palaeoecol.*, **122**, pp. 1–26.
- Overpeck, J., Wheeler, W., Shanahan, T., Cole, J., Scholz, C., Arko, J. and Sharp, E., 2003, A new perspective on hydrologic change in West Africa over the last 800 years. *CLIVAR Workshop*, Tucson, Nov. 2003, 2 p.
- Patricola, C.M. and Cook, K.H., 2007, Dynamics of the West African monsoon under mid-Holocene precessional forcing: regional climate model simulations. *J. Climate*, **20**, pp. 694–716.
- Pefontan, Lt., 1922, Histoire de Tombouctou, de sa fondation au XIIème s. à 1893. *Bull. Com. Et. Hist. Sc. Afr. Occid. Fr.*, **7**, pp. 81–113.
- Petit-Maire, N., 1992, Environnements et climats de la ceinture tropicale nord-africaine depuis 140.000 ans. *Bull. Soc. Géol. France*, **160**, pp. 27–34.
- Petit-Maire, N., Faure, M., Gayet, M. and Guerin, C., 1991, Importance des données paléontologiques pour l'étude des changements climatiques globaux: macropaléontologie et paléoclimats sahariens. *Bull. Soc. Géol. France*, **162**, pp. 707–711.
- Pias, J. and Barbery, J., 1964, Notice explicative. Cartes pédologiques de reconnaissance au 1/200.000 ème. Feuilles de Fort-lamy, Massenya, Mogroum. *Publ. ORSTOM*, Fort-Lamy, 103 p.
- Pias, J., 1967, Quatre deltas successifs du Chari au Quaternaire (Rép. Du Tchad et du Cameroun). *C.R. Acad. Sc.*, Paris, **264**, pp. 2357–2360.
- Pias, J., 1970, Les Formations sédimentaires Tertiaires et Quaternaires de la Cuvette Tchadienne et les sols qui en dérivent. *Mémoire ORSTOM*, **43**, Paris, 407 p.
- Prell, W.L. and Kutzbach, J.E., 1987, Monsoon variability over the past 150.000 years. *J. Geophys. Res.*, **92**, pp. 8411–8425.
- Rasse, M., Soriano, S., Tribolo, C., Stokes, S. and Huysecom, E., 2004, La Séquence Pléistocène supérieur d'Ounjougou (Pays Dogon, Mali, Afrique Ouest): Evolution géomorphologique, enregistrements sédimentaires et changements culturels. *Quaternaire*, **15**, pp. 329–341.
- Rasse, M., Ballouche, A., Huysecom, E., Tribolo, C., Ozainne, S., Le Drezen, Y., Stokes, S. and Neumann, K., 2006, Evolution géomorphologique, enregistrements sédimentaires et dynamiques paléoenvironnementales holocènes à Ounjougou (Plateau Dogon, Mali, Afrique de l'Ouest). *Quaternaire*, **17**, pp. 61–74.

- Raynal, J.P., Alaoui, F.Z., Geraads, D., Magoga, L. and Mohi, A., 2001, The earliest occupation of North-Africa: the Moroccan perspective. *Quat. Intern.*, **75**, pp. 65–75.
- Reimer, P.J., Baillie, M.G.L., Bard, E. et Bayliss, A., Beck, J.W., Bertrand, C.J.H., Blackwell, P.G., Buck, C.E., Burr, G.S., Cutler, K.B., Damon, P.E., Edwards, R.L., Fairbanks, R.G., Friedrich, M., Guilderson, T.P., Hogg, A.G., Hughen, K.A., Kromer, B., McCormac, G., Manning, S., Ramsey, C.B., Reimer, R.W., Remmele, S., Southon, J.R., Stuiver, M., Talamo, S., Taylor, F.W., van der Plicht, J. and Weyhenmeyer, C.E., 2004, INTCAL04 Terrestrial Radiocarbon age calibration, 0–26 cal kyr BP. *Radiocarbon*, **46**, pp. 1029–1058.
- Rendell, H.M., Clarke, M.L., Warren, A. and Chappell, A., 2003, The timing of climbing dune formation in Southwestern Niger: fluvio-aeolian interactions and the role of sand supply. *Quat. Sc. Rev.*, **22**, pp. 1059–1065.
- Retallack, G.J., 2001, Cenozoic expansion of grasslands and climatic cooling. *J. Geology*, **109**, pp. 407–426.
- Retallack, G.J., 1992, Middle Miocene fossil plants from Fort Ternan (Kenya) and evolution of African grasslands. *Palaeobiology*, **18**, pp. 383–400.
- Ritchie, J.C. and Haynes, C.V., 1987, Holocene vegetation zonation in the eastern Sahara. *Nature*, **330**, pp. 645–647.
- Rodrigues, D., Abell, P.I. and Kröpelin, S., 2000, Seasonality in the Early Holocene climate of Northwest Sudan: interpretation of *Etheria elliptica* shell isotopic data. *Global and Planet. Ch.*, **26**, pp. 181–187.
- Rognon, P., 1967, Le Massif de l'Atakor et ses bordures (Sahara central) Etude géomorphologique. *CNRS édit., série Géologie*, **9**, 560 p.
- Rognon, P., 1989, Variations de l'aridité au Sahara depuis 125.000 BP en relation avec les "contraintes" orbitales et glaciaires. *Bull. Soc. Géol. France* (sér.8), **5**, pp. 13–20.
- Rognon, P., 1996, Climatic change in the African deserts between 130.000 and 10.000 yr BP. *C.R. Acad. Sc., Paris*, sér. 2a, **323**, pp. 549–561.
- Rohling, E.J. and Palike, H., 2005, Centennial-scale climate cooling with a sudden cold event around 8.200 years ago. *Nature*, **434**, pp. 975–979.
- Sahnouni, M., 2005, Point des connaissances du Paléolithique ancien d'Afrique du Nord et la question de la première occupation humaine au Maghreb. In: *Le Paléolithique en Afrique: l'histoire la plus longue*. Publ. Errance, Paris, pp. 99–128.
- Said, R., 1993, *The River Nile. Geology, hydrology and utilization*. Oxford.
- Salard-Cheboldaëff, M., 1981, Palynologie Maestrichienne et Tertiaire du Cameroun. *Rev. Palaeobot. and Palyno.*, **32**, pp. 401–439.
- Sarnthein, M., 1978, Sand deserts during glacial maximum and climatic optimum. *Nature*, **272**, pp. 43–46.
- Sarnthein, M., Thiede, J., Pflaumann, U., Erlenkeuser, H., Fütterer, D., Koopmann, B., Lange, H. and Seibold, E., 1982, Atmospheric and oceanic circulation patterns of Northwest Africa during the past 25 Million years. In *Geology of Northwest African continental margin*. Edited by von Rad, U., Hinz, K., Sarnthein, M., Seibold, E., Springer-Verlag, Berlin, pp. 545–604.
- Satabie, B., 1994, Biosystématique et vicariance dans la flore Camerounaise. *Bull. Jard. Bot. Nat. Belg.*, **63**, pp. 125–170.
- Schild, R. and Wendorf, F., 2001, Geoarchaeology of the Holocene climatic optimum at Nabta Playa, southwestern desert, Egypt. *Geoarchaeology*, **16**, pp. 7–28.
- Schneider, J.L., 1969, Evolution du dernier lacustre et peuplements préhistoriques aux Pays-Bas du Tchad. *Bull. Inst. F. Afr. Noire*, sér. A, **31**, pp. 259–263.
- Schrire, B.D., Lavin, M. and Lewis, G.P., 2005, Global distribution patterns of the Leguminosae: insights from recent phylogenies. *Biologische Schrifter*, **55**, pp. 375–422.

- Schuster, M., 2002, Sédimentologie et paléocéologie des séries à vertébrés du paléolac Tchad depuis le Miocène supérieur. *Thèse Science*, Univ. Strasbourg, 152 p.
- Schuster, M., Düringer, P., Ghienne, J.F., Vignaud, P., Beauvilain, A., Mackaye, H.T. and Brunet, M., 2003, Coastal conglomerates around the Hadjer el Khamis inselbergs (Western Chad, Central Africa): new evidence for lake Mega-Chad episodes. *Earth Surf. Process Landform*, **28**, pp. 1059–1069.
- Schuster, M., Roquin, C., Düringer, P., Brunet, M., Caugy, M., Fontugne, M., Mackaye, H.T., Vignaud, P. and Ghienne, J.F., 2005, Holocene lake Mega-Chad palaeoshorelines from space. *Quat. Sc. Rev.*, **24**, pp. 1821–1827.
- Schuster, M., Düringer, P., Ghienne, J.F., Vignaud, P., Mackaye, H.T., Likius, A. and Brunet, M., 2006, The age of the Sahara desert. *Science*, **311**, p. 821 and pp. 1138–1139.
- Schuster, M., Düringer, P., Ghienne, J.F., Roquin, C., Sepulchre, P., Moussa, A., Lebatard, A.E., Mackaye, H.T., Likius, A., Vignaud, P. and Brunet, M., 2009, Chad Basin: Palaeoenvironments of the Sahara since the Late Miocene. *C.R. Geoscience*, **341**, pp. 603–611.
- Seager, R., Graham, N., Herweijer, C., Gordon, A.L., Kushnir, Y. and Cook, E., 2007, Blueprints for Medieval hydroclimate. *Quat. Sc. Rev.*, **26**, pp. 2322–2336.
- Segalen, L., Lee-Thorp, J.A. and Cerling, T., 2007, Timing of C₄ grass expansion across sub-Saharan Africa. *J. Human Evol.*, **53**, pp. 549–559.
- Seignobos, C., 1993, Des traditions Fellata et de l'assèchement du lac Tchad. In *Datation et Chronologie dans le Bassin du lac Tchad*. Edited by Barreteau, D., von Graffenried, C., Série *Colloques and Séminaires ORSTOM*, pp. 165–182.
- Sepulchre, P., Schuster, M., Ramstein, G., Krinner, G., Girard, J.F., Fluteau, F., Vignaud, P. and Brunet, M., 2008, Simulating the Holocene Lake Mega Chad with an AGCM coupled with a lake model: a preliminary approach. *Glob. and Plan. Ch.*, **61**, pp. 41–48.
- Sepulchre, P., Ramstein, G. and Schuster, M., 2009, Modelling the impact of tectonics, surface conditions and sea surface temperatures on Saharan and sub-Saharan climate evolution. *C.R. Geoscience*, **341**, pp. 612–620.
- Servant, M., 1973, Séquences continentales et variations climatiques: Evolution du bassin du Tchad au Cénozoïque supérieur. Thèse Sc., Paris, *Travaux and Documents ORSTOM*, **159**(1983).
- Servant, M., Ergenzinger, P. and Coppens, Y., 1969, Datations absolues sur un delta lacustre quaternaire au sud du Tibesti (Angamma). *C.R. Séances Soc. Géol. France*, **8**, pp. 313–314.
- Servant, M. and Servant-Vildary, S., 1980, L'environnement quaternaire du bassin du Tchad. In *The Sahara and the Nile*. Edited by Williams, M.A.J. and Faure, H., A.A. Balkema Publ., Rotterdam, pp. 133–162.
- Servant, M. and Servant-Vildary, 2003, Holocene precipitation and atmospheric changes inferred from river palaeowetlands in the Bolivian Andes. *Palaeogeogr., Palaeoclimato., Palaeoeco.*, **194**, pp. 187–206.
- Servant-Vildary, S., 1973, Le Plio-Quaternaire ancien du Tchad: évolution des associations de diatomées, stratigraphie, paléocéologie. *Cahier ORSTOM, série Géologie*, **5**, pp. 217–234.
- Servant-Vildary, 1978, Etude des diatomées et paléolimnologie du bassin tchadien au Cénozoïque supérieur. Thèse Sc., Paris, *Travaux and Documents ORSTOM*, **84**.
- Shanahan, T.M., Overpeck, J.T., Anchukaitis, K.J., Beck, J.W., Cole, J.E., Dettman, D.L., Peck, J.A., Scholz, C.A. and King, J.W., 2009, Atlantic forcing of persistent drought in West Africa. *Science*, **324**, pp. 377–380.
- Shindell, D.T., Faluvegi, G., Miller, R.L., Schmidt, G.A. and Hansen, J.E., 2006, Solar and anthropogenic forcing of tropical hydrology. *Geophys. Res. Lett.*, **33**, pp. L24706.

- Sieffermann, G., 1970, Variations climatiques au Quaternaire dans le sud-ouest de la cuvette tchadienne. *C.R. 92^e Cong. Nat. Soc. Savantes*, **2**, Strasbourg, pp. 485–494.
- Smith, J.R., Giegengack, R. and Schwarcz, H.P., 2004, Constraints on Pleistocene pluvial climates through stable-isotope analysis of fossil-spring tufas and associated gastropods, Kharga Oasis, Egypt. *Palaeogeogr., Palaeoclimato., Palaeoeco.*, **206**, pp. 157–175.
- Smith, J.R., Hawkins, A.L., Asmeron, Y., Polyak, V. and Giegengack, R., 2007, New age constraints on the Middle Stone Age occupations of Kharga Oasis, western desert, Egypt. *J. Human Evol.*, **52**, pp. 690–701.
- Sonntag, C., Thorweihe, U., Rudolph, J., Lohnert, E.P., Junghans, C., Munnich, K.O., Klitzsch, E., El Shazly, E.M. and Swailem, F.M., 1980, Isotopic identification of Saharian groundwaters, groundwater formation in the past. *Palaeoecology Africa*, **12**, pp. 159–171.
- Stager, J.C., Ryves, D., Cumming, B.F., Meeker, L.D. and Beer, J., 2005, Solar variability and the levels of Lake Victoria, East Africa, during the last Millennium. *J. Palaeolimnology*, **33**, pp. 243–251.
- Stebbins, G.L., 1974, Flowering plants. Evolution above the species level. *Harvard Univ. Press*.
- Stein, R. and Sarnthein, M., 1984, Late Neogene events of atmospheric and oceanic circulation offshore Northwest Africa: high-resolution record from deep-sea sediments. *Palaeoecology of Africa*, **16**, pp. 9–36.
- Stokes, S., Bailey, R.M., Fedoroff, N. and O'Marah, K.E., 2004, Optical dating of aeolian dynamism on the West African Sahelian margin. *Geomorphology*, **59**, pp. 281–291.
- Stott, L., Poulsen, C., Lund, S. and Thunell, R., 2002, Super ENSO and global climate oscillations at millennial time scales. *Nature*, **297**, pp. 222–226.
- Sultan, M., Sturchio, N., Hassan, F.A., Hamdan, M.A., Mahmood, A.M., El Alfy, Z. and Stein, T., 1997, Precipitation source inferred from stable isotopic composition of Pleistocene groundwater and carbonate deposits in the western desert of Egypt. *Quat. Res.*, **48**, pp. 29–37.
- Szabo, B.J., Haynes, C.V. and Maxwell, T.A., 1995, Ages of Quaternary pluvial episodes determined by Uranium-series and radiocarbon dating of lacustrine deposits of eastern Sahara. *Palaeogeogr., Palaeoclimato., Palaeoeco.* **113**, pp. 227–242.
- Thepenier, R.M. and Cruette, D., 1981, Formation of cloud bands associated with the American Subtropical Jet Stream and their interaction with midlatitude synoptic disturbances reaching Europe. *Month. Weather Rev.*, **109**, pp. 2209–2220.
- Thomas, H., 1977, Géologie et paléontologie du gisement Acheuléen de l'Erg Tihodaine. *Mém. Cent. Rech. Anthropol. Préhist. et Ethno.* **27**, Alger.
- Thomas, H. and Picq, P., 2001, Des singes à la conquête du monde des arbres. In *Aux origines de l'humanité. I-De l'apparition de la vie à l'homme moderne*. Edited by Coppens, Y., and Picq, P., Publ. Fayard, Paris, pp. 72–119.
- Thomas, M.F. and Thorp, M.B., 1992, Landscape dynamics and surface deposits arising from Late Quaternary fluctuations in the forest-savanna boundary of West Africa. In *Nature and dynamics of forest-savanna boundaries*. Edited by Furley, P.A., Proctor, J., and Ratter J.A., Chapman and Hall Publ., London, pp. 215–253.
- Tilho, J., 1925, Sur l'aire probable d'extension maxima de la mer paléotchadienne. *C.R. Acad. Sc.*, **181**, Paris, pp. 643–646.
- Tillet, T., 1989, L'Atérien saharien: essai sur le comportement d'une civilisation paléolithique face à l'accroissement de l'aridité. *Bull. Soc. Géol. France*, (sér.8) **5**, pp. 91–97.
- Torrent, H., 1966, Carte hydrogéologique de reconnaissance de la République du Tchad au 1/500.000^{ème} (Feuille BONGOR). Rapport de synthèse. *Minist. Trav. Publ. and Serv. Hydraul. Tchad and BRGM, Orléans*.

- Trauth, M.H., Larrasoana, J.C. and Mudelsee, M., 2009, Trends, rhythms and events in Plio-Pleistocene African climate. *Quat. Sc. Rev.*, **28**, pp. 399–411.
- Treinen-Claustre, F., 1982, Sahara et Sahel à l'Age du Fer. Borkou, Tchad. *Mém. Soc. Africanistes*, Paris, 214 p.
- Van Peer, P., 1998, The Nile corridor and the Out-of-Africa model. *Current Anthropology*, **39**, pp. 115–140.
- Van Peer, P. and Vermeersch, P.M., 2007, The place of Northeast Africa in the early history of modern Humans: new data and interpretations on the Middle Stone Age. In *Rethinking the Human evolution*. Edited by Mellars, P. et al., Cambridge, McDonald Inst. of Archaeology, pp. 187–198.
- Vermeersch, P.M., Paulissen, E., Otte, M. and Gijssels, G., 2000, Nag Ahmed el Khalifa, an Acheulean site. In *Palaeolithic living sites in Upper and Middle Egypt*. Edited by Vermeersch, P.M., Leuven Univ. Press, Belgique, pp. 57–73..
- Vermeersch, P.M., Van Neer, W. and Gullentops, F., 2006, El Abadiya 3, Upper Egypt, a Late Palaeolithic site on the shore of a large Nile Lake. In *Archaeology of Early Northeastern Africa. Studies in African Archaeology*, **9**, Poznam Archaeology Museum, pp. 404–424.
- Vermeersch, P.M., 2006, La vallée du Nil et le Sahara oriental: une population préhistorique fluctuante sous l'effet des variations climatiques. *C.R. Palevol.*, **5**, pp. 255–262.
- Vernet, R., 1993, *Préhistoire de la Mauritanie*. Publ., Sépia, Paris.
- Verschuren, D., Laird, K.R. and Cumming, B.F., 2000, Rainfall and drought in equatorial East Africa during the past 1.100 years. *Nature*, **403**, pp. 410–413.
- Vignaud, P., Düringer, P., Mackaye, H.T., Likius, A., Blondel, C., Boisserie, J.R., De Bonis, L., Eisenmann, V., Etienne, M.E., Geraads, D., Guy, F., Lehmann, T., Lihoreau, F., Martinez, N.L., Mourer-Chauvire, C., Otero, O., Rage, J.C., Schuster, M., Viriot, L., Zazzo, A. and Brunet, M., 2002, Geology and palaeontology of the Upper Miocene Toros-Menalla hominid locality, Chad. *Nature*, **418**, pp. 152–155.
- Vincens, A., Buchet, G., Servant, M. and Ecofit Mbalang collaborators, 2010, Vegetation response to the African Humid Period termination in central Cameroon (7°N)—new pollen insight from Lake Mbalang. *Climate of Past Discuss.*, **5**, pp. 2577–2606.
- Vizy, E.K. and Cook, K.H., 2002, Development and application of a mesoscale climate model for the tropics: influence of sea surface temperature anomalies on the West African monsoon. *J. Geophys. Res.*, **107**, pp. 1–22.
- von Grafenstein, U., Erlenkeuser, H., Muller, J., Jouzel, J. and Johnsen, S., 1998, The cold event 8.200 years ago documented in oxygen isotope records of precipitation in Europe and Greenland. *Climate Dynamics*, **14**, pp. 73–81.
- Wendorf, F., Close, A.E., Schild, R., Gautier, A., Schwarcz, H.P., Miller, G.H., Kowalski, K., Krolik, H., Bluszcz, A., Robins, D. and Grun, R., 1990, Le dernier Interglaciaire dans le Sahara oriental. *L'Anthropologie*, **94**, pp. 361–391.
- Wendorf, F., Schild, R. and Close, A.E., 1993, Egypt during the last Interglacial. The Middle Palaeolithic of Bir Tarfawi and Bir Sahara East. *Plenum Press*, New York, 596 p.
- Wendorf, F. and Schild, R., 2005, Le Paléolithique moyen d'Afrique du Nord: un bref survol. In: *Le Paléolithique en Afrique: l'histoire la plus longue*. Publ. Errance, Paris, pp. 157–204.
- Williams, M.A.J., Abell, P.I. and Sparks, B.W., 1987, Quaternary landforms, sediments, depositional environments and gastropod isotope ratios at Adrar Bous, Tenere Desert of Niger, south-central Sahara. In *Desert sediments: ancient and modern*. Edited by Frostick, L. and Reid, I., Geol. Soc. Sp. Publ., London, **35**, pp. 105–125..
- Williams, M.A.J., Adamson, D.A., Cock, B. and McEvedy, R., 2000, Late Quaternary environments in the White Nile region, Sudan. *Global and Plan. Ch.*, **26**, pp. 305–316.

- Williams, M.A.J., Talbot, M., Aharon, P., Abdl Salaam, Y., Williams, F. and Brendeland, K.I., 2006, Abrupt return of the summer monsoon 15.000 years ago: new supporting evidence from the lower Nile valley and Lake Albert. *Quat. Sc. Rev.*, **25**, pp. 2651–2665.
- Wrinn, P.J. and Rink, W.J., 2003, ESR dating of tooth enamel from Aterian levels at Mugharet el Aliya (Tangier, Marocco). *J. Archaeo. Sc.*, **30**, pp. 123–133.
- Zachos, J., Pagani, M., Sloan, L., Thomas, E. and Billups, K., 2001, Trends, rhythms, and aberrations in global climate 65 Ma to present. *Science*, **292**, pp. 686–693.
- Zazo, A., Bocherens, H., Brunet, M., Beauvilain, A., Billiou, D., Mackaye, H.T., Vignaud, P. and Mariotti, A., 2000, Herbivore palaeodiet and palaeoenvironmental changes in Chad during the Pliocene using stable isotope ratios of tooth enamel carbonate. *Palaeobiology*, **26**, pp. 294–309.
- Zeltner, J.C., 1980, Pages d'histoire du Kanem. L'Harmattan, Paris, 275 p.
- Zhang, R. and Delworth, T.L., 2005, Simulated tropical response to a substantial weakening of the Atlantic thermohaline circulation. *J. Clim.*, **18**, pp. 1853–1860.

CHAPTER 13

An assessment of the spatial and temporal distribution of natural hazards in Central Africa

Ine Vandecasteele, Jan Moeyersons & Philippe Trefois
Musée Royal de l'Afrique Centrale, Tervuren, Belgique

ABSTRACT: The Central African region of the Democratic Republic of Congo (DRC), Rwanda and Burundi is little known in international geomorphic and natural hazard literature. In an attempt to gather some primary information for this 2.400.000 km² white patch on the map, the geomorphology and remote sensing division of the RMCA has recently launched the “Natural Hazards Database for Central Africa”, which integrates information from diverse sources on natural hazards having occurred in the region since 1910. The database records some 241 events for the period 1910–2009, having resulted in 1959 deaths and affected over 12,2 million people. The database forms a basis for investigation into the spatial and temporal trends in hazard occurrence in Central Africa. Preliminary results show that the region of the Congo Basin is more geomorphologically active than first thought, and that there is an especially high frequency of events along the Albertine rift zone encompassing the Kivu provinces in DRC, Rwanda and Burundi. It is not so much the magnitude of events, but their frequency that has resulted in widespread material and human losses. Events of hydrological origin such as mass movements and flash and wash floods are becoming increasingly important, and the number thereof has been seen to rise exponentially since 2000. Although it has not as yet been included in our databank, fieldwork suggests that urban gullying also forms an increasingly important threat. We attribute this increase in frequency of events to the accelerated urbanisation in the region over the last few decades.

13.1 INTRODUCTION

Central Africa receives only limited attention as a naturally hazardous region. Even though the area is prone to a wide variety and high frequency of natural hazards, very little is known about the nature and consequences thereof.

Various studies have already been carried out on the occurrence of natural hazards globally (Dilley *et al.*, 2005) and in Africa (UN/ISDR 2004; ICSU, 2007), but as yet there has been no extended study of the central African region. Figure 1 shows an extract of the natural hazards map for Africa compiled by the UNESCO-IHDR. The map gives an overview of hazards present in the region, but demonstrates at the same time the complete lack of information for the Congo Basin.

The natural hazards database for central Africa has been set up as a synthesis of existent information on the area, allowing identification of particular high-risk regions, and investigation into the temporal trends in hazard occurrence. It is a first attempt at coverage of this region, which remains vacant on most risk maps. The International Disaster Database maintained by the Université Catholique de Louvain (EM-DAT) was consulted and used in the initial data collection. The collection of data would also not be possible without the Réseau de Correspondants (RéCO), a network of scientists

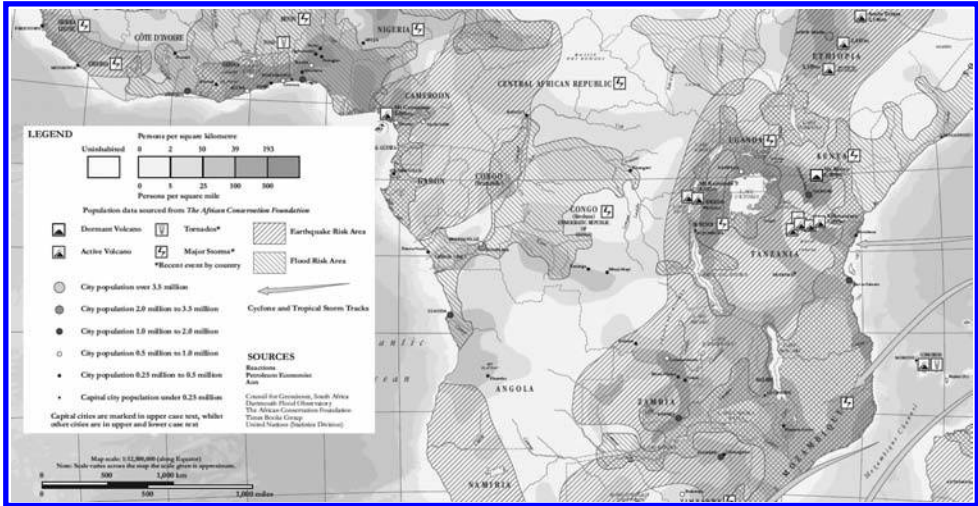


Figure 1. Extract from the natural hazards map for Africa compiled by the UNSCO-IHDR, covering the region of interest (UNESCO-IHDR, 2009).

set up in 2009 to share information within Rwanda, Burundi, and the Democratic Republic of Congo. These local experts continue to provide us with up-to-date and detailed information on natural hazards occurring in the region, which is vital, since many events fall below the radar of the international media.

Although the events reported in this article cover a wide range of natural hazard types, our focus is on events of geomorphological origin. These include all mass movement and flooding events. Field studies carried out in the region show that gullying is also an important hazard in most urban areas. Examples of extreme gullying have already been noted in the towns of Kinshasa, Butembo, Mbuji-Mayi, Kikwit, Lisala, and Bujumbura. Little information is currently available on the extension and related damages caused by this type of erosion, however, and further field investigation is necessary before these events can be included in the databank.

This article presents the Natural Hazards Database for Central Africa and gives a first account of the geographic and temporal distributions of the recorded events and their causal factors.

13.2 MATERIALS AND METHODS

13.2.1 The database

Definition and classification of natural hazards

The term “natural hazard” is used to describe a phenomenon of natural origin which affects a population, resulting in human casualties or material damage. The definition of a naturally-occurring phenomenon as a “hazard” varies according to the source. An event is usually only classified as a natural hazard if it has a significant impact on the human population. This may be in terms of human deaths, injuries, or material damages to property, constructions, livestock, or crops. A high frequency of events leading to a loss in soil fertility, for example, may also be considered a “hazard”.

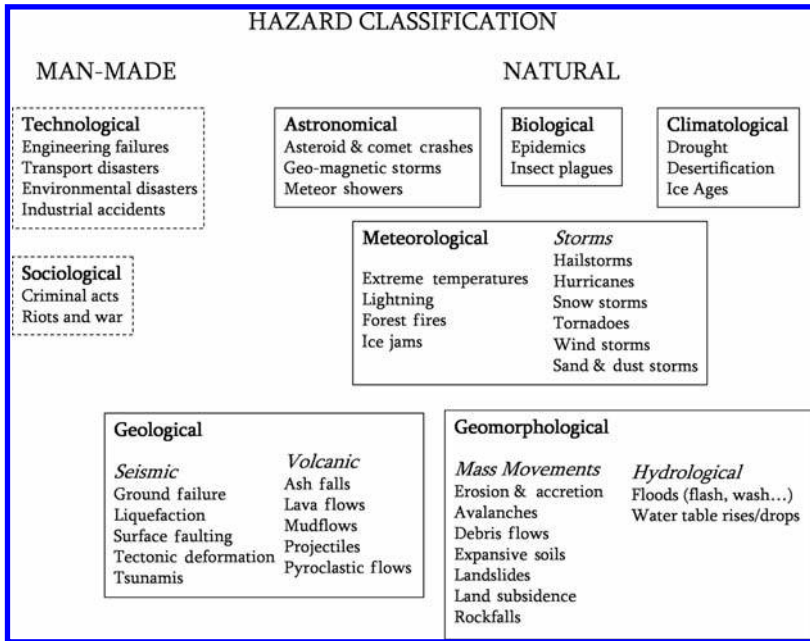


Figure 2. A classification of hazard types according to their origin/nature. (Source: Alexander, 1993; Smith & Petley, 2009, reworked by authors).

Figure 2 gives an overview of the classification of hazards, which may be identified as either natural or man-made, although there is often an overlap. We focus on natural phenomena, and classify events according to their origin. The classification of natural hazards is greatly disputed, and our overview is by no means the only possible approach, nor is it exhaustive.

The database includes only the natural hazards of which there is evidence in at least one of the three countries. It should be noted that where there has been doubt as to the classification of an event, it has been defined according to the manner in which it has been reported. The following natural phenomena were included in the database:

- Volcanic activity—lava flows, gas emissions and explosive eruptions.
- Seismic activity—all reported earthquakes of a magnitude of 4 or higher on the Richter scale, and/or where the population is affected.
- Drought—prolonged periods of low or absent rainfall.
- Storms—tropical storms, hailstorms, torrential rainstorms and strong winds.
- Flooding—reported inundations having resulted in material or human losses.
- Mass movements—all transport of superficial material, including landslides, mudflows and rock falls, as well as gully erosion.

Data collection

In order to include as much information as possible from 1900 onwards, a wide variety of sources were consulted. The archives of the Royal Museum for Central Africa were searched for historical reports detailing events (Devroey, 1962; De Bremaecker, 1957), and the GeoRef database was used to find relevant scientific publications mentioning

hazard events. Although not many articles have been published on the subject matter, this did provide us with some interesting information (Byers, 1992; Laraque *et al.* 1998; Runge and Nguimalet, 2005; Shako, 2007). Reliable news agencies were also consulted, including IRIN (www.irinnews.org/), BBC (www.bbc.co.uk), and Le potentiel (www.lepotentiel.com/). NGO reports made available online also proved helpful, especially those compiled by the UN, the Red Cross, Doctors without borders, FAO, and those posted on Reliefweb (www.reliefweb.com).

We also consulted several existing natural hazard databases, notably the emergency database EM-DAT (www.emdat.be/) maintained by the Centre for Research on the Epidemiology of Disasters (CRED) of the Université Catholique de Louvain. A few other internet sources, including Catastrophes Naturelles (www.catnat.net/) Dartmouth Flood Observatory (www.dartmouth.edu/~floods/) and Glide number (www.glidenumber.net/) provided useful information. A number of entries are also based on personal communication in the field, or that shared by the members of the RéCO. The following information was included in the database for each event:

- Disaster ID—this is a specific identification number given to an event; it has been compiled from the year in which the event occurred, the number (or letter) of the event in that year, and the country code (e.g. 1998-A-BDI).
- Location—the country, province, and specific coordinates of the event were noted where possible. Georeferencing was carried out using a system developed by the CRED.
- Hazard type—this is disputable, since often a hazardous event may be classed under different categories, or involves more than one actual hazard simultaneously. The hazard type as reported was consequently noted.
- Secondary hazards—any additional hazards related to the reported event.
- Start & End date—as specifically as possible, though the start and end dates of longer term hazards such as droughts were difficult to define.
- Magnitude—this gives an idea of the scale of the event, where it has been measured.
- Number of people affected—the sum of the reported number of people left homeless and those injured during an event.
- Number of people killed—the number of deaths directly resulting from an event.
- Structural damage—includes all material damage that may have occurred, such as loss of crops and destruction of buildings.
- River Basin—where relevant the name of the river along which the event has taken place.
- Additional Information—any extra information that has been included in the reports found, but does not fit the above categories.
- Source—the original source of the information. An entry has been noted to be more reliable the more sources it has.

Criteria for entry in the database

The entries originating from the CRED (EM-DAT) are based on the following criteria: more than 100 people were affected by the event; more than 10 people killed; or a state of emergency was declared. We have used less strict criteria to enable us to include as many significant events as possible. Our basic criteria is that an event is included if there has been any evidence of material damage (houses or crop losses) and/or human loss.

13.2.2 Study area

The database has been compiled for the Democratic Republic of Congo (DRC), Rwanda and Burundi, located between longitudes 12,1 and 31,3, and latitudes 5,4 and -13,5 (Figure 3). The region is bounded by the Republic of Congo (Brazzaville), the Central African Republic, Sudan, Uganda, Tanzania, Zambia and Angola, with only about 40 kilometers of coastline.

The border between the DRC and Rwanda and Burundi is formed by the Albertine Rift, the western branch of the East African Rift Valley. The largest part of the DRC is drained by the Congo River, whose basin extends into the neighbouring countries in the north, and with an area of 3.630.000 km² forms the second largest drainage basin in the world after the Amazon (Summerfield and Hulton, 1994). The Congo Basin itself is relatively flat, at an elevation between 300 and 600 meters above sea level (Figure 3). In the East, it is bounded by a more outspoken topography towards the Kivu Provinces and the Albertine Rift. To the West, the Congo River cuts itself a way to the Atlantic Ocean through the Cristal Mountains along rapids and chutes. Sandy deposits like the Kalahari and the Yangambi sands cover the central and southern part of the basin. Palaeozoic formations are exposed in the East, in Rwanda-Burundi and in the Cristal Mountains (Robert, 1948; Cahen, 1954). The vegetation found in the region varies greatly from tropical forests in the North and centre through to open savannah in the South. The climatic conditions range from tropical in Northern DRC to temperate in the mountainous regions of the Kivu Provinces, Rwanda and Burundi (Bultot, 1971, see also Figure 8).

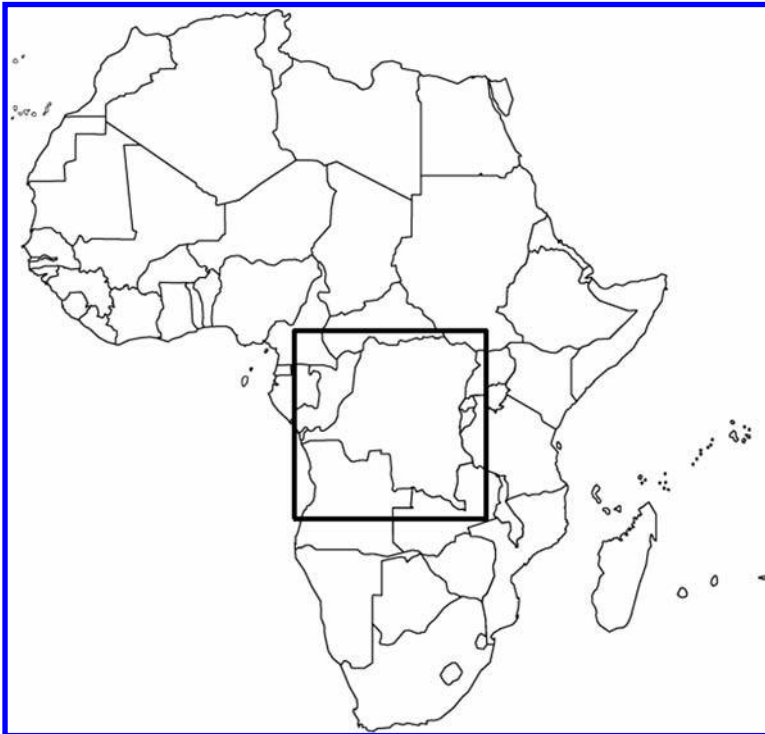


Figure 3A. The location of Rwanda, Burundi and the DRC in Africa.

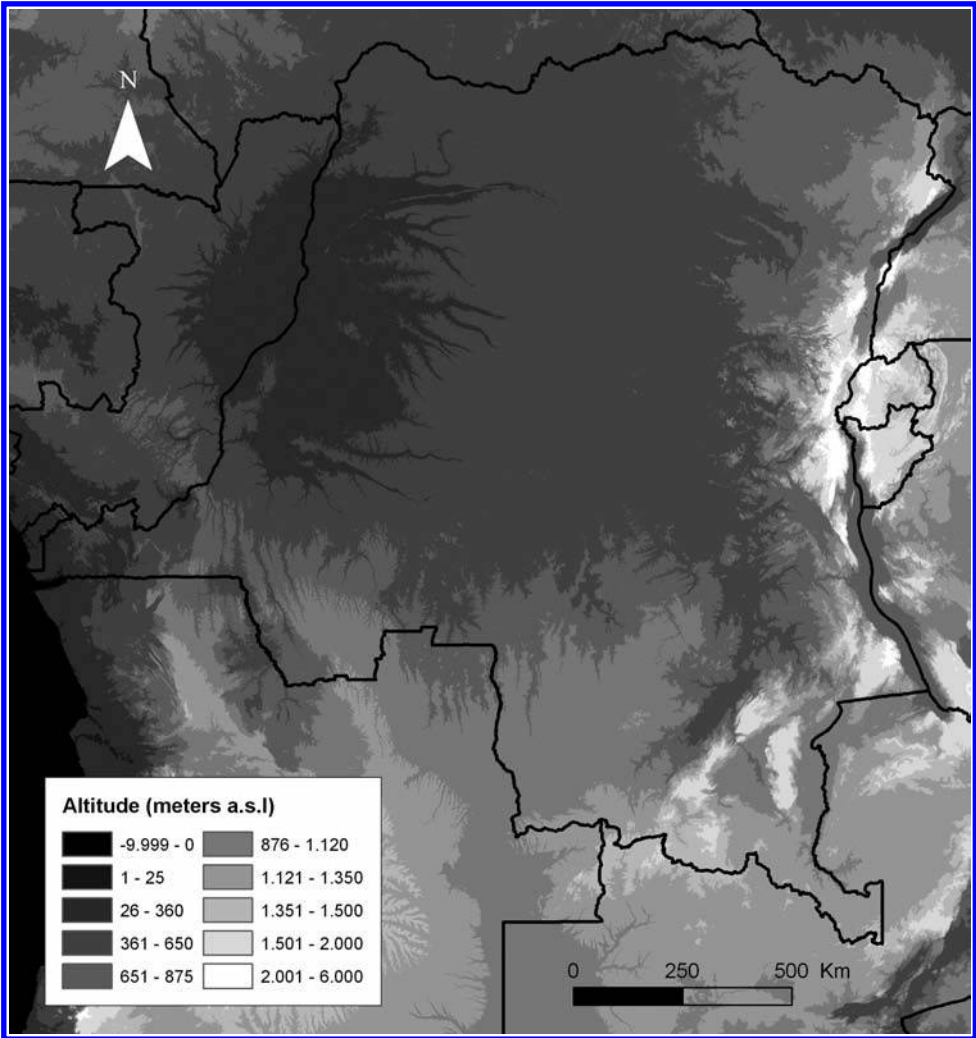


Figure 3B. Map of the altitudes of the study area (in meters above sea level).

The countries have seen rapid urbanization over the last few decades, further accelerated by political instability, especially in the eastern Kivu provinces, Rwanda and Burundi.

13.3 RESULTS

13.3.1 The database

Table 1 gives an overview of all the hydrological and meteorological events entered in the database so far. There have been several notably large events, such as the countrywide flooding in Rwanda in 1974, which affected 1,9 million people; the eruption of the Nyiragongo Volcano (Komorowski, *et al.*, 2003), Eastern DRC in 2002, which

Table 1. Extract from the database, showing the location, start year, type of hazard, and the number of people affected or killed for events of hydrological or meteorological origin.

Country	Location	Year	Hazard type	No. affected	No. killed
RWA	Nzaza	1910	Drought	0	0
DRC	Zongo	1916	Flood	0	0
DRC	Matadi, Mbandaka, Kisangani	1961	Flood	0	0
DRC	Maniema	1962	Flood	0	0
DRC	Zongo	1962	Flood	0	0
RWA	Rwankeri	1963	Landslide	0	0
DRC	Mandwe	1968	Landslide	768	154
DRC	Bukavu	1971	Landslide	0	0
DRC	Muhanga	1972	Landslide	0	22
DRC	Bukavu	1973	Landslide	0	0
RWA	Countrywide	1974	Flood	1.900.000	0
DRC	Bukavu	1976	Landslide	0	0
RWA	Widespread	1976	Drought	1.700.000	0
DRC	Bas-Congo	1978	Drought	500.000	0
DRC	Maniema	1979	Flood	0	0
DRC	Kinshasa	1984	Flood	0	0
DRC	Kivu provinces	1984	Drought	300.000	0
RWA	Widespread	1984	Drought	420.000	0
DRC	Uvira	1986	Flood	0	0
DRC	Kalimabenge, Mulongwe, Kanyabululu	1986	Flood	0	0
DRC	Kinshasa	1987	Flood	0	0
RWA	Base	1987	Landslide	0	0
DRC	Uvira	1988	Landslide	0	0
RWA	Ruhengeri, Gitarama, Gisenyi, Gikongoro, Kibuye	1988	Flood	21.678	48
RWA	Nyakinama	1988	Landslide	0	0
DRC	Maniema	1989	Flood	0	0
DRC	Kalundu, Kasenga	1989	Flood	0	0
BDI	Bujumbura	1989	Flood	3.600	12
DRC	South-Kivu	1989	Landslide	148	0
DRC	Likasi	1989	Flood	0	0
RWA	South, west of Kigali	1989	Drought	60.000	237
DRC	Kinshasa	1990	Flood	27.500	23
DRC	Uvira	1991	Flood	0	0
DRC	Kinshasa	1991	Flood	0	0
DRC	Bandundu	1992	Flood	0	0
DRC	Bukavu	1992	Landslide	0	0
BDI	Lake Tanganyika	1992	Drought	0	0
DRC	Uvira	1993	Landslide	0	0
DRC	Kinshasa	1994	Flood	0	0
BDI	Lake Tanganyika	1994	Drought	0	0
DRC	Bukavu	1994	Flood	50	39
DRC	Bukavu	1995	Landslide	0	0

(Continued)

Table 1. (Continued).

Country	Location	Year	Hazard type	No. affected	No. killed
RWA	Ginkongoro	1996	Drought	82.000	0
DRC	Kinshasa	1997	Flood	0	0
DRC	Kinshasa	1997	Flood	0	0
DRC	Murhala	1997	Landslide	0	0
DRC	Kisangani	1997	Flood	35.506	0
DRC	Bagira	1997	Landslide	0	0
DRC	Kivu Provinces	1998	Flood	0	0
DRC	Equateur	1998	Flood	22.500	70
DRC	Zongo	1999	Flood	0	0
BDI	Kayanza	1999	Storm	30.810	0
DRC	Kindu, Kisangani, Kinshasa	1999	Flood	0	0
BDI	Bugabira, Busoni, Kirundo, Ntega, Gitega, Ruyigi, Karuzi, Rutana, Makamba, Muyinga, Cankuzo, Moso, Imbo	1999	Drought	650.000	6
RWA	Umutara, Kibungo, Kigali Rural, Gitarama, Butare, Gikongoro	1999	Drought	894.545	0
DRC	Kinshasa	1999	Flash flood	78.000	2
RWA	Umutara, Kibungo, Kigali Rural, Gitarama, Butare, Muyinga, Kirundo	2000	Drought	0	0
BDI	Bugabira, Busoni, Kirundo, Ntega, Muyinga, Cankuzo, Moso, Imbo	2000	Drought	0	0
RWA	Karambo and Nyundo	2000	Flood	1.000	0
BDI	Bujumbura	2000	Flood	500	0
DRC	Kinshasa	2001	Flood	0	0
BDI	Kirundo, Muyinga	2001	Drought	0	0
DRC	Mbanza Ngungu	2001	Storm	0	0
DRC	Kinshasa	2001	Flood	26	50
RWA	Nshili, Nyaruguru, Mushubi	2001	Flash flood	0	10
RWA	Ruhengeri, Gisenyi, Gikongoro, Kibuye, Byumba	2001	Flood	3.000	2
DRC	Mbandaka	2001	Flood	13.000	0
DRC	Nord-Kivu	2001	Landslide	0	12
DRC	Mashango village, Muyunyi-Karuba	2001	Landslide	0	12
DRC	Uvira	2002	Flood	2.540	40
DRC	Goma	2002	Storm	0	11
BDI	Buringa	2002	Flood	2.000	0
RWA	Kigali, Gisenyi, Byumba, Bweyete, Rusenyi	2002	Flood	20.000	69
BDI	Bujumbura	2002	Flood	6.000	0
DRC	North and Central	2002	Flood	3.000	0

(Continued)

Table 1. (Continued).

Country	Location	Year	Hazard type	No. affected	No. killed
DRC	Plateau, Cuvette & Sangha	2002	Flood	3.000	0
DRC	Kivu, South-West	2003	Flood	0	0
DRC	Yumbi, Bombala, Maboka, Bongembe	2003	Storm	22.500	17
RWA	Umutara, Kibungo, Gitarama, Butare, Gikongoro, Bugesera, Gashora	2003	Drought	1.000.000	0
DRC	Hongo, Bukavu	2003	Landslide	0	0
DRC	Kasheke and Tchofi Villages, Kahele	2003	Landslide	0	9
BDI	Widespread	2003	Drought	0	0
DRC	Kisangani	2003	Flood	600	0
DRC	Bikoro	2003	Storm	73	11
RWA	Umutara, Byumba	2003	Flood	7.016	0
DRC	Matadi	2003	Landslide	0	11
DRC	Lufutoto, Kwilu-Ngongo	2003	Flood	881	1
DRC	Kinshasa	2004	Flood	0	0
BDI	Senga	2004	Storm	300	0
BDI	Mpanda Commune	2004	Storm	500	0
BDI	Kinama	2004	Storm	15.000	0
BDI	Rugazi	2004	Flash flood	10.000	0
DRC	Kinshasa	2004	Flood	1	13
DRC	Wakabangu, Pangi	2004	Drought	0	0
DRC	Kitanu	2004	Flood	0	0
DRC	Kinshasa	2005	Flood	0	0
BDI	Bugabira, Busoni, Kirundo, Ntega; Muyinga and Cankuzo Provinces, Ruyigi, Rutana	2005	Drought	2.150.000	120
BDI	Gatumba, Imbo, Kinyinya Hill, Waribondo Hill, Mushasha, Muyange	2005	Flash flood	5.000	0
DRC	Uvira Region	2005	Storm	5.389	8
RWA	Widespread	2005	Drought	0	0
DRC	Moukondozi and Kintsaka	2005	Storm	0	2
DRC	Kindu	2005	Storm	0	0
DRC	Kindu	2005	Storm	0	0
DRC	Mbuji-Mayi	2005	Storm	5	9
DRC	Kinshasa	2005	Flood	0	0
DRC	Minova	2005	Landslide	101	8
RWA	Kigali	2005	Flood	3	2
DRC	Kisantu	2005	Flood	0	0
DRC	Walikale	2005	Storm	0	6
DRC	Boma	2005	Storm	0	0
DRC	Kintanu, Inkisi	2005	Flood	0	0
DRC	Sud-Kivu: Fizi, Uvira, Ruzizi	2005	Drought	325	3

(Continued)

Table 1. (Continued).

Country	Location	Year	Hazard type	No. affected	No. killed
BDI	North and West	2006	Drought	430.000	0
BDI	Muyinga, Karusi, Ruyigi Province	2006	Drought	0	120
BDI	Gatumba	2006	Storm	1.505	0
DRC	Lukaya District	2006	Flood	3.870	0
BDI	Murwi Commune, Buhayira	2006	Flash flood	1.200	1
RWA	Umutara, Kibungo, Gitarama, Butare, Gikongoro, Bugesera	2006	Drought	1.011.200	0
DRC	Bukavu	2006	Flood	0	4
DRC	Oicha	2006	Storm	75.066	3
DRC	Kimbanseke, Kisenso, Limete, Masina, Matete Councils, Kinshasa	2006	Flood	5.500	1
BDI	Muramvya, Bururi	2006	Flood	5.000	20
BDI	Muheka	2006	Flood	5.000	1
BDI	Gihanga Commune, Imbo, Bujumbura Province, Bubanza Province	2006	Flash flood	2.000	9
BDI	Muramvya Province	2006	Flood	1.000	11
DRC	Bagira (Bukavu)	2006	Landslide	0	0
BDI	Kibago and Kayogoro Communes	2006	Flood	1.500	0
DRC	Kisangani, Mbuji-Mayi	2006	Flood	68.000	6
DRC	Maniema	2006	Flood	20.000	0
DRC	Kinshasa	2006	Storm	0	0
RWA	Northern part	2006	Flood	25.000	25
RWA	Rulindo District	2006	Landslide	2.000	24
BDI	Cibitoke, Ruyigi, Bubanza, Muramvya, Karusi, Kanyanza Districts	2006	Flood	4.105	0
DRC	Bumba, Basoko	2006	Flood	3.600	0
DRC	Bukavu	2006	Landslide	0	5
DRC	Kisantu	2006	Flood	1.000	0
DRC	Isangi	2006	Flood	1.060	0
RWA	Bigogwe	2007	Flood	1.670	18
BDI	Bujumbura, Bubanza, Cibitoke, Karuzi, North and Central	2007	Flood	23.000	4
BDI	Gatumba	2007	Flood	10.000	0
RWA	Rubavu, Nyabihu	2007	Flood	500	10
BDI	Bujumbura (Kinindo, Kanyosha, Musaga)	2007	Storm	125	0
DRC	Inongo	2007	Storm	0	0
DRC	Kinshasa	2007	Flood	2	0
DRC	Mbuji-Mayi	2007	Landslide		4
RWA	Rubavu, Nyabihu	2007	Flood	4.000	20
RWA	Bigogwe	2007	Flood	2.810	18

(Continued)

Table 1. (Continued).

Country	Location	Year	Hazard type	No. affected	No. killed
RWA	Ruhengeri, Byumba	2007	Flood	1.000	15
DRC	Ndaro	2007	Flood	0	0
BDI	Bujumbura, Cibitoke, Bururi	2007	Flood	2.701	1
DRC	Kisenge	2007	Storm	0	1
DRC	Bandalungwa, Bumbu, Kalamu, Kisenso, Lemba, Limete, Masina, Matete, Mont Ngafula, Ngaba, Ngaliema, Selembao	2007	Flood	1.600	32
BDI	Buterere, Bujumbura	2007	Storm	1.005	1
DRC	Kikwit	2007	Flood	0	0
DRC	Kikwit	2007	Flood	0	15
DRC	Kalehe	2008	Landslide	0	0
DRC	Kikwit	2008	Storm	8	10
DRC	Katuba, Lubumbashi	2008	Flood	0	2
DRC	Inongo	2008	Storm	1	0
DRC	Bukavu	2008	Landslide	0	5
DRC	Bandundu, Kasai Occidental	2008	Flood	502	15
DRC	Commune Mososo, Limete, Kinshasa	2008	Flood	0	0
BDI	Mugina, in Cibitoke	2008	Storm	5.000	0
DRC	Luebo	2008	Flood	250	0
BDI	Bujumbura Rural, Cibitoke, Ngozi	2008	Flood	2.770	0
BDI	Bugarama, Nyamurenza	2008	Storm	5	3
RWA	Rubavu, Kirehe, Ngoma, Nyamasheke	2008	Flood	500	0
DRC	Kindu	2008	Storm	0	0
DRC	Maniema	2008	Flood	6.625	0
RWA	West region	2008	Flood	0	0
DRC	Kinshasa	2008	Storm	0	0
RWA	Western regions	2008	Flood	2.500	0
BDI	Cibitoke	2008	Storm	1.000	0
DRC	Kinshasa (Binza, Lukunga)	2008	Storm	0	0
DRC	Kindu	2008	Flood	10	2
DRC	Road Kalemie-Nyunzu	2008	Flood	0	0
DRC	Kasheke	2008	Landslide	0	0
DRC	Kinshasa	2009	Flood	0	0
DRC	Kilimani Refugee Camp, Masisi	2009	Landslide	0	8
DRC	Bienga	2009	Landslide	0	5
BDI	Bujumbura, Buterere, Maramvya	2009	Flood	8.000	0
DRC	Kinshasa (Selembao)	2009	Landslide	0	4
RWA	Cyamuhinda	2009	Landslide	0	0
RWA	Rubavu, Nyabihu	2009	Flood	0	0
DRC	Butembo	2009	Flood	0	0
BDI	Gihanga	2009	Flood	1.070	0
BDI	Bujumbura	2009	Flood	3.585	0
DRC	Kabare, Kalehe, Bukavu	2009	Flood	0	20

killed 200 people, and left over 110.000 homeless; and the widespread drought in Northern Burundi in 2005 which affected some 2,1 million people. It should be noted, however, that the especially high frequency of smaller-scale events, such as landslides and local flooding make them equally devastating over time (Vandecasteele *et al.*, 2009).

A detailed discussion of the volcanic and seismic activity in the region falls beyond the scope of this article, but may be consulted in Ebinger, 1989 and Smets, 2010. The information has been simplified and listed in chronological order for reference.

13.3.2 Impact of hazards/quantification

The consequences of the natural hazards included in the database are expressed in terms of human losses, the number of people affected (those rendered homeless or injured), and material damages (constructions as well as crops damaged or destroyed). Figure 4 shows the total number of events of each type of hazard for the 3 countries included in the database, and the corresponding number of people killed and affected per event. It should be noted that these figures are most likely to be greatly underestimated due to the communication limitations in the region.

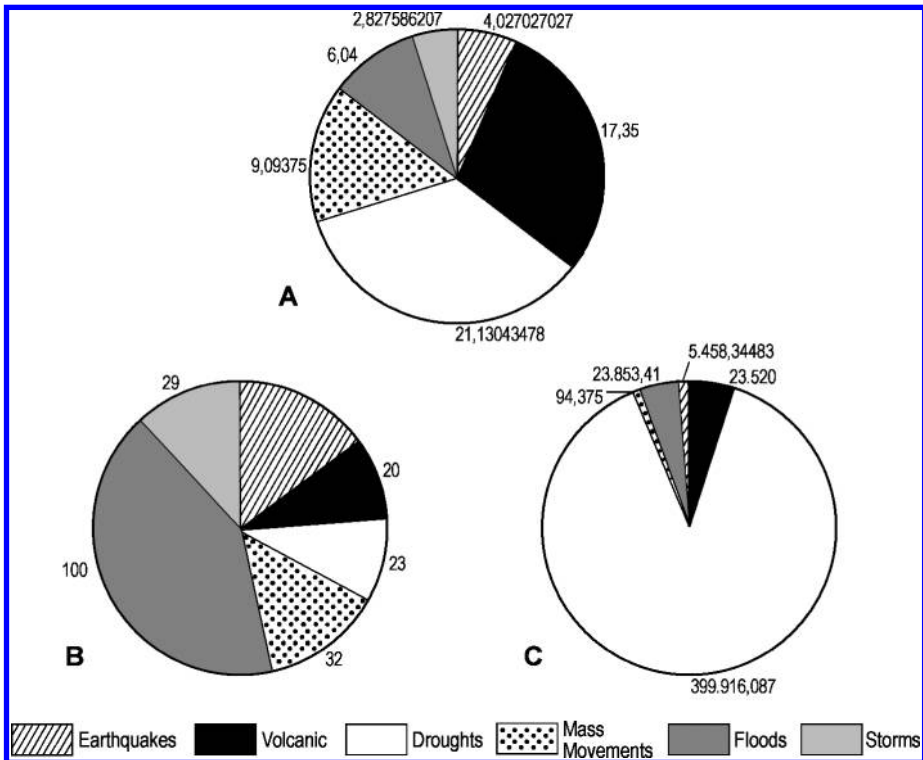


Figure 4. The total number of events of each type included in the databank (A), with the number of deaths per event (B), and the number of people affected per event (C) for each hazard type.

Floods are the most common events recorded in the region; their high frequency means that this type of hazard has led to the highest total number of deaths in the region, and affected over 2 million people. Although droughts are less frequent, they show both the highest number of deaths and people affected per event, presumably due to the prolonged nature of the events, and the related widespread damage to agriculture and livestock.

Table 2 gives the total number of events, deaths, and people affected per country. The database includes 241 events for the period 1910–2009, having resulted in 1959 reported hazard-related deaths, and some 12,2 million people affected. Taking the sizes of the countries into account, hazardous events seem to be concentrated in Rwanda, Burundi, and the Kivu provinces (see Figures 7 and 8), with Rwanda having the highest number of hazard-related deaths and number of people affected by events.

13.3.3 Temporal evolution

There is a general increase in the absolute number of hazard events (Figure 5), which can partially be explained by improved communication over the last few decades, but which, nevertheless, does reflect the increasing exposure of populations to natural hazards. In addition, due to rising population densities, smaller events, perhaps previously not affecting any people, may now cause increasing damages and be reported as natural hazards.

The CRED database confirms the same increase in absolute number of reported disasters globally (Figure 6). Personal communication in the field has also suggested that there has been an increase in the frequency and consequences of natural hazards in the region. This is especially outspoken as of the late 1990s, which is an indication

Table 2. The total number of events, deaths, and people affected by all hazard types for the three countries.

	DRC	Rwanda	Burundi	TOTAL
No. Events	161	37	43	241
No. Killed	1.092	554	313	1.959
No. Affected	1.393.477	7.458.468	3.383.447	12.235.392

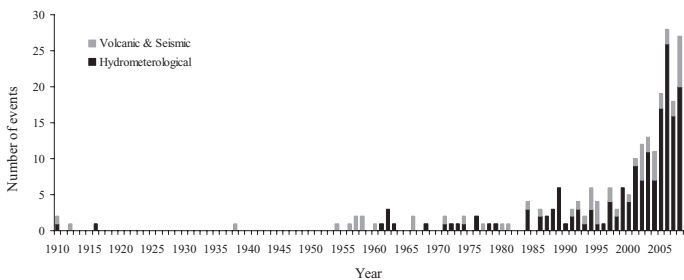


Figure 5. Graph showing the trend in occurrence of natural hazards for the period 1910 to 2009 in Rwanda, Burundi and the DRC. Hazards are classed as being of hydrometeorological (drought, storms, flooding and mass movements) or of volcanic and seismic origin.

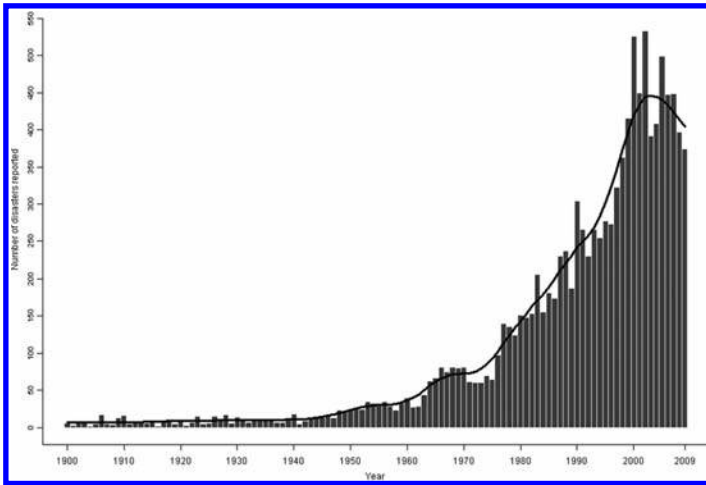


Figure 6. The global trend in number of natural disasters reported for the period 1900 to 2008. (Source: EM-DAT: The OFDA/CRED International Disaster Database, www.emdat.be, Université Catholique de Louvain).

that the rise in absolute reported number of events is not solely related to improving communication.

Although we do suggest that there is an important increase in events, it is important to keep in mind that there are also historical encounters of large events affecting great numbers of people. This is the case, for example, for the major flooding along the Congo River in 1961 (Devroey, 1962). An extreme amount of discharge was generated in the Kivu provinces, after which the overbank flow propagated along the Congo stream at a velocity of 0,5 m/s, all the way to Kinshasa, about 1.500 kilometers further downstream, inundating numerous villages along the way.

13.3.4 Spatial distribution

Figure 7 plots the data collected on flooding and mass movements on a base map of the population density for 2000 (UNEP/GRID).

Note that georeferencing of the events was carried out based on the reported information, so that the specific location of an event has been defined as the region or town(s) where human or material loss has been recorded. Almost all the reported hydrogeological events took place in urban areas (areas with high population densities on Figure 7). Although events are more likely to be reported if they take place in urban areas due to the damages they may cause, our field observations in and around Kinshasa, Bujumbura, Kigali, Butembo, Bukavu, Uvira, Mbuji-Mayi, Kikwit and Lisala confirm that hydrogeological hazards occur more frequently and with greater intensity within urbanised areas. This emphasizes the influence of urbanisation on the occurrence of events such as flooding and mass movements.

Figure 8 plots the storm and drought events in the region for the period 1910–2009, on a map of the average yearly precipitation and temperature (Bultot, 1971).

Storms tend to occur between 2° North and 7° South within the tropical belt. Droughts are frequent in the south of Rwanda and Burundi, where total precipitation

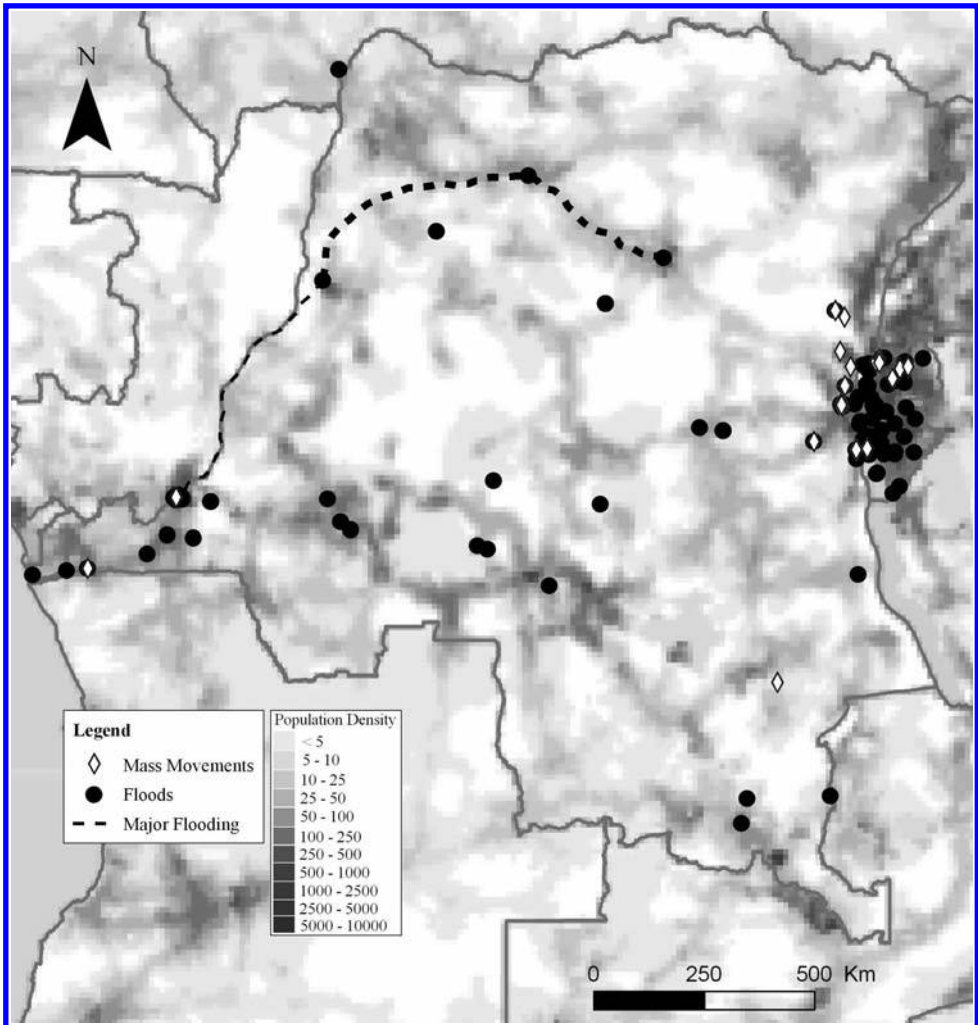


Figure 7. The distribution of mass movements and flood events included in the databank on a base map of the population density for 2000 (UNEP/GRID).

is lower, and population density greatest. There is a concentration of events along the Albertine Rift zone, which can be related to an accentuated topography, tectonic activity, and a high population density.

The Congo Basin itself is, however, equally a geomorphologically active, dynamic area, prone to flooding, storms, and mass movements. Flooding occurs mostly along the main tributary of the Congo River, and frequently in Rwanda and Burundi. The trajectory of large flooding events in 1941, 1961, and 1997 is indicated by a broken line in Figure 7. During these years, overbank flow events propagated along the length of the river, originating in the more mountainous Kivu Provinces, and inundating towns along the Congo in the provinces of Maniema, Tshopo, Mongala, Equateur, Mai-Ndombe, and Kinshasa.

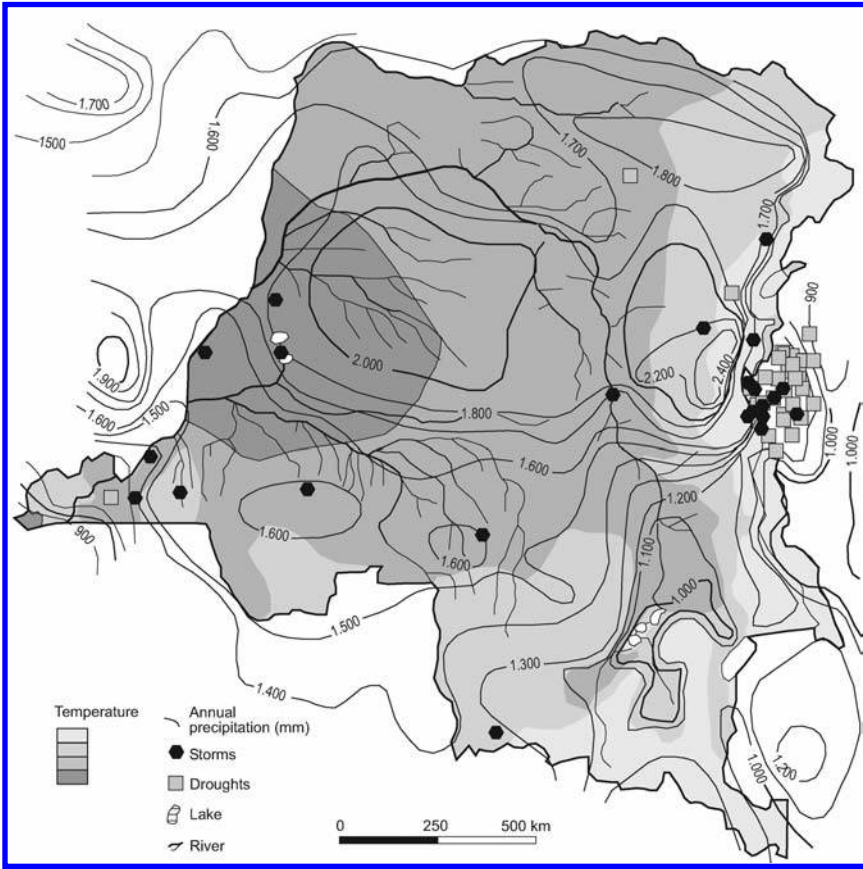


Figure 8. Spatial distribution of storms and droughts, on a map of average annual precipitation and temperature (after Bultot, 1971).

13.4 DISCUSSION

13.4.1 Limitations of the database

One of the main limitations in developing the database is the discrepancy in availability of information. Reports on hazardous events are readily available in large towns where NGO's are active, and this may give a skewed perception of the distribution of events in space and time.

With the introduction of telephone lines, national newspapers, radio and, of course, internet, information has become increasingly more accessible. This may partly explain why we see an exponential rise in number of recorded events over the concerned period of time. Figure 9 compares images of a flooding event in Ubandu, DRC, that we assume occurred in 1941 based on historical reports, of which there is very little information, to images of a recent landslide in the refugee camp of Masisi, North Kivu, DRC, which was recorded by various aid organizations on the 9th of February 2009, killing 8 people, injuring 3, and destroying numerous houses.



Figure 9. A) Flooding along the Congo River in Ubundu, 1941. B) Landslide in Masisi Refugee Camp, 2009.

The reliability of source data may sometimes also be questionable. Often figures related to human and material loss are estimates, and reports do not always include all the desired information on an event. That is why we try to include as many sources as possible.

So far entries have been classified according to how they are referred to in written reports. This may be problematic in certain cases since the event may involve more than one type of hazard. A storm may be related to flooding as well as several types of mass movements, for example, which means it is unclear as to how the event should be recorded.

One of the main problems we are now facing is how to integrate information on observed gullying into the database. Although gullying is undoubtedly the most common hazard in the region, affecting numerous people, and causing extensive destruction of property in urban areas, very few events are reported.

13.4.2 Causative factors

The factors leading to a high frequency of events in the Central African region are numerous. There are a number of natural characteristics of a terrain that make it susceptible to hazards. These natural factors may in turn be influenced by human actions (anthropogenic factors), which often lead to a more frequent occurrence of an event in that region, or in greater human and material loss resulting from an event.

Climate change may also influence the frequency of natural hazards, and is a result of both natural and anthropogenic factors. The changing vulnerability of the population with respect to natural hazard events is also an important factor in determining the consequences of an event.

It should be noted that events are often 'offsite effects'. For example, high population pressures and deforestation in the Kivu provinces (Wils, 1986) may increase surface runoff and river discharge further downstream. This is assumed to be the case for the major flooding along the course of the Congo River in 1941, 1961, and 1997.

13.4.2.1 Factors influencing spatial distribution

The spatial distribution of hazards is mostly defined by natural factors, although anthropogenic factors such as land use and urbanisation influence the concentration of hazards in urban areas.

Topography

Relief plays an important role in determining slope stability. There is an inverse relationship between the gradient of a slope and its stability for a uniform substrate. Most landslides have been located on the Albertine rift shoulders, where the relief energy is most outspoken.

Lithology and soil type

The type of substrate is important in determining the susceptibility of terrain to flooding and mass movements. Volcanic material, clays and loose rock are most susceptible to landslides, whilst impermeable material such as compact clays and marl will accelerate the occurrence of a flood. The Kalahari Sands and other sands of Pleistocene age (Cahen, 1954) covering almost the entire southern half of our study area are prone to rapid erosion and gulying. The easternmost provinces of the DRC, Rwanda, and Burundi are situated on crystalline bedrock, and the boundary with the overlying clays commonly forms the slip surface.

Tectonic activity

The Albertine rift is the only tectonically active region in the study area. The seismic activity within the rift can also trigger mass movements (Jibson and Keefer, 1993; Moeyersons *et al.*, 2004). Volcanic eruptions in the Virunga Range may also go paired with mass movements and the release of lethal gases (Favalli *et al.*, 2008; Wafula *et al.*, 2007).

13.4.2.2 Factors influencing temporal evolution

The factors leading to the observed increase in frequency of natural hazards are mostly anthropogenic in nature.

Climate change and hydrological regime

Although there is no clear trend to an increase or decrease in the absolute amount of precipitation in the region over time, considerable changes have been noted in the variability of the rainfall, as well as indications that the intensity of rainfall events is increasing (Muhigwa, 1999). Figure 10 compares the average monthly rainfall in Bukavu, North Kivu, for the periods 1930 to 1946 and 1988 to 2003 (Ndyambo *et al.*, 2009).

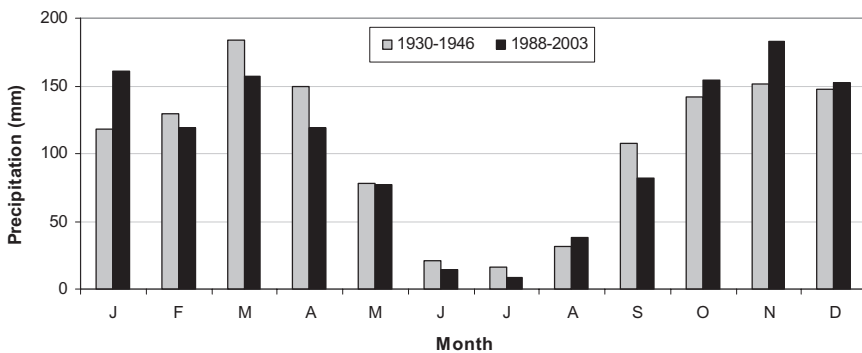


Figure 10. Monthly Average Precipitation for Bukavu, DRC, for the periods 1930–1946 and 1988–2003. (Source: Ndyambo *et al.*, 2009).

The large changes in monthly averages (increases from October to January, and decreases from February to July) between the two periods indicate a shift in the rainfall regime which may in part be responsible for the increasing numbers of landslides and floods in the city. Another indicator of a change in the pluviometric regime is a decrease in the level of Lake Kivu (Wafula *et al.*, 2007), which has had a direct impact on the production of the Rusizi hydroelectric power stations.

There is evidence for a change in river regime in Central Africa (Moeyersons and Trefois, 2008). Instead of a gradual rise in spring discharges following a rainfall event, there is an increasing high surface runoff which arrives directly in the river bed. The reasons for this change are mainly anthropogenic (deforestation, urbanisation, overgrazing and cultivation increase the runoff coefficient) but may also be in a smaller part due to climate change (higher intensity precipitation). The concentration of rainfall in the rainy season, and the intensity of rain showers increase the amount of surface runoff during the season, resulting in high erosion rates and flooding where the water is not effectively drained.

Land use

The type of land use in a region has a large influence on the hydrological properties of the substrate, and the amount of water transported as surface runoff. Forest cover has been proven to reduce the risk of flooding (Rwilima and Faugère, 1981; Bradshaw *et al.*, 2007). In the Congo Basin the deforestation rate has been estimated at 0,21% per year (Duveiller *et al.*, 2008), and is expected to increase to 1% by the year 2050 (Zhang *et al.*, 2006). Where surface water is effectively drained or infiltrates into the subsurface the risk of flooding and gully erosion is reduced. So, large portions of land left fallow or forested can reduce the risk of this type of natural hazard.

The exponential growth of the population in the region over the last few decades has lead to the rapid urbanisation of large areas of land. This has been observed on aerial photos and satellite images in the towns of Kinshasa, Kigali, Bujumbura, Butembo, Uvira, and Bukavu. Figure 11 shows the evolution of Butembo by comparing 3 satellite images from 1975, 1987, and 2001. The city's population increased from about 50.000 to 400.000 inhabitants between 1975 and 2001, with the surface area of the city increasing fivefold in the same period.

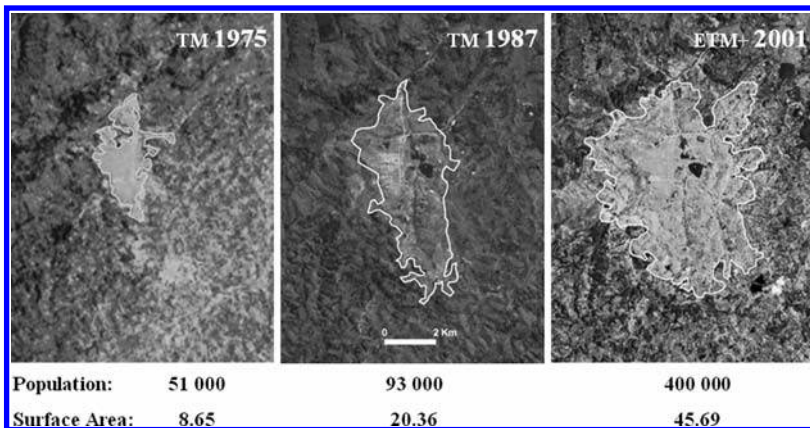


Figure 11. Growth of the town of Butembo, North Kivu between 1975 and 2001. The white line indicates the extension of the urban area on each image.

The construction of urban areas leads to an increase in runoff coefficients, which in turn increases the risk of flooding, gullying and mass movements. The construction of roads especially has been observed to be the cause of new gullies as well as the reactivation or acceleration of mass movements.

13.5 CONCLUSIONS

The Natural Hazard Database for Central Africa shows, for the first time in literature, that Central Africa is at present a geomorphologically active region. There is a concentration of events in the Kivu provinces, Rwanda, and Burundi due to the proximity of the rift valley with its related tectonic activity, high annual rainfall, accentuated topography, and high population density. The Congo Basin itself is equally active, with frequent flooding along the main waterways, and extreme erosion and gully formation.

There has been a large increase in frequency of reported hydrogeological events since the 1990s. Almost all recorded events occurred in urban areas, indicating that the increase is largely due to the accelerated urbanisation in the region over the last few decades.

The limitations faced with respect to the spatial and temporal data collection should be reduced by retrieving more complete information through the Réseau de Correspondants (RéCO) which has been set up for the three countries. Gullying having caused significant material damage will also be included in the databank with the aid of information provided by the RéCO, further field work in the region, and the consultation of satellite imagery.

REFERENCES

- Alexander, D., 1993 *Natural disasters*. London, UCL Press. 631 p.
- Alcántara-Ayala, I., 2002, Geomorphology, natural hazards, vulnerability and prevention of natural disasters in developing countries, *Geomorphology*, **47**, 2–4, pp. 107–124.
- Bradshaw, C., Sodhi, N., Peh, K., and Brook B., 2007, Global evidence that deforestation amplifies flood risk and severity in the developing world. *Global Change Biology*, **13**, pp. 2379–2395.
- Bultot, F., 1971, Atlas Climatique du Bassin Congolais, *Publications de l'Institut National pour l'Etude Agronomique du Congo (I.N.E.A.C)*.
- Byers, A.C., 1992, Soil Loss and Sediment Transport During the Storms and Landslides of May 1988 in Ruhengeri Prefecture, Rwanda, *Natural Hazards*, **5**, pp. 279–292.
- Cahen, L., 1954, *Géologie du Congo belge*. Liège, p. 577.
- De Bremaecker, J.Cl., 1957, Letter to the editor: Recent Volcanic Eruption in Belgian Congo, *Transactions, American Geophysical Union*, **38**, 6.
- Dilley, M., Chen, R.S., Deichmann, U., Lerner-Lam, A.L., Arnold M, Agwe, J., Buys, P., Kjekstad, O., Lyon, B., and Yetman, G., 2005, *Natural Disaster Hotspots: A Global Risk Analysis*. World Bank, Washington, D.C.
- Devroey, E-J., 1962, La crue exceptionnelle de 1961–1962 du fleuve Congo. *Extrait du Bulletin de l'Académie royale des Sciences d'Outre-Mer*, N.S., **VIII**, pp. 285–292.
- Duveiller, G., Defourny, P., Desclée, B., and Mayaux, P., 2008, Deforestation in Central Africa: Estimates at regional, national and landscape levels by advanced processing of systematically-distributed Landsat extracts, *Remote Sensing of Environment*, **112**, 5, pp. 1969–1981.

- Ebinger, C.J., 1989. Tectonic development of the western branch of the East African rift system. *Geological Society of America Bulletin*, **101**, pp. 885–903.
- EM-DAT: The OFDA/CRED International Disaster Database, www.emdat.be, Université Catholique de Louvain, Brussels, Belgium.
- Favalli, M., Chirico, G.D., Papale, P., Pareschi, M.T. and Boschi, E., 2008, Lava flow hazard at Nyiragongo Volcano, D.R.C., *Bulletin Volcanology*, DOI 10.1007/s00445-008-0233-y.
- ICSU Regional Office for Africa, 2007, *Natural and Human-induced Hazards and Disasters in sub-Saharan Africa*.
- Jibson, R.W. and Keefer, D.K., 1993, Analysis of the seismic origin of landslides: Examples from the New Madrid seismic zone. *Geological Society of America Bulletin*, **105**, 4, pp. 521–536.
- Komorowski, J.-C., Tedesco, D., Kasereka, M., Allard, P., Papale, P., Vaselli, O., Durieux, J., Baxter, P., Halbwachs, M., Akumbe, M., Baluku, B., Briole, P., Ciraba, M., Dupin, J.-C., Etoy, O., Garcin, D., Hamaguchi, H., Houlié, N., Kavotha, K.S., Lemarchand, A., Lockwood, J., Lukaya, N., Mavonga, G., de Michele, M., Mpore, S., Mukambilwa, K. and Munyololo F., 2003, The January 2002 flank eruption of Nyiragongo Volcano (Democratic Republic of Congo): chronology, evidence for a tectonic rift trigger, and impact of lava flows on the city of Goma, *Acta Vulcanologica*, **14**(1–2), pp. 27–62.
- Laraque, A., Orange, D., Maziezoula, B., and Olivry, J.-Cl., 1998, Origine des variations de débits du Congo à Brazzaville Durant le 14ème siècle, Water Resources Variability in Africa during the 14th Century, *Proceedings of the Abidjan '98 Conference held at Abidjan, Cote d'Ivoire, November 1998*. IAHS Publ. **252**.
- Moeyersons, J., Tréfois, P., Lavreau, J., Alimasi, D., Badriyo, I., Mitima, B., Mundala, M., Munganga, D.O. and Nahimana, L., 2004, A geomorphological assessment of landslide origin at Bukavu, Democratic Republic of the Congo. *Engineering Geology*, **72**, 1–2, pp. 73–87.
- Moeyersons, J., and Trefois, P., 2008, Desertification and changes in river regime in Central Africa: possible ways to prevention and remediation In: Gabriels, D., Cornelis, W., Eyletters, M., Hollebosch, P., Combating desertification? Assessment, adaptation and mitigation strategies. *Proceedings of the Conference on Desertification, Ghent*, **23**, UNESCO Centre for Eremology, Ghent University, Belgium, pp. 144–156.
- Muhigwa, J.-B., 1999, Analyse des perturbations dans le régime pluviométrique du Sud-Kivu durant les 50 dernières années. *Musée Royale d'Afrique centrale, Département de Géologie Min., Rapport Annuel 1997 & 1998*, pp. 112–121.
- Ndyanbo, S., Vandecasteele, I., Moeyersons, J., and Trefois, P., 2009, Climate-related Natural Hazards in Bukavu. *International Symposium: developing countries facing global warming: a post-Kyoto assessment*. United Nations Brussels, Royal Academy Overseas Sciences, Brussels, 12–13 June, Abstract, p. 72.
- Robert, M., 1948, *Le Congo physique*. *The Journal of Geology*, **56**, 3, pp. 247–247.
- Runge, J., and Nguimalet, C.-R., 2005, Physiogeographic features of the Oubangui catchment and environmental trends reflected in discharge and floods at Bangui 1911–1999, Central African Republic, *Geomorphology*, **70**, pp. 311–324
- Rwilima, Ch., and Faugère, T., 1981, Evolution entre 1958 et 1979 du couvert forestier et du débit des sources dans trois régions naturelles du Rwanda. *GEOMINES-SOMIRWA*, A.I.D.R. Kigali, 14 p.
- Shako, A.O., 2007, Seismicity and Recent Seismic Disasters in the D.R.-Congo, *Bulletin of HSEE*, **41**, pp. 43–54.

- Smets, B., Wauthier, C. and d'Oreye, N. A new map of the lava flow field of Nyamulagira (D.R.Congo) from satellite imagery. *Journal of African Earth Sciences*, AVCoR Special Issue, in press.
- Smith, K. and Petley, D.N., 2009, *Environmental Hazards: Assessing Risk and Reducing Disaster*, 5th Edition, Taylor & Francis, 383 p.
- Summerfield, M., and Hulton, N., 1994, Natural controls of fluvial denudation rates in major world drainage basins, *Journal of Geophysical Research*, **99**, B7, pp. 13.871–13.883.
- United Nations Environment Programme/Global Resource Information Database (UNEP/GRID) Spatial Data (Sioux Falls Dataset, Africa Population Distribution Database), 2000 Population Density, <http://na.unep.net/globalpop/africa/afpopd00.gif>
- UN/ISDR, 2004, *Towards Sustainable Development in Africa: A report on the status of disaster risk management and disaster risk assessment in Africa*. UN/ISDR, Africa Development Bank, African Union, New Partnership for Africa's Development.
- UNESCO-IHDR, 2009, *African Natural Hazards Map*.
- Vandecasteele, I., Byizigiro, V., Nkurunziza, D., Sahani, M., Nahimana, L., Lutumba, I., Ndyababo, S., Trefois, P., and Moeyersons, J., 2009, Spatial and temporal distribution of geomorphological hazards: the new "Natural Hazards Database for Central Africa". *Proceedings IAG Conference Melbourne 6–11 July 2009*.
- Wafula, D.M., Yalire, M., Kasereka, M., Ciraba, M., Kwetuenda, M. and Hamaguchi, H., 2007, Natural disasters and hazards in the Lake Kivu Basin, Western Rift Valley of Africa. <http://iugg-georisk.org/presentations/pdf/Lake-Kivu-hazards.pdf>
- Wils, W., Carael, M. and Tondeur, G., 1986, Le Kivu montagneux, Surpopulation—Sousnutrition—Erosion du sol (Etude prospective par simulations mathématiques), *Académie Royale des Sciences d'Outre-mer, Classe des Sciences naturelles et médicales*, Mémoires in-8°, Nouvelle Série, **21**, 3, Bruxelles.
- Zhang, Q., Justice, C.O., Jiang, M., Brunner, J. and Wilke, D.S., 2006, A GIS-based assessment on the vulnerability and future extent of the tropical forests of the Congo basin, *Environmental Monitoring and Assessment*, **114**, pp. 107–121.